Université de Montréal

Des complexes métalliques avec des ligands hydroxyamidines/ amidines oxydes (AMOXs) – synthèse, caractérisation et investigation de leurs applications

par

Mihaela Cibian

Département de chimie

Faculté des arts et des sciences

Thèse présentée à la Faculté des études supérieures et postdoctorales
en vue de l'obtention du grade de Philosophiae Doctor (Ph. D.)
en chimie

Décembre 2015

Résumé

La motivation initiale de ce travail provient de l'importance que les composés de coordination ont dans notre vie quotidienne. Leurs propriétés les rendent attrayants pour un large éventail d'applications, dans des domaines allant de la catalyse et de la conversion et stockage de l'énergie solaire jusqu'au domaine des matériaux et des sciences de la vie. Poussée par l'évolution et le progrès général de notre société, la recherche en chimie de coordination moderne évolue vers *la complexité au niveau moléculaire*, où la Nature représente une source majeure d'inspiration, comme dans le cas de la photosynthèse artificielle et de la chimie métallo-supramoléculaire. Dans le même temps, l'étude des complexes de coordination nourrit la curiosité scientifique et les approches pluridisciplinaires ouvrent de nouveaux mondes fascinants, tout en repoussant les frontières de la connaissance à des niveaux sans précédent.

En continuité avec l'étude et le développement de composés de coordination pour des applications spécifiques, le thème central de cette thèse est l'interaction Métal - Ligand et les moyens de la moduler par le design du ligand, afin de générer les propriétés nécessaires pour les applications ciblées. Le design de complexes de coordination est considéré comme un «ensemble de composants modulables» – le ligand: les groupes fonctionnels des atomes donneurs, les substituants et leurs effets électroniques et stériques, le type et la dimension du cycle chélate; l'ion métallique; l'environnement.

Les ligands étudiés ici sont les oxydes d'amidines *N,N'*-disubstitués (AMOXs) (aussi appelés α-aminonitrones ou hydroxyamidines). L'influence du motif de substitution du ligand sur les propriétés des composés est étudiée pour des complexes bis(AMOX) de cobalt(II) et de zinc(II). Les bis(chélates) de cobalt(II) sont plan carré (bas spin) à l'état solide, mais présentent une isomérisation de la structure plan carré (bas spin) vers une structure tétraédrique (haut spin) en solution dans des solvants non-coordinants. L'équilibre d'isomérisation est fortement influencé par le motif de substitution sur le ligand, du fait d'une combinaison de facteurs stériques et électroniques.

Une approche théorique (DFT/ TD-DFT) et expérimentale combinée a montré que, dans la famille des chélates bis(AMOX) de zinc(II), le gap optique peut être finement modulé

pour de potentielles applications dans des dispositifs optoélectroniques par la modification spécifique des ligands.

Un cas spécial de solvatomorphisme a été identifié: des modifications de la géométrie et de l'état de spin sont induites par la présence ou l'absence de liaisons hydrogènes dans un même composé de cobalt(II). L'influence de l'environnement est ainsi illustrée. Les interactions faibles sont les principaux facteurs responsables pour la stabilisation du système vers une combinaison spécifique géométrie - état de spin à l'état fondamental, de façon similaire au contrôle allostérique et aux interactions hôte-invité dans les systèmes biologiques.

Des études préliminaires vers des systèmes supramoléculaires à base des ligands AMOX ont été effectuées (assemblées multimétalliques vers des matériaux fonctionnels et des systèmes photocatalytiques pour conversion d'énergie solaire, en particulier la photocatalyse pour la production de H2).

J'espère que les résultats et les perspectives présentées dans cette thèse incitent à la poursuite de la chimie de coordination des AMOXs.

Mots-clés: chimie de coordination, complexe métallique, cobalt, zinc, ligands N,O-donneurs, amidine *N*-oxyde/ α-aminonitrone/ hydroxyamidine, détermination de structure à l'état solide, stéréochimie, isomérisation, effets des substituants, solvatomorphisme, cristallographie aux rayons X, théorie de la fonctionnelle de la densité, électrochimie, photophysique.

Note: Pour les chapitres écrits en français, la traduction en anglais est disponible dans les Annexes.

Abstract

The underlying motivation for this work stems from the importance that coordination compounds play in our daily lives. Their properties make them suitable and attractive for a wide range of applications in fields going from catalysis and solar energy conversion/ storage to materials and life sciences. Driven by the general progress of our society, research in modern coordination chemistry evolves *toward complexity at the molecular level*, with Nature representing a major source of inspiration as shown by artificial photosynthesis and metallosupramolecular chemistry. At the same time, the study of coordination complexes nurtures scientific curiosity, and multidisciplinary approaches are opening fascinating new worlds, while pushing the frontiers of knowledge to unprecedented depths.

In line with the study and the development of coordination compounds for specific applications, the central theme of this thesis is the Metal-Ligand interaction and how it can be modulated through ligand design to generate the properties targeted for particular applications. The design of coordination complexes is seen as a '*collection of adjustable components*' (e.g. the ligand: the donor atoms and their functional groups, the type and the size of the chelating ring, the ring substituents and their electronic and steric effects; the metal-ion; the environment).

The ligands under study are the *N,N'*-disubstituted amidine oxides (AMOXs) (also known as α-aminonitrones/ hydroxyamidines). The influence of the ligand substitution pattern on the properties of the compounds is investigated in series of cobalt(II) and zinc(II) bis(AMOX) complexes. The cobalt(II) bis(chelates) are square-planar (low spin) in the solid state, but show square-planar (low spin) to tetrahedral (high spin) isomerization in solution of non-coordinating solvents. The isomerization equilibrium is highly sensitive to the substitution pattern on the ligand due to a combination of steric and electronic influences. A combined experimental and theoretical approach [DFT and time dependent (TD-DFT)] has shown that in the family of zinc(II) bis(AMOX) chelates, by specific modification of the ligands, the optical band gap can be fine-tuned for potential applications in optoelectronic devices.

A special case of hydrogen-bonding-induced geometry and spin change at a cobalt(II) centre within a same cobalt(II) bis(chelate) has been identified. It highlights the influence of the environment on the properties of the complex. Weak interactions are the main factors responsible for biasing the system toward a specific geometry – spin state combination in the ground state, in a similar fashion to allosteric control and host-guest interactions in biological systems.

Preliminary studies were conducted toward AMOX-based supramolecular systems: multimetallic assemblies toward functional materials and photocatalytic systems for solar energy-conversion (in particular photocatalysis for H_2 production).

It is my hope that the above results and the perspectives presented in this work motivate further developments in AMOX coordination chemistry.

Keywords : coordination chemistry, coordination complex, cobalt, zinc, N,O ligands, amidine *N*-oxide/ α-aminonitrone/ hydroxyamidine, structure elucidation, stereochemistry, isomerization, substituent effects, solvatomorphism, X-ray crystallography, density functional theory, electrochemistry, photophysics.

Note: The English translation of the chapters written in French is available in Appendix.

Table des matières

Liste des tableaux

ANNEXES / APPENDIX

Liste des figures

ANNEXES / APPENDIX

Liste des schémas

Liste des abréviations

Å	Angström
ACN	Acetonitrile
AcOEt	Acetate d'éthyle
AMOX	Amidine oxide
ATR	Attenuated Total Reflectance
B3LYP	Becke, three-parameter, Lee-Yang-Parr exchange-correlation functional
bpy	2,2'-bipyridyne
br	Broad
BTZ	2-(2-benzothiazolyl)phenolato
CCD	Charged-Coupled Device
cif	Crystallographic Information File
CSD	Cambridge Structural Database
CV	Cyclic Voltammetry
cyt b6f	Complexe cytochrome b6f
d	Doublet
DCM	Dichlorométhane
dd	Doublet of doublet
deg	Degré
DFT	Density Funtional Theory
DMF	*N,N'*-diméthylformamide
DMSO	Diméthylsulfoxyde
DSPEC	Dye-sensitized photoelectrosynthesis cell
DSSC	Dye Sensitized Solar Cells
EA	Elemental Analysis
ED	Electron Donor
EDG	Electron-Donating Group
EPR/ ESR	Electron Paramagnetic Resonance/ Electron Spin Resonance
eq.	Equivalent
equiv.	Equivalent
ESI-MS	Electrospray Ionization Mass Spectrometry
EtOH	Ethanol
EW	Electron Withdrawing
EWG	Electron-Withdrawing Group
Fd	Ferrodoxine
FT-IR	Fourier Transform Infrared
GC	Gas Chromatography
GOF	Goodness of fit

HER	Hydrogen Evolving Reaction
HOMO	Highest Occupied Molecular Orbital
HRMS	High Resolution Mass Spectrometry
HS	High spin
I	Luminescence intensity
IR	Infrared
LANL2DZ	Los Alamos National Laboratory 2 double ζ
LC	Ligand-centered transition
LLIVCT	Ligand-to-ligand intervalence charge transfer
LMCT	Ligand-to-metal charge transfer
LS	Low spin
LUMO	Lowest occupied molecular orbital
m	Multiplet
M(II)	Metal(II) ion
m/z	Mass over charge ratio
MCD	Magnetic Circular Dichroism
m-CPBA	meta-Chloroperoxibenzoic acid
MALDI	Matrix Assisted Laser Desorption/Ionization
Me	Methyl
MLCT	Metal-to-ligand charge transfer
MOF	Metal-Organic Framework
MO	Molecular Orbital
MW	Microwave irradiation
NIR	Near Infrared
NMR	Nuclear Magnetic Resonance
NO	Nitric oxide/ nitrosyl
NTO	Natural Transition Orbital
OEC	Oxygen evolving centre
OLED	Organic Light Emitting Diodes
ORTEP	Oak Ridge Thermal Ellipsoid Program
PC	Plastocyanine
PCM	Polarized Continuum Model
PEC	Photoelectrochemical cell
Ph	Phenyl
ppm	Part par million
POM(s)	Polyoxométalate(s)
PPSE	Polyphosphoric acid trimethyl ester
PQH	Plastoquinol
PS	Photosensitisateur
PSI	Photosystème I

PSII	Photosystème II
PV	Photovoltaics
py	Pyridine or pyridyl
s	Singlet
SCE	Standard Calomel Electrode
SED	Sacrificial electron donor
sept	Septet
sh	Shoulder
SOMO	Singly occupied molecular orbital
SWV	Square-Wave Voltammetry
t	Triplet
TBABr	Tetrabutylammonium bromide
TBABr3	Tetrabutylammonium tribromide
TBAP	Tetrabutylammonium hexafluorophosphate
TD-DFT	Time-dependent Density Functional Theory
TEA	Triéthylamine
TEOA	Triéthanolamine
TGA	Thermogravimetric analysis
THF	Tetrahydrofurane
TLC	Thin layer chromatography
TOF	Turnover Frequency
TON	Turnover Frequency
UNC EFRC	University of North Carolina Energy Frontier Research Center
UV	Ultraviolet
vis	Visible
WO	Water oxidation
WOLED	White Organic Light Emitting Diode
XAS	X-ray absorption spectroscopy
XPS	X-ray photoelectron spectroscopy
XRD	X-ray diffraction
Z	Number of molecules per unit cell

To my family

Remerciements/ Acknowledgements

First and foremost I would like to thank Professor Garry Hanan. Thank you for your unique way of guiding without taking one's independence and for constantly motivating me to surpass myself. Thank you for opening my eyes to new perspectives on myself and on the world around. Your advice, your continuous support, and the fact that you believed in me have helped me to become a better student, a better scientist, and a better person. Thank you!

My thanks are also going to all the personnel and services at Université de Montréal: **XRD Laboratory**: Professor Frank Schaper, Dr. Michel Simard, Françine Bélanger-Gariépy and Dr. Thierry Maris; **Elemental Analysis Service**: Elena Nadezhina and Françine Bélanger-Gariépy; **Mass Spectrometry Service**: Dr. Alexandrea Furtos, Marie-Christine Tang, and Karine Venne; **NMR Spectroscopy Service**: Dr. Minh Tan Phan Viet, Dr. Cédric Malveau, Sylvie Bilodeau and Antoine Hamel; **Materials Characterization Laboratory**: Pierre Ménard-Tremblay, Sylvain Essiembre, Patricia Moraille, and Dr. Samir Elouatik; **Teaching Laboratory**: Huguette Dinel, Gaétan Caron, Denis Deschenes, Amira Khoury, Medgine Lindor-Ménard, and Sylvie Marceau; **Workshop**: Jean-François Myre, Louis Beaumont, and Cédric Ginart. Thank you for all your help, your enthusiasm, and the patience you guided me with into the captivating world of research.

I am particularly grateful to Professor André Beauchamp, Professor Frank Schaper, and Dr. Michel Simard as well as to Françine Bélanger-Gariépy and Dr. Thierry Maris for introducing me to the fascinating field of X-ray crystallography. An additional thanks to Françine Bélanger-Gariépy and Elena Nadezhina for giving me the opportunity to learn and practice the technique of elemental analysis. I am also grateful to Dr. Alexandra Furtos for the training and advice in mass spectrometry.

I would also like to thank Professor Ken Sakai and his research group from Kyushu University, Japan. The internship in your group was a wonderful professional and personal experience.

I am very grateful to all the graduate students and postdoctoral fellows I had the chance to work with during the years: Dr. Daniel Chartrand, Dr. Michael Cooke, Dr. Marie-Pierre

I will forever be grateful to Mrs. Ruxandra Arghius, my first chemistry teacher. You have the special gift to touch the minds and souls of your students, thank you!

I thank all the others who helped me in any way during the time of my PhD. Finally, I thank my friends and my family for their unconditional love and support.

Chapitre 1: Introduction

1.1. Le contexte général: 'La chimie de coordination moléculaire et supramoléculaire' – les complexes de coordination et leurs applications

1.1.1. Le rôle des composés de coordination: dès succès passés aux défis actuels et futurs – des tendances dans la chimie de coordination moderne

L'étude et le développement de composés de coordination pour des applications spécifiques, tangibles est la motivation sous-jacente pour le présent travail. Il découle de l'importance que ces composés jouent dans notre vie quotidienne.[1] En combinant les caractéristiques des ions métalliques avec celles des ligands organiques, les complexes de coordination présentent des propriétés intrinsèques qui peuvent être plus facilement adaptables par rapport à celles des matériaux inorganiques purs, tout en possédant une meilleure stabilité et robustesse versus les substances organiques.[2] Par conséquent, leurs propriétés les rendent attrayants pour un large éventail d'applications, dans des domaines allant de la catalyse et de la conversion et stockage de l'énergie solaire jusqu'au domaine des matériaux et des sciences de la vie.[1] La recherche sur les composés de coordination a prospéré au cours des dernières décennies, résultant dans des aperçus fascinants et des développements sans précédent, contribuant à l'évolution des connaissances.[3] Ainsi, la chimie de coordination moderne a vu le jour et s'est établie comme un important domaine de recherche qui apporte des solutions pratiques nécessaires pour répondre aux plus grands défis de l'humanité: l'énergie, l'eau, l'alimentation, l'environnement, la pauvreté et les maladies.[3-4] Des exemples de composés de coordination dans diverses applications sont mis en évidence dans le Tableau 1.1-1 et la Figure 1.1-1. Les complexes de coordination sont idéalement placés du point de vue de leurs propriétés photophysiques, photochimiques, électrochimiques (redox) et magnétiques pour être utilisés dans des applications comme: des colorants et des pigments (p. ex. **1-2**, Tableau 1.1-1);[5] des extractants pour l'industrie de l'extraction et l'hydrométallurgie (p. ex. **3-5**,

Tableau 1.1-1);[6] des catalyseurs dans des procédés catalytiques homogènes d'importance industrielle (p. ex. **6-12**, Tableau 1.1-1);[7] des médicaments pour la thérapie anticancer (p.ex. **13-15**, Tableau 1.1-1),[8] la thérapie de chélation (p. ex. **16-19**, Tableau 1.1-1),[9] le traitement de la polyarthrite rhumatoïde (p. ex. **20**, Tableau 1.1-1),[10] et des agents de diagnostique (p. ex. **21-22**, Tableau 1.1-1)[11] en médecine. En outre, l'utilisation de complexes de coordination dans les technologies émergentes telles que les dispositifs récolteurs et de conversion de l'énergie solaire (p. ex. Dye Sensitized Solar Cells (DSSCs) (p. ex. **23-26**, Tableau 1.1-1)),[12] les applications à base d'Organic Light Emitting Diodes (OLEDs) (p. ex. **27-31**, Tableau 1.1-1),[13] et les applications à base de Metallic-Organic Framework (MOF) (p. ex. **32-33**, Tableau 1.1-1)[14] a suscité un intérêt accru pour la recherche. Des résultats concrets ont été obtenus: produits prototypes (p. ex. réservoir de carburant à base de MOFs et matériaux de filtration à base de MOFs;[14a] dispositifs d'éclairage à base de DSSCs (p. ex. Hana-Akari lamp by Sony)[12b, 15]) ainsi que des produits qui ont déjà été introduits sur le marché (panneaux d'éclairage à base d'OLEDs (OSRAM, Mitsubishi, Pioneer, LG Chem) téléviseurs à base d'OLEDs (p. ex. LG, Sony, Panasonic) et smartphones (p. ex. Samsung Galaxy), les feux arrière à base d'OLEDs (BMW)).[16]

Tableau 1.1-1. Des exemples de composés de coordination dans diverses applications (voir la Figure 1.1-1 pour les structures des systèmes/ composés)

Composé (Fig. 1)	Type d'application	Domaine	Référence
1	Colorant	industrie des colorants et pigments, du textile, du papier et du bois	[5]
2	Pigment		
3 – 5	extractants pour les métaux	industrie de l'extraction et de l'hydrométallurgie	[6]
6	catalyseur – hydroformylation	production industrielle des aldéhydes	[7a, 7f]
7	catalyseur – procédé Monsanto	production industrielle de l'acide acétique	[7a, 7f]
8	catalyseur – procédé Cativa		
9	catalyseur – procédé SHOP (Shell higher olefin process)	industrie pétrochimique – oligomérisation des oléfines (production des oléfines linéaires C6-C20)	[7a, 7b]
10	catalyseur –hydrogénation asymétrique des cétones	industrie pharmaceutique	[7c-e]
11 – 12	catalyseur – cross-coupling	synthèse des produits organiques	[7a, 7g, 7h]
13 – 15	médicaments anticancéreux cliniquement approuvés au niveau mondial	médecine: thérapie contre le cancer	[8a, 8b]
16 – 17	des agents chélateurs de fer	médecine: thérapie de la surcharge en fer	[9a-c]
18	des agents chélateurs de métaux lourds (M = Hg, As, Au)	médecine: thérapie pour empoisonnement aux métaux lourds (approuvé par FDA)	[9a]
19	des agents chélateurs de plomb		
20	médicament contre l'arthrite rhumatoïde	médecine: thérapie (approuvé par FDA)	[10]
21	agent de contraste (MRI)	médecine: imagerie diagnostique (approuvé par FDA)	[11a]
22	gamma-emitting radio-nuclide bone imaging agent		[11b, 17]
23 – 26	DSSC (colorants)	récolte et conversion de l'énergie solaire	[12a-c, 12e, 18]
27 – 31	OLEDs	optoélectroniques	[13]
32 – 33	stockage de carburant/ gaz: réservoir de carburant à base de MOFs	transportation	[14]
33	matériaux filtrants	industrie alimentaire et textile	
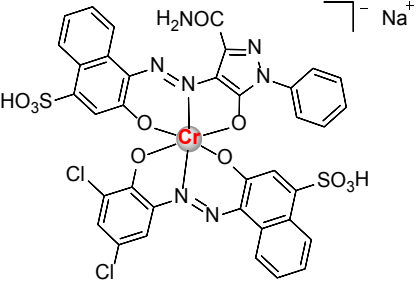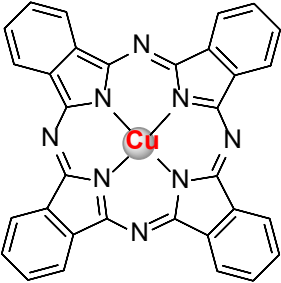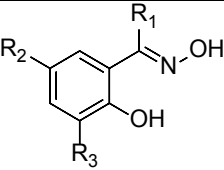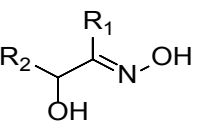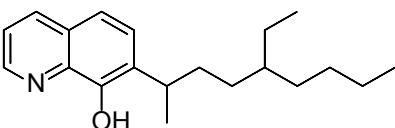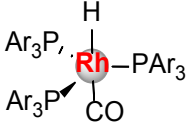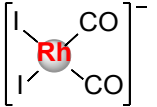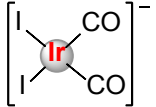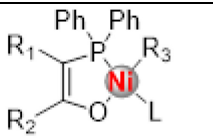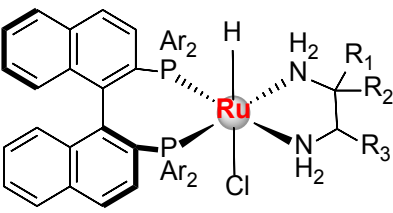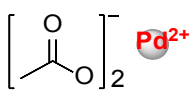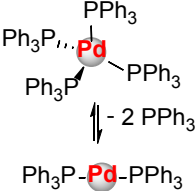
colorant azo à base de Cr (CI Acid Violet 121)	phthalocyanine de cuivre (CI Pigment Blue 15)
1[5]	**2**[5]

R_1 = H, alkyl, Ph, benzyl R_2 = alkyl R_3 = H, Cl	R_1 = R_2 = 2-ethyl-phenyl	
extractants de métaux de type oxime phénolique	extractants de métaux de type α-hydroxyoxime	Kelex 100 extractant de métaux de type 8-hydroxyquinoline
3[6]	**4**[6]	**5**[6]

catalyseur à base de Rh (hydroformylation)	catalyseur à base de Rh (Monsanto)	catalyseur à base d'Ir (Cativa)
6[7f]	**7**[7f]	**8**[7f]

R_1 = CF$_3$, C$_3$F$_7$, C$_6$F$_5$ R_2 = CO$_2$Et R_3 = Ph L = PPh3	
catalyseur à base de Ni (SHOP)	RuHCl(BINAP)(diamine)
9[7b]	**10**[7e]

précatalyseur/ catalyseur à base de Pd (cross coupling reactions)	
11[7a]	**12**[7a]

Figure 1.1-1. Des exemples de composés de coordination dans diverses applications

cisplatine	*carboplatine*	*oxaliplatine*
13[8a]	**14**[8a]	**15**[8a]
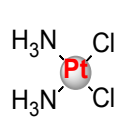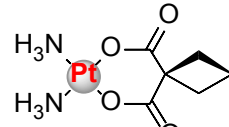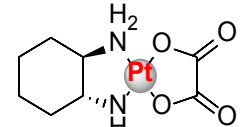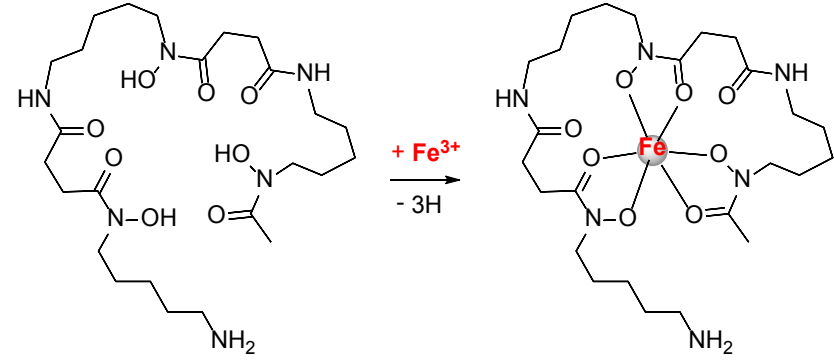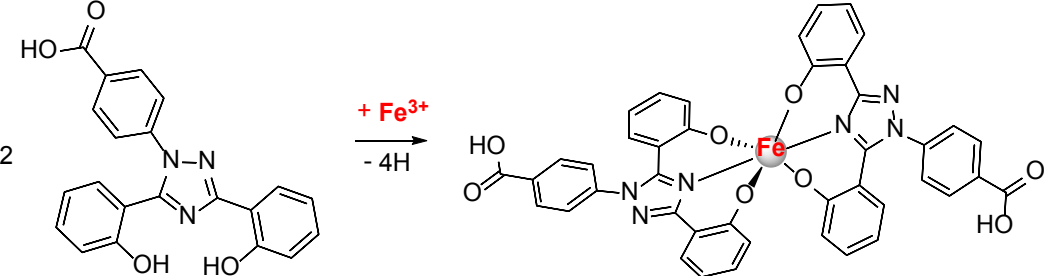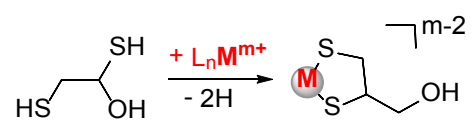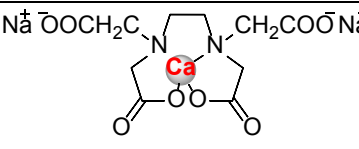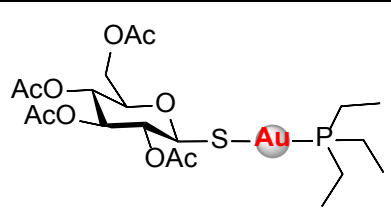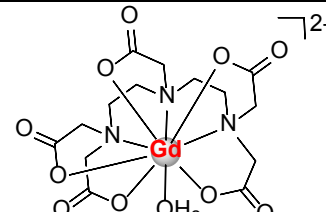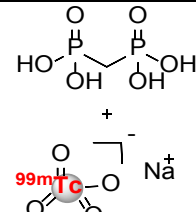
deferoxamine/ desferrioxamine-B (Desferal)		*ferrioxamine B*
16[9a-c]		**16-i**[9a-c]

deferasirox (Exjade)		*complexe Fe(deferasirox)₂*
17[9a-c]		**17-i**[9a-c]

dimercaprol/ British Anti Lewisite (BAL)	*M(dimercaprol)$^{m-2}$ complex M = Hg, As, Au*	*calcium disodium EDTA (utilisé dans l'empoisonnement au plomb)*
18[19]	**18-i**	**19**[9a]

auranofin (Ridaura)	*[Gd(DTPA)(H₂O)]²⁻(Magnevist)*	*⁹⁹ᵐTc medronate*
20[10]	**21**[20]	**22**[17]

Figure 1.1-1. Des exemples de composés de coordination dans diverses applications – (suite)

N3 (colorant DSSC)	K19 (colorant DSSC)
23[12c]	**24**[12c]

TFRS-52 (colorant DSSC)	SM315 (colorant DSSC)
25[12e]	**26**[18]

Λ-fac-Ir(ppy)₃	Δ-fac-Ir(ppy)₃	Λ-FIrpic	Δ-FIrpic
27[13e]		**28**[13e]	

Ir(ppy)₂(diketonate)	Eu(dbm)₃(phen)	mer-Alq₃	fac-Alq₃
29[13a]	**30**[13d]	**31**[13f]	
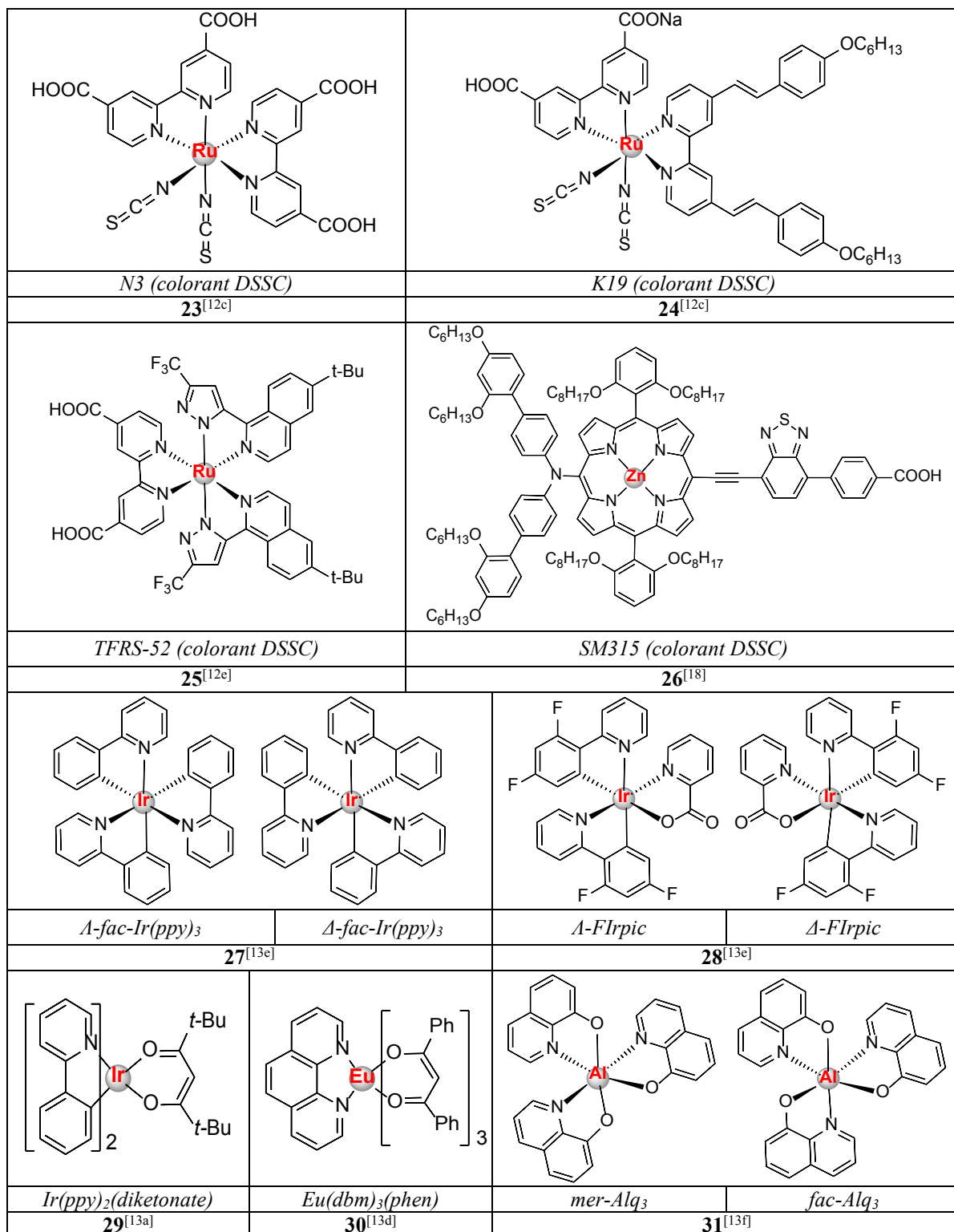
Figure 1.1-1. Des exemples de composés de coordination dans diverses applications – (suite).
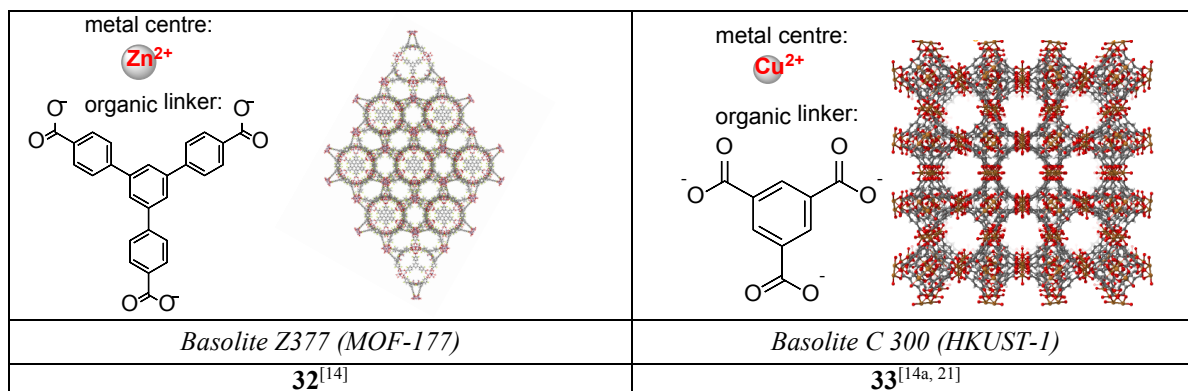
Figure 1.1-1. Des exemples de composés de coordination dans diverses applications – (suite).

L'évolution de notre société au niveau mondial se caractérise par le processus cyclique de type cause-effet: défis ↔ (mènent au) progrès. En conséquence, la tendance générale suivante a émergé dans la recherche, le développement et la mise en œuvre des applications réelles (dispositifs et processus): *plus robuste - plus efficace en termes d'énergie et de l'espace - plus vert*. Du point de vue des composés utilisés dans de telles applications, cette tendance a engendré une évolution *vers le niveau moléculaire*: être en mesure de générer, de modifier et d'adapter les propriétés des composés en ajustant, contrôlant, ainsi que de prédire et de concevoir au niveau moléculaire.[3, 22] Une description plus compréhensive de cette tendance est *vers la complexité au niveau moléculaire*, car elle se compose en fait de deux directions simultanées: i) *la spécialisation* (l'étude poussée des composants individuels afin de comprendre les fondements, leurs spécificités, leurs propriétés, et d'en tirer des modèles) et ii) *des approches interdisciplinaires et multidisciplinaires* (d'un point de vue général, on peut le considérer comme un système combinant des composants de nature différente, et/ ou divers «outils de connectivité», et/ ou méthodologies, pour renforcer la complémentarité et les effets synergiques, pour gagner en efficacité totale et en stabilité).[3, 22-23] Une présentation schématique est mise en évidence dans la Figure 1.1-2.

La direction *spécialisation* peut être décrite par une approche de type «boîte noire», l'évolution d'un premier rapport d'un système (I) vers l'étude et le développement de ses différents composants (II), et d'autres études systématiques de chaque composant (III). On peut considérer les *approches multidisciplinaires* suivantes: les méthodes de caractérisation expérimentales combinées (1); le développement des modèles théoriques, l'utilisation de calculs théoriques, ainsi que la validation des modèles par comparaison avec les résultats

expérimentaux (2); le développement des systèmes hybrides (3); l'application du composé / système dans un dispositif et l'évaluation de sa performance (4).
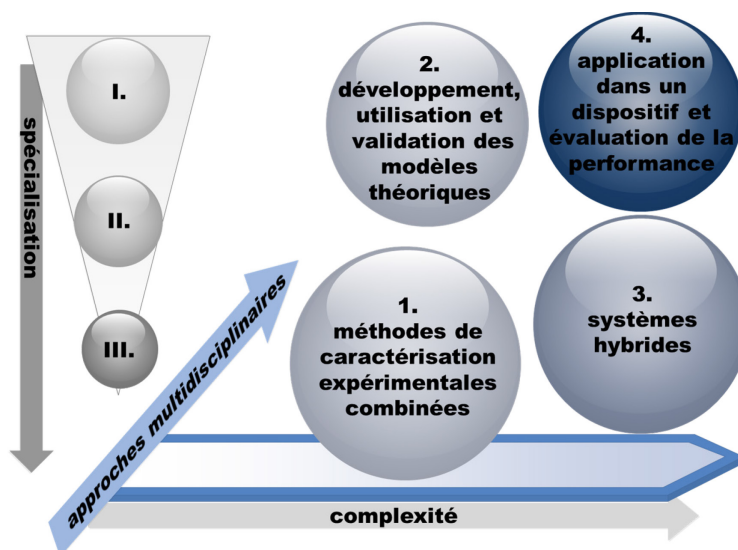
Figure 1.1-2. La tendance *vers la complexité au niveau moléculaire* dans la chimie de coordination moderne: spécialisation et approches multidisciplinaires.

L'évolution de la chimie de coordination moderne *vers la complexité au niveau moléculaire* n'est pas un processus aléatoire. Dans la Nature, les composés de coordination existent en tant que ses composants [10] et sont utilisés dans divers processus.[24] Les mondes minéral et biologique sont des modèles de maîtrise de la complexité au niveau moléculaire. Par conséquent, la nature a représenté la source d'inspiration pour le développement et l'utilisation des composés de coordination, ce qui a conduit au développement du *bio-mimétisme*, et des *approches bio-inspirées*.[25] Le *bio-mimétisme* en chimie de coordination vise à développer des composés /systèmes qui imitent les parties de ceux biologiques, en mettant l'accent sur l'étude, l'élucidation et la modélisation du rôle des ions métalliques et leurs environnements de coordination dans les systèmes biologiques.[26] Ces approches présentent un intérêt particulier pour le développement de médicaments et la catalyse.[27] Comprendre le rôle des ions métalliques dans les bactéries peut aussi être d'une grande importance industrielle et agricole.[3] L'intérêt de la recherche dans ce sens est confirmé par la récente «Unified Microbiome Initiative (UMI)»: '*décrypter les gènes et les chimies microbiens*' est identifié comme un besoin essentiel pour '*accélérer la découverte de base et l'implémentation dans des*

applications'[28] L'objectif des *approches bio-inspirées* est de reproduire le fonction, et non la complexité des systèmes biologiques.[29] Ainsi, des systèmes hybrides étudiant les performances des composés synthétiques dans un milieu biologique (p. ex. les hydrogénases artificielles à base de cobaloximes),[30] ainsi que les performances des espèces biologiques en milieu/ environnement synthétique (p. ex. des enzymes et des cultures microbiennes dans les dispositifs solaires et à combustible)[31] ont étés mis au point, conduisant à d'importants avancements des connaissances.

Parmi les approches bio-inspirées, la photosynthèse artificielle est primordiale dans la perspective d'un avenir énergétique durable.[29, 32] C'est pourquoi il est important d'évaluer le rôle que les complexes de coordination jouent / puissent jouer dans cette direction.[33] Dans le contexte de la croissance de la population mondiale et l'augmentation du niveau de vie à travers le monde, l'explosion de la demande pour l'énergie, qui en résulte, engendrera davantage la consommation de combustibles fossiles.[32d, 34] Par conséquent, l'épuisement des ressources non renouvelables de la Terre et en particulier l'augmentation associée des émissions de gaz à effet de serre, auront des coûts extrêmement négatifs sur l'environnement.[35] Le développement des ressources d'énergie alternatives et renouvelables est devenu l'un des défis les plus importants de l'humanité.[29, 32] Parmi les sources d'énergie alternatives existantes, l'énergie solaire reçoit une attention particulière en raison de sa disponibilité et de son abondance.[29, 32] Les principales formes de conversion de l'énergie solaire sont la chaleur, l'électricité et les carburants. Trois stratégies principales de recherche peuvent être identifiées dans ce sens: i) la conversion directe en énergie électrique par des dispositifs photovoltaïques; ii) la production de biocarburants à partir de la biomasse; iii) la photosynthèse artificielle.[32f] La photosynthèse naturelle est un système idéal pour générer et stocker de l'énergie en utilisant des ressources qui sont disponibles et abondantes (la lumière du soleil, l'eau et le dioxyde de carbone) (Figure 1.1-3a).[36] L'énergie solaire est récoltée et transférée par des unités chromophores de photosystème II (PSII). La séparation de charge a lieu, suivie par le transfert de trous et d'électrons. Des trous sont transférés au centre d'évolution de l'oxygène (OEC – oxygen evolving centre), où l'eau est décomposée en oxygène (libéré dans l'atmosphère) et en quatre protons. Des cofacteurs redox (p. ex. le plastoquinol PQH2, la plastocyanine PC), le complexe cytochrome b6f (cyt b6f) et la ferrodoxine (Fd) transfèrent des électrons au photosystème I (PSI) et à la réductase

ferrodoxine-NADP⁺ (FNR), qui les utilise pour la réduction de protons sous forme de NADPH. L'hydrogène est combiné dans une étape suivante avec du dioxyde de carbone pour former des hydrates des carbone riches en énergie.[32g, 36]
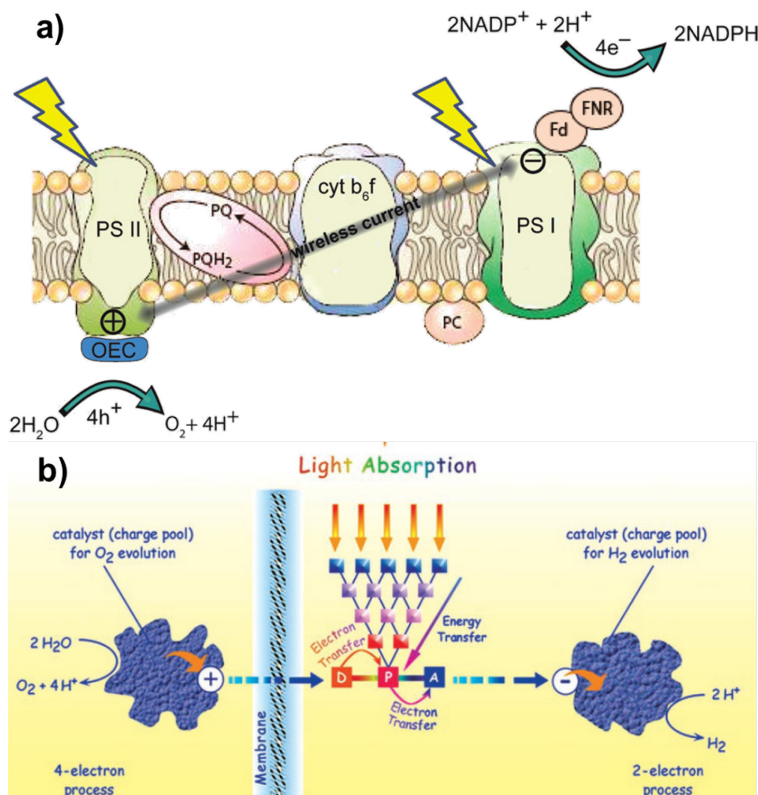
Figure 1.1-3. a) Schéma simplifié de la photosynthèse naturelle (reproduit avec permission de la référence [36]) b) Schéma simplifié des processus clés dans la photosynthèse artificielle (figure reproduite avec permission, référence [32i])

Le développement d'un dispositif artificiel qui fonctionne sur les mêmes principes (p. ex. la récolte de la lumière, le transfert d'énergie, la séparation de charge, le transfert d'électrons, la catalyse pour le clivage de l'eau) (Figure 1.1-3b) est considéré comme une solution viable au problème énergétique.[29, 32] Cependant, le défi dans un système artificiel est d'intégrer des systèmes de récolte et de conversion de lumière qui génèrent un électron /trou à la fois avec des processus catalytiques redox multiélectroniques (4 électrons pour l'oxydation de l'eau et deux électrons pour la réduction des protons), ainsi que des (auto)mécanismes de régénération nécessaire dans un système efficace.[36] Le rôle du chimiste est donc d'imaginer et de synthétiser des composés capables d'effectuer ces tâches, et d'intégrer ces composés dans

des systèmes fonctionnels, afin de convertir des molécules pauvres en énergie dans des molécules riches en énergie, en utilisant la lumière du soleil (p. ex. H_2 à partir de H_2O ou méthanol à partir de H_2O et CO_2), dans le but d'aider à la transformation globale d'une société basée sur les combustibles fossiles à une société basée sur des combustibles solaires.[29, 32]

Motivée par les préoccupations environnementales urgentes,[32d, 35] ainsi que par l'initiative et des consensus politiques sans précédent,[32d, 37] la recherche dans la photosynthèse artificielle a prospéré pendant la dernière décennie. Depuis le rapport historique de Honda et Fujishima sur le clivage de l'eau avec du TiO_2 et de la lumière UV,[38] des progrès significatifs ont été réalisés en utilisant des semi-conducteurs dopés comme récolteurs de lumière et/ ou catalyseurs dans des systèmes photovoltaïques,[39] électrochimiques,[40] photocatalytiques et photoélectrochimiques.[32d, 41] Cependant, la stabilité réduite de ces systèmes lorsqu'ils sont en contact prolongé avec des électrolytes aqueux reste à résoudre.

En outre, l'utilisation des complexes de coordination (comme photosensibilisateurs et/ ou catalyseurs) dans des systèmes photosynthétiques artificiels a également été exploitée, car ils possèdent les propriétés photophysiques et redox nécessaires pour être employés comme alternative ou complément aux matériaux semi-conducteurs dans de tels systèmes.[32d, 33, 42] Les cellules solaires à colorant (dye-sensitized solar cells (DSSCs)),[39] les cellules photoélectrochimiques (à colorant) ((dye-synthesized) photoelectrochemical cells (PECs)),[33, 42a, 43] et les cellules photoélectrosynthétiques à colorant (dye-sensitized photoelectrosynthesis cells (DSPECs))[32d] sont des exemples de tels dispositifs hybrides qui couplent des photosensibilisateurs moléculaires et/ ou des catalyseurs à des semi-conducteurs ou d'autres hôtes macromoléculaires (p. ex. des oligomères et des matériaux polymères). Le prototype DSPEC développé par UNC EFRC (North Carolina Energy Frontier Research Center on Solar Fuels) (Figure 1.1-4a) intègre un système chromophore - catalyseur moléculaire avec des matériaux d'oxydes semi-conducteurs pour effectuer le clivage de l'eau comme suit: (1) l'absorption de la lumière; (2) l'injection de l'électron dans la bande de conduction du semi-conducteur; (3) le transfert de l'électron injecté à la cathode par l'intermédiaire d'un circuit externe; (4) le transfert de l'électron du catalyseur au chromophore – activation du catalyseur; (5) les étapes 1-4 sont répétées quatre fois pour construire les quatre équivalents oxydants nécessaires pour l'oxydation de l'eau et l'évolution de l'oxygène à la photoanode. À la cathode,

la réduction H_2O/H^+ a lieu (l'application de $\sim$0.2 V est nécessaire pour complétion).[32d] Des exemples de systèmes chromophores - catalyseurs utilisés dans ce dispositif sont montrés dans la Figure 1.1-4b. Le clivage de l'eau est réalisé en utilisant le composé **B** avec un rendement de conversion du photon absorbé de 4,4 %.[32d] L'objectif final est de développer des cellules en tandem en combinant photoanodes pour l'oxydation de l'eau avec photocathodes pour le clivage de l'eau ou la réduction du CO_2 en formate/ acide formique ou *syngas* (gaz de synthèse H_2:CO – la matière première pour la production d'hydrocarbures par le procédé Fischer-Tropsch).[32d] À ce jour (décembre 2015), des PECs intégrant systèmes moléculaires chromophores - catalyseurs pour la photoanode et la photocathode ont été rapportés par Sun *et al.* (Figure 1.1-4c), avec une efficacité de transformation de l'énergie solaire en hydrogène de moins de 1 %.[44] Des complexes de coordination utilisés comme chromophores dans DSSCs[45], ainsi que des photosensibilisateurs et des catalyseurs moléculaires dans PECs[33, 42a, 43] et des assemblages photosensibilisateur - catalyseur[46] dans DSPECs (Figure 1.1-4b) ont été récemment passés en revue.
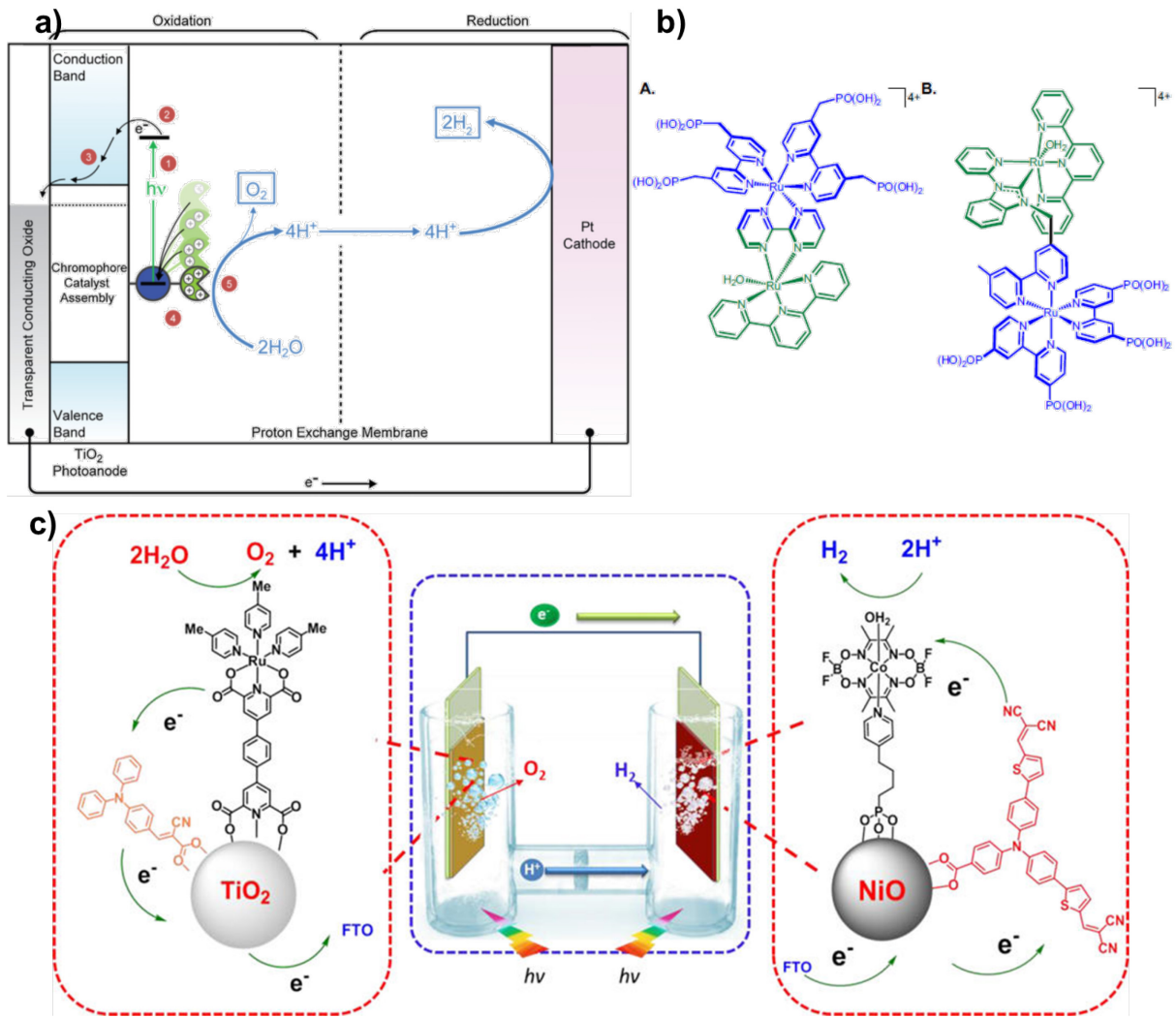
Figure 1.1-4. a) Représentation schématique du prototype DSPEC développé par UNC EFRC. b) Exemple de systèmes chromophore – catalyseur utilisés (chromophore en bleu et catalyseur en vert) (figure reproduite avec permission, référence [32d]). c) PEC moléculaire complète rapporté par Sun *et al*. (figure reproduite avec permission, référence [44])
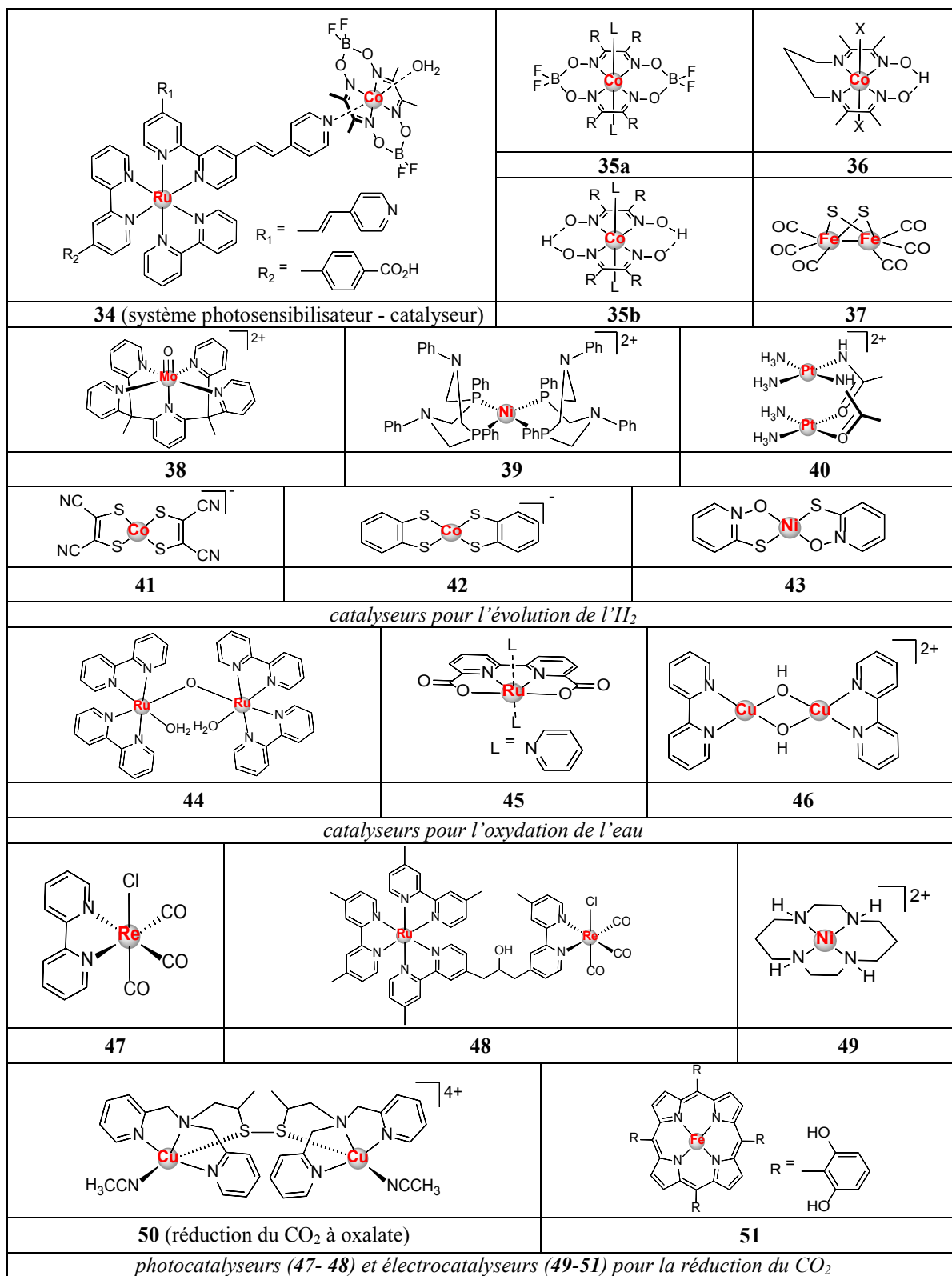
Figure 1.1-5. Photocatalyseurs et/ ou électrocatalyseurs moléculaires pour la réduction des protons,[47] l'oxydation de l'eau,[33] et la réduction du CO₂.[48]

Afin de surmonter le degré élevé de complexité d'un système photosynthétique artificiel complètement homogène, l'étude des demi-réactions (p. ex., l'oxydation de l'eau (water oxidation (WO)) et la réduction des protons (hydrogen evolving reaction (HER)) dans le cas du clivage de l'eau), à l'aide des donneurs/ accepteurs sacrificiels d'électrons, a été privilégiée, dans la quête de mieux comprendre chaque processus.[33, 49] Ces systèmes sont souvent testés dans des solvants organiques ou dans des mélanges organiques aqueux, afin de surmonter les problèmes de solubilité. Ainsi, les avantages offerts par les systèmes moléculaires par rapport à ceux hétérogènes sont exploités: investigations mécanistiques accessibles et une plus facile adaptabilité (tunability) grâce à un kit d'outils de synthèse bien développé; ainsi, la capacité d'analyser les relations structure-fonction et d'utiliser les connaissances obtenues dans la conception des systèmes améliorés sont acquis.[32a, 33]

Les chromophores synthétiques à base de complexes de coordination sont bien développés, aidés par les progrès des DSSCs.[39] Cependant, leur stabilité à long terme et la performance globale dans des milieux aqueux sont encore à être optimisées, et les mécanismes dans les systèmes photocatalytiques homogènes sont encore à être sondés et mieux compris. En outre, la plupart de ces chromophores sont basés sur des ions de métaux nobles, qui sont rares et coûteux (p. ex **23-25**, Figure 1.1-1; composés Figure 1.1-4; **34**, **44**, **45**, **47**, **48,** Figure1.1-5). L'une des avancées les plus récentes dans ce sens est le rapport d'un photosensibilisateur à base de Fe.[50]

En dépit des progrès importants (p. ex. Figure 1.1-4 et Figure 1.1-5), des catalyseurs moléculaires pour les procédés de conversion de l'énergie solaire en combustible qui fonctionnent en milieu aqueux et qui soient robustes, efficaces et rentables et à base de métaux non nobles, sont encore à être développés.[32a] Cela a un impact négatif sur le développement des systèmes photocatalytiques homogènes. Afin de résoudre les inconvénients liés à la rareté et le coût prohibitif des composés à base de métaux nobles, des catalyseurs (électrocatalyseurs et photocatalyseurs) à base d'ions plus abondants et de moins chers métaux de transition de la première rangée,[33, 47a] (Fe,[51] Co,[52] Ni,[53] Cu,[54]), ainsi que des systèmes chromophore-catalyseur sans métaux nobles[47e, 55] ont été rapportés pour la réduction des protons (p. ex. **35-39** et **41-43**, Figure 1.1-5),[47] l'oxydation de l'eau (p. ex. **46**, Figure 1.1-5),[33] et la réduction du CO_2 (p. ex. **49-51**, Figure 1.1-5).[48] Néanmoins, l'efficacité de conversion de l'énergie

solaire en combustible et/ ou la durée de vie (stabilité/ robustesse) des systèmes moléculaires rapportés à ce jour, ne répondent pas aux paramètres qui permettent leur application à grande échelle.[32a, 33, 53a] Les exigences très complexes en termes de conception et d'ingénierie d'un dispositif de conversion de l'énergie solaire en combustible qui fonctionne complétement sur des processus homogènes sont également des facteurs prohibitifs.[32a]

Ainsi, les dispositifs photosynthétiques artificiels complets et fonctionnels pour la conversion de l'énergie solaire en combustible chimique sont à base de semi-conducteurs[32d, 36, 56] (les plus performants à ce jour) ou hybrides (p. ex. composés moléculaires/ semi-conducteurs,[32d, 33, 42a, 43] composés biologiques/ semi-conducteurs[31b]), dans de nombreux cas intégrant les sous-systèmes individuels les plus développés.[32a, 33] Cependant, en dépit des progrès importants, ces dispositifs sont encore au niveau du prototype. Le coût de l'hydrogène solaire produit par PECs a été évalué en 2012 à plus de 100 USD/ kg (contre 3,64 USD/ kg pour l'hydrogène éolien et 7,62 USD/ kg pour l'hydrogène photovoltaïque (en diminution constante)).[57] Atteindre la compétitivité en termes des coûts pour l'hydrogène solaire produit par PECs se traduirait dans des temps de vie de dispositifs de 25 ans à des rendements (énergie solaire à combustible) de 15 %.[32d] Ces paramètres sont loin de ceux des prototypes existants (plus hauts temps de vie d'ordre de mois).[32d] Ainsi, la recherche fondamentale est nécessaire, afin d'ajuster les nombreux paramètres impliqués dans les systèmes complets de conversion de d'énergie solaire en combustible pour accroître leur efficacité et leur temps de vie, et guider leur progression vers la viabilité commerciale et leur application à grande échelle dans l'industrie.[32a, 32d, 33] Cependant, les prototypes PEC et DSPEC démontrent l'utilisation réussie de complexes moléculaires de coordination dans les dispositifs photosynthétiques artificiels. Ils prouvent que les composés de coordination pourraient contribuer à ce domaine, et représentent un encouragement pour poursuivre les recherches dans cette direction.

Les 'approches bio-inspirées' se trouvent également à la base de la chimie supramoléculaire.[24, 58] (Une brève description du concept est présentée dans la section 1.2 *vide infra*). Quant à la *complexité au niveau moléculaire* dans une perspective supramoléculaire, la définition de Steed et Atwood d'un '*dispositif supramoléculaire*' revêt une importance particulière car il se concentre '*sur les interactions fonctionnelles entre les composants plutôt que sur la nature chimique de leur connectivité*'.[22] En conséquence, si une

seule molécule a des propriétés de nature supramoléculaire, elle est considérée comme un '*dispositif supramoléculaire*' (une présentation plus complète de ce concept est donnée dans la section 1.2 *vide infra*).[22] Encore une fois, les propriétés intrinsèques de la liaison de coordination (force de liaison intermédiaire) permettent aux composés de coordination d'être utilisés dans ce domaine.[23] Ainsi, le sous-domaine de la chimie métallosupramoleculaire s'est développé.[59] Des avancées majeures ont été réalisées et des théories importantes ont été mises au point par rapport à l'(auto-) assemblage des composés de coordination en solution,[60] aux interfaces,[61] sur les surfaces,[62] et à l'état solide.[63] Des exemples ont été passés en revue de manière approfondie, couvrant des ensembles discrets,[64] des réseaux de solides (MOFs/ polymères de coordination),[64b, 65] des cristaux liquides, des nanomatériaux,[66] et des aspects liés au crystal engineering.[67] Leur importance particulière émerge en science des matériaux (capteurs,[22, 68] électronique moléculaire,[22, 69] stockage de l'énergie et du gaz/ combustible,[14b, 70] matériaux magnétiques[71]), catalyse,[72] et médecine.[8c, 73]

En conclusion, les exemples de composés de coordination présentés dans cette section ont été choisis pour illustrer: *i) leur importance dans notre vie quotidienne* – les complexes de coordination sont bien établis dans certaines applications (p. ex. l'industrie des colorants et des pigments, l'hydrométallurgie et l'industrie d'extraction, la catalyse et la médecine); ils jouent également un rôle important dans des domaines émergents comme en témoigne leur utilisation dans OLEDs, DSSCs et des applications basées sur MOF; *ii) les défis et les opportunités* – il y a des domaines (p. ex. la photosynthèse artificielle, les dispositifs moléculaires, les nouvelles méthodes de diagnostic et de thérapie) dans lesquels l'utilisation de complexes de coordination est seulement au niveau de la recherche fondamentale ou prototype, mais dans le développement futur desquels ils pourraient jouer un rôle important.

Des tendances dans l'étude des complexes de coordination et leurs applications ont également été identifiées. Poussée par l'évolution générale/ progrès de notre société, la recherche en chimie de coordination moderne évolue *vers la complexité au niveau moléculaire*, la nature représentant une source majeure d'inspiration, comme le montre la photosynthèse artificielle et la chimie métallosupramoleculaire. L'évolution à partir de l'étude fondamentale des complexes de coordination et des preuves de principe dans la recherche universitaire, vers des prototypes et des applications à grande échelle peut être extrêmement

lente (p. ex. approbation clinique de nouveaux médicaments) ou très rapide (p. ex. OLEDs). Cependant, il n'y a aucun doute que les composés de coordination peuvent présenter des réponses aux problèmes réels. Une vision innovante est donc nécessaire pour réaliser de nouvelles découvertes et pour utiliser ce qui a déjà été découvert de façons nouvelles et originales. Dans le même temps, l'étude des complexes de coordination nourrit la curiosité scientifique, et les approches multidisciplinaires ouvrent de nouveaux mondes fascinants, tout en repoussant les frontières de la connaissance à des profondeurs sans précédent.

1.1.2. Des concepts clés – le cadre théorique

Le contexte de ce travail d'un point de vue conceptuel/ théorique est présentée à la Figure 1.1-6. Des concepts pertinents sélectionnés sont mis en évidence dans cette section: composé de coordination/ complexe métallique; liaison/ interaction métal-ligand; design du ligand; propriétés des complexes de coordination (expérimentales *vs.* calculées); relation structure - propriétés; approches du point de vue moléculaire/ supramoléculaire; systèmes à valence mixte ; architectures de coordination supramoléculaires

▪ Le terme **composé de coordination** est utilisé en accord avec la définition IUPAC d'une ***entité de coordination***:[74] '*un ensemble constitué d'un **atome central** (généralement métallique) sur lequel un réseau d'autres groupes d'atomes (**ligands**) est attaché*'. En chimie inorganique/ de coordination, **l'atome central** est un **ion métallique** et le ligand est '**les atomes ou les groupes d'atomes reliés à l'atome central**'.[75] Les termes composé de coordination et complexe de coordination sont utilisés comme synonymes dans ce travail. Quant à la distinction entre les composés organométalliques ('*composés ayant des liaisons entre un ou plusieurs atomes métalliques et un ou plusieurs atomes de carbone d'un groupe organyle*'[76]) et les composés de coordination, le principe de classification donnée dans *Comprehensive Coordination Chemistry II* est formellement adopté: '*n'importe quel composé de coordination dans lequel le nombre de liaisons métal-carbone est d'au moins la moitié du nombre de coordination du métal est considéré comme «organométallique»*'[77] Cependant, comme des outils théoriques et expérimentaux de plus en plus avancés sont désormais disponibles pour sonder en profondeur la nature de la liaison métal-ligand, il pourrait être utile d'abandonner ces classifications/ distinctions de niveau intermédiaire, en faveur de nouvelles

terminologies permettant l'évaluation directe des spécificités d'un système dans un cadre conceptuel général .

▪   La définition IUPAC de la **liaison chimique** pourrait être considérée pour définir le type de cadre conceptuel général mentionné ci-dessus: '*Il y a une liaison chimique entre deux atomes ou groupes d'atomes dans le cas où les forces qui agissent entre eux sont de nature à conduire à la formation d'un agrégat avec une stabilité suffisante pour que le chimiste le considère comme une «espèce moléculaire» indépendante.*'[78] Dans ce concept général, **la liaison dans les composés de coordination** a comme base la notion de **l'interaction métal-ligand**.
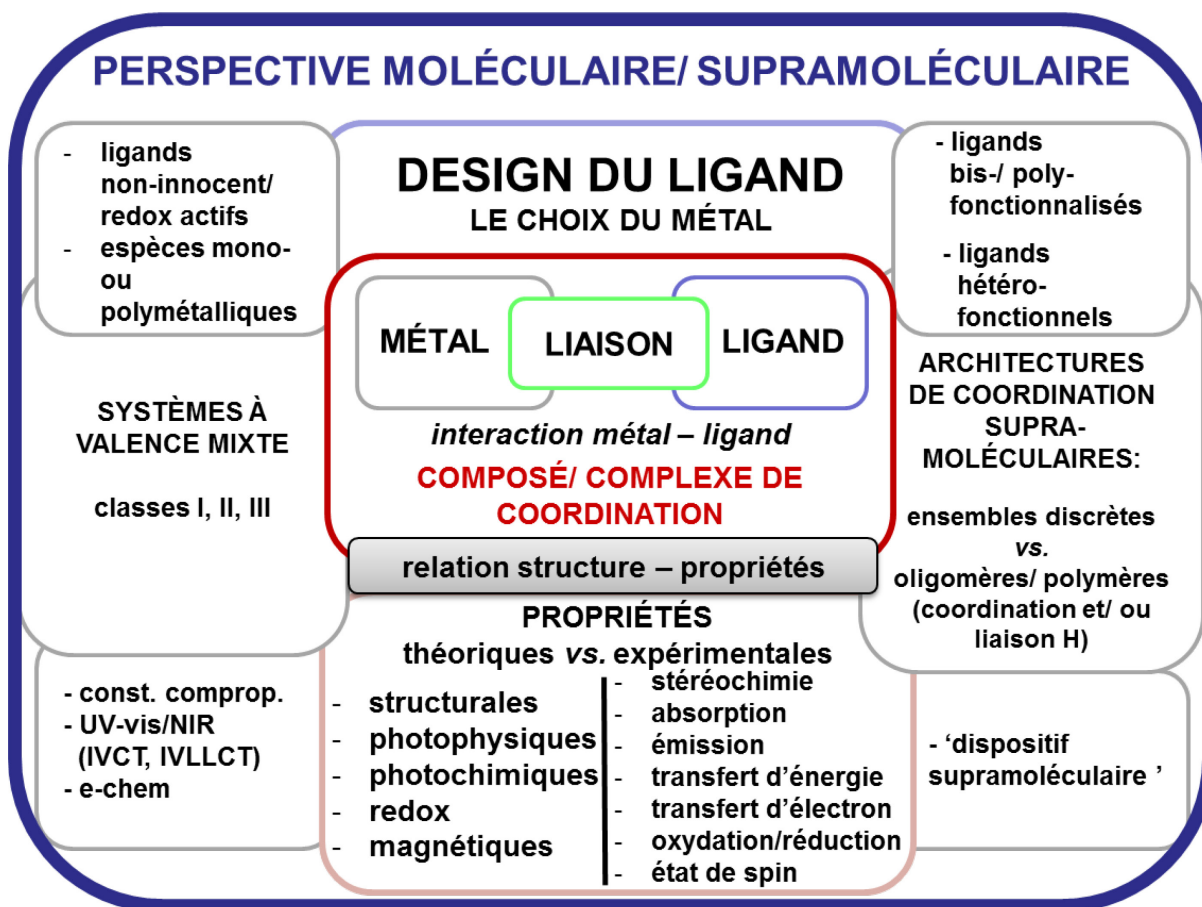
Figure 1.1-6. Le cadre conceptuel/ théorique de cette thèse

L'une des principales nécessités est donc de sonder et de décrire adéquatement cette interaction et son influence sur la structure et les propriétés des composés (géométrie; stéréochimie; état de spin, propriétés photophysiques et redox, stabilité/ réactivité; chimie).

Des aspects de la théorie du champ cristallin, du champ des ligand, et des orbitales moléculaires (molecular orbital (MO))[79] seront utilisées pour décrire et discuter les spécificités des systèmes à l'étude. Du point de vue classique, l'interaction métal-ligand peut être considérée comme une combinaison de contributions spécifiques du métal, du ligand, et de l'environnement/ milieu (Figure 1.1-7).
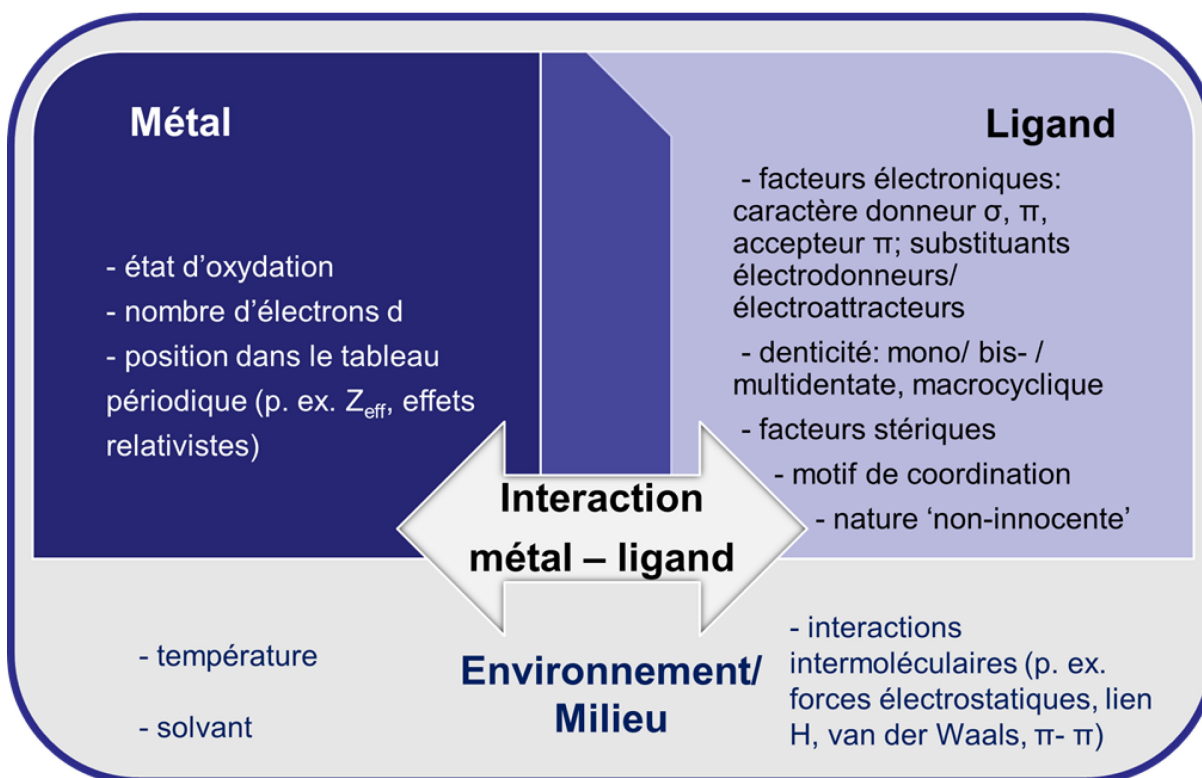
Figure 1.1-7. L'interaction métal-ligand: les facteurs liés au métal, au ligand et à l'environnement

En outre, des techniques de caractérisation expérimentales multidisciplinaires (p. ex. cristallographie rayons X, résonance magnétique nucléaire (RMN), résonance paramagnétique électronique (RPE),[80] spectroscopie vibrationnelle (IR/ Raman),[81] spectroscopie d'absorption UV/vis/NIR et rayons X (XAS),[82] spectroscopie Mössbauer, X-ray photoelectron spectroscopy (XPS), dichroïsme circulaire magnétique (DCM), magnétométrie SQUID, techniques électrochimiques (p. ex. voltammétrie cyclique, spectroélectrochimie) et outils avancés de chimie théorique[83] (p. ex. DFT,[84] TD-DFT))[85] permettent de sonder, d'interpréter, et de complétement décrire les spécificités de la liaison métal-ligand et les

propriétés dans chaque cas individuel. Ceci est particulièrement nécessaire et apporte de l'information importante dans le cas des complexes de coordination avec des ligands présentant un comportement *non-innocent* (p. ex. NO, quinones/ semiquinones/ catécholates, α-diimines, α-dithiolènes, porphyrines, chlorines, corroles, ligands azo).[86] Le terme *non-innocent* décrit des cas particuliers de composés de coordination dans lesquels il y a de l'incertitude quant à l'état d'oxydation du centre métallique, car les ligands impliqués sont actifs redox dans la même gamme des potentiels électrochimiques.[86c] Toutefois, le comportement *innocent* ou *non-innocent* d'un ligand dépend des conditions et de la situation de coordination.[86c, 87] En conséquence, la nécessité d'utiliser des termes tels que un *comportement non-innocent* plutôt que un *ligand non-innocent* est soulignée.[86c] La description de la liaison dans les complexes avec des ligands actifs redox a été débattue depuis longtemps[86a], mais un succès significatif a été obtenu dans la dernière décennie en utilisant la combinaison mentionnée ci-dessus des techniques expérimentales multidisciplinaires et des calculs théoriques.[86b, 88] Les propriétés de ces complexes (p. ex. réservoirs d'électrons, transfert d'électrons) les suggèrent comme des sujets importants de recherche du moment, et les indiquent comme des candidats potentiels pour des applications en catalyse[89] et dans la chimie des matériaux.[90]

L'influence de l'interaction métal-ligand sur la structure des composés de coordination est déterminée par une combinaison de facteurs électroniques du métal et du ligand, ainsi que par des effets stériques. Ces derniers concernent les répulsions au niveau des ligands, résultant dans la stabilisation de la géométrie de la plus faible énergie.[91] Bien que possible, c'est assez complexe de traduire les effets électroniques et stériques des ligands dans des modèles accessibles (p. ex. les états d'oxydation métriques de Brown pour les ligands actifs redox,[92] le paramètre électrochimique de Lever pour les ligands[93]). Par contre, les facteurs électroniques du métal peuvent être interprétés facilement en se basant sur la théorie du champ cristallin. Ainsi, les préférences de géométrie en fonction de l'état d'oxydation du métal/ nombre d'électrons d ont été identifiées,[91] (Figure 1.1.-8) et ont été confirmées expérimentalement.[91, 94] Une grande partie de la recherche se concentre également sur la prévision et le contrôle de la stéréochimie et des états de spin (Figure 1.1-9).[94b]
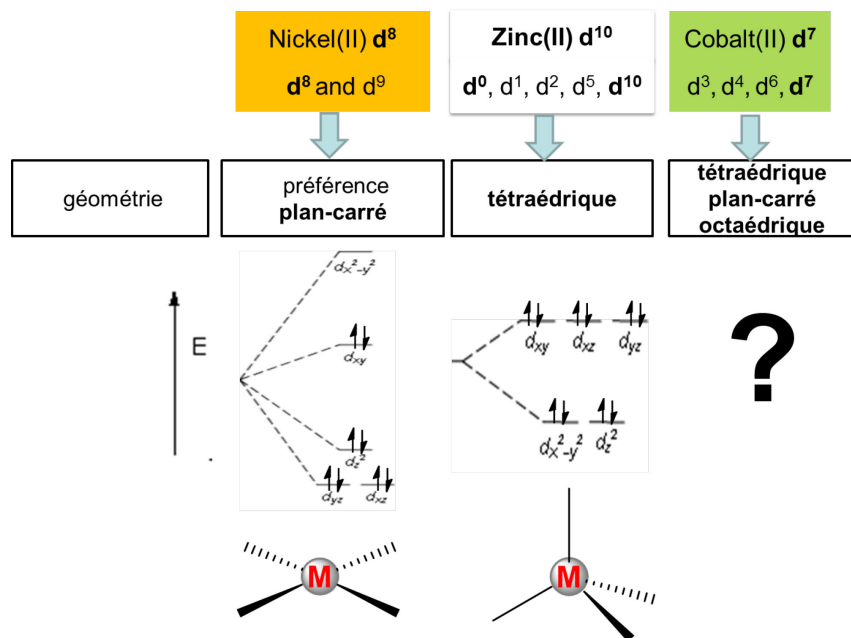
Figure 1.1-8. Les préférences de géométrie en fonction de l'état d'oxydation/ nombre d'électrons d du métal.[79a, 94]

▪ **Le design du ligand** est l'un des thèmes centraux dans la chimie de coordination et il est aussi un concept clé dans cette thèse. Il est défini par Collins comme '*le processus par lequel les composants sont variés, soit pour satisfaire la curiosité ou pour contrôler les propriétés d'un système ciblé*'.[95] Le design du ligand est vu par le même auteur comme '*une collection de composants modulables*':[95] le type d'anneau chélate (macrocyclique/ cyclique; denticité) et sa taille; les substituants et leurs effets électroniques et stériques; les atomes donneurs et les groupes fonctionnels des atomes donneurs; les site(s) de coordination (Figure 1.1-10 gauche). Le réglage (tuning) de ces paramètres entraîne la modulation de **la capacité** intrinsèque **de chélation** du ligand pour différents ions métalliques. Si 'le choix du métal' est ajouté en tant que composant supplémentaire à cette trousse d'outils, le concept peut être étendu au **design de complexes de coordination** (Figure 1.1.-10). Le choix de l'ion métallique génère des propriétés spécifiques, qui sont peaufinées (fine-tuned) par le design du ligand. Le design des ligands actifs redox a récemment reçu une attention particulière.[87a, 96] L'environnement/ milieu (Figure 1.1-7) peut également être considéré comme un composant modulable.
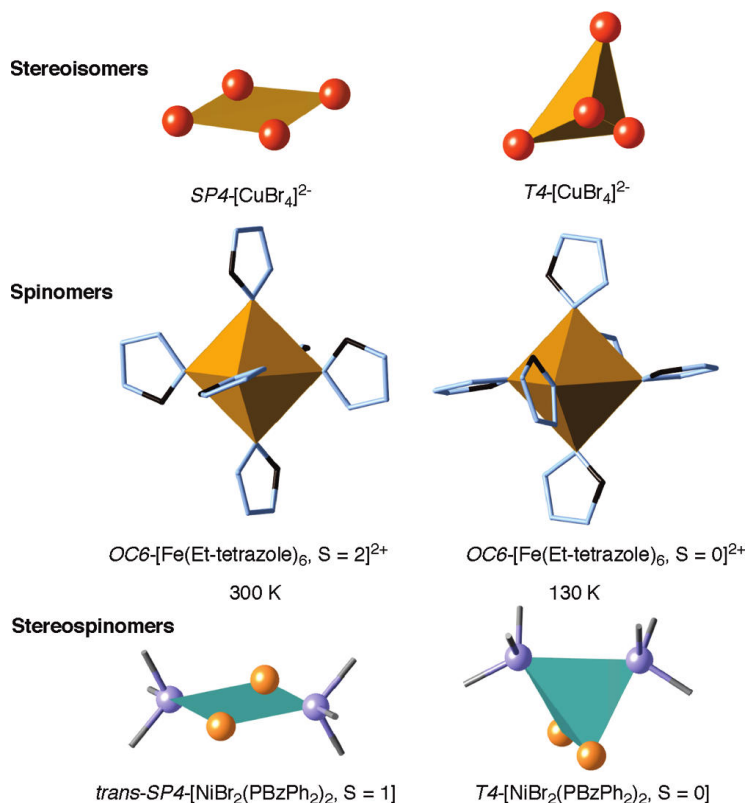
Figure 1.1-9. Des exemples d'isomérie: des isomères de géométrie de coordination (stéréoisomères), des isomères de spin (spinomères), et les deux types d'isomérie (stéréospinomères). (figure reproduite avec permission, référence [94b])
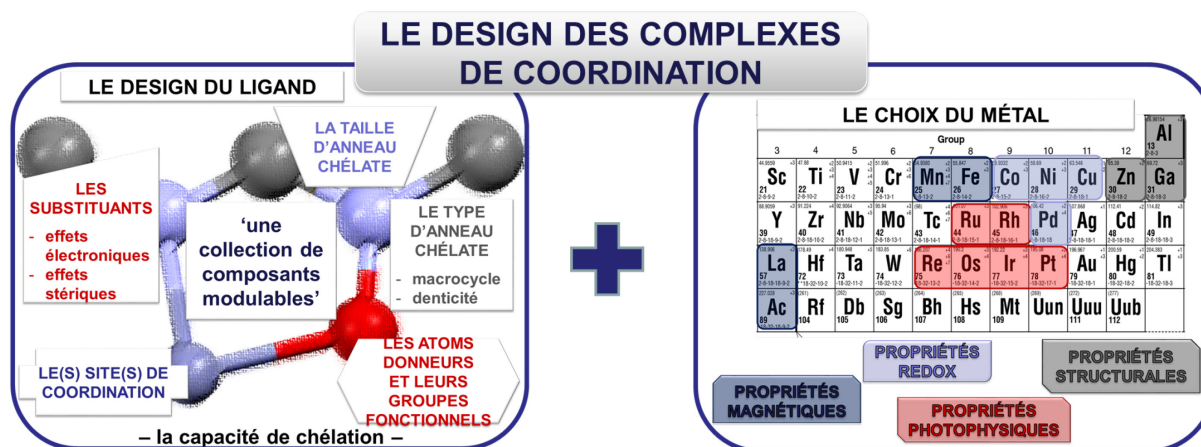
Figure 1.1-10. Le design des complexes de coordination comme '*une collection des composants modulables*'[95] (figure conçue en utilisant des concepts de référence [95])

▪ Comme souligné dans la section 1.1.1, les complexes de coordination sont attirants en raison de leurs **propriétés** spécifiques, qui les rendent des candidats intéressants pour une grande variété d'applications. Par conséquent, leur propriétés photophysiques, photochimiques, redox et magnétiques ont été étudiées en profondeur par des méthodes expérimentales et/ ou théoriques.[97] Des théories ont été développées et des **relations structure – propriétés** ont été établies pour différentes classes de composés, dans le but de synthétiser des complexes avec des propriétés ciblées pour des applications spécifiques. Les processus induits par la lumière dans les complexes de coordination (p. ex. la séparation de charge) sont parmi les plus pertinents dans leur étude et leur application (dispositifs et procédés). Une représentation schématique des concepts fondamentaux de photophysique est donnée dans la Figure 1.1-11.

▪ En raison de leurs propriétés optiques, électriques et magnétiques,[98] les complexes de coordination impliquant deux ou plusieurs centres actifs redox (composés à valence mixte) sont également d'intérêt côté applications, ainsi que du point de vue de la recherche fondamentale. Trois types de comportement peuvent être identifiés pour ces composés, en fonction du degré d'interaction électronique entre les centres redox: aucune interaction/ localisation (classe I), interaction partielle/ localisation partielle (classe II), et interaction forte/ délocalisation complète (classe III).[22, 98] Pour les composés de classe II, de nouvelles propriétés résultant de l'interaction de type 'intervalence' entre les centres redox peuvent être confirmées par des techniques spectroélectrochimiques (des transitions optiques caractéristiques de type intervalence (IV)). [22, 98] Les théories de complexes à valence mixte ont été développées initialement pour les espèces bi- et multi-métalliques, prenant en considération l'interaction électronique entre les centres métalliques. Cependant, la notion a été étendue pour englober les cas des composés de coordination avec deux ou plusieurs ligands actifs redox, dans lesquels l'interaction électronique a lieu entre des ligands radicaux 'pontés' par le métal. Des transitions caractéristiques de transfert de charge 'intervalence' ligand-à-ligand (ligand-to-ligand intervalence charge transfer (LLIVCT) transitions) sont observées dans ces systèmes de type classe II.[86c]

▪ Comme mentionné brièvement dans la section précédente (1.1.1), il est intéressant de considérer les approches moléculaires/ supramoléculaires de Atwood et Steed illustrées par le concept de '*dispositif supramoléculaire*',[22] du point de vue des composés de coordination. La

base 'structurelle' de la définition classique de la chimie supramoléculaire est étendue pour englober un composant 'fonctionnel'. Une exemplification, en utilisant des critères photochimiques et électrochimiques de classification, est présentée dans la Figure 1.1-12.[22]
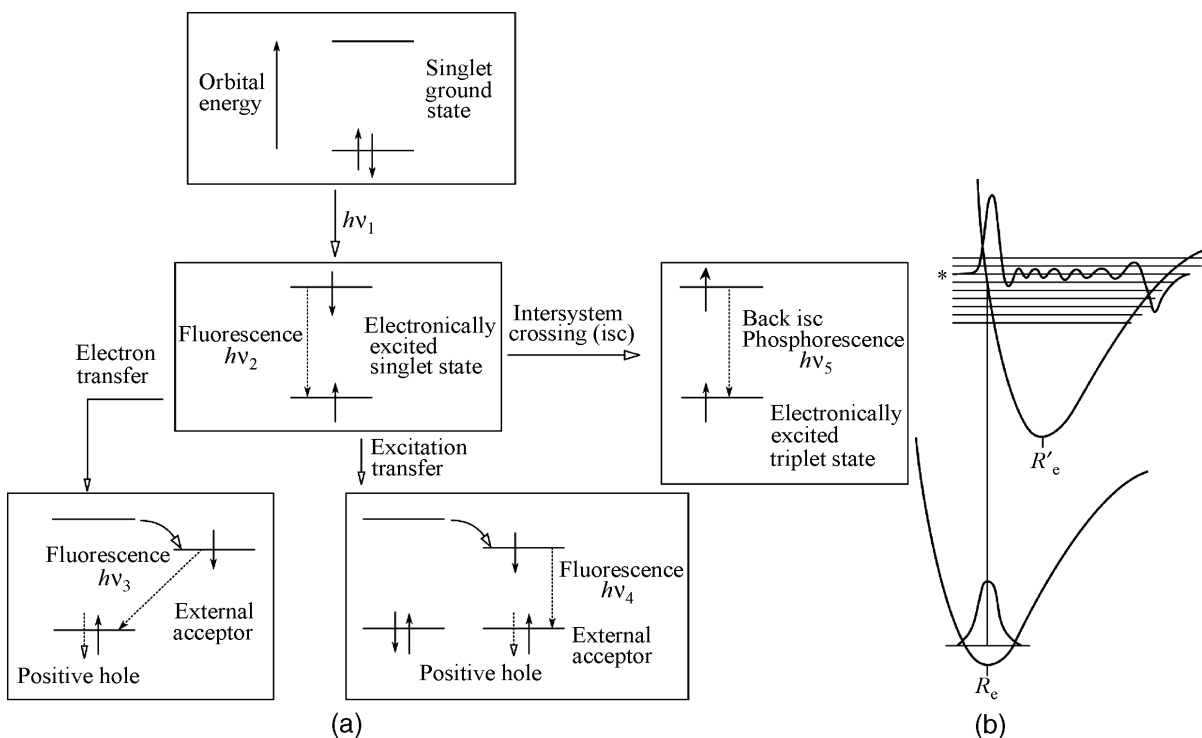
Figure 1.1-11. (a) La photoexcitation et les possibles processus radiatifs à l'état excité, (b) Après la photoexcitation, un électron est promu dans un niveau vibrationnel de l'état excité. (figure reproduite avec permission, référence [22]).

'Si l'excitation d'une molécule par la lumière (♦ ↔ ●) aboutit à la formation des états excités qui sont essentiellement localisés sur l'une des deux composantes (♦ ou ●) ou provoque le transfert d'électrons de l'une à l'autre, la molécule est dite être supramoléculaire. Si l'état excité est sensiblement délocalisé à travers les deux composants, le complexe est mieux pensé comme étant simplement une grosse molécule unique. Des arguments analogues s'appliquent aux processus redox.'[22] Si on regarde les complexes à valence mixte de ce point de vue, ceux dans les classes I et II sont considérés supramoléculaires, tandis que ceux dans la classe III sont de grosses molécules. Les complexes de coordination avec les ligands actifs redox présentant des charges localisées et partiellement localisées deviennent ainsi des 'entités supramoléculaires' au sein de cette approche.
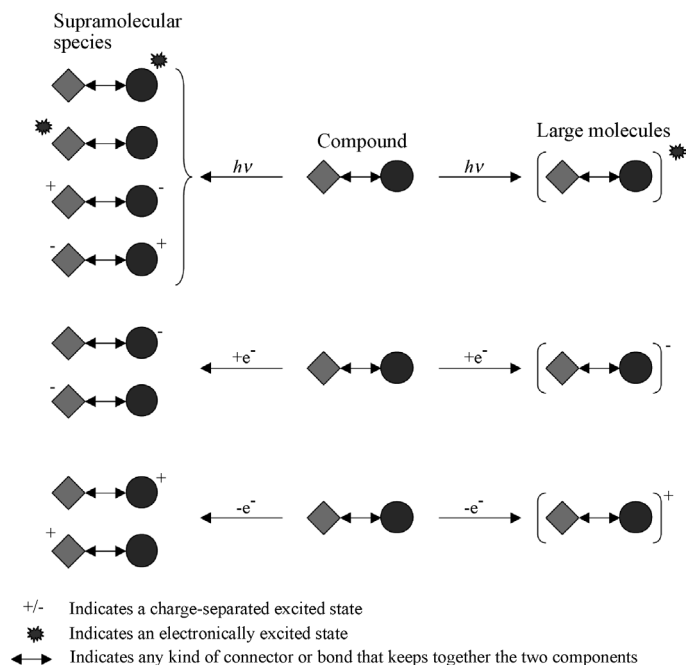
Figure 1.1-12. Dispositif supramoléculaire *versus* grosse molécule: critères photochimiques et électrochimiques de classification. (figure reproduite avec permission, référence [22])

En considérant la définition classique de J. M. Lehn de la chimie supramoléculaire: '*la chimie au-delà de la molécule, portant sur des entités organisées de complexité plus élevée résultant de l' association de deux ou plusieurs espèces chimiques maintenues ensemble ...*',[99] les liaisons de coordination peuvent être identifiées dans la trousse d'outils des interactions supramoléculaires, à côté des interactions ion-ion, ion-dipôle, et dipôle-dipôle, les liaisons hydrogène,[100] les interactions cation-π , anion-π, π-π, les forces van der Waals et 'crystal packing' et les interactions 'closed shell' (p. ex. les interactions métalophilique, les liaisons halogène,[101]).[23, 60a]

Les outils et les stratégies générales de la chimie hôte-invité et de la chimie d'auto-assemblage (reconnaissance au niveau moléculaire, l'utilisation des affinités/ compatibilités préexistantes, la pré-organisation et la complémentarité, la réversibilité) ont été appliqués avec succès à des composés de coordination, ce qui a eu comme résultat le développement du domaine fascinant de chimie métallosupramoléculaire.[23, 59-60, 99] Les sous-domaines associés et les références bibliographiques correspondantes ont été présentés à la fin de la section 1.1.1 (page 17), ainsi que leur pertinence pour différents types d'applications. Il est également important de souligner l'importance du design du ligand du point de vue de la chimie

supramoléculaire[59] Des exemples de stratégies de recherche dans ce sens sont: cibler la spécificité et la sélectivité par le design (hétéro) ligands multifonctionnels;[102] identifier et exploiter l'effet de la coordination métal-ligand sur le réglage (tuning) des interactions intermoléculaires;[103] utiliser la complémentarité de la combinaison liaisons de coordination/ liaisons hydrogène, afin d'exploiter la synergie, coopérativité et l'émergence résultant de cette association.[104]

Les concepts théoriques clés discutés ici seront exemplifiés dans la section 1.2 avec des systèmes ion métallique – ligands N,O, visant à établir le contexte spécifique du travail présenté dans cette thèse.

1.2. Le contexte spécifique: 'préparer la voie pour les AMOXs' – des exemples pertinents de complexes de coordination avec des ligands N,O

1.2.1. Examiner le concept du 'design des complexes de coordination comme *une collection des composants modulables*' avec des exemples de la chimie de coordination des ligands N,O

Des aspects de la chimie de coordination des ligands N,O seront présentés du point de vue du design des complexes de coordination comme '*un ensemble de composants modulables*'[95] (Figure 1.1-10, section 1.1.2) . Les 'composants modulables' suivants seront mis en évidence: le design du ligand (le type du cycle chélate (denticité, cyclique/ macrocyclique) et la taille du cycle chélate, les atomes donneurs et les groupements fonctionnels des atomes donneurs, les substituants du cycle et leurs effets électroniques et stériques, le(s) site(s)/ mode(s) de coordination); le choix de l'ion métallique; l'environnement/ le milieu (p. ex. les interactions secondaires, le solvant) .

La diversité de types et de tailles du cycle chélate dans la chimie de coordination des ligands N,O est mise en évidence par des exemples choisis de complexes métalliques classiques de cette classe (Figure 1.2-1). Dans la catégorie de cycle chélate à 6 atomes, les complexes avec des ligands de type salicylaldimine (**52**),[105] β-ketoaminato (**53**),[106] et salen (**54**)[107] sont parmi les plus étudiés, en particulier dans la catalyse.[108] Des complexes macrocycliques de type [N_2O_2] (**55**)[109] ont également suscité l'intérêt de la recherche.[109-110] Des exemples typiques dans la classe de cycle chélate à 5 atomes comprennent les complexes avec des ligands de type quinolin-8-olato (**56**)[111] *o*-aminophenolato (**57**),[87a, 90, 112] pyridine-2-carboxylato,[113] pyridine-2,6-dicarboxylato (**58**).[114] Il existe également des ligands N,O qui forment des cycles chélates à quatre et à trois atomes avec des ions métalliques (p. ex. Ti(IV) (**59**),[115] Co(II) (**59**,[116] **60**,[117] **61**[118]), Zn(II) (**60**,[119] **61**[120]). Toutes ces classes de composés ont été amplement passées en revue (plusieurs références sont données ci-dessus). La classe de cycle chélate à cinq atomes sera discutée dans la section 1.2.2.

Pour évaluer l'influence/ l'impact de la nature des atomes donneurs et des groupements fonctionnels des atomes donneurs, sur les propriétés des complexes, l'exemple des études sur l'activité anti-cancer des complexes arènes d'iridium et de ruthénium avec des ligands bidentates (N,N'), (N,O) et (O,O') a été choisi. Dans ces études, il a été constaté que la cytotoxicité du complexe (dans certains cas comparable à celle du cisplatine (**13**, Figure 1.1-1) est en corrélation avec le type de ligand bidentate.[121] Les effets de la coordination des ligands bidentates (N,N') versus (N,O) ont également été étudiés en ce qui concerne l'activation des complexes carbonyles de manganèse(I) et de rhénium(I) pour substitution. Il a été trouvé que les ligands donneurs anioniques (N,O) (p. ex. 2-picolinate; 2,4-quinolinate) activent le centre métallique plus rapidement que les ligands neutres (N,N') (p. ex. 1,10- phénanthroline; 2,2'-bipyridine).[122] L'influence des atomes donneurs sur des propriétés différentes des complexes a aussi été sondée par des études théoriques. Par exemple, dans la série électronique $[Ru(en)_2L_{NN}]^{n+}$ (n = +2, +1, 0), (L_{NN} = *o*-phenylenediamide), le remplacement du NH dans L_{NN} avec des atomes d'oxygène dans L_{NO} et L_{OO} a généré une réduction plus facile avec 0,5 V par substitution NH/ O (expliquée par les auteurs par l'électronégativité plus grande de l'oxygène par rapport à l'azote).[87a]

52	53	54	55
		cycle chélate à 6 atomes	

56	57	58	59	60	61
cycle chélate à 5 atomes			*cycle chélate à 4 atomes*		*cycle chélate à 3 atomes*
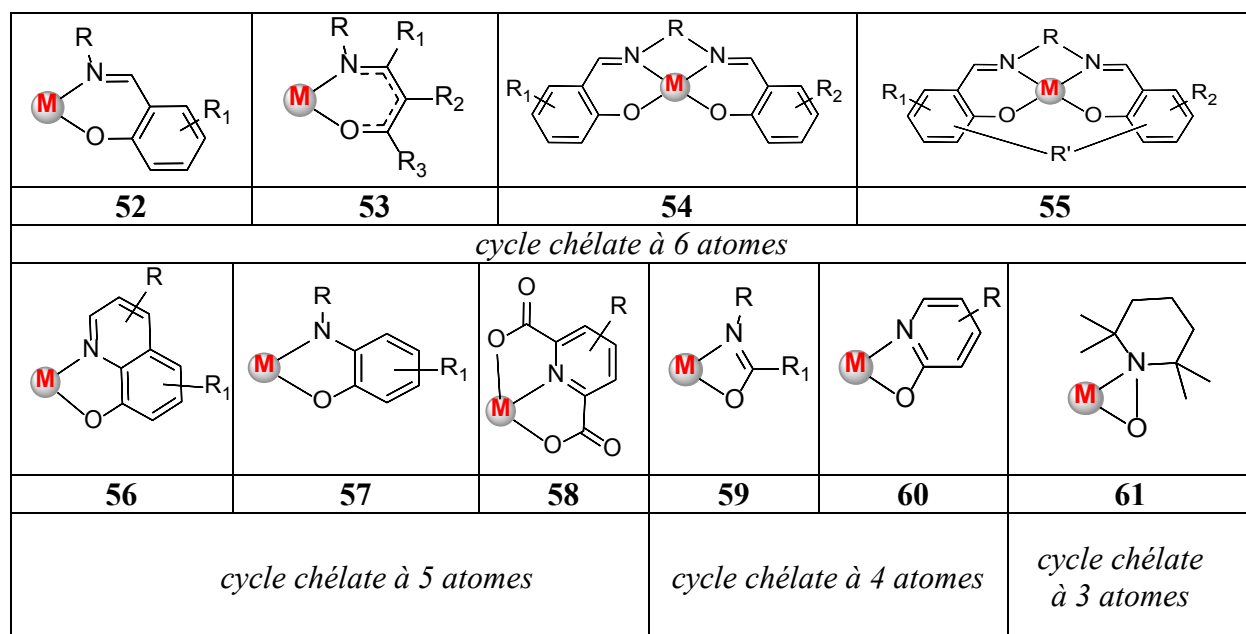
Figure 1.2-1 Des structures des complexes avec des ligands N,O mettant en évidence de divers types et de tailles de cycles chélates (cyclique/ macrocyclique, différentes denticités)

Les composés les plus significatifs pour définir le contexte spécifique de ce travail sont les complexes bis(chélates) monomères homoleptiques tétracoordinés des ligands N,O bidentates, formant des cycles chélates à 5 avec l'ion métallique (voir Figure 1.3-1). Par conséquent, l'effet des groupements fonctionnels des atomes donneurs, l'influence des substituants et leurs effets électroniques et stériques, ainsi que l'importance du choix de l'ion métallique et l'effet de l'environnement/ milieu seront analysés au sein de cette classe de composés (section 1.2.2)

1.2.2. Des complexes des métaux de transitions avec des ligands N,O bidentates de la catégorie bis(chélates) homoleptiques tétracoordinés formant des cycles chélates à cinq

1.2.2.1. Recherche CSD – sommaire, classification et discussion des résultats

Afin d'identifier les composés d'intérêt, une recherche dans la base de données Cambridge Structural Database (CSD)[123] a été effectuée en utilisant les critères présentés dans la Figure 1.2-2a. La procédure de sélection des données est donnée dans le titre de la figure.
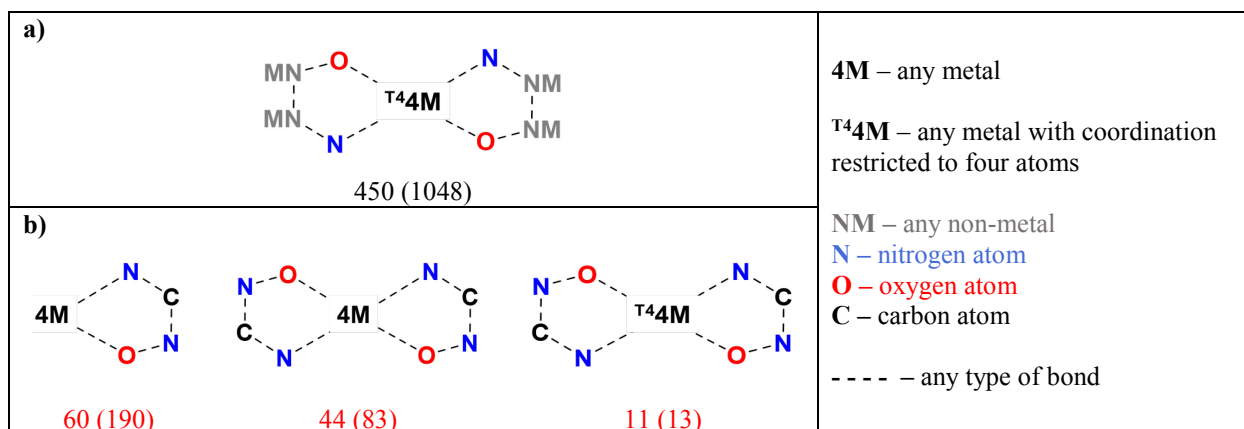
Figure 1.2-2 – Les critères de recherche CSD[124] avec le nombre de résultats après et avant la sélection des données (le nombre total des résultats est donné entre parenthèses). La procédure de sélection des données: les résultats sans coordonnés 3D n'ont pas été considérés; seulement les structures monométalliques avec des ligands bidentates N,O ont été retenues (les structures multimétalliques et les structures des polymères de coordination ont été exclues – des

systèmes dinucléaires et de nucléarité plus élevée choisis sont présentés dans la section 1.2.2.2); les déterminations multiples de la même structure ont été enlevées manuellement.

Ainsi, 450 structures des complexes bis(chélates) monomères homoleptiques tétracoordinés des ligands N,O bidentates, formant des cycles chélates à 5 avec l'ion métallique ont été identifiées après la sélection des données. La majorité des structures contiennent des ligands mono-anioniques, générant des bis(chélates) neutres avec les ions métalliques(II), [M(II)]. La répartition des résultats par type d'ion métallique est illustrée dans la Figure 1.2-3. Plus de 90 % des composés contiennent des ions des métaux de transition des groupes 10, 11 et 12. Les complexes de cuivre(II) comptent pour près de la moitié des structures (47 %) , suivis par ceux de Pd(II) (18 %), Ni(II) (10 %) et Pt (II) (8 %). 3 % des résultats ont été trouvés pour chacun des ions cobalt(II) et zinc(II).

Metal	Nb. of structures
Cu	211
Pd	83
Ni	43
Pt	38
Ag	22
Co	15
Zn	12
Sn	8
Ge	4
Pb	3
Hg	2
Cr	2
Mn	2
Au	2
Be	1
In	1
Fe	1
Sb	1
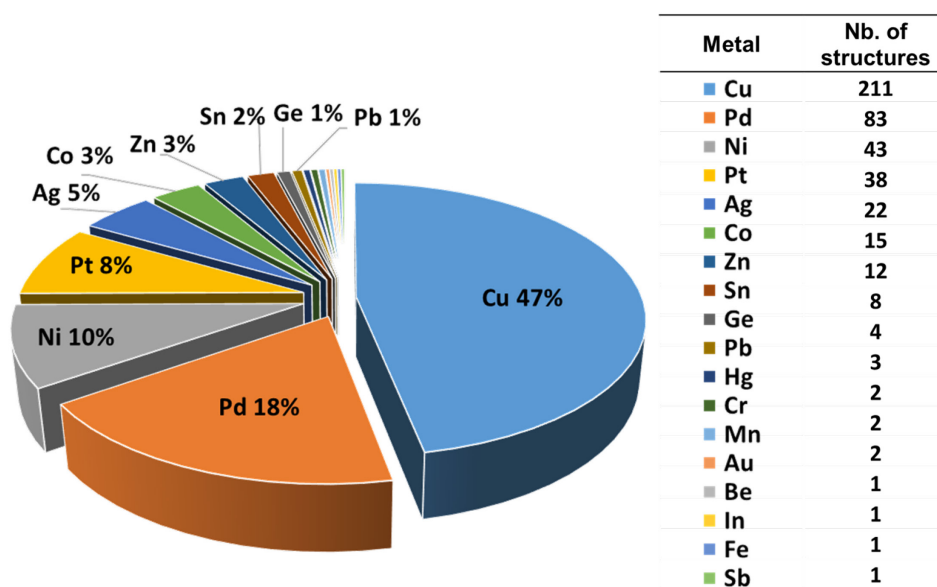
Figure 1.2-3. La distribution des résultats de la recherche CSD (Figure 1.2.-2) par type de métal.

La distribution des résultats par la nature du cycle chélate et par le type de ligand est présentée dans les Figures 1.2-4 et 1.2-5. La nature du cycle chélate κ^2-(N,O) a été définie à partir de l'identité des deux autres atomes du cycle, comme suit: OCCN; OCNN; ONNN; ONCN; autres/ others (OCPN, OPCN, OSCN)). La classification par type de ligands N,O

considère la nature chimique du ligand. Ainsi, plus de 20 catégories génériques ont été identifiées (Figure 1.2-5 et Appendix-1.2).

En 1971, dans leur étude sur la stéréochimie de complexes bis(chélate) des ions métallique(II), dans un même type d'analyse structurelle, Holm et O'Connor ont identifié seulement trois catégories de ligands N,O (tous de type OCCN: 8-hydroxyquinoline; α-hydroxyamidine, and alkanolamine). Ils ont également noté à l'époque que '*la chimie de ce groupe* [M-N_2O_2 bis(chélates) formant des cycles chélates à 5] *est mal développée*'.[106a] Par conséquent, les 450 structures à l'état solide rapportées en ce moment (octobre 2015) attestent de l'avancement dans la chimie de cette classe de complexes au cours des 45 dernières années. L'analyse de la répartition par type de ligand montre que les complexes avec des ligands type aminoacides (1) représentent la majorité, suivis par ceux de 8-hydroxyquinolines (2). Ceci est en ligne avec l'étude approfondie de ces complexes en médecine (1 et 2)[111b, 111f, 125] en matériaux[111c, 126] et dans l'industrie d'extraction (2).[6] Les trois prochaines classes, dans l'ordre décroissant mais avec des nombres similaires de structures, sont les ligands de type pyridine-2-carboxylato et ses dérivés (3), alkanolamine (4) et amido-phénolato (5). Les composés carbohydrazonato (12) sont la classe la plus importante de la classe de type OCNN, alors que les complexes de type triazene-1-oxyde (14) sont les seules de type ONNN. Le plus petit nombre de composés se trouve dans la catégorie ONCN. Ce sont des bis(chélates) des structures 15 à 19 (Figure 1.2-5; 17 = structure de type nitroimidazolato).

Chelate ring type	Nb. of structures
■ OCCN	371
■ OCNN	47
■ ONNN	18
■ ONCN	11
■ other	3
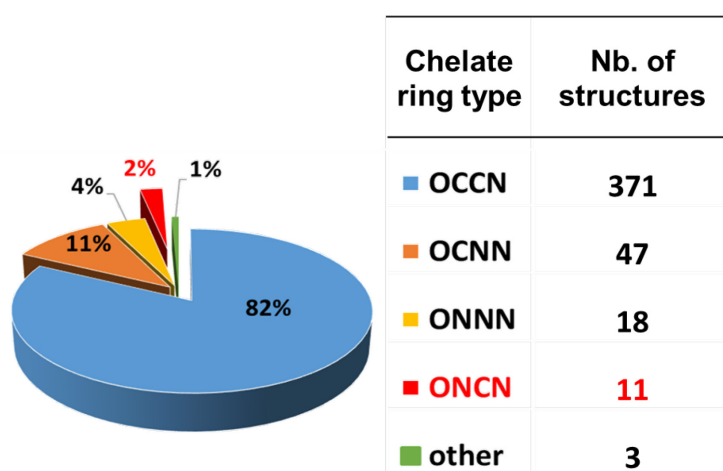
Figure 1.2-4. La distribution des résultats de la recherche CSD (Figure 1.2-2) par type de cycle chélate (OCCN; OCNN; ONNN; ONCN; others (OCPN, OPCN, OSCN))

Les études des séries systématiques de complexes avec le même ion métallique, mais avec différents motifs de substitution du ligand permettent d'en tirer des relations structure-propriétés. Le rôle des substituants et leurs effets électroniques et stériques est ainsi déterminé. L'étude de la famille des complexes de cobalt(II) triazène-1-oxydes est un exemple dans cette direction et il est important quant à la prévision et le contrôle de la stéréochimie et de l'état de spin dans les complexes tétracoordinés. L'isomérisation de la géométrie plan carré (spin bas) à la géométrie tétraédrique (haut spin) est observée pour cette classe de composés et il a été montré que dans des solutions de solvants non-coordinants (p. ex. le dichlorométhane) l'équilibre du processus d'isomérisation est contrôlé par la nature des substituants.[127] L'importance de l'environnement/ milieu (solvant non-coordinant) est aussi montrée.

L'impact du choix du métal sur les propriétés des composés est mis en évidence par l'étude de complexes du même ligand avec différents ions métalliques. Le type de métal donne, par ses caractéristiques intrinsèques, des propriétés spécifiques (mais pas mutuellement exclusives) au complexe (p. ex. Re(I), Ru(II), Ir(III), Eu(III) – propriétés photophysiques; Co(II /III), Ni(II) , Cu(II) – propriétés redox; Mn (II/ III), Fe (II/ III), Gd(III) – propriétés magnétiques). Dans des séries de complexes avec le même ligand et différents ions métalliques (dans le même environnement/ milieu), la structure du complexe (géométrie/ mode de coordination) et sa réactivité sont révélées être dépendantes de l'ion métallique.[128] Il a également été démontré que la nature de l'ion métallique peut influencer le degré de comportement non-innocent du ligand.[88k]

Le type de groupement fonctionnel des atomes donneurs (la nature des atomes, saturé *vs* insaturé, neutre *vs* chargé) détermine le degré de délocalisation de la densité électronique dans le cycle chélate et sur le ligand, permettant la modulation de la capacité de donation σ, donation π ou acceptation π. Cela a un effet direct sur l'interaction métal-ligand, et donc sur les propriétés du composé. La variation des propriétés structurelles de différents groupements fonctionnels des atomes donneurs (Table 1.2-1) est suivie dans une série de complexes de cuivre(II) avec des ligands de type ONCN, les classes 15 et 18: 2-aminopyridine-1-oxydo et *N*-R-*N*-(2-pyridyl)hydroxylamine (Figure 1.2-5).[129] Des différences significatives sont observées au niveau des longueurs de liaison dans le cycle chélate parmi les complexes

étudiés. Les variations sont en accord avec la nature des liens, le degré de délocalisation électronique, la géométrie au centre métallique, et la charge du complexe.
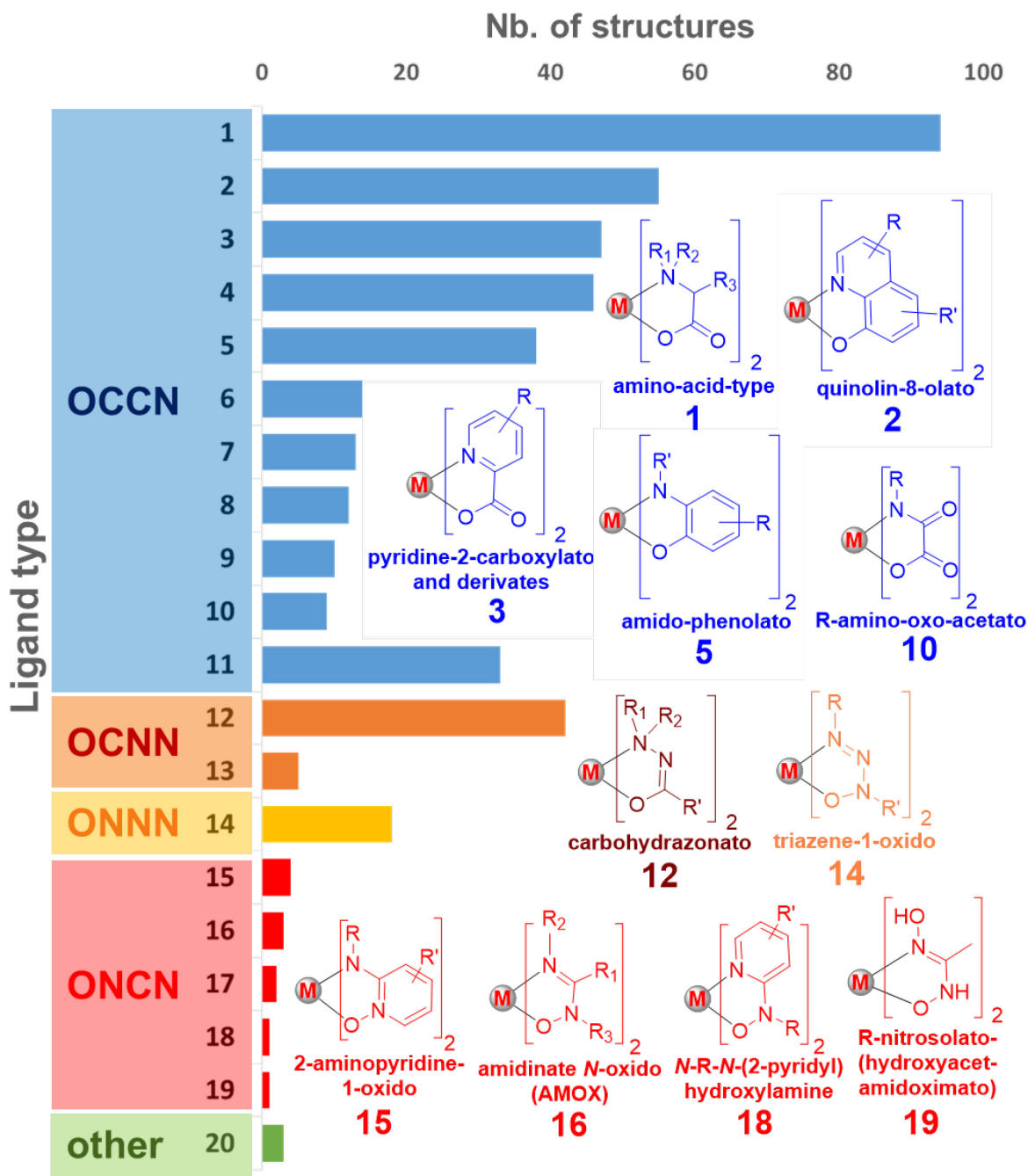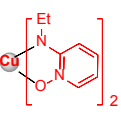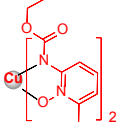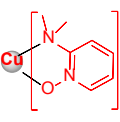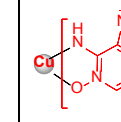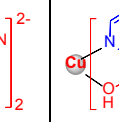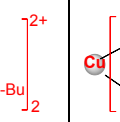
Figure 1.2-5. La distribution des résultats de la recherche CSD (Figure 1.2-2) par type de ligand. Les structures génériques sont données pour des classes choisies de composés. Pour la

liste complète des structures voir Appendix-1.2. La catégorie 11 regroupe plusieurs types de ligands ('other/ autres OCCN').

D'autre part, les 'bite angles' et les 'bite distances' ont des valeurs similaires (même si pas tous statistiquement équivalents), en accord avec le fait que tous les complexes contiennent des cycles chélates à 5 de type ONCN. En relation avec les complexes de cuivre(II) avec des ligands de type 18, il est important de mentionner que les analogues avec des ligands radicaux 2-pyridyl-nitroxyde (les deux ligands L• et des composés à valence mixte avec un ligand L• et un autre ligand L⁻) ont été préparés et étudiés pour leurs propriétés magnétiques.[129-130] La longueur de liaison N-O dans les complexes radicaux (1.29-1.30Å) est distinctement plus courte que celles dans les complexes de cuivre(II) avec des ligands de type 15 et 18.

Tableau 1.2-1. La variation des propriétés structurales dans une série des complexes de cuivre(II) avec des ligands de type ONCN.[131]

Bond lengths (Å) / angles (°)						
	Cu(15-1)₂	Cu(15-2)₂	[Cu(15-3)₂]⁺ 2(ClO₄)⁻	[Cu(15-4)₂]⁻ 2(Na)⁺	[Cu(18-1)₂]⁺ 2(BF₄)⁻	Cu(18-2)₂
Ref. CSD	DUKNUS	HATNEV	MAPOCU	CUHJUK	YUKCOX	YUKCOX
Cu-O1	1.917(3)	1.906(5)ᵃᵛ	1.987(1)	1.949(3)	1.923(2)	1.917(2)
Cu-N2	1.900(3)	1.941(3) 1.916(3)	2.052(1)	1.898(3)	1.930(2)	1.936(2)
N1-C1	1.312(3)	1.375(7) ᵃᵛ	1.435(1)	1.304(5)	1.353(2)	1.348(2)
C1-N2	1.378(3)	1.372(4) 1.412(5)	1.352(10	1.384(4)	1.415(2)	1.419(2)
N1-O1	1.350(3)	1.330(5) 1.356(4)	1.351(1)	1.377(4)	1.440(2)	1.444(2)
Bite distance	2.543(2)	2.252(4) 2.543(5)	2.624(4)	2.564(3)	2.542(2)	2.543(2)
Bite angle	83.5(1)	82.2(1) 83.3(1)	83.2(1)	83.6(1)	82.6(1)	82.7(1)
τ_4	0.00	0.33	0.00	0.00	0.00	0.00

Compte tenu de la pertinence des complexes de type ONCN pour le travail dans cette thèse, une recherche CSD[123] a également été réalisée, dans ce cas particulier, pour des bis(chélates) métalliques sans restriction sur le nombre de coordination, ainsi que pour des monochélates métalliques (Figure 1.2. -2b), afin d'identifier toutes les structures reportées contenant des ligands N,O bidentates de type ONCN, complexés aux ions métalliques dans le

mode κ2-(N,O). En plus des structures de type 15 - 19, des complexes métalliques avec des ligands de type nitropyrazolato,[132] 1,8-naphthyridine-1-oxyde,[133] et amidoxime-type[134] ont été identifiés.

1.2.2.2. Systèmes dinucléaires et de nucléarité plus élevée avec des ligands N,O formant des cycles chélates à 5

Pour cette classe de composés, un grand nombre (environ 500) de complexes monomères avec des ligands polydentates, dimères, trimères, tétramères, et des espèces de nucléarité plus élevés, ainsi que des polymères de coordination est rapporté dans la CSD. Ces structures présentent les types des ligands N,O discutés précédemment, mais qui sont conçus/ connectés pour générer de multiples sites de coordination (p. ex. des unités chélatantes (identiques ou non) pontées (voir les ligands type bis-R-amino-oxo-acetato, Figure 1.2-6a); des combinaisons de groupements fonctionnels dans le ligand pour générer des sites supplémentaires de liaison pour des métaux (p. ex. les ligands pyridine-di-carboxylate, pyridine-amidoxime, pyrimidine-amidoxime ligands, Figure 1.2-6b)). Des stratégies de chimie supramoléculaire sont également utilisés: le type d'assemblage est induit par la géométrie de l'ion métallique, en combinaison avec les vecteurs de coordination du ligand (p. ex. ion métallique octaédrique + vecteurs de coordination parallèles = assemblage de type grille Figure 1.2-6c).

La capacité de chélation des sites de coordination, la 'compatibilité' avec le métal (considéré dans le cadre de la théorie HSAB des acides et bases durs et mous), ainsi que l'effet de l'environnement/ milieu déterminent les modes de coordination et la stéréochimie dans les composés mono/ oligo/ et polymétalliques. Les tendances suivantes ont été observées en criblant les structures multimétalliques de composés dans cette classe. Les ligands macrocycliques forcent la géométrie plan carré; les unités de ligands N,O pontées, mettant en évidence un motif de coordination tétradentate M(NO)$_2$(NO)$_2$ ont généralement la forme *cis* lors de la complexation (Figure 1.2-6a, e). Pour les complexes monomériques des ligands bidentates N,O, la forme *trans* est généralement la norme, mais il y a cependant des cas où la forme *cis* est stabilisée par des interactions entre les atomes donneurs du cycle chélate avec

des cations (Figure 1.2-6d), ou par liaisons hydrogène et/ ou d'autre type de 'packing forces' – ces situations soulignent également le rôle important de l'environnement/ milieu.
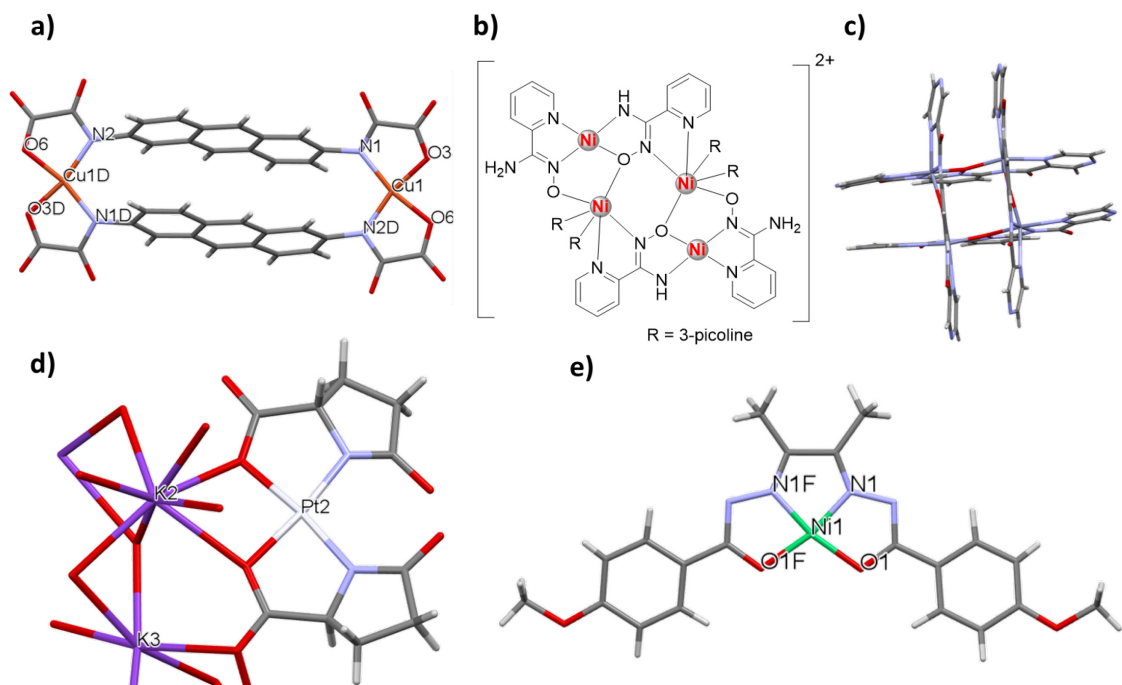
Figure 1.2-6. Des exemples choisis des systèmes mononucléaires, dinucléaires et de nucléarité plus élevée: a) unités de type amino-oxo-acetato pontées et la structure dimérique formée avec des ions de cuivre(II)[135] – cette famille de composés est d'intérêt pour les propriétés magnétiques;[136] b) le tétramère de nickel(II) formé en utilisant les multiple modes de coordination du ligand pyridine-amidoxime;[137] c) composé grille à base de zinc(II);[138] d) structure monomérique avec des ligands N,O bidentates dans laquelle la forme *cis* est stabilisée par des interactions entre les atomes d'O du cycle chélate et des ions K$^+$;[139] e) des ligands N,O pontés, résultant dans un motif de coordination tétradentate M(NO)$_2$(NO)$_2$ avec l'imposition de la forme *cis* du complexe et de la géométrie plan carré.[140]

1.2.3. La présentation des ligands amidine *N*-oxydes (AMOX)

Les oxydes d'amidine/ amidine oxydes (AMOXs), aussi connus comme α-aminonitrones, sont les formes tautomériques des hydroxyamidines et des amidoximes. (Figure 1.2-7b).[141] Les amidoximes sont les hydroxyamides des acides imidiques, qui sont des tautomères des carboxyamides (Figure 1.2-7a). Ainsi, les amidoximes sont formellement

classifiées comme des dérivés de carboximides.[141] Les structures des AMOXs sont présentées dans la Figure 1.2-7b, classifiées en fonction du degré de substitution (p. ex. non-substitués, *N*-substitués, *N,N*-disubstitués, *N,N'*-disubstitués).
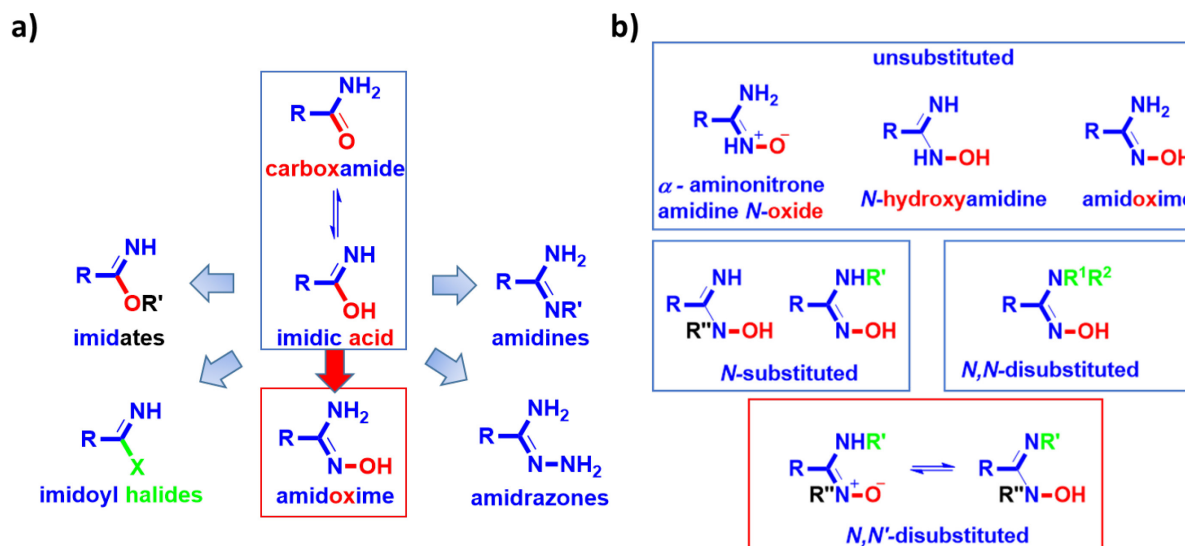
Figure 1.2-7. La famille des amidoximes: a) leurs précurseurs; b) les formes tautomériques et la classification en fonction du degré de substitution.

L'évolution du nombre de publications contenant l'un des termes: *amidine oxide*, *hydroxyamidine*, *aminonitrone*, *amidoxime* montre une tendance ascendante constante au cours de la période 1900 à 2015 (Figure 1.2-8a). Toutefois, lorsque le nombre total de publications sur des composés de type AMOX est comparé aux résultats obtenus pour les composés de type 2,2' -bipyridine et 8 -hydroxyquinoline, on peut voir que la recherche basée sur les AMOX est à ses débuts (Figure 1.2 -8b). À cet égard, il est important de noter que très récemment, les amidoximes et leurs complexes de coordination ont été passés en revue en détail par Kukushkin *et al*.[142]
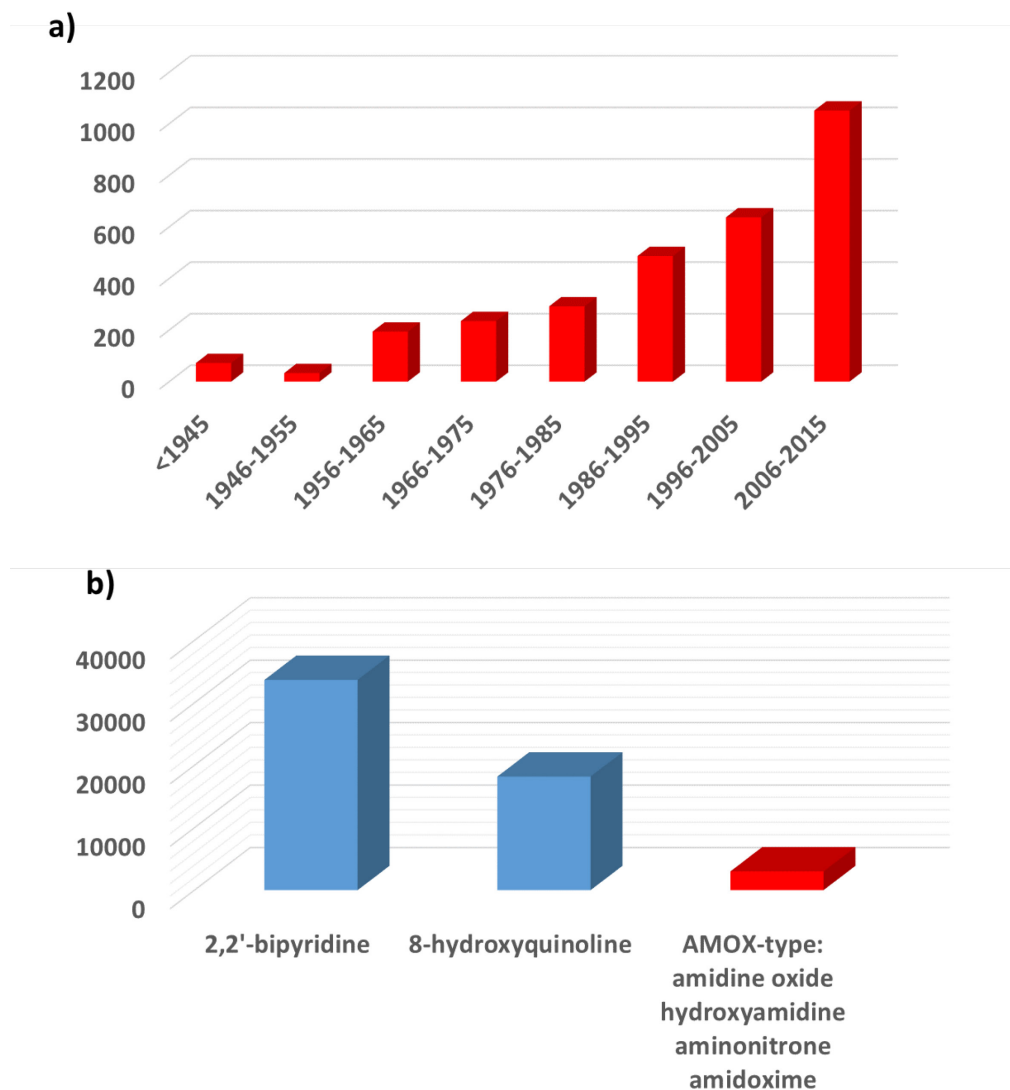
Figure 1.2-8. Le nombre de publications contenant au moins l'un des termes: *amidine oxide*, *hydroxyamidine*, *aminonitrone*, *amidoxime* (Scifinder, December 2015): a) l'évolution du nombre de publications pendant 1900-2015; b) la présentation comparative *vs.* les résultats obtenus pour les terms *2,2'-bipyridine* et *8-hydroxyquinoline*.

1.3. L'objectif de la recherche, les directions de recherche et la méthodologie

1.3.1. L'objectif de la recherche et les directions de recherche

L'objectif général des travaux rapportés dans cette thèse est l'étude des ligands amidine *N*-oxydes (AMOX) *N,N′*-disubstitués (également connu sous le nom de *N*- hydroxyamidines/ α-aminonitrones *N,N′*-disubstitués, Figure 1.2-7) du point de vue de la chimie de coordination et de la chimie supramoléculaire (Figure 1.3-1 gauche). Comme choix des métaux, les ions des métaux de transitions de la droite de la première rangée sont ciblés, notamment le cobalt(II) et le zinc(II).
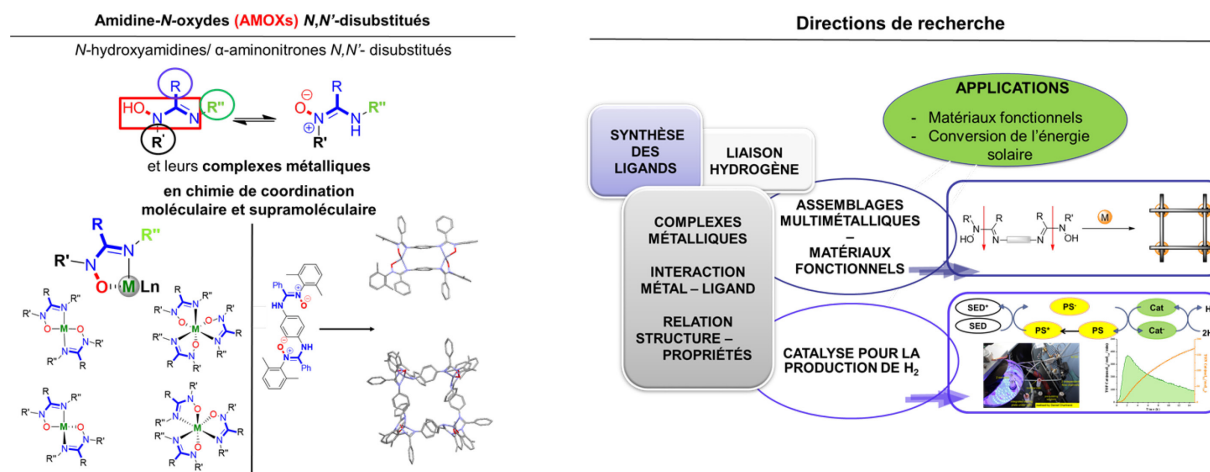
Figure 1.3-1. L'objectif général de la thèse et les directions de recherche

Les axes de recherche suivants ont été poursuivis (Figure 1.3-1 droite):

▪ les ligands: la synthèse et la caractérisation

▪ les complexes métalliques: la synthèse et la caractérisation; l'étude de l'influence du motif de substitution des ligands sur l'interaction métal-ligand et l'identification des relations structure - propriétés

▪ les composés à base des ligands AMOXs dans des systèmes supramoléculaires: des assemblages multimétalliques – vers des matériaux fonctionnels et des systèmes photocatalytiques pour la conversion d'énergie solaire (plus spécifiquement la photocatalyse

pour la production de H$_2$). L'étude des motifs des liaisons hydrogène dans les composés à base des AMOXs est également un point d'intérêt.

1.3.2. Note sur la méthodologie

La méthodologie utilisée dans cette thèse est décrite dans la Figure 1.3-2 (gauche). Les techniques spécifiques utilisées pour la caractérisation des composés et l'étude de leurs propriétés sont indiquées dans la Figure 1.3-2 (droite).
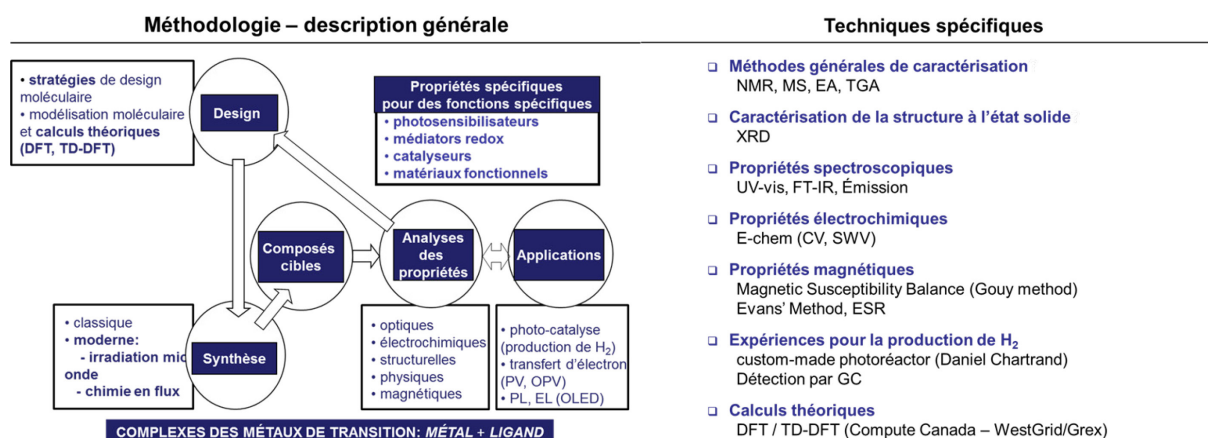
Figure 1.3-2. La méthodologie: les grandes lignes (gauche) et des techniques spécifiques (droite)

Les tests de la performance des complexes AMOX à base de zinc(II) dans OLEDs sont faits en collaboration avec d'autres groupes de recherche. Le travail est en cours et les résultats, ainsi que la méthodologie seront décrits dans des futures publications. Les résultats préliminaires sont cependant présentés dans le chapitre 5.

1.4. Le plan de la thèse

La thèse est divisée en six chapitres

Chapitre 1. Pour définir le contexte général de ce travail, l'importance des composés de coordination dans les applications est soulignée. Les tendances et les opportunités futures dans leur étude et leur utilisation dans des applications sont aussi identifiées. Les concepts clés pertinents de chimie de coordination moléculaire et supramoléculaire sont également présentés (section 1.1). Le contexte spécifique de cette recherche est mis en évidence par des aspects

choisis de la chimie de coordination des ligands N,O (section 1.2). L'objectif général de la recherche, les directions de recherche et la méthodologie sont également décrites (section 1.3), ainsi que le plan de la thèse (section 1.4).

Chapitre 2. Ce chapitre présente: les propriétés des ligands AMOX (section 2.1.2), un aperçu général sur la stratégie de synthèse utilisée (section 2.1.3), et les résultats obtenus sur la famille de *N*-hydroxyformamidines *N,N'*-disubstitués (section 2.2).

Chapitre 3. Les complexes de cobalt(II) avec des ligands *N,N'*- diarylformamidinate *N*-oxydes stériquement encombrés sont introduits (section 3.2) et l'influence du motif de substitution des ligands sur les propriétés des complexes est évaluée (section 3.3).

Chapitre 4. Ce chapitre met en évidence un cas particulier de changement de géométrie et de spin, induit par des interactions de type liaison hydrogène dans un composé chélate de cobalt(II) bis(AMOX). L'influence de l'environnement sur les propriétés du complexe est ainsi révélée: les interactions faibles sont les principaux facteurs responsables de la stabilisation du système dans une combinaison spécifique géométrie - état de spin à l'état fondamental.

Chapitre 5. Les résultats sur la chimie de coordination des ligands AMOX avec des ions métalliques zinc(II) ions métalliques sont présentés. Premièrement, la relation structure – propriétés dans la famille de complexes Zn(AMOX)$_2$ (AMOX = *N,N'*-diarylformamidinate-*N*-oxyde) est déterminée (section 5.2). L'étude théorique (DFT/ TD-DFT) réalisée pour la série Zn(AMOX)$_2$ (AMOX = *N,N'*-diarylbenzamidinate-*N*-oxyde) afin d'évaluer l'influence du motif de substitution du ligand sur le band gap des complexes (section 5.3.1) est ensuite présentée. Au final, les composés dimériques de type [Zn(AMOX)$_2$]$_2$ (AMOX = *N,N'*-diarylbenzamidinate-*N*-oxyde (section 5.3.2) et le polymère de coordination à base des ligands bis-AMOX et d'ions zinc(II) sont décrits (section 5.3.3).

Chapitre 6. Les conclusions générales de la thèse (section 6.1) et les perspectives des ligands AMOXs dans la chimie de coordination moléculaire et supramoléculaire (section 6.2), ainsi que des observations finales (section 6.3) sont présentées.

1.5. Références

[1] M. D. Ward, in *Comprehensive Coordination Chemistry II* (Ed.: Meyer, J. A.; McCleverty, T. J.), Pergamon, Oxford, **2003**, pp. xv-xvi.

[2] C. E. Housecroft, A. G. Sharpe, in *Inorganic Chemistry, 4th Ed.*, Pearson, Harlow; New York, **2012**, pp. 639-847.

[3] J. A. Meyer; T. J. McCleverty, in *Comprehensive Coordination Chemistry II* (Ed.: Meyer, J. A.; McCleverty, T. J.), Pergamon, Oxford, **2003**, pp. xix-xx.

[4] R. Smalley, Humanity's top ten problems for next 50 years; http://cnst.rice.edu/content.aspx?id=246; accessed 10/2015.

[5] a) P. Gregory, in *Comprehensive Coordination Chemistry II* (Ed.: Meyer, J. A.; McCleverty, T. J.), Pergamon, Oxford, **2003**, pp. 549-579; b) J. Kent, in *Riegel's Handbook of Industrial Chemistry* (Ed.: Kent, J.), Springer US, **2003**, pp. 880-962.

[6] P. A. Tasker, P. G. Plieger, L. C. West, in *Comprehensive Coordination Chemistry II* (Ed.: Meyer, J. A.; McCleverty, T. J.), Pergamon, Oxford, **2003**, pp. 759-808.

[7] a) C. E. Housecroft, A. G. Sharpe, in *Inorganic Chemistry, 4th Ed.*, Pearson, Halrow, **2012**, pp. 940-975; b) V. C. Gibson, E. L. Marshall, in *Comprehensive Coordination Chemistry II* (Ed.: Meyer, J. A.; McCleverty, T. J.), Pergamon, Oxford, **2003**, pp. 1-74; c) C. Pettinari, F. Marchetti, D. Martini, in *Comprehensive Coordination Chemistry II* (Ed.: Meyer, J. A.; McCleverty, T. J.), Pergamon, Oxford, **2003**, pp. 75-139; d) R. H. Morris, *Acc. Chem. Res.* **2015**, *48*, 1494-1502; e) R. Noyori, M. Yamakawa, S. Hashiguchi, *J. Org. Chem.* **2001**, *66*, 7931-7944; f) P. W. N. M. Van Leeuwen, C. Claver, in *Comprehensive Coordination Chemistry II* (Ed.: Meyer, J. A.; McCleverty, T. J.), Pergamon, Oxford, **2003**, pp. 141-206; g) S. Hübner, J. G. de Vries, V. Farina, *Advanced Synthesis & Catalysis* **2016**, *358*, 3-25; h) I. P. Beletskaya, A. V. Cheprakov, in *Comprehensive Coordination Chemistry II* (Ed.: Meyer, J. A. and McCleverty, T. J.), Pergamon, Oxford, **2003**, pp. 305-368.

[8] a) J. J. Wilson, S. J. Lippard, *Chem. Rev.* **2014**, *114*, 4470-4495; b) N. Farrell, in *Comprehensive Coordination Chemistry II* (Ed.: Meyer, J. A. and McCleverty, T. J.), Pergamon, Oxford, **2003**, pp. 809-840; c) A. Erxleben, in *Reference Module in Chemistry, Molecular Sciences and Chemical Engineering*, Elsevier, **2015**.

[9] a) K. J. Franz, *Curr. Opin. Chem. Biol.* **2013**, *17*, 143-149; b) P. V. Bernhardt, *Dalton Trans.* **2007**, 3214-3220; c) http://www.rsc.org/education/eic/issues/2009Jan/iron-antibiotic-siderophore-oxygen-microbe.asp#; consulted december 2015; d) S. J. S. Flora, in *Comprehensive Inorganic Chemistry II (Second Edition)* (Ed.: Poeppelmeier, J. R.), Elsevier, Amsterdam, **2013**, pp. 987-1013.

[10] I. Bertini, H. B. Gray, S. J. Lippard, J. S. Valentine, *Bioinorganic Chemistry*, Univ. Sci. Books, **1994**, 505 - 583

[11] a) É. Tóth, L. Helm, A. E. Merbach, in *Comprehensive Coordination Chemistry II* (Ed.: Meyer, J. A. and McCleverty, T. J.), Pergamon, Oxford, **2003**, pp. 841-881; b) S. Z. Lever, J. D. Lydon, C. S. Cutler, S. S. Jurisson, in *Comprehensive Coordination Chemistry II* (Ed.: Meyer, J. A. M. J.), Pergamon, Oxford, **2003**, pp. 883-911; c) É. Tóth, L. Helm, A. E. Merbach, in *Reference Module in Chemistry, Molecular Sciences and Chemical Engineering*, Elsevier, **2015**; d) A. Duatti, in *Reference Module in Chemistry, Molecular Sciences and Chemical Engineering*, Elsevier, **2013**.

[12]   a) M. Nazeeruddin, M. Grätzel, in *Comprehensive Coordination Chemistry II* (Ed.: Meyer, J. A. and McCleverty, T. J.), Pergamon, Oxford, **2003**, pp. 719-758; b) K. Kalyanasundaram, *Dye-sensitized Solar Cells*, EFPL Press, **2010**, ; c) http://www.dyesol.com/products/dsc-materials/dyes.html; consulted november 2015; d) S. Mathew, A. Yella, P. Gao, R. Humphry-Baker, F. E. CurchodBasile, N. Ashari-Astani, I. Tavernelli, U. Rothlisberger, K. NazeeruddinMd, M. Grätzel, *Nat. Chem.* **2014**, *6*, 242-247; e) K.-L. Wu, W.-P. Ku, J. N. Clifford, E. Palomares, S.-T. Ho, Y. Chi, S.-H. Liu, P.-T. Chou, M. K. Nazeeruddin, M. Gratzel, *Energy Environ. Sci.* **2013**, *6*, 859-870.

[13]   a) I. Omae, *Coord. Chem. Rev*; b) E. Holder, B. M. W. Langeveld, U. S. Schubert, *Advanced Materials* **2005**, *17*, 1109-1121; c) Sigma Aldrich; OLED eFabricator; http://www.sigmaaldrich.com/materials-science/learning-center/oled-efabricator.html?cm_sp=Insite-_-MatSci-_-oledPDP; consulted december 2015; d) R. C. Evans, P. Douglas, C. J. Winscom, *Coord. Chem. Rev.* **2006**, *250*, 2093-2126; e) T.-Y. Li, Y.-M. Jing, X. Liu, Y. Zhao, L. Shi, Z. Tang, Y.-X. Zheng, J.-L. Zuo, *Scientific Reports* **2015**, *5*, 14912; f) C. Pérez-Bolívar, S.-y. Takizawa, G. Nishimura, V. A. Montes, P. Anzenbacher, *Chem. Eur. J.* **2011**, *17*, 9076-9082.

[14]   a) P. Silva, S. M. F. Vilela, J. P. C. Tome, F. A. Almeida Paz, *Chem. Soc. Rev.* **2015**, *44*, 6774-6803; b) Y.-B. Zhang, H. Furukawa, N. Ko, W. Nie, H. J. Park, S. Okajima, K. E. Cordova, H. Deng, J. Kim, O. M. Yaghi, *J. Am. Chem. Soc.* **2015**, *137*, 2641-2650; c) A. U. Czaja, N. Trukhan, U. Muller, *Chem. Soc. Rev.* **2009**, *38*, 1284-1293.

[15]   http://www.sony.net/Products/SC-HP/cx_news_archives/img/pdf/vol_56/sideview56.pdf; consulted december 2015.

[16]   a) http://www.digitaltrends.com/home-theater/value-electronics-tv-shootout-2015-lg-oled-winner/; consulted december 2015; b) http://www.displaymate.com/Galaxy_S6_ShootOut_1.htm; consulted december 2015; c) http://www.oled-info.com/history; consulted december 2015.

[17]   a) PubChem, http://pubchem.ncbi.nlm.nih.gov/compound/157443#section=Top; accessed 21-12-2015; b) http://www.accessdata.fda.gov/scripts/cder/drugsatfda/index.cfm?fuseaction=Search.SearchAction&SearchType=BasicSearch&searchTerm=NET&Search_Button=Submitaccessed; accessed on 21-12-2015.

[18]   S. Mathew, A. Yella, P. Gao, R. Humphry-Baker, F. E. CurchodBasile, N. Ashari-Astani, I. Tavernelli, U. Rothlisberger, K. NazeeruddinMd, M. Grätzel, *Nat Chem* **2014**, *6*, 242-247.

[19]   http://www.remm.nlm.gov/dimercaprol.htm

[20]   Information on Gadolinium-based Contrast Agents (GBCA): http://www.fda.gov/Drugs/DrugSafety/PostmarketDrugSafetyInformationforPatientsandProviders/ucm142882.htm; consulted 22-12-2015

[21]   http://www.chemtube3d.com/solidstate/MOF-home.html; consulted december 2015.

[22]   J. W. Steed, J. L. Atwood, in *Supramolecular Chemistry*, John Wiley & Sons, Ltd, **2009**, pp. 707-775.

[23]   J. W. Steed, J. L. Atwood, in *Supramolecular Chemistry*, John Wiley & Sons, Ltd, **2009**, pp. 1-48.

[24]   J. W. Steed, J. L. Atwood, in *Supramolecular Chemistry*, John Wiley & Sons, Ltd, **2009**, pp. 49-104.

[25]   a) G. F. Swiegers, in *Bioinspiration and Biomimicry in Chemistry* (Ed.: Swiegers, G. F.), John Wiley & Sons, Inc., **2012**, pp. i-xxvii; b) J. W. Steed, J. L. Atwood, in *Supramolecular Chemistry*, John Wiley & Sons, Ltd, **2009**, pp. 777-827; c) M. Zhang, Z.-Y. Gu, M. Bosch, Z. Perry, H.-C. Zhou, *Coord. Chem. Rev.* **2015**, *293–294*, 327-356.

[26]   a) W. Lubitz, H. Ogata, O. Rüdiger, E. Reijerse, *Chem. Rev.* **2014**, *114*, 4081-4148; b) T. Xu, D. Chen, X. Hu, *Coord. Chem. Rev.* **2015**, *303*, 32-41; c) G. Berggren, A. Adamska, C. Lambertz, T. R. Simmons, J. Esselborn, M. Atta, S. Gambarelli, J. M. Mouesca, E. Reijerse, W. Lubitz, T. Happe, V. Artero, M. Fontecave, *Nature* **2013**, *499*, 66.

[27]   M. Hoarau, C. Hureau, E. Gras, P. Faller, *Coord. Chem. Rev.* **2016**, *308*, 445-459.

[28]   A. P. Alivisatos, M. J. Blaser, E. L. Brodie, M. Chun, J. L. Dangl, T. J. Donohue, P. C. Dorrestein, J. A. Gilbert, J. L. Green, J. K. Jansson, R. Knight, M. E. Maxon, M. J. McFall-Ngai, J. F. Miller, K. S. Pollard, E. G. Ruby, S. A. Taha, *Science* **2015**, *350*, 507-508.

[29]   H. B. Gray, *Nat. Chem.* **2009**, *1*, 7.

[30]   a) G. Caserta, S. Roy, M. Atta, V. Artero, M. Fontecave, *Curr. Opin. Chem. Biol.* **2015**, *25*, 36-47; b) M. Bacchi, G. Berggren, J. Niklas, E. Veinberg, M. W. Mara, M. L. Shelby, O. G. Poluektov, L. X. Chen, D. M. Tiede, C. Cavazza, M. J. Field, M. Fontecave, V. Artero, *Inorg. Chem.* **2014**, *53*, 8071.

[31]   a) T. W. Woolerton, S. Sheard, Y. S. Chaudhary, F. A. Armstrong, *Energy Environ. Sci.* **2012**, *5*, 7470-7490; b) E. M. Nichols, J. J. Gallagher, C. Liu, Y. Su, J. Resasco, Y. Yu, Y. Sun, P. Yang, M. C. Y. Chang, C. J. Chang, *Proc. Natl. Acad. Sci.* **2015**, *112*, 11461-11466.

[32]   a) J. R. McKone, N. S. Lewis, H. B. Gray, *Chem. Mater.* **2014**, *26*, 407-414; b) C. E. Lubner, R. Grimme, D. A. Bryant, J. H. Golbeck, *Biochemistry* **2010**, *49*, 404-414; c) N. S. Lewis, D. G. Nocera, *Proc. Natl. Acad. Sci. U. S. A.* **2006**, *103*, 15729-15735; d) R. L. House, N. Y. M. Iha, R. L. Coppo, L. Alibabaei, B. D. Sherman, P. Kang, M. K. Brennaman, P. G. Hoertz, T. J. Meyer, *J. Photochem. Photobiol. C: Photochem. Rev.* **2015**, *25*, 32-45; e) L. Hammarström, S. Hammes-Schiffer, *Acc. Chem. Res.* **2009**, *42*, 1859-1860; f) R. Eisenberg, *Science* **2009**, *324*, 44-45; g) J. Barber, *Chem. Soc. Rev.* **2009**, *38*, 185-196; h) V. Balzani, A. Credi, M. Venturi, *ChemSusChem* **2008**, *1*, 26-58; i) N. Armaroli, V. Balzani, *Angew. Chem., Int. Ed.* **2007**, *46*, 52-66.

[33]   S. Berardi, S. Drouet, L. Francas, C. Gimbert-Surinach, M. Guttentag, C. Richmond, T. Stoll, A. Llobet, *Chem. Soc. Rev.* **2014**, *43*, 7501-7519.

[34]   J. D. Hughes, *Nature* **2013**, *494*, 307-308.

[35]   K. R. Ramsayer, C., http://climate.nasa.gov/news/2364/; consulted 12-2015.

[36]   D. G. Nocera, *Acc. Chem. Res.* **2012**, *45*, 767-776.

[37]   H. Shaftel, http://climate.nasa.gov/news/2373/; consulted december 2015.

[38]   A. Fujishima, K. Honda, *Bull. Chem. Soc. Jap.* **1971**, *44*, 1148-1150.

[39]   A. Hagfeldt, G. Boschloo, L. Sun, L. Kloo, H. Pettersson, *Chem. Rev.* **2010**, *110*, 6595-6663.

[40]   Y. Jiao, Y. Zheng, M. Jaroniec, S. Z. Qiao, *Chem. Soc. Rev.* **2015**, *44*, 2060-2086.

[41]   a) F. E. Osterloh, *Chem. Soc. Rev.* **2013**, *42*, 2294-2320; b) T. Hisatomi, J. Kubota, K. Domen, *Chem. Soc. Rev.* **2014**, *43*, 7520-7535; c) J. Ronge, T. Bosserez, D. Martel, C. Nervi, L. Boarino, F. Taulelle, G. Decher, S. Bordiga, J. A. Martens, *Chem. Soc. Rev.*

2014, *43*, 7963-7981; d) Z. Li, W. Luo, M. Zhang, J. Feng, Z. Zou, *Energy Environ. Sci.* **2013**, *6*, 347-370.

[42]   a) L. Sun, F. Li, Z. Yu, *Energy Environ. Sci.* **2015**, *8*, 760-775; b) M. Wang, K. Han, S. Zhang, L. Sun, *Coord. Chem. Rev.* **2015**, *287*, 1-14; c) V. Artero, M. Fontecave, *Chem. Soc. Rev.* **2013**, *42*, 2338.

[43]   N. Queyriaux, N. Kaeffer, A. Morozan, M. Chavarot-Kerlidou, V. Artero, *J. Photochem. Photobiol., C* **2015**, Ahead of Print.

[44]   F. Li, K. Fan, B. Xu, E. Gabrielsson, Q. Daniel, L. Li, L. Sun, *J. Am. Chem. Soc.* **2015**, *137*, 9153-9159.

[45]   P. Chawla, M. Tripathi, *International Journal of Energy Research* **2015**, *39*, 1579-1596.

[46]   D. L. Ashford, M. K. Gish, A. K. Vannucci, M. K. Brennaman, J. L. Templeton, J. M. Papanikolas, T. J. Meyer, *Chem. Rev.* **2015**, *115*, 13006-13049.

[47]   a) M. Wang, L. Sun *ChemSusChem* **2010**, *3*, 551-554; b) M. Wang, L. Chen, L. Sun, *Energy Environ. Sci.* **2012**, *5*, 6763-6778; c) V. S. Thoi, Y. Sun, J. R. Long, C. J. Chang, *Chem. Soc. Rev.* **2013**, *42*, 2388-2400; d) T. Lazarides, T. McCormick, P. Du, G. Luo, B. Lindley, R. Eisenberg, *J. Am. Chem. Soc.* **2009**, *131*, 9192-9194; e) J. L. Dempsey, J. R. Winkler, H. B. Gray, in *Comprehensive Inorganic Chemistry II (Second Edition)* (Ed.: Poeppelmeier, J. R.), Elsevier, Amsterdam, **2013**, pp. 553-565.

[48]   a) M. E. Louis, T. G. Fenton, J. Rondeau, T. Jin, G. Li, *Comments on Inorganic Chemistry* **2016**, *36*, 38-60; b) W.-H. Wang, Y. Himeda, J. T. Muckerman, G. F. Manbeck, E. Fujita, *Chem. Rev.* **2015**; c) M. Rakowski Dubois, D. L. Dubois, *Acc. Chem. Res.* **2009**, *42*, 1974-1982; d) R. Angamuthu, P. Byers, M. Lutz, A. L. Spek, E. Bouwman, *Science* **2010**, *327*, 313-315; e) C. Costentin, M. Robert, J.-M. Saveant, *Chem. Soc. Rev.* **2013**, *42*, 2423-2436.

[49]   M. D. Kärkäs, O. Verho, E. V. Johnston, B. Åkermark, *Chem. Rev.* **2014**, *114*, 11863-12001.

[50]   T. C. B. Harlang, Y. Liu, O. Gordivska, L. A. Fredin, C. S. Ponseca Jr, P. Huang, P. Chábera, K. S. Kjaer, H. Mateos, J. Uhlig, R. Lomoth, R. Wallenberg, S. Styring, P. Persson, V. Sundström, K. Wärnmark, *Nat. Chem.* **2015**, *7*, 883-889.

[51]   a) P. Zhang, M. Wang, Y. Na, X. Q. Li, Y. Jiang, L. C. Sun, *Dalton Trans.* **2010**, *39*, 1204-1206; b) M. Wang, L. Chen, X. Li, L. Sun, *Dalton Trans.* **2011**, *40*, 12793-12800.

[52]   a) N. Queyriaux, R. T. Jane, J. Massin, V. Artero, M. Chavarot-Kerlidou, *Coord. Chem. Rev.* **2015**, *304-305*, 3-19; b) V. Artero, M. Chavarot-Kerlidou, M. Fontecave, *Angew. Chem., Int. Ed.* **2011**, *50*, 7238-7266.

[53]   a) A. Das, Z. Han, W. W. Brennessel, P. L. Holland, R. Eisenberg, *ACS Catalysis* **2015**, *5*, 1397-1406; b) S. Wiese, U. J. Kilgore, M.-H. Ho, S. Raugei, D. L. DuBois, R. M. Bullock, M. L. Helm, *ACS Catal.* **2013**, *3*, 2527-2535.

[54]   a) H. Lei, H. Fang, Y. Han, W. Lai, X. Fu, R. Cao, *ACS Catalysis* **2015**, *5*, 5145-5153; b) X. Liu, H. Zheng, Z. Sun, A. Han, P. Du, *ACS Catalysis* **2015**, *5*, 1530-1538.

[55]   a) X. Li, M. Wang, D. Zheng, K. Han, J. Dong, L. Sun, *Energy Environ. Sci.* **2012**, *5*, 8220-8224; b) T. M. McCormick, B. D. Calitree, A. Orchard, N. D. Kraut, F. V. Bright, M. R. Detty, R. Eisenberg, *J. Am. Chem. Soc.* **2010**, *132*, 15480-15483.

[56]   E. Verlage, S. Hu, R. Liu, R. J. R. Jones, K. Sun, C. Xiang, N. S. Lewis, H. A. Atwater, *Energ. Environ. Sci.* **2015**, *8*, 3166-3172.

[57]   J. Newman, P. G. Hoertz, C. A. Bonino, J. A. Trainham, *J. Electrochem. Soc.* **2012**, *159*, A1722-A1729.

[58]   J.-M. Lehn, in *Constitutional Dynamic Chemistry, Vol. 322* (Ed.: Barboiu, M.), Springer Berlin Heidelberg, **2012**, pp. 1-32.

[59]   E. C. Constable, C. E. Housecroft, in *Comprehensive Inorganic Chemistry II (Second Edition)* (Ed.: Poeppelmeier, J. R.), Elsevier, Amsterdam, **2013**, pp. 1-29.

[60]   a) J. W. Steed, J. L. Atwood, in *Supramolecular Chemistry*, John Wiley & Sons, Ltd, **2009**, pp. 591-706; b) K. Harris, Q. F. Sun, M. Fujita, in *Comprehensive Inorganic Chemistry II (Second Edition)* (Ed.: Poeppelmeier, J. R.), Elsevier, Amsterdam, **2013**, pp. 31-57.

[61]   J. W. Steed, J. L. Atwood, in *Supramolecular Chemistry*, John Wiley & Sons, Ltd, **2009**, pp. 829-859.

[62]   M. R. Axet, O. Dechy-Cabaret, J. Durand, M. Gouygou, P. Serp, *Coord. Chem. Rev.* **2016**, *308*, 236-345.

[63]   L. Valade, D. de Caro, C. Faulmann, K. Jacob, *Coord. Chem. Rev.* **2016**, *308*, 433-444.

[64]   a) R. Chakrabarty, P. S. Mukherjee, P. J. Stang, *Chem. Rev.* **2011**, *111*, 6810-6918; b) T. R. Cook, Y.-R. Zheng, P. J. Stang, *Chem. Rev.* **2013**, *113*, 734-777; c) T. R. Cook, P. J. Stang, *Chem. Rev.* **2015**, *115*, 7001-7045; d) M. Yoshizawa, J. K. Klosterman, M. Fujita, *Angew. Chem. Intl. Ed.* **2009**, *48*, 3418-3438; e) R. S. Forgan, J.-P. Sauvage, J. F. Stoddart, *Chem. Rev.* **2011**, *111*, 5434-5464.

[65]   a) N. A. Khan, S. H. Jhung, *Coord. Chem. Rev.* **2015**, *285*, 11-23; b) A. Karmakar, A. V. Desai, S. K. Ghosh, *Coord. Chem. Rev.* **2016**, *307, Part 2*, 313-341; c) J. W. Steed, J. L. Atwood, in *Supramolecular Chemistry*, John Wiley & Sons, Ltd, **2009**, pp. 537-589; d) M. Li, D. Li, M. O'Keeffe, O. M. Yaghi, *Chem. Rev.* **2014**, *114*, 1343-1370; e) H. Furukawa, K. E. Cordova, M. O'Keeffe, O. M. Yaghi, *Science* **2013**, *341*; f) S. Kitagawa, K. Uemura, *Chem. Soc. Rev.* **2005**, *34*, 109.

[66]   a) C. Amiens, D. Ciuculescu-Pradines, K. Philippot, *Coord. Chem. Rev*; b) J. W. Steed, J. L. Atwood, in *Supramolecular Chemistry*, John Wiley & Sons, Ltd, **2009**, pp. 899-939.

[67]   J. W. Steed, J. L. Atwood, in *Supramolecular Chemistry*, John Wiley & Sons, Ltd, **2009**, pp. 441-536.

[68]   A. J. McConnell, C. S. Wood, P. P. Neelakandan, J. R. Nitschke, *Chem. Rev.* **2015**, *115*, 7729-7793.

[69]   a) M. D. Manrique-Juárez, S. Rat, L. Salmon, G. Molnár, C. M. Quintero, L. Nicu, H. J. Shepherd, A. Bousseksou, *Coord. Chem. Rev*; b) P. G. Lacroix, I. Malfant, C. Lepetit, *Coord. Chem. Rev*; c) A. Bianchi, E. Delgado-Pinar, E. García-España, F. Pina, in *Comprehensive Inorganic Chemistry II (Second Edition)* (Ed.: Poeppelmeier, J. R.), Elsevier, Amsterdam, **2013**, pp. 969-1037.

[70]   L. Wang, Y. Han, X. Feng, J. Zhou, P. Qi, B. Wang, *Coord. Chem. Rev.* **2016**, *307, Part 2*, 361-381.

[71]   a) A. K. Bar, C. Pichon, J.-P. Sutter, *Coord. Chem. Rev*; b) L. K. Thompson, L. N. Dawe, *Coord. Chem. Rev.* **2015**, *289–290*, 13-31; c) M. Castellano, R. Ruiz-García, J. Cano, J. Ferrando-Soria, E. Pardo, F. R. Fortea-Pérez, S.-E. Stiriba, W. P. Barros, H. O. Stumpf, L. Cañadillas-Delgado, J. Pasán, C. Ruiz-Pérez, G. de Munno, D. Armentano, Y. Journaux, F. Lloret, M. Julve, *Coord. Chem. Rev.* **2015**, *303*, 110-138.

[72] a) C. J. Brown, F. D. Toste, R. G. Bergman, K. N. Raymond, *Chem. Rev.* **2015**, *115*, 3012-3035; b) P. Ballester, P. van Leeuwer, A. Vidal-Ferran, in *Reference Module in Chemistry, Molecular Sciences and Chemical Engineering*, Elsevier, **2015**.

[73] G.-Y. Li, R.-L. Guan, L.-N. Ji, H. Chao, *Coord. Chem. Rev.* **2014**, *281*, 100-113.

[74] IUPAC Golden Book: (http://goldbook.iupac.org/C01330.html); consulted 10-2015

[75] IUPAC Golden Book: (http://goldbook.iupac.org/L03518.html); consulted 10-2015

[76] IUPAC Golden Book: (http://goldbook.iupac.org/O04328.html; consulted 12-2015

[77] J. A. McCleverty, T. J. Meyer, in *Comprehensive Coordination Chemistry II* (Ed.: Meyer, J. A. M. J.), Pergamon, Oxford, **2003**, pp. xv-xxiv.

[78] IUPAC Golden Book: (http://goldbook.iupac.org/B00697.html); consulted 10-2015

[79] a) J. R. Gispert, in *Coordination Chemistry*, Wiley, **2008**, pp. 3-29; b) C. Lepetit, V. Maraval, Y. Canac, R. Chauvin, *Coord. Chem. Rev.*

[80] M. Goswami, A. Chirila, C. Rebreyend, B. de Bruin, *Top. Catal.* **2015**, *58*, 719-750.

[81] M. Wächtler, J. Guthmuller, L. González, B. Dietzek, *Coord. Chem. Rev.* **2012**, *256*, 1479-1508.

[82] G. Smolentsev, V. Sundström, *Coord. Chem. Rev.* **2015**, *304–305*, 117-132.

[83] C. Daniel, *Coord. Chem. Rev.* **2015**, *282–283*, 19-32.

[84] a) A. Caneschi, D. Gatteschi, F. Totti, *Coord. Chem. Rev.* **2015**, *289–290*, 357-378; b) A. C. Tsipis, *Coord. Chem. Rev.* **2014**, *272*, 1-29; c) M. Bruschi, C. Greco, P. Fantucci, L. De Gioia, *Inorg. Chem.* **2008**, *47*, 6056-6071; d) M. Atanasov, C. Daul, H. U. Güdel, T. A. Wesolowski, M. Zbiri, *Inorg. Chem.* **2005**, *44*, 2954-2963; e) A. C. Tsipis, A. T. Chaviara, *Inorg. Chem.* **2004**, *43*, 1273-1286.

[85] C. Adamo, T. Le Bahers, M. Savarese, L. Wilbraham, G. García, R. Fukuda, M. Ehara, N. Rega, I. Ciofini, *Coord. Chem. Rev.* **2015**, *304–305*, 166-178.

[86] a) B. Butschke, K. L. Fillman, T. Bendikov, L. J. W. Shimon, Y. Diskin-Posner, G. Leitus, S. I. Gorelsky, M. L. Neidig, D. Milstein, *Inorg. Chem.* **2015**, *54*, 4909-4926; b) K. Ray, T. Petrenko, K. Wieghardt, F. Neese, *Dalton Trans.* **2007**, 1552-1566; c) W. Kaim, *Inorg. Chem.* **2011**, *50*, 9752-9765.

[87] a) G. Skara, B. Pinter, P. Geerlings, F. De Proft, *Chem. Sci.* **2015**, *6*, 4109-4117; b) W. Kaim, *Eur. J. Inorg. Chem.* **2012**, *2012*, 343-348.

[88] a) M. M. Khusniyarov, E. Bill, T. Weyhermueller, E. Bothe, K. Wieghardt, *Angew. Chem., Int. Ed.* **2011**, *50*, 1652-1655, S1652/1651-S1652/1610; b) P. J. Chirik, K. Wieghardt, *Science* **2010**, *327*, 794-795; c) K. Ray, S. DeBeer George, E. I. Solomon, K. Wieghardt, F. Neese, *Chem. Eur. J.* **2007**, *13*, 2783-2797; d) R. Kapre, K. Ray, I. Sylvestre, T. Weyhermueller, S. DeBeer George, F. Neese, K. Wieghardt, *Inorg. Chem.* **2006**, *45*, 3499-3509; e) K. Ray, E. Bill, T. Weyhermueller, K. Wieghardt, *J. Am. Chem. Soc.* **2005**, *127*, 5641-5654; f) S. Kokatam, T. Weyhermuller, E. Bothe, P. Chaudhuri, K. Wieghardt, *Inorg. Chem.* **2005**, *44*, 3709-3717; g) K. S. Min, T. Weyhermueller, K. Wieghardt, *Dalton Trans.* **2004**, 178-186; h) K. S. Min, T. Weyhermueller, E. Bothe, K. Wieghardt, *Inorg. Chem.* **2004**, *43*, 2922-2931; i) D. Herebian, E. Bothe, F. Neese, T. Weyhermueller, K. Wieghardt, *J. Am. Chem. Soc.* **2003**, *125*, 9116-9128; j) D. Herebian, E. Bothe, E. Bill, T. Weyhermueller, K. Wieghardt, *J. Am. Chem. Soc.* **2001**, *123*, 10012-10023; k) P. Chaudhuri, C. N. Verani, E. Bill, E. Bothe, T. Weyhermueller, K. Wieghardt, *J. Am. Chem. Soc.* **2001**, *123*, 2213-2223; l) B. De Bruin, E. Bill, E. Bothe, T. Weyhermueller, K. Wieghardt, *Inorg. Chem.* **2000**, *39*, 2936-2947; m) A. Das, P. Ghosh, S. Plebst, B. Schwederski, S. M.

Mobin, W. Kaim, G. K. Lahiri, *Inorg. Chem.* **2015**, *54*, 3376-3386; n) A. Paretzki, M. Bubrin, J. Fiedler, S. Zalis, W. Kaim, *Chem. Eur. J.* **2014**, *20*, 5414-5422; o) M. M. R. Choudhuri, W. Kaim, B. Sarkar, R. J. Crutchley, *Inorg. Chem.* **2013**, *52*, 11060-11066; p) A. K. Das, R. Hubner, B. Sarkar, J. Fiedler, S. Zalis, G. K. Lahiri, W. Kaim, *Dalton Trans.* **2012**, *41*, 8913-8921; q) A. B. P. Lever, *Coord. Chem. Rev.* **2010**, *254*, 1397-1405; r) D. Kalinina, C. Dares, H. Kaluarachchi, P. G. Potvin, A. B. P. Lever, *Inorg. Chem.* **2008**, *47*, 10110-10126; s) S. I. Gorelsky, A. B. P. Lever, M. Ebadi, *Coord. Chem. Rev.* **2002**, *230*, 97-105; t) R. Santana da Silva, S. I. Gorelsky, E. S. Dodsworth, E. Tfouni, A. B. P. Lever, *Dalton Trans.* **2000**, 4078-4088; u) A. B. P. Lever, S. I. Gorelsky, *Coord. Chem. Rev.* **2000**, *208*, 153-167; v) R. A. Metcalfe, A. B. P. Lever, *Inorg. Chem.* **1997**, *36*, 4762-4771; w) H. Masui, A. B. P. Lever, E. S. Dodsworth, *Inorg. Chem.* **1993**, *32*, 258-267; x) M. Haga, E. S. Dodsworth, A. B. P. Lever, *Inorg. Chem.* **1986**, *25*, 447-453; y) R. Sarkar, K. K. Rajak, *J. Organomet. Chem.* **2015**, *779*, 1-13; z) N. Deibel, M. G. Sommer, S. Hohloch, J. Schwann, D. Schweinfurth, F. Ehret, B. Sarkar, *Organometallics* **2014**, *33*, 4756-4765; aa) N. Deibel, S. Hohloch, D. Schweinfurth, F. Weisser, A. Grupp, B. Sarkar, *Chem. Eur. J.* **2014**, *20*, 15178-15187; ab) S. Bellinger-Buckley, T.-C. Chang, S. Bag, D. Schweinfurth, W. Zhou, B. Torok, B. Sarkar, M.-K. Tsai, J. Rochford, *Inorg. Chem.* **2014**, *53*, 5556-5567.

[89]   a) O. R. Luca, R. H. Crabtree, *Chem. Soc. Rev.* **2013**, *42*, 1440-1459; b) V. Lyaskovskyy, B. de Bruin, *ACS Catal.* **2012**, *2*, 270-279.

[90]   D. L. J. Broere, R. Plessius, J. I. van der Vlugt, *Chem. Soc. Rev.* **2015**, *44*, 6886-6915.

[91]   J. R. Gispert, *Coordination Chemistry*, Wiley, **2008**, 59-93

[92]   S. N. Brown, *Inorg. Chem.* **2012**, *51*, 1251-1260.

[93]   A. B. P. Lever, *Inorg. Chem.* **1990**, *29*, 1271-1285.

[94]   a) J. R. Gispert, Wiley, **2008**, pp. 59-93; b) J. Cirera, P. Alemany, S. Alvarez, *Chem. - Eur. J.* **2004**, *10*, 190-207; c) J. Cirera, E. Ruiz, S. Alvarez, *Inorg. Chem.* **2008**, *47*, 2871-2889.

[95]   T. J. Collins, *Acc. Chem. Res.* **1994**, *27*, 279-285.

[96]   J. W. Jurss, R. S. Khnayzer, J. A. Panetier, K. A. El Roz, E. M. Nichols, M. Head-Gordon, J. R. Long, F. N. Castellano, C. J. Chang, *Chem. Sci.* **2015**, *6*, 4954-4972.

[97]   Comprehensive Coordination Chemistry II (Ed.: J. A. McCleverty, J. Meyer), Pergamon, Oxford, 2003

[98]   J. R. Gispert, in *Coordination Chemistry*, Wiley, **2008**, pp. 403-435.

[99]   J. R. Gispert, in *Coordination Chemistry*, Wiley, **2008**, pp. 439-476.

[100] G. R. Desiraju, T. Steiner, *The Weak Hydrogen Bond in Structural Chemistry and Biology*, **2001**,

[101] L. C. Gilday, S. W. Robinson, T. A. Barendt, M. J. Langton, B. R. Mullaney, P. D. Beer, *Chem. Rev.* **2015**, *115*, 7118-7195.

[102] a) L. Zhang, Y.-J. Lin, Z.-H. Li, G.-X. Jin, *J. Am. Chem. Soc.* **2015**, *137*, 13670-13678; b) R. Sheng, L. Tang, L. Jiang, L. Hong, Y. Shi, N. Zhou, Y. Hu, *ACS Chem. Neurosci.* **2015**.

[103] Y. Gao, X. Zhang, C. Ma, X. Li, J. Jiang, *J. Am. Chem. Soc.* **2008**, *130*, 17044-17052.

[104] a) U. Gellrich, J. Huang, W. Seiche, M. Keller, M. Meuwly, B. Breit, *J. Am. Chem. Soc.* **2011**, *133*, 964-975; b) S. K. Sommer, L. N. Zakharov, M. D. Pluth, *Inorg. Chem.* **2015**, *54*, 1912-1918; c) S. K. Sommer, E. A. Henle, L. N. Zakharov, M. D. Pluth, *Inorg. Chem.* **2015**, *54*, 6910-6916.

[105] a) A. D. Garnovskii, I. S. Vasilchenko, D. A. Garnovskii, B. I. Kharisov, *J. Coord. Chem.* **2009**, *62*, 151-204; b) A. Blagus, D. Cincic, T. Friscic, B. Kaitner, V. Stilinovic, *Macedonian Journal of Chemistry and Chemical Engineering* **2010**, *29*, 117-138.

[106] a) R. H. Holm, M. J. O'Connor, *Progr. Inorg. Chem.* **1971**, *14*, 241-401; b) R. H. Holm, G. W. Everett, Jr., A. Chakravorty, *Prog. Inorg. Chem.* **1966**, *7*, 83-214.

[107] C. J. Whiteoak, G. Salassa, A. W. Kleij, *Chem. Soc. Rev.* **2012**, *41*, 622-631.

[108] a) K. C. Gupta, A. K. Sutar, *Coord. Chem. Rev.* **2008**, *252*, 1420-1450; b) R. Drozdzak, B. Allaert, N. Ledoux, I. Dragutan, V. Dragutan, F. Verpoort, *Coord. Chem. Rev.* **2005**, *249*, 3055-3074; c) T. Katsuki, *Chem. Soc. Rev.* **2004**, *33*, 437-444; d) P. G. Cozzi, *Chem. Soc. Rev.* **2004**, *33*, 410-421; e) D. J. Darensbourg, *Chem. Rev.* **2007**, *107*, 2388-2410; f) H. Chen, Z. Sun, S. Ye, D. Lu, P. Du, *J. Mater. Chem. A* **2015**, *3*, 15729-15737.

[109] S. Akine, T. Nabeshima, *Dalton Trans.* **2009**, 10395-10408.

[110] a) E. L. Gavey, M. Pilkington, *Coord. Chem. Rev.* **2015**, *296*, 125-152; b) M. Rezaeivala, H. Keypour, *Coord. Chem. Rev.* **2014**, *280*, 203-253.

[111] a) Y. n. Song, H. Xu, W. Chen, P. Zhan, X. Liu, *MedChemComm* **2015**, *6*, 61-74; b) V. Prachayasittikul, S. Prachayasittikul, S. Ruchirawat, V. Prachayasittikul, *Drug. Des. Devel. Ther.* **2013**, *7*, 1157-1178; c) N. Thejo Kalyani, S. J. Dhoble, *Renewable Sustainable Energy Rev.* **2012**, *16*, 2696-2723; d) Z. Yin, B. Wang, G. Chen, M. Zhan, *J. Mater. Sci.* **2011**, *46*, 2397-2409; e) P. J. Jadhav, B. N. Limketkai, M. A. Baldo, *Adv. Polym. Sci.* **2010**, *223*, 29-44; f) W.-Q. Ding, S. E. Lind, *IUBMB Life* **2009**, *61*, 1013-1018; g) M. Elhabiri, A.-M. Albrecht-Gary, *Coord. Chem. Rev.* **2008**, *252*, 1079-1092; h) M. Albrecht, M. Fiege, O. Osetska, *Coord. Chem. Rev.* **2008**, *252*, 812-824.

[112] a) B. Sarkar, D. Schweinfurth, N. Deibel, F. Weisser, *Coord. Chem. Rev.* **2015**, *293–294*, 250-262; b) E. Bill, E. Bothe, P. Chaudhuri, K. Chlopek, D. Herebian, S. Kokatam, K. Ray, T. Weyhermuller, F. Neese, K. Wieghardt, *Chem. Eur. J.* **2005**, *11*, 204-224; c) X. Sun, H. Chun, K. Hildenbrand, E. Bothe, T. Weyhermüller, F. Neese, K. Wieghardt, *Inorg. Chem.* **2002**, *41*, 4295-4303.

[113] P. Teo, T. S. A. Hor, *Coord. Chem. Rev.* **2011**, *255*, 273-289.

[114] P. Banerjee, *Coord. Chem. Rev.* **1999**, *190-192*, 19-28.

[115] P. R. Payne, R. K. Thomson, D. M. Medeiros, G. Wan, L. L. Schafer, *Dalton Trans.* **2013**, *42*, 15670-15677.

[116] J. Li, C. Wang, X. Li, H. Sun, *Dalton Trans.* **2012**, *41*, 8715-8722.

[117] A. J. Blake, L. M. Gilby, S. Parsons, J. M. Rawson, D. Reed, G. A. Solan, R. E. P. Winpenny, *J. Chem. Soc., Dalton Trans.* **1996**, 3575-3581.

[118] P. Jaitner, W. Huber, A. Gieren, H. Betz, *J. Organomet. Chem.* **1986**, *311*, 379-385.

[119] C. G. Mowat, S. Parsons, G. A. Solan, R. E. P. Winpenny, *Acta Crystallogr. Sect. C* **1997**, *53*, 282-283.

[120] Z. Zhu, J. C. Fettinger, M. M. Olmstead, P. P. Power, *Organometallics* **2009**, *28*, 2091-2095.

[121] a) S. J. Lucas, R. M. Lord, R. L. Wilson, R. M. Phillips, V. Sridharan, P. C. McGowan, *Dalton Trans.* **2012**, *41*, 13800-13802; b) A. Habtemariam, M. Melchart, R. Fernández, S. Parsons, I. D. H. Oswald, A. Parkin, F. P. A. Fabbiani, J. E. Davidson, A. Dawson, R. E. Aird, D. I. Jodrell, P. J. Sadler, *J. Med. Chem.* **2006**, *49*, 6858-6868.

[122] a) T. N. Twala, M. Schutte-Smith, A. Roodt, H. G. Visser, *Dalton Trans.* **2015**, *44*, 3278-3288; b) A. Brink, H. G. Visser, A. Roodt, *Inorg. Chem.* **2013**, *52*, 8950-8961; c) M. Schutte, G. Kemp, H. G. Visser, A. Roodt, *Inorg. Chem.* **2011**, *50*, 12486-12498.

[123] F. Allen, *Acta Crystallogr. Sect. B* **2002**, *58*, 380-388.

[124] CSD search performed in october 2015

[125] T. Storr, in *Ligand Design in Medicinal Inorganic Chemistry*, John Wiley & Sons, Ltd, **2014**, pp. i-xvii.

[126] P. K. Petrova, R. L. Tomova, R. T. Stoycheva-Topalova, InTech, **2011**, pp. 161-193.

[127] J. A. Wolny, M. F. Rudolf, Z. Ciunik, K. Gatner, S. Wolowiec, *J. Chem. Soc., Dalton Trans.* **1993**, 1611-1622.

[128] L. C. Kalutarage, P. D. Martin, M. J. Heeg, C. H. Winter, *J. Am. Chem. Soc.* **2013**, *135*, 12588-12591.

[129] A. Okazawa, T. Ishida, *Chem. Phys. Lett.* **2009**, *480*, 198-202.

[130] a) A. Okazawa, D. Hashizume, T. Ishida, *J. Am. Chem. Soc.* **2010**, *132*, 11516-11524; b) A. Okazawa, Y. Nagaichi, T. Nogami, T. Ishida, *Inorg. Chem.* **2008**, *47*, 8859-8868.

[131] a) D. X. West, S. F. Pavkovic, J. N. Brown, *Acta Crystallogr. Sect. B* **1980**, *36*, 143-145; b) D. X. West, E. J. Zaluzec, S. F. Pavkovic, *Acta Crystallogr. Sect. C* **1994**, *50*, 173-175; c) P. Knuuttila, H. Knuuttila, *Acta Crystallogr. Sect. C* **1986**, *42*, 989-991; d) E. Sletten, T. Marthinsen, J. Sletten, *Inorg. Chimica Acta* **1984**, *93*, 37-41.

[132] F.-Q. Z. Ying-Lei Wang, Yue-Ping Ji, Jian-Hua Yi, Ting An, Wei-Xiao Liu, *Chinese Chemical Letters* **2014**, *25*, 902-906.

[133] T. Minyu, *Bull. Chem. Soc. Jpn.* **1989**, *62*.

[134] A. Krajete, G. Steiner, H. Kopacka, K.-H. Ongania, K. Wurst, Marc O. Kristen, P. Preishuber-Pflügl, B. Bildstein, *Eur. J. Inorg. Chem.* **2004**, *2004*, 1740-1752.

[135] M. Castellano, J. Ferrando-Soria, E. Pardo, M. Julve, F. Lloret, C. Mathoniere, J. Pasan, C. Ruiz-Perez, L. Canadillas-Delgado, R. Ruiz-Garcia, J. Cano, *Chem. Comm.* **2011**, *47*, 11035-11037.

[136] M. Castellano, R. Ruiz-García, J. Cano, J. Ferrando-Soria, E. Pardo, F. R. Fortea-Pérez, S.-E. Stiriba, M. Julve, F. Lloret, *Acc. Chem. Res.* **2015**, *48*, 510-520.

[137] H.-Z. Kou, G.-Y. An, C.-M. Ji, B.-W. Wang, A.-L. Cui, *Dalton Trans.* **2010**, *39*, 9604-9610.

[138] W.-J. Ma, Z.-Y. Gao, S. Zhu, B.-L. Wu, *Polyhedron* **2014**, *73*, 59-66.

[139] B. Viossat, N. Rodier, N.-H. Dung, O. Guillard, *Acta Crystallogr. Sect. C* **1986**, *42*, 659-662.

[140] A. Bacchi, M. Carcelli, O. Francescangeli, F. Neve, P. Pelagatti, C. Pelizzi, *Inorg. Chem. Commun.* **1999**, *2*, 255-257.

[141] *The Chemistry of amidines and imidates / edited by Saul Patai*, Wiley, London ; New York, **1975**, 85-155

[142] D. S. Bolotin, N. A. Bokach, V. Y. Kukushkin, *Coord. Chem. Rev.* **2016**, *313*, 62-93.

Chapitre 2: Les ligands AMOXs *N,N'*-disubstitués

2.1. Introduction

2.1.1. Plan du chapitre

Ce chapitre présente:

▪ la réponse à la question *Pourquoi les ligands AMOXs N,N'-disubstitués*? **(section 2.1.2)**

▪ un survol des stratégies synthétiques utilisées **(section 2.1.3)**

▪ les résultats obtenus pour la famille des hydroxyformamidines *N,N'*-disubstituées, qui ont été publiés dans l'article suivant:

Synlett, **2011**, 3, 405-409 – *Communication* **(section 2.2)**

2.1.2. Pourquoi les ligands AMOXs *N,N'*-disubstitués?

L'intérêt pour les ligands AMOXs *N,N'*-disubstitués découle de leurs propriétés (Figure 2.1-1). La même perspective de design du ligand comme '*une collection des composants modulables*'[1] sera utilisée pour mettre en évidence ces propriétés.

Les ligands AMOXs *N,N'*-disubstitués sont des ligands bidentates qui forment des cycles chélates à 5 atomes avec des ions métalliques. Du point de vue des atomes donneurs et des groupements fonctionnels des atomes donneurs, les AMOXs combinent le caractère donneur σ des atomes d'oxygène et d'azote, avec le caractère donneur π de l'atome d'oxygène et les propriétés d'accepteur π de la fonction amidine. Les ligands AMOXs présentent une délocalisation de la densité électronique dans le squelette ONCN. La modulation du degré de délocalisation électronique ainsi que la modulation de l'encombrement stérique sont possibles en modifiant le motif de substitution sur le ligand. Des substituants peuvent être introduits dans trois positions (les deux atomes d'azote et l'atome de carbone central) directement sur le squelette ONCN (positions de substitution 'primaires'). Des positions de substitution 'secondaires' peuvent également être identifiées (p ex. celles sur les substituants *N,N'*-

diaryles, *N,N'*-dialkyes ou *C*-aryles, *C*-alkyles). De plus, les AMOXs sont robustes et présentent des avantages pour la synthèse de leurs analogues substitués, par rapport aux ligands cycliques de type 8-hydroxyquinoline.

Figure 2.1-1. Pourquoi les ligands AMOXs?

Les ligands AMOXs *N,N'*-disubstitués présentent des '*composants modulables*' supplémentaires dans le 'tool-kit' du design: leurs propriétés acido-basiques riches (la basicité de l'atome N de l'oxime, la basicité du groupement OH et la basicité de l'atome N');[2] la tautomérie (hydroxyamidine *N,N'*-disubstituée / α-aminonitrone *N,N'*-disubstituée (amidine-*N*-oxyde *N,N'*-disubstituée)[2] (Figure 1.2-7), ainsi que la rotation limitée sur le groupement amidine résultant en isomères EE/EZ/ZE/ZZ).[3] De plus, les ligands AMOXs sont de très bons agents de chélation (ils ont été utilisés pour tracer des ions métalliques en chimie analytique). Il y a, donc, une opportunité de modulation directe de leur capacité de chélation pour des cibles spécifiques.

2.1.3. Les strategies synthétiques utilisées – survol

Les stratégies synthétiques utilisées pour obtenir les ligands AMOXs présentés dans ce travail sont montrées dans la Figure 2.1-2 (en haut).
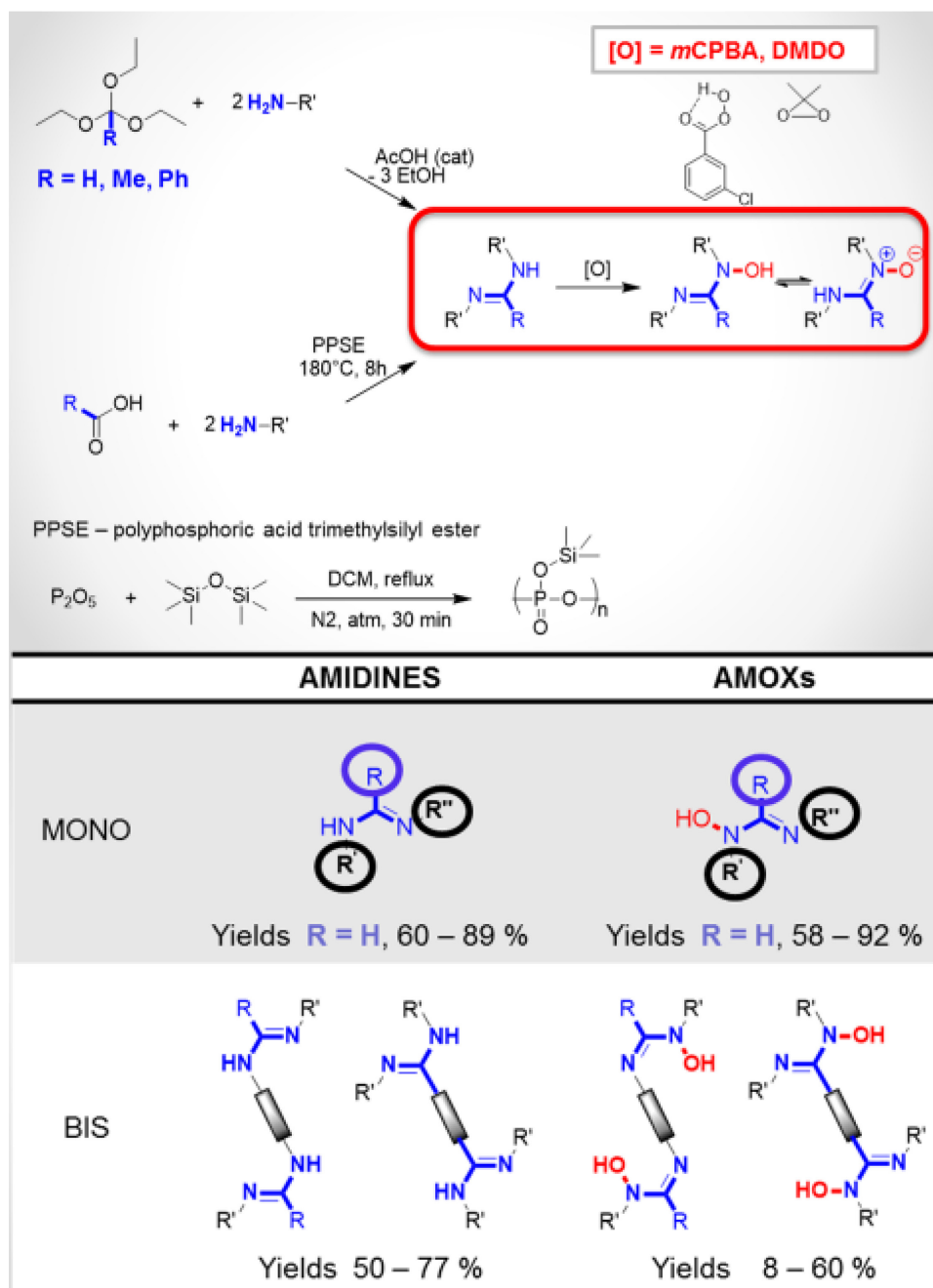
Figure 2.1-2. Les stratégies synthétiques (en haut) utilisées pour obtenir les ligands AMOXs (en bas)

La *N*-oxydation des amidines *N,N'*-disubstituées avec du *m*-CPBA[4] a été développée comme la méthode de choix pour la synthèse des AMOXs correspondants. Cette méthode a été intégrée avec différentes techniques de préparation des amidines parents (la condensation classique des orthoesters avec des amines (par distillation ou adaptée à l'activation par micro-ondes) et la condensation directe des acides carboxyliques (ou des amides) avec des amines en utilisant le 'polyphosphoric acid trimethyl ester' (PPSE)).[5] Ainsi, une 'stratégie synthétique' générale pour la préparation des ligands AMOXs a été établie. La méthode a été initialement utilisée pour la synthèse de mono-AMOXs, mais elle a été étendue avec succès pour la préparation des ligands bis-AMOXs pontés par les atomes d'azote et les ligands bis-AMOXs pontés par les atomes de carbone (Figure 2.1-2 (en bas)). Les ligands AMOXs pontés par les atomes d'azote et leurs précurseurs bis-amidines sont présentés dans la section 5.3.3 du chapitre 5, ainsi que leur chimie de coordination avec les ions de zinc(II).

Le problème majeur pour la réaction de *N*-oxydation des amidines avec du *m*-CPBA est la protonation du substrat par l'acide produit, avec la formation d'une paire d'ions très stable (Figure 2.1-3). Cela empêche qu'une conversion totale soit atteinte. En conséquence, l'efficacité de la méthode de *N*-oxydation est très dépendante du substrat. Les tentatives de *N*-oxydation des amidines portant des groupes alkyles comme substituants sur les atomes d'azote ont échoué, car ces substrats sont trop basiques et ils forment des sels de peracide en présence du *m*-CPBA. La méthode a été principalement utilisée pour la synthèse des AMOXs symétriques. Son applicataion pour la *N*-oxydation des amidines non-symétriques apporterai de l'information sur la sur la sélectivité de cette méthode. Le mécanisme proposé pour la réaction de *N*-oxydation des amidines avec du *m*-CPBA est illustré dans la Figure 2.1-4. Il a été adapté à partir du mécanisme d'époxydation des alcènes.[6]
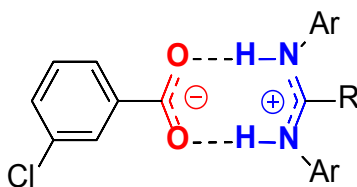
Figure 2.1-3. La voie d'inhibition proposé pour la réaction de *N*-oxydation des amidines avec du *m*-CPBA
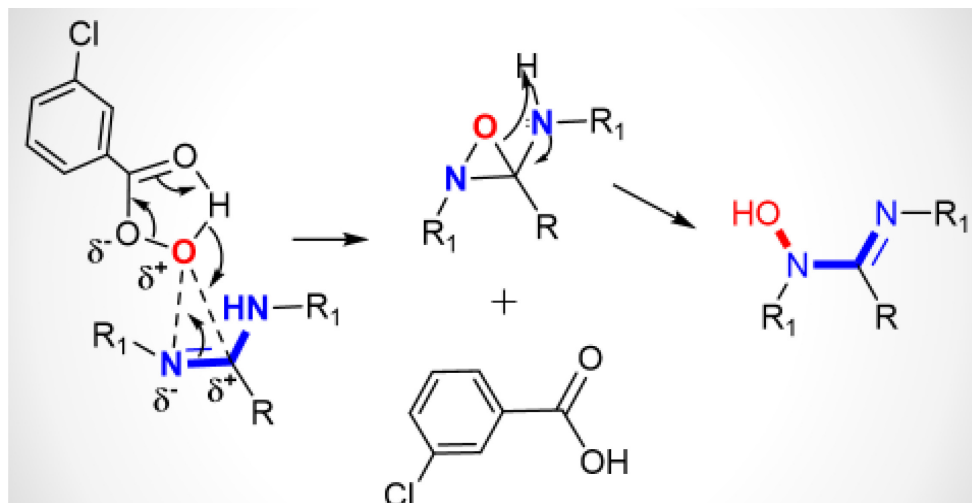
Figure 2.1-4. Le mécanisme proposé pour la *N*-oxydation des amidines avec du *m*-CPBA[6]

Il est important de préciser que l'objectif principal de cette thèse est l'étude de la chimie de coordination des AMOXs. La synthèse et la caractérisation des ligands AMOXs a été une partie importante du travail et des efforts ont été investis dans l'optimisation des protocoles de synthèse. Par contre, une investigation complète des ligands (la clarification des processus de tautoméries, des processus d'isomérisation, des mécanismes de réaction, etc.) a été considérée d'une importance secondaire pour ce projet. Plusieurs rapports sur ces sujets existent dans la littérature, en particulier pour les amidoximes,[3] mais ces thèmes de recherche ne sont pas complètement clarifiés dans le cas des ligands AMOXs *N,N'*-disubstitués. Par conséquent, il serait intéressant d'éventuellement les poursuivre comme futurs développements du projet.

2.1.4. References

[1]   T. J. Collins, *Acc. Chem. Res.* **1994**, *27*, 279-285.
[2]   *The Chemistry of amidines and imidates / edited by Saul Patai*, Wiley, London ; New York, **1975**, 85-155
[3]   D. S. Bolotin, N. A. Bokach, V. Y. Kukushkin, *Coord. Chem. Rev.* **2016**, *313*, 62-93.
[4]   a) E. Baranowska, I. Panfil, C. Belzecki, *Bull. Acad. Pol. Sci., Ser. Sci. Chim.* **1977**, *25*, 93-99; b) C. Belzecki, I. Panfil, *Bull. Acad. Pol. Sci., Ser. Sci. Chim.* **1975**, *23*, 119-123.
[5]   a) M. Kakimoto, S. Ogata, A. Mochizuki, Y. Imai, *Chem. Lett.* **1984**, 821-824; b) S. Ogata, A. Mochizuki, M. Kakimoto, Y. Imai, *Bull. Chem. Soc. Jpn.* **1986**, *59*, 2171-2177.
[6]   P. D. Bartlett, *Rec. Chem. Prog.,* **1950**, 11 47.

2.2. Facile Synthesis of Hydroxyformamidines by the N-Oxidation of Their Corresponding Formamidines

2.2.1. Résumé

La *N*-oxydation des amidines *N,N'*-disubstituées avec *m*-CPBA (acide *meta*-chloroperoxybenzoïque) représente une voie douce, rapide et efficace vers les hydroxyamidines correspondantes. Cette voie synthétique nouvelle pour la préparation des hydroxyamidines *N,N'*-disubstituées offre une alternative attrayante versus la voie classique. Il a été trouvé que l'efficacité de la réaction de *N*-oxydation et la stabilité des hydroxyformamidines sont influencées par le mode de substitution des groupements *N,N'*-diaryles: des rendements plus élevés (jusqu'à 92%) et des produits plus stables sont obtenus pour les composés ayant des groupements phényles 2,6-disubstitués. Les techniques spectroscopiques de RMN ^{1}H et ^{13}C, la spectrométrie de masse haute résolution et/ ou l'analyse élémentaire ont été utilisées pour caractériser les produits.

Contribution:

Mihaela Cibian: synthèses optimisées et caractérisation de quatorze composés, rédaction de l'article

Sophie Langis-Barsetti: synthèse et caractérisation de quatre composés

Garry S. Hanan: supervision, révision de l'article

Facile Synthesis of Hydroxyformamidines by the N-Oxidation of Their Corresponding Formamidines

Mihaela Cibian, Sophie Langis-Barsetti, Garry S. Hanan*

Département of Chemistry, Université de Montréal, Montréal, Québec, H3T-1J4, Canada

*: E-mail: garry.hanan@umontreal.ca. Fax: 1-514-343-2468

2.2.2. Table of Content Graphic

2.2.3. Abstract

The *N*-oxidation of *N,N'*-disubstituted amidines with *m*-CPBA (*meta*-chloroperoxibenzoic acid) affords a mild, rapid and efficient route to the corresponding hydroxyamidines. This novel synthetic route for the preparation of *N,N'*-disubstituted hydroxyamidines provides an attractive alternative to the classical one. It was found that the efficiency of the *N*-oxidation reaction and the stability of the hydroxyformamidines are influenced by the substitution on the *N,N'*-diaryl rings, e.g., higher yields (up to 92%) and more stable products are obtained for the compounds bearing substituents in the 2,6-positions of the phenyl rings. ^{1}H NMR and ^{13}C NMR, HRMS and/ or elemental analysis were used to characterize the products.

2.2.4. Introduction

N,N'-Disubstituted hydroxyamidines/ amidoximes have been studied for their biological activity (antituberculars, hypotensives) and their pharmacological properties (bactericidal, fungicidal, local anaesthetics)[1] and also as precursors in the synthesis of cyclic compounds.[2] Their propensity to form stable five-membered chelate rings with metal ions was exploited for tracing metals in analytical chemistry.[3]
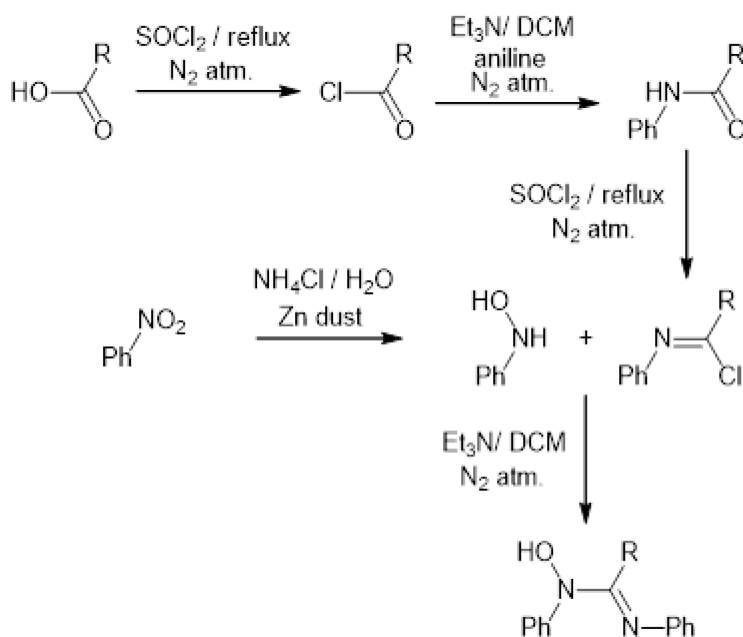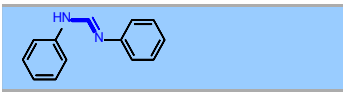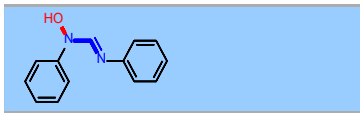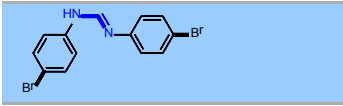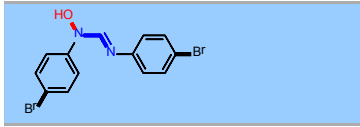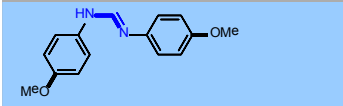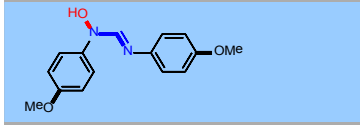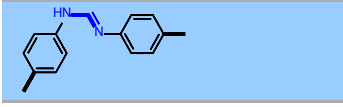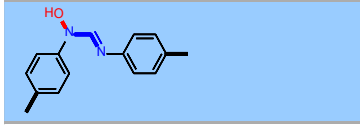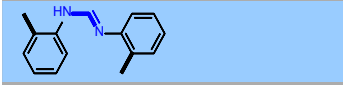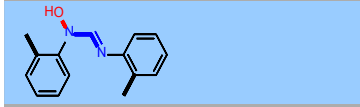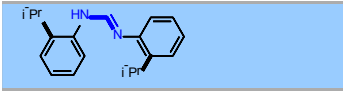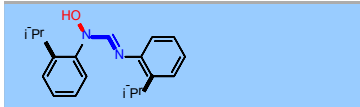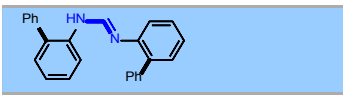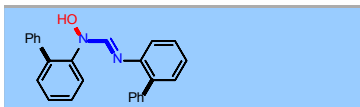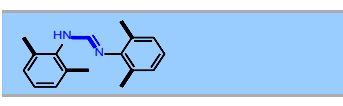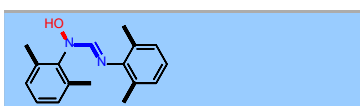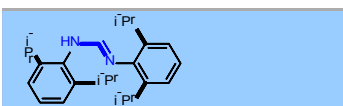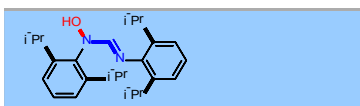
Scheme 2.2-1. Synthesis of hydroxyamidines *via* a classic route.[5]

They also show good electronic delocalization through the ligand backbone and have interesting design possibilities as far as multiple functionalization is concerned. Due to these properties, the *N,N'*-disubstituted hydroxyamidines/ amidoximes and their mononuclear complexes are interesting candidates for incorporation into supramolecular assemblies based on coordination chemistry and hydrogen bonding. They could also present potential applications in catalysis, as recently many catalysts containing *N,O*-bidentate ligands have been developed.[4] Surprisingly none of these aspects of their chemistry have received much attention in the literature. In this context, our main objective is to synthesize and characterize *N,N'*-diaryl-*N*-hydroxyamidine ligands and their different metal complexes, in order to study their properties and their possible applications in the above-mentioned fields. We have developed and optimized a new route for the synthesis of the hydroxyamidines – the *N*-oxidation of the parent amidines with *m*-CPBA – as a more efficient alternative to the classical one (Scheme 2.2-1). We report herein the results obtained using different functionalized formamidines **2a-i** as substrates (Scheme 2.2-2).
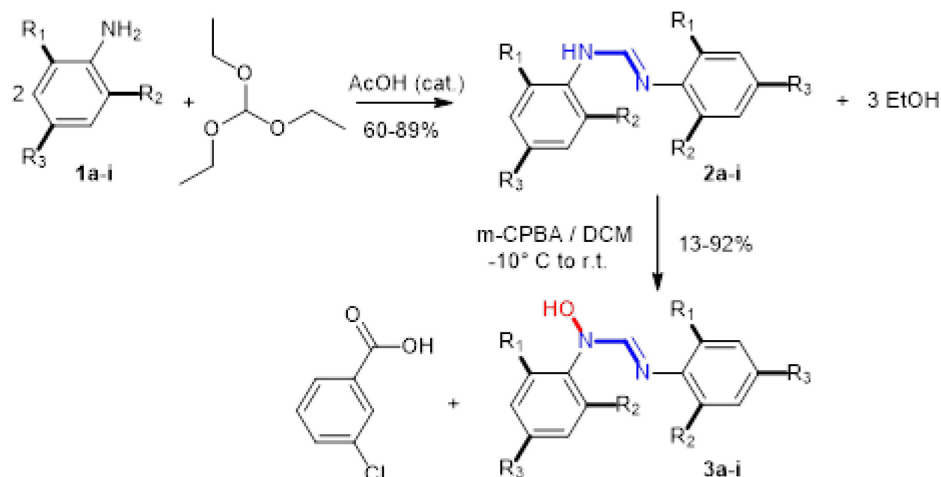
Scheme 2.2-2 The two-step synthesis of hydroxyformamidines: step 1: synthesis of the formamidines **2a-i** from a mixture of **1a-i** and triethylorthoformate (2:1) with AcOH (cat.); step 2: synthesis of **3a-i** *via* the *N*-oxidation of formamidines **2a-i** with *m*-CPBA. **(a)** R₁=R₂=R₃=H; **(b)** R₁=R₂=H, R₃=Br; **(c)** R₁=R₂=H, R₃=OMe; **(d)** R₁=R₂=H, R₃=Me; **(e)** R₁=Me, R₂=R₃=H; **(f)** R₁=iPr, R₂=R₃=H; **(g)** R₁=Ph, R₂=R₃=H; **(h)** R₁=R₂=Me, R₃=H; **(i)** R₁=R₂=iPr, R₃=H.

Table 2.2-1. Specific conditions and yields for the synthesis of the formamidines **2a-i** and hydroxyamidines **3a-i**

Cpd.	Formamidines **2**	Yield[a,b,c] , %	Hydroxyformamidines **3**	Yield[i] , %
a		81 (85)		20
b		82 (-)		13
c		80 (-)		15
d		89 (-)		22
e		85[d] (80)		41[j]
f		78 (66)		59[k]
g		85[e] (81)		58[k]
h		85[f](60[g])		92[l]
i		66[h] (75)		88[l]

[a] Isolated yields.
[b] Yield obtained by microwave (MW) irradiation (method B), using the general procedure[6], unless otherwise mentioned.

[c] Yields in brackets obtained using the general procedure (method A),[7-8] unless otherwise mentioned.
[d] Modified reaction time (30 minutes).
[e] Modified reaction time and temperature (140-160 °C, 15 min).
[f] Modified reaction time and temperature (140 °C, 1 hour).
[g] Modified reaction time (1 hour)
[h] Modified reaction time and temperature (140 °C, 2 hours).
[i] Yields obtained by the general method,[9] unless otherwise mentioned.
[j] Modified reaction temperature (-10°C to r.t) and diisopropylethylamine used instead of NaHCO$_3$
[k] Modified reaction temperature (-10°C to r.t).[10-11]
[l] Modified reaction time (15-30 min) and no NaHCO$_3$ used.[12-13]

2.2.5. Results and discussion

Generally, hydroxyamidines are prepared from the corresponding carboxylic acids, aniline and hydroxyaniline, by the multi-step procedure showed in Scheme 2.2-1.[5] Most of the steps are performed under an inert atmosphere and are relatively time-consuming. Also, the synthesis of hydroxyanilines can be considered as the limiting step due to their instability, leading to low overall yields. Besides offering an alternative to their difficult classical synthesis, the new two-step preparation method for hydroxyamidines (Scheme 2.2-2) presents added advantages: rapidity, ease of manipulations and improved overall efficiency. It also avoids the use of chlorination agents (SOCl$_2$ or PCl$_5$), which are toxic and corrosive. The idea of preparing the amidines first is part of our synthetic strategy, which takes advantage of their facile synthesis,[14] and at the same time, eliminates the use of hydroxyanilines. The proposed procedure can be applied to different amidine substrates (different substitution on the central carbon: formamidines, acetamidines, benzamidines and/ or different substitution on the *N,N'*-diaryl rings). The specific reaction conditions and yields are reported in Table 2.2-1.

The synthesis of the parent formamidines (**2a-i**) (Scheme 2.2-2 – step 1) was done in one-step using commercially available starting materials. The first procedure (method A)[7] employed the classical distillation of ethanol from a mixture of aniline, triethylorthoformate (2:1) and a catalytic amount of glacial acetic acid.[14] The second procedure was a modified microwave reaction (MW) (method B)[6] of the same mixture of compounds.[15] Molecular sieves (4Å) were used in this second case to displace the equilibrium to the products by

removing the resulting ethanol. Both procedures give good yields (60 – 89%) (Table 2.2-1), but the MW reactions proved to be particularly easy to set-up and manipulate, as well as very fast and more efficient. In most cases the reaction times for MW reactions are 10-30 minutes (1 h and 2 h for the more bulky compounds **2h** and **2i,** respectively) *vs.* a few hours to overnight for distillations. Also, similar or better yields are generally obtained by MW reactions *vs.* distillation. The only exception is the compound **2i** (R1=R2=iPr and R3=H), the bulkiest in the series, which requires a longer reaction time due to steric hindrance caused by the *ortho* substituents.

The synthesis of the hydroxyformamidines (**3a-i**) by the *N*-oxidation of the corresponding amidines is a mild, rapid and fairly efficient procedure. The limit of this approach is the ease with which the amidine is protonated by the *m*-chlorobenzoic acid produced during the reaction. An ion pair is formed and stabilized through H bonding.[16] Several approaches were tried in order to overcome this issue. The most successful ones proved to be: i) the use of the amidine as its own base, ii) the use of other organic bases (e.g. diisopropylethylamine), and iii) the addition of $NaHCO_3$ at the beginning of the reaction. The use of stronger inorganic bases was limited by their poor solubility in DCM. Biphasic reactions were also tried when using inorganic bases, but the overall yield wasn't improved as the stability of formamidines substrates and hydroxyformamidines products toward nucleophilic attack on the central carbon started to play an important role, which resulted in the formation of the corresponding amide as a side-product. The *N*-oxidation reaction of amidines with *m*-CPBA may undergo a similar mechanism as epoxidation[17], with the formation of an intermediate of oxaziridine ring type, which could also explain the formation of arylamides as a side-product of the reaction.[18]

The efficiency of the *N*-oxidation reaction is influenced by the substitution on the *N,N'*-aryl rings. The substrates with electron-donating bis-*o*-substituents (**3h-i**) give good yields (88-92%), while moderate yields (41-59%) are obtained for the compounds bearing electron-donating mono-*o*-substituants (**3e-g**). The absence of *o*-substitution (**3a-d**) results in poor yields (13-22%), as the compounds also decompose during purification.[19] As the yields were calculated for the isolated products, the effect of *o*-substitution on the efficiency of the reaction could be explained by the higher stability of the *o*-substituted compounds, as the

central carbon is best protected on steric grounds.[20] Electron-donating *o*-substituents also increase the basicity of the imido-nitrogen, which has the determining role in driving the *N*-oxidation reaction by electronic considerations. For the very bulky *o*-substituted substrates, steric hindrance starts to have an influence on the *N*-oxidation reaction as well (**3i** *vs.* **3h**).

The newly synthesized hydroxyformamidines were characterized by ^{1}H NMR and ^{13}C NMR, HRMS and/ or elemental analysis (SI). A common feature in the ^{1}H-NMR of the hydroxyamidines *vs.* their corresponding amidines is the splitting of the signals due to the asymmetry introduced in the molecule by the presence of the hydroxyl group (Figure S2; Appendix-2.2-SI).

2.2.6. Conclusion

In conclusion the *N*-oxidation of amidines with *m*-CPBA is a straightforward method for synthesizing their corresponding hydroxyamidines. This method was successfully used with different functionalized formamidines, the *ortho*-substituted ones giving the best results. *N*-Oxidation with *m*-CPBA of functionalized acetamidines and benzamidines substrates is currently under investigation, as well as the application of the method to aliphatic and unsymmetrical formamidines.

2.2.7. Experimental Section

Full experimental details are given as Supplementary Information (SI) – Appendix-2.2.-SI. Partial experimental information can be found in section 2.2.10. References and Notes (as they appeared in the article.)

2.2.8. Acknowledgements

2.2.9. Supporting Information

Supporting Information for this article is available online at http://www.thieme-connect.de/ejournals/toc/synlett. In this thesis, the same material is found in Appendix-2.2-SI.

2.2.10. References and Notes

[1]   (a) Srivastava, R. M.; Brinn, I. M.; Machuca-Herrera, J. O.; Faria, H. B.; Carpenter, G. B.; Andrade, D.; Venkatesh, C. G.; de Morais, L. P. F. *J. Mol. Struct.* **1997,** *406*, 159. (b) Clement, B. *Drug Metab. Rev.* **2002,** *34*, 565.

[2]   (a) Durust, N.; Akay, M. A.; Durust, Y.; Kilic, E. *Anal. Sci.* **2000,** *16*, 825. (b) Dueruest, Y.; Akcan, M.; Martiskainen, O.; Siirola, E.; Pihlaja, K. *Polyhedron* **2008,** *27*, 999.

[3]   (a) Kharsan, R. S.; Mishra, R. K. *Bull. Chem. Soc. Jpn.* **1980,** *53*, 1736. (b) Kharsan, R. S.; Patel, K. S.; Mishra, R. K. *Indian J. Chem., Sect. A* **1980,** *19A*, 499. (c) Agarwal, C.; Patel, K. S.; Mishra, R. K. *Asian Environ.* **1990,** *12*, 29. (d) Deb, M. K.; Mishra, N.; Patel, K. S.; Mishra, R. K. *Analyst* **1991,** 116, 323.

[4]   (a) Desjardins, S. Y.; Cavell, K. J.; Jin, H.; Skelton, B. W.; White, A. H. *J. Organomet. Chem.* **1996,** *515*, 233. (b) Lee, A. V.; Schafer, L. L. *Eur. J. Inorg. Chem.* **2007**, *16*, 2243. (c) Batten, M. P.; Canty, A. J.; Cavell, K. J.; Ruether, T.; Skelton, B. W.; White, A. H. *Inorg. Chim. Acta* **2006,** *359*, 1710. (d) John, A.; Katiyar, V.; Pang, K.; Shaikh, M. M.; Nanavati, H.; Ghosh, P. *Polyhedron* **2007,** *26*, 4033. (e) Ding, F.; Sun, Y.; Monsaert, S.; Drozdzak, R.; Dragutan, I.; Dragutan, V.; Verpoort, F. *Curr. Org. Synth.* **2008,** *5*, 291. (f) Ledoux, N.; Allaert, B.; Schaubroeck, D.; Monsaert, S.; Drozdzak, R.; Van Der Voort, P.; Verpoort, F. *J. Organomet. Chem.* **2006,** *691*, 5482.

[5]   (a) Briggs, L. H.; Cambie, R. C.; Dean, I. C.; Rutledge, P. S. *Aust. J. Chem.* **1976,** *29*, 357. (b) Krajete, A.; Steiner, G.; Kopacka, H.; Ongania, K.-H.; Wurst, K.; Kristen, M. O.; Preishuber-Pfluegl, P.; Bildstein, B. *Eur. J. Inorg. Chem.* **2004**, *8*, 1740. (c) Tian, L.; Xu, G.-Y.; Ye, Y.; Liu, L.-Z. *Synthesis* **2003**, *9*, 1329. (d) Kamm, O.; Marvel, C. S. *Org. Synth.*, **1941**, *1*, 445

[6]   **General Procedure**[14] – **Method A:** The ethanol was distilled from a mixture of aniline, triethylorthoformate (2:1), and a catalytic amount of glacial acetic acid at 120-160 °C. The reactions times ranges form 1h (**2h**) to overnight. Solids were formed which where further purified as described in reference 7.

[7]   **General Procedure**[15] – **Method B**: A mixture of aniline, triethylorthoformate (2:1), and a catalytic amount of glacial acetic acid (molecular sieves 4 Å were also added) was microwave activated at 130 °C for 10 minutes. At the end of the reactions, oily solids were obtained, which were taken in DCM (**2a-e** and **2g-i**) or hexane (**2f**). The solvents were evaporated under vacuum to afford solids or oils that were further purified by recrystallization in DCM/ hexane (1:1) (**2a-e** and **2g**), boiling hexane (**2f, 2i**) or by trituration/ sonication with hexane (**2h**). Colourless solids were obtained in all cases.[8]

[8]   Except for compound **2f**, all of the formamidines are known compounds, and their characterization is similar to reported data.[14]
       2f: Compound **1f** (7.5 ml, 51 mmol, 2 eq.), triethylorthoformate (4.0 ml, 25 mmol, 1 eq.) and a catalytic amount of glacial acetic acid (0.30 ml, 5.1 mmol, 0.2 eq.) were reacted following the general procedure described in reference 7. After purification by

trituration with cold pentane and recrystallization in hot hexane, colorless crystals were obtained. Yield = 5.56 g, 78%. ^{1}H-NMR (CDCl$_3$, 300 MHz) δ, ppm: 8.00 (s, 1H, -NH-C**H**=N-), 7.29 (d, J^d = 8 Hz, 2H, -C$_6$**H**$_4$), 7.20-7.08 (m, 4H, -C$_6$**H**$_4$), 7.02 (d, J^d = 8 Hz, 2H, -C$_6$**H**$_4$), 3.29 (sept, J^{sept} = 7 Hz, 2H, –C**H**(CH$_3$)$_2$), 1.26 (d, J^d = 7 Hz, 12H, -CH(C**H**$_3$)$_2$). ^{13}C-NMR (CDCl3, 75 MHz) δ, ppm: 148.6, 139.5, 126.7, 125.9, 124.0, 118.7, 27.73, 23.21. Elemental Analysis: *calc.* (%) for C$_{19}$H$_{24}$N$_2$: C 81.38, H 8.63, N 9.99; *found*: C 81.62, H 9.27, N 10.17.

[9] **General Procedure – *N*-oxidation of amidines with *m*-CPBA:** A solution of *m*-CPBA (1eq.) in DCM was added drop wise by addition funnel to a solution of amidine (1 eq.) and NaHCO$_3$ (1.0-1.5 eq.) in the same solvent, at 0 °C (ice bath) to room temperature. The reaction mixture was stirred for other 30 to 60 minutes at room temperature and was washed with an aqueous solution of K$_2$CO$_3$ (5%) (2 *x* 25 mL). The combined organic fractions were dried over anhydrous MgSO$_4$ or Na$_2$SO$_4$ and filtered. The solvent was removed by evaporation, to afford solids or oils that were further purified by recrystallization or flash chromatography on silica.

[10] **Compound 3f:** Compound **2f** (2.0 g, 7.1 mmol, 1 eq.) and NaHCO$_3$ (0.61 g, 7.1 mmol, 1 eq.) in DCM (50 mL) and *m*-CPBA (1.6 g, 7.1 mmol, 1 eq.) in DCM (50 mL) were reacted following the general procedure described in reference 9, and modified as specified in Table 1 footnote k. After purification by flash chromatography on silica (gradient of eluants: hexane/ AcOEt (2:8), AcOEt/ MeOH (9:1), DCM 100%) and recrystallization in hot hexane, a colorless solid was obtained. Yield = 0.92 g, 58%. ^{1}H-NMR (CDCl$_3$, 300 MHz) δ, ppm: 7.93 (s, 1H, -NH-C**H**=N-), 7.45-7.39 (m, 2H, -C$_6$**H**$_4$), 7.34-7.31 (m, 2H, -C$_6$**H**$_4$), 7.28-7.08 (m, 3H, -C$_6$**H**$_4$), 6.96 (d, J^d = 8 Hz, 1H, -C$_6$**H**$_4$), 3.67 (bs, O**H**), 3.40 (sept, J^{sept} = 7 Hz, 1H, -C**H**(CH$_3$)$_2$), 3.27 (sept, J^{sept} = 7 Hz, 1H, -C**H**(CH$_3$)$_2$), 1.33-1.29 (m, 12H, -CH(C**H**$_3$)$_2$). ^{13}C-NMR (CDCl3, 75 MHz) δ, ppm: 145.0, 142.1, 137.4, 136.2, 135.4, 130.1, 127.1, 127.0, 126.7, 126.6, 125.5, 124.3, 116.2, 28.12, 27.61, 24.27 (2C), 23.08 (2C). MS (ESI-HRMS DCM) (m/z): [M+H]$^+$ C$_{19}$H$_{25}$N$_2$O: *calc.* 297.1961; *found* 297.1971. Elemental Analysis: *calc.* (%) for C$_{19}$H$_{24}$N$_2$O: C 76.99, H 8.16, N 9.45; *found*: C 76.80, H 8.23, N 9.40.

[11] **Compound 3g:** Compound **2g** (1.5 g, 4.3 mmol, 1 eq.) and NaHCO$_3$ (0.38 g, 4.3 mmol, 1 eq.) in DCM (50 mL) and *m*-CPBA (0.96 g, 4.3 mmol, 1 eq.) in DCM (50 mL) were reacted following the general procedure described in reference 9, and modified as specified in Table 1 footnote k. After purification by flash chromatography on silica (gradient of eluants: hexane/ AcOEt (2:8), AcOEt/ MeOH (9:1), DCM 100%) and recrystallization in DCM/ hexane (1:1), a colorless solid was obtained. Yield = 0.93 g, 59%. ^{1}H-NMR (CDCl$_3$, 400 MHz) δ, ppm: δ 7.85 – 7.78 (m, 1H, -C$_6$**H**$_4$), 7.55 – 7.32 (m, 14H, -C$_6$**H**$_5$, -C$_6$**H**$_4$ and -NH-C**H**=N-), 7.21 (dd, J = 7, 2 Hz, 1H, -C$_6$**H**$_4$), 7.11 (td, J = 8, 2 Hz, 1H, -C$_6$**H**$_4$), 7.05 (td, J = 7, 1 Hz, 1H, -C$_6$**H**$_4$), 6.17 (d, J = 8 Hz, 1H, -C$_6$**H**$_4$), 3.67 (bs, O**H**). ^{13}C-NMR (CDCl3, 75 MHz) δ, ppm: 142.0, 138.2, 137.5, 136.9, 135.7, 135.2, 131.7, 131.40, 130.7, 129.4 (2C), 129.24 (2C), 129.19 (2C), 129.1 (2C), 128.8, 128.6, 128.5 (2C), 128.3, 128.1, 126.1, 123.7, 115.4. MS (ESI-HRMS DCM) (m/z): [M+H]$^+$ C$_{25}$H$_{21}$N$_2$O: *calc.* 365.1648; *found* 365.1655 Elemental Analysis: *calc.* (%) for C$_{25}$H$_{20}$N$_2$O: C 82.39, H 5.53, N 7.69; *found*: C 82.33, H 5.52, N 7.73.

[12] **Compound 3h:** Compound **2h** (1.0 g, 4.0 mmol, 1 eq.) in DCM (20 mL) and *m*-CPBA (0.89 g, 4.0 mmol, 1 eq.) in DCM (20 mL) were reacted following the general procedure described in reference 9, and modified as specified in Table 1 footnote l. After

recrystallization in DCM/ hexane (1:1) at -10 °C, a colorless solid was obtained. Yield = 0.98 g, 92%. ^{1}H-NMR (CDCl$_3$, 400 MHz) δ 7.34 (s, 1H, -NH-C$\boldsymbol{H}$=N-), 7.20 (t, J^t = 8 Hz, 1H, -C$_6\boldsymbol{H}_3$), 7.15-7.06 (m, 5H, -C$_6\boldsymbol{H}_3$), 3.51 (bs, O$\boldsymbol{H}$), 2.38 (d, J^d = 3 Hz, 12H, -C$\boldsymbol{H}_3$). ^{13}C-NMR (CDCl3, 75 MHz) δ, ppm: 142.1, 140.4, 135.8, 134.8 (2C), 133.4, 129.3, 129.0 (2C), 128.6 (2C), 126.7, 18.81 (2C), 17.26 (2C). MS (ESI - DCM) (m/z): 269.2 [M+H]$^+$ (100%). Elemental Analysis: *calc.* (%) for (C$_{17}$H$_{20}$N$_2$O)$_2$CH$_2$Cl$_2$: C 67.62, H 6.81, N 9.01; *found*: C 68.19, H 6.81, N 9.00.

[13] **Compound 3i:** Compound **2i** (1.5 g, 4.1 mmol, 1eq.) in DCM (10 mL) and *m*-CPBA (0.9 g, 4.1 mmol) in DCM (40 mL) were reacted following the general procedure described in reference 9, and modified as specified in Table 1 footnote l. The green-white solid obtained after solvent evaporation was taken in EtOH, as the formamidine **2i** has low solubility in this solvent. After filtration, EtOH evaporation, and drying under vacuum, a pale-yellow solid was obtained. Yield = 1.4 g, 88%. m.p. 165-167 °C. ^{1}H-NMR (CDCl$_3$, 300 MHz) δ, ppm: 7.39 – 7.32 (m, 1H, C$_6\boldsymbol{H}_3$), 7.32 – 7.26 (m, 1H, C$_6\boldsymbol{H}_3$), 7.25 – 7.21 (m, 2H, C$_6\boldsymbol{H}_3$ and -NH-C$\boldsymbol{H}$=N-), 7.20 (d, J^d = 2 Hz, 2H, C$_6\boldsymbol{H}_3$), 7.18 (d, J^d = 1 Hz, 1H, C$_6\boldsymbol{H}_3$), 3.37 (sept, J^{sept} = 7 Hz, 2H, –C$\boldsymbol{H}$(CH$_3$)$_2$), 3.25 (sept, J^{sept} = 7 Hz, 2H, –C$\boldsymbol{H}$(CH$_3$)$_2$), 1.37 (d, J^d = 7 Hz, 6H, -CH(C$\boldsymbol{H}_3$)$_2$), 1.23 (d, J^d = 7 Hz, 12H, -CH(C$\boldsymbol{H}_3$)$_2$), 1.18 (d, J^d = 7 Hz, 6H, -CH(C$\boldsymbol{H}_3$)$_2$). ^{13}C-NMR (CDCl3, 75 MHz) δ, ppm: 146.6 (2C), 146.0 (2C), 141.7, 133.2, 132.5, 130.6, 128.8 (2C), 124.8 (2C), 124.7 (2C), 29.28 (2C) 29.10 (2C), 25.98 (2C), 25.05 (2C), 24.87 (4C). MS (ESI - DCM) (m/z): 381.3 [M+H]$^+$ (100%). Elemental Analysis: *calc.* (%) for C$_{25}$H$_{36}$N$_2$O: C 78.90, H 9.53, N 7.36; *found*: C 78.79, H 9.43, N 7.21.

[14] (a) Hirano, K.; Urban, S.; Wang, C.; Glorius, F. *Org. Lett.* **2009,** *11*, 1019. (b) Krahulic, K. E.; Enright, G. D.; Parvez, M.; Roesler, R. *J. Am. Chem. Soc.* **2005,** *127*, 4142. (c) Roberts, R. M. *J. Org. Chem.* **1949,** *14*, 277. (d) Cole, M. L.; Deacon, G. B.; Forsyth, C. M.; Konstas, K.; Junk, P. C. *Dalton Trans.* **2006**, *27*, 3360 (e) Cole, M. L.; Junk, P. C.; Louis, L. M. *Dalton Trans.* **2002,** *20*, 3906.

[15] Harding, P.; Harding, D. J.; Adams, H.; Youngme, S. *Synth. Commun.* **2007,** *37*, 2655.

[16] Kraft, A.; Peters, L.; Powell, H. R. *Tetrahedron* **2002,** *58*, 3499.

[17] Bartlett, P. D. *Record Chem. Progress* **1950,** *11*, 47.

[18] Srivastava, R.; Pereira, M.; Faustino, W.; Coutinho, K.; dos Anjos, J.; de Melo, S. *Monatshefte für Chemie / Chemical Monthly* **2009,** *140*, 1319.

[19] For **3a-d** pure products are obtained only by recrystallization as decomposition on silica column occurs. Attempts to maximize the yield by repeated evaporations-recrystallizations were unsuccessful, as the decomposition product (amide) starts to be observed after 1-2 cycles.

[20] Also observed by ^{1}H NMR, as the shielding of formamidine H decreases in the series **3i**, **3h**, **3g**, **3f**, **3e**, **3c**, **3d**, **3b**, **3a** (see Figure S1, Appendix-2.2-SI).

Chapitre 3: Des complexes de cobalt(II) avec des ligands encombrés *N,N'*-diaryle-formamidinate-*N*-oxydes

3.1. Plan du chapitre

Ce chapitre présente les résultats obtenus pour les complexes de cobalt(II) avec des ligands encombrés *N,N'*-diarylformamidinate-*N*-oxydes. Ces résultats ont été publiés dans les articles suivants:

- *Dalton Trans.*, **2011**, *40,* 1038-1040 – *Communication* (**section 3.2**)

- *Eur. J. Inorg. Chem*, **2015**, 73-82 – *Full Paper* (**section 3.3**).

3.2. Synthesis and Crystal Structure of a Rare Square-Planar Cobalt(II) Complex of a Hydroxyamidinate Ligand

3.2.1. Résumé

Des nouveaux complexes de cobalt(II) avec des ligands formamidinate *N*-oxydes sont présentés, ainsi que leurs propriétés électrochimiques et spectroscopiques. Une coordination plan-carré existe autour du centre métallique, ce qui est assez rare pour un ion cobalt(II) d^7. Cela a été confirmé par oxydation chimique à l'espèce cobalt(III). Le complexe de cobalt(II) est difficile à réduire, mais son oxydation facile le suggère comme potentiel donneur d'électrons dans des réactions photo-redox.

Contribution:

Mihaela Cibian: synthèse et caractérisation totale du ligand, synthèse des complexes et leurs caractérisations partielles, rédaction finale de l'article

Sofia Derossi: caractérisation partielle des complexes, structures cristallines des complexes, mesure de la constate d'association et expériences d'oxydation chimique, rédaction partielle

Garry S. Hanan: supervision, révision de l'article

Synthesis and Crystal Structure of a Rare Square-Planar Co(II) Complex of a Hydroxyamidinate Ligand

Mihaela Cibian, Sofia Derossi, and Garry S. Hanan*

Département of Chemistry, Université de Montréal, Montréal, Québec, H3T-1J4, Canada

*: E-mail: garry.hanan@umontreal.ca. Fax: 1-514-343-7056

3.2.2. Table of content graphic
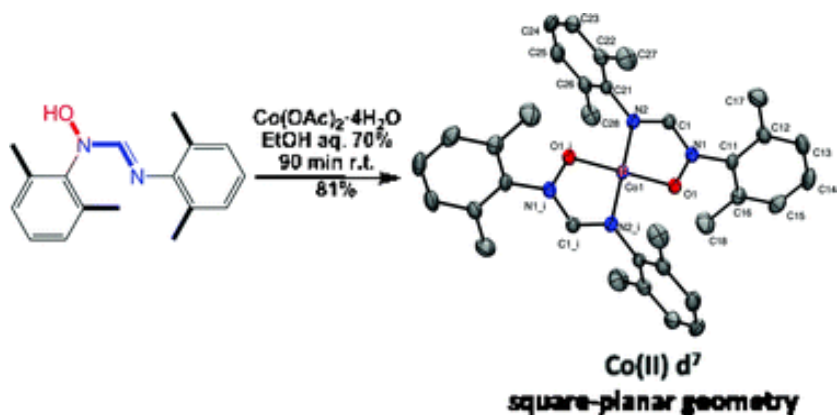
3.2.3. Abstract

Novel hydroxyamidinate complexes of cobalt(II) are presented, together with their electrochemical and spectroscopic properties. An unusual d^7 square-planar coordination around the cobalt(II) center exists and was confirmed by chemical oxidation to its cobalt(III) species. The cobalt(II) complex is difficult to reduce, but its facile oxidation suggests that it may be useful as an electron donor in photoredox reactions.

3.2.4. Introduction

N-Hydroxyamidines are excellent bidentate ligands that form stable 5-membered rings with metal ions. Their transition-metal complexes have found intensive application as antifungal drugs as well as sequestrating agents.[1,2] They also present various positions for functionalization, *e.g.*, different substituents on the central carbon: formamidines, acetamidines, benzamidines; and different substituents on the amidine nitrogens. Thus, the electronic and steric properties of the ligands can be fine-tuned, which in turn allows their complexes to be fine-tuned as well. In spite of these advantages, their use in coordination and supramolecular chemistry or catalysis has so far received little attention.[3,4] This is surprising, considering the versatility and robustness offered by these ligands and their complexes. Therefore, our research focuses on the synthesis and characterization of *N,N'*-diaryl-*N*-hydroxyamidine ligands and their different metal complexes, in order to study their properties and their possible applications in the above-mentioned fields.

In this work, we present the ligand *N*-hydroxy-*N,N'*-bis(2,6-dimethylphenyl)-formamidine, **2** and its homoleptic Co(II) complex, compound **3**, as the result of preliminary studies of a new family of cobalt complexes based on the hydroxyamidine motif (Scheme 3.2-1). The choice of metal ion is in line with general research efforts to find alternatives to the noble metals in photocatalysis. At the same time, Co(II) complexes are currently in the limelight, due to their potential applications in fuel cells (where inexpensive metals are required, which combine good reducing properties and thermal stability) and as redox mediators in dye-sensitized solar cells (DSSC).[5,6]

3.2.5. Results and Discussion

3.2.5.1. Synthesis

The *N*-hydroxy-*N,N'*-bis(2,6-dimethylphenyl)formamidine ligand was prepared by a facile synthetic method in which the amidine precursor **1** is first isolated and subsequently *N*-oxidized with *m*-CPBA (*meta*-chloroperoxybenzoic acid) to give ligand **2** in 92% yield (Scheme 3.2-1).[7] Complex **3** was easily obtained upon mixing 2 equivalents of **2** with Co(II) acetate in aqueous ethanol, at room temperature. Immediate formation of a pale green precipitate was observed, and the product was isolated in good yield (81%) as a pale-green powder (Scheme 3.2.-1). Complex **3** has been characterized by different spectroscopic techniques, high resolution mass spectrometry, microanalysis and X-ray diffraction analysis. (Electronic supplementary information (ESI) available in Appendix-3.2-SI)
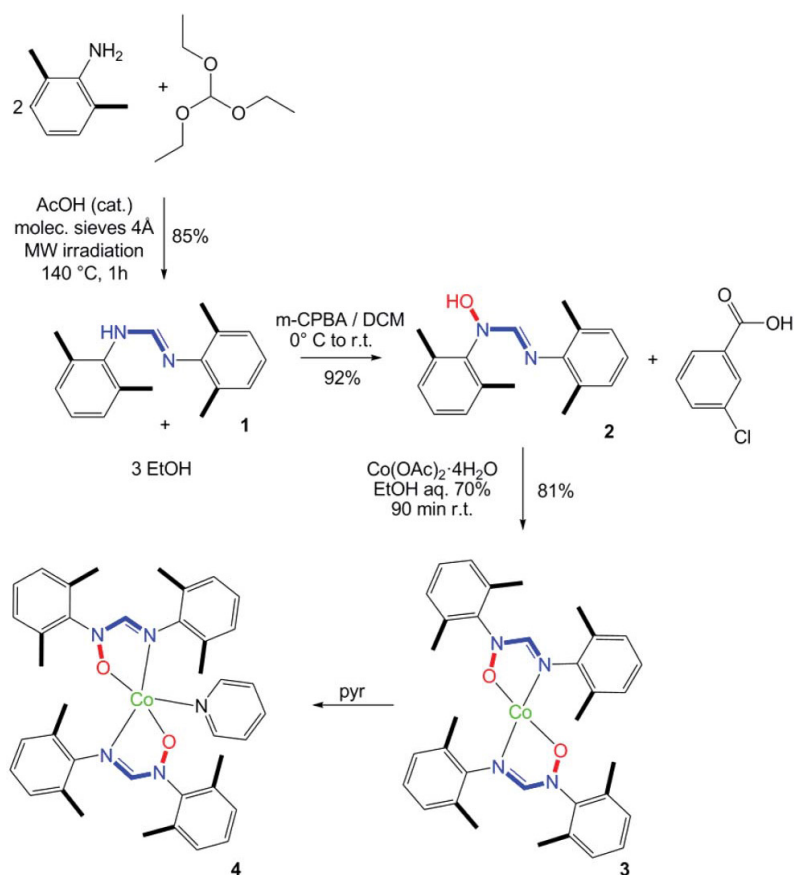
Scheme 3.2-1 Synthesis of the ligand *N*-hydroxy-*N,N'*-bis(2,6-dimethylphenyl)formamidine, **2**, its homoleptic Co(II) complex **3**, and the Co(II) complex's pyridine adduct **4**.

3.2.5.2. ^{1}H NMR Spectroscopy

The ^{1}H-NMR spectrum of **3** is characteristically expanded due to paramagnetism (50 to -50 ppm), in line with the oxidation state of the metal [Co(II), d^7]. The ^{1}H NMR resonances were assigned based on the integration ratio, COSY experiments and correlation with the X-ray crystal structure in order to establish the proximity of the protons to the metal center. (Appendix-3.2-SI)

3.2.5.3. X-ray Diffraction

X-ray quality crystals of **3** were obtained by diffusion of hexane into DCM (1 : 1) at -10 °C (Figure 3.2-1a).
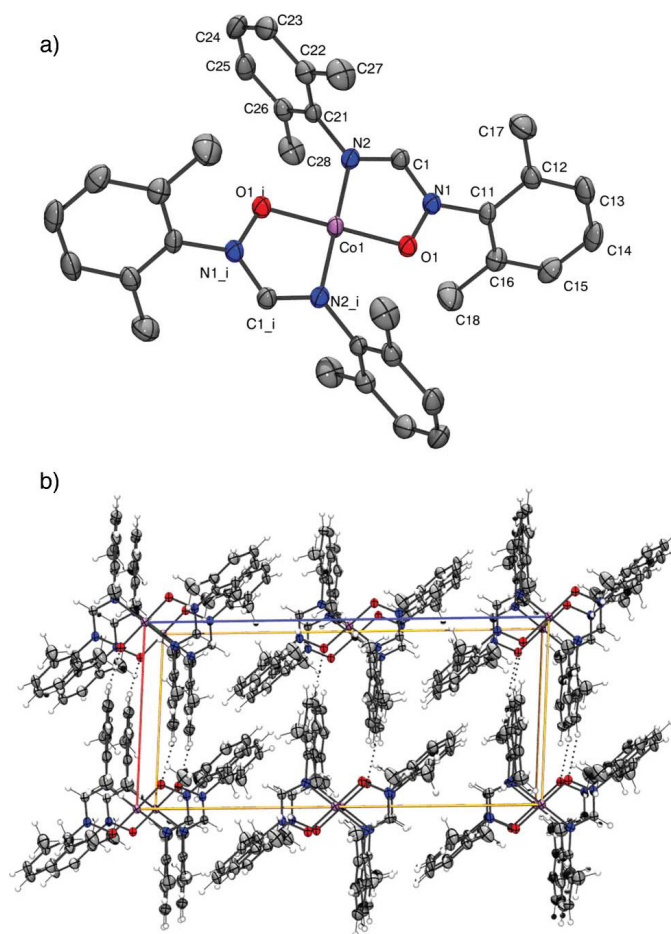
Figure 3.2-1 (a) ORTEP view of **3** with *Ci* symmetry. Ellipsoids are shown at 50% probability level. Hydrogen atoms were removed for clarity. (b) Packing diagram of **3** showing the intermolecular interactions.

The crystal structure highlights a tetracoordinated cobalt(II), sitting on an inversion center. The geometry around the metal is square-planar, with the two five-membered chelate rings being coplanar and no solvent molecule coordinated axially. This feature is quite rare as only 8 crystal structures are reported for four-coordinated square-planar Co(II) complexes with bidentate N,O-ligands.‡ Axial coordination is usually present, to offer the preferred octahedral geometry of the metal center,[8] as in the typical examples of Co(dmg)$_2$ and Co(acac)$_2$.[9,10] The bite angle of the ligand (O1–Co1–N2) is 84(1)°. The Co–O and Co–N bond lengths are comparable with the values observed in the Schiff base–cobalt(II) compounds and in other cobalt complexes displaying square-planar geometry.[11,12] Electron density is delocalized over the amidine bridge resulting in the almost equal C1–N1 and C1–N2 bonds (1.319 (2) and 1.312(2) Å , respectively). However, only partial orbital overlap exists between the aryl and the amidine π-systems, as the aryl rings are twisted from the mean plane of the hydroxyamidine by 79.4° and 59.1°. The absence of axial interactions is particularly encouraging from a supramolecular point of view, as the complex offers two sites for coordination. Examination of the packing for **3** showed weak intermolecular C(π)–H···O interactions (d = 2.45 Å and $θ$ = 162°) between one of the *meta* aryl hydrogens and the oxygen atom of an adjacent molecule (Figure 3.2-1b).

Crystals of compound **4** were grown by slow evaporation of a pyridine solution. The structure of **4** shows the presence of a pyridine adduct of **3**, in which only one pyridine is coordinated to the cobalt, resulting in a pentacoordinated metal centre with a distorted square-pyramidal geometry (Figure 3.2-2). The two ligands are no longer coplanar, but form an angle of 41(1)°, and the deviation of the metal atom from the mean plane, O(1)O(1_i)N(2)N(2_i), is 0.40(1) Å. This rearrangement blocks the second axial coordination site, compared to the square planar case, which prevents access of a second pyridine molecule to the cobalt(II) center (Figures 3.2-2 and 3.2-3). The Co–O and Co–N bond lengths in **4** are slightly longer than those in **3**, while the N–O bonds are slightly shorter. The delocalization over the amidine backbone is also influenced by the axial coordination of the pyridine, as both aryl rings are forced to adopt a position closer to orthogonality with respect to the hydroxyamidine bridge (in **4**, the tilt angle of aryls and the mean plane of the hydroxyamidine are 77.4° and 78.9° *vs.* 79.4° and 59.1° in **3**). Hence, the partial orbital overlap between the aryl and the amidine p-

systems is reduced in comparison with **3**, resulting in different C1–N1 and C1–N2 bond distances (1.321(4) and 1.296(4) Å, respectively). The Co–N5 (N of the pyridine) bond length is comparable with what it is reported for similar structures.[13]
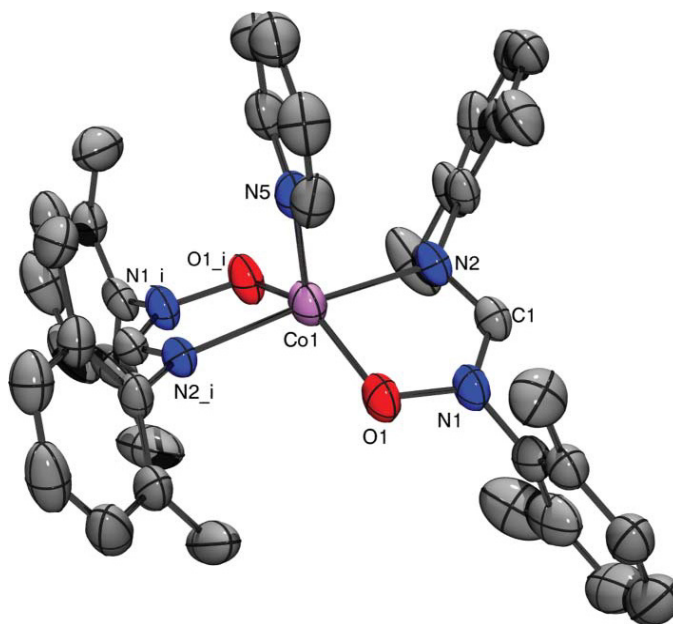
Figure 3.2-2 ORTEP view of **4** with C_2 symmetry. Ellipsoids are shown at 50% probability level. Hydrogen atoms were removed for clarity.
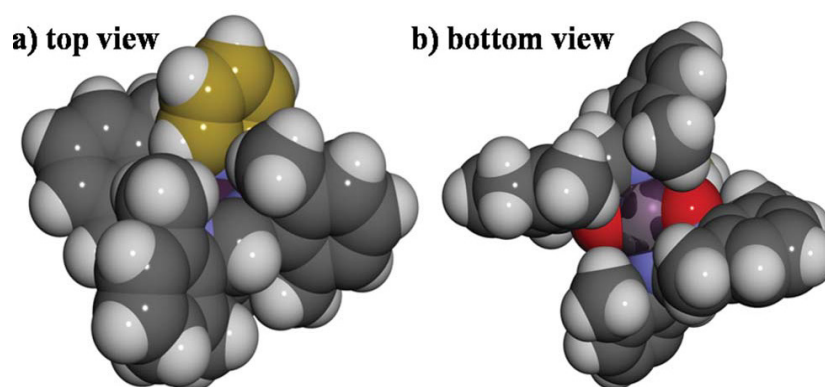
Figure 3.2-3 Space-filling models of **4**: (a) top view of pyridine (yellow) gaining access to the Co(II) center; and (b) bottom view in which methyl groups restrict access to the Co(II) centre.

3.2.5.4. Spectroscopic and electrochemical properties, and chemical oxidation experiments

In order to establish the behavior of **3** in the presence of pyridine, the association constant for the **3**–pyridine assembly was calculated by UV-vis titration to be $K = 3$ M^{-1}, Thus, the square-planar geometry of **3** is preferred even in the presence of relatively good ligands such as pyridine.

The UV-vis spectrum of **3** in DCM shows a featureless visible region, with a very intense band centered at higher energies than the solvent cut-off. There are weak bands in the NIR region, of extinction coefficients below 80 M^{-1}cm^{-1}, corresponding to forbidden *d–d* transitions (Figure 3.2-4).
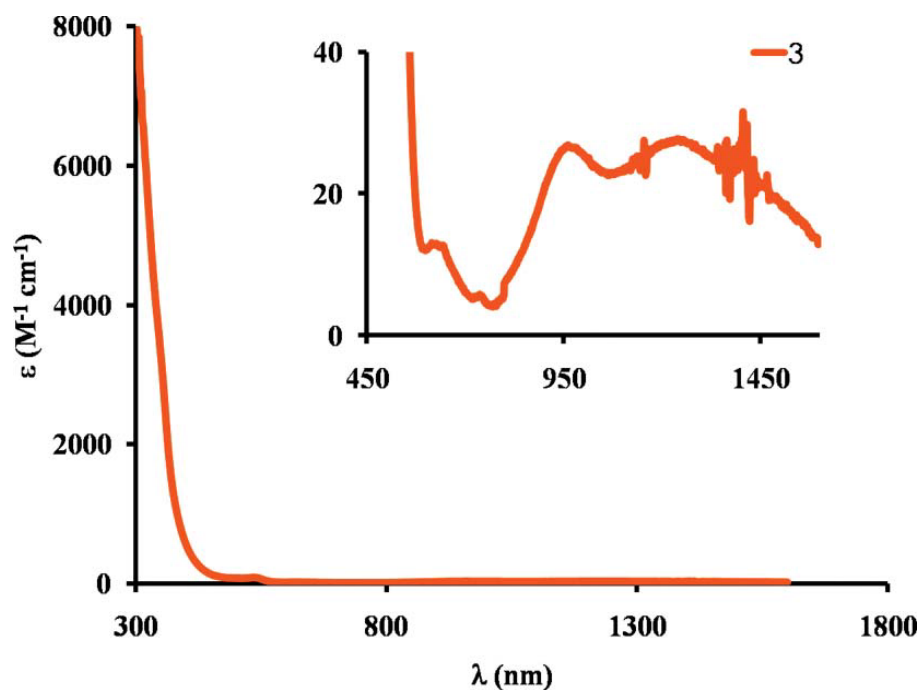
Figure 3.2- 4 UV-vis-NIR spectrum of **3** ([**3**] = 5.9 x 10^{-4} M) in DCM [λ, nm (ε, M^{-1} cm^{-1})]: 540 (79), 622 (12), 942 (29), 1233 (27).

The cyclic voltammogram of complex **3** showed a reversible oxidation process at +0.47 V *vs*. SCE, corresponding to the Co$^{II/III}$ couple, but no sign of the Co$^{I/II}$ wave was found on scanning in the negative potential region. A further irreversible process, at +1.70 V, was assigned to ligand oxidation. The oxidation of **3** resulted in a dramatic change in the appearance of the solution, giving a dark green coloration. An '*in situ*' chemical oxidation

experiment, followed by UV-vis spectroscopic analyses, was performed in order to establish the oxidation state of the metal. The oxidizing agent TBABr$_3$ (tetrabutylammonium tribromide) was added to **3**, which led to the growth of a strong band centered at *ca.* 630 nm, with a molar absorptivity of 3200 $M^{-1}cm^{-1}$ (Figure 3.2-5). However, when the non-oxidizing salt TBABr (tetrabutylammonium bromide) was added, no significant change was observed in comparison with the spectrum of pure **3**, which excludes that this effect is due to the simple coordination of Br$^-$ to the complex. The appearance of a band at 630 nm in the oxidized form of **3** has not yet been clarified, however, it may be due to an allowed ligand-to-metal charge transfer from Br lone-pair to the Co(III), explaining the intense green color also exhibited by other Co(III)-Br complexes.[14–16]
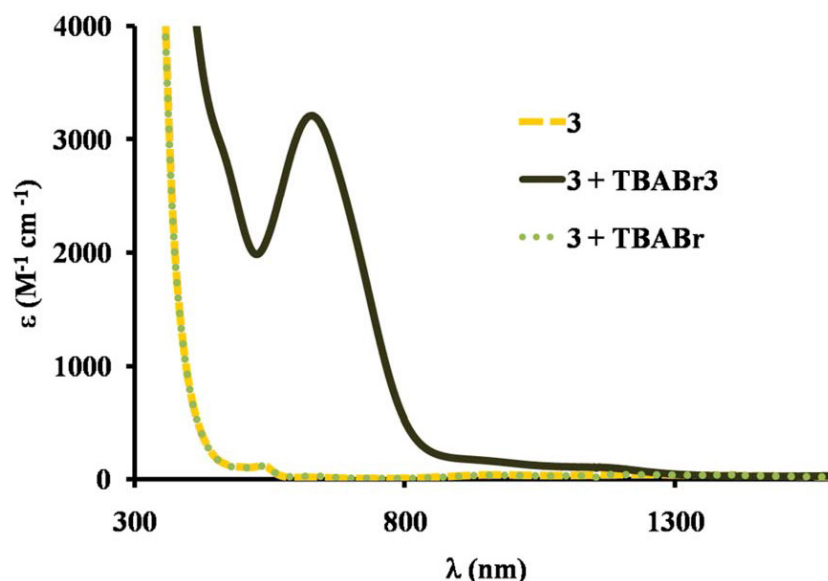
Figure 3.2-5 UV-vis-NIR spectrum of pure **3** ([**3**] = 5.9 x 10^{-4} M) in DCM (yellow dashes); **3** in the presence of TBABr (green dots); and (b) **3** in the presence of TBABr$_3$ (black line).

3.2.6. Conclusion

In conclusion, complex **3** is very stable and its study provides good insight into the basic properties of the rare square-planar Co(II) complexes and this promising family of hydroxyamidine complexes. The electronic properties of the metal–ligand interaction and the steric hindrance generated by the 2,6-substituents on the ligand are perfectly combined to

induce the rare square-planar geometry around the Co(II) center. Their close resemblance with the well known Co(salen)$_2$ and Co(dmg)$_2$ compounds, widely employed in catalytic and photocatalytic applications, gives hope for the possibility to tune the redox potential of the hydroxyamidinate cobalt complexes for oxygen transport or catalysis for hydrogen production.[16–18]

3.2.7. Experimental Section

Full experimental details are given in Appendix 3.2-SI.

Complex 3: A solution of the ligand **2** (0.10 g, 0.37 mmol, 2 eq.) in aq. EtOH 90% was slowly added to a solution of metal salt Co(OAc)$_2$·4H$_2$O (0.046 g, 0.19 mmol, 1 eq.) in water. The formation of a green precipitate is observed almost instantly. After stirring for 90 min. at r.t., water was added and the reaction mixture was kept at 4°C for 2 h, before being filtered. The resulted solid was washed with hot water and aq. EtOH 50%, and was taken in DCM and dried over MgSO$_4$. A second filtration and solvent evaporation yielded the desired product as a green powder. X-ray quality crystals obtained by slow diffusion of hexane in DCM at -10 °C. Yield: 0.090 g, 81%. ^{1}H NMR paramagnetic compound Co(II) d^7: (CDCl$_3$, 300 MHz) δ, ppm: 47,39; 36,92; 23,20; 7,28; -0,31; -5,62; -45,38; -50,84. IR (ATR, solid sample, cm^{-1}) 3008, 2968, 2947, 2913, 2851, 1601, 1578, 1466, 1269, 1227, 1202, 1092, 987, 928, 918, 892, 821, 777, 755, 741, 694, 639, 527, 497, 488. Elemental Analysis: calc. (%) for C$_{34}$H$_{38}$CoN$_4$O$_2$: C 68.79, H 6.45, N 9.44; found: C 68.52, H 6.42, N 9.27. MS (ESI-HRMS DCM – no acid) (m/z): [M]$^+$ C$_{34}$H$_{38}$CoN$_4$O$_2$: calc. 593.2321; found 593.2305. [M+Na]$^+$ C$_{34}$H$_{38}$CoN$_4$NaO$_2$: calc. 616.2219; found 616.2212. UV-vis: (DCM, 5 x 10^{-4} M) [λ, nm (ε, M^{-1}cm^{-1})]: 540 (79), 622 (12), 942 (29), 1233 (27). E-chem (values vs. SCE) (in 0.1 M TBAPF$_6$ in DCM; scan rate is 100 mV s^{-1}) Co$^{II/III}$, +0.47 V (r) ; ligand, +1.70 V (irr); no reduction observed.

3.2.8. Acknowledgments

3.2.9. Supporting Information

Electronic supplementary information (ESI) available: synthesis of **2** and **3** and key crystallographic data (CCDC reference numbers 796317 and 796318). For ESI and crystallographic data in CIF or other electronic format see DOI: 10.1039/c0dt01365j. In this thesis, the same material is found in Appendix-3.2-SI

3.2.10.   References

‡ CSD search, November 2010.
[1]   L. H. Briggs, R. C. Cambie, I. C. Dean and P. S. Rutledge, *Aust. J. Chem.*, **1976**, *29*, 357–66.
[2]   R. S. Kharsan, K. S. Patel, R. K. Mishra and L. R. Malewar, *Proc. Indian Acad. Sci., Chem. Sci.*, **1980**, *89*, 411–15.
[3]   A. Krajete, G. Steiner, H. Kopacka, K.-H. Ongania, K. Wurst, M. O. Kristen, P. Preishuber-Pfluegl and B. Bildstein, *Eur. J. Inorg. Chem.*, **2004**, 1740–1752.
[4]   A. N. Verma, S. B. Gholse and S. P. Sangal, *J. Indian Chem. Soc.*, **1995**, *72*, 685–688.
[5]   S. Caramori, J. Husson, M. Beley, C. Bignozzi, R. Argazzi and P. Gros, *Chem.–Eur. J.*, **2010**, *16*, 2611–2618.
[6]   H.Wang, P.G. Nicholson, L. Peter, S. M. Zakeeruddin and M. Grätzel, *J. Phys. Chem. C*, **2010**, *114*, 14300–14306.
[7]   M. Cibian, S. Langis-Barsetti andG. S.Hanan, *Synlett*, **2010**, accepted for publication.
[8]   E. K. Brechin, O. Cador, A. Caneschi, C. Cadiou, S. G. Harris, S. Parsons, M. Vonci and R. E. P. Winpenny, *Chem. Commun.*, **2002**, 1860–1861.
[9]   V. D. Vreshch, J.-H. Yang, H. Zhang, A. S. Filatov and E. V. Dikarev, *Inorg. Chem.*, **2010**, *49*, 8430–8434.
[10]   P. N. Bourosh, O. A. Bologa, Y. A. Simonov, G. Bocelli and N. V. Gerbeleu, *Russ. J. Coord. Chem.*, **2005**, *31*, 641–644.
[11]   W.-B. Yuan, H.-Y. Wang, J.-F. Du, S.-W. Chen and Q. Zhang, *Acta Crystallogr., Sect. E: Struct. Rep. Online*, **2006**, *62*, m3504–m3505.
[12]   L.-J. Zhang, X.-L. Zhao, P. Cheng, J.-Q. Xu, X. Tang, X.-B. Cui, W. Xu and T.-G. Wang, *Bull. Chem. Soc. Jpn.*, **2003**, *76*, 1179–1184.
[13]   X. Y. Qiu, S. L. Yang,W. S. Liu and H. L. Zhu, *Acta Crystallogr., Sect. E: Struct. Rep. Online*, **2006**, *62*, m1320–m1321.
[14]   H. El-Ghamry, R. Issa, K. El-Baradie, S. Masaoka and K. Sakai, *Acta Crystallogr., Sect. E: Struct. Rep. Online*, **2009**, *65*, m1378–m1379.
[15]   C. T. Cohen, C. M. Thomas, K. L. Peretti, E. B. Lobkovsky and G.W. Coates, *Dalton Trans.*, **2006**, 237–249.
[16]   A. Kilic, E. Tas, B. Deveci and I. Yilmaz, *Polyhedron*, **2007**, *26*, 4009–4018.
[17]   A. Fihri, V. Artero,M. Razavet, C. Baffert,W. Leibl and M. Fontecave, *Angew. Chem., Int. Ed.*, **2008**, *47*, 564–567.
[18]   D. H. Busch and N. W. Alcock, *Chem. Rev.*, **1994**, *94*, 585–623.

3.3. Influence of Ligand Substitution Pattern on Structure in Cobalt(II) Complexes of Bulky *N,N'*-Diarylformamidinate *N*-Oxides

3.3.1. Résumé

Des complexes de cobalt(II) avec des ligands encombrés *N,N'*-diarylformamidinate *N*-oxydes ont été synthétisés et caractérisés. Leurs structures cristallines ont aussi été obtenues. Les bis(chélates) de cobalt(II) sont plan carré (bas spin) à l'état solide, comme le démontrent leurs structures cristallines et leurs moments magnétiques (μ_{eff} = 1.8 to 2.1 μ_B). Néanmoins, ces composés montrent l'isomérisation d'une structure plan-carré (bas spin) à une structure tétraédrique (haut spin: μ_{eff} = 3.5 to 4.7 μ_B) dans des solutions de solvants non-coordinants. Le processus d'isomérisation a été prouvé par différentes techniques spectroscopiques. L'équilibre de l'isomérisation est beaucoup influencé par le motif de substitution du ligand, suite à une combinaison des effets stériques et électroniques.

Contribution:

Mihaela Cibian: synthèse optimisée des complexes et caractérisation complète, études d'absorption UV-vis à température variable, études de l'équilibre d'isomérisation, mesures des moments magnétiques, résolution d'une structure cristalline, modélisation des molécules par DFT et rédaction de l'article

Sophie Langis-Barsetti: synthèse préliminaire et caractérisation partielle des composés

Fernanda Gomes De Mendonça: synthèse des ligands

Sammy Touaibia: caractérisation partielle des complexes (confirmation de leurs propriétés rédox)

Sofia Derossi: structure cristalline et caractérisation partielle d'un complexe

Denis Spasyuk: structure cristalline d'un complexe

Garry S. Hanan: supervision, révision de l'article

Influence of Ligand Substitution Pattern on Structure in Cobalt(II) Complexes of Bulky *N,N'*-Diarylformamidinate *N*-Oxides

Mihaela Cibian, Sophie Langis-Barsetti, Fernanda Gomes de Mendonça, Sammy Touaibia, Sofia Derossi, Denis Spasyuk, and Garry S. Hanan*

Département of Chemistry, Université de Montréal, Montréal, Québec, H3T-1J4, Canada

*: E-mail: garry.hanan@umontreal.ca. Fax: 1-514-343-7586

3.3.2. Table of content graphic

Square planar (LS) (solid state) ⇌ Square planar (LS) ⇌ Tetrahedral (HS) (solution)
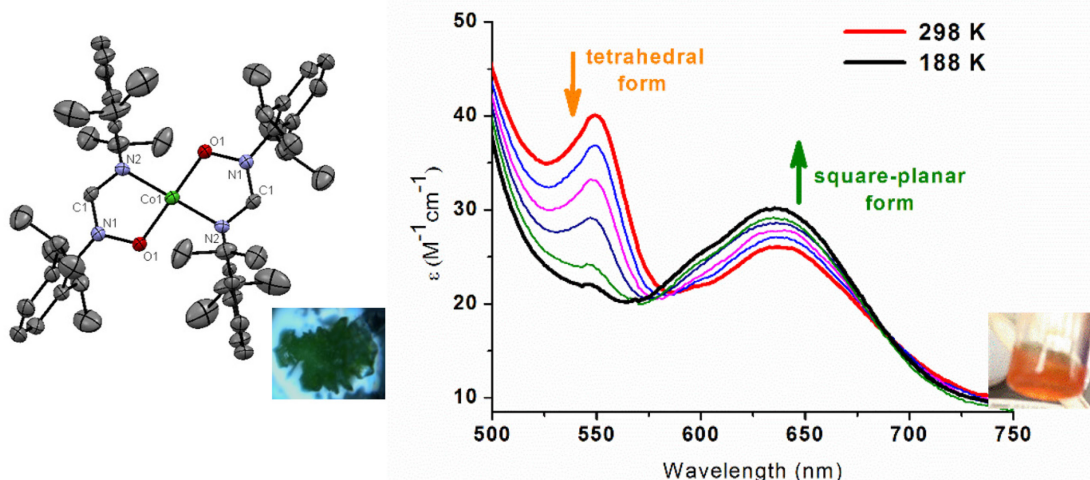
Cobalt(II) bis(chelates) of bulky *N,N'*-diarylformamidinate *N*-oxide ligands show isomerization from square-planar low-spin (in the solid state) to tetrahedral high-spin (in solutions of noncoordinating solvents).

3.3.3. Abstract

Cobalt(II) complexes of bulky *N,N'*-diarylformamidinate-*N*-oxide ligands were synthesized and structurally characterized. The cobalt(II) bis-chelates are square-planar (low spin) in the solid state, according to XRD and magnetic measurements (μ_{eff} = 1.8 to 2.1 μ_B), but show square-planar (low spin) to tetrahedral (high spin – μ_{eff} = 3.5 to 4.7 μ_B) isomerization in solution of non-coordinating solvents, as demonstrated by different spectroscopic techniques. The isomerization equilibrium is highly sensitive to the substitution pattern on the ligand due to a combination of steric and electronic influences.

3.3.4. Introduction

Several reports related to amidine-*N*-oxide (AMOX, also called α-aminonitrones and *N*-hydroxyamidines) ligands and their transition metal complexes exist in the literature.[1] However, investigation of their properties from a coordination and supramolecular chemistry perspective has received little attention. Amidinate ligands are closely related to the *N*-

hydroxyamidinate ligands and have been intensively explored in organometallic and coordination chemistry over the past decades, resulting in applications in catalysis and materials.[2] AMOX ligands are good chelators for metal ions and exhibit good electronic delocalization in the amidine backbone. Furthermore, they offer the possibility of modulating and fine-tuning their electronic and steric properties by varying the substitution pattern on the three atoms of the amidine moiety.[1a, 1d] Our goal is to fine-tune the properties of their corresponding metal complexes for applications in catalysis and magnetic materials.

Our preliminary results regarding the Co(II)L$_2$ complex (**2a**) (Scheme 3.3-1), where HL = N-hydroxy-N,N'-bis(2,6-dimethylphenyl)formamidine (**1a**), highlight an interesting consequence of the metal-ligand interaction: steric and electronic effects combine to offer a rare square-planar geometry around the d^7 Co(II) centre in a bis-bidentate environment, while permitting facile oxidation of the metal ion.[3] In solutions of noncoordinating solvents, a square-planar to tetrahedral isomerization can be observed. For a tetra-coordinate cobalt(II) system this is particularly interesting, because the structural change is also accompanied by a change in spin.[4] Investigation of such systems affords detailed information concerning their coordination number and geometry, which is needed to predict and control the architecture and properties of the transition-metal complexes for application purposes.[5]
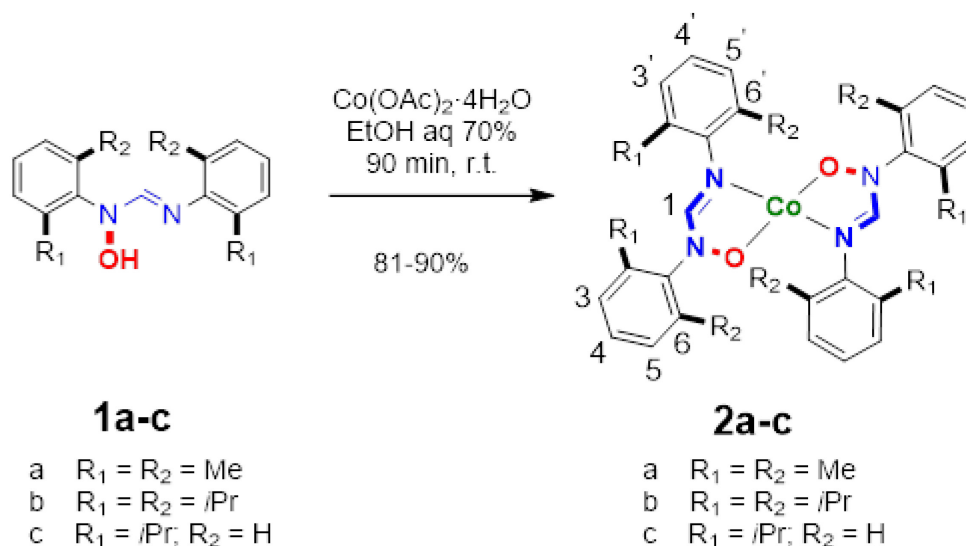
Scheme 3.3-1. Synthesis of Co(AMOX)$_2$ complexes **2a-c**.

The square-planar to tetrahedral isomerisation of a series of bis-chelate metal(II) compounds was previously studied by Holm.[5a, 6] In cobalt-based systems, this process was investigated for organometallic complexes,[7] and for cobalt complexes of triazene-1-oxides[8], tropocoronand macrocycles,[9] and iminopyrrolyl ligands.[10] These studies revealed the importance of the electronic and steric properties of the ligand on the structural preference of the complex. Recently, the same type of process was also reported for cobalt complexes of α-imino alkoxide ligands.[11] However, examples of square-planar to tetrahedral isomerization in five-membered ring metal complexes of *N,O*-bidentate ligands are scarce.[5a, 8, 11-12] The cobalt bis(chelates) of sterically demanding AMOX ligands offer a new opportunity to explore the effect of ligand-metal interactions on their structural, spectroscopic, and electrochemical properties.

3.3.5. Results and discussion

3.3.5.1. Synthesis

Homoleptic complexes of cobalt(II) (**2b-c**, Scheme 3.3-1) with the following AMOX ligands: *N*-hydroxy-*N,N'*-bis(2,6-diisopropylphenyl)formamidine (**1b**) and *N*-hydroxy-*N,N'*-bis(2-isopropylphenyl)formamidine (**1c**) were synthesized and characterized. The syntheses of ligands **1a-c** and complex **2a** were previously reported.[3, 13] Complexes **2b** and **2c** were also straightforward to prepare by reacting two equivalents of the corresponding ligand with cobalt(II) acetate in aqueous ethanol at room temperature. A green precipitate formed in each case, and the products were isolated in good yields (81-90%) as air-stable powders (Scheme 1). The solids are air-stable for months without decomposition and readily dissolve in chlorinated solvents to give yellow-orange solutions, but are poorly soluble in polar solvents. The compounds undergo oxidation over a period of days when left in solution. Complexes **2a-c** were characterized by X-ray crystallography, ^{1}H-NMR and UV-vis spectroscopy, mass spectrometry and elemental analysis.

3.3.5.2. X-ray diffraction

Green X-ray quality crystals were obtained by recrystallization of **2a** and **2c** from DCM/ hexane (1:1 v/v) at -20°C and/or room temperature and from AcOEt/ hexane at room

temperature for **2b**. X-Ray structures and data are presented in Figures 3.3-1 – 3.3-2 and Tables 3.3-1 – 3.3-2. As for **2a**,[3] the metal ions in **2b** and **2c** display a square-planar geometry (Figures 3.3-1 and 3.3-2). In all cases the metal ion is sitting on an inversion center, and the two five-membered chelate rings are coplanar, with no axially coordinated solvent molecule. There are few examples of square-planar coordination geometries reported for cobalt(II) complexes of bidentate ligands,[3, 6a-c, 10-11, 12c, 14] as tetrahedral geometry is favoured on steric grounds in bis(bidentate) four-coordinate environments. In some cases, axial coordination of solvent molecules is present, which offers the preferred octahedral geometry around the metal center, as for Co(acac)$_2$.[15] Stabilization of the square-planar geometry can usually be achieved in the presence of macrocyclic ligands[16] or by a special combination of steric and electronic factors.[3, 10, 12c, 14b, 14d] Square-planar cobalt(II) complexes with bidentate *N,O*-ligands that form 5-membered chelate rings are rare and only ten (including **2a**) crystal structures of this type are reported in the CCDC.[17]
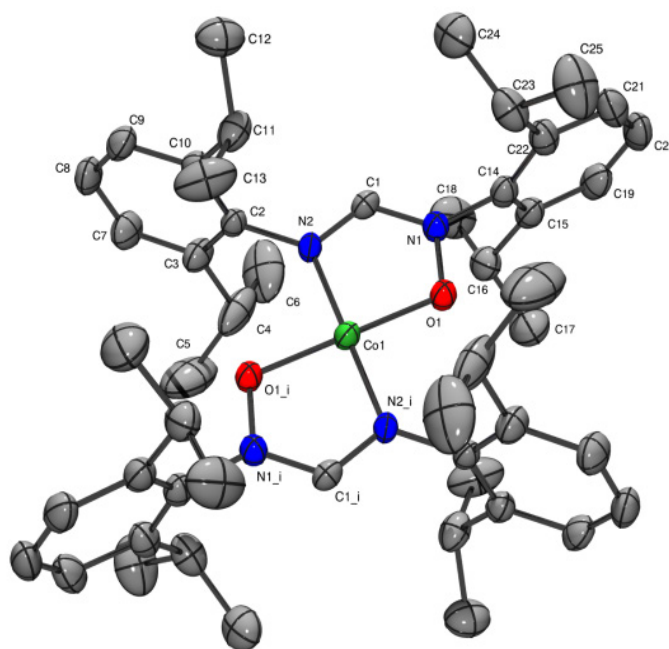
Figure 3.3-1. ORTEP view of **2b** with C_i symmetry. Ellipsoids are shown at 50% probability level. Hydrogen atoms were removed for clarity.

Five of these structures correspond to cobalt complexes of redox active *o*-aminophenol-type ligands and can be considered as a special case due to the 'non-innocent' nature of the ligand.[14b, 14d, 18] In one other case the stabilization of the square-planar geometry

at the Co center is assisted by two intramolecular interactions of X−H···Co type.[19] This leaves only three other types of *N,O*-ligands, except the AMOXs, able to stabilize square-planar geometry of cobalt(II) bis(chelates) with five-membered chelate rings: α-imino alkoxide[11], carbohydrazide[14e], and triazene-1-oxide derivatives[12c].

Table 3.3-1. Solid state structure and refinement data for compounds **2a-c**.

Compound	2a[a]	2b	2c
Formula	$C_{34}H_{38}CoN_4O_2$	$C_{50}H_{70}CoN_4O_2$	$C_{38}H_{46}CoN_4O_2$
M_w (g/mol)	593.61	818.03	649.72
Temperature (K)	200	150	150
Wavelength (Å)	0.71073	1.54178	1.54178
Crystal System	Monoclinic	Triclinic	Monoclinic
a (Å)	8.8879(12)	10.6229(3)	7.5524(2)
b (Å)	8.3485(11)	10.6858(2)	24.9130(7)
c (Å)	20.363(3)	11.8393(2)	9.3964(3)
α (°)	90	109.052(1)	90
β (°)	93.057(2)	105.705(1)	104.449(1)
γ (°)	90	99.860(1)	90
Unit cell volume (Å^3)	1508.8(3)	1172.06(4)	1712.04(9)
Space Group	P2$_1$/c	P-1	P2$_1$/c
Z	2	1	2
$d_{calcd.}$ (g/cm^3)	1.307	1.159	1.260
μ (mm^{-1})	0.606	3.177	4.223
F(000)	626	441	690
Reflections collected	36660	18441	34923
Independent reflections	4749	18441	3218
GoF	0.975	1.046	1.060
R1(F) [I > 2σ(I)]	0.0367	0.0327	0.0298
wR(F^2) [I > 2σ(I)]	0.1008	0.0829	0.0860
R1(F) (all data)	0.0512	0.0341	0.0313
wR(F^2) (all data)	0.1066	0.0841	0.0869
Largest diff. peak/ hole (e/Å^3)	0.858/ -0.336	0.153/ -0.293	0.272/ -0.478

[a]from ref.[3].

Table 3.3-2. Selected bond distances (Å) and angles (°) for 2a-c and chosen examples of cobalt complexes from literature **3-8**

Cpd.	τ_4[i]	Bond distances (Å)					Angle (°)	Tilt (°)	angle[k]
		Co-O1	Co-N2	C1-N1	C1-N2	O1-N1	O1-Co-N2	Ar(NO)	ArN
2a[a]	0	1.834(1)	1.886(1)	1.319(2)	1.312(2)	1.392(1)	84.5(1)	59(1)	79(1)
2b	0	1.841(2)	1.883(1)	1.319(2)	1.306(3)	1.389(2)	84.9(1)	84(1)	87(1)
2c	0	1.833(1)	1.898(1)	1.316(2)	1.316(2)	1.387(1)	84.6(1)	60(1)	60(1)
3[b]	0	1.805(3)	1.856(3)	-	-	1.339(4)	81.9(1)	-	39(1)
4[c]	0.02	1.823(3)[j]	1.836(3)[j]	-	-	-	85.7(1)	-	90(1)
5[d]	0	1.828(1)	1.840(1)	-	-	-	85.7(1)	-	69(1)
6[e]	0.02	1.848(3)[j]	1.841(4)[j]	-	-	-	94.1(1)	-	-
7[f]	0	1.848(1)[j]	1.967(1)[j]	-	-	-	84.3(1)	-	-
8[g]	0	1.846(1)	1.938(1)	-	-	-	84.5(1)	-	-
2a-sqpl[h] **(DFT optimized CH₂Cl₂)**	0	1.839	1.890	1.324	1.317	1.398	84.4	74	89

[a] from ref.[3]; [b] **3**: Co(L)₂, L = triazene 1-oxide-type,[12c] [c] **4**: Co(L)₂, L=*o*-aminophenol-type,[14d] [d] **5**: Co(L)₂, L=*o*-aminophenol-type,[14b] [e] **6**: Co(L)₂, L=[N₂O₂]-Schiff base type ligand;[20] [f] **7**: Co(L)₂, L=*α*-imino alkoxide-type,[11] [g] **8**: Co(L)₂, L=carbohydrazide-type.[14e] [h] Theory level: uB3LYP/ LANL2DZ, CPCM: CH₂Cl₂. [i] as defined by Houser.[21] [j] Average value. [k] Angle between the plane of the aromatic ring and the plane of the -N-C=N- moiety.

Table 3.3-3. Chemical shift values (ppm) for ^{1}H NMR spectra[a] of complexes **2a-c**[b]

Cpd.	1	3'	3	4'	4	5'	5	6'	6	-C*H*'-CH$_3$	-C*H*-CH$_3$	-C*H*$_3$'	-C*H*$_3$
2a	-0.7	-1.6	30.8	-34.3	19.6	-1.6	30.8	-	-	-	-	-40.1	37.0
2b	0.5	8.8	14.8	- 3.7	11.5	8.8	14.8	-	-	-26.9	18.1	-2.5	8.0
												-16.5	0.5
2c	0.1	-9.5	30.3	-34.1	20.1	11.6	33.3	-200	69.2	-22.7	51.1	-29.0	8.9

[a] see Scheme 3.3-1 for the notation of the H. [b] in CD$_2$Cl$_2$.
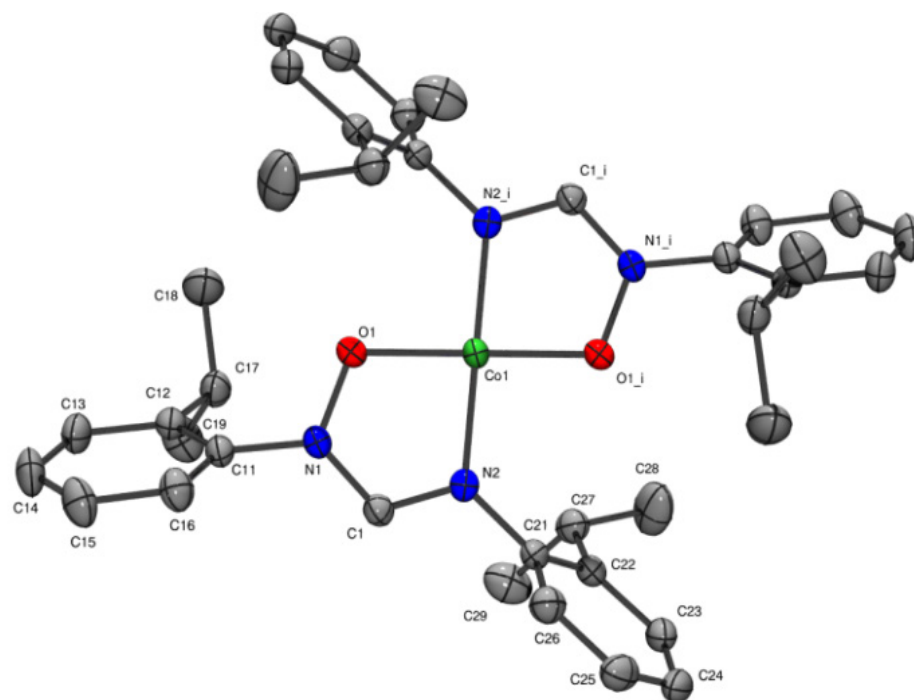
Figure 3.3-2. ORTEP view of **2c** with C_i symmetry. Ellipsoids are shown at 50% probability level. Hydrogen atoms were removed for clarity.

The Co–O bond lengths in **2a-c** are similar and their values are closer to those observed in cobalt complexes of Schiff base-type, α-imino alkoxide-type, and carbohydrazide-type ligands (cpd. **6**, **7**, and **8**; Table 2) rather than the triazen-1-oxide analogues (**3**; Table 3.3-2) or the cobalt(II) complexes of redox-active ligands (**4**, **5**; Table 3.3-2). The Co–N bonds are also similar within the **2a-c** series, but they differ from those in the compounds **3-8** (Table 3.3-2), as result of the differences in the five-member chelate rings (type of atoms, substituents, electronic delocalization).

All three structures **2a-c** show electron density delocalized over the amidine bridge, resulting in equal (within 3σ) C1–N1 and C1–N2 bonds. However, only partial orbital overlap exists between the aryl and the amidine π-systems, since the aryl rings are twisted from the mean plane of the –N–C=N– moiety in order to accommodate the steric bulk generated by the 2,6-substituents. The values of the tilt angles are shown in Table 3.3-2, and are indicative of the degree of delocalization in the molecule. Among **2a-c**, the largest ArN and Ar(NO) dihedral angles are observed for **2b**. This fact is in accordance with **1b** being the most sterically demanding ligand. Examination of the packing in the three structures shows weak

C(π)–H $\cdots$O (d = 2.45 Å, θ = 162°) and C(π)–H $\cdots\pi$ intermolecular interactions for **2a** and **2c**, respectively.

3.3.5.3. ^{1}H-NMR spectroscopy

The ^{1}H NMR spectra of **2a-c** are shifted due to paramagnetic effects (δ = 69 ppm to δ = -200 ppm, Table 3.3-3 and Figure S1, Appendix-3.3-SI), which is consistent with the oxidation state of the metal ion [cobalt(II), d^7]. They exhibit characteristically broadened signals, without coupling constants, albeit with accurate integrations. Thus, it was possible to assign the ^{1}H NMR resonances based on the integration ratio, 2D COSY and T1 relaxation time measurement experiments, and to correlate these results with the proximity of the protons to the metal centre. The aryl ring on the *N*-Co is closer to the metal centre, and thus more influenced than the aryl ring which sits on the *NO*-Co.[22] As a consequence, the *para* H4' are paramagnetically more shifted than the *para* H4 (see Scheme 3.3.-1 for the notation of H). In the case of **2a** this is also supported by the T1 relaxation time values of 22.7 ms for H4 vs. 34.4 ms for H4'. For **2a** (substituted with methyl groups in the 2,6-positions), the two broad signals at δ = +37.0 and -40.1 ppm integrate to 6H, corresponding to the -C*H$_3$* protons. They are positioned in close proximity of the cobalt centre due to the tilt of the aryl rings with respect to the amidine oxide plane. Their short T1 relaxation time values of 1.3 and 1.7 ms are also in line with their position close to the paramagnetic centre. In the case of **2b**, the –C*H*-CH$_3$ protons are the ones close to the metal centre, and their resonances are thus the most shifted due to paramagnetism, being observed as broad signals at δ = +18.1 and -26.9 ppm. For compound **2c** (monosubstituted in position 2), protons H6, H6' (in the *ortho* position) and H4' (in the *para* position) are the most influenced by the metal centre, and thus appear at δ = 69.2, -200, and -34.1 ppm, respectively.

3.3.5.4. Square-planar (LS) to tetrahedral (HS) isomerization

In four-coordinate cobalt(II) systems, the square-planar to tetrahedral structural change is also accompanied by a change in spin.[4] The solution and solid state effective magnetic moments for **2a-c** are shown in Table 3.3-4. The solid state magnetic moments have the characteristic low spin (LS, S=1/2)) values (1.8-2.2 μ_B) expected for cobalt(II) in square-planar geometry.[4, 7]   These values are in line with the square-planar geometry of the

compounds as shown by XRD structural characterization. For **2a**, the solution-phase (CH$_2$Cl$_2$) magnetic moment (4.7 μ_B) corresponds to a tetrahedral configuration of the cobalt(II) d^7 centre: high-spin, S=3/2. This value is higher than the spin-only one (3.89 μ_B) due to spin-orbit coupling.[23] The values of the magnetic moment determined in solution for **2b** (3.5 μ_B) and **2c** (4.0 μ_B) are between the accepted high spin (4.2–5.2 μ_B) and low spin (1.8–2.2 μ_B) values[4] for cobalt(II) complexes, suggesting an equilibrium between the LS square-planar and HS tetrahedral forms.[6a, 6c, 8, 22a]

Table 3.3-4. Effective magnetic moments μ_{eff} (μ_B) for complexes **2a-c**, measured in solution[a] and solid[b] phase.

Cpd.	μ_{eff} solution[c] (μ_B)	μ_{eff} solid state[c] (μ_B)
2a	4.67 ± 0.16	1.84 ± 0.21
2b	3.54 ± 0.14	1.86 ± 0.16
2c	4.03 ± 0.06	2.10 ± 0.09

[a]measured by Evans' method in CD$_2$Cl$_2$ (10% v/v TMS) at 298 K; [b]measured by magnetic susceptibility balance at 295 K. [c]the measurements were done at least in triplicate and the reported error represents the confidence interval at 95% probability.

The thermodynamic parameters for this equilibrium for **2a-c** are presented in Table 3.3-5. They were derived based on variable temperature (193 – 298 K) magnetic susceptibility measurements. This method was previously reported for similar systems.[6a, 6c, 8, 24] The magnetic moment increased with increasing temperature for **2a-c**, with the highest variation in 193 – 298 K temperature range being observed for **2b**, followed by **2c** and **2a** (Figure S3, Appendix-3.3-SI). By using $\mu_{eff} = 2.83(\chi^M T)^{1/2}$ (1), the free energy changes (ΔG) were evaluated from the temperature dependence of the magnetic susceptibility (χ^M – molar magnetic susceptibility) and hence the corresponding effective magnetic moments:

$$\Delta G = RTln((\chi^M_t - \chi^M_{obs})/(\chi^M_{obs} - \chi^M_p)) \qquad (2).$$

Expression 2 was derived using Equations (3) - (7).

$$\Delta G = -RTlnK \qquad (3)$$

$$\chi^M_{obs} = N_t\chi^M_t + N_p\chi^M_p \qquad (4)$$

$$K = N_t/N_p \qquad\qquad\qquad (5)$$

$$N_t + N_p = 1 \qquad\qquad\qquad (6)$$

$$N_t = (1 + e^{\Delta G/RT})^{-1} \qquad\qquad (7)$$

The equilibrium constant (K) of the isomerization process square-planar to tetrahedral is defined as in (5), with N_t and N_p representing the mole fractions of the tetrahedral and square-planar form, respectively. The magnetic moments determined for **2a-c** in solid form (100% square-planar) were used as magnetic moments of the pure square-planar form (μ_p). For the pure tetrahedral form (μ_t), magnetic moments of 4.85 μ_B were assumed, based on literature reports of similar systems. [4, 8]

Table 3.3-5. Thermodynamic parameters related to the isomerization equilibrium: tetrahedral high-spin (HS) to square-planar low spin (LS) for **2a-c** in non-coordinating solvents[a]

Cpd.	ΔG^{298} (kJ mol^{-1})	ΔH (kJ mol^{-1})	ΔS (J K^{-1} mol^{-1})	N_t[b]
2a	-5 ± 0.8	5 ± 0.9	34 ± 6.1	0.9 ± 0.16
2b	1 ± 0.2	11 ± 2.0	32 ± 5.8	0.4 ± 0.07
2c	-1 ± 0.2	5 ± 0.9	18 ± 3.2	0.6 ± 0.11
Co(RN$_3$Ar)$_2$[c]	-	1 - 15	5 - 30	-
Co(L)$_2$[d]	-	0 - 12	6 - 32	-

[a]derived from magnetic susceptibility measurements performed by Evans' method in CD$_2$Cl$_2$, at variable temperatures (193–298 K); corrections for the change in solvent density with temperature were applied[25], [26]; errors are estimated as follows: ±4% for the magnetic moments; ±15% for ΔG values (considering an error of 10% on the magnetic moment assumed for the pure tetrahedral form); ±18% for ΔH, ΔS and N_t values[27]; [b]N_t – mole fraction of the tetrahedral form at 298 K; [c]cobalt(II) complexes of triazene-1-oxide-type ligands[14a]; [d]L is a β-ketoamine or β-iminoamine-type ligand.[5a]

The ΔG values for **2a-c** varied linearly with temperature (Figure S2, Supporting Information). By using $\Delta G = \Delta H - T\Delta S$ (8), the changes in enthalpy (ΔH) and entropy (ΔS) were obtained from the least square fit of ΔG vs. T (Table 3.3-5, Figure S2, Appendix-3.3-SI). The values of the thermodynamic parameters obtained for the bis(AMOX) cobalt chelates are

in the same order of magnitude with those previously reported for cobalt complexes of triazene-1-oxide-type[8] and β-ketoamine-type[5a] ligands. For **2a** and **2c**, the values of N_t at 298 K (0.9 and 0.6) indicate a preference for tetrahedral geometry in CH_2Cl_2 solution. Interestingly, in the case of **2b,** the square-planar form is slightly stabilized ($N_t = 0.4$). Thus, the thermodynamic data suggest a high sensitivity of the isomerization equilibrium to the substitution pattern on the ligand. The higher proportion of the square-planar form (LS) in **2b** vs. **2a** and **2c** also correlates with the UV/Vis spectroscopic data (*vide infra*), and the chemical shifts in ^{1}H-NMR, which are the paramagnetically least shifted in the case of **2b**. The preference of **2a** for the tetrahedral form is also supported by DFT calculations (*vide infra*). To eliminate the possibility of five- or six-coordinate low spin species, and hence their influence on the observed magnetic moments, the adherence of the Beer-Lambert law was confirmed in the range of concentrations over the magnetic and spectroscopic properties were measured (10^{-5} – 10^{-3} M).[6b] This would not be the case if dimerization promoted octahedral coordination at higher concentrations.

As for the other cases of square-planar-to-tetrahedral isomerization, positive values are obtained for ΔH, which can be attributed to the endothermic weakening of the metal–ligand bonds in the isomerization process.[5a, 8] The highest value of ΔH is observed for **2b**, indicating a higher degree of stabilization for the square-planar form in this case. The high steric bulk of the 2,6-di-*i*Pr substituents on the aryl rings pushes the phenyl rings almost perpendicular to the plane of the amidine backbone (tilt angles of 84º and 87º; see Table 3.3-2), therefore, the electronic density of the anionic –O–N–C=N– AMOX linkage is less delocalized on the aromatic moieties of the ligand thereby generating a stronger ligand field for the metal centre.

The total entropy change ΔS is considered to have three contributions: the change in spin multiplicity, the difference in solvation, and the change in vibrational entropy between the two isomers.[16] While the change in spin multiplicity (doublet to quartet) is the same for all three compounds, it is difficult to distinguish between the specific contributions in terms of solvation and vibrational entropy due to the bulky substituents on the aryl rings. Complexes **2a** and **2b** are *ortho*-disubstituted on the aryl rings and present similar values for the entropy change *vs*. *ortho*-monosubstituted **2c**, for which a decrease of ΔS is observed.

3.3.5.5. UV/vis spectroscopic properties

The spectroscopic properties of **2a-c** are presented in Table 3.3-6. Their UV/Vis spectra in CH_2Cl_2 show low-intensity bands in the visible and NIR region, with intense bands centred at higher energies than the solvent cut-off point (Figure 3.3-3 and Figure S4, Appendix-3.3-SI). The absorption bands in the visible and NIR region correspond to spin-allowed and Laporte-forbidden dd transitions. They present characteristic low molar absorptivity values.[23, 28] The bands at 540-550 nm, 940-980 nm, and 1230 nm are characteristic of the tetrahedral form.[5a, 8] Similar features were identified for tetrahedral cobalt(II) complexes of triazene-1-oxides[8] and β-ketoamine[5a] ligands. These three transitions could be tentatively assigned, based on Orgel diagram for tetrahedral metal complexes, to $^4A_2(F) \rightarrow ^4T_1(P)$, $^4A_2(F) \rightarrow ^4T_1(F)$, and $^4A_2(F) \rightarrow ^4T_2(F)$, respectively. [23, 28] The analysis of the electronic spectra of **2a** and **2c** shows that the UV-vis spectroscopy also supports tetrahedral geometry in solution of non-coordinated solvents for these complexes at room temperature.

Table 3.3-6 Spectroscopic data for complexes **2a-c** and their corresponding ligands **1a-c**.[a]

Cpd.	λ_{max} [nm] (ε x 10^2 [$M^{-1}cm^{-1}$])
1a	286(130)
1b	280(110)
1c	293sh(120), 313(154)
2a	247sh(239), 265sh(209), 350(32), 540(0.97), 622(0.32), 942(0.29); 1233(0.27)
2b	260sh(253), 340(55), 550(0.40), 635(0.24), 945(0.15), 1000sh(0.11), 1310 (0.11)
2c	290(196), 305(176), 540(0.57), 644sh(0.18), 987(0.16), 1247(0.20)

[a]measured in dichloromethane, at room temperature; sh = shoulder
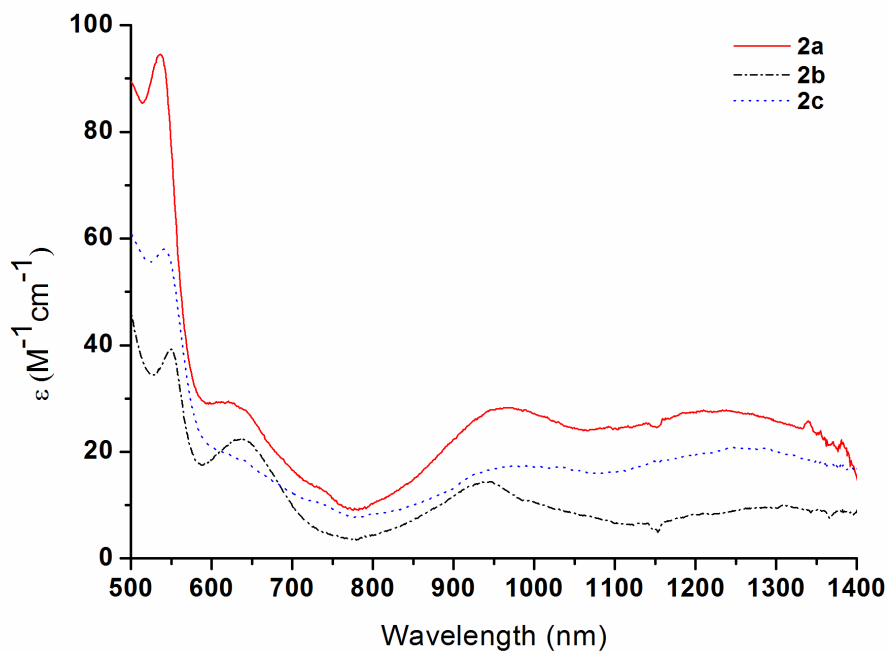
Figure 3.3-3. Electronic spectra of **2a-c** in CH_2Cl_2 at room temperature.
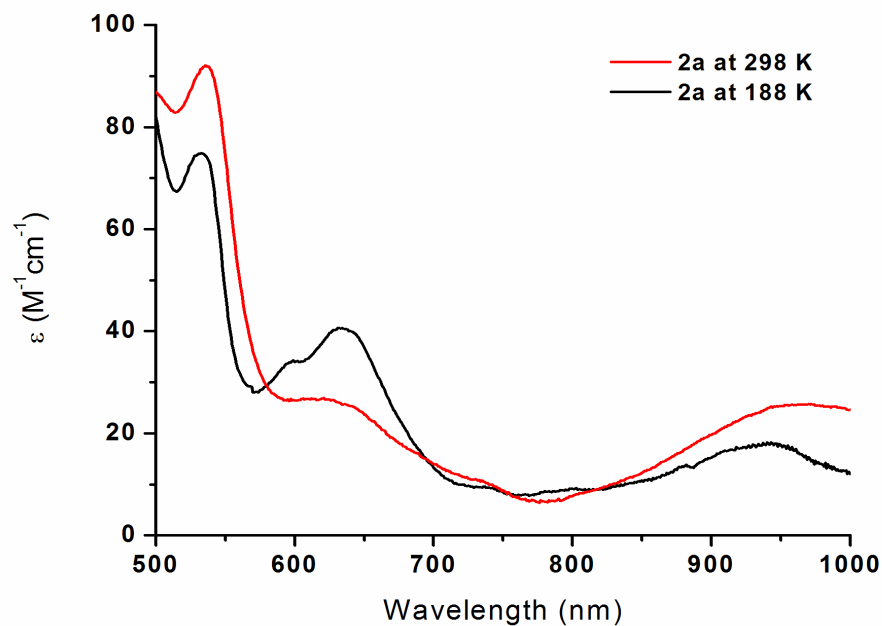
Figure 3.3-4. Electronic spectra of **2a** in CH_2Cl_2 at 298 K (red) and 188 K (black)

Figure 3.3-4 presents the comparison of the electronic spectra of **2a** recorded in CH_2Cl_2 at 298 K and 188 K. The band at 620-640 nm is indicative of the square-planar form. A second band characteristic of the square-planar isomer appears at 900-1000 nm, but overlaps with the signal identified for the tetrahedral form.[6c, 8] The square planar form is stabilized with decreasing temperature.

The absorption spectrum of **2b** confirms that the square-planar form is present in a higher proportion compared with **2a** and **2c** at room temperature. The variable temperature UV/Vis analysis for **2b** further indicates an increase in the square-planar form with decreasing temperature (Figure 3.3-5). Its comparison with the absorption spectrum of **2b** in the solid state (Figure 3.3-6) confirms the assignment of the band at 620-640 nm to the square-planar form.
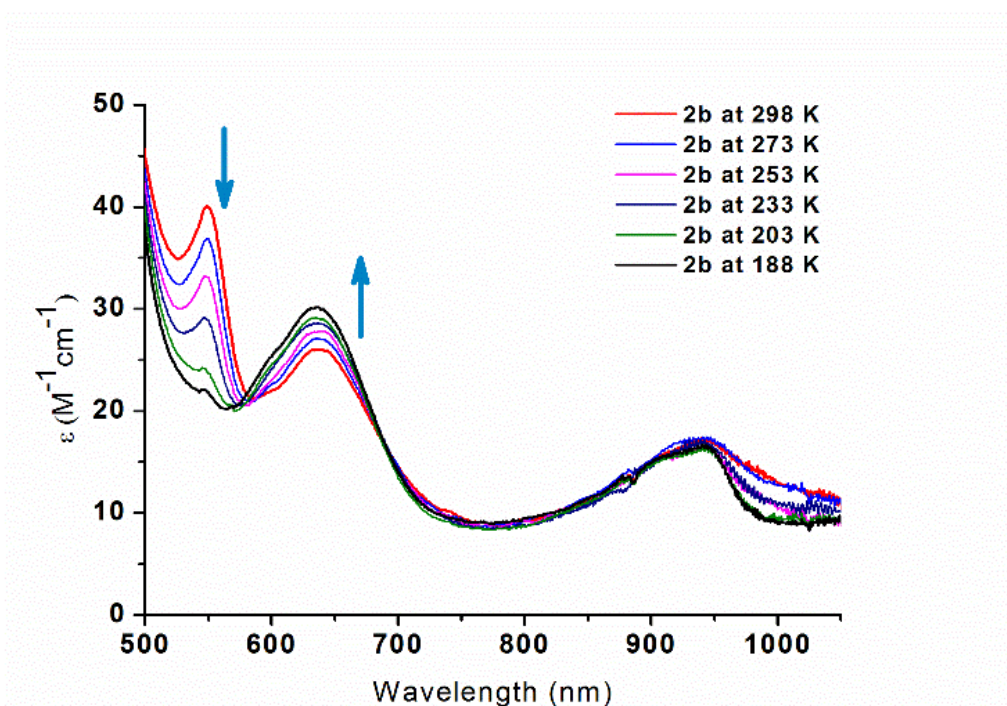
Figure 3.3-5. Electronic spectra of **2b** in CH_2Cl_2 at variable temperature.

For the AMOX ligands **1a-c** the electronic spectra display the characteristic ligand-centred (LC) π-π* transitions in the UV region, with high molar absorptivity coefficients (Figure S4, Appendix-3.3-SI).[23, 28]
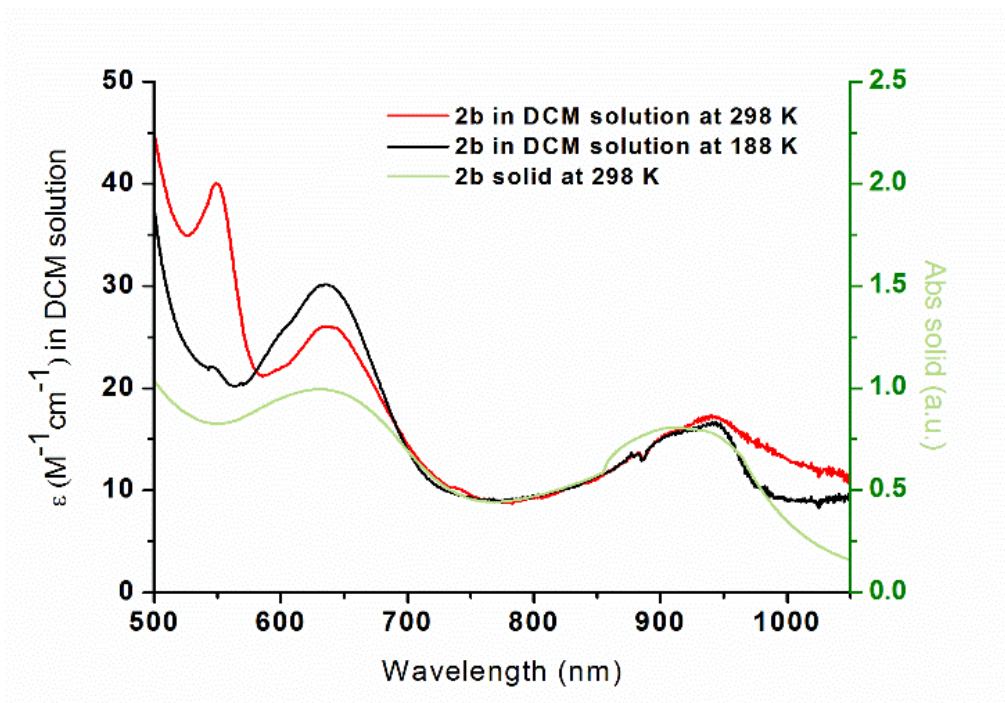
Figure 3.3-6. Electronic spectra of **2b** in CH_2Cl_2 at 298 K (red), 188 K (black), and in the solid state (green).

3.3.5.6. DFT calculations

The optimized structures of **2a** for the two forms [square-planar (S=1/2, doublet) (**2a-sqpl**) and tetrahedral (S=3/2, quadruplet) (**2a-tetra**)] in dichloromethane (spin-unrestricted uB3LYP/ LANL2DZ theory level, CPCM: CH_2Cl_2) are illustrated in Figure 3.3.-7a. The optimized calculated structure of **2a-sqpl** is in good agreement with the XRD data (Table 3.3.-2). The comparison of the energy values of the two isomers **2a-sqpl** and **2a-tetra** (Table S1, Appendix-3.3-SI) shows a slight stabilization (4.3 kcal/ mol), of the tetrahedral form, which is in accordance with the experimental observations and the values of the thermodynamic parameters.

In an effort to account for the preference for the square-planar form in the case of **2b**, DFT calculations using the same theory level were also run for its two isomers **2b-sqpl** (S=1/2, doublet) and **2b-tetra** (S=3/2, quadruplet) (Tables S1-S3, S6, S7, Appendix-3.3-SI). Non-convergence of the **2b-sqpl** frequency calculation does not allow us to conclude if this structure is at its minimum, therefore, the energy comparison is inconclusive in this

case.Figure 3.3-7b displays the spin-density plots for each of the two isomers of **2a**. The corresponding values are illustrated in Table S2, Appendix-3.3-SI. The unpaired electrons are concentrated on the metal centre (d_{yz} orbital for the square-planar form; d_{xy}, d_{xz} and d_{yz} orbitals for the tetrahedral form). The same observation stands for **2b**.
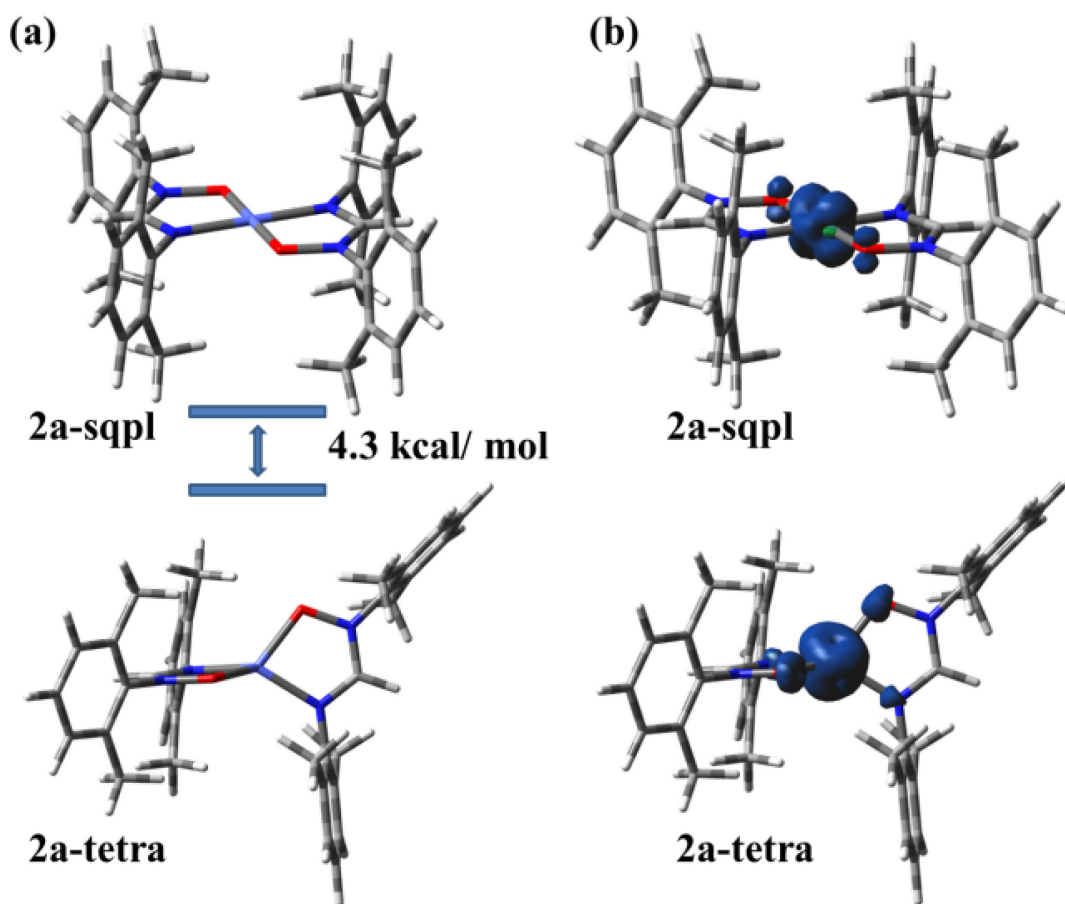
Figure 3.3-7. (a) DFT optimized structures (uB3LYP/LANL2DZ, CPCM: CH_2Cl_2) for the square-planar (S=1/2, doublet) and the tetrahedral (S=3/2, quadruplet) form of **2a**; (b) electron-spin density plots for the two isomers of **2a**.

3.3.5.7. Electrochemisty

Table 3.3-7. Electrochemical data for compounds **2a-c** in dry DCM and DMF.[a],[b]

Cpd.	$E_{1/2}$[c]		E_{pa}(irr)		E_{pc}(irr)	
	DCM	DMF	DCM	DMF	DCM	DMF
2a	0.47 (70)	0.14 (62)	1.70[d]	1.06; 1.22; 1.57	_[e]	-2.27
2b	0.41 (80)	0.17 (76)	1.88	1.15; 1.38; 1.56	_[e]	-2.34
2c	0.46 (82)	0.09 (86)	1.56	0.92; 1.21	_[e]	-2.16

E (V) *vs.* SCE

[a] [nBu$_4$N]PF$_6$ (0.1 M), compound concentration about 1mM, glassy carbon electrode, scan rate 100 mV/s, room temperature, Ar atmosphere, ferrocene used as internal reference. [b] All potentials are reported in V, *vs.* SCE (Fc/Fc$^+$ *vs.* SCE was considered 0.46V in DCM and 0.45 in DMF.[29]). [c] the difference E_{pc}-E_{pa} is given in parentheses. [d] From ref.[3]. [e] No process is observed.

Table 3.3-7 presents the electrochemical data for **2a-c** in DCM and DMF. The CVs (Figure S5, Appendix-3.3.-SI) display a one-electron reversible process, assigned to the Co(II/III) couple, followed by irreversible ligand-based oxidation processes. The easier oxidation of **2a-c** in DMF (0.09 – 0.17 V) than in DCM (0.41 – 0.47 V) can be seen as a consequence of the difference in coordination capacity and polarity of the two solvents. It is worth mentioning that no reduction wave can be observed for **2a-c** in the electrochemical window of DCM (down to -1.8 V). The same observation was reported for the cobalt(II) complexes of triazene-1-oxides.[8] The difficult reduction is in line with the anionic character of the ligand, enhanced by the effect of the electron-donating substituents. However, an irreversible reduction process can be observed in DMF, in the -2.16 – -2.34 V potential range. This process is absent in the CV of the free ligand (Figure S5, Appendix-3.3-SI), and it is therefore tentatively assigned to the Co(II/I) reduction.

3.3.6. Conclusions

New bis(AMOX) cobalt(II) complexes were synthesised and characterised. They are a new family of compounds that isomerise from square-planar LS in the solid state to tetrahedral HS in solution of non-coordinating solvents. This process was probed by the crystal structures of the compounds showing square-planar geometry at the metal centre, and the magnetic moments in solid state with values characteristic of the LS form. NMR spectroscopic data, values of solution magnetic moments and UV/Vis data are in agreement with the existence of an equilibrium between the square-planar and tetrahedral form in solution of non-coordinating solvents. The thermodynamic parameters for the isomerization equilibrium were determined. They suggest a major influence of the ligand substitution pattern on the isomerization equilibrium by a subtle interplay of steric and electronic factors. Very bulky substituents in 2,6-positions of the aryl rings of the ligand favour the square-planar (LS) form in solid state, and in solution of non-coordinating solvents. An extended delocalization of the electron density of the amidine *N*-oxide moiety is hindered in this case by steric reasons (tilt angles formed by the aryl planes and the five-membered chelate ring plane are close to 90°). As observed, slightly less bulky substituents (2-*i*PrPh and 2,6-diMePh) still stabilize the square-planar form in solid state. In solution of non-coordinating solvents at room temperature, however, they allow tilt angles more favourable to an enhanced delocalization of the electron density of the amidine *N*-oxide moiety, reducing the field strength of the corresponding ligands and stabilizing the tetrahedral form. This is also confirmed by DFT calculations, in the case of 2,6-diMePh substituents. The fact that the square-planar form stabilises with decreasing solution temperature is in line with the explanations given above.

The extra substitution position available on the central C atom in the AMOX ligand system can be seen as an advantage in term of steric modularity and electronic tuning (e.g. compared with the triazene 1-oxides analogues). We are extending the family of AMOX based metallic complexes in order to better assess and understand the interplay of steric and electronic factors and their influence on the properties in these systems.

3.3.7. Experimental section

Materials and instrumentation

The metal salts, the anilines and the triethylorthoformate were purchased from Aldrich, and the *m*-CPBA 77% was purchased from Acros, and were used without further purification. ACS grade solvents were purchased from VRW and Fisher and were removed under reduced pressure using a rotary evaporator, unless otherwise stated. Nuclear magnetic resonance (NMR) spectra were recorded in CD_2Cl_2 and $CDCl_3$ at 25°C, on the following spectrometers: Bruker AV-400, AV-500, and DRX-400. Chemical shifts (δ) are reported in part per million (ppm) relative to TMS, and are referenced to the residual solvent signal (5.35 ppm for CD_2Cl_2 and 7.26 ppm for $CDCl_3$). Variable temperature NMR spectra and T1 relaxation time measurements were performed at the NMR Spectroscopy Service at Université de Montréal. Absorption spectra were measured in dichloromethane (previously distilled), between 230 and 1400 nm, at room temperature (r.t.), on a Cary 500i UV-Vis-NIR spectrophotometer. Absorption spectra at variable temperature were measured on a Cary 6000i UV-vis-NIR spectrophotometer, using an Oxford Instrument cryostat and temperature controller. Solution samples were prepared in concentration range 10^{-5} to 10^{-3} M. Absorption spectrum of **2b** in solid form was measured on the latter instrument, using a microcrystal mounted on a solid sample holder. Electrochemical measurements were carried out in argon-purged dry DCM, at room temperature, with a BAS CV50W multipurpose equipment interfaced to a PC. The working electrode was a glassy carbon electrode. The counter electrode was a Pt wire, and the pseudo-reference electrode was a silver wire. The reference was set using an internal 1 mM ferrocene/ferrocenium sample at 460 mV and 450 mV *vs*. SCE in DCM and DMF, respectively.[29] The concentration of the compounds was about 1 mM. Tetrabutylammonium hexafluorophosphate (TBAP) was used as supporting electrolyte and its concentration was 0.10 M. Cyclic voltammograms were obtained at scan rates of 50, 100, 200, and 500 mV/s. For irreversible oxidation processes, the anodic peak was used as *E*. Experimental uncertainties are as follows: absorption maxima, ±2 nm; molar absorption coefficient, 10%; redox potentials, ± 10 mV. The microanalyses and the mass spectrometry analyses were performed at the Elemental Analysis Service and the Regional Mass Spectrometry Centre at Université de Montréal. Magnetic susceptibility measurements in solution were performed by

the Evans' method,[24] in CD_2Cl_2, using 10% vol.-% TMS, at 298 K. The sample concentration was in the order of 10^{-3} M. In the solid state, the measurements were carried out on powder or microcrystalline samples (10-20 mg), at 295 K, using a Johnson-Matthey magnetic susceptibility balance and $HgCo(NCS)_4$ as calibrant.[30] The measurements were performed at least in triplicate, and the confidence interval at 95% probability is given as error. The standard diamagnetic corrections using Pascal constants were applied.[31] Magnetic moments were calculated using: $\mu_{eff} = 2.83(\chi^M T)^{1/2}$ (1). As previously reported[6a, 6c, 8, 24] and succinctly presented in Results and Discussion part, magnetic susceptibility measurements in solution (Evans' method) were performed at variable temperature (193 – 298 K) in order to derive thermodynamic parameters for the isomerization equilibrium discussed in this paper.

X-ray structure determination

Crystal structure determination and refinement data for **2a-c** are given in Tables 3.3-1 – 3.3-2 and Figures 3.3-1 – 3.3-2. Full details are provided in Appendix-3.3-SI. CCDC-963737 (for **2b**) and -963738 (for **2c**) contain the supplementary crystallographic data for this paper. These data can be obtained free of charge from The Cambridge Crystallographic Data Centre via www.ccdc.cam.ac.uk/data_request/cif.

Computational details

Gaussian09, Revision D.01[32] was used for all theoretical calculations discussed herein, with spin-unrestricted B3LYP[33] DFT method, LANL2DZ ECP[34] basis set, and CPCM (CH_2Cl_2) solvation model. Initial atom coordinates for geometry optimization were taken from XRD data (cif) of the corresponding square-planar structures. For the tetrahedral isomers, XDR data of the Zn analogues (of tetrahedral geometry) were used, with the Zn atom changed for a Co atom. No symmetry constraints were used for the geometry optimization. Details on optimized structures are given in Tables S4-S7, Appendix-3.3-SI. No imaginary frequencies were obtained when frequency calculations on optimized geometries were performed, except for **2b-sqpl** (see DFT calculations part in the article and Appendix-3.3-SI). The values of $<S^2>$ were monitored, and didn't show major spin contamination (Table S3, Appendix-3.3-SI). The total energy values used for calculating energy differences between isomers were obtained from single point calculations on the optimized structures using a

mixed basis set: LANL2DZ ECP for the Co atom, and 6-311g(d,p) for the N, O, C, H atoms. GaussView 3.0.9[35] and Chemissian 2.200[36] software were used for data analysis, visualisation, and surface plots.

Synthesis

The syntheses of the ligands **1a-c** and complex **2a** were previously reported.[3, 13]

Synthesis of complexes

General procedure.[1c, 3] A solution of the ligand (2 eq.) in aqueous ethanol 90% was added to a solution of metal salt (1 eq.) in water. The formation of precipitate is observed almost instantly. The reaction mixture was stirred at room temperature before water was added (reaction times are specified below for each compound), and was kept at 4°C for 1-2 h before being filtered. The resulted solid was washed with hot water and aqueous ethanol 50%, and was taken in DCM and dried over MgSO$_4$. A second filtration and the solvent evaporation yielded the desired products as solids. When necessary, further purification by recrystallization was performed.

Bis(*N,N'*-bis(2,6-diisopropylphenyl)-*N*-oxidoformamidinate) of cobalt(II) (2b) – The following reagents were combined according to the general procedure: *N*-hydroxy-*N,N'*-bis(2,6-diisopropylphenyl)formamidine (**1b**) (0.40 g, 1.1 mmol, 2 eq.) and cobalt(II) acetate tetrahydrate (0.13 g, 0.51 mmol, 1 eq.). Reaction time: 90 min. Yield 0.33 g, 83%. Green crystals (X-ray quality) were obtained after recrystallization in AcOEt/ hexane (1:1).

^{1}H-NMR (CD$_2$Cl$_2$, 400 MHz) δ, ppm: 18.13 (s, 2H, -C**H**-CH$_3$); 14.79 (s, 2H, -*m*-C$_6$**H**$_3$); 11.49 (s, 1H, -*p*-C$_6$**H**$_3$); 8.83 (s, 2H, -*m*-C$_6$**H**$_3$); 8.00 (s, 6H, -CH-C**H**$_3$); 0.54 (s, 7H, -CH-C**H**$_3$ and –N-C**H**=N-); -2.50 (s, 6H, -CH-C**H**$_3$); -3.71 (s, 1H, -*p*-C$_6$**H**$_3$); -16.45 (s, 6H, -CH-C**H**$_3$); -29.91 (s, 2H, -C**H**-CH$_3$). Elemental Analysis: *calc.* (%) for C$_{50}$H$_{70}$CoN$_4$O$_2$: C 73.41, H 8.62, N 6.85; *found*: C 73.41, H 8.90, N 6.87. MS (ESI, DCM) (m/z): 817.4 [M]$^+$. IR (ATR, solid sample, cm^{-1}): 3066, 3028, 2959, 2927, 2864, 1608, 1586, 1461, 1442, 1404, 1380, 1360, 1327, 1306, 1270, 1254, 1214, 1191, 1178, 1099, 1060, 1043, 992, 930, 886, 820, 801, 770, 756, 731, 689, 642, 620, 599, 546, 534, 497, 485, 427.

Bis(*N,N'*-bis(2-isopropylphenyl)-*N*-oxidoformamidinate) of cobalt(II) (2c) – The following reagents were combined according to the general procedure: *N*-hydroxy-*N,N'*-bis(2-isopropylphenyl)formamidine (**1c**) (0.29 g, 1.0 mmol, 2 eq.) and cobalt(II) acetate tetrahydrate (0.13 g, 0.51 mmol, 1 eq.). Reaction time: 90 min. Product obtained as green powder. Yield 0.29 g, 87%. Recrystallization in DCM/ hexane (1:1) at room temperature afforded X-ray quality green crystals.

^{1}H-NMR (CD$_2$Cl$_2$, 400 MHz) δ, ppm: 69.21 (s, 1H, -*o*-C$_6$**H**$_4$), 51.14 (s, 1H, -C**H**-CH$_3$), 33.29 (s, 1H, -*m*-C$_6$**H**$_4$), 30.32 (s, 1H, -*m*-C$_6$**H**$_4$), 20.10 (s. 1H, -*p*-C$_6$**H**$_4$), 11.66 (s, 1H, -*m*-C$_6$**H**$_4$), 8.87 (s, 6H, -CH-C**H**$_3$), 0.12 (s, 1H, -N-C**H**=N-), -9.54 (s, 1H, -*m*-C$_6$**H**$_4$), -28.99 (s, 6H, -CH-C**H**$_3$), -32.67 (s, 1H, -C**H**-CH$_3$), -34.12 (s, 1H, -*p*-C$_6$**H**$_4$), -200.6 (s, 1H, -*o*-C$_6$**H**$_4$). Elemental Analysis: *calc.* (%) for C$_{38}$H$_{46}$CoN$_4$O$_2$: C 70.25, H 7.14, N 8.62; *found*: C 70.43, H 7.13, N 8.60. MS (ESI, DCM) (m/z): 650.2 [M+H]$^{+}$. IR (ATR, solid sample, cm^{-1}): 3066, 3027, 2955, 2927, 2859, 1605, 1586, 1572, 1495, 1484, 1446, 1407, 1379, 1360, 1295, 1276, 1243, 1227, 1198, 1162, 1113, 1093, 1085, 1035, 997, 938, 888, 863, 823, 775, 755, 679, 638, 628, 538, 507, 468, 436.

3.3.8. Acknowledgments

3.3.9. Supporting Information

Supporting Information for this article is available on the WWW under http://dx.doi.org/10.1002/ejic.201402895. In this thesis, the same material is found in Appendix-3.3-SI.

3.3.10. References

[1]   a) A. Krajete, G. Steiner, H. Kopacka, K.-H. Ongania, K. Wurst, M. O. Kristen, P. Preishuber-Pfluegl, B. Bildstein, *Eur. J. Inorg. Chem.* **2004**, 1740-1752; b) A. Mishra, M. H. Mohabey, *Asian J. Chem.* **2002**, *14*, 1794-1796; c) A. N. Verma, S. B. Gholse, S. P. Sangal, *J. Indian Chem. Soc.* **1995**, *72*, 685-688; d) L. H. Briggs, R. C. Cambie, I. C. Dean, P. S. Rutledge, *Aust. J. Chem.* **1976**, *29*, 357-366.

[2]   a) F. T. Edelmann, *Chem. Soc. Rev.* **2009**, *38*, 2253-2268; b) F. T. Edelmann, *Adv. Organomet. Chem.* **2008**, *57*, 183-352; c) S. Collins, *Coord. Chem. Rev.* **2011**, *255*, 118-138; d) S. T. Barry, *Coord. Chem. Rev.* **2013**, *257*, 3192-3201.

[3]   M. Cibian, S. Derossi, G. S. Hanan, *Dalton Trans.* **2011**, *40*, 1038-1040.

[4]   H. A. Goodwin*, Vol. 234* (Eds.: P. Gütlich, H. A. Goodwin), Springer Berlin / Heidelberg, **2004**, pp. 786-786.

[5]   a) R. H. Holm, M. J. O'Connor, *Progr. Inorg. Chem.* **1971**, *14*, 241-401; b) J. Cirera, P. Alemany, S. Alvarez, *Chem. Eur. J.* **2004**, *10*, 190-207.

[6]   a) G. W. Everett, Jr., R. H. Holm, *J. Am. Chem. Soc.* **1965**, *87*, 5266-5267; b) G. W. Everett, Jr., R. H. Holm, *Inorg. Chem.* **1968**, *7*, 776-785; c) G. W. Everett, Jr., R. H. Rholm, *J. Am. Chem. Soc.* **1966**, *88*, 2442-2451; d) D. H. Gerlach, R. H. Holm, *Inorg. Chem.* **1969**, *8*, 2292-2297; e) R. H. Holm, A. Chakravorty, L. J. Theriot, *Inorg. Chem.* **1966**, *5*, 625-635; f) A. H. Maki, N. Edelstein, A. Davison, R. H. Holm, *J. Am. Chem. Soc.* **1964**, *86*, 4580-4587.

[7]   R. Poli, *Chem. Rev.* **1996**, *96*, 2135-2204.

[8]   J. A. Wolny, M. F. Rudolf, Z. Ciunik, K. Gatner, S. Wolowiec, *J. Chem. Soc., Dalton Trans.* **1993**, 1611-1622.

[9]   B. S. Jaynes, L. H. Doerrer, S. Liu, S. J. Lippard, *Inorg. Chem.* **1995**, *34*, 5735-5744.

[10]   S. A. Carabineiro, L. C. Silva, P. T. Gomes, L. C. J. Pereira, L. F. Veiros, S. I. Pascu, M. T. Duarte, S. Namorado, R. T. Henriques, *Inorg. Chem.* **2007**, *46*, 6880-6890.

[11]   L. C. Kalutarage, P. D. Martin, M. J. Heeg, C. H. Winter, *Journal of the American Chemical Society* **2013**, *135*, 12588-12591.

[12]   a) Z. Ciunik, J. A. Wolny, M. F. Rudolf, *Acta Crystallogr., Sect. C: Cryst. Struct. Commun.* **1991**, *47*, 2539-2541; b) Z. Ciunik, J. A. Wolny, M. F. Rudolf, S. Wolowiec, *J. Chem. Soc., Dalton Trans.* **2002**, 885-895; c) M. F. Rudolf, J. Wolny, Z. Ciunik, P. Chmielewski, *J. Chem. Soc., Chem. Commun.* **1988**, 1006.

[13]   a) M. Cibian, S. Langis-Barsetti, G. S. Hanan, *Synlett* **2011**, 405-409; b) M. Cibian, S. Derossi, G. S. Hanan, *Acta Crystallogr., Sect. E: Struct. Rep. Online* **2009**, *65*, o2485; c) E. Baranowska, I. Panfil, C. Belzecki, *Bull. Acad. Pol. Sci., Ser. Sci. Chim.* **1977**, *25*, 93-99; d) C. Belzecki, I. Panfil, *Bull. Acad. Pol. Sci., Ser. Sci. Chim.* **1975**, *23*, 119-123.

[14]   a) J. A. Wolny, M. F. Rudolf, Z. Ciunik, K. Gatner, S. Wolowiec, *J. Chem. Soc., Dalton Trans.* **1993**, 1611-1622; b) A. L. Smith, L. A. Clapp, K. I. Hardcastle, J. D. Soper, *Polyhedron* **2010**, *29*, 164-169; c) B. S. Manhas, B. C. Verma, S. B. Kalia, *Polyhedron* **1995**, *14*, 3549-3556; d) E. Bill, E. Bothe, P. Chaudhuri, K. Chlopek, D. Herebian, S. Kokatam, K. Ray, T. Weyhermuller, F. Neese, K. Wieghardt, *Chem. Eur. J.* **2005**, *11*, 204-224; e) M. C. Karunarathne, T. J. Knisley, G. S. Tunstull, M. J. Heeg, C. H. Winter, *Polyhedron* **2013**, *52*, 820-830.

[15]   V. D. Vreshch, J.-H. Yang, H. Zhang, A. S. Filatov, E. V. Dikarev, *Inorg. Chem.* **2010**, *49*, 8430-8434.

[16]   R. D. Jones, D. A. Summerville, F. Basolo, *Chem. Rev.* **1979**, *79*, 139-179.

[17]   CCDC search on Septembre 09, 2014

[18]   A. I. Poddel'sky, V. K. Cherkasov, G. K. Fukin, M. P. Bubnov, L. G. Abakumova, G. A. Abakumov, *Inorganica Chimica Acta* **2004**, *357*, 3632-3640.

[19]   F. Di Salvo, F. Teixidor, C. Viñas, J. G. Planas, M. E. Light, M. B. Hursthouse, N. Aliaga-Alcalde, *Cryst. Growth Des.* **2012**, *12*, 5720-5736.

[20]   W.-B. Yuan, H.-Y. Wang, J.-F. Du, S.-W. Chen, Q. Zhang, *Acta Crystallogr., Sect. E: Struct. Rep. Online* **2006**, *62*, m3504-m3505.

[21]   L. Yang, D. R. Powell, R. P. Houser, *Dalton Trans.* **2007**, 955-964.

[22]   a) K. C. D. Robson, C. D. Phillips, B. O. Patrick, W. S. McNeil, *Dalton Trans.* **2010**, *39*, 2573-2578; b) I. S. Tidmarsh, B. F. Taylor, M. J. Hardie, L. Russo, W. Clegg, M. D. Ward, *New Journal of Chemistry* **2009**, *33*, 366.

[23]   F. A. Cotton, G. Wilkinson, C. A. Murillo, M. Bochmann, *Advanced Inorganic Chemistry*, 6th ed., Wiley, **1999**, 820-821

[24]   D. F. Evans, *J. Chem. Soc.* **1959**, 2003-2005.

[25]   D. Ostfeld, I. A. Cohen, *J. Chem. Educ.* **1972**, *49*, 829.

[26]   D. R. Lide, *CRC Handbook of Chemistry and Physics - Internet Version, 9th edition* **2014**, 6-158 - 156-162.

[27]   The error associated with this method is relatively high, therefore only the results that are different within at least 2σ are compared and discussed.

[28]   C. Housecroft, A. Sharpe, *Inorganic Chemistry, 4th ed.*, Pearson, Harlow, **2012**, 687-699

[29]   N. G. Connelly, W. E. Geiger, *Chem. Rev.* **1996**, *96*, 877-910.

[30]   R. P. Sharma, K. K. Bhasin, *Bull. Chem. Soc. Jpn.* **1986**, *59*, 1603-1604.

[31]   C. J. O'Connor, *Prog. Inorg. Chem.* **1982**, *29*, 203-283.

[32]   G. W. T. M. J. Frisch, H. B. Schlegel, G. E. Scuseria, M. A. Robb, J. R. Cheeseman, G. Scalmani, V. Barone, B. Mennucci, G. A. Petersson, H. Nakatsuji, M. Caricato, X. Li, H. P. Hratchian, A. F. Izmaylov, J. Bloino, G. Zheng, J. L. Sonnenberg, M. Hada, M. Ehara, K. Toyota, R. Fukuda, J. Hasegawa, M. Ishida, T. Nakajima, Y. Honda, O. Kitao, H. Nakai, T. Vreven, J. A. Montgomery, Jr., J. E. Peralta, F. Ogliaro, M. Bearpark, J. J. Heyd, E. Brothers, K. N. Kudin, V. N. Staroverov, R. Kobayashi, J. Normand, K. Raghavachari, A. Rendell, J. C. Burant, S. S. Iyengar, J. Tomasi, M. Cossi, N. Rega, J. M. Millam, M. Klene, J. E. Knox, J. B. Cross, V. Bakken, C. Adamo, J. Jaramillo, R. Gomperts, R. E. Stratmann, O. Yazyev, A. J. Austin, R. Cammi, C. Pomelli, J. W. Ochterski, R. L. Martin, K. Morokuma, V. G. Zakrzewski, G. A. Voth, P. Salvador, J. J. Dannenberg, S. Dapprich, A. D. Daniels, Ö. Farkas, J. B.

Foresman, J. V. Ortiz, J. Cioslowski, and D. J. Fox, **2013,** *Gaussian09, Revision D.01,* Gaussian, Inc.; Wallingford CT.

[33]   a) C. Lee, W. Yang, R. G. Parr, *Phys. Rev. B: Condens. Matter* **1988**, *37*, 785-789; b) B. Miehlich, A. Savin, H. Stoll, H. Preuss, *Chem. Phys. Lett.* **1989**, *157*, 200-206.

[34]   a) P. J. Hay, W. R. Wadt, *J. Chem. Phys.* **1985**, *82*, 270-283; b) P. J. Hay, W. R. Wadt, *J. Chem. Phys.* **1985**, *82*, 299-310; c) T. H. H. Dunning, P. J., in *Methods of Electronic Structure Theory, Vol. 2* (Ed.: H. F. Schaefer), Plenum Press, New York, **1977**; d) W. R. Wadt, P. J. Hay, *J. Chem. Phys.* **1985**, *82*, 284-298.

[35]   T. K. R. D. K. Dennington II, J. Millam, K. Eppinnett, W. L. Hovell, R. Gilliland, **2003,** *GaussView 3.0.9,* Semichem, Inc.; Shawnee Mission, KS.

[36]   L. Skripnikov, **2005 - 2011,** *Chemissian V2.200.*

Chapitre 4: Geometry and Spin Change at the Heart of a Cobalt(II) Complex: A Special Case of Solvatomorphism

4.1. Résumé

Des études structurales et spectroscopiques montrent un cas spécial de solvatomorphisme: des modifications de la géométrie et de l'état de spin sont induites par liaisons hydrogènes, dans une même composé, le bis(chelate) de cobalt(II). Les structures à l'état solide sont présentées pour les deux formes du complexe: la forme tétraédrique et la forme plan carré solvatée. Les mesures du moment magnétique ainsi que les analyses spectroscopiques EPR confirment l'état haut spin de la forme tétraédrique (μ_{eff} = 4.7 μ_B) et l'état bas spin du solvatomorphe plan carré. Des interactions par liaisons hydrogènes spécifiques entre les molécules de solvant et les atomes des cycles chélates du complexes (O1$\cdots$H-CHCl$_2$ (d = 2.26 Å, D = 3.24 Å, θ = 173°); O2$\cdots$H-CHCl$_2$ (d = 2.22 Å, D = 3.19 Å, θ = 165°)) jouent un rôle primordial dans la stabilisation du système vers un état fondamental bas spin.

Contribution:

Mihaela Cibian: tous les travaux présentés dans l'article et la rédaction de l'article

Garry S. Hanan: supervision, révision de l'article

Geometry and Spin Change at the Heart of a Cobalt(II) Complex: A Special Case of Solvatomorphism

Mihaela Cibian and Garry S. Hanan*

Département of Chemistry, Université de Montréal, Montréal, Québec, H3T-1J4, Canada

*: E-mail: garry.hanan@umontreal.ca. Fax: 1-514-343-7586

4.2. Table of content graphic

What makes this heart beat?

Hydrogen bonding induces geometry and spin change within a same *N,O*-(bis)chelate of cobalt(II), as proved by complete structural characterization and spectroscopic methods. The system offers important insights into the role of the weak recognition forces and co-operative effects with respect to stereochemistry and spin preferences in four-coordinated metal complexes.

4.3. Abstract

Structural analysis and spectroscopic methods reveal a special case of solvatomorphism: hydrogen-bonding-induced geometry and spin change within a same *N,O*-(bis)chelate of cobalt(II). Solid state structures are presented for both the tetrahedral and the solvated square-planar forms of the complex. Magnetic moment measurements and ESR spectroscopy confirm the high-spin state of the tetrahedral form (μ_{eff} = 4.7 μ_B) and the low-spin state of the square-planar solvatomorph. Specific hydrogen-bonding interactions between the solvent molecules and the complex chelate ring (O1···H-CHCl$_2$ (d = 2.26 Å, D = 3.24 Å, θ = 173°); O2···H-CHCl$_2$ (d = 2.22 Å, D = 3.19 Å, θ = 165°)) play a pivotal role in biasing the system toward the low-spin ground state.

4.4. Introduction

Theoretical rules to predict the stereochemistry and spin state of a particular metal ion – ligand combination may open the doors to new magnetic materials, however, their validation by comparison with experimental data is also necessary.[1] Considerable research focuses on studying metal-ligand interactions and their influence on molecular structure, physical properties, and chemical reactivity,[2] but the prediction and control of stereochemistry and spin-states are still far from being achieved.[1a-d] For specific d^n metal configurations (d^3,d^4,d^6,d^7) in four-coordinated ligand environments, it was established that both square-planar and tetrahedral geometries are possible.[1a, 1b] More specifically, for cobalt(II) d^7 bis-chelates, the configurational equilibrium between square-planar and tetrahedral forms was previously reported for several ligand types: β-ketoamines,[3] iminopyrrolyl,[4] α-imino alkoxides,[5] triazene 1-oxides,[6] and amidine *N*-oxides (AMOXs).[7]

These systems exhibit not only stereoisomerism but also spin isomerism from high spin (HS), tetrahedral cobalt(II) complexes (S = 3/2) to low spin (LS), square-planar cobalt(II) complexes, (S = 1/2),[2d, 2e, 8] although a few exceptions exist.[9] The square-planar form is usually observed in the solid state, while the tetrahedral form (or an equilibrium between the two forms) is found in solution of non-coordinating solvents. In all such systems, the specific geometry/ spin state combination in the ground state was shown to be mainly determined by

the properties of the ligand, and to be particularly sensitive to the ligand substitution pattern.[3-7] However, within a given metal complex, factors other than those directly linked to the metal and/ or the ligand have to be considered: reaction conditions, solvent, temperature, and secondary interactions. Examples of the same metal complex being isolated and characterized in both forms in the solid state are rare In the case of cobalt bis-chelates of iminopyrrolyl-type ligands[4] and triazene-1-oxides[6], the two forms were isolated in the solid state, but structural evidence is presented only for one of the isomers.

The results of a Cambridge Structural Database (CSD)[10] search for cobalt complexes with the same bis(chelate) ligand environment and different geometries at the metal centre are presented in Table S1, Supplementary Information (SI) (Appendix-4-SI). The analysis of these results indicates that three categories of factors play an important role in the change of geometry: i) the substitution pattern of the ligand; ii) the oxidation state of the metal and/ or the ligand; iii) the secondary interactions (e. g., hydrogen bonding, electrostatic interactions). This third category is also central to the spin and structure changes in catalytic processes of biological systems,[11] as well as in areas of solid-state chemistry, such as polymorphic/ solvatomorphic[12] and magnetic[13] materials. For example, anionic cobalt(II) complexes of fluorinated alkoxide ligands were shown to display varying geometries at the metal center depending on their interactions with different cations.[9a, 14] These examples highlight how the subtle differences in the structure invoked by weak interactions result in different coordination geometries, albeit with no spin change in these cases.

In the same vein, the present work explores the effect of metal–ligand interaction on the structure of complex **1** and its properties, while examining the critical effect that weak forces and stimuli (e.g., hydrogen bonding, solvation, temperature) have on its final structure(s). We report a special case of solvatomorphism by structurally characterizing **1** in its two forms (Figures 4-1 - 4-4): the orange tetrahedral form (**1-orange**) and the green square-planar bis-dichloromethane solvatomorph (**1-green**). The spin change associated with the structural transformation in this system is also demonstrated.
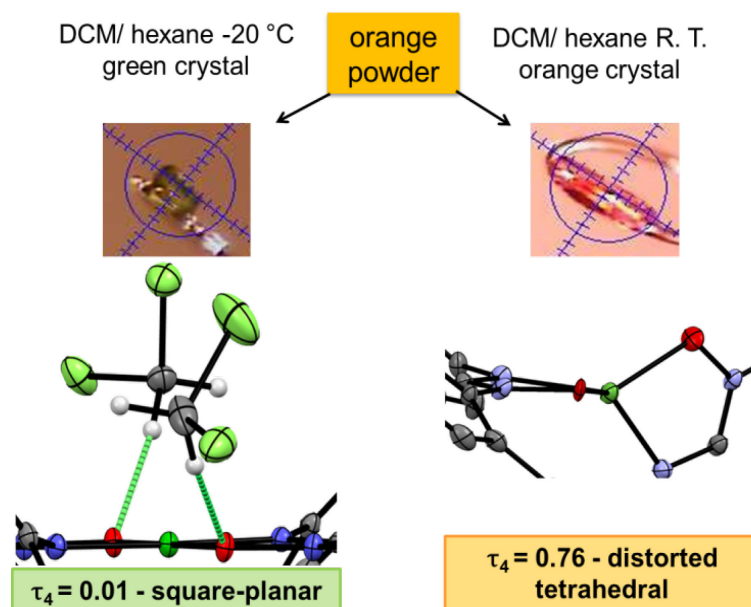
Figure 4-1. The two forms of **1** with different geometries at the metal centre.

4.5. Results and Discussion

4.5.1. Synthesis
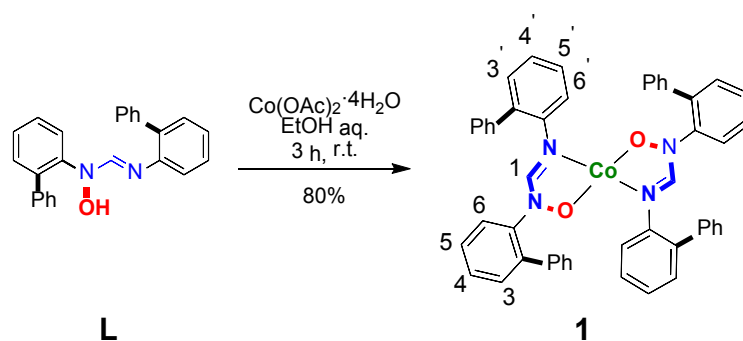
Scheme 4-1. Synthesis of bis[*N,N'*-bis(2-biphenyl)-*N*-oxidoformamidinate] cobalt(II) (**1**).

Complex **1** was readily synthesized in 80% yield by allowing two equivalents of the ligand **L** to react with the cobalt acetate salt in ethanol at room temperature (Scheme 4-1), and

it was isolated as an air-stable orange powder. In accordance with its neutral nature, it is poorly soluble in alcohols and other polar solvents. Recrystallization from DCM/ hexane by slow evaporation at different temperatures gave the two types of crystals (Figure 4-1). Upon evaporation of a DCM solution of **1** at room temperature, a mixture of **1-orange** and **1-green** was obtained, although it was found that the formation of **1-green** is favoured at low temperatures. Qualitative observations are presented in Figure 4-2.

Figure 4-2. Thermal transformations of **1-orange** and **1-green** over time.

The two forms were isolated independently in solid state as both powders and crystals, and were fully characterized. The **1-green** powder was obtained by evaporation from a DCM solution of **1**, at $0 - 5$ °C. However, at room temperature **1-green** slowly converts back to **1-orange** over time with loss of DCM. Neither cooling of **1-orange** nor its exposure to DCM vapour results in the formation of **1-green**.

4.5.2. X-ray Diffraction and Thermogravimetric Analyses

The solid state structures of **1-green** and **1-orange** highlight the square-planar ($\tau_4{}^{[15]} = 0.01$) and pseudo-tetrahedral ($\tau_4 = 0.76$) geometries at the cobalt centre, respectively (Figure 4-3, Figure 4-4, Table 4-1, and Figures S1-S4, Table S2; Appendix-4-SI).

The periplanar angle between the two chelate rings are $2(1)°$ and $85(1)°$ in **1-green** and **1-orange**, respectively. Selected bond lengths and angles of the two structures are
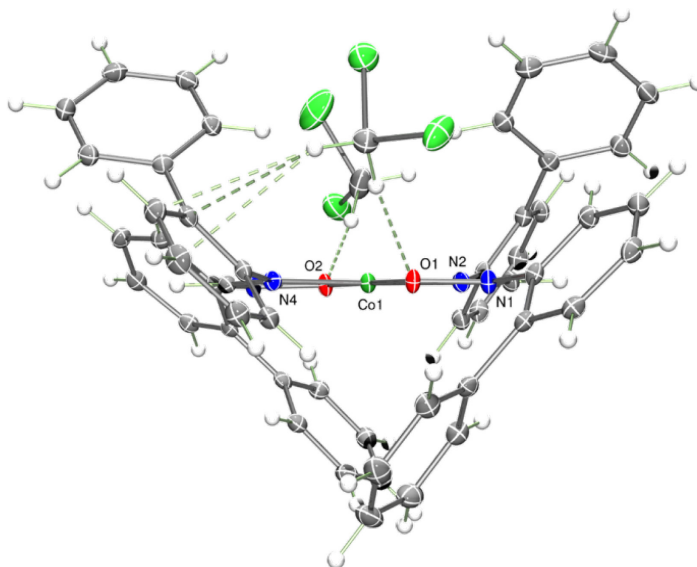
Figure 4-3. The solid state structure of **1-green**: ORTEP view highlighting the hydrogen-bonding between the co-crystallized DCM molecules and the compound – ellipsoids are shown at 50% probability level.
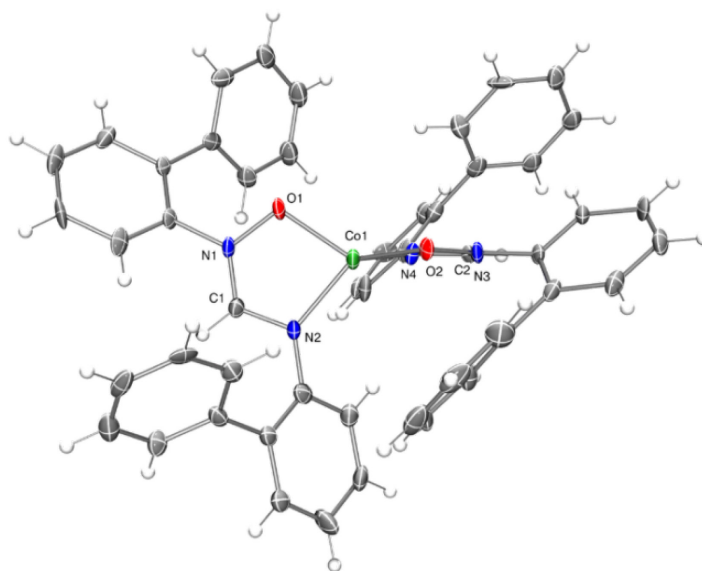
Figure 4-4. The solid state structure of **1-orange**: ORTEP view with ellipsoids shown at 50% probability level.

compared in Table 4-1. The mean Co–O and Co–N bond lengths of 1.840(2) Å and 1.900(1) Å in **1-green** are comparable to the corresponding values in previously reported square-planar (LS) Co(AMOX)$_2$ complexes[7] (cpds. **2-4**, Table 4-1), being identical[16] with those found in compound **4** (1.8433(1) Å and 1.898(1) Å), which has a similar mono *ortho*-substitution pattern. Both Co–O and Co–N bond lengths in **1-green** are significantly longer than those found in square-planar cobalt(II) (LS) complexes of triazene 1-oxide ligands (cpd. **5**, Table 4-1) and *o*-aminophenol-redox-active-type ligands (cpd. **6**, Table 4-1).

The Co–O bond length in **1-green** is also comparable with those found in cobalt complexes of α-imino alkoxide-[5] and carbohydrazide-type[17] ligands (cpds. **7** and **8**, Table 4-1), while the Co–N bond is longer in **1-green** versus **7** and **8**. In **1-orange**, the mean Co–O bond length (1.951(7) Å) is similar to the corresponding values reported for tetrahedral (HS) cobalt(II) complexes of fluorinated alkoxide ligands[14a] (1.952(3) Å), and α-iminoketone-type ligands (cpd. **10**, Table 4-1). The mean Co–N bond length 1.989(8) Å is comparable to those found in tetrahedral cobalt complexes of triazene 1-oxide ligands[6] (cpd. **9**, Table 4-1), and β-ketoaminato ligands[18] (cpd. **11**, Table 4-1). The Co-O and Co-N bond lengths are longer by 0.11(1) and 0.09(1) Å in **1-orange** (tetrahedral) *vs.* **1-green** (square-planar), as expected based on crystal- and ligand-field theory.[19] This point is also reflected in the expansion of the O–N–C angle in **1-orange** (119.5(8)°) *vs.* **1-green** (115.7(1)°), but not in the value of the endocyclic O–Co–N angle (84.3(3)°), which is identical[17] in both forms of **1**. The tightening of this angle with respect to the ideal values is imposed by the strain of the five-membered chelate ring. For **1-green**, examination of the interactions between the two co-crystallized DCM molecules and **1** (Figure 4-3) shows that the DCM protons (of a same molecule) participate in hydrogen bonding: one DCM proton interacts with one O atom from the metal chelate ring (O1···H-CHCl$_2$ (d = 2.26 Å, D = 3.24 Å, θ = 173°), O2···H-CHCl$_2$ (d = 2.22 Å, D = 3.19 Å, θ = 165°) while the other DCM proton is implicated in a H···πC(sp^2) type weak interaction (d = 2.6 – 2.8 Å). Hydrogen bonding of Cl···*p*-H-C(sp^2) type (d = 2.93 Å, D = 3.61 Å, θ = 130°; Figure S4, SI) is also observed. A CSD[10] search for intermolecular O···H-CHCl$_2$ contacts, with O atom part of a five- or six-membered metal chelate ring, and directly linked to the metal ion, revealed that **1-green** has the shortest interaction of this type reported for a four-coordinated cobalt complex (Table S3; Appendix-4-SI).

Table 4-1. Selected bond distances (Å) and angles (°) for **1-green** and **1-orange**, and for chosen cobalt *N,O*-bischelates **2-11**

Cpd.	$\tau_4^{[k]}$	Bond distances (Å)					Angle (°)	Tilt angle[l] (°)	
		Co-O1	Co-N2	C1-N1	C1-N2	O1-N1	O1-Co-N2	Ar(NO)	ArN
1-green	0.01	1.837(1) 1.843(1)	1.900(1)[m]	1.314(2)[m]	1.317(2)[m]	1.389(2)[m]	84.7(1)[m]	47(1)[m]	50(1) 56(1)
1- orange	0.76	1.951(7)[m]	1.989(8)[m]	1.319(14)[m]	1.330(13)[m]	1.378(11)[m]	83.8(3)[m]	42(1)[m]	45(1)[m]
1-green⊃2DCM [a] **(DFT – gas-phase)**	0.05	1.876	1.940	1.342	1.331	1.428	84.6	53	54
1-green⊃2DCM [b] **(DFT – CH₂Cl₂)**	0.02	1.884	1.940	1.341	1.331	1.433	84.4	59	58
1-green[a] **(DFT – gas-phase)**	0.04	1.888	1.950	1.340	1.330	1.431	84.2	55	52
1-green[b] **(DFT – CH₂Cl₂)**	0.02	1.893	1.953	1.339	1.331	1.433	84.1	59	54
1-orange[a] **(DFT – gas-phase)**	0.72	1.983	2.007	1.344	1.336	1.414	83.5	53	66
1-orange[b] **(DFT – CH₂Cl₂)**	0.73	2.004	2.022	1.342	1.338	1.417	82.9	56	53

Cpd.	$\tau_4^{[k]}$	Bond distances (Å)					Angle (°)	Tilt angle[l] (°)	
		Co-O1	Co-N2	C1-N1	C1-N2	O1-N1	O1-Co-N2	Ar(NO)	ArN
2[c]	0	1.834(1)	1.886(1)	1.319(2)	1.312(2)	1.392(1)	84.5(1)	59(1)	79(1)
3[c]	0	1.841(2)	1.883(1)	1.319(2)	1.306(3)	1.389(2)	84.9(1)	84(1)	87(1)
4[c]	0	1.833(1)	1.898(1)	1.316(2)	1.316(2)	1.387(1)	84.6(1)	60(1)	60(1)
5[d]	0	1.805(3)	1.856(3)	-	-	1.339(4)	81.9(1)	-	39(1)
6[e]	0.02	1.823(3)[m]	1.836(3)[m]	-	-	-	85.7(1)[m]	-	90(1)
7[f]	0	1.848(1)[m]	1.967(1)[m]	-	-	-	84.3(1)[m]	-	-
8[g]	0	1.846(1)	1.938(1)	-	-	-	84.5(1)	-	-
9[h]	0.73	1.965(4)[m]	1.978(4)[m]	-	-	1.348(5)[m]	79.7(1)[m]		8(1)[m]
10[i]	0.76	1.955(1)	1.954(1)	-	1.326(2)	-	83.9(1)	-	26(1)[n]
11[j]	0.87	1.929(4)	1.966(4)	-	-	-	96.3(1)	-	-

[a] theory level: uB3LYP/ LANL2DZ, gas-phase; [b] theory level: uB3LYP/ LANL2DZ, PCM: CH_2Cl_2; [c] **2-4**: Co(L)$_2$, L=amidine-oxide-type[7]; [d] **5** Co(L)$_2$, L=triazene 1-oxide-type (GESTED)[20]; [e] **6**: Co(L)$_2$, L=o-aminophenol-type (FESFAL)[21]; [f] **7**: Co(L)$_2$, L=α-imino alkoxide-type (GIFJIQ)[5]; [g] **8**: Co(L)$_2$, L=carbohydrazide-type (DOBYEA)[17]; [h] **9**: Co(L)$_2$, L=triazene 1-oxide-type (YANWOZ)[6]; [i] **10**: Co(L)$_2$, L=α-iminoketone-type (YIPHIP)[22]; [j] **11**: Co(L)$_2$, L=β-ketoaminato-type (WAYLOZ)[18]; [k] as defined by Houser[15]; [l] angle between the plane of the aromatic ring and the plane of the -N-C=N- moiety; [m] average value; [n] the Ar substituent is positioned on the C atom of the α-iminoketone ligand.

The participation of the O atoms in hydrogen bonding interactions lowers their π-donation character and combined with the overall packing interactions contributes to the stabilization of the square-planar form of **1**. Further examination of the packing for **1-green** also shows non-classical intermolecular interactions of H···πC(sp^2) and πC(sp^2)···πC(sp^2) type (Figure S3; Appendix-4-SI). For **1-orange** only non-classical hydrogen bonding of H···π C(sp^2) type is observed (Figure S4; Appendix-4-SI).

Thermogravimetric analyses were performed for both **1-orange** and **1-green** (Figures S5-S7; Appendix-4-SI) in the 25 – 600 °C temperature range. A weight loss of 14% is observed for **1-green** between 25 – 90 °C, corresponding to the loss of 1.6 DCM molecules. This value is also confirmed by elemental analysis, and suggests that the solvated square-planar form contains traces of the unsolvated tetrahedral form, as shown by the magnetic moment values (*vide infra*).[23] The temperature of the DCM loss (43 – 90 °C, with the maximum at 70 °C) is indicative of the strong interaction of the DCM with the complex in the solid state, in agreement with packing analysis of the X-ray structure.

4.5.3. Magnetic, Spectroscopic and Electrochemical properties

In four-coordinate cobalt(II) systems, the square-planar to tetrahedral structural change is usually accompanied by a change in spin.[8] The values of the magnetic moments obtained in the solid state at room temperature for **1-orange** (4.7 μB) and **1-green** (2.6 μB) confirm the spin change. The value of 4.7 μB is in the range for high spin magnetic moments (4.2-5.2 μB) expected for cobalt(II) in tetrahedral geometry,[2e, 8] higher than the spin-only value (3.89 μB) due to spin-orbit coupling.[24] The same value of 4.7 μB is measured by Evans' method at room temperature for the solution-phase (CD_2Cl_2) magnetic moment of **1**. The value of 2.6 μB is slightly higher than expected for the square-planar low spin cobalt(II) (1.8 -2.2 μB). [2e, 25] The results of thermogravimetric and elemental analyses indicate that a trace amount of **1-orange** (HS) is present, which would raise the magnetic moment of **1-green**.

ESR spectra recorded for **1-green** and **1-orange** solids at room temperature (Figure 4-5) are broad, characteristic for pure solid samples due to dipolar interactions.[26] The square-planar LS form of **1-green** is confirmed by the signal obtained, typical for cobalt(II) d^7 (S=1/2).[27] The form of the signal and the *g* values ($g_1 = 2.70$ and $g_2 \approx g_3 = 2.15$) are
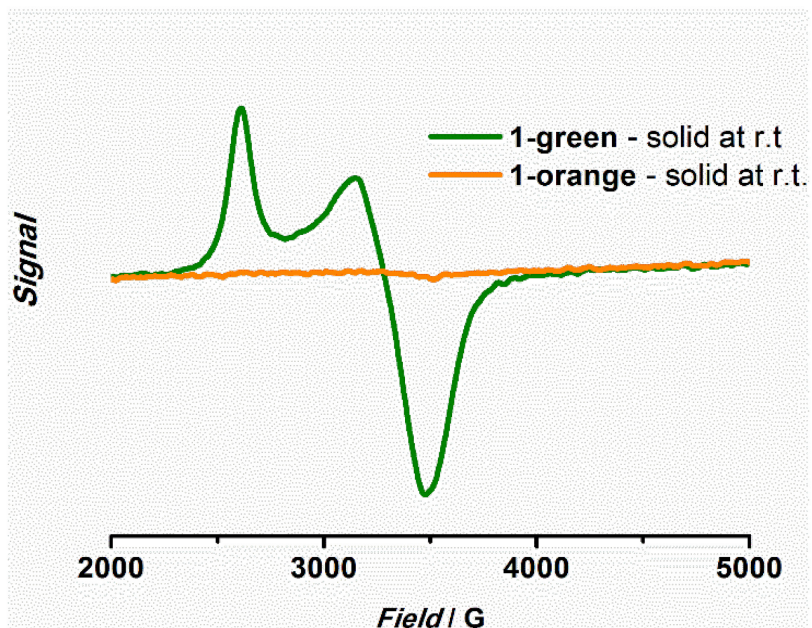
Figure 4-5. X-Band ESR spectra of **1-green** (green line) (g_1 = 2.70, $g_2 \approx g_3$ = 2.15) and **1-orange** (orange line) in the solid state, at room temperature. Conditions: frequency 9.8800 GHz, power 2 mW, modulation 0.5 mT/ 100 kHz.
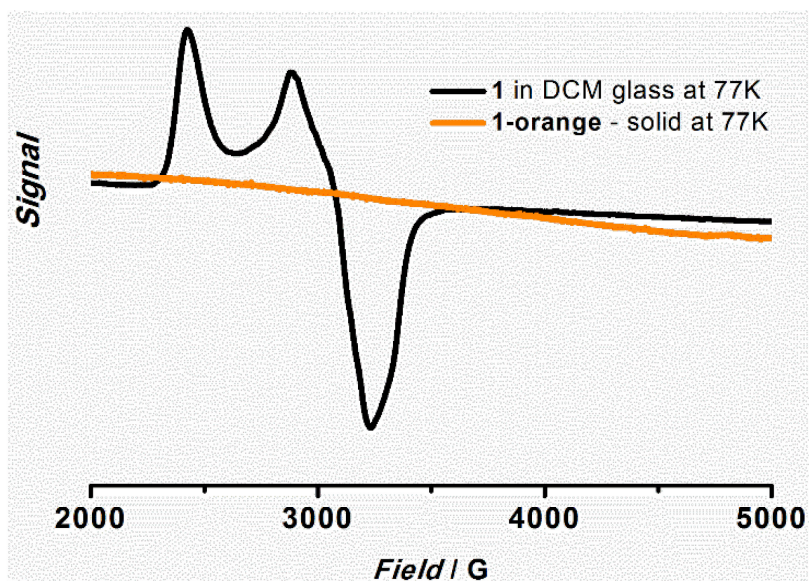
Figure 4-6. X-Band ESR spectrum of **1** in frozen DCM measured at 77 K (in black) with g_1 = 2.70, $g_2 \approx g_3$ = 2.12, and X-band ESR spectrum of **1-orange** solid measured at 77 K (in orange). Conditions: frequency 9.177 GHz, power 1 mW, modulation 2 mT/100kHz.

indicative of square-planar LS cobalt(II) without axial coordination, with significant delocalization along one axis.[27d, 28] Despite the difficulty to clearly differentiate between the g_2 and the g_3 values, a ground state $(d_{yz})^1$ is proposed, which is also confirmed by DFT calculations (*vide infra*, Figure 4-10, Figure S12; Appendix-4-SI), and is in line with the anionic nature of the AMOX ligands.[27] The **1-orange** solid is silent in ESR at room temperature as expected for cobalt(II) HS S=3/2 above 40 K.[9b, 29]. The solution of **1** in DCM is also silent in ESR at room temperature, but when cooled at 77 K, it gives the signal characteristic for the cobalt(II) square-planar LS (g_1 = 2.70 and g_2 = 2.12) (Figure 4-6). Nevertheless, when the ESR spectrum of **1-orange** solid is recorded at 77 K, no signal is observed. This strongly suggests that the change in spin is the result of a change from tetrahedral to square-planar geometry, which is induced by the stabilization of the square-planar form by the interactions of the compound with the DCM.

In the electronic spectra of **1-green** and **1-orange**, recorded in the solid state at room temperature (Figure 4-7), the bands at 644 and 944 nm are indicative of the square-planar form, while the bands at 540 and 970 nm are characteristic of the tetrahedral form.[3b, 6] The variable temperature UV-vis analysis for **1** indicates that the square-planar form is stabilized with decreasing temperature (Figure 4-8). Its comparison with the absorption spectrum of **1-green** in the solid state (Figure 4-7) confirms the assignment of the band at 620-650 nm as the square-planar form. The UV-vis-NIR spectrum of **1** in DCM (Figure. S8; Appendix-4-SI) shows low intensity bands in the visible and NIR region, corresponding to spin allowed and Laporte forbidden *d-d* transitions. They present characteristic low molar absorptivity values.[19, 24] The bands at 540 nm, 970 nm, and 1266 nm are indicative of the tetrahedral form.[6, 30] Similar features were identified for tetrahedral cobalt(II) *N,O*-bis-chelates of AMOXs,[7, 31] triazene-1-oxides,[6] and β-ketoamine[30] ligands. Thus, the electronic absorption spectra of **1** support the stabilization of the tetrahedral geometry in DCM solution at room temperature. [25]
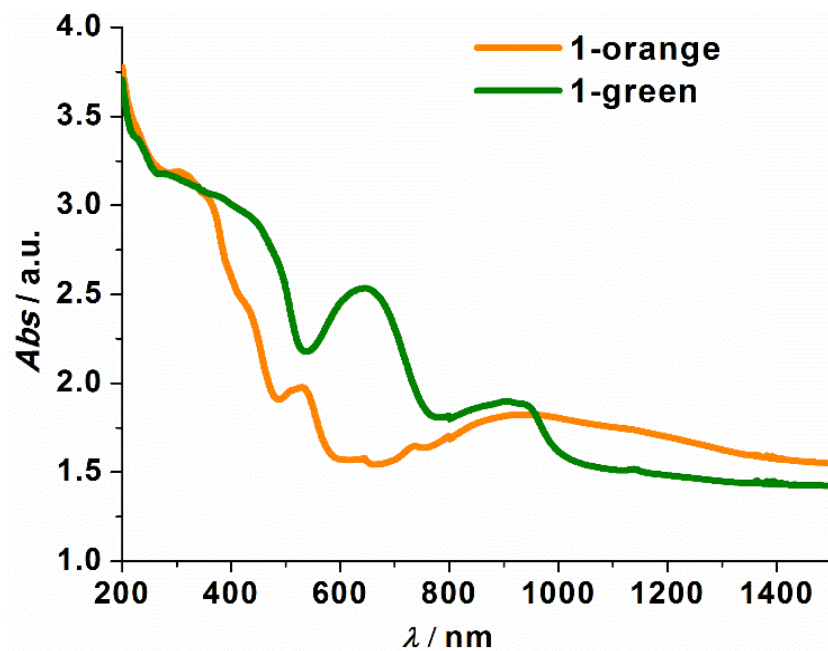
Figure 4-7. Reflectance spectra of **1-green** (green line) and **1-orange** (orange line) in the solid state. Absorbance is derived from % reflectance.
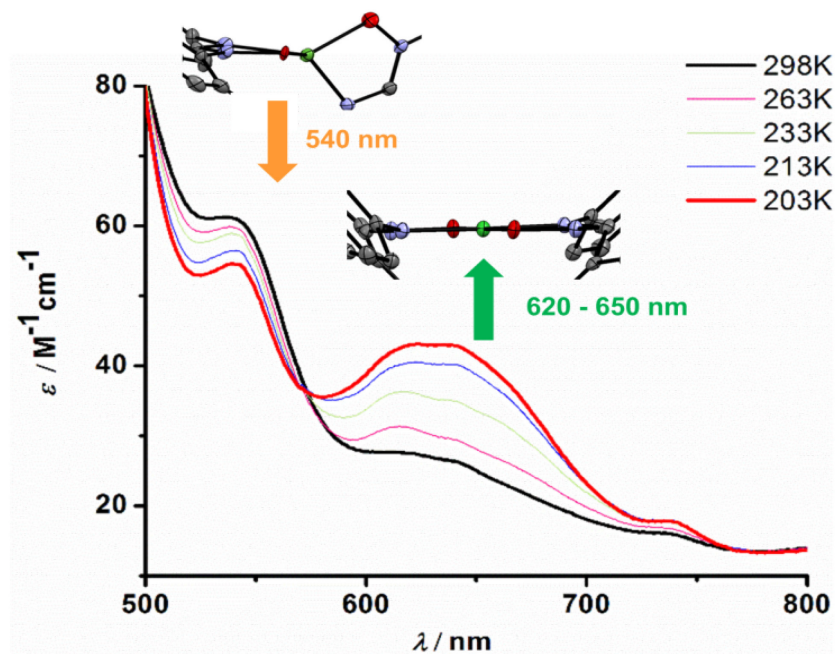
Figure 4-8. Electronic spectra of **1** in DCM at variable temperature.

The ^{1}H NMR spectrum of **1** (Figure 4-9) in CD$_2$Cl$_2$ shows broadened signals between 56 and -100 ppm with accurate integrations. The paramagnetic nature of the compound allows tentative assignment of the ^{1}H NMR resonances based on the integration ratio, 2D COSY and T_1 relaxation time measurement experiments, as well as correlation with the proximity of the protons to the metal centre. The aryl ring bonded to the *N*-Co is more influenced because of its proximity to the metal centre than the aryl ring on the *NO*-Co.[18, 32] As a consequence, the *ortho*-H6' is more paramagnetically shifted (-99.6 ppm) than the *ortho*-H6 (55.9 ppm) (see Scheme 4-1 and Figure 4-9 for the notation of H). Their close proximity to the cobalt centre is due to the tilt of the aryl rings with respect to the amidine-oxide plane. Their short T_1 relaxation times of 0.53 ms (H6') and 1.16 ms (H6) are consistent with their position close to the paramagnetic centre.
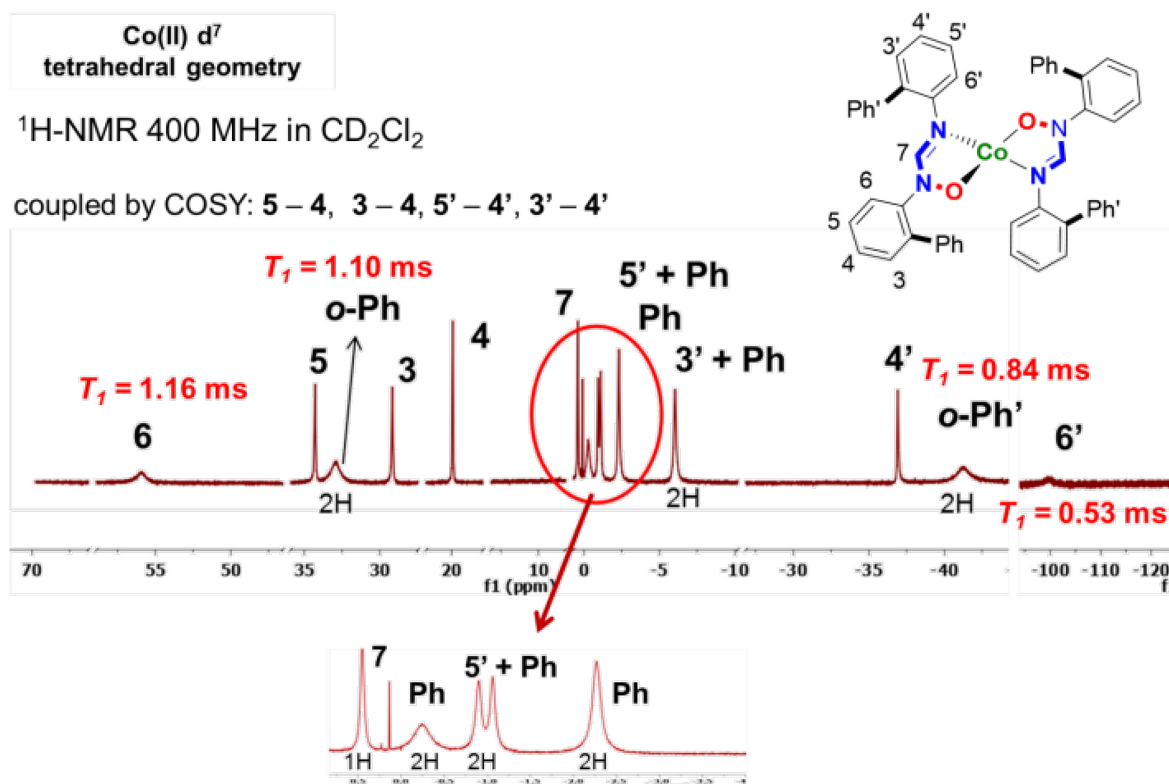
Figure 4-9. ^{1}H NMR spectrum of **1** in CD$_2$Cl$_2$ with tentative assignment of ^{1}H signals.

The electrochemical properties of **1** were also investigated. The cyclic voltammograms (CVs) of **1** in dry DMF (Figure S9; Appendix-4-SI) display a one-electron reversible process at 0.14 V *vs*. SCE, assigned to the Co(II/III) couple, followed by irreversible ligand-based oxidation processes at more positive values (1.00 V and 1.21 V *vs*. SCE). The relatively facile oxidation of the metal is in line with the anionic character of the ligand. In addition, an irreversible reduction process is observed at -2.10 V *vs*. SCE. The absence of this event in the CV of the zinc analogue (Figure S9; Appendix-4-SI), suggests that it can be tentatively assigned to the Co(II/I) reduction. The difficult reduction, also consistent with the anionic character of the ligand, and a $(d_{yz})^1$ ground state of the complex, was also reported for cobalt complexes of electron-donating AMOX ligands (-2.16 to -2.34 V *vs*. SCE potential range),[7] as well as for cobalt complexes of triazene-1-oxides.[6]

4.5.4. DFT calculations

DFT optimized structures of **1** were calculated for **1-green** (square-planar structure, with the two DCM molecules; S = 1/2, doublet), **1-orange** (tetrahedral structure; S = 3/2, quadruplet), and **1-green⊃2DCM** (square-planar structure without the two DCM molecules; S = 1/2, doublet) (Figure S10-S12 and Tables S4-S15; Appendix-4-SI).
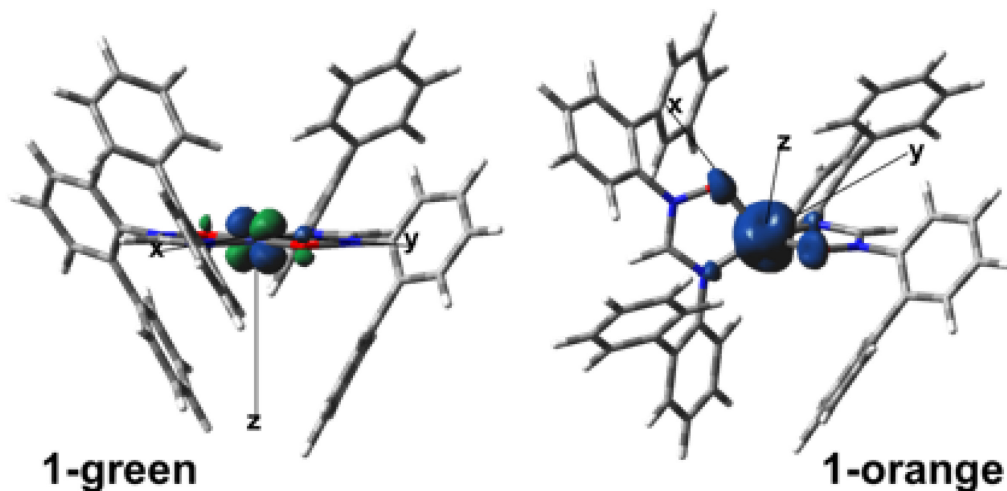
Figure 4-10. DFT optimized structures (uB3LYP/ LANL2DZ, PCM: DCM) for **1-green** and **1-orange** with the electron spin density plots.

The optimized calculated structures (Figure S10) are in agreement with the XRD data (Table 4-1). All of the three forms were found to be very close in energy (Tables S4-S5 and Figure S11; Appendix-4-SI). **1-green** and **1-orange** are both slightly stabilized *versus* **1-green⊃2DCM** (in gas phase and with the solvation model), confirming the stabilizing nature of the interactions between **1** and the guest DCM molecules. A slight stabilization

(7 kcal mol^{-1}) for the **1-green** versus the **1-orange** is also obtained in the gas phase, while using the solvation model, the energies of these two forms differ by only 1 kcal mol^{-1}. This result is in accordance with the existence of both forms at room temperature, as observed experimentally.

The spin density plots (Figure 4-10 and Tables S6-S7; Appendix-4-SI) indicate the concentration of unpaired electrons on the metal centre. The $(d_{yz})^1$ ground state configuration of **1-green** is thus supported by DFT calculations. The raising of d_{yz} orbital above the d_{z2} (Figure S12; Appendix-4-SI) may be interpreted as a result of the π-donation properties of the AMOX ligand.[27f, 28]

4.6. Conclusion

In conclusion, solid-state structures are presented for complex **1** in both its HS tetrahedral form and its LS square-planar solvated form, as confirmed by magnetic moment measurements and ESR. To the best of our knowledge, this is the first report with complete structural evidence of a hydrogen-bonding-induced geometry and spin change at a cobalt(II) centre within a same cobalt(II) bis(chelate). In the previously reported systems of cobalt bis-chelates with iminopyrrolyl-type ligands[4] and triazene-1-oxides[6], the solvent effect was found to be essential in biasing the system toward a specific geometry/ spin state combination in the ground state. However, no direct proof was given for how this effect occurs. In **1**, the weak interactions with the solvent molecules (the overall host-guest interactions: hydrogen bonding and packing forces) are identified as the main factors responsible for determining the stereochemistry and the spin state of the complex. The unique feature of this system is the combination of electronic and steric properties of the ligand and the ligand-metal interaction to give specific hydrogen-bonding patterns and host-guest recognition events. The synergistic effect of all these factors results in a delicate balance of energy for the tetrahedral and square-

planar forms. The geometry and spin change in the solvatomorph is thus possible, without directly acting upon the metal ion by coordination/ de-coordination, but in a similar fashion to allosteric control with host-guest interactions in biological systems. The study of **1** offers the opportunity to better understand the role of weak intermolecular forces and co-operative effects with respect to stereochemistry and spin preferences in four-coordinated metal complexes, which bodes well for further advances in catalysis and magnetic materials.

4.7. Experimental section

Materials and Instrumentation

The metal salt, the aniline and the triethylorthoformate were purchased from Aldrich, and the *m*-CPBA 77% was purchased from Acros, and were used without further purification. ACS grade solvents were purchased from VRW and Fisher and were removed under reduced pressure using a rotary evaporator, unless otherwise stated. Nuclear magnetic resonance (NMR) spectra were recorded in CD_2Cl_2 and $CDCl_3$ at 25°C, on the following spectrometers: Bruker AV-400, AV-500, and DRX-400. Chemical shifts (δ) are reported in part per million (ppm) relative to TMS, and are referenced to the residual solvent signal (5.35 ppm for CD_2Cl_2 and 7.26 ppm for $CDCl_3$). Variable temperature NMR spectra and $T1$ relaxation time measurements were performed at the NMR Spectroscopy Service at Université de Montréal. Absorption spectra were measured in dichloromethane (previously distilled), between 230 and 1400 nm, at room temperature (r.t.), on a Cary 500i UV-Vis-NIR spectrophotometer. Absorption spectra at variable temperature were measured on a Cary 6000i UV-vis-NIR spectrophotometer, using an Oxford Instrument cryostat and temperature controller. Solution samples were prepared in concentration range 10^{-5} to 10^{-3} M. Reflectance spectra of **1** were measured on the latter instrument, using a Praying-Mantis accessory. X-Band ESR spectra were collected on a Bruker Super XFT spectrometer (frequency: 9.8800 GHz, microwave power: 2 mW, modulation frequency: 100 kHz, modulation amplitude: 5 G) at room temperature, and on a JEOL JES-FA spectrometer (frequency: 9.1770 GHz, microwave power: 1 mW, modulation frequency: 100 kHz, modulation amplitude: 20 G) at 77 K, for solid samples and 5 mM dichloromethane solutions of **1**. The solid samples were prepared under N_2 atmosphere, and the solutions were degassed by the freeze-pump-thaw technique.

Electrochemical measurements were carried out in argon-purged dry DMF, at room temperature, with a BAS CV50W potentiostat. The working electrode was a glassy carbon electrode. The counter electrode was a Pt wire, and the pseudo-reference electrode was a silver wire. The reference was set using an internal 1 mM ferrocene/ferrocenium sample at 450 mV *vs*. SCE in DMF.[33] The concentration of the compounds was 1 mM. Tetrabutylammonium hexafluorophosphate (TBAP) was used as supporting electrolyte and its concentration was 0.10 M. Cyclic voltammograms were obtained at scan rates of 50, 100, 200, and 500 mV/s. For irreversible oxidation processes, the cathodic peak was used as E. Experimental uncertainties are as follows: absorption maxima, ±2 nm; molar absorption coefficient, 10%; redox potentials, ± 10 mV. The microanalyses and the mass spectrometry analyses were performed at the Elemental Analysis Service and the Regional Mass Spectrometry Centre at Université de Montréal. Magnetic susceptibility measurements were performed in solution by the Evans' method,[34] in CD_2Cl_2, using 10% v/v TMS, at 298 K. The sample concentration was in the order of 10^{-3} M. In the solid state, the measurements were carried out on powder or microcrystalline samples (10-20 mg), at 295 K, using a Johnson-Matthey magnetic susceptibility balance and $HgCo(NCS)_4$ as calibrant.[35] The measurements were performed at least in triplicate, and the confidence interval at 95% probability is given as error. The standard diamagnetic corrections using Pascal constants were applied.[36] Magnetic moments were calculated using: $\mu_{eff} = 2.83(\chi^M T)^{1/2}$. Thermogravimetric analyses (TGA) were carried out on a TA Q-500 thermogravimetric analyzer (TA Instruments) under N_2 atmosphere, in the 25 – 600 °C temperature range, at a heating rate of 10 °C/ min.

X-ray Structure Determination

Crystallographic data for **1-green** and **1-orange** (Table S2; Appendix-4-SI) were collected at 100 K, using a Bruker smart diffractometer equipped with an APEX II CCD Detector, a Incoatec IMuS source and a Quazar MX mirror. The crystal-to-detector distance was 4.0 cm, and the data collection was carried out in 512 x 512 pixel mode. The initial unit cell parameters were determined by a least-squares fit of the angular setting of strong reflections, collected by a 180.0 degree scan in 180 frames over three different parts of the reciprocal space. For data collection, determination of cell parameters, cell refinement, and data reduction *APEX2* and *SAINT* (Bruker, 2007) were used.[37] Absorption corrections were

applied using *SADABS* and *TWINABS* (Bruker 2001).[38] Structure solution was performed using direct methods with *SHELXS* or *SHELXT* (Sheldrick, 2008) and refined on F^2 by full-matrix least squares using *SHELXL2014* (Sheldrick, 2008).[39] *OLEX2* (Dolomanov *et al.*, 2009)[40] and *ORTEP-3 for Windows* (Farrugia, 2012)[41] were used for molecular graphics. The material was prepared for publication with *publCIF* (Westrip, 2010).[42] CCDC 1041637 (for **1-green**) and CCDC 1041638 (for **1-orange**) contain the supplementary crystallographic data for this paper. These data can be obtained free of charge from The Cambridge Crystallographic Data Centre via www.ccdc.cam.ac.uk/data_request/cif. **1-orange** was a twinning case and was treated accordingly in the refinement of the structure. Details are provided in Supporting Information (Appendix-4-SI) and in the crystallographic information file (.CIF).

Computational Details

Gaussian09, Revision D.01[43] was used for all theoretical calculations discussed herein, with restricted open shell and spin-unrestricted B3LYP[44] DFT methods and LANL2DZ ECP[45] basis set. The calculations were performed for the ground states, in gas-phase and using the PCM (CH_2Cl_2) solvation model. Initial atom coordinates for geometry optimization were taken from XRD data (cif) of the corresponding structures. No symmetry constraints were used for the geometry optimization. Details on optimized structures are given in Tables S5-S16 (Appendix-4-SI). No imaginary frequencies were obtained when frequency calculations on optimized geometries were performed. The values of $<S^2>$ were monitored, and didn't show major spin contamination (Tables S9-S10, Appendix-4-SI). The total energy values used for calculating energy differences were obtained from single point calculations on the optimized structures using a mixed basis set: LANL2DZ ECP for the Co atom, and 6-311g(d,p) for the N, O, C, H, Cl atoms. GaussView 3.0.9[46] and Chemissian 2.200[47] software were used for data analysis, visualisation, and surface plots.

Synthesis

The syntheses of ligand **L** was previously reported.[48]

Bis[*N*,*N'*-bis(2-biphenyl)-*N*-oxidoformamidinate) of cobalt(II) (1). To a solution of cobalt(II) acetate tetrahydrate (0.21 g, 0.82 mmol, 1 eq.) in ethanol (20 mL) (brought to pH 8

by addition of NaOH aq. 20%) was added a solution of the ligand *N*-hydroxy-*N,N'*-bis(2-biphenyl)formamidine (**L**) (0.60 g, 1.64 mmol, 2 eq.) in ethanol (10 mL). The reaction mixture was stirred at room temperature for 3h. Water (10 mL) was added to the orange suspension. The suspension was kept at 4°C for 1h to afford an orange precipitate. After filtration, an orange powder was obtained, which was dried under vacuum. Yield 0.52 g, 80%. X-Ray quality **orange** crystals (very thin needles) were obtained from DCM/ hexane (1:1) at room temperature. X-Ray quality **green** crystals were obtained from the same solvent mixture at -20 °C. ^{1}H NMR (CD$_2$Cl$_2$, 400 MHz) δ, ppm: 55.90 (s, 1H, *o*-C$_6$*H*$_4$-(NO); (**H6**)), 34.28 (s, 1H, *m*-C$_6$*H*$_4$-(NO); (**H5**)), 32.93 (s, 2H, *o*-C$_6$*H*$_5$-C$_6$H$_4$-(NO); (***o*-Ph**)), 29.16 (s, 1H, *m*-C$_6$*H*$_4$-(NO); (**H3**)), 19.92 (s, 1H, *p*-C$_6$*H*$_4$-(NO); (**H4**)), 0.41 (s, 1H, -N-C*H*=N-; (**H7**)) -0.29 (s, 2H, C$_6$*H*$_5$-C$_6$H$_4$-; (**Ph or Ph'**)), -0.94 and -1.10 (s, s, 2H, *m*-C$_6$*H*$_4$-(N); (**H5'**) and C$_6$*H*$_5$-C$_6$H$_4$-; (**Ph or Ph'**)), -2.31 (s, 2H, C$_6$*H*$_5$-C$_6$H$_4$-; (**Ph or Ph'**)), -6.04 (s, 2H, *m*-C$_6$*H*$_4$-(N); (**H3'**) and C$_6$*H*$_5$-C$_6$H$_4$-; (**Ph or Ph'**)), -36.32 (s, 1H, *p*-C$_6$*H*$_4$-(N); (**H4'**)), -41.34 (s, 2H, *o*-C$_6$*H*$_5$-C$_6$H$_4$-(N); ***o*-Ph'**), -99.52 (s, 1H, *o*-C$_6$*H*$_4$-(N) (**H6'**)). MS (ES, DCM) (m/z): 785.4 [M]$^+$. Magnetic moment: (**1-green** in solid state): 2.6 ± 0.1 µB, (**1-orange** in solid state): 4.7 ± 0.1 µB; in solution: 4.70 ± 0.1 µB. Elemental Analysis: for **1-green** *calc.* (%) for C$_{50}$H$_{38}$CoN$_4$O$_2$(CH$_2$Cl$_2$)$_{1.6}$ (921.70): C 67.24, H 4.51, N 6.08; *found* (%): C 67.12, H 4.35, N 6.08; for **1-orange** *calc.* (%) for C$_{50}$H$_{38}$CoN$_4$O$_2$ (785.81): C 76.42, H 4.87, N 7.13;. *found* (%) C 76.24, H 4.77 , N 7.13.

4.8. Acknowledgments

4.9. Supporting Information

Supporting Information for this article is available on the WWW under http://dx.doi.org/10.1002/chem.201500852. In this thesis, the same material is found in Appendix-4-SI.

4.10. References

[1]   a) J. Cirera, P. Alemany, S. Alvarez, *Chem. Eur. J.* **2004**, *10*, 190-207; b) J. Cirera, E. Ruiz, S. Alvarez, *Inorg. Chem.* **2008**, *47*, 2871-2889; c) S. Alvarez, J. Cirera, *Angew. Chem., Int. Ed.* **2006**, *45*, 3012-3020; d) G. Aullon, S. Alvarez, *Theor. Chem. Acc.* **2009**, *123*, 67-73; e) S. Alvarez, *J. Am. Chem. Soc.* **2003**, *125*, 6795-6802.

[2]   a) S. Alvarez, A. A. Palacios, G. Aullon, *Coord. Chem. Rev.* **1999**, *185-186*, 431-450; b) L. H. Doerrer, M. T. Bautista, S. J. Lippard, *Inorg. Chem.* **1997**, *36*, 3578-3579; c) R. A. Friesner, M.-H. Baik, B. F. Gherman, V. Guallar, M. Wirstam, R. B. Murphy, S. J. Lippard, *Coord. Chem. Rev.* **2003**, *238-239*, 267-290; d) B. S. Jaynes, L. H. Doerrer, S. Liu, S. J. Lippard, *Inorg. Chem.* **1995**, *34*, 5735-5744; e) R. Poli, *Chem. Rev.* **1996**, *96*, 2135-2204; f) H. Xu, R. Chen, Q. Sun, W. Lai, Q. Su, W. Huang, X. Liu, *Chem. Soc. Rev.* **2014**, *43*, 3259-3302.

[3]   a) G. W. Everett, Jr., R. H. Holm, *J. Am. Chem. Soc.* **1965**, *87*, 5266-5267; b) G. W. Everett, Jr., R. H. Rholm, *J. Am. Chem. Soc.* **1966**, *88*, 2442-2451.

[4]   S. A. Carabineiro, L. C. Silva, P. T. Gomes, L. C. J. Pereira, L. F. Veiros, S. I. Pascu, M. T. Duarte, S. Namorado, R. T. Henriques, *Inorg. Chem.* **2007**, *46*, 6880-6890.

[5]   L. C. Kalutarage, P. D. Martin, M. J. Heeg, C. H. Winter, *J. Am. Chem. Soc.* **2013**, *135*, 12588-12591.

[6]   J. A. Wolny, M. F. Rudolf, Z. Ciunik, K. Gatner, S. Wolowiec, *J. Chem. Soc., Dalton Trans.* **1993**, 1611-1622.

[7]   M. Cibian, S. Langis-Barsetti, F. G. De Mendonça, S. Touaibia, S. Derossi, D. Spasyuk, G. S. Hanan, *Eur. J. Inorg. Chem.* **2014**, 10.1002/ejic.201402895.

[8]   H. A. Goodwin, *Top. Curr. Chem.* **2004**, *234*, 23-47.

[9]   a) S. A. Cantalupo, S. R. Fiedler, M. P. Shores, A. L. Rheingold, L. H. Doerrer, *Angew. Chem., Int. Ed.* **2012**, *51*, 1000-1005; b) D. M. Jenkins, A. J. Di Bilio, M. J. Allen, T. A. Betley, J. C. Peters, *J. Am. Chem. Soc.* **2002**, *124*, 15336-15350.

[10]   F. Allen, *Acta Crystallogr., Sect. B: Struct. Sci.* **2002**, *58*, 380-388.

[11]   a) M. F. Perutz, A. J. Wilkinson, M. Paoli, G. G. Dodson, *Annu. Rev. Biophys. Biomol. Struct.* **1998**, *27*, 1-34; b) A. Dey, T.-a. Okamura, N. Ueyama, B. Hedman, K. O. Hodgson, E. I. Solomon, *J. Am. Chem. Soc.* **2005**, *127*, 12046-12053.

[12]   a) H. G. Brittain, *J. Pharm. Sci.* **2011**, *100*, 1260-1279; b) H. G. Brittain, *Drugs Pharm. Sci.* **2008**, *178*, 185-228; c) H. G. Brittain, *J. Pharm. Sci.* **2012**, *101*, 464-484; d) H. G. Brittain, K. R. Morris, S. X. M. Boerrigter, *Drugs Pharm. Sci.* **2009**, *192*, 233-281.

[13]   a) D. Maspoch, D. Ruiz-Molina, K. Wurst, N. Domingo, M. Cavallini, F. Biscarini, J. Tejada, C. Rovira, J. Veciana, *Nat. Mater.* **2003**, *2*, 190-195; b) B. Li, R.-J. Wei, J. Tao, R.-B. Huang, L.-S. Zheng, Z. Zheng, *J. Am. Chem. Soc.* **2010**, *132*, 1558-1566; c)

J. S. Costa, S. Rodríguez-Jiménez, G. A. Craig, B. Barth, C. M. Beavers, S. J. Teat, G. Aromí, *J. Am. Chem. Soc.* **2014**, *136*, 3869-3874.

[14] a) X. Wurzenberger, C. Neumann, P. Klüfers, *Angew. Chem., Int. Ed.* **2013**, *52*, 5159-5161; b) L. Tahsini, S. E. Specht, J. S. Lum, J. J. M. Nelson, A. F. Long, J. A. Golen, A. L. Rheingold, L. H. Doerrer, *Inorg. Chem.* **2013**, *52*, 14050-14063.

[15] L. Yang, D. R. Powell, R. P. Houser, *Dalton Trans.* **2007**, 955-964.

[16] within 3σ

[17] M. C. Karunarathne, T. J. Knisley, G. S. Tunstull, M. J. Heeg, C. H. Winter, *Polyhedron* **2013**, *52*, 820-830.

[18] K. C. D. Robson, C. D. Phillips, B. O. Patrick, W. S. McNeil, *Dalton Trans.* **2010**, *39*, 2573-2578.

[19] C. Housecroft, A. Sharpe, *Inorganic Chemistry, 4th ed.*, Pearson, Harlow, **2012**, pp. 665-712

[20] M. F. Rudolf, J. Wolny, Z. Ciunik, P. Chmielewski, *J. Chem. Soc., Chem. Commun.* **1988**, 1006.

[21] E. Bill, E. Bothe, P. Chaudhuri, K. Chlopek, D. Herebian, S. Kokatam, K. Ray, T. Weyhermuller, F. Neese, K. Wieghardt, *Chem. Eur. J.* **2005**, *11*, 204-224.

[22] C. C. Lu, E. Bill, T. Weyhermüller, E. Bothe, K. Wieghardt, *Inorg. Chem.* **2007**, *46*, 7880-7889.

[23] **1-green** was freshly prepared by evaporation of a DCM solution of **1-orange** at 0 - 5 deg. C. The green powder obtained was air-dried for two hours before being subjected to thermogravimetric and elemental analyses. It is therefore impossible to determine if the traces of **1-orange** in the **1-green** compound are the result of an incomplete conversion or a loss of DCM molecules over time.

[24] F. A. Cotton, G. Wilkinson, C. A. Murillo, M. Bochmann, *Advanced Inorganic Chemistry*, 6th ed., Wiley, New York, **1999**, pp. 820-821

[25] Y. Nishida, S. Kida, *Bull. Chem. Soc. Jap.* **1972**, *45*, 461-465.

[26] E. I. Solomon, A. B. P. Lever, *Inorganic Electronic Structure and Spectroscopy, Methodology, Vol. 1*, Wiley, New York, **1999**, 129-131

[27] a) Y. Nishida, S. Kida, *Bull. Chem. Soc. Jpn.* **1978**, *51*, 143-149; b) F. L. Urbach, R. D. Bereman, J. A. Topich, M. Hariharan, B. J. Kalbacher, *J. Am. Chem. Soc.* **1974**, *96*, 5063-5069; c) P. Pietrzyk, M. Srebro, M. Radon, Z. Sojka, A. Michalak, *J. Phys. Chem. A* **2011**, *115*, 2316-2324; d) A. Ceulemans, M. Dendooven, L. G. Vanquickenborne, *Inorg. Chem.* **1985**, *24*, 1159-1165; e) M. A. Hitchman, *Inorg. Chem.* **1977**, *16*, 1985-1993; f) Y. Nishida, K. Hayashida, A. Sumita, S. Kida, *Bull. Chem. Soc. Jpn.* **1980**, *53*, 271-272.

[28] M. P. Marshak, M. B. Chambers, D. G. Nocera, *Inorg. Chem.* **2012**, *51*, 11190-11197.

[29] A. Palma, J. F. Gallagher, H. Muller-Bunz, J. Wolowska, E. J. L. McInnes, D. F. O'Shea, *Dalton Trans.* **2009**, 273-279.

[30] R. H. Holm, M. J. O'Connor, *Progr. Inorg. Chem.* **1971**, *14*, 241-401.

[31] M. Cibian, S. Derossi, G. S. Hanan, *Dalton Trans.* **2011**, *40*, 1038-1040.

[32] I. S. Tidmarsh, B. F. Taylor, M. J. Hardie, L. Russo, W. Clegg, M. D. Ward, *New J. Chem.* **2009**, *33*, 366.

[33] N. G. Connelly, W. E. Geiger, *Chem. Rev.* **1996**, *96*, 877-910.

[34] D. F. Evans, *J. Chem. Soc.* **1959**, 2003-2005.

[35] R. P. Sharma, K. K. Bhasin, *Bull. Chem. Soc. Jpn.* **1986**, *59*, 1603-1604.

[36]   C. J. O'Connor, *Prog. Inorg. Chem.* **1982**, *29*, 203-283.

[37]   Bruker, **2007,** *APEX2 and SAINT,* Bruker AXS Inc., Madison, Wisconsin, USA.

[38]   Bruker, **2001,** *SADABS and TWINABS,* Bruker AXS Inc., Madison, Wisconsin, USA.

[39]   G. M. Sheldrick, *Acta Crystallogr., Sect. A: Found. Crystallogr.* **2008**, *64*, 112-122.

[40]   O. V. Dolomanov, Bourhis, L. J., Gildea, R. J., Howard, J. A. K., Puschmann, H., *J. Appl. Cryst.* **2009**, *42*, 339-341.

[41]   L. J. Farrugia, *J. Appl. Crystallogr.* **1997**, *30*, 565.

[42]   S. P. Westrip, *J. Appl. Crystallogr.* **2010**, *43*, 920-925.

[43]   G. W. T. M. J. Frisch, H. B. Schlegel, G. E. Scuseria, M. A. Robb, J. R. Cheeseman, G. Scalmani, V. Barone, B. Mennucci, G. A. Petersson, H. Nakatsuji, M. Caricato, X. Li, H. P. Hratchian, A. F. Izmaylov, J. Bloino, G. Zheng, J. L. Sonnenberg, M. Hada, M. Ehara, K. Toyota, R. Fukuda, J. Hasegawa, M. Ishida, T. Nakajima, Y. Honda, O. Kitao, H. Nakai, T. Vreven, J. A. Montgomery, Jr., J. E. Peralta, F. Ogliaro, M. Bearpark, J. J. Heyd, E. Brothers, K. N. Kudin, V. N. Staroverov, R. Kobayashi, J. Normand, K. Raghavachari, A. Rendell, J. C. Burant, S. S. Iyengar, J. Tomasi, M. Cossi, N. Rega, J. M. Millam, M. Klene, J. E. Knox, J. B. Cross, V. Bakken, C. Adamo, J. Jaramillo, R. Gomperts, R. E. Stratmann, O. Yazyev, A. J. Austin, R. Cammi, C. Pomelli, J. W. Ochterski, R. L. Martin, K. Morokuma, V. G. Zakrzewski, G. A. Voth, P. Salvador, J. J. Dannenberg, S. Dapprich, A. D. Daniels, Ö. Farkas, J. B. Foresman, J. V. Ortiz, J. Cioslowski, and D. J. Fox, **2009,** *Gaussian09, Revision D.01,* Gaussian, Inc.; Wallingford CT.

[44]   a) C. Lee, W. Yang, R. G. Parr, *Phys. Rev. B: Condens. Matter* **1988**, *37*, 785-789; b) B. Miehlich, A. Savin, H. Stoll, H. Preuss, *Chem. Phys. Lett.* **1989**, *157*, 200-206.

[45]   a) P. J. Hay, W. R. Wadt, *J. Chem. Phys.* **1985**, *82*, 270-283; b) P. J. Hay, W. R. Wadt, *J. Chem. Phys.* **1985**, *82*, 299-310; c) T. H. Dunning, Hay, P. J., in *Methods of Electronic Structure Theory, Vol. 2* (Ed.: H. F. I. Schaefer), Plenum Press New York, **1977**; d) W. R. Wadt, P. J. Hay, *J. Chem. Phys.* **1985**, *82*, 284-298.

[46]   R. D. K. Dennington II, T.; Millam, J.; Eppinnett, K.; Hovell, W. L.; Gilliland, R., **2003,** *GaussView 3.0.9,* Semichem, Inc.; Shawnee Mission, KS.

[47]   L. Skripnikov, **2005 - 2014,** *Chemissian V4.01,*

[48]   a) M. Cibian, S. Langis-Barsetti, G. S. Hanan, *Synlett* **2011**, 405-409; b) M. Cibian, S. Derossi, G. S. Hanan, *Acta Crystallogr., Sect. E: Struct. Rep. Online* **2009**, *65*, o2485; c) E. Baranowska, I. Panfil, C. Belzecki, *Bull. Acad. Pol. Sci., Ser. Sci. Chim.* **1977**, *25*, 93-99; d) C. Belzecki, I. Panfil, *Bull. Acad. Pol. Sci., Ser. Sci. Chim.* **1975**, *23*, 119-123.

Chapitre 5: Des complexes de zinc(II) avec des ligands *N,N'*-diaryl-R-amidinate-*N*-oxydes

5.1. Plan du chapitre

Ce chapitre présente:

▪ les résultats obtenus pour la chimie de coordination des ligands encombrés *N,N'*-diarylformamidinate-*N*-oxydes avec des ions métalliques de zinc(II); ces résultats ont été publiés dans l'article suivant:

Eur. J. Inorg. Chem, **2016**, 177-185 – *Full Paper* (**section 5.2**).

▪ des résultats additionnels, non-publiés, sur les complexes de zinc(II) avec des ligands *N,N'*-diaryl-bezamidinate *N*-oxydes

5.2. The Relationship between Structure and Properties in Zinc(II) complexes of Bulky *N,N'*-Diarylformamidinate *N*-Oxides

5.2.1. Résumé

Des complexes homoleptiques de zinc(II) (**3a-3d**) avec des ligands encombrés *N,N'*-diarylformamidinate *N*-oxydes (*N*-hydroxy-*N,N'*-bis(2,6-diisopropylphenyl)formamidine (**2a**), *N*-hydroxy-*N,N'*-bis(2,6-dimethylphenyl)formamidine (**2b**), *N*-hydroxy-*N,N'*-bis(2-isopropyl-phenyl)formamidine (**2c**), and *N*-hydroxy-*N,N'*-bis(2-biphenyl)formamidine (**2d**)) ont été synthétisés et caractérisés. Leurs structures à l'état solide sont présentées, ainsi que leurs propriétés en solution, étudiées par spectroscopies RMN et UV/Vis et par voltampérométrie cyclique. Des calculs théoriques (DFT et TD-DFT) ont été effectués pour évaluer et rationaliser l'influence de la modification des ligands sur les propriétés des complexes: la HOMO, localisée sur la partie NCNO de la molécule est peu influencée par le motif de substitution des ligands, tandis que la LUMO, localisée sur le groupement aryl-N-O est directement affectée. La différence d'énergie HOMO-LUMO peut ainsi être ajustée en vue des applications potentielles.

Contribution:

Mihaela Cibian: synthèse optimisée des composés et caractérisation totale, résolution de deux structures cristallines, modélisation des molécules par DFT/ TD-DFT et rédaction de l'article

Sophie Langis-Barsetti: synthèse préliminaire et caractérisation partielle des composés

Janaina Ferreira: résolution d'une structure cristalline

Garry S. Hanan: supervision, révision de l'article

The Relationship between Structure and Properties in Zinc(II) Complexes of Bulky *N,N'*-Diarylformamidinate *N*-Oxides

Mihaela Cibian, Sophie Langis-Barsetti, Janaina Ferreira, and Garry S. Hanan*

Département of Chemistry, Université de Montréal, Montréal, Québec, H3T-1J4, Canada

*: E-mail: garry.hanan@umontreal.ca. Fax: 1-514-343-7586

5.2.2. Table of Content Graphic
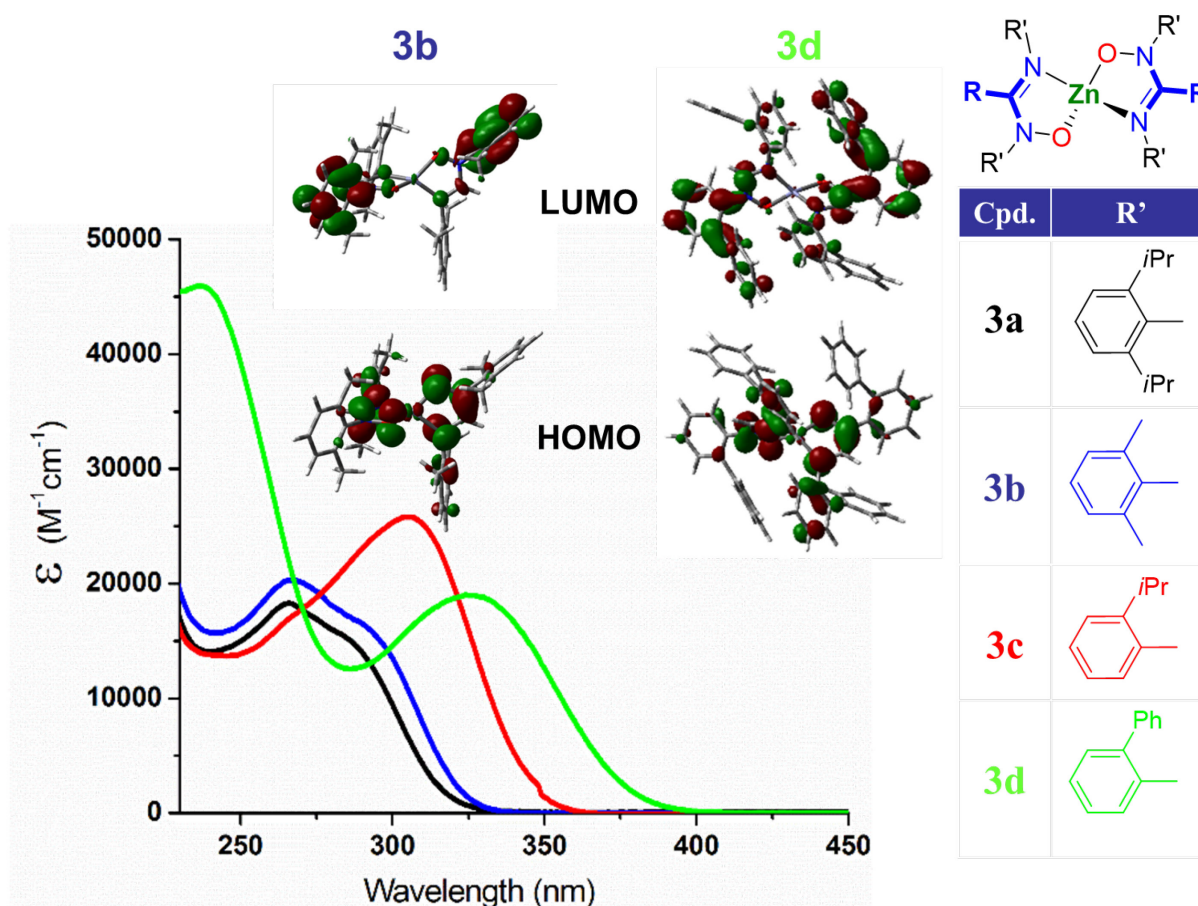
In the zinc(II) bis-chelates of bulky *N,N'*-diarylformamidine-*N*-oxide ligands the HOMO is localized on the N=C-N-O moiety, and hence less influenced by the substitution pattern, while the LUMO, localized on the aryl ring with the O-N moiety is directly affected, allowing the HOMO-LUMO bandgap to be fine-tuned.

5.2.3. Abstract

Homoleptic zinc(II) complexes (**3a-d**) of the bulky *N,N'*-diarylformamidinate-*N*-oxide ligands *N*-hydroxy-*N,N'*-bis(2,6-diisopropylphenyl)formamidine (**2a**), *N*-hydroxy-*N,N'*-bis(2,6-dimethylphenyl)formamidine (**2b**), *N*-hydroxy-*N,N'*-bis(2-isopropylphenyl)formamidine (**2c**), and *N*-hydroxy-*N,N'*-bis(2-biphenyl)formamidine (**2d**) were synthesized and characterized. Their solid state structures are presented, together with their solution properties, as examined by NMR and UV/vis spectroscopy, and cyclic voltammetry. Theoretical calculations [DFT and time dependent (TD-DFT)] were performed to assess and to rationalize the influence of ligand modification on the properties of the complexes: the highest occupied molecular orbital (HOMO), localized on the NCNO moiety, is less influenced by the substitution pattern, whereas the lowest unoccupied molecular orbital (LUMO), localized on the aryl ring with the O-N moiety, is directly affected; therefore the optical bandgap can be fine-tuned for potential applications.

5.2.4. Introduction

The N-donor ligands 2,2'-bipyridine[1] and 2,2':6',2''-terpyridine[2] have been widely used in coordination chemistry as they form stable five-membered chelate rings upon metal-ion coordination. The metal complexes thus formed are typically cationic owing to the charge neutrality of the ligands, which makes them less useful in applications such as metal organic frameworks.[3] The use of anionic ligands allows the formation of neutral metal complexes with favourable interactions between the metal ion and the ligand, which can be extended to oligo- or polymetallic assemblies. An appealing class of anionic ligands is the amidine *N*-oxide type (AMOX, also known as α-aminonitrones and *N*-hydroxyamidines; Figure 5.2-1),[4] which has attracted relatively little attention from a coordination and supramolecular chemistry perspective. AMOXs are bidentate anionic ligands, good chelators for metal ions, and exhibit good electronic delocalization in the amidine backbone. Furthermore, their electronic and steric properties can be modulated and fine-tuned by variation of the substitution pattern on the amidine moiety (Figure 5.2-1).[4a, 4d]
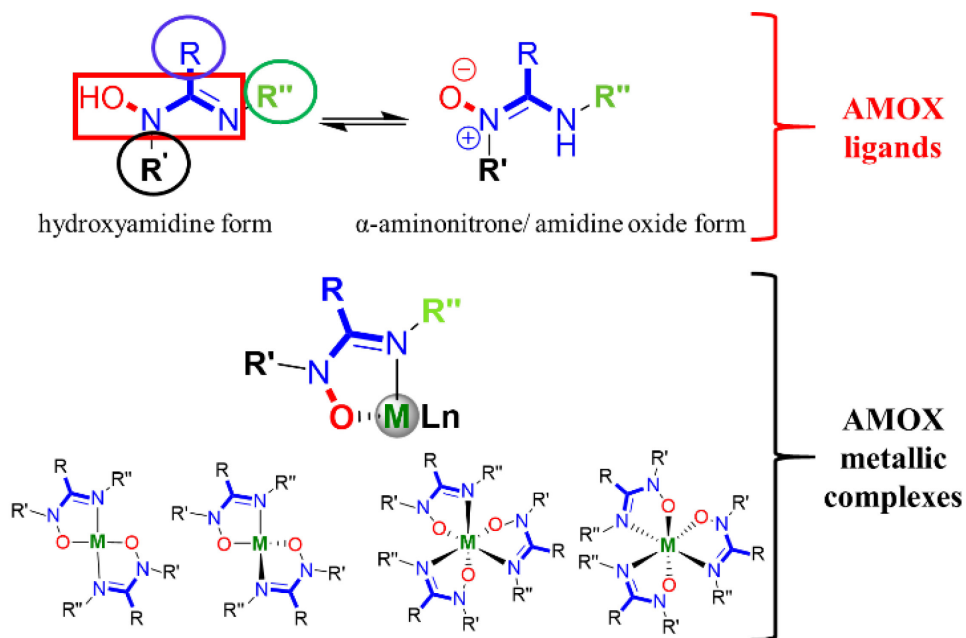
Figure 5.2-1. AMOX ligands and their metallic complexes

We are interested in the metal complexes of AMOX ligands because we can fine-tune the properties of the ligands to alter the corresponding properties of the complexes for applications in catalysis as well as luminescent and magnetic materials. For the AMOX-based metallic complexes, the electron density at the metal ion can be influenced by changing the substituents on the N atoms, the central carbon of the amidine or both. By varying the donor ability of the N,O chelators (by using electron-withdrawing or -donating groups, steric stimuli, or both), the metal-ligand interaction is modulated to produce changes in the structure and geometry of the complexes, and hence, their properties. Our preliminary studies with $Co^{II}(AMOX)_2$ complexes showed that a rare square-planar geometry exists with a d^7 cobalt(II) centre in a bis-bidentate environment.[5] Isomerization from square-planar to tetrahedral geometry accompanied by a change in spin was also identified for these compounds.[6]

Herein, a combined experimental and theoretical analysis of a zinc(II) family of bis(AMOX)chelates is used to examine ligand influence in bis(AMOX)zinc(II) complexes. As electronic factors do not produce a preferred coordination geometry for zinc(II) ions, the tetrahedral geometry is favoured on steric grounds in a 4-coordinate environment.[7] Furthermore, zinc(II) is highly abundant and non-toxic, which bodes well for its incorporation into photoluminescent compounds for optoelectronic applications,[8] as has already been

demonstrated by the studies on zinc(II) complexes of *N*-salicylidene-*N'*-aroylhydrazine ligands,[9] 8-hydroxyquinoline-type ligands,[10] benzothiazole and its derivatives[11] and 2-oxazolylphenolate ligands.[12] Therefore, a theoretical approach, validated by comparison with experimental data, will allow us to develop the tools for the analysis of a broad family of AMOX-based compounds, towards the identification and synthesis of the right candidates for final use in device applications.

5.2.5. Results and Discussion

5.2.5.1. Synthesis

Formamidines **1a-1d** were synthesized from the corresponding anilines and triethyl-orthoformates as previously described.[13] The syntheses of ligands **2a-2d** were realized in moderate-to-good yields (69-92%) by the *N*-oxidation of their corresponding parent amidines with *meta*-chloroperoxybenzoic acid (*m*-CPBA), in dichloromethane (Scheme 5.2-1).[5, 13e, 14]
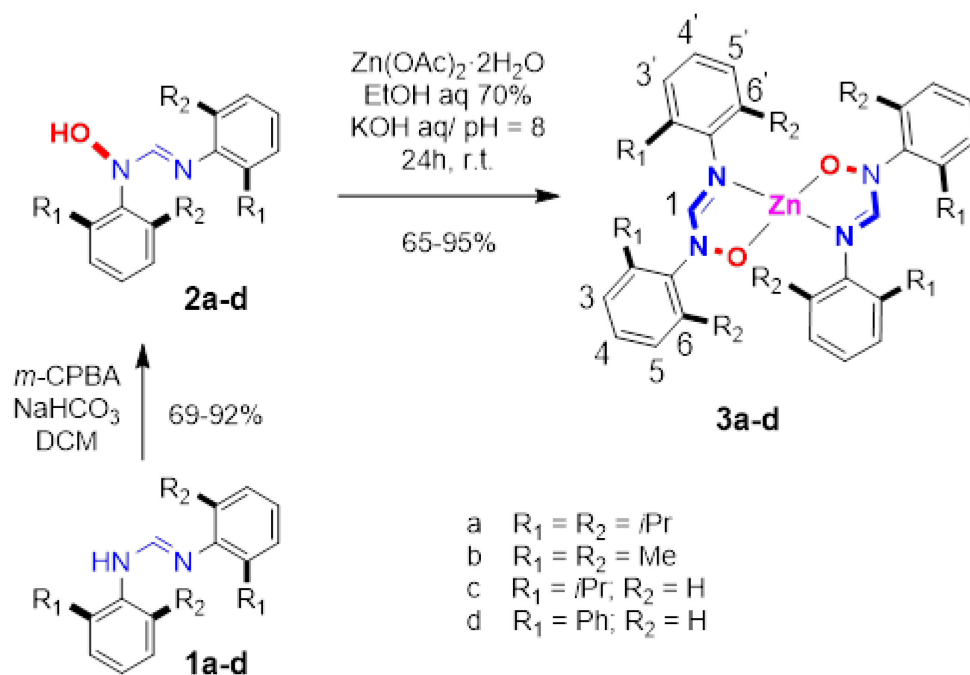
Scheme 5.2-1. Synthesis of AMOX ligands **2a-2d** and their corresponding Zn(AMOX)$_2$ complexes **3a-3d**.

Complexes **3a-3d** were prepared by reacting zinc(II) acetate with two equivalents of the corresponding ligand in aqueous ethanol at room temperature. The desired complexes readily precipitated in each case, and the products were isolated in good to excellent yields (65-95%) as beige powders (Scheme 5.2.-1). The solids are air-stable for months without decomposition. They readily dissolve in chlorinated solvents to give pale-yellow solutions, but are less soluble in polar solvents such as alcohols, DMF, and DMSO. The formation of the zinc bis(chelates) **3a-3d** was confirmed by mass spectrometry (MALDI) and elemental analysis. The complexes were also characterized in solid state by X-ray crystallography (**3a**, **3b** and **3d**), and their properties in solution were investigated by ^{1}H NMR and UV-vis spectroscopy as well as cyclic voltammetry.

5.2.5.2. ^{1}H NMR Spectroscopy

The ^{1}H NMR spectra for **3a-d** are presented in Figure 5.2-2. Compounds **3a**, **3b**, and **3c** exhibit the characteristic doublet signals of the –CH-C***H***$_3$ protons in the aliphatic region (δ = 1.0 to 2.2 ppm). The appearance of four doublet signals for the –CH-C***H***$_3$ protons in **3a** upon complexation is in line with the diastereotopic nature of the protons. In addition, **3a** and **3c** show septet signals at chemical shifts between 3.2 to 4.0 ppm, for the -C***H***-CH$_3$ protons. The differences in ^{1}H and ^{13}C NMR chemical shifts for the complexes with respect to the free ligands are indicative of the effect of metal ion complexation. In all three cases, the signal corresponding to the C atom of the –N-***C***H=N- moiety appears downfield in the spectra of the complexes (149-151 ppm) in comparison with the same signal for the free ligands (142-147 ppm), as a result of the deshielding effect produced on coordination of the zinc(II) ion. The assignment of the ^{1}H NMR resonances was based on the integration ratio, 2D COSY, NOESY and HMQC experiments, as well as the proximity of the protons to the metal centre.

The distinction between the *para*-H4 and *para*-H4' protons (see Scheme 5.2-1 for the numbering) was proposed on consideration that the aryl ring attached to N-Zn is bound to a chelating N atom and is thus more influenced by the metal centre than the aryl ring bound to NO-Zn. As a consequence, the *para*-H4' is more deshielded than the *para*-H4. In the spectrum of **3a** (Figure S1, Appendix 5.2-SI), the resonance of the –N-C***H***=N- (H1) proton is shifted downfield and those of the aliphatic substituents are shifted upfield with respect to those of **2a**.
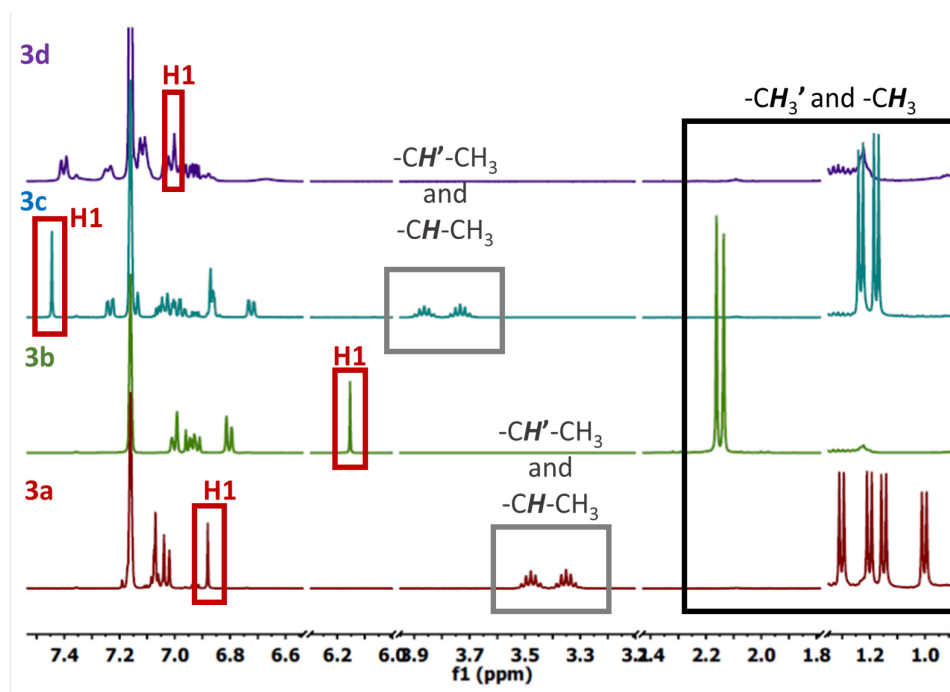
Figure 5.2-2. ^{1}H NMR spectra for **3a-3d** in C$_6$D$_6$

The same trend is maintained for **3b** and **2b** (Figure S2, Appendix 5.2-SI). However, for **3c** and **2c** (Figure S3, Appendix 5.2-SI), the signals of the –N-C**H**=N- protons (H1) appear at similar chemical shifts, and the resonances of the aliphatic protons appear downfield. The deshielding influence of the coordination of the metal cation is combined with the shielding/ deshielding effects resulting indirectly from the steric strain generated upon the formation of the complex, as the changes in the tilt angles between the plane of the –N=C–N-O– AMOX linkage and the planes of the *N*-aryl substituents dictate the degree of electron-density delocalization in the molecule (see X-ray diffraction section). The difference in the substitution pattern on the aryl rings (2,6-disubstitution *versus* 2-mono substitution) are important factors governing interannular twist.

5.2.5.3. X-ray Diffraction

Complexes **3a**, **3b** and **3d** were recrystallized from methanol (**3a** and **3b**) and DCM (**3d**) to afford colourless X-ray-quality crystals. The molecular structures are shown in Figures 5.2-3 − 5.2-5 and Figures S4-S10, Appendix-5.2-SI, and the crystal data, data collection and structure refinement details are summarized in Table 5.2-1. Selected bond lengths and angles

for **3a**, **3b** and **3d**, as well as other relevant zinc(II) bis(chelates) reported previously (**4-8**) are presented in Table 5.2-2. Compound **3b** crystallized with two independent molecules in the asymmetric unit (Figure 5.2-4). All three structures display monomeric zinc(II) ions in a pseudotetrahedral geometry, with no coordinated solvent molecule or other strong interactions with atoms in their proximity. As mentioned previously, closed-shell d^{10} metal ions, especially those with bulky ligands, typically favour tetrahedral geometry on steric grounds in bis-bidentate four-coordinate environments.[7, 15] However, a CSD[16] search for tetrahedral zinc(II) complexes with bidentate N,O ligands in five-membered chelate rings yielded only eight crystal structures of this type,[17] in comparison with over 800 structures for their penta- or hexacoordinated analogues, and over 200 structures for zinc(II) complexes with bidentate N,O ligands in 6-membered chelate rings.
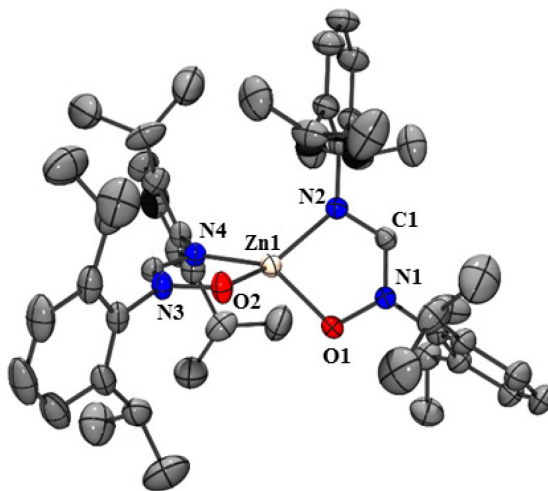
Figure 5.2-3. ORTEP view of **3a** with C_i symmetry. Ellipsoids are shown at 50% probability level. Hydrogen atoms and co-crystallized solvent molecules are omitted for clarity.[18]
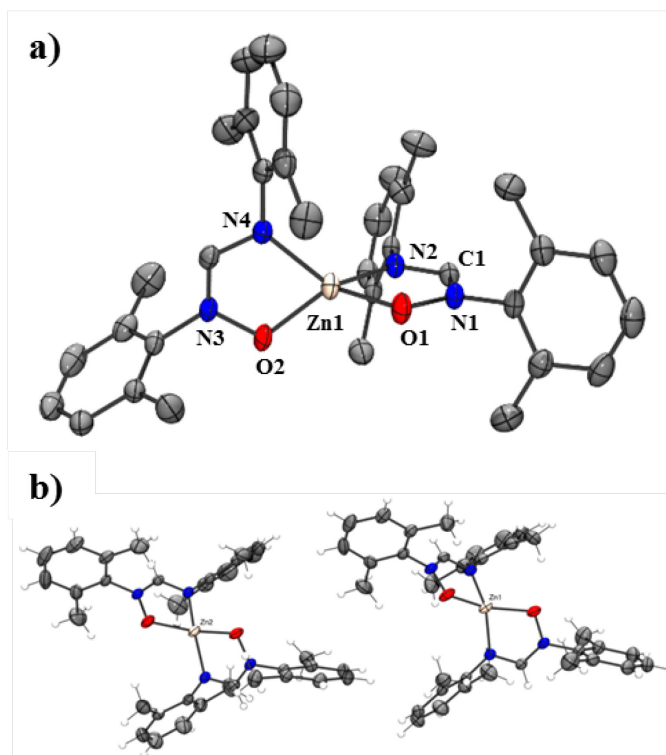
Figure 5.2-4. (a) ORTEP view of **3b**. Ellipsoids are shown at 50% probability level. Hydrogen atoms are omitted for clarity. (b) The two molecules in the asymmetric unit.[15]
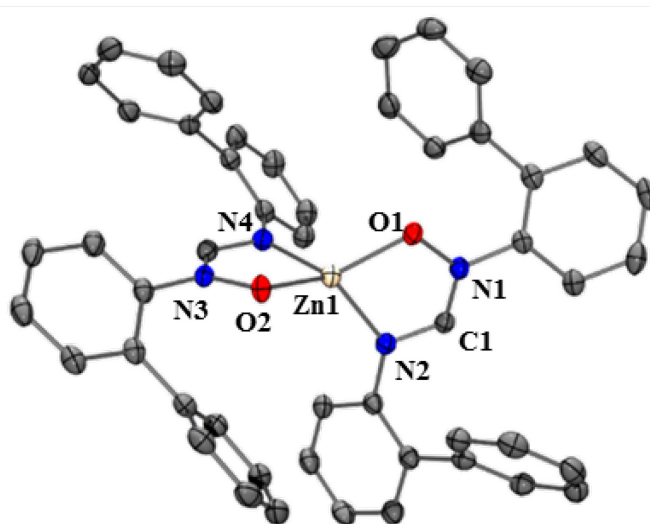
Figure 5.2-5. ORTEP view of **3d**. Ellipsoids are shown at 50% probability level. Hydrogen atoms are omitted for clarity.[15]

Four of these eight structures correspond to zinc complexes of redox-active ligands of *o*-aminophenol[19] and phenoxazin-1-one types.[20] In addition to the AMOXs, the other N,O ligands, that form five-membered (bis)chelates of tetrahedral geometry with zinc(II) ions are: [(Me₃Si)N(*i*-Pr₂PCO₂)]⁻,[21] triazene-1-oxide-type ligands,[22] and sterically demanding 8-hydroxyquinoline derivatives.[23] The τ_4[24] values are 0.73 for **3a**, 0.72 for **3b,** and 0.77 for **3d**, and the periplanar angle (γ; Table 5.2-2) between the two five-membered chelate rings are 70(1)°, 80(1)° and 85(1)°, respectively. These values are indicative of a similar degree of distortion from a perfect tetrahedron in **3a** and **3b** (disubstitution pattern), and are also comparable with those for zinc(II) bis(chelates) of triazen-1-oxides[22] and 8-hydroxyquinoline derivatives[23b] (**4** and **6**; Table 5.2-2). Furthermore, **3d** (monosubstitution pattern) is closer to the perfect tetrahedron, as are the corresponding zinc(II) complexes of *o*-aminophenol[19a] and *β*-ketoamine-type[25] ligands (**5** and **8**; Table 5.2-2). The Zn–O and Zn–N bond lengths are significantly different within the series of Zn(AMOX)₂ complexes reported herein, but they are still comparable within the series and with those found for similar structures.[22-23, 25-26] In **3a**, the mean Zn–O bond length is 1.977(1) Å whereas the same bond lemgths in **3b** range between 1.987(1) Å – 1.992(1) Å (for the two molecules in the asymmetric unit). These values are close to those reported for tetrahedral zinc complexes of triazen-1-oxides[22] and 8-hydroxyquinoline derivatives[23b] (**4** and **6**; Table 5.2-2).

Table 5.2-1. Solid state structure and refinement data for compounds **3a**, **3b**, and **3d**.

Compound	3a	3b	3d
Formula	$C_{50}H_{70}N_4O_4Zn$ $\cdot 2(CH_3OH)_2$	$C_{34}H_{38}ZnN_4O_2$	$C_{50}H_{38}ZnN_4O_2$
M_w (g/mol)	888.55	600.05	792.23
Temperature (K)	200	150	100
Wavelength (Å)	1.54178	1.54178	1.34139
Crystal System	Triclinic	Monoclinic	Orthorhombic
a (Å)	11.6191(2)	8.7240(3)	19.3727(6)
b (Å)	11.9438(3)	30.8185(11)	7.8496(2)
c (Å)	21.8727(4)	24.0226(8)	24.8195(7)
α (°)	98.728(1)	90	90
β (°)	94.086(1)	99.443(2)	90
γ (°)	117.556(1)	90	90
Unit cell volume (Å^3)	2625.0(1)	6371.2(4)	3774.3(1)
Space Group	P-1	P21/n	Pca2$_1$
Z	2	8	4
$d_{calcd.}$ (g/cm^3)	1.124	1.251	1.394
μ (mm^{-1})	0.985	1.340	0.800
F(000)	960	2528	1648
Reflections collected	33981	82669	69171
Independent reflections	9932	12500	8671
GoF	1.086	0.943	1.040
R1(F) [I > 2σ(I)]	0.0491	0.0352	0.0404
wR(F^2) [I > 2σ(I)]	0.1262	0.0912	0.0970
R1(F) (all data)	0.0542	0.0458	0.0515
wR(F^2) (all data)	0.11298	0.0951	0.1035
Largest diff. peak/ hole (e/Å^3)	0.414 and -0.549	0.269 and -0.435	1.17 and -0.22
Flack parameter	-	-	0.49(3)

Table 5.2-2. Selected bond distances (Å) and angles [°] for **3a**, **3b**, and **3d** obtained from XRD, their optimized structures as well as examples of previously reported zinc bis(chelates) (**4-8**).

Cpd.	τ_4[g]	Bond distances (Å)					Angle (°)	Tilt angles (°)		
		Zn-O	Zn-N	C1-N1	C1-N2	O1-N1	O-Zn-N	Ar(NO)[j]	ArN[j]	γ[k]
3a	0.73	1.977(1)[h]	1.981(1)[h]	1.320(4)[h]	1.314(3)[h]	1.384(2)[h]	84.1(1)[h]	81(1)[h]	70(1)[h]	75(1)
3b	0.72	1.987(1) - 1.992(1)[i]	1.963(1)- 1.971(1)[i]	1.314(4)[h]	1.319(4)[h]	1.378(4)[h]	84.2(2)[h]	78(1)- 89(1)[i]	70(1)- 76(1)[i]	80(1)[h]
3d	0.77	1.953(3)[h]	2.004(4)[h]	1.320(6)[h]	1.324(6)	1.378(5)[h]	84.5(1)[h]	42(1)[h]	45(1)[h]	85(1)
4[a]	0.74	1.967(4)[h]	1.968(4)[h]	-	-	1.330(4)[h]	80.3(1)[h]	-	7(1)[h]	86(1)
5[b]	0.77	1.924(1)[h]	2.052(1)[h]	-	-	-	85.7(1)[h]	-	-	84(1)
6[c]	0.68	1.997(3)[h]	2.037(4)[h]	-	-	-	83.5(1)[h]	-	-	85(1)
7[d]	0.09	1.851(1)[h]	1.871(1)[h]	-	-	-	91.2(1)[h]	-	-	37(1)
8[e]	0.79	1.953(1)- 1.958(1)[i]	1.966(1)[h]	-	-	-	96.4(1)- 97.3(1)[i]	-	-	85(1)
3a-dft[f]	0.73	1.98[h]	2.02[h]	1.33[h]	1.32[h]	1.38[h]	84[h]	81-90[i]	70[h]	80
3b-dft[f]	0.78	1.99[h]	2.01[h]	1.33[h]	1.32[h]	1.38[h]	84[h]	83[h]	73[h]	90
3d-dft[f]	0.78	1.97[h]	2.02[h]	1.33[h]	1.32[h]	1.37[h]	84[h]	47[h]	43[h]	90

[a] **4**: Zn(RN$_3$Ar)$_2$ – (ZOSMUP)[22]; [b] **5**: Zn(L)$_2$, L=*o*-aminophenol-type ligand (YAVGIN)[19a]; [c] **6**: Zn(L)$_2$, L=8-hydroxyquinoline-type ligand (KEHPEU)[23b]; [d] **7**: Zn(L)$_2$, L=[N$_2$O$_2$]-Schiff base type ligand (MAHZUR)[27]; [e] **8**: Zn(L)$_2$, L=*β*-ketoamine-type ligand (FEXNON)[25]; [f] optimized structures, theory level: B3LYP/ 6-31g(d, p), PCM: CH$_2$Cl$_2$; [g] as defined by
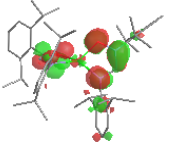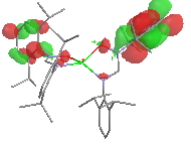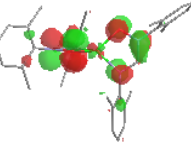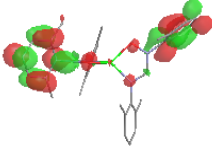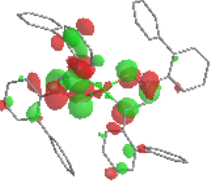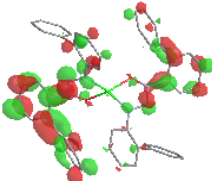
Houser[24]; [h] average value; [i] range of values for the two molecules in the asymmetric unit; [j] angle between the plane of the -N-C=N- moiety and the plane of the aromatic ring; [k] periplanar angle between the two five-membered chelate rings.

Table 5.2-3. Photophysical,[a] electrochemical,[b] and theoretical[c] data for **3a-3d**.

Cpd.	Experimental data						Theoretical data		
	λ_{max} [nm] (ε x 10^2 [$M^{-1}cm^{-1}$])	E_{pa}(irr) [V] *vs*. SCE	E_{ox_onset} [V]	HOMO[d] [eV]	LUMO[e] [eV]	E_g[f] [eV] (λ_{abs_onset} [nm])	HOMO[g] [eV]	LUMO[h] [eV]	E_g(TD-DFT)[i] [eV]
3a	270 (178), 287 (148) sh	1.17; 1.44; 1.63	1.04	-5.44	-1.54	3.90 (318)	-5.13	-1.17	3.96 (313)
3b	267 (208), 296 (150) sh	1.18; 1.41; 1.73	1.07	-5.47z	-1.64	3.83 (324)	-5.20	-1.33	3.87 (320)
3c	270 (177), 304 (252)	0.98; 1.31; 1.70	0.86	-5.26	-1.98	3.60 (344)	-	-	-
3d	237 (460), 325 (190)	1.03; 1.30; 1.81	0.88	-5.28	-2.10	3.28 (378)	-5.15	-1.66	3.49 (355)

[a] the photophysical data were obtained in CH_2Cl_2, at room temperature; [b] the electrochemical data were obtained under the following conditions: dry CH_2Cl_2, [nBu_4N]PF_6 0.1M, compound concentration about 1mM, glassy carbon electrode, scan rate 100 mV/s, room temperature, Ar atmosphere, ferrocene used as internal reference; Fc/Fc$^+$ *vs*. SCE was considered 0.46V in DCM[28]; [c] theory level: B3LYP/ 6-31g(d, p), PCM: CH_2Cl_2. [d] the HOMO level was determined with the equation: E_{HOMO} [eV] = -(4.4 + E_{ox_onset}); [e] no reduction process is observed; LUMO level was determined with the equation: E_{LUMO} [eV] = E_{HOMO} + E_g; [f] E_g was obtained through the absorption edge technique[10c]: E_g = 1240/λ_{abs_onset}; [g] the HOMO level was obtained from DFT optimization, theory level: B3LYP/ 6-31g(d, p), PCM: CH_2Cl_2; [h] LUMO level was obtained using E_{LUMO} [eV] = E_{HOMO} (DFT) + E_g(TD-DFT); [i] E_g(TD-DFT) is the TD-DFT calculated first singlet, which corresponds to the HOMO-LUMO transition; theory level: B3LYP/ 6-31g(d, p), PCM: CH_2Cl_2.

Table 5.2-4. TD-DFT calculated lowest-energy singlet transitions for **3a-3d** with plots of corresponding natural transition orbitals [NTOs; theory level: B3LYP/ 6-31g(d, p), PCM: CH_2Cl_2].

Cpd.	λ/ nm (Oscillator strength)	Transition (% contribution)	NTO surfaces	
			'Hole'	'Particle'
3a	313 (0.0033)	HOMO->LUMO (76) H-1->L+1 (19)		
3b	320 (0.0089)	HOMO->LUMO (75) H-1->L+1 (23)		
3d	355 (0.0902)	HOMO->LUMO (67) H-1->L+1 (30)		

The Zn–N bond lengths in **3a** and **3b** [1.981(1) Å and 1.963(1) Å – 1.971(1) Å, respectively] are comparable with the corresponding values in **4**, as well as with those in previously reported tetrahedral zinc complexes of β-ketoamine-type[25] ligands (**8**; Table 5.2-2). In **3d**, the mean Zn–O bond length [1.953(3) Å] is significantly shorter than in **3a** and **3b** and is similar to the values reported for tetrahedral zinc(II) complexes of β-ketoamine-type[25] ligands [1.953(1) – 1.958(1) Å], (**8**, Table 5.2-2). The mean Zn–N bond length of 2.004(4) Å (in **3d**) is longer than those in **3a** and **3b**, and is in the same range with those found in tetrahedral zinc complexes of o-aminophenol[19a] and 8-hydroxyquinoline derivatives[23b] (**5** and **6**, Table 5.2-2). The Zn–O and Zn–N bond lengths in **3a**, **3b** and **3d** are significantly longer than those reported for zinc complexes of Schiff base-type ligands[27] (**7**, Table 5.2-2); planar geometry is forced by the macrocyclic nature of the ligand in the latter (the value of τ_4[24] is 0.09).

The different Zn–O and Zn–N bond lengths in **3a**, **3b** and **3d** is not reflected in the expansion/ contraction of the O–N–C and N-C-N angles, which are equivalent in the three structures. Furthermore, the endocyclic O–Zn–N angles are also identical in all three compounds [84.1(1), 84.2(2), and 84.5(1)°, respectively]. The bite angle of the ligand and the strain of the five-membered chelate ring determine the contraction of this angle with respect to the ideal values.

The mean O–N bond lengths are identical in **3a**, **3b** and **3d**, and they are longer that those in triazene-1-oxides zinc complexes. All the bond lengths in the AMOX moiety are identical for the three compounds; this supports the idea of the delocalization of electron density in the –N=C-N-O– AMOX linkage, and allows the influence of the substituents on the Zn–O and Zn–N bonds and the geometry around the zinc(II) ion to be assessed. To accommodate the steric bulk generated by the 2,6-substituents of the aryl rings, the phenyl rings are pushed almost perpendicular to the plane of the chelate ring [the tilt angles in **3a** and **3b** are in the range of 70(1)° - 89(1)°], therefore, the electron density of the –N=C-N-O– AMOX linkage is less delocalized on the aromatic moieties of the ligand in **3a** and **3b**, whereas the 2-biphenyl substituted **3d** analogue has more delocalization on the aromatic rings, as supported by values of the tilt angles of 42(1)°for Ar(NO) and 45(1)° for Ar(N) substituents. The smaller tilt angles in **3a** [81(1)° for Ar(NO) and 70(1)° for Ar(N)) relative to

those of **3b** [78(1)° - 89(1)°for Ar(NO) and 70(1)° - 76(1)° for Ar(N)] are explained by greater repulsive interactions between the 2,6-diisopropyl substituents in **3a** than between the 2,6-dimethyl substituents in **3b**, for which the tilt angles are close to perpendicularity.

In both **3a** and **3b**, the O atoms from the metal chelate rings are implicated in simple and bifurcated intra- and intermolecular hydrogen bonding. This type of interaction is a common feature for zinc(II) complexes having an O atom as at least one of the chelating atoms: 57 results were obtained in CSD[16] for five-membered ring zinc(II) chelates of this type.[29] In **3a**, the O atoms interact with the ArN isopropyl protons (–C**H**-CH$_3$) (d = 2.61 Å, D = 3.35 Å, θ = 131°, intramolecular) and with the -O**H** protons of the co-crystallised methanol molecules (d = 1.98 Å, D = 2.80 Å, θ = 167°; Figure S8, Appendix 5.2-SI). In **3b**, the ArN methyl protons form intramolecular hydrogen bonds with the O atoms (d = 2.56 Å, D = 3.44 Å, θ = 152°), while the ArNO methyl (d = 2.47 Å, D = 3.38 Å, θ = 157°) and *m*-H-C(sp2) protons (d = 2.62 Å, D = 3.46 Å, θ = 150°) are implicated in weak intermolecular interactions of the same type (Figure S9; Appendix-5.2-SI). The participation of the O atoms in hydrogen-bonding interactions lowers their π-donation character and combined with the overall packing interactions, and the steric bulk of the ligands, contributes to the observed pseudotetrahedral geometry around the zinc(II) ion, in combination with the overall packing interactions and the steric bulk of the ligands. In **3d** the O atoms are not implicated in hydrogen-bonding. This, as well as the presence of attractive intramolecular interactions of the C(sp2)–H···πC(sp2) type (d = 2.6 – 3.5 Å; Figure S10, Appendix 5.2-SI), could explain the shorter Zn–O bond in this structure relative to those in **3a** and **3b**. Further examination of the packing interactions reveals intermolecular non-classical hydrogen-bonding of the πC(sp2)···πC(sp2) type for **3b**, and C(sp2)–H···π C(sp2) type for both **3b** and **3d**.

5.2.5.4. UV/vis Spectroscopic Properties

The spectroscopic data for the zinc(II) complexes **3a-3d** are summarized in Table 5.2-3. Their UV/vis spectra in DCM are shown in Figure 5.2-6, together with those of the corresponding AMOX ligands **2a-2d**. The electronic spectra of the compounds display the characteristic ligand-centred/ intraligand (LC/ IL) π-π* transitions in the UV region with high molar absorptivity coefficients, as expected for complexes with closed-shell d^{10} zinc(II) ions.

Upon complexation, slight red shifts of the lowest-energy absorption bands relative to those of the free ligands can be identified for **3a** and **3b**, whereas minor blue shifts are observed for **3c** and **3d**. For the same lowest-energy absorption band, a progressive red shift is observed across the **3a-3d** series. The intensity of this band varies as follows: the highest absorptivity coefficients are found for **3c** (25200 $M^{-1}cm^{-1}$) and **3d** (19000 $M^{-1}cm^{-1}$), followed by **3b** (15000 $M^{-1}cm^{-1}$) and **3a** (14800 $M^{-1}cm^{-1}$). The interpretation of the electronic spectra was greatly aided by TD-DFT calculations (*vide infra*).
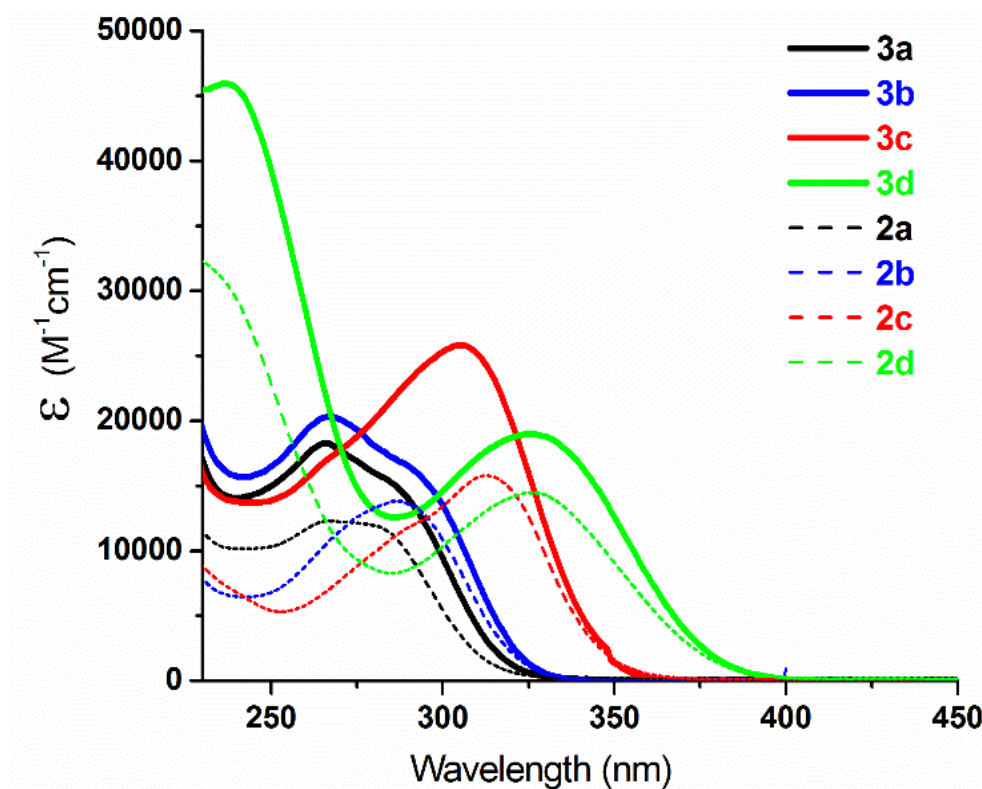
Figure 5.2-6. Electronic spectra of **3a-3d** and their corresponding ligands **2a-2d** in CH_2Cl_2 at room temperature. (λ_{max} [nm] (ε x 10^2 [$M^{-1}cm^{-1}$])) **2a**: 280 (110); **2b**: 286 (130); **2c**: 293sh (120), 313 (154); **2d**: 231 (321), 324 (145).

5.2.5.5. Electrochemistry

The redox properties of the Zn(AMOX)$_2$ complexes were also examined and the data are reported in Table 5.2-3. The cyclic voltammograms (CVs) of **3a-3d** in dry DCM (Figure S11, Appendix-5.2-SI) display three irreversible ligand-based oxidation processes. The first two oxidations appear at similar potentials within the series [0.98 V – 1.18 V and 1.30 V –

1.44 V (vs. SCE), respectively], which indicates that substitution effects are minor. The third oxidation is the easiest in **3a** (1.63 V), followed by **3b** and **3c** (at similar potentials: 1.73 V and 1.70 V respectively), and then **3d** at 1.81 V; this series follows the increase in the electron-donating character of the ligands. It is important to mention that no reduction wave were observed for **3a-d** in the electrochemical window of DCM; therefore the LUMOs are at high energies. The difficult reduction is in line with the anionic character of the ligand, enhanced by the effect of the electron-donating substituents, and was also reported for zinc(II) complexes of benzothiazole derivatives,[11] cobalt(II) complexes of electron-donating AMOX ligands,[30] as well as for cobalt complexes of triazene-1-oxides.[31] From the CVs of the compounds, the experimental energies of their HOMOs were determined (Figure 5.2-7, Table 5.2.-3) from the onset potential of the first oxidation wave (E_{ox_onset}), using the data vs. SCE, and the formula: E_{HOMO} [eV] $= -(4.4 + E_{ox\_onset})$.[9-12] As no reduction was observed for the compounds reported herein, the energies of the LUMOs were determined by using the equation: E_{LUMO} [eV] $= E_{HOMO} + E_g$, where E_g is the optical band gap, obtained through the absorption-edge technique ($E_g = 1240/\lambda_{abs\_onset}$).[10c, 32]

5.2.5.6. DFT and TD-DFT calculations

DFT and TD-DFT calculations were performed for **3a**, **3b**, and **3d** in dichloromethane [theory level B3LYP/ 6,31-g(d,p), PCM: CH_2Cl_2]. This simple theoretical model has been applied to similar systems.[9-12, 33] The optimized calculated structures are in good agreement with the XRD data (Table 5.2-2). The DFT and TD-DFT results support the experimental observations and are in very good agreement with the values obtained experimentally (Tables 5.2-2 – 5.2-4, Figures 5.2-7 – 5.2-9, and Figures S12-S15, Appendix 5.2-SI). In all three structures, the HOMO is localized on the –N=C-N-O– AMOX moiety (Figure 5.2-8, Table S1, Appendix 5.2-SI), without contribution from the zinc(II) ion. As expected for a closed shell d^{10} metal ion, the zinc-based orbitals are very stable and are not involved in the redox or optical properties.

The localization of the HOMO on the AMOX moiety explains the substituent effect in agreement with the electrochemical data. The LUMO is localized on Ar(NO) (the aryl ring with the N-O moiety attached, Figure 5.2.-8, Table S1, Appendix 5.2-SI), and is, therefore,

directly influenced by the substitution pattern and the degree of electron-density delocalization on the respective aryl ring. Enhanced delocalization lowers the LUMO level and, therefore, decreases the band gap. Thus, the DFT and TD-DFT results confirm and explain the red shift of the lowest-energy electronic transition observed in the UV/vis spectra of **3a-3d**, in line with the higher degree of delocalization in **3d** and **3c** vs. **3a** and **3b** (Tables 5.2-3 − 5.2-4 and Figures 5.2-7 − 5.2-9; Figures S12-S15 and Tables S2-S4, Appendix 5.2-SI).
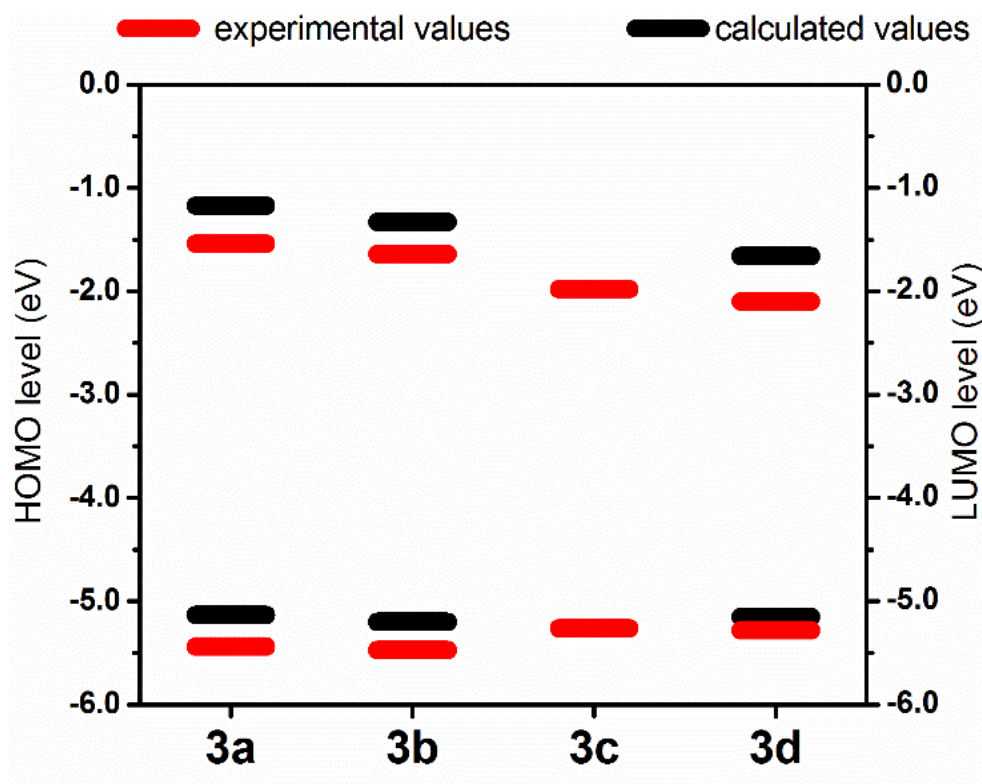
Figure 5.2-7. Experimental *versus* calculated band gaps for **3a-3d**

The trend is consistent with the values of the tilt angles between the N=C-N plane and the aryl rings attached to the N (ArN) and N-O (Ar(NO)) moieties and the bulkiness of the substituents (Table 5.2-2).

The order of increasing intensity of the electronic transitions (**3a** < **3b** < **3d**) is also reproduced by the TD-DFT calculations: the oscillator strength calculated for **3a** is the lowest, followed by **3b** and **3d** (Tables 5.2-3 − 5.2-4 and Figure 5.2-9; Tables S2-S5 and Figures S12-S15, Appendix 5.2-SI). In addition, the change in ligand conformation upon metal-ion

complexation increases the energy of the LUMO relative to those for the free ligands, because the electron-density delocalization is decreased owing to the 'decoupling' of the Ar(NO) ring from the π system of the AMOX, as indicated by the tilt angle of $78° – 89°$ for **3a** and **3b**, and $42°$ for **3d**.

Cpd.	Molecular orbital (MO) surfaces	
	HOMO	LUMO
3a		
3b		
3d		
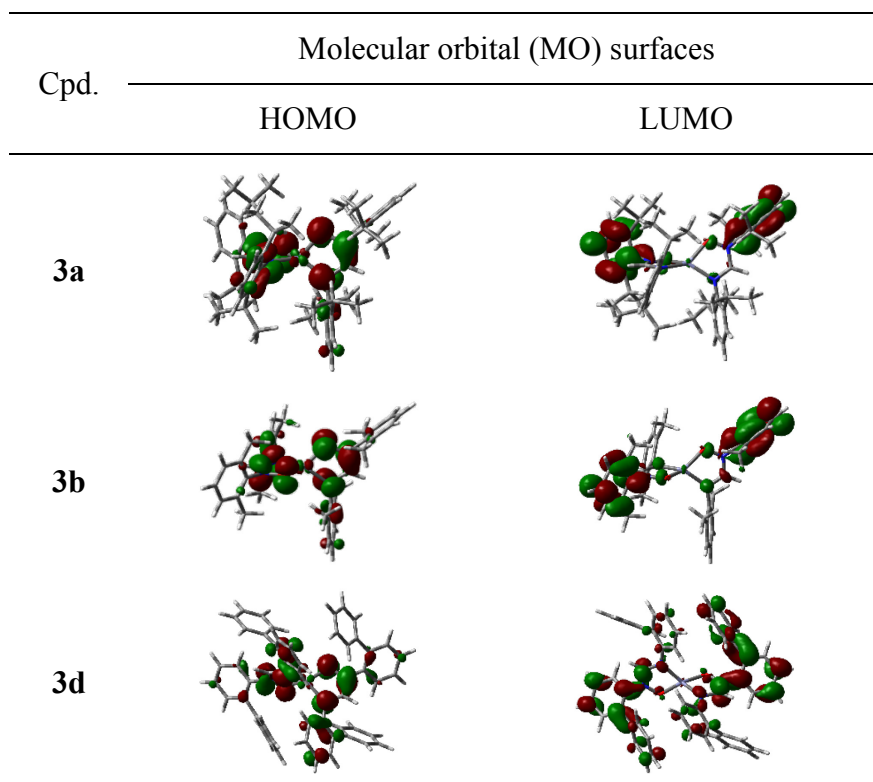
Figure 5.2-8. DFT-optimized structures of **3a-3d** with surfaces of the frontier molecular orbitals (MOs)

The complexation influence on the energy of the HOMO with respect to the free ligands is the result of combined phenomena of opposite effects: the presence of increased electron density with reduced delocalization leads to destabilization, whereas stabilization is generated as the zinc(II) cation withdraws electron density from the –N=C-N-O– AMOX bridge. Further analysis of the TD-DFT calculations (Table 5.2-4 and Figure 5.2-9; Tables S2-S4 and Figures S12-S15, Appendix-5.2-SI) indicates a strong correlation of the experimental data with the corresponding calculated transitions. The assignment of the electronic transitions for complexes **3a**, **3b**, and **3d** confirms the nature of the lowest energy transition (HOMO-LUMO, Table 5.2-4). The subsequent electronic transitions at higher energies are also well modeled, and their detailed descriptions are presented in Tables S2-S4, Appendix 5.2-SI.
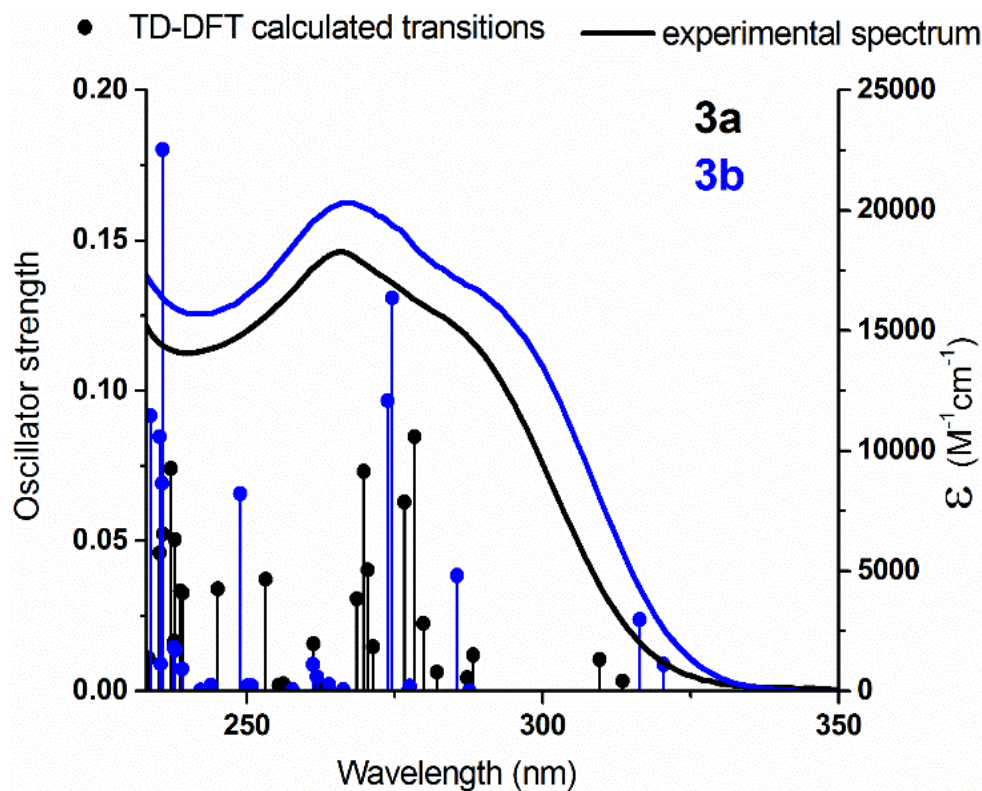
Figure 5.2-9. Electronic spectra of **3a** (in black) and **3b** (in blue) in CH$_2$Cl$_2$: experimental spectra and TD-DFT calculated transitions (vertical lines), theory level: B3LYP/ 6,31-g(d,p), PCM: CH$_2$Cl$_2$

5.2.6. Conclusions

The AMOX complexes described herein allowed the effect of *N*- substitution on the metal-ligand interaction as well as their structural, spectroscopic, and electrochemical properties to be examined. Bulky substituents in the 2,6 positions increase the electronic density in the amidine-oxide backbone, by disrupting its delocalization on the *N*-moieties of the molecule (electronic effect induced by steric modification). This substitution pattern also prevents additional coordination to the metal ion, and contributes to an enhanced solubility of the compounds. The theoretical calculations (DFT and TD-DFT) undertaken allowed the assessment and the rationalization of the influence of ligand modification on the properties of the complexes. The AMOX ligand family shows great promise to prepare a wide variety of transition metal complexes with predictable and tunable properties.

5.2.7. Experimental Section

Materials and instrumentation

The metal salts, the anilines and the triethylorthoformate were purchased from Aldrich, and the *m*-CPBA 77% was purchased from Acros, and all were used without further purification. ACS grade solvents were purchased from VRW and Fisher and were removed under reduced pressure using a rotary evaporator, unless otherwise stated. Nuclear magnetic resonance (NMR) spectra were recorded in DMSO-d_6, C_6D_6, and $CDCl_3$ at 25°C, on the following spectrometers: Bruker AV-400, AV-500, and DRX-400. Chemical shifts (δ) are reported in part per million (ppm) relative to TMS, and are referenced to the residual solvent signal (2.50 ppm for DMSO-d_6, 7.16 ppm for C_6D_6, and 7.26 ppm for $CDCl_3$). Absorption spectra were measured in dichloromethane (previously distilled), between 230 and 1400 nm, at room temperature (r.t.), on a Cary 500i UV-Vis-NIR spectrophotometer. Solution samples were prepared in concentration range 10^{-5} to 10^{-3} M. Electrochemical measurements were carried out in argon-purged dry DCM, at room temperature, with a BAS CV50W multipurpose potentiostat. The working electrode was a glassy carbon electrode. The counter electrode was a Pt wire, and the pseudo-reference electrode was a silver wire. The reference was set using an internal 1 mM ferrocene/ferrocenium sample at 460 mV *vs*. SCE in DCM.[28] The concentration of the compounds was about 1 mM. Tetrabutylammonium hexafluorophosphate (TBAP) was used as supporting electrolyte and its concentration was 0.10 M. Cyclic voltammograms were obtained at scan rates of 50, 100, 200, and 500 mV/s. For irreversible oxidation processes, the anodic peak was used as *E*. Experimental uncertainties are as follows: absorption maxima, ±2 nm; molar absorption coefficient, 10%; redox potentials, ± 10 mV. The microanalyses and the mass spectrometry analyses were performed at the Elemental Analysis Service and the Regional Mass Spectrometry Centre at Université de Montréal.

X-ray structure determination

The crystal structure determination and refinement data for **3a**, **3b**, and **3d** are given in Tables 5.2-1 and 5.2-2 and Figures 5.2-3 – 5.2-5. Full details are provided in Appendix-5.2-SI. CCDC-963739 (for **3b**), -963740 (for **3a**) and -1426815 (for **3d**) contain the supplementary

crystallographic data for this paper. These data can be obtained free of charge via www.ccdc.cam.ac.uk/data_request/cif.

Computational details

Gaussian09, Revision D.01[34] was used for all theoretical calculations discussed herein, with B3LYP[35] DFT method, 6,31-g(d,p)[36] basis set, and PCM[37] (CH_2Cl_2) solvation model. Initial atom coordinates for geometry optimization were taken from XRD data (cif) of the corresponding structures. No symmetry constraints were used for the geometry optimization. Details on optimized structures are given in Tables S5-S7, Appendix-5.2-SI. No imaginary frequencies were obtained when frequency calculations on optimized geometries were performed. TD-DFT[38] calculations (for the first 30 (**3a**, **3b**) and 50 (**3d**) singlet states) were performed, starting with the optimized geometries of the ground states. GaussView 3.0.9[39] Gaussum[40] and Chemissian V.4.36[41] software were used for data analysis, visualisation, and surface plots.

Synthesis

The syntheses of the AMOX ligands **2a-d**[5, 13e, 14] and their parent amidines **1a-d**[13] were previously reported.

Synthesis of complexes

General procedure.[4c, 5] A solution of the ligand (2 eq.) in aqueous ethanol 90% was added to a solution of metal salt (1 eq.) in water, previously brought to pH 8 with an aqueous solution of KOH or NaOH. The formation of precipitate is observed almost instantly. The reaction mixture was stirred at room temperature before water was added (reaction times are specified below for each compound), and was kept at 4°C for 1-2 h before being filtered. The resulted solid was washed with hot water and aqueous ethanol 50%, and was dissolved in DCM and dried over $MgSO_4$. A second filtration and evaporation of the solvent yielded the desired products as solids. When necessary, further purification by recrystallization was performed.

Bis(*N,N'*-bis(2,6-diisopropylphenyl)-*N*-oxidoformamidinate) of zinc(II) (3a) − The following reagents were combined according to the general procedure: *N*-hydroxy-*N,N'*-bis(2,6-diisopropylphenyl)formamidine (0.26 g, 0.69 mmol, 2 eq.) and Zn(II) acetate · 2 H_2O (0.08 g, 0.35 mmol, 1 eq.). Reaction time: 24 h. The resulting colourless solid was

recrystallized in hot methanol to afford colorless crystals. Yield: 0.27 g, 95%. X-Ray quality crystals were obtained using the same recrystallization procedure.

^{1}H NMR (C$_6$D$_6$, 400 MHz): δ=7.19 (m, 1H, *p*-C$_6$**H**$_3$-(*N*); (**H4'**)), 7.11-7.02 (m, 5H, -*m*-C$_6$**H**$_3$-(*NO*); (**H3 and H5**) and -*p*-C$_6$**H**$_3$-(*NO*); (**H4**) and -*m*-C$_6$**H**$_3$-(*N*); (**H3' and H5'**)), 6.89 (s, 1H, -N-C**H**=N-; (**H1**)) 3.48 (hept, *J* = 7 Hz, 2H, -C**H**-CH$_3$ or -C**H'**-CH$_3$), 3.35 (hept, *J* = 7 Hz, 2H, -C**H**-CH$_3$ or -C**H'**-CH$_3$), 1.30 (d, *J* = 7 Hz, 6H, -CH-C**H**$_3$ or -CH-C**H**$_3$'), 1.20 (d, *J* = 7 Hz, 6H, -CH-C**H**$_3$ or -CH-C**H**$_3$'), 1.15 (d, *J* = 7 Hz, 6H, -CH-C**H**$_3$ or -CH-C**H**$_3$'), 1.00 (d, *J* = 7 Hz, 6H, -CH-C**H**$_3$ or -CH-C**H**$_3$'). ^{13}C NMR (C$_6$D$_6$, 101 MHz): δ=150.0 (1C, -N-**C**H=N-), 147.7 (2C, -*o*-**C**$_6$H$_3$), 143.4 (2C, -*o*-**C**$_6$H$_3$), 143.2 (1C, -**C**$_6$H$_3$), 138.5 (1C, -**C**$_6$H$_3$), 129.8 (1C, -*p*-**C**$_6$H$_3$), 125.3 (1C, -*p*-**C**$_6$H$_3$), 123.8 (2C, -*m*-**C**$_6$H$_3$), 123.3 (2C, -*m*-**C**$_6$H$_3$), 28.86 (2C, -**C**H-CH$_3$), 28.19 (2C, -**C**H-CH$_3$), 24.96 (2C, -CH-**C**H$_3$), 24.65 (2C, -CH-**C**H$_3$), 24.59 (2C, -CH-**C**H$_3$), 23.12 (2C, -CH-**C**H$_3$). Elemental Analysis: *calc.* (%) for C$_{50}$H$_{70}$N$_4$O$_2$Zn (824.51g/mol): C 72.84, H 8.56, N 6.80; *found*: C 72.19, H 8.63, N 6.76. MS (MALDI) (m/z): 823.49 [M+H]$^+$. IR (ATR, solid sample, cm^{-1}): 3065, 3009, 2961, 2927, 2867, 1606, 1581, 1459, 1439, 1382, 1361, 1324, 1304, 1254, 1215, 1191, 1164, 1147, 1100, 1059, 1044, 998, 928, 816, 803, 761, 729, 682, 618, 582, 532, 491, 476, 456, 432.

Bis(*N,N'*-bis(2,6-dimethylphenyl)-*N*-oxidoformamidinate) of zinc(II) (3b) – The following reagents were combined according to the general procedure: *N*-hydroxy-*N,N'*-bis(2,6-diisopropylphenyl)formamidine (0.50 g, 1.9 mmol, 2 eq.) and Zn(II) acetate · 2 H$_2$O (0.20 g, 0.9 mmol, 1 eq.). Reaction time: 24 h. The resulting colourless solid was recrystallized in DCM/hexane to afford a pale beige powder. Yield: 0.37 g, 65%. X-Ray quality crystals were obtained from methanol/water by slow diffusion at 4 °C and from dmso-d$_6$ by slow evaporation.

^{1}H NMR (C$_6$D$_6$, 400 MHz): δ=7.00 (d, *J* = 7 Hz, 2H, -*m*-C$_6$**H**$_3$-(*N*); (**H3' and H5'**)), 6.96-6.91 (m, 2H, -*p*-C$_6$**H**$_3$-(*N*) and -*p*-C$_6$**H**$_3$-(*NO*); (**H4' and H4**)), 6.81 (d, *J* = 7 Hz, 2H, -*m*-C$_6$**H**$_3$-(*N*); (**H3 and H5**)), 6.16 (s, 1H, -N-C**H**=N-; (**H1**)), 2.16 (s, 6H, -C**H**$_3$), 2.14 (s, 6H, -C**H**$_3$'). ^{1}H-NMR (DMSO-*d*$_6$, 400 MHz) δ, ppm: 7.84 (s, 1H, -N-C**H**=N-; (**H1**)), 7.19 (t, *J* = 8 Hz, 1H, -*p*-C$_6$**H**$_3$-(*N*); (**H4'**)), 7.11 (d, *J* = 8 Hz, 2H, -*m*-C$_6$**H**$_3$-(*N*); (**H3' and H5'**)), 6.98 (d, *J* = 8 Hz, 2H, -*m*-C$_6$**H**$_3$-(*NO*); (**H3 and H5**)), 6.88 (t, *J* = 8 Hz, 1H, -*p*-C$_6$**H**$_3$-(*NO*); (**H4**)), 2.17 (s, 6H, -C**H**$_3$'), 1.97 (s, 6H, -C**H**$_3$). ^{13}C-NMR (DMSO-*d*$_6$, 75 MHz): 149.6 1C, -N-**C**H=N-), 145.1 (1C,

-C₆H₃), 140.3 (1C, **-C₆H₃**), 135.9 (2C, **-o-C₆H₃**), 132.0 (2C, **-o-C₆H₃**), 128.5 (1C, **-p-C₆H₃**), 127.9 (2C, **-m-C₆H₃**), 127.7 (2C, **-m-C₆H₃**), 123.7 (1C, **-p-C₆H₃**), 18.11 (2C, **-C**H₃), 16.90 (2C, **-C**H₃). Elemental Analysis: *calc.* (%) for C₃₄H₃₈N₄O₂Zn (600.08 g/mol): C 68.05, H 6.38, N 9.34; *found*: C 67.65, H 6.90, N 9.30. MS (MALDI) (m/z): 599.24 [M+H]⁺. IR (ATR, solid sample, cm⁻¹): 2917, 1611, 1582, 1470, 1373, 1306, 1203, 1089, 994, 929, 765, 687, 591, 531

Bis(*N,N'*-bis(2-isopropylphenyl)-*N*-oxidoformamidinate) of zinc(II) (3c) – The following reagents were combined according to the general procedure: *N*-hydroxy-*N,N'*-bis(2-isopropylphenyl) formamidine (0.2 g, 0.7 mmol, 2 eq.) and Zn(II) acetate · 2 H₂O (0.07 g, 0.33 mmol, 1 eq.). Reaction time: 24 h. A colourless solid was obtained. Yield: 0.07 g, 78%.

¹H NMR (C₆D₆, 300 MHz, TMS): δ=7.44 (s, 1H, -N-C***H***=N-, (**H1**)), 7.23 (d, *J* = 7 Hz, 1H, *o*-C₆***H***₃-(*N*); (**H6'**)), 7.13 (d, 1H, *o*-C₆***H***₃-(*NO*); (**H6**)), 7.10 – 6.94 (m, 3H, *m*-C₆***H***₃-(*NO*); (**H5**) and *m*-C₆***H***₃-(*N*); (**H5'**) and *p*-C₆***H***₃-(*N*); (**H4'**)), 6.89 – 6.83 (m, 2H, *p*-C₆***H***₃-(*NO*); (**H4**) and *m*-C₆***H***₃-(*NO*); (**H3**)), 6.72 (d, *J* = 7 Hz, 1H, *m*-C₆***H***₃-(*N*); (**H3'**)), 3.86 (hept, *J* = 7 Hz, 1H, -C***H***-CH₃ or -C***H'***-CH₃), 3.72 (hept, *J* = 7.0 Hz, 1H, -C***H***-CH₃ or -C***H'***-CH₃), 1.23 (d, *J* = 7 Hz, 6H, -CH-C***H***₃ or -CH-C***H***₃'), 1.18 (d, *J* = 7 Hz, 6H, -CH-C***H***₃ or -CH-C***H***₃'). ¹³C NMR (C₆D₆, 101 MHz, TMS): δ = 149.00 (1C, -N-***C***H=N-), 146.32 (1C, **-C₆**H₄), 145.76 (1C, **-C₆**H₄), 141.92 (1C, **-C₆**H₄), 141.12 (1C, **-C₆**H₄), 128.95 (1C, **-o-C₆**H₄ or **-p-C₆**H₄), 126.97 (1C, **-o-C₆**H₄), 126.67 (1C, **-o-C₆**H₄ or **-p-C₆**H₄), 126.42 (1C, **-o-C₆**H₄), 126.30 (1C, **-o-C₆**H₄ or **-p-C₆**H₄), 124.56 (1C, **-o-C₆**H₄ or **-p-C₆**H₄), 123.26 (1C, **-m-C₆**H₃), 28.55 (1C, **-C**H-CH₃), 27.69 (1C, **-C**H-CH₃), 24.07 (2C, -CH-***C***H₃), 24.00 (2C, -CH-***C***H₃). Elemental Analysis: *calc.* (%) for C₃₈H₄₆N₄O₂Zn (656.19 g/mol): C 69.56, H 7.07, N 8.54; *found*: C 69.52, H 6.92, N 8.53. IR (ATR, solid sample, cm⁻¹): 3053, 3028, 2961, 2926, 2867, 1609, 1587, 1571, 1487, 1446, 1386, 1360, 1341, 1326, 1282, 1240, 1195, 1163, 1085, 1036, 1002, 942, 905, 760, 751, 725, 665, 621, 603, 576, 534, 507, 478, 459.

Bis(*N,N'*-bis(2-biphenyl)-*N*-oxidoformamidinate) of zinc(II) (3d) – The following reagents were combined according to the general procedure: *N*-hydroxy-*N,N'*-bis(2-biphenyl)formamidine (0.22g, 0.62 mmol, 2 eq) and Zn(II) acetate · 2 H₂O (0.07g, 0.31 mmol, 1 eq). Reaction time: 24 h. The resulting colourless solid was recrystallized in DCM/hexane. Yield: 0.22 g, 88%. ¹H NMR (C₆D₆, 400 MHz, TMS): δ=7.40 (d, *J* = 7 Hz, 2H), 7.38 – 7.30 (m, 1H), 7.24 (d, *J* = 7 Hz, 2H), 7.14 – 7.09 (m, 6H), 7.04 – 6.93 (m, 6H), 6.88 (t, *J* = 7.0 Hz,

1H), 6.67 (s, 1H). ^{13}C NMR (C$_6$D$_6$, 101 MHz, TMS): δ = 149.72, 141.07, 139.12, 136.97, 135.35, 131.33, 130.86, 129.90, 128.98, 128.92, 128.67, 123.80. Elemental Analysis: *calc.* (%) for C$_{50}$H$_{38}$N$_4$O$_2$Zn (792.26 g/mol): C 75.80, H 4.83, N 7.07; *found*: C 76.30, H 4.95, N 7.14.

5.2.8. Acknowledgments

Supporting Information for this article is available on the WWW under http://dx.doi.org/10.1002/ejic.201501106. In this thesis, the same material is found in Appendix-5.2-SI: ^{1}H NMR spectra of **2a/3a**, **2b/3b** and **2c/3c**; ORTEP views, spacefill views, H-bonding and intramolecular interactions of **3a**, **3b** and **3d**; cyclic voltammograms of **3b** and **3c**; molecular orbital surfaces for **3a**, **3b** and **3d**; electronic spectra of **3a**, **3b** and **3d**; TD-DFT-calculated singlet transitions for **3a**, **3b** and **3d**; atomic coordinates for DFT optimization of **3a**, **3b** and **3d**.

5.2.9. References

[1]   C. Kaes, A. Katz, M. W. Hosseini, *Chem. Rev. (Washington, DC, U. S.)* **2000**, *100*, 3553-3590.

[2]   U. S. Schubert, A. Winter, G. R. Newkome, in *Terpyridine-Based Materials*, Wiley-VCH Verlag GmbH & Co. KGaA, **2011**, pp. 65-127.

[3]   H. Furukawa, K. E. Cordova, M. O'Keeffe, O. M. Yaghi, *Science* **2013**, *341*.

[4]   a) A. Krajete, G. Steiner, H. Kopacka, K.-H. Ongania, K. Wurst, M. O. Kristen, P. Preishuber-Pfluegl, B. Bildstein, *Eur. J. Inorg. Chem.* **2004**, 1740-1752; b) A. Mishra, M. H. Mohabey, *Asian J. Chem.* **2002**, *14*, 1794-1796; c) A. N. Verma, S. B. Gholse, S. P. Sangal, *J. Indian Chem. Soc.* **1995**, *72*, 685-688; d) L. H. Briggs, R. C. Cambie, I. C. Dean, P. S. Rutledge, *Aust. J. Chem.* **1976**, *29*, 357-366.

[5]   M. Cibian, S. Derossi, G. S. Hanan, *Dalton Trans.* **2011**, *40*, 1038-1040.

[6]   H. A. Goodwin, *Top. Curr. Chem.* **2004**, *234*, 23-47.

[7]   J. Cirera, P. Alemany, S. Alvarez, *Chem. Eur. J.* **2004**, *10*, 190-207.

[8]   H. Xu, R. Chen, Q. Sun, W. Lai, Q. Su, W. Huang, X. Liu, *Chem. Soc. Rev.* **2014**, *43*, 3259-3302.

[9]   a) F. Borbone, U. Caruso, M. Causa, S. Fusco, B. Panunzi, A. Roviello, R. Shikler, A. Tuzi, *Eur. J. Inorg. Chem.* **2014**, *2014*, 2695-2703; b) U. Caruso, B. Panunzi, A. Roviello, A. Tuzi, *Inorg. Chem. Commun.* **2013**, *29*, 138-140.

[10]   a) G. Yu, S. Yin, Y. Liu, Z. Shuai, D. Zhu, *J. Am. Chem. Soc.* **2003**, *125*, 14816-14824; b) X. Xu, Y. Liao, G. Yu, H. You, C. a. Di, Z. Su, D. Ma, Q. Wang, S. Li, S. Wang, J. Ye, Y. Liu, *Chem. Mater.* **2007**, *19*, 1740-1748; c) R. Wang, L. Deng, M. Fu, J. Cheng, J. Li, *Journal of Materials Chemistry* **2012**, *22*, 23454-23460.

[11]   a) H.-P. Zeng, G.-R. Wang, G.-C. Zeng, J. Li, *Dyes Pigm.* **2009**, *83*, 155-161; b) L. S. Sapochak, F. E. Benincasa, R. S. Schofield, J. L. Baker, K. K. C. Riccio, D. Fogarty, H. Kohlmann, K. F. Ferris, P. E. Burrows, *J. Am. Chem. Soc.* **2002**, *124*, 6119-6125.

[12]   H.-J. Son, W.-S. Han, J.-Y. Chun, B.-K. Kang, S.-N. Kwon, J. Ko, S. J. Han, C. Lee, S. J. Kim, S. O. Kang, *Inorg. Chem.* **2008**, *47*, 5666-5676.

[13]   a) M. L. Cole, G. B. Deacon, C. M. Forsyth, K. Konstas, P. C. Junk, *Dalton Trans.* **2006**, 3360-3367; b) K. Hirano, S. Urban, C. Wang, F. Glorius, *Org. Lett.* **2009**, *11*, 1019-1022; c) P. Harding, D. J. Harding, H. Adams, S. Youngme, *Synth. Commun.* **2007**, *37*, 2655; d) K. E. Krahulic, G. D. Enright, M. Parvez, R. Roesler, *J. Am. Chem. Soc.* **2005**, *127*, 4142-4143; e) M. Cibian, S. Langis-Barsetti, G. S. Hanan, *Synlett* **2011**, 405-409.

[14]   a) M. Cibian, S. Derossi, G. S. Hanan, *Acta Crystallogr., Sect. E: Struct. Rep. Online* **2009**, *65*, o2485; b) E. Baranowska, I. Panfil, C. Belzecki, *Bull. Acad. Pol. Sci., Ser. Sci. Chim.* **1977**, *25*, 93-99; c) C. Belzecki, I. Panfil, *Bull. Acad. Pol. Sci., Ser. Sci. Chim.* **1975**, *23*, 119-123.

[15]   J. Cirera, E. Ruiz, S. Alvarez, *Inorg. Chem.* **2008**, *47*, 2871-2889.

[16]   F. Allen, *Acta Crystallogr., Sect. B: Struct. Sci.* **2002**, *58*, 380-388.

[17]   CCDC search on August 15 , 2015

[18]   The labelling of the chelate rings is chosen in order to help the discussion on the X-ray structures. For some of the atoms, it may differ from the labelling in the corrresponding cif. The structure with full labelling from the cif is presented in SI.

[19]   a) Y.-I. Kim, S.-J. Yun, I.-H. Hwang, D.-Y. Kim, S. K. Kang, *Acta Crystallogr., Sect. E: Struct. Rep. Online* **2012**, *68*, m504-m505; b) A. I. Poddel'sky, I. V. Smolyaninov, A. A. Skatova, A. N. Lukoyanov, G. K. Fukin, N. T. Berberova, V. K. Cherkasov, G. A. Abakumov, *Zeitschrift für anorganische und allgemeine Chemie* **2008**, *634*, 1154-1160; c) A. D. Garnovskii, A. S. Antsyhkina, G. G. Sadikov, I. S. Vasil'chenko, D. A. Garnovskii, A. I. Uraev, M. A. Porai-Koshits, *Zh. Neorg. Khim.* **1995**, *40*, 1977-1980.

[20]   E. P. Ivakhnenko, A. G. Starikov, K. A. Lyssenko, V. I. Ovcharenko, A. S. Bogomyakov, S. L. Veber, V. I. Minkin, *Inorg. Chim. Acta* **2014**, *410*, 144-149.

[21]   D. A. Dickie, R. P. Ulibarri-Sanchez Iii, P. J. Jarman, R. A. Kemp, *Polyhedron* **2013**, *58*, 92-98.

[22]   J. Wolny, Z. Ciunik, M. Rudolf, *J. Chem. Crystallogr.* **1995**, *25*, 407-412.

[23]   a) M. Czugler*, R. Neumann, E. Weber*, *Inorg. Chim. Acta* **2001**, *313*, 100-108; b) J. Sanmartin-Matalobos, C. Portela-Garcia, L. Martinez-Rodriguez, C. Gonzalez-Bello, E. Lence, A. M. Garcia-Deibe, M. Fondo, *Dalton Trans.* **2012**, *41*, 6998-7004.

[24]   L. Yang, D. R. Powell, R. P. Houser, *Dalton Trans.* **2007**, 955-964.

[25]   C. Di Iulio, M. Middleton, G. Kociok-Köhn, M. D. Jones, A. L. Johnson, *Eur. J. Inorg. Chem.* **2013**, *2013*, 1541-1554.

[26] H.-J. Son, W.-S. Han, J.-Y. Chun, B.-K. Kang, S.-N. Kwon, J. Ko, S. J. Han, C. Lee, S. J. Kim, S. O. Kang, *Inorganic Chemistry* **2008**, *47*, 5666-5676.

[27] C.-B. Wu, *Acta Crystallogr., Sect. E: Struct. Rep. Online* **2004**, *60*, m1580-m1581.

[28] N. G. Connelly, W. E. Geiger, *Chem. Rev.* **1996**, *96*, 877-910.

[29] CCDC search on September 8 , 2015

[30] M. Cibian, S. Langis-Barsetti, F. G. De Mendonça, S. Touaibia, S. Derossi, D. Spasyuk, G. S. Hanan, *Eur. J. Inorg. Chem.* **2014**, *2015*, 73-82.

[31] J. A. Wolny, M. F. Rudolf, Z. Ciunik, K. Gatner, S. Wolowiec, *J. Chem. Soc., Dalton Trans.* **1993**, 1611-1622.

[32] a) J.-L. Bredas, *Mater. Horiz.* **2014**, *1*, 17-19; b) P. I. Djurovich, E. I. Mayo, S. R. Forrest, M. E. Thompson, *Org. Electron.* **2009**, *10*, 515-520.

[33] C. Adamo, D. Jacquemin, *Chem. Soc. Rev.* **2013**, *42*, 845-856.

[34] M. J. Frisch, G. W. Trucks, H. B. Schlegel, G. E. Scuseria, M. A. Robb, J. R. Cheeseman, G. Scalmani, V. Barone, B. Mennucci, G. A. Petersson, H. Nakatsuji, M. Caricato, X. Li, H. P. Hratchian, A. F. Izmaylov, J. Bloino, G. Zheng, J. L. Sonnenberg, M. Hada, M. Ehara, K. Toyota, R. Fukuda, J. Hasegawa, M. Ishida, T. Nakajima, Y. Honda, O. Kitao, H. Nakai, T. Vreven, J. A. Montgomery, J. E. Peralta, F. Ogliaro, M. Bearpark, J. J. Heyd, E. Brothers, K. N. Kudin, V. N. Staroverov, R. Kobayashi, J. Normand, K. Raghavachari, A. Rendell, J. C. Burant, S. S. Iyengar, J. Tomasi, M. Cossi, N. Rega, J. M. Millam, M. Klene, J. E. Knox, J. B. Cross, V. Bakken, C. Adamo, J. Jaramillo, R. Gomperts, R. E. Stratmann, O. Yazyev, A. J. Austin, R. Cammi, C. Pomelli, J. W. Ochterski, R. L. Martin, K. Morokuma, V. G. Zakrzewski, G. A. Voth, P. Salvador, J. J. Dannenberg, S. Dapprich, A. D. Daniels, O. Farkas, J. B. Foresman, J. V. Ortiz, J. Cioslowski, D. J. Fox, *Gaussian 09*, **2009**,

[35] a) C. Lee, W. Yang, R. G. Parr, *Phys. Rev. B: Condens. Matter* **1988**, *37*, 785-789; b) B. Miehlich, A. Savin, H. Stoll, H. Preuss, *Chem. Phys. Lett.* **1989**, *157*, 200-206.

[36] M. M. Francl, W. J. Pietro, W. J. Hehre, J. S. Binkley, M. S. Gordon, D. J. DeFrees, J. A. Pople, *J. Chem. Phys.* **1982**, *77*, 3654-3665.

[37] J. Tomasi, B. Mennucci, R. Cammi, *Chem. Rev.* **2005**, *105*, 2999-3094.

[38] a) M. E. Casida, C. Jamorski, K. C. Casida, D. R. Salahub, *J. Chem. Phys.* **1998**, *108*, 4439-4449; b) R. E. Stratmann, G. E. Scuseria, M. J. Frisch, *J. Chem. Phys.* **1998**, *109*, 8218-8224.

[39] R. D. K. Dennington II, T.; Millam, J.; Eppinnett, K.; Hovell, W. L.; Gilliland, R., **2003**, *GaussView 3.0.9*, Semichem, Inc.; Shawnee Mission, KS.

[40] N. M. T. O'Boyle, A. L.; Langner, K. M., *J. Comp. Chem.* **2008**, *29*, 839-845.

[41] L. Skripnikov, **2005 - 2015**, *Chemissian V.4.36,*

5.3. Des résultats additionnels, non-publiés, sur les complexes de zinc(II) avec des ligands *N,N'*-diaryl-bezamidinate *N*-oxydes

5.3.1. Zn(AMOX)₂ (AMOX = *N,N'*-diarylbenzamidinate-*N*-oxyde) – étude théorique

Afin d'évaluer et de rationaliser l'effet du motif de substitution des ligands AMOX sur la largeur du gap optique des complexes, l'étude théorique (DFT/ TD-DFT) effectuée pour la famille des complexes Zn(AMOX)₂ (AMOX = *N,N'*-diarylformamidinate-*N*-oxyde) et décrit dans la section 5.2, a été étendue à la série des complexes de zinc(II) avec des ligands AMOX = *N,N'*-diarylbenzamidinate-*N*-oxydes (Tableau 5.3-1). Les détails sur les calculs théoriques et sur les structures optimisées sont donnés dans l'Annexe-5.3-EXP. Les représentations des orbitales moléculaires (HOMO et LUMO) pour les composés **Zn1 – Zn6** et **Zn8 – Zn10** sont illustrées dans la Figure 5.3-1. Comme dans le cas des composés **3** (section 5.2), la HOMO se trouve sur la partie ONCN de la molécule. Par contre, la localisation de la LUMO change sur le substituent *C*-aryle.

Tableau 5.3-1. Les composés analysés dans cette étude

Composé	Substituants *C*-aryle R	Substituants *N,N'*-diaryles R'	Obs.
Zn1	Ph	2,6-diiPrPh	
Zn2	Ph	2,6-diMePh	
Zn3	4-BrPh	2,6-diMePh	
Zn4	4-py	2,6-diMePh	
Zn5	4-CF₃Ph	2,6-diMePh	
Zn6	4-OMePh	2,6-diMePh	
Zn7	4-N(Me₂)Ph	2,6-diMePh	*pas convergé*
Zn8	4-py	2,6-diiPrPh	
Zn9	4-py	2-py	
Zn10	4-py	C₆F₅	
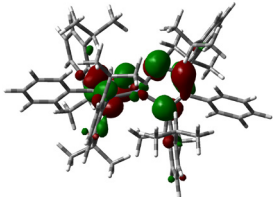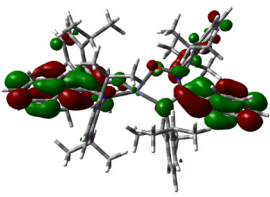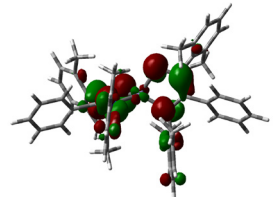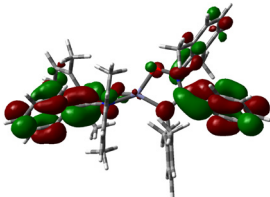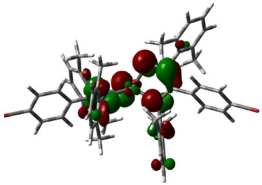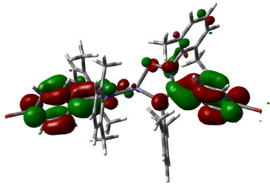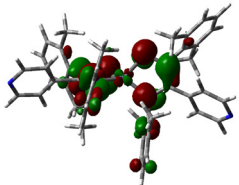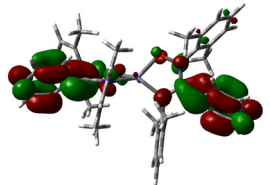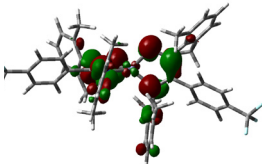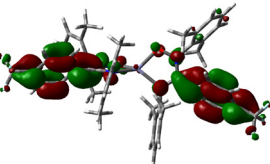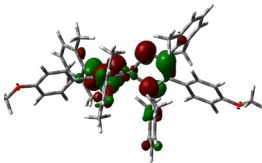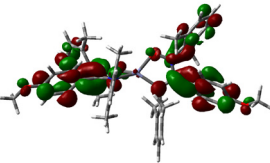
Composé	Représentations des orbitales moléculaires	
	HOMO	LUMO
Zn1		
Zn2		
Zn3		
Zn4		
Zn5		
Zn6		

Figure 5.3-1a Les représentations des orbitales moléculaires (HOMO et LUMO) pour les composés **Zn1 – Zn6**

Composé	Représentations des orbitales moléculaires	
	HOMO	LUMO/ LUMO+1
Zn8		
Zn9		
Zn10		
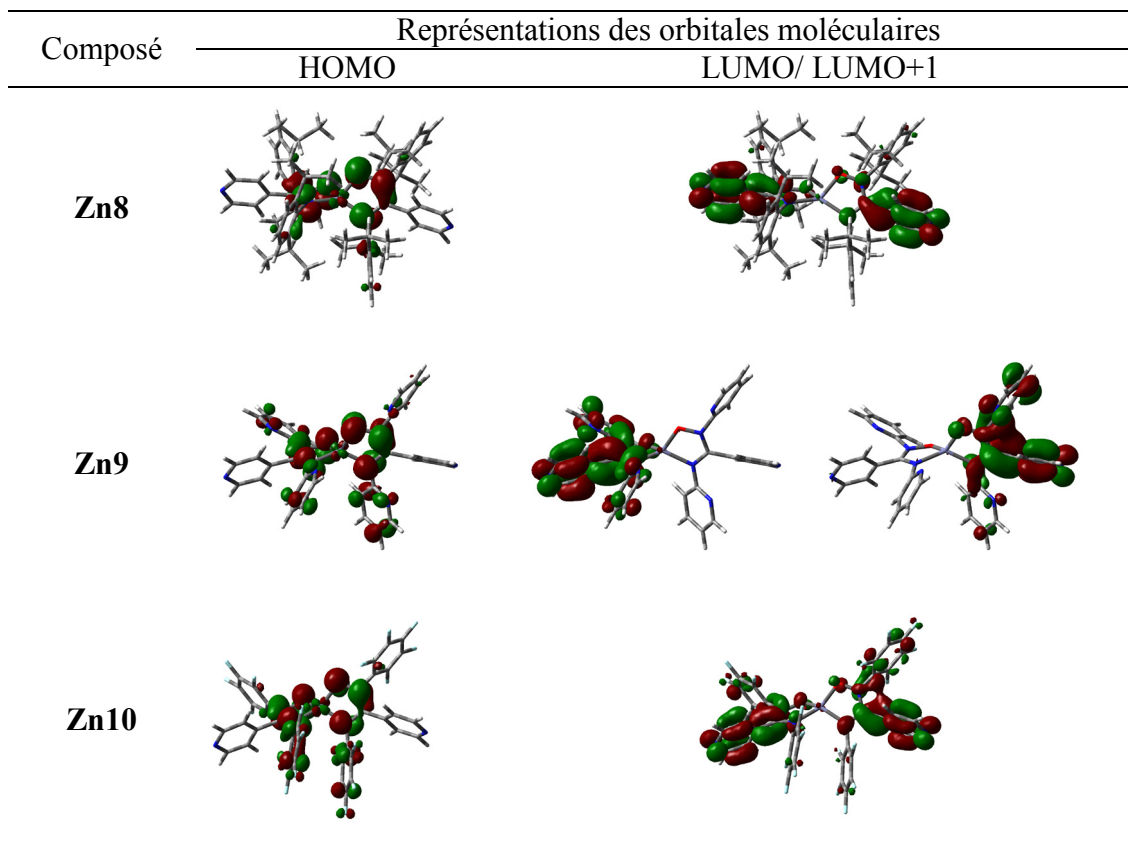
Figure 5.3-1b Les représentations des orbitales moléculaires (HOMO et LUMO) pour les composés **Zn8 – Zn10**

Les résultats sont résumés dans le Tableau 5.3-2, la Figure 5.3-2 (l'influence de la substitution sur le *C*-aryle) et la Figure 5.3-3 (l'influence de la substitution sur les *N,N'*-aryles).

Tableau 5.3-2. Les niveaux énergétiques de la HOMO et de la LUMO pour **Zn1** – **Zn6** et **Zn8** – **Zn10** – valeurs théoriques

Composé	E_{HOMO}[a] (eV)	E_{LUMO}[b] (eV)	$E_{g\ (TD\text{-}DFT)}$[c] (eV)	Composé	E_{HOMO} (eV)	E_{LUMO} (eV)	$E_{g\ (TD\text{-}DFT)}$ (eV)
Zn1	-5.05	-1.51	3.54	**Zn6**	-5.03	-1.38	3.65
Zn2	-5.09	-1.56	3.53	**Zn8**	-5.21	-1.99	3.22
Zn3	-5.17	-1.76	3.41	**Zn9**	-5.38	-2.21	3.17
Zn4	-5.25	-2.04	3.21	**Zn10**	-5.87	-2.42	3.45
Zn5	-5.21	-1.97	3.24				

[a] E_{HOMO} a été obtenue par optimisation DFT, niveau de théorie: B3LYP/ 6-31g(d, p), PCM: CH₂Cl₂; [b] E_{LUMO} (eV) = E_{HOMO} (DFT) + $E_{g(TD\text{-}DFT)}$; [c]E_g(TD-DFT) est le premier singulet calculé par TD-DFT, qui correspond à la transition HOMO-LUMO; niveau de théorie B3LYP/ 6-31g(d, p), PCM: CH₂Cl₂.

La stabilisation des niveaux énergétiques des LUMOs augmente avec la force du substituant électroattracteur (EW – electron withdrawing) (un degré de délocalisation électronique plus importante sur le *C*-aryle) (Figure 5.3-2). Il a également été constaté que la substitution sur le *C*-aryle a un effet mineur sur le niveau d'énergie de la HOMO et un effet plus important sur le niveau d'énergie de la LUMO. L'effet de la substitution sur les *N,N'*-aryles peut être observé dans la Figure 5.3-3. La stabilisation des deux niveaux d'énergie de la HOMO et de la LUMO a lieu. Le degré de stabilisation est également en corrélation avec la nature du substituant ED/ EW (ED – electron donating; EW – electron withdrawing). Le gap optique des complexes Zn(AMOX)₂ a été aussi comparé à celui du Zn(BTZ)₂ (BTZ = 2-(2-benzothiazolyl)phenolato), qui est un composé utilisé avec succès dans des applications type OLED.[1]
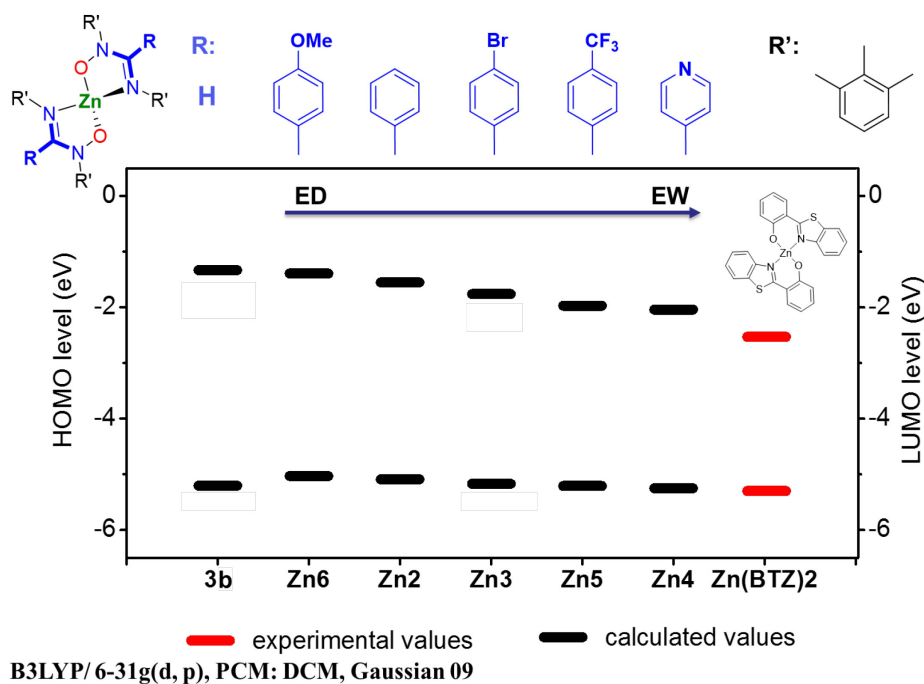
Figure 5.3-2. Le gap optique calculé pour **Zn2 – Zn6**. (L'influence de la substitution sur le *C*-aryle.)
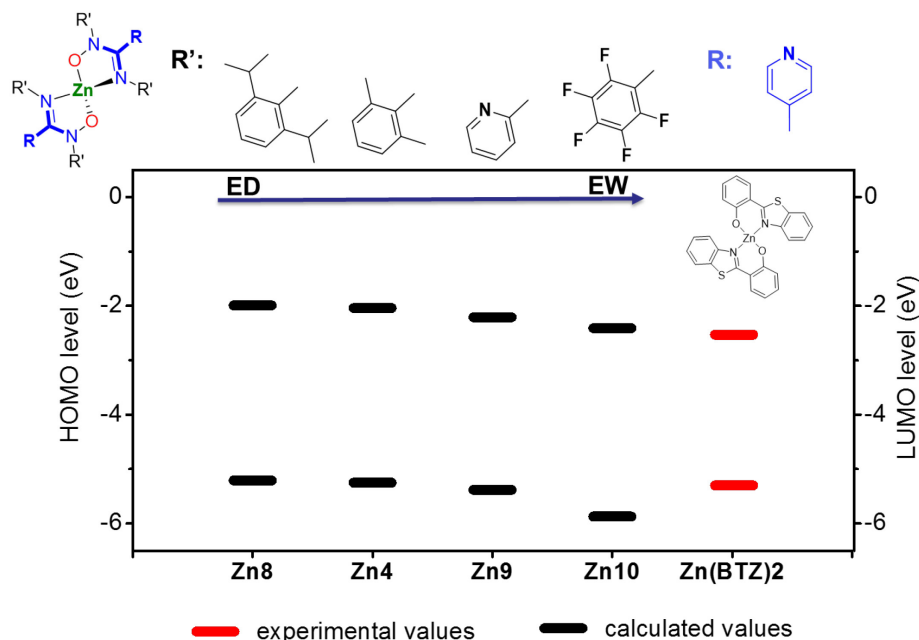
Figure 5.3-3. Le gap optique calculé pour **Zn4**, **Zn8**, **Zn9**, **Zn10**. (L'influence de la substitution sur les *N,N'*-aryles.)

5.3.2. Les dimères [Zn(AMOX)₂]₂ (AMOX = *N,N'*-diarylbenzamidinate-*N*-oxyde)

La Figure 5.3-4 et le Tableau S31 de l'Annexe-5.3-EXP illustrent les propriétés des composés dimères de zinc(II) [Zn(AMOX)₂]₂ avec des ligands AMOX = *N,N'*-diarylbenzamidinate-*N*-oxyde: **D1** ([Zn(AMOX)₂]₂ avec AMOX = 4-bromo-*N,N'*-diphenylbenzamidinate-*N*-oxyde) et **D2** ([Zn(AMOX)₂]₂ avec AMOX = 4-cyano-*N,N'*-diphenylbenzamidinate-*N*-oxyde). Les détails expérimentaux sont donnés dans l'Annexe-5.3-EXP. Pour **D1**, la structure à l'état solide a été obtenue (Figure 5.3-4a et Tableaux S16-S18 de l'Annexe-5.3-EXP). Les centres Zn(II) ont une coordination cinq et une géométrie pseudo-pyramide à base carrée. Les ligands AMOX présentent deux modes de coordination aux ions de zinc(II): μ-AMOX-κN,κO:κO et AMOX-κN,κO. Ces complexes présentent de l'intérêt potentiel dans des applications de type OLED.[2] Les calculs DFT pour ce type de composés montrent la localisation de la HOMO sur la partie ONCN de la molécule, tandis que la LUMO se trouve sur les substituants *C*-aryles (Figure 5.3-4b). Cette distinction indique que le niveau

énergétique de la LUMO peut être finement modulé en modifiant le substituant *C*-aryle (introduire des groupements EW/ED). En effet, la stabilisation de la LUMO a été observée pour **D2** vs. **D1**, en ligne avec le meilleur caractère EW du groupement -CN (**D2**) vs. –Br (**D1**). Pour **D1**, valeur de son gap optique déterminée par calculs théoriques DFT/TD-DFT est en accord avec la valeur trouvée expérimentalement (Figure 5.3-4c). De plus, la valeur trouvée expérimentalement est proches de celle du Zn(BTZ)₂ (BTZ = 2-(2-benzothiazolyl)phenolato), un composé utilisé avec succès dans la fabrication des OLEDs.[1] Bien que **D1** soit faiblement luminescent en solution à des basses concentrations, il est émissif à l'état solide. Son spectre d'émission se caractérise par la présence d'une large bande d'émission (400 – 800 nm) (Figure 5.3-4d). Le phénomène d'émission induite par agrégation (AIE – Aggregation Induced Emission) est proposé pour expliquer ce comportement et des investigations sont en cours pour le prouver. La performance de ces composés comme luminophores dans WOLEDs (White OLEDs) est testée en collaboration avec le groupe de recherche du Pr. Nunzi à Queens University. Un exemple des résultats préliminaires pour **D1** est montré dans la Figure 5.3-4e.
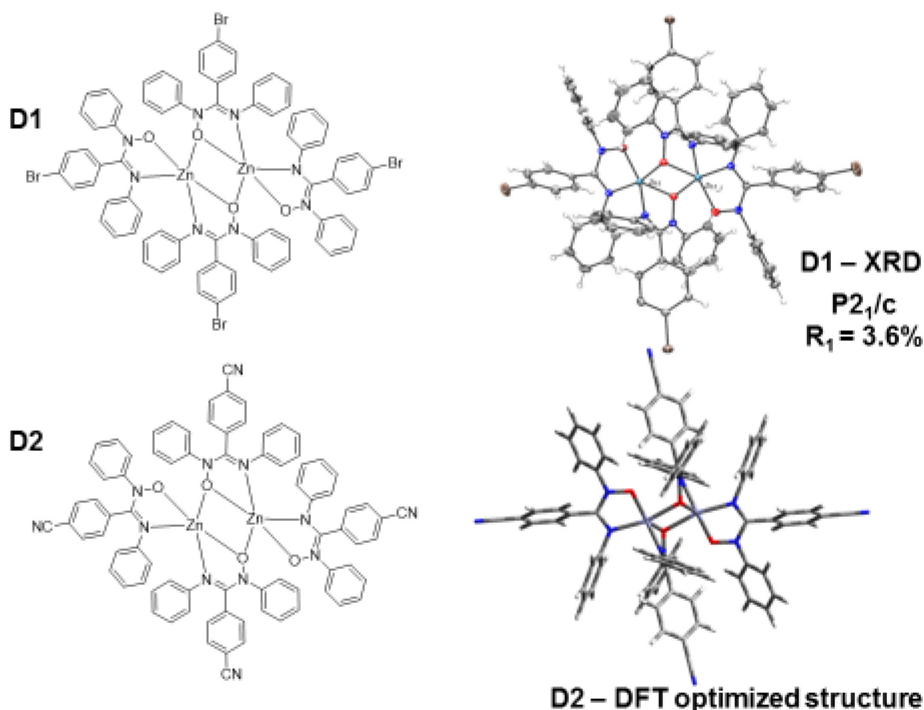
Figure 5.3-4a. Les structures ChemDraw des **D1** et **D2**, la structure à l'état solide du **D1** (cristallographie par Janaina Ferreira) et la structure optimisé par DFT du **D2**

HOMO LUMO

D1

D2

B3LYP/ 6-31g(d, p), PCM: DCM, Gaussian 09
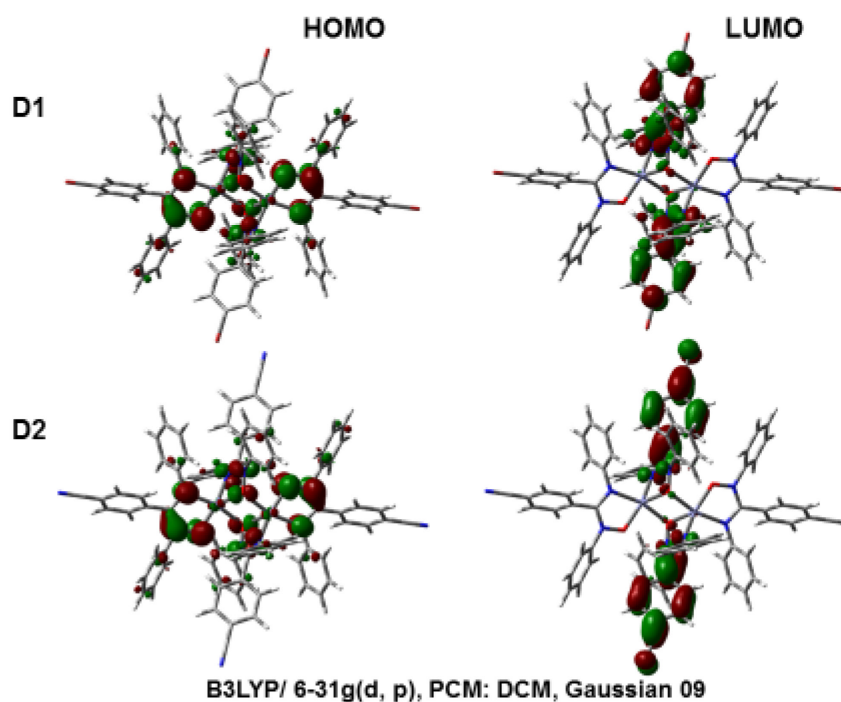
Figure 5.3-4b. Les représentations des orbitales moléculaires (HOMO et LUMO) pour **D1** et **D2**
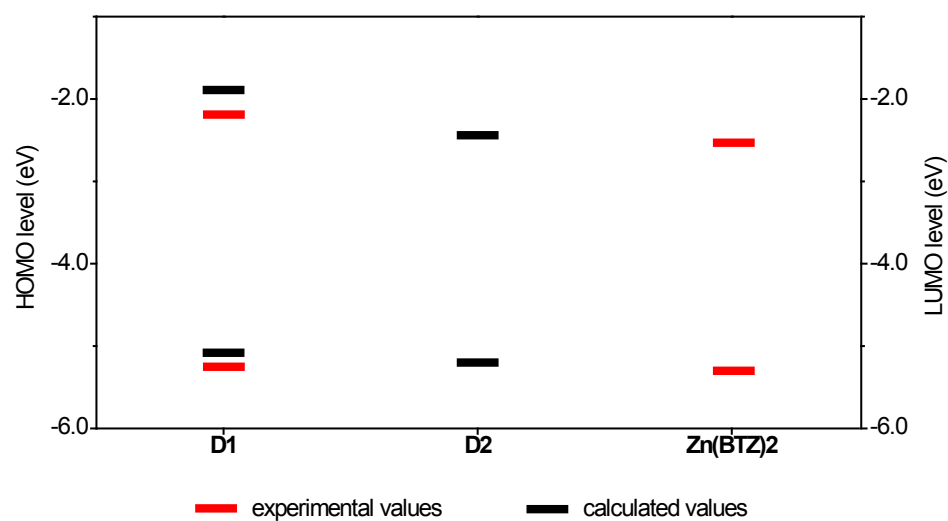
Figure 5.3-4c. Les gaps optiques pour **D1** (valeur calculée et valeur déterminée expérimentalement) et pour **D2** (valeur calculée); comparaison avec Zn(BTZ)$_2$

Cpd.	D1 (4-BrPh)
$\lambda_{max\ em}$ (nm)	556

λ_{exc} (nm) = 350
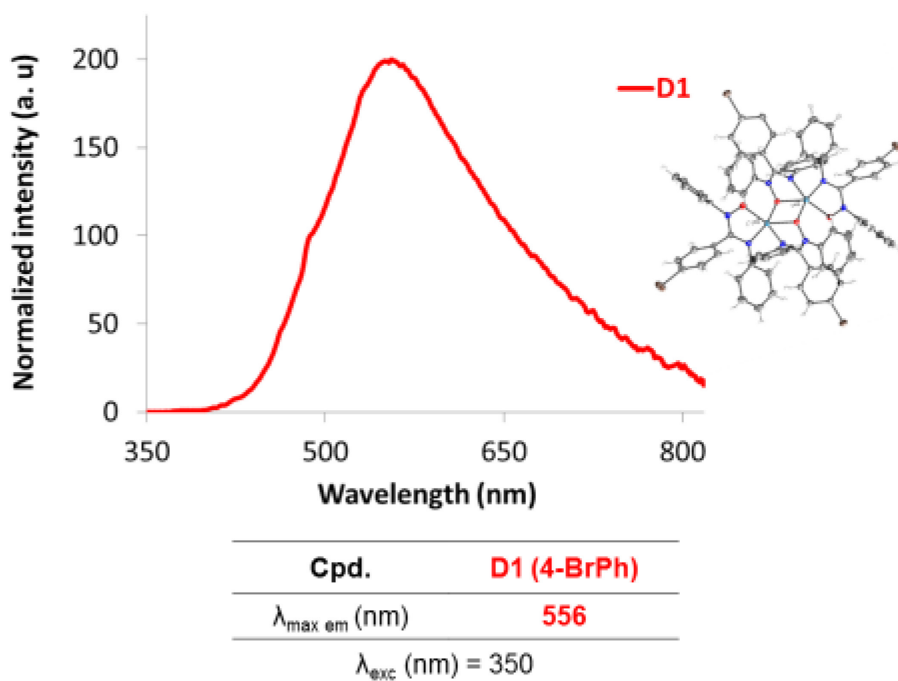
Figure 5.3-4d. Le spectre d'émission à l'état solide (en poudre) pour **D1**

Device structure of the Wight OLED (WOLED)

Al (180 nm)	Cathode
Alq3 (40 nm)	EIL
BCP (8 nm)	ETL/HBL
PVK-l (66.7 wt%): PBD (30 wt%): D1 (3 wt%)	EML
PVK-h	HTL/EBL
PEDOT:PSS	HIL
ITO	Anode
Glass	

Work by Afshin Shahalizad, Nunzi Group, Queens University
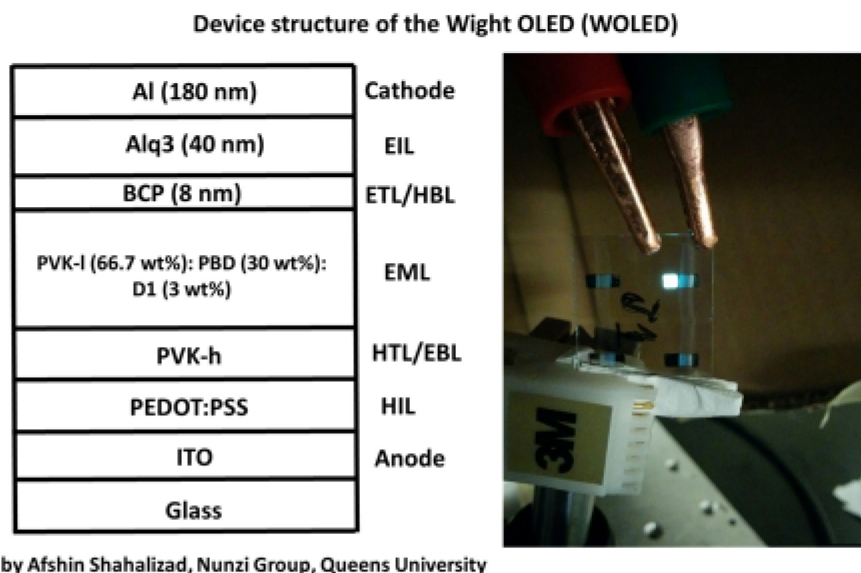
Figure 5.3-4e. Le test dans WOLEDs pour **D1**

5.3.3. La coordination des ligands bis-AMOXs pontés par les atomes d'azote avec des ions de zinc(II)

Des ligands bis-AMOXs pontés par les atomes d'azote ont été synthétisés (Figure 5.3-5) afin d'être utilisés comme briques pour des architectures supramoléculaires. Les détails expérimentaux sont donnés dans l'Annexe-5.3-EXP.
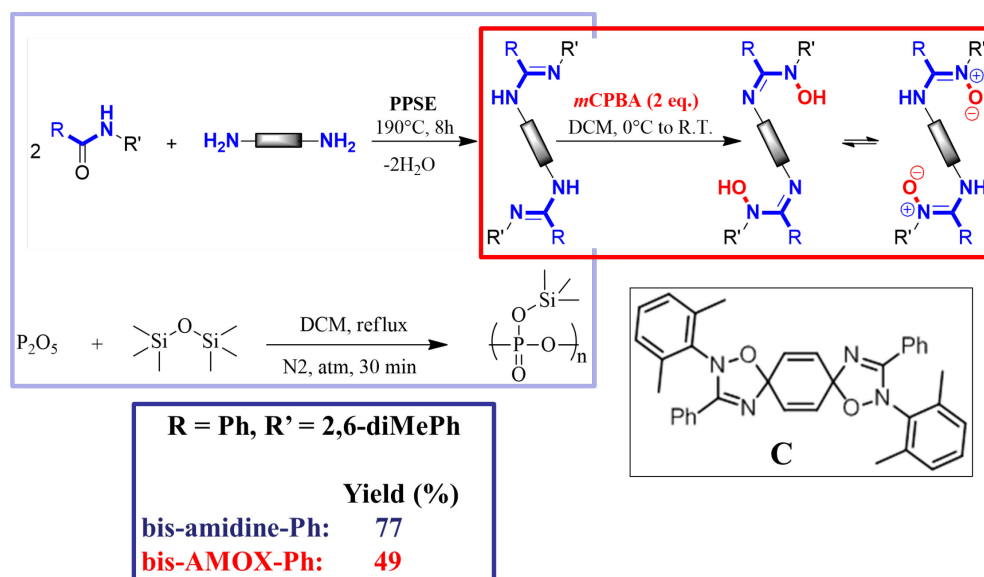
Figure 5.3-5. La synthèse des ligands bis-AMOXs pontés par les atomes d'azote et des leurs précurseurs bis-amidines

La synthèse des composés bis-AMOXs pontés par les atomes d'azote en utilisant PPSE a été optimisée aux conditions présentées ci-dessus (8h et 190°C); aux temps de réaction plus courts, de l'amide est présente et aux temps de réaction plus longues des produits secondaires sont formés. La purification des bis-AMOXs est faite par chromatographie flash sur SiO$_2$, en utilisant le gradient d'éluants: hexane/AcOEt 5/5, AcOEt 100%, AcOEt/EtOH 5/5, EtOH 100%. Les produits secondaires identifiés sont: du mono-AMOX et du bis-AMOX oxydé (produit **C**, Figure 5.3-5 – sa structure à l'état solide est présentée dans la Figure 5.3-8). Les spectres RMN ^{1}H de la **bis-amidine-Ph** et du **bis-AMOX-Ph**, avec l'assignation des résonances des protons sont montrés dans la Figure 5.3-6. Les structures à l'état solide de la **bis-amidine-Ph**, du **bis-AMOX-Ph** et du composé **C** ont été obtenues et sont présentée dans les Figures 5.3-7, 5.3-8, 5.3-9 et les Tableaux S19-S27 de l'Annexe-5.3-EXP.
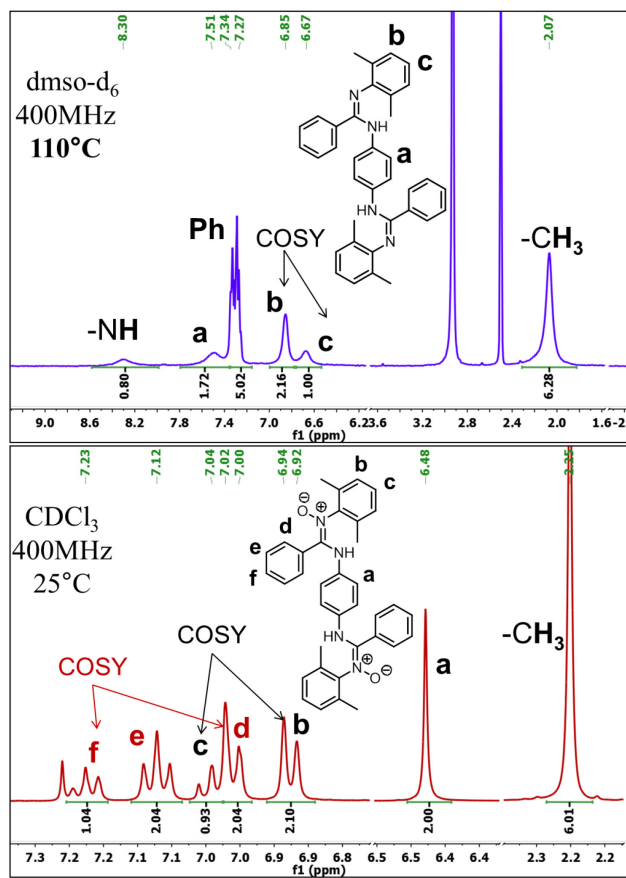
Figure 5.3-6. Le spectre RMN ^{1}H de la **bis-amidine-Ph** (en haut) et du **bis-AMOX-Ph** (en bas) avec l'assignation des résonances des protons.
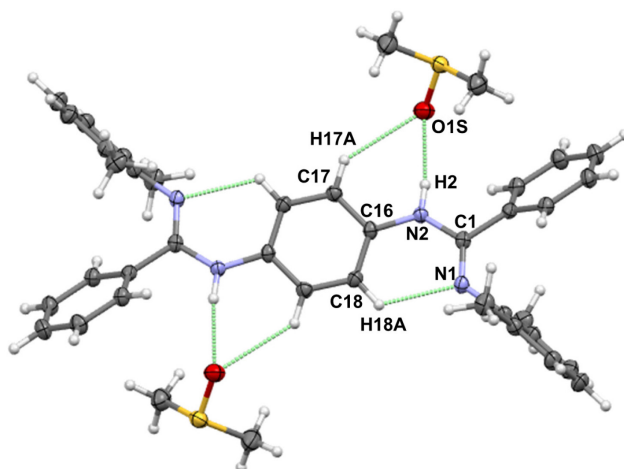
Figure 5.3-7. La structure du **bis-amidine-Ph** à l'état solide: représentation ORTEP avec les ellipsoïdes à 50% niveau de probabilité; le motif formé par les liens hydrogène (intramoléculaires et avec le solvant co-cristallisé) est aussi présenté.
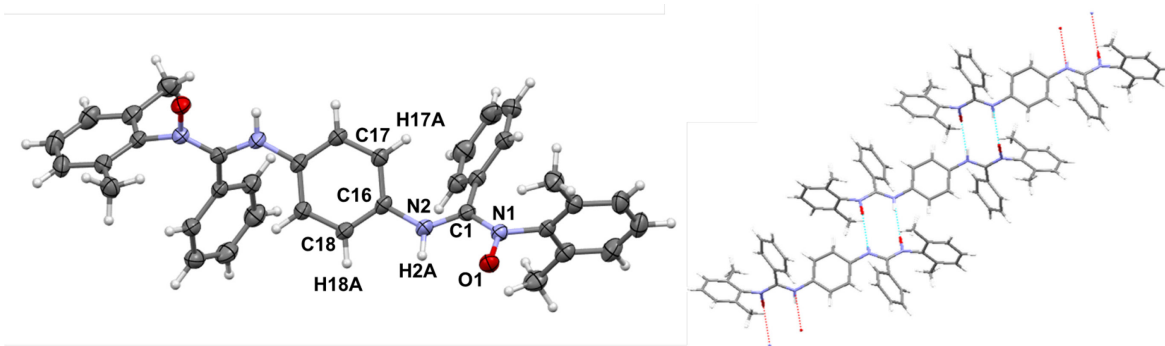
Figure 5.3-8. La structure du **bis-AMOX-Ph** à l'état solide: représentation ORTEP avec les ellipsoïdes à 50% niveau de probabilité (à gauche) et le motif formé par les liens hydrogène (à droit) – des dimères cycliques *via* des liens N-H⋯O (*d* = 1.977(1)
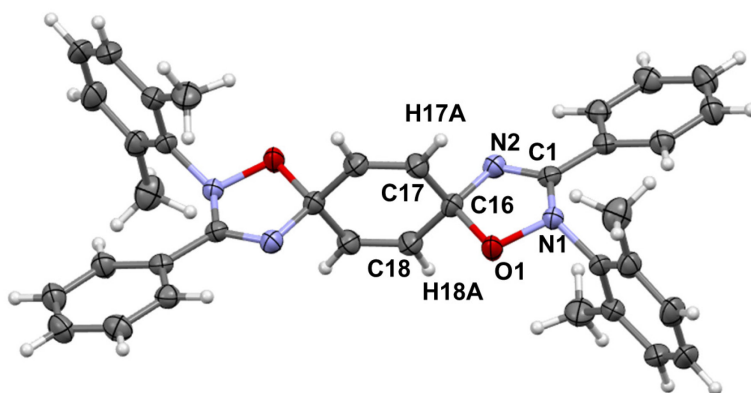
Figure 5.3-9. La structure du composé **C** à l'état solide: représentation ORTEP avec les ellipsoïdes à 50% niveau de probabilité

La complexation du ligand bis-AMOX ponté par les atomes d'azote (**bis-AMOX-Ph**) (qui peut présenter des vecteurs parallèles de coordination) avec des ions métalliques de zinc(II) (géométrie tétraédrique) a été réalisée pour tenter d'obtenir des composés de type grille moléculaire (Figure 5.3-10).
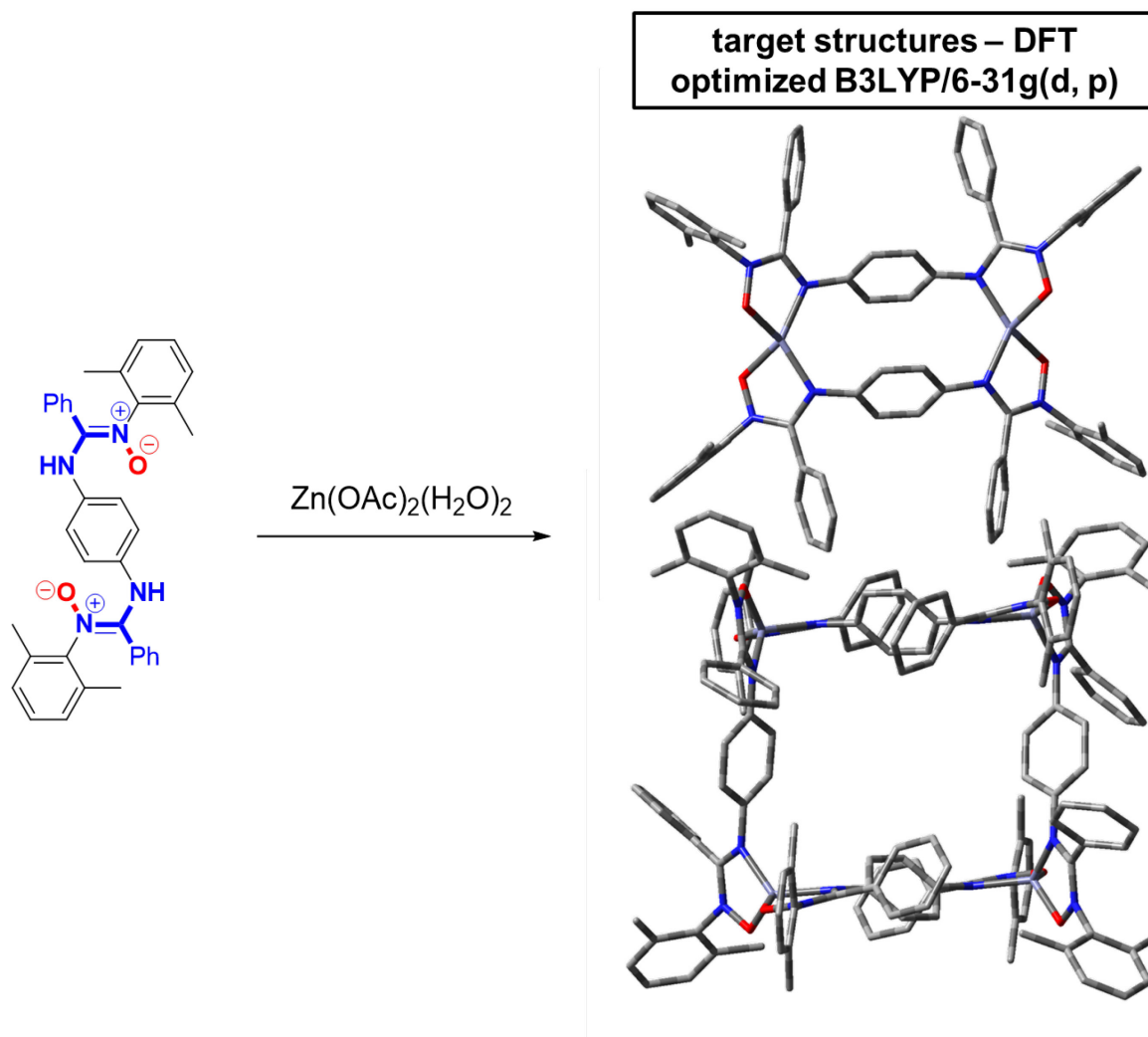
Figure 5.3-10. La complexation du ligand bis-AMOX (**bis-AMOX-Ph**) avec des ions métalliques de zinc(II): les composés attendus (modèles)

Par contre, un composé métallo-polymérique 1D a été obtenu, comme prouvée par sa structure à l'état solide (Figure 5.3-11 et Tableaux S28-S30 de l'Annexe-5.3-EXP). Le composé a été obtenu comme une poudre jaune, très insoluble. Des cristaux de très mauvaise qualité (des aiguilles très fines) ont été obtenus par évaporation lente d'une solution du composé dissout à chaud dans toluène. La structure à l'état solide montre un polymère de coordination 1D, avec une distance Zn---Zn de 9.6 Å. Les ions métalliques de zinc(II) ont une géométrie pseudo-tétraédrique ($\tau_4 = 0.74$).[3]
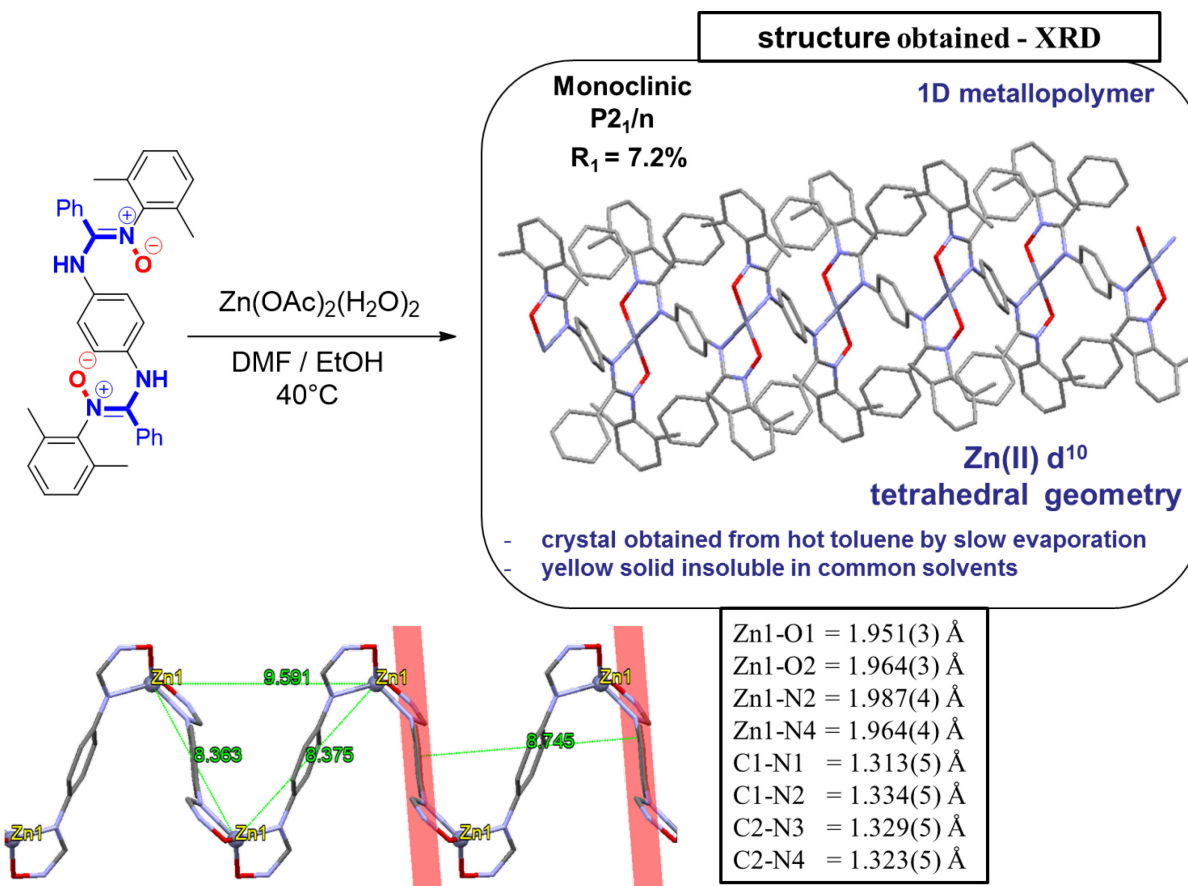
Figure 5.3-11. La synthèse du métallopolymere de zinc(II) et sa structure à l'état solide. Les atomes d'hydrogène et les molécules de toluènes co-cristallisées ont été omis pour clarté.

L'insolubilité du polymère nuit à sa caractérisation complète. Le spectre électronique du composé est montré dans la Figure 5.3-12 ensemble avec ceux du ligand bis-AMOX et de la bis-amidine parent. Le métallopolymère de zinc(II) est émissif (Figure 5.3-13) et il a une bonne stabilité (la TGA montre une température de décomposition Td (mesurée à 5% perte de masse) de 320 °C (Figure 5.3-14)).
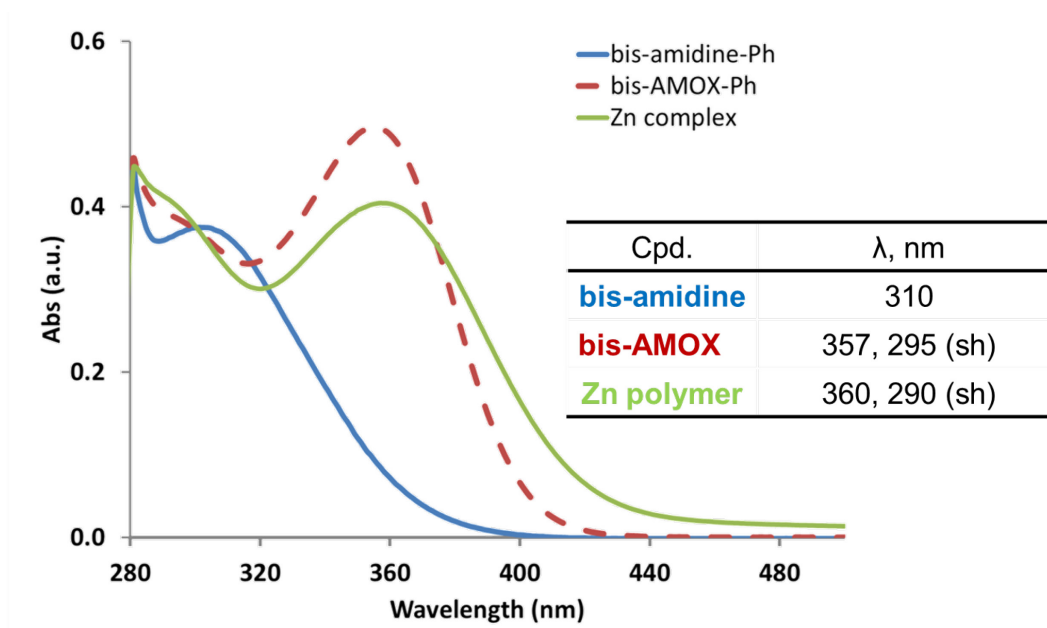
Figure 5.3-12. Les spectres électroniques du métallopolymère de zinc(II), le ligand bis-AMOX correspondant et son précurseur bis-amidine (dans toluène)
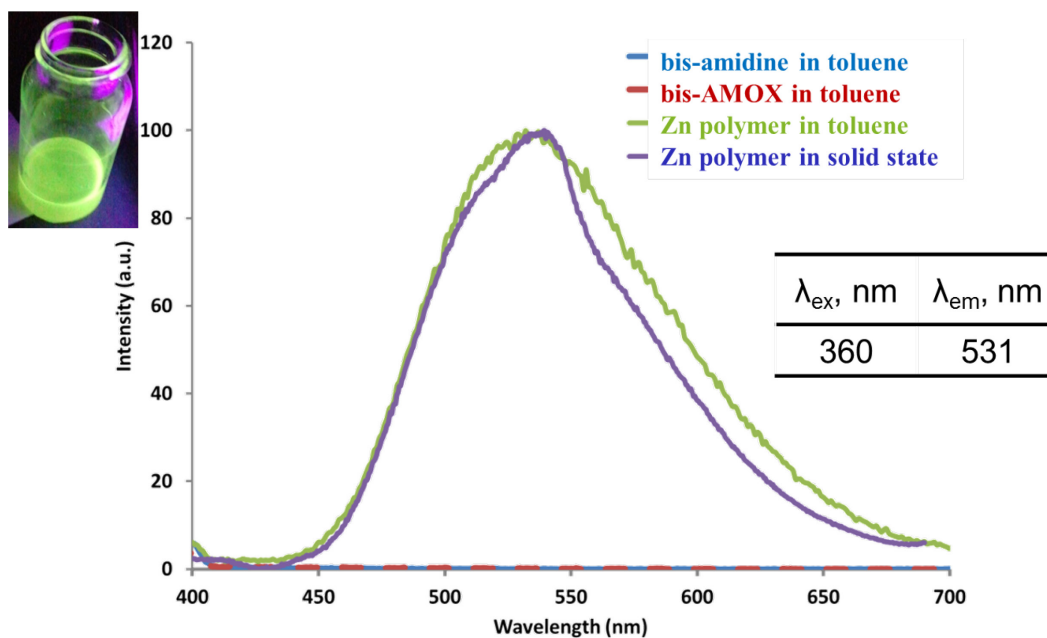
Figure 5.3-13. Les spectres d'émission du métallopolymère de zinc(II) (dans toluène et à l'état solide), du ligand bis-AMOX et de son précurseur bis-amidine (dans toluène).
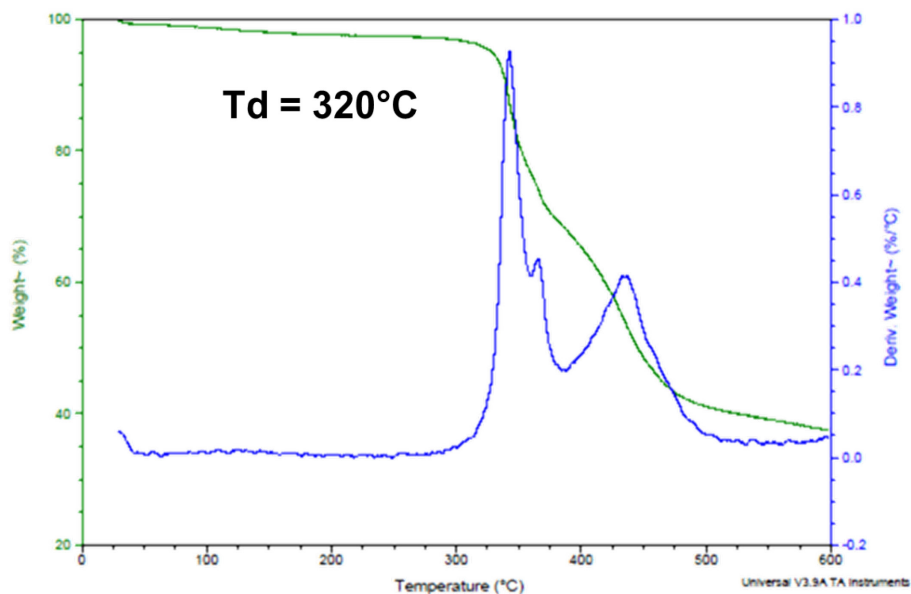
Figure 5.3-14. Le profile TGA pour le métallopolymer de zinc(II) (Td calculée à 5% perte de masse).
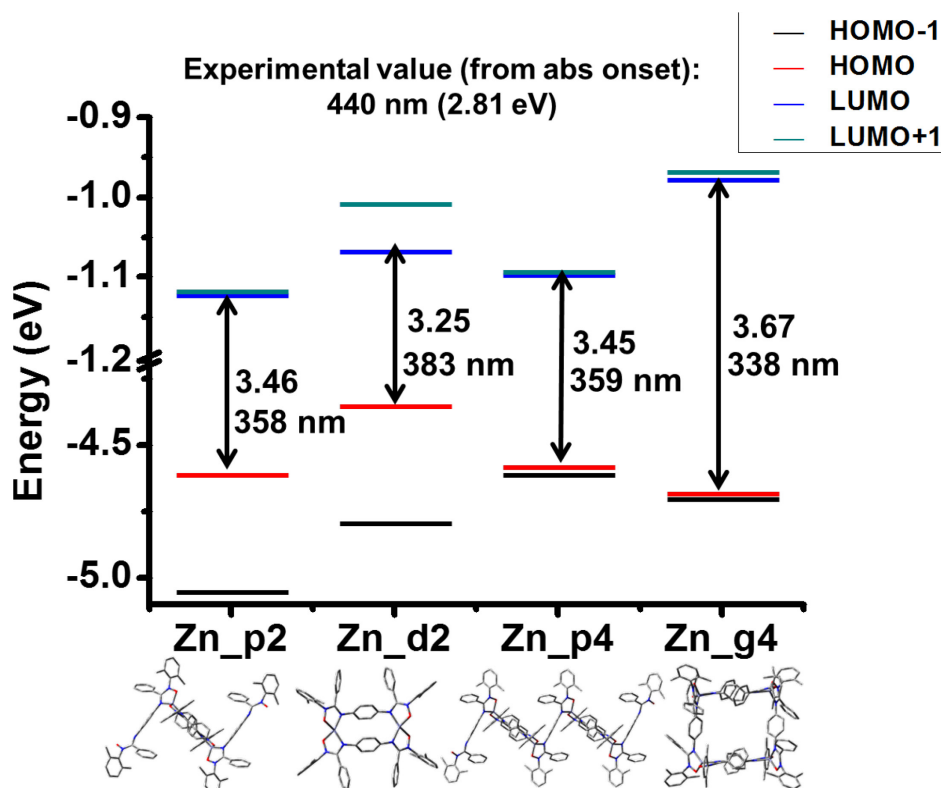
Figure 5.3-15. Les gaps optiques calculés pour des composés de zinc(II) bis-AMOX de type assemblages discrets et oligomériques.

Les gaps optiques calculés pour des composés de zinc(II) bis-AMOX de type assemblages discrets et oligomériques sont présentés dans la Figure 5.3-15 et les représentations des orbitales moléculaires (HOMO et LUMO) sont illustrées dans la Figure 5.3-16. La localisation de la LUMO sur le substituant *C*-aryle est observée dans tous les cas, ce qui indique que le gap optique de ce type de composés peut aussi être finement modulé par la modification de ce substituant spécifique.

DFT - B3LYP/ 6-31g(d, p)
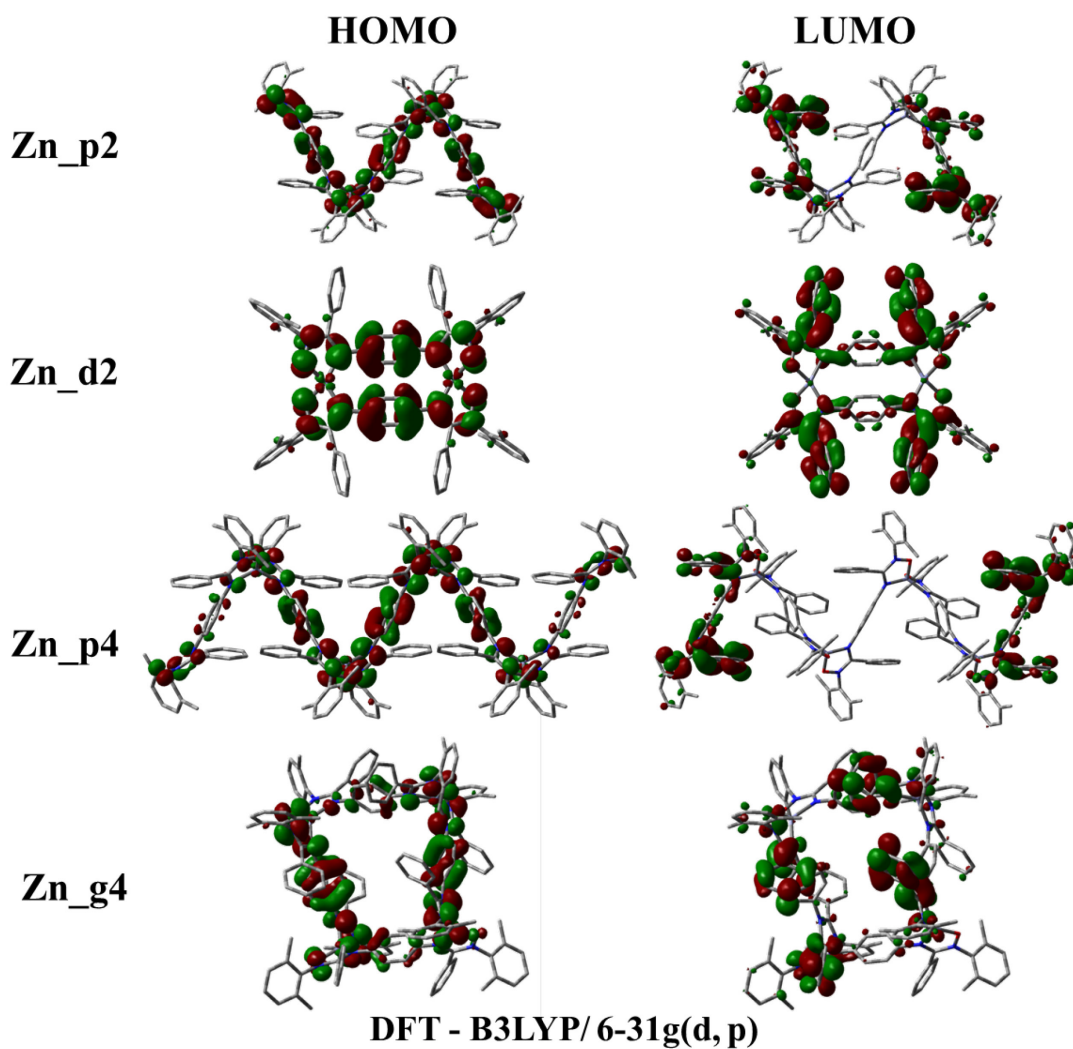
Figure 5.3-16. Les représentations des orbitales moléculaires (HOMO et LUMO) pour des composés de zinc(II) bis-AMOX de type assemblages discrets et oligomériques.

5.3.4. Références

[1]   R. Wang, L. Deng, M. Fu, J. Cheng, J. Li, *J. Mat. Chem.* **2012**, *22*, 23454-23460.
[2]   F. Borbone, U. Caruso, M. Causa, S. Fusco, B. Panunzi, A. Roviello, R. Shikler, A. Tuzi, *Eur. J. Inorg. Chem.* **2014**, *2014*, 2695-2703.
[3]   L. Yang, D. R. Powell, R. P. Houser, *Dalton Trans.* **2007**, 955-964.

Chapitre 6: Conclusions et perspectives

D'après le format de 'thèse par articles', des observations finales sont présentées à la fin de chaque chapitres/ sections décrivant des résultats publiés. Dans ce dernier chapitre, un résumé de ces observations est donné, en mettant en évidence les principales conclusions de la thèse (**section 6.1**). En plus, les perspectives du projet et des informations sur les travaux en cours sont présentées (**section 6.2**), ainsi que quelques remarques finales (**section 6.3**).

6.1. Sommaire

Grâce à leurs propriétés, les composés de coordination sont utilisés dans un large éventail d'applications dans des domaines allant de la catalyse aux matériaux et aux sciences de la vie. Des exemples de composés de coordination dans des applications (dans des domaines bien établis, des domaines émergents et au niveau de prototype/ recherche fondamentale) ont été donnés (Tableau 1.1-1 et Figure 1.1.-1, chapitre 1) afin d'illustrer leur importance dans notre vie quotidienne. Des tendances dans la chimie de coordination moléculaire ont également été identifiées. Poussée par le progrès général de notre société, la recherche évolue *vers la complexité au niveau moléculaire*, la nature représentant une source majeure d'inspiration comme montré par la photosynthèse artificielle et la chimie métallosupramoléculaire. Ces exemples établissent le contexte général pour les travaux présentés dans cette thèse.

Le cadre théorique de ce travail a été fixé par des concepts clés, tels que: complexe composé/ métallique/ de coordination; liaison/ interaction métal-ligand; design du ligand; propriétés des complexes de coordination (expérimentales *vs.* calculées); relation structure – propriétés; approches moléculaires/ supramoléculaires; systèmes à valence mixte; et architectures supramoléculaires de coordination. Le design des complexes de coordination est considéré comme une '*collection de composants modulables*' (p. ex. le ligand: les atomes donneurs et les groupements fonctionnels des atomes donneurs, les substituants et leurs effets électroniques et stériques, le type et la taille cycle chélate; les ions métalliques; l'environnement/ le milieu). Ce concept a été illustré avec des aspects de la chimie de

coordination des ligands N,O, afin d'établir le contexte spécifique de la thèse. Le même concept a été ensuite appliqué à la recherche dans cette thèse.

Premièrement, les propriétés des ligands utilisés (amidine oxydes (AMOXs)/ α-aminonitrones/ hydroxyamidines *N,N'*-disubstitués) sont présentées dans la même perspective du design du ligand comme collection des composants modulables. Deuxièmement, l'influence du motif de substitution des ligands sur les propriétés des complexes est étudiée à l'intérieur de la série des complexes bis(AMOX) avec différents ions métalliques (cobalt(II) et zinc(II)). Les complexes bis(chélates) de cobalt (II) sont plan carré (bas spin) à l'état solide, mais montrent l'isomérisation de la géométrie plan carré (bas spin) à la géométrie tétraédrique (haut spin) dans des solutions de solvants non-coordinants. L'équilibre d'isomérisation est très sensible au motif de substitution des ligands en raison d'une combinaison de facteurs stériques et électroniques. L'intégration des études théoriques (DFT/ TD-DFT) avec des résultats expérimentaux, pour la validation des modèles, a montré que, dans la famille de bis(AMOX) chélates de zinc (II), par la modification spécifique des ligands, le gap optique des complexes peut être ajusté (tuned) pour des applications potentielles dans des dispositifs optoélectroniques. Troisièmement, l'effet de l'environnement sur les propriétés des composés est exploré dans le cas d'un complexe de cobalt(II) bis(AMOX), en examinant l'effet que les forces faibles (p. ex. liaison hydrogène, solvatation, température) ont sur sa structure. Un changement de géométrie et de spin au centre cobalt(II) est induit par des liaisons hydrogène. Les interactions faibles sont ainsi identifiées comme étant les principaux facteurs responsables pour amener le système vers une combinaison spécifique géométrie–état de spin, de façon similaire aux interactions hôte-invité et le contrôle allostérique dans les systèmes biologiques. Ainsi, le système offre des informations importantes sur le rôle des interactions de reconnaissance faibles et les effets de coopération sur les préférences de stéréochimie et de spin dans les complexes métalliques tétracoordinés. Compte tenu de la pertinence des complexes de cobalt tétracoordinés en catalyse (p. ex. la polymérisation radicalaire, la production d'hydrogène, le transport d'oxygène) et pour des matériaux magnétiques, l'information offerte par ce système pourrait servir aux nouveaux développements dans ces domaines.

De plus, des études préliminaires ont été menées vers des systèmes supramoléculaires à base des ligands AMOXs: des assemblages multimétalliques vers des matériaux fonctionnels (sections 5.3.2, 5.3.3 et 6.2.3) et des systèmes photocatalytiques pour la conversion d'énergie solaire (en particulier la photocatalyse pour la production de H_2) (section 6.2.3).

6.2. Perspectives et travaux en cours

Cette section couvre les perspectives du projet et des informations sur les travaux en cours. Les résultats présentés convergent vers le but général de la thèse, mentionné dans l'introduction: l'étude des ligands amidines *N*-oxydes *N,N'*-disubstitués (AMOXs), du point de vue de la chimie de coordination et supramoléculaire. Il y a trois directions principales de recherche qui ont été identifiées pour poursuivre le projet: les ligands AMOXs (section 6.2.1), les composés de coordination des ligands AMOXs (section 6.2.2), et les systèmes supramoléculaires à base des ligands AMOXs (des assemblages multimétalliques vers des matériaux fonctionnels et des systèmes photocatalytiques pour la conversion d'énergie solaire, en particulier la photocatalyse pour la production de H_2) (section 6.2.3). Les progrès réalisés dans chacune de ces directions, ainsi que les perspectives de développement seront présentés.

6.2.1. Les ligands AMOXs

La *N*-oxydation des amidines *N,N'*-disubstituées avec du *m*-CPBA a été optimisée et utilisée comme la méthode de choix pour **la synthèse des ligands AMOXs** correspondants. L'intégration de cette méthode avec différentes techniques de préparation des amidines parents a conduit à une 'stratégie synthétique' générale pour l'obtention des AMOXs (Figure 2.1-2, Chapitre 2). Cela englobe des techniques de synthèse classiques (p. ex. la distillation, les réactions thermiques) ainsi que des techniques de synthèse modernes (p. ex. l'activation micro-ondes). Des variations spécifiques de cette stratégie générale permettent son application à une large gamme de substrats (p. ex. des groupements fonctionnels différents et différents degrés d'encombrement stérique). Cette méthode a été initialement utilisée pour la synthèse des mono-AMOXs, mais elle a été étendue avec succès pour la préparation des bis-AMOXs pontés par les atomes d'azote et des bis-AMOXs pontés par les atomes de carbone. (Figure 2.1-2, Chapitre 2). De nouveaux ligands AMOXs ont ainsi été synthétisés et caractérisés, ce

qui a permis le développement de cette classe de composés et l'investigation ultérieure de leur chimie de coordination.

Comme développement futur, la méthode pourrait être facilement adaptée pour la synthèse combinatoire, ce qui ouvrirait la possibilité de criblage d'une banque de composés afin d'identifier les meilleurs candidats ayant les propriétés souhaitées. Des essais préliminaires ont été effectués pour adapter l'étape de *N*-oxydation à la synthèse en flux continu ('flow chemistry').[1]. Le problème majeur pour la réaction de *N*-oxydation des amidines avec du *m*-CPBA est la protonation du substrat par l'acide produit, avec la formation d'une paire d'ions stable, ce qui empêche que la conversion totale soit atteinte. La technique de synthèse en flux continu offre la possibilité d'augmenter le degré de conversion en optimisant les paramètres suivants: concentration/ stœchiométrie/ temps de résidence dans le réacteur/ température. L'utilisation de cette technique pourrait apporter des avantages supplémentaires pour la synthèse des composés bis-AMOXs. Dans ces réactions, outre le problème de protonation, l'analogue mono-AMOX est formé. De plus, à des concentrations de 0.1 M, la formation (en majorité) du produit cyclique oxydé (le composé **C**, Figure 5.3-5 et Figure 5.3-9 section 5.3.3) est observée. En utilisant la technique de synthèse en flux continu, les conditions de dilution nécessaires pour maximiser la formation du composé bis-AMOX peuvent être créées et la formation du produit mono-AMOX peut aussi être minimisée grâce à un meilleur contrôle des paramètres de réaction.

En ce qui concerne **les structures cristallines des ligands AMOXs**, des études sont en cours pour identifier les facteurs (p. ex. les effets de substitution: stériques et/ou électroniques, d'autres types d'interactions supramoléculaires) qui génèrent des motifs spécifiques de liens hydrogène: des dimères cycliques *via* des liens –O-H---O– et –N-H---N– avec l'existence des deux tautomères hydroxyamidine et α-aminonitrone (type 1); des dimères cycliques *via* des liens –O-H---N– avec l'existence de la forme hydroxamidine seulement (type 2); des dimères cycliques *via* des liens –N-H---O– avec l'existence de la forme α-aminonitrone seulement (type 3); des dimères non-cycliques *via* des liens –O-H---O- avec l'existence des deux tautomères hydroxyamidine et α-aminonitrone (type 4).[2] La compréhension et la rationalisation d'une telle relation cause-effet sont importantes pour pouvoir utiliser efficacement les liaisons hydrogène comme outil de 'crystal engineering'. Des études

théoriques (p. ex. des calculs DFT) sont également prévues dans ce sens, pour la comparaison avec les résultats expérimentaux.

D'autres avenues possibles à explorer avec des ligands AMOXs sont: leur réactivité et des tests en catalyse; leur étude sur des surfaces; des systèmes hybrides: l'incorporation dans des polymères (p. ex. comme adsorbant pour des ions toxiques); AMOX-QD (quantum dots); AMOX-nanoparticules; AMOXs ancrés sur TiO_2 ou POMs (des études récentes présentent l'ancrage des ligands N,O aux semi-conducteurs[3] et aux POMs);[4] la modulation de la capacité de chélation pour des applications en médecine (thérapie de chélation),[5] l'industrie d'extraction;[6] la versatilité dans la coordination – la catalyse assisté par le ligand; d'autres processus dynamiques dans des applications biomédicales.

6.2.2. Les composés de coordination des ligands AMOXs

Des avenues à explorer en ce qui concerne les composés de coordination des ligands AMOXs sont brièvement souligné ci-dessous.

a) les complexes de ligands AMOXs avec des ions de Co(II) et Co(III) – dans les complexes **Co(AMOX)₂** (AMOX = *N,N'*-bis(aryl)-formamidinate-*N*-oxyde), la stabilisation de la géométrie plan carré au centre de cobalt(II) dépend de la présence de substituants dans les positions 2, 6 des *N*-aryles, ainsi que de l'encombrement stérique de ces substituants. Quand seulement 2-méthylephényle est utilisé comme substituant, le complexe pseudo-octaédrique de Co(III) est obtenu (Figure S1, Annexe-6.2-EXP). Les propriétés électrochimiques des complexes Co(AMOX)₂, avec la réversibilité du couple Co(II/III), ainsi que leurs spectres UV/vis sans transitions intenses dans le visible et l'encombrement stérique des ligands AMOX suggèrent que ces composés pourraient être des candidats appropriés pour être utilisés comme médiateurs redox dans des DSSCs.[7a] La caractérisation de la famille des composés **Co(III)(AMOX)₂X (X = halogène)** est en cours. Des résultats préliminaires indiquent un intérêt possible dans leurs propriétés magnétiques. Des tests préliminaires avec des complexes Co(AMOX)₂ comme catalyseurs pour la production de H_2 dans des systèmes photocatalytiques ont été realisés. Les conclusions et les perspectives sur ce sujet sont présentées dans la section 6.2.3.

b) les dimères [Zn(AMOX)₂]₂ (Figure 5.3-4a-e, section 5.3.2) – représentent une autre classe de composés AMOXs avec de l'intérêt potentiel dans des applications. Ce sont des composés stables et leur solubilité dans des solvants organiques représente un avantage pour leur processabilité dans la fabrication des dispositifs. La performance de ce type de composés comme luminophores dans les White OLEDs (WOLEDs) est actuellement étudiée en collaboration avec le groupe de recherche du prof. Nunzi de Queens University. L'exemple d'un résultat préliminaire est présenté dans la Figure 5.3-4e, section 5.3.2. Le travail est en cours pour développer cette famille de composés. Comme montré à la section 5.3.2, les calculs DFT, validés par les résultats expérimentaux, indiquent que le gap optique de ces complexes peut être finement modulé en modifiant le substituent *C*-aryle (introduire des groupements EW/ED), afin d'obtenir des composés ayant les propriétés désirés.

c) les complexes Al(AMOX)₃ – sont aussi des composés prometteurs pour des applications de type OLED. Le travail sur cette famille de complexes est en cours. Les résultats préliminaires obtenus pour Al(AMOX)₃ (AMOX = *N,N'*-diphenyl-benzamidinate-*N*-oxyde) suggèrent que ces complexes sont solubles dans les solvants organiques, sont facilement processables en films, sont stables et sont émissifs à l'état solide. La comparaison du gap optique du Al(AMOX)₃ (AMOX = *N,N'*-diphenyl-benzamidinate-*N*-oxyde) avec ceux du Alq₃ et Zn(BTZ)₂ (des composés classiques utilisés dans OLEDs)[7b] est présentée dans la Figure S2, Annexe-6.2-EXP. Des études DFT/ TD-DFT préliminaires suggèrent que, de même que pour les complexes de zinc(II), le gap optique des complexes d'aluminium(III) peut être finement modulé en modifiant le substituent *C*-aryle du ligand AMOX.

d) la chimie du Ru(II)/Re(I) avec des ligands AMOXs – est d'intérêt pour la synthèse des photosensibilisateurs et/ou catalyseurs (p. ex. pour l'oxydation de l'eau, la réduction du CO_2); des composés de Ru(II/III) avec des ligands AMOXs pouraient être utilisés comme photosensibilisateurs dans DSSCs – des calculs DFT pour $[Ru(AMOX)(bpy)_2]^+$ (Figure S3, Annexe-6.2-EXP) montrent la HOMO localisée partiellement sur le ligand AMOX et la LUMO sur le fragment bpy (qui est ancré au semi-conducteur) – cela suggère fortement la possibilité d'injection d'électron dans le semi-conducteur, tout en disposant d'une possibilité d'ajuster le niveau d'énergie de la HOMO par des modifications des substituants sur le ligand AMOX).

D'autres projets comprennent: des complexes de Ni(II) et Cu(II) avec des ligands AMOXs – ces projets sont en cours; des ions lanthanides et actinides avec des ligands AMOX; d'autres ions métalliques (Fe(II/III), Mn(II/III/IV), Pt(II), Pd(II), Ir(III) etc.) avec des ligands AMOXs. De plus, des ligands AMOXs substitués par de longues chaînes alkyles, qui forment des complexes neutres avec des ions métalliques, pourraient être exploités dans le domaine des cristaux liquides. Il serait également utile d'explorer davantage la réactivité des complexes à base des ligands AMOXs en catalyse et/ ou dans des réactions de type 'modification *sur le complexe*'.

6.2.3. Les systèmes supramoléculaires à base des ligands AMOXs

6.2.3.1. Des systèmes multimétalliques – vers des matériaux fonctionnels

Différentes architectures multimetalliques ont été obtenues lors de la complexation des ligands bis-AMOX pontés par les atomes d'azote, avec des ions métalliques: un métallopolymère-1D avec des ions de Zn(II) (présenté dans le chapitre 5, section 5.3.3) qui est émissif, et un ensemble discrét dinucléaire avec des ions de Ni(II) (travail en cours – la structure à l'état solide du Ni$_2$(bis-AMOX-Ph)$_2$ est montrée comparativement à la structure du polymère de coordination (Figure S4, l'Annexe-6.2-EXP) à titre d'exemple pour souligner les perspectives du projet sur la direction de la chimie supramoléculaire des systèmes basés sur les ligands AMOX. La caractérisation complète du composé Ni$_2$(bis-AMOX-Ph)$_2$ reste à être finalisée. Des composés analogues, avec des métaux paramagnétiques (p. ex. Cu(II)), peuvent être synthétisés et étudiés pour leurs propriétés magnétiques. Les composés de type grille avec des ions de Zn(II) sont encore à obtenir – le criblage des différentes conditions (solvant/ température/ stœchiométrie) est en cours. L'étude des liens pont hydrogène dans les ligands bis-AMOX ainsi que l'étude des effets de coopérativité coordination – liens hydrogène dans des composés de type AMOX-amidine pontés sont aussi d'intérêt du point de vue du 'crystal engineering'. L'extension du design du ligand à des AMOXs multifonctionnels par variation structurelle (p. ex. l'introduction de substituants de type pyridine(s), phosphine(s) sur les ligands AMOX) et la coordination avec différents ions métalliques pourrait conduire à de nouvelles architectures métallosupramoléculaires; le design spécifique du ligand pour mener à la sélectivité des ions métalliques serait également d'intérêt.

6.2.3.2.   Des systèmes photocatalytiques pour la production de H₂

Des complexes Co(AMOX)₂ (AMOX = *N,N'*-bis(2.6-dimethylphenyl)-formamidinate-*N*-oxyde (**Co(2,6-diMe)₂**) et *N,N'*-bis(2-biphenyl)-formamidinate-*N*-oxyde (**Co(2-Ph)₂**) ont été étudiés comme catalyseurs pour la production de H₂ dans des systèmes photocatalytiques à base de photosensibilisateurs (PS) de Re(I) et Ir(III) (Figure 6.2-1, Figure 6.2-2 et Figures S5-S11, l'Annexe-6.2-EXP).[8] Un bref survol de ces résultats préliminaires est fait ici, dans le but d'introduire les perspectives du projet dans cette direction.

La production de H₂ a été suivie en temps réel, par des expériences en flux continu, en utilisant la chromatographie en phase gazeuse. (Figures S8-S9, l'Annexe-6.2-EXP).[9] Le criblage des différentes combinaisons: système de solvant – source de protons, donneur sacrificiel d'électrons (sacrificial electron donor (SED)), photosensibilisateur (PS) et catalyseur, a été réalisé (Figures S7, l'Annexe-6.2-EXP).

Comme observation générale, les complexes Co(AMOX)₂ catalyse la production de H₂ dans des systèmes photocatalytiques à base de PS de Re(I) et Ir(III), mais avec des bas TONs (turnover numbers). La performance du système est très dépendante des conditions expérimentales. Les meilleurs résultats (TON 170) ont été obtenus avec un PS à base de Ir(III), TEA comme SED et Co(2-Ph)₂, dans DMF, pour une stœchiométrie PS:Cat 5:1 (1:0.2) (Figure 6.2-2). Comme montré par des tests d'addition de PS, les catalyseurs Co(AMOX)₂ sont robustes (Figure S6, l'Annexe-6.2-EXP). Par contre, le principal problème est représenté par leur réduction Co(II/I) difficile. Il a été établi dans la littérature, par des études expérimentales et théoriques, que l'analogue de Co(I) photogénéré est l'espèce d'entrée dans le cycle catalytique de la production de H₂ à base des catalyseurs de cobalt. (Figure S11, l'Annexe-6.2-EXP).[8a, 8c-e, 10] Dans des conditions photocatalytiques, l'espèce de Co(I) peut être généré par des processus de quenching oxydatif ou réductif.[11] Pour des systèmes Ir/TEA et Re/TEOA, il a été montré que le processus de quenching réductif a habituellement lieu (Figure 6.2-1).[8] Toutefois, dans les systèmes étudiés dans ce travail, les deux processus (oxydatif et réductif) sont thermodynamiquement défavorables pour le transfert d'électron nécessaire pour générer l'espèce Co(I) (Table S3, l'Annexe-6.2-EXP). Le système le plus performant (Ir-PS avec Co(2-Ph)₂) est celui qui a la plus petite barrière d'énergie (0.68 V).
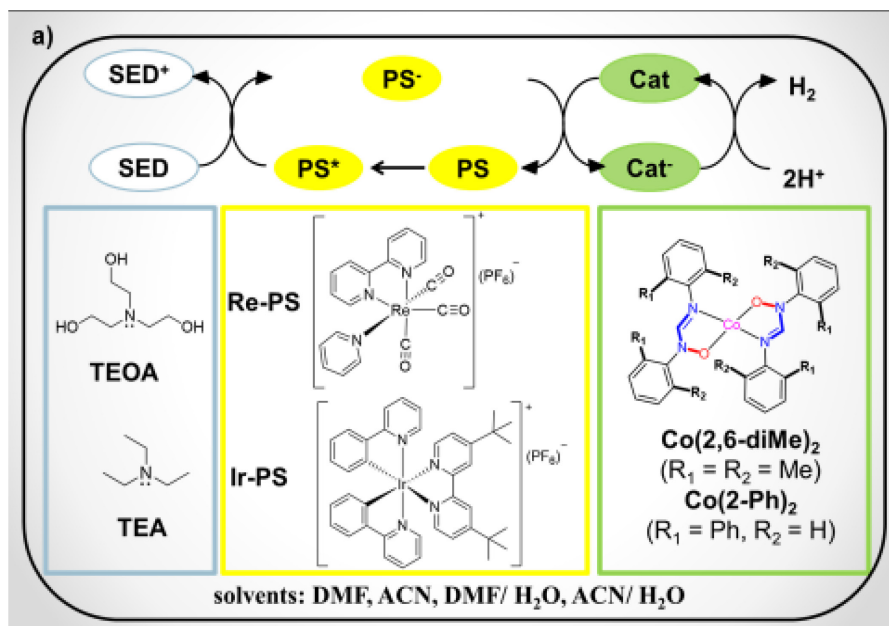
Figure 6.2-1. Les systèms photocatalytiques étudiés [8]
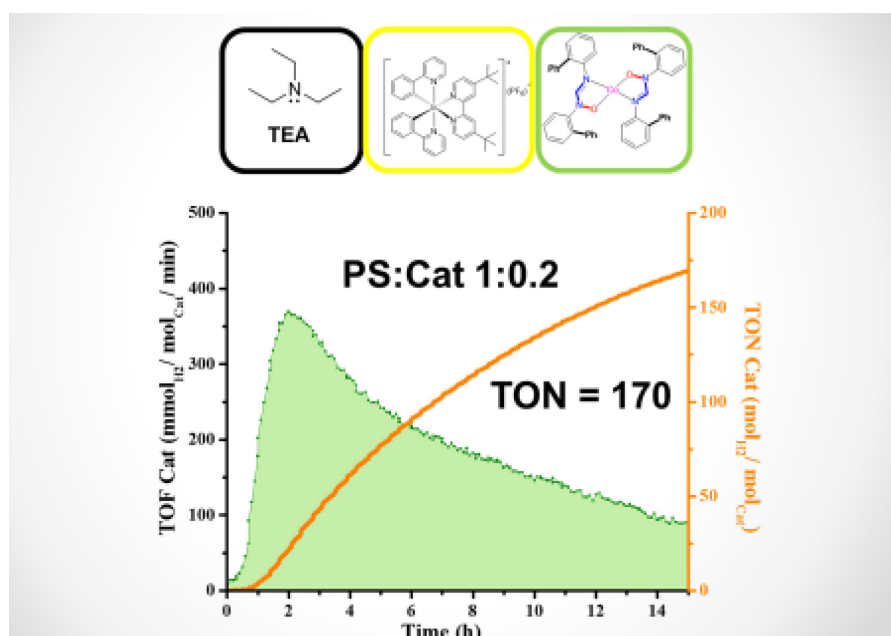
Figure 6.2-2. Le système le plus performant pendant cet étude: production photocatalytique de H_2 dans 7.5 mL d'une solution de DMF contenant TEA 1M, PS 0.1 mM, et une stœchiométrie PS:Cat 5:1 (1:0.2), à 20^{0}C (irradiation pendant 15 h à 394 nm). Dans l'expérience 'contrôle' (seulement PS sans catalyseur, mêmes conditions) seulement des traces de H_2 ont été produites.

Par conséquent, afin d'améliorer les performances de ces systèmes, il est nécessaire de modifier le potentiel de réduction des complexes Co(AMOX)$_2$ vers des valeurs plus positives. Cela peut être fait par l'introduction de groupes EW sur le ligand AMOX. La modification des ligands AMOX afin de rendre leurs complexes solubles dans l'eau est une autre direction pour le développement de ce projet, car le but final est la production de H$_2$ dans des systèmes aqueux.

6.3. Remarques finales

La nature exploratoire de ce projet et les résultats intéressants trouvés jusqu'ici ont conduit à de multiples directions de recherche qui peuvent être poursuivies (section 6.2). J'espère que les résultats et les perspectives présentés dans ce travail motivent de futurs développements dans la chimie de coordination des ligands AMOXs.

Comme ce projet est directement lié à la chimie de coordination moderne, des orientations/ stratégies dans l'étude des complexes de coordination et leur utilisation dans des applications sont présentées comme observations finales. Elles sont basées sur les résultats obtenus, ainsi que sur l'expérience de recherche et les connaissances accumulées au cours de ce projet:

-    le développement des stratégies de design pour les complexes de coordination, en mettant l'accent sur le design du ligand; l'objectif final est de faire usage des relations structure–propriétés pour concevoir et synthétiser avec succès des composés ayant les propriétés voulues

-    l'intégration des études théoriques (calculs théoriques p. ex. méthodes DFT et TD-DFT) les travaux expérimentaux pour valider les modèles théoriques

-    l'utilisation des systèmes de criblage/ approches combinatoires pour mener des études systématiques sur les complexes de coordination, ainsi que des enquêtes systématiques de leurs performances dans des dispositifs spécifiques

-    l'utilisation d'approches multidisciplinaires dans la synthèse, les méthodes de caractérisation et la fabrication de dispositifs pour générer des systèmes hybrides qui

exploitent les principes de pré-design et de complémentarité ainsi que les effets synergiques, afin de gagner en efficacité

- **le développement de stratégies et de méthodes plus efficaces pour lier (design/ prédiction/ réglage (tuning)/ adaptation) les propriétés des complexes métalliques avec leurs performances dans les applications (dispositifs et procédés)**

- la poursuite du contrôle au niveau moléculaire; la nécessité de mieux comprendre le comportement des molécules au niveau des interfaces et sur les surfaces, la solubilité des complexes de coordination dans l'eau/ solvant organique

- le développement de nouvelles stratégies pour intégrer les nouvelles découvertes (p. ex. l'utilisation des ligands redox-actifs).

Et sur un plan plus général:

- l'amélioration des outils existants et le développement de nouveaux outils (bases de données, outils de recherche, logiciels, etc.), en intégrant les nouvelles technologies, dans le but de faire face à la recherche extensive et à l'énorme progrès, ainsi qu'à l'explosion d'information reportée

- la recherche pour des tendances dans l'étude des composés de coordination et pour des leçons du passé et du présent; le développement d'une approche globale, holistique pour l'étude des complexes de coordination en fonction des besoins réels de la société et des valeurs qui respectent l'éthique et considèrent comme priorités 'la vie' et 'l'environnement' – l'extension de cette approche à l'éducation dans la chimie de coordination et aux initiatives de collaboration (milieu universitaire – gouvernement – industrie)

- l'investissement dans la recherche fondamentale, car les percées scientifiques se produisent par le biais de la recherche fondamentale.

~ ~ ~

'*Il y a des choses qu'on ne sait pas qu'on ne sait pas*' (Donald Rumsfeld, dans une conférence de presse au siège de l'OTAN, Bruxelles, Belgique, 2002); ainsi, comme

chercheur, il est important de continuer à observer, de continuer à garder un esprit ouvert et alerte, d'être prêt à (rece)voir la sérendipité. Il est également important de changer de perspective, de penser dynamiquement et de chercher 'la grande image' dans des situations ponctuelles et les spécificités dans des tendances générales, parce que:

'*LA SCIENCE, À SON MEILLEUR, NOUS FOURNIT DE MEILLEURES QUESTIONS, PAS DE RÉPONSES ABSOLUES*' (Norman Cousins, 1976) **et** '*LE VÉRITABLE VOYAGE DE LA DÉCOUVERTE NE CONSISTE PAS À CHERCHER DE NOUVEAUX PAYSAGES, MAIS À AVOIR DE NOUVEAUX YEUX*' (Marcel Proust)**.**

6.4. References

[1]   D. T. McQuade, P. H. Seeberger, *J. Org. Chem.* **2013**, *78*, 6384-6389.

[2]   a) M. Cibian, S. Derossi, G. S. Hanan, *Acta Crystallogr. Sect. E* **2009**, *65*, o2485-o2485; b) A. Krajete, G. Steiner, H. Kopacka, K.-H. Ongania, K. Wurst, Marc O. Kristen, P. Preishuber-Pflügl, B. Bildstein, *Eur. J. Inorg. Chem.* **2004**, *2004*, 1740-1752.

[3]   L. Zhang, J. M. Cole, *ACS Appl. Mat. & Interf.* **2015**, *7*, 3427-3455.

[4]   B. Artetxe, S. Reinoso, L. San Felices, P. Vitoria, A. Pache, J. Martín-Caballero, J. M. Gutiérrez-Zorrilla, *Inorg. Chem.* **2015**, *54*, 241-252.

[5]   a) G. Crisponi, V. M. Nurchi, J. I. Lachowicz, M. Crespo-Alonso, M. A. Zoroddu, M. Peana, *Coord. Chem. Rev.* **2015**, *284*, 278-285; b) K. J. Franz, *Curr. Op. in Chem. Biol.* **2013**, *17*, 143-149; c) S. J. S. Flora, in *Comprehensive Inorganic Chemistry II (Second Edition)* (Ed.: Poeppelmeier, J. R.), Elsevier, Amsterdam, **2013**, pp. 987-1013.

[6]   P. A. Tasker, P. G. Plieger, L. C. West, in *Comprehensive Coordination Chemistry II* (Ed.: Meyer, J. A. and McCleverty, T. J.), Pergamon, Oxford, **2003**, pp. 759-808.

[7]   a) T. W. Hamann, *Dalton Trans.* **2012**, *41*, 3111; b) R. Wang, L. Deng, M. Fu, J. Cheng, J. Li, *J. Mat. Chem.* **2012**, *22*, 23454-23460.

[8]   a) P. Zhang, P.-A. Jacques, M. Chavarot-Kerlidou, M. Wang, L. Sun, M. Fontecave, V. Artero, *Inorg. Chem.* **2012**, *51*, 2115-2120; b) A. M. Soliman, D. Fortin, P. D. Harvey, E. Zysman-Colman, *Chem. Commun.* **2012**, *48*, 1120-1122; c) B. Probst, M. Guttentag, A. Rodenberg, P. Hamm, R. Alberto, *Inorg. Chem.* **2011**, *50*, 3404-3412; d) B. Probst, A. Rodenberg, M. Guttentag, P. Hamm, R. Alberto, *Inorg. Chem.* **2010**, *49*, 6453-6460; e) B. Probst, C. Kolano, P. Hamm, R. Alberto, *Inorg. Chem.* **2009**, *48*, 1836-1843.

[9]   D. Chartrand, PhD Thesis: *Vers des assemblages de complexes métalliques oligonucléaires, servant d'antenne solaire au niveau moléculaire*, Université de Montréal, **2013**

[10]   a) S. Berardi, S. Drouet, L. Francas, C. Gimbert-Surinach, M. Guttentag, C. Richmond, T. Stoll, A. Llobet, *Chem. Soc. Rev.* **2014**, *43*, 7501-7519; b) B. H. Solis, Y. Yu, S. Hammes-Schiffer, *Inorg. Chem.* **2013**, *52*, 6994-6999; c) J. L. Dempsey, J. R. Winkler,

H. B. Gray, in *Comprehensive Inorganic Chemistry II (Second Edition)* (Ed.: Poeppelmeier, J. R.), Elsevier, Amsterdam, **2013**, pp. 553-565.

[11] V. Artero, M. Chavarot-Kerlidou, M. Fontecave, *Angew. Chem., Int. Ed.* **2011**, *50*, 7238-7266.

ANNEXES/ APPENDIX

Annexe-1 / Appendix-1 – Chapter 1: Introduction

1.1. General Context: 'Molecular and Supramolecular Coordination Chemistry' – Coordination Complexes and Their Applications

1.1.1. The Role of Coordination Compounds: From Past and Present Successes to Present and Future Challenges – Trends in Modern Coordination Chemistry

The study and the development of coordination compounds for specific, tangible applications is the underlying motivation for the present work. It stems from the importance these compounds play in our daily lives.[1] By combining the characteristics of metal-ions with those of organic ligands, metal-organic (cf., coordination complexes) complexes present intrinsic properties with enhanced tunability *versus* the pure inorganic materials, while gaining in stability and robustness, with respect to the organic substances.[2] Therefore, their properties make them suitable and attractive for a wide range of applications in fields going from catalysis and solar energy conversion/ storage to materials and life sciences.[1] Consequently, research on coordination compounds has flourished over the past decades, resulting in fascinating insights into knowledge and unprecedented developments.[3] Thus, modern coordination chemistry has emerged and established an important field of research that contributes the practical solutions needed to respond to humanity's top challenges: energy, water, food, environment, poverty, and disease.[3-4] Selected successes of coordination compounds in various applications are highlighted in Table 1.1-1 and Figure 1.1-1. Coordination complexes are ideally placed from the point of view of their photophysical, photochemical, electrochemical (redox) and magnetic properties to perform in well-established applications as: dyes and pigments (e.g. **cpds. 1-2**, Table 1.1-1);[5] extractants for hydrometallurgy and extraction industry (e.g. **cpds. 3-5**, Table 1.1-1);[6] catalysts in homogeneous catalytic processes of industrial importance (e.g. **cpds. 6-12**, Table 1.1-1);[7] drugs in anticancer therapy (e.g. **cpds. 13-15**, Table 1.1-1),[8] chelation therapy (e.g. **cpds. 16-**

19, Table 1.1-1),[9] rheumatoid arthritis therapy (e.g. **cpd. 20**, Table 1.1-1),[10] and diagnostic agents (e.g. **cpd. 21-22**, Table 1.1-1)[11] in medicine. In addition, the use of coordination complexes in emergent technologies such as solar energy harvesting and conversion devices (e.g. Dye Sensitized Solar Cells (DSSCs) (e.g. **cpds. 23-26**, Table 1.1-1)),[12] Organic Light Emitting Diodes (OLEDs) (e.g. **cpds. 27-31**, Table 1.1-1),[13] and Metallic-Organic Framework (MOF)-based applications (e.g. **cpd. 32-33**, Table 1.1-1)[14] has attracted increased research interest. Concrete results were achieved: prototype products (e.g. MOF-based fuel tank and MOF-based filter materials;[14a] DSSC-based lighting devices (e.g. Hana-Akari lamp by Sony)[12b, 15]) as well as products which have already been introduced on the market (OLED-based lighting panels (OSRAM, Mitsubishi, Pioneer, LG Chem) OLED TVs (e.g. LG, Sony, Panasonic) and smartphones (e.g. Samsung Galaxy), OLED-based taillights (BMW)).[16]

Table 1.1-1. Selected examples of coordination compounds in applications (see Figure 1.1-1 for the structures of the system/ compound(s))

Cpd. (Fig. 1)	Application type	Field	Reference
1	Dye	dyes, pigments, textile, paper, and wood industry	[5]
2	Pigment		
3 – 5	metal extractants	hydrometallurgy and extraction	[6]
6	catalyst – hydroformylation	industrial production of aldehydes	[7a, 7f]
7	catalyst – Monsanto process	industrial production of acetic acid	[7a, 7f]
8	catalyst – Cativa process		
9	catalyst – Shell higher olefin process (SHOP)	petrochemical industry – olefin oligomerization (production of C6-C20 linear olefins)	[7a, 7b]
10	catalyst – asymmetric hydrogenation of ketones	pharmaceutical industry	[7c-e]
11 – 12	catalyst – cross-coupling	organic products synthesis	[7a, 7g, 7h]
13 – 15	worldwide clinically approved anticancer drugs	medicine: cancer therapy	[8a, 8b]
16 – 17	iron chelating agents	medicine: iron overload therapy	[9a-c]
18	heavy metal chelating agent (M = Hg, As, Au)	medicine: chelation therapy for heavy metal poisoning (FDA approved)	[9a]
19	lead chelating agent		
20	rheumatoid arthritis drug	medicine: therapy (FDA approved)	[10]
21	MRI contrast agent	medicine: diagnostic imaging (FDA approved)	[11a]
22	gamma-emitting radio-nuclide bone imaging agent		[11b, 17]
23 – 26	DSSC (dyes)	solar-energy harvesting and conversion	[12a-c, 12e, 18]
27 – 31	OLEDs	Optoelectronics	[13]
32 – 33	fuel/ gas storage: MOF-enhanced fuel tank	Transportation	[14]
33	filter material	textile and food industry	
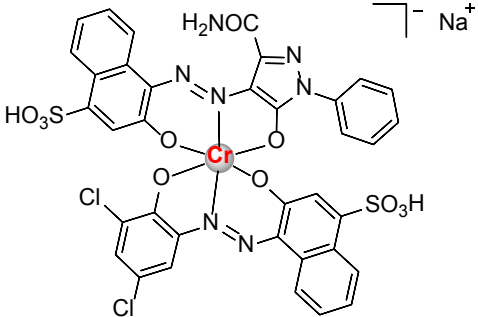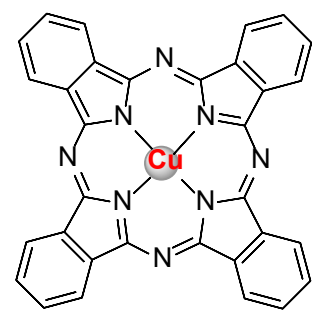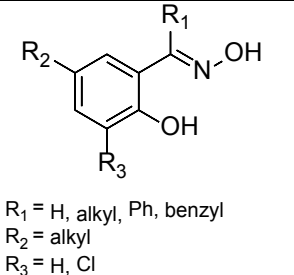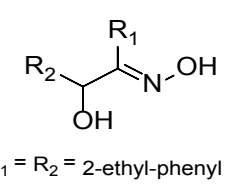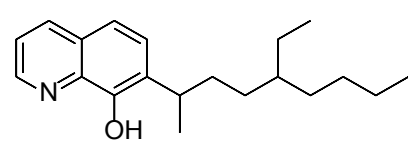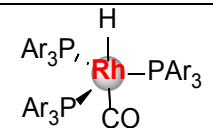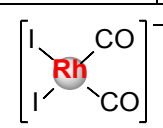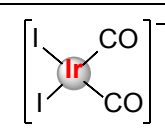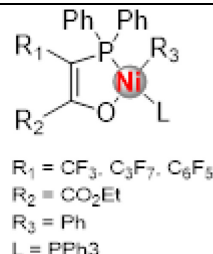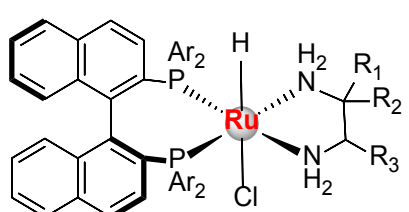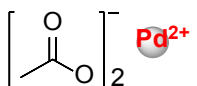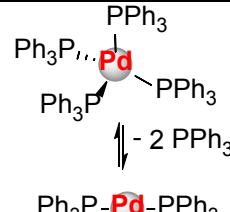
Cr-based azo dye (CI Acid Violet 121)	*copper phthalocyanine (CI Pigment Blue 15)*
1[5]	**2**[5]

R$_1$ = H, alkyl, Ph, benzyl R$_2$ = alkyl R$_3$ = H, Cl	R$_1$ = R$_2$ = 2-ethyl-phenyl	
phenolic oxime-type metal extractants	*α-hydroxyoxime-type metal extractants*	*Kelex 100* *8-hydroxyquinoline-type metal extractant*
3[6]	**4**[6]	**5**[6]

Rh-based catalyst (hydroformylation)	*Rh-based catalyst (Monsanto)*	*Ir-based catalyst (Cativa)*
6[7f]	**7**[7f]	**8**[7f]

R$_1$ = CF$_3$, C$_3$F$_7$, C$_6$F$_5$ R$_2$ = CO$_2$Et R$_3$ = Ph L = PPh3	
Ni-based catalysts (SHOP)	*RuHCl(BINAP)(diamine)*
9[7b]	**10**[7e]

	- 2 PPh$_3$
Pd-based precatalyst/ catalyst (cross coupling reactions)	
11[7a]	**12**[7a]

Figure 1.1-1. Selected examples of coordination compounds in applications
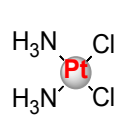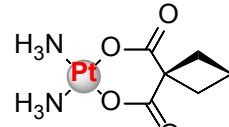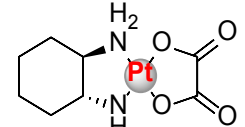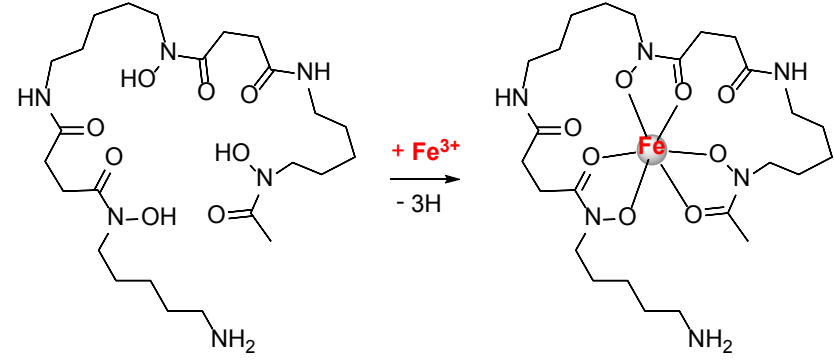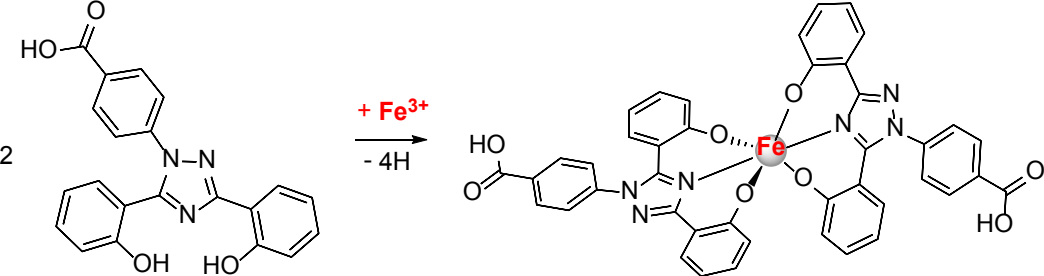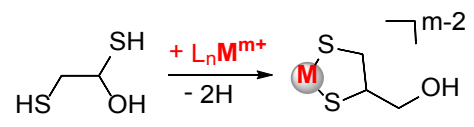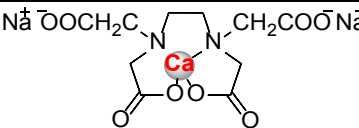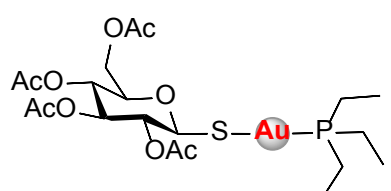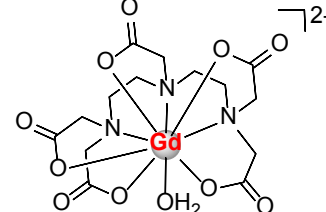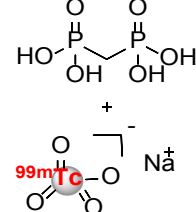
Cisplatin	*Carboplatin*	*oxaliplatin*
13[8a]	**14**[8a]	**15**[8a]

deferoxamine/ desferrioxamine-B (Desferal)	*ferrioxamine B*
16[9a-c]	**16-i**[9a-c]

deferasirox (Exjade)	*Fe(deferasirox)₂ complex*
17[9a-c]	**17-i**[9a-c]

dimercaprol/ *British Anti Lewisite (BAL)*	*M(dimercaprol)^{m-2} complex* *M = Hg, As, Au*	*calcium disodium EDTA* *(used in lead poisoning)*
18[19]	**18-i**	**19**[9a]

auranofin (Ridaura)	*[Gd(DTPA)(H₂O)]^{2-} (Magnevist)*	*^{99m}Tc medronate*
20[10]	**21**[20]	**22**[17]

Figure 1.1-1. Selected examples of coordination compounds in applications – (cont)
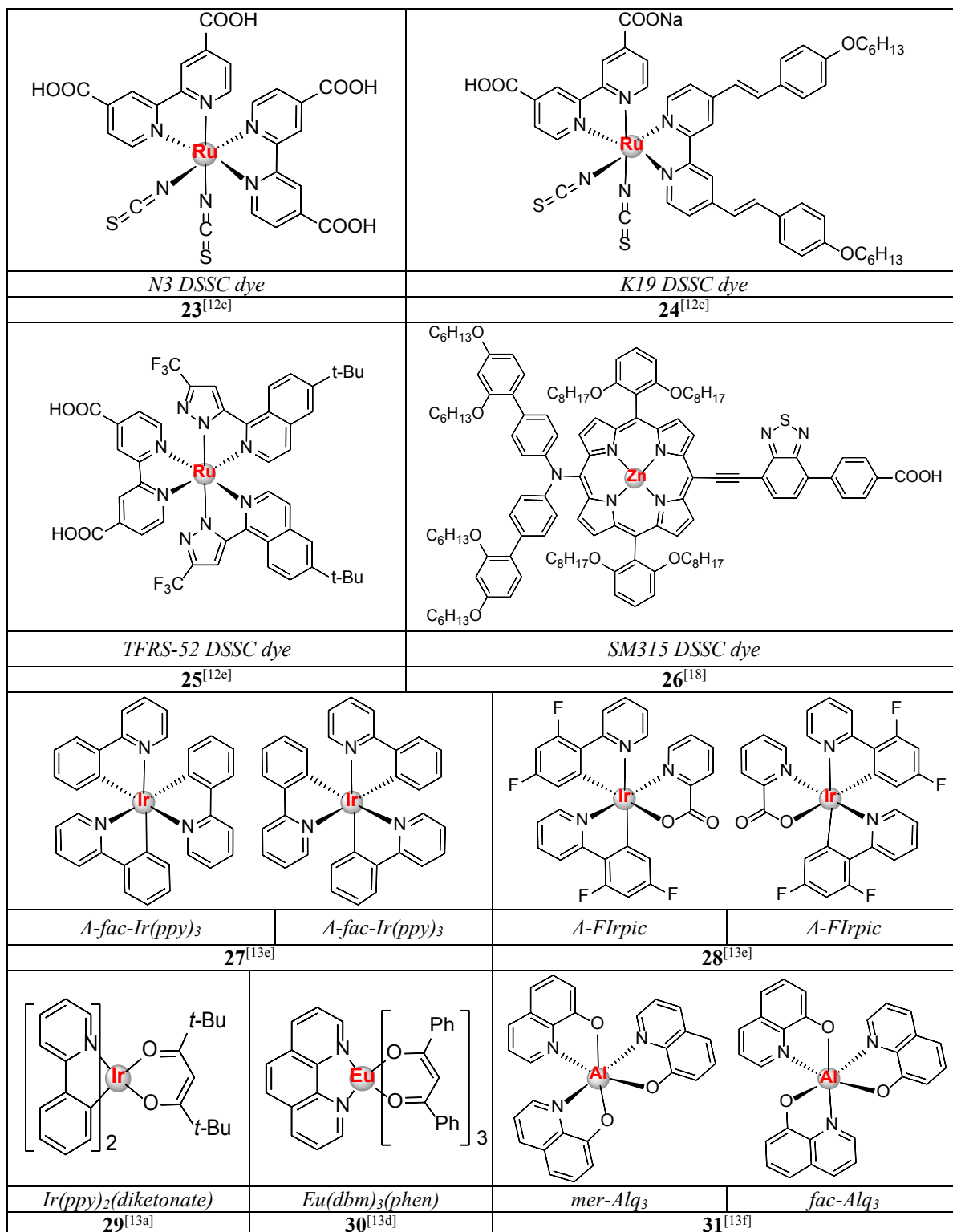
N3 DSSC dye	*K19 DSSC dye*
23[12c]	**24**[12c]
TFRS-52 DSSC dye	*SM315 DSSC dye*
25[12e]	**26**[18]

Λ-fac-Ir(ppy)₃	*Δ-fac-Ir(ppy)₃*	*Λ-FIrpic*	*Δ-FIrpic*
27[13e]		**28**[13e]	

Ir(ppy)₂(diketonate)	*Eu(dbm)₃(phen)*	*mer-Alq₃*	*fac-Alq₃*
29[13a]	**30**[13d]	**31**[13f]	

Figure 1.1-1. Selected examples of coordination compounds in applications – (cont).

metal centre: Zn²⁺ organic linker:	metal centre: Cu²⁺ organic linker:
Basolite Z377 (MOF-177)	*Basolite C 300 (HKUST-1)*
32[14]	**33**[14a, 21]
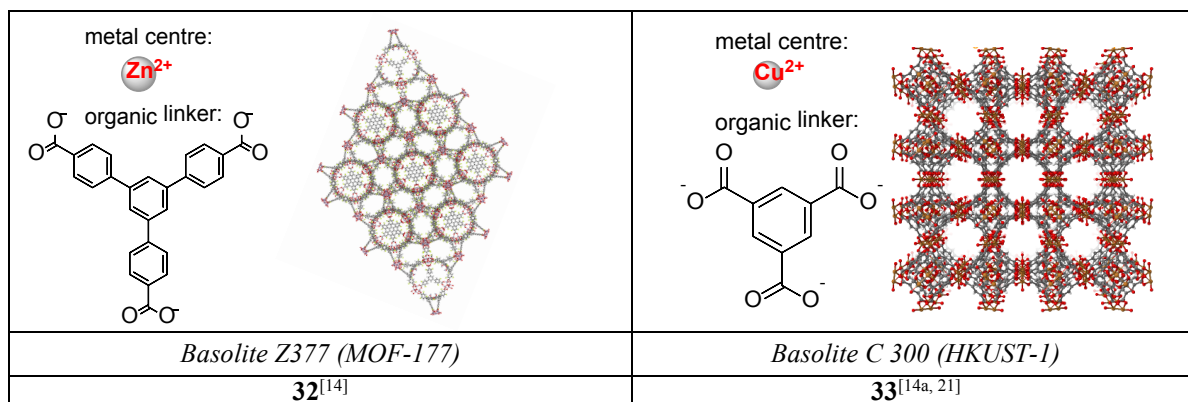
Figure 1.1-1. Selected examples of coordination compounds in applications – (cont).

The evolution of our society at a global level is characterized by the cyclical cause-and-effect process: challenges ↔ (lead to) progress. As a result, the following general trend*: more robust – more energy and space efficient – greener* has emerged in research, development and implementation of real applications (both devices and processes). From the perspective of compounds used in such applications, this trend has engendered an evolution *toward the molecular level: to be able to generate, modify, and adapt properties of compounds by tuning, controlling, as well as predicting and designing at the molecular level.*[3, 22] A more comprehensive description of this tendency is *toward complexity at the molecular level*, as it actually consists of two simultaneous directions: i) *specialization* (the in-depth study of the individual components in order to understand the fundamentals, their specificities, their properties, and to derive models) and ii) *inter- and multidisciplinary approaches* (from a general perspective, it can be seen as a system combining components of different nature, and/ or diverse 'connectivity tools', and/ or methodologies, to enhance complementarity and synergic effects, to gain in total efficiency and stability).[3, 22-23] A schematic presentation is highlighted in Figure 1.1-2. The *specialization* direction can be described by a 'black-box' approach, from the evolution of the first report of a system (I) toward the study and development of its individual components (II), and further systematic studies of each component (III). As *multidisciplinary approaches*, the following can be considered: the combined experimental characterization methods (1); the development of theoretical models, the use of theoretical calculations and the validation of these models by comparison with the experimental results (2); the development of hybrid systems (3); the application of the compound/ system in a device and assessment of its performance (4).
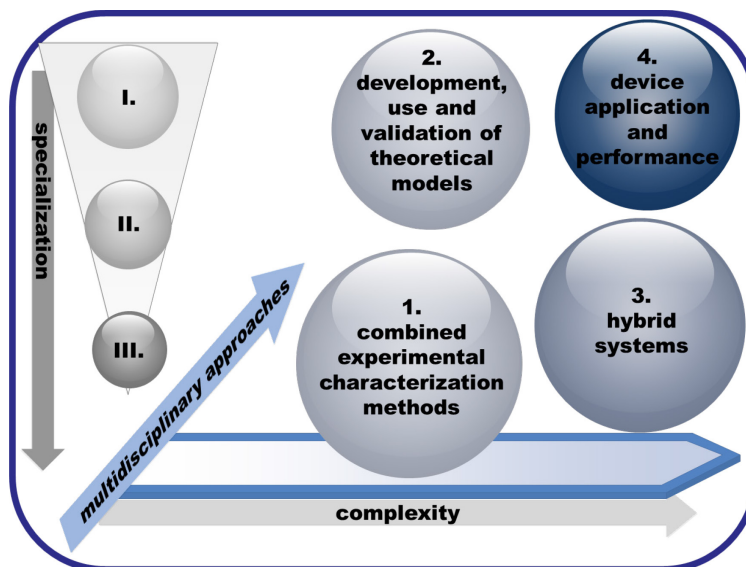
Figure 1.1-2. The trend *toward complexity at the molecular level* in modern coordination chemistry: specialization and multidisciplinary approaches

The evolution of modern coordination chemistry *toward complexity at the molecular level* is not an aleatory process. In Nature, coordination compounds exist as its components[10] and are used in various processes.[24] Both the mineral and the biological realms are state-of-the-art models of mastering complexity at the molecular level. Consequently, Nature has represented the source of inspiration for the development and use of coordination compounds, leading to the development of bio-mimicry, and bio-inspired approaches.[25] *Bio-mimicry* in coordination chemistry aims to develop compounds/ systems which mimic parts of biological ones, with focus on studying, elucidating and modeling the role of metal-ions and their coordination environments in the biological systems.[26] These approaches have particular relevance for drug development and catalysis.[27] Understanding the role of metal-ions in bacteria could also be of high industrial and agricultural significance.[3] Increasing research interest is shown in this direction, as proved by the recent Unified Microbiome Initiative (UMI): '*decrypting microbial genes and chemistries*' is identified as a key need and opportunity in order '*to accelerate basic discovery and translation to applications*'.[28] *The objective of the bio-inspired approaches* is to reproduce the function, not the complexity of the biological systems.[29] Thus, hybrid systems, studying the performance of synthetic compounds in biological environment (e.g. cobaloxime-based artificial hydrogenases)[30] as

well as the performance of biological species in synthetic medium/ environment (e.g. enzymes and microbial cultures in solar-fuel devices).[31] have been developed, leading to important advancement of knowledge.

Among the bio-inspired approaches, artificial photosynthesis is paramount from the perspective of a sustainable energy future.[29, 32] Therefore, it is important to assess the role coordination complexes play/ could play in this direction.[33] In the context of the world's population growth and the increase in the standard of living across the globe, the accompanying explosion in demand for energy will engender further consumption of fossil-fuels.[32d, 34] Consequently, the depletion of Earth's non-renewable resources, and especially the associated augmentation of greenhouse gas emissions will have extremely negative environmental costs.[35] The development of alternative and renewable energy resources has become one of the most important challenges facing humanity.[29, 32] Among the existent alternative energy sources, solar energy receives particular attention due to its availability and abundance.[29, 32] The main forms of solar energy conversion are heat, electricity and fuels, and three principal research strategies can be identified in this direction: i) direct conversion into electrical energy by photovoltaic devices; ii) production of biofuels using biomass; iii) artificial photosynthesis.[32f] The natural photosynthesis is the most successful system in generating and storing energy, using resources which are available and abundant (sunlight, water and carbon dioxide) (Figure 1.1-3a).[36] The solar energy is harvested and transferred by chromophore units in photosystem II (PSII). Charge separation takes place followed by hole and electron transfer. Holes are transferred to the oxygen evolving centre (OEC) which splits water into oxygen (released in atmosphere) and four protons. Redox-active cofactors (e.g., plastoquinol PQH2, plastocyanin PC), the cytochrome b6f complex (cyt b6f) and ferrodoxin (Fd) transfer electrons to photosystem I (PSI), and the ferrodoxin-NADP$^+$ reductase (FNR) which uses them for reducing protons in form of NADPH. Hydrogen is combined in a further step with carbon dioxide to make energy rich carbohydrates.[32g, 36]
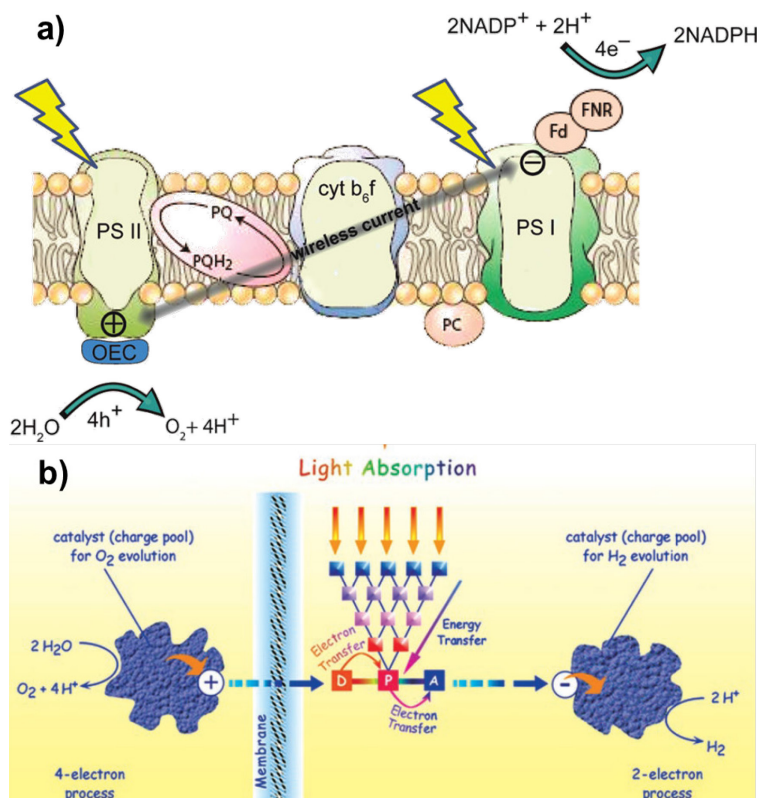
Figure 1.1-3. a) Simplified scheme of natural photosynthesis (reproduced with permission from reference [36]) b) Simplified scheme of key processes in artificial photosynthesis (reproduced with permission from reference [32i])

The development of an artificial device working on the same principles (e.g. light harvesting, energy transfer, charge separation, electron transfer, catalysis for water splitting) (Figure 1.1-3b) is considered a viable solution to the energy problem.[29, 32] However, the challenge in an artificial system is to integrate light harvesting and conversion systems which generate one electron/ hole at a time with catalytic multi-electron redox processes (4 electrons for water oxidation and two electrons for proton reduction), as well as the (auto)regeneration mechanisms needed in an efficient system.[36] Therefore, the role of the chemist is to imagine and synthesize compounds able to perform these tasks, and to integrate them in functional systems, in order to convert energy-poor molecules into energy-rich ones using sun light (e.g. H_2 from H_2O or methanol from H_2O and CO_2), and to assist in the global transformation from a fossil-fuel-based society to a solar-fuel-based one.[29, 32]

Motivated by urgent environmental concerns[32d, 35] and unprecedented political initiative and consensus,[32d, 37] research in artificial photosynthesis has flourished for the past decade and continues to be in the spotlight. Since the historical report of splitting water with TiO_2 and UV-light by Honda and Fujishima,[38] significant advances have been realized in using doped-semiconductors as light harvesters and/or catalysts in photovoltaic,[39] electrochemical,[40] photocatalytic and photoelectrochemical systems.[32d, 41] However, the reduced stability of these systems when they are in prolonged contact with aqueous electrolytes remains to be resolved.

Moreover, the use of coordination complexes (as photosensitizer and/ or catalysts) has also been exploited in artificial photosynthetic systems, as they possess the necessary photophysical and redox properties to be used as alternatives or as complements to semiconductor materials in such systems.[32d, 33, 42] Dye-sensitized solar cells (DSSCs),[39] (dye-synthesized) photoelectrochemical cells (PECs),[33, 42a, 43] and dye-sensitized photoelectrosynthesis cells (DSPECs)[32d] are examples of such hybrid devices coupling molecular photosensitizers and/ or catalysts with semiconductors or other macromolecular hosts (e.g. oligomeric and polymeric materials). The prototype DSPEC developed by the University of North Carolina Energy Frontier Research Center (UNC EFRC) on Solar Fuels (Figure 1.1-4a) integrates a molecular chromophore–catalyst system with oxide semiconductor materials to perform water splitting as follows: (1) light absorption; (2) electron injection into the conduction band of the semiconductor; (3) transfer of the injected electron to the cathode through an external circuit; (4) electron transfer from the catalyst to the chromophore – activation of the catalyst; (5) steps 1–4 are repeated four times to build up the four oxidative equivalents necessary for water oxidation and oxygen evolution at the photoanode. At the cathode, the H_2O/H^+ reduction takes place (an applied bias of ~0.2 V is required to drive it to completion.) [32d] Examples of chromophore–catalyst systems used in this device are showed in Figure 1.1-4b. Water splitting is realized using compound **B** with an absorbed photon conversion efficiency of 4.4%.[32d] The final objective is to develop tandem cells by combining photoanodes for water oxidation with photocathodes for water splitting or CO_2 reduction to formate/ formic acid or to *syngas* (H_2:CO synthesis gas – the feedstock for hydrocarbon production by Fischer–Tropsch process).[32d] To date, tandem PECs integrating molecular

chromophore-catalysts systems for both photoanode and photocathode were reported by Sun and coworkers (Figure 1.1-4c), with solar to hydrogen efficiency less than 1%.[44] Coordination complexes used as chromophores in DSSCs[45] as well as molecular photosensitizers and catalysts in PECs[33, 42a, 43] and photosensitizer-catalyst assemblies[46] in DSPECs, Figure 1.1-4b) were recently reviewed.
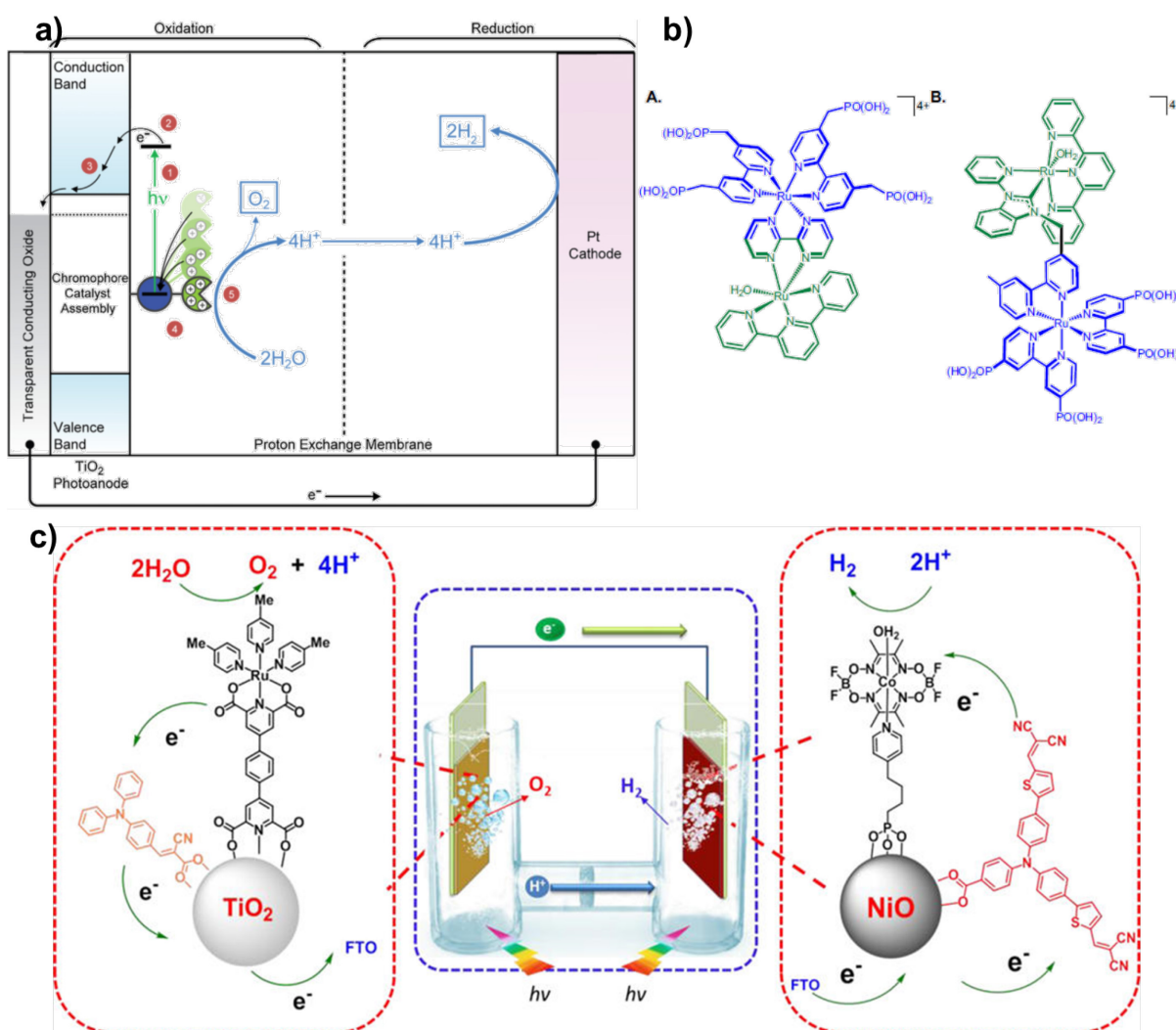
Figure 1.1-4. a) Schematic representation of the prototype DSPEC developed by UNC EFRC. b) Example of chromophore–catalyst systems used (chromophore in blue and catalyst in green). (Reproduced with permission from reference [32d]). c) Complete molecular PEC reported by Sun and co-workers. Reproduced with permission form reference [44].
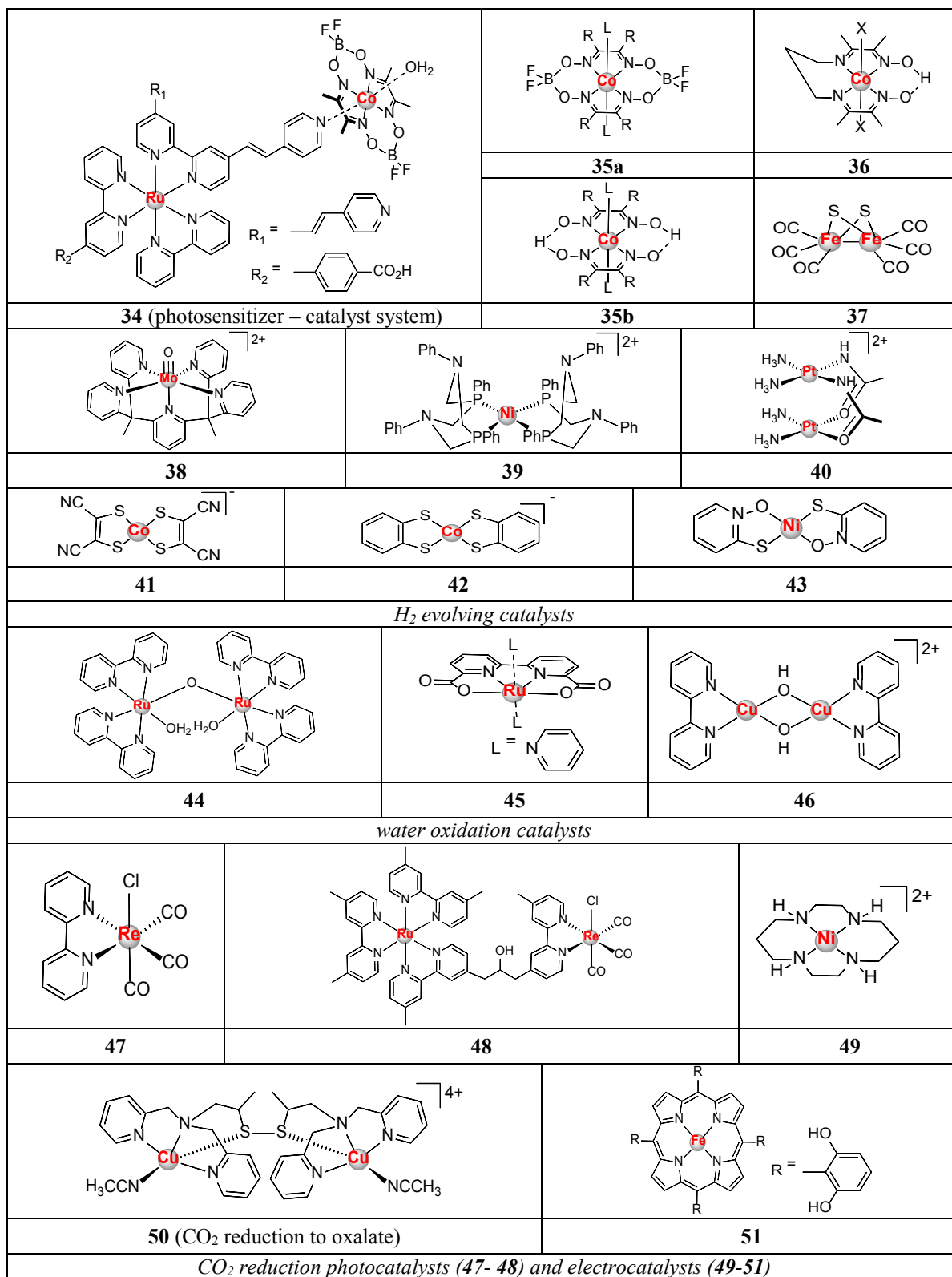
Figure 1.1-5. Selected molecular photocatalysts and/ or electrocatalysts for proton reduction,[47] water oxidation, [33] and CO$_2$ reduction.[48]

In order to overcome the high degree of complexity of a fully homogeneous artificial photosynthetic system, the study of half-reactions (e.g. water oxidation (WO) and proton reduction (hydrogen evolving reaction (HER)) in case of water splitting) using sacrificial electron donors/ acceptors has been privileged, in the quest to better access and understand each process.[33, 49] Often these systems are tested in organic solvents or in organic-aqueous mixtures in order to overcome solubility problems. Thus, the advantages offered by the molecular systems over the heterogeneous ones are exploited: accessible mechanistic investigations and easier tunability through a well-developed synthetic tool-kit; this translates into the capacity to analyse structure-function relationships and to use the resulting knowledge in the design of improved systems.[32a, 33]

The synthetic chromophores based on coordination complexes are well developed, aided by the advances in DSSCs.[39] However, their long-term stability and overall performance in aqueous media are still to be optimized, and mechanisms in homogeneous photocatalytic systems are still to be fully understood and probed. In addition, they are based on noble metal-ions, which are scarce and expensive (e.g. **cpds. 23-25**, Figure 1.1-1; cpds. Figure 1.1-4; **cpds**. **34**, **44**, **45**, **47**, **48,** Figure1.1-5). One of the most recent breakthroughs in this direction is the report of a Fe-based photosensitizer.[50]

On the catalyst side, despite substantial progress (e.g. Figure 1.1-4 and Figure 1.1-5), energy-efficient, robust, and cost-effective (non-noble metal) molecular catalysts for solar-fuel conversion processes in aqueous media are still lacking.[32a] This fact impacts on the development of homogeneous photocatalytic systems as well. In order to solve the drawbacks associated to the scarcity and prohibitive cost of noble metal-based compounds, catalysts (electrocatalysts and photocatalysts) based on more abundant and less expensive first row transition metal-ions[33, 47a] (Fe,[51] Co,[52] Ni,[53] Cu,[54]) as well as noble-metal free chromophore-catalyst systems[47e, 55] have been reported for proton reduction (e.g. **cpds. 35-39 and 41-43**, Figure 1.1-5),[47] water oxidation (e.g. **cpd. 46**, Figure 1.1-5),[33] and CO_2 reduction (e.g. **cpds. 49-51**, Figure 1.1-5).[48] Nevertheless, the solar to fuel conversion efficiency and/ or the life-time (stability/ robustness) of the molecular systems reported to date do not meet the parameters that allow their large-scale application.[32a, 33, 53a] The very complex design and

engineering requirements for a solar-fuel device based on fully homogeneous processes are also prohibitive factors.[32a]

Thus, completely functional artificial photosynthetic devices for the conversion of solar energy into chemical fuel are semiconductor-based[32d, 36, 56] (the best performing so far) or hybrid (e.g. molecular compounds/ semiconductors,[32d, 33, 42a, 43] biological compounds/ semiconductors[31b]) in many cases integrating the most developed individual sub-systems.[32a, 33] However, despite important advances, they are still at the prototype level. The cost of solar hydrogen produced by PEC was evaluated in 2012 at over 100 USD/ kg (versus 3.64 USD/ kg for wind hydrogen and 7.62 USD/ kg for PV hydrogen (steadily decreasing)).[57] Reaching cost competitiveness for PEC solar hydrogen would translate in life times of 25 years at solar-to-fuel efficiencies of 15%.[32d] These parameters are far from those of the existent prototypes (highest life times of months).[32d] Thus, more basic research is needed, in order to adequately tune the numerous parameters involved in complete solar-to-fuel systems toward increased efficiency and life times, and thereby guide their advancement toward commercial viability and their full establishment in industry.[32a, 32d, 33] However, the PEC and DSPEC prototypes demonstrate the successful use of molecular coordination complexes in solar-to-fuel artificial photosynthetic devices. They prove that coordination compounds could contribute to this field, and represent an encouragement for further research in this direction.

'Bio-inspiration' also lies at the foundation of supramolecular chemistry.[24, 58] (a brief description of the concept is presented in section 1.2. *vide infra*). Related to '*the complexity at the molecular level*' from a supramolecular perspective, Steed and Atwood's definition of a '*supramolecular device*' is of particular significance as it focuses '*on the functional interactions between the components rather than the chemical nature of their connectivity*'.[22] Therefore, if a single molecule has properties of supramolecular nature, it is considered a '*supramolecular device*' (a more comprehensive presentation of this concept is given in section 1.2. *vide infra*).[22] Once again, the intrinsic properties of coordination bond (intermediate strength bonding interactions) allow coordination compounds to be used in this field.[23] Thus, the subfield of metallosupramolecular chemistry has evolved.[59] Major breakthroughs have been achieved and important theories have been developed with respect to the (self-) assembly of coordination compounds in solution,[60] at interfaces,[61] on surfaces,[62]

and in the solid state.[63] Examples have been extensively reviewed, and span discrete assemblies,[64] network solids (MOFs/ coordination polymers),[64b, 65] liquid crystals, nanomaterials,[66] and aspects related to crystal engineering.[67] Their particular relevance emerges in materials science (sensors,[22, 68] molecular electronics,[22, 69] energy and gas/ fuel storage,[14b, 70] magnetic materials[71]), catalysis,[72] and medicine.[8c, 73]

In conclusion, the examples of coordination compounds presented in this section were chosen in order to illustrate: *i) their importance in our daily life* – coordination complexes are well-established in applications (e.g., dye and pigments, hydrometallurgy and extraction industry, catalysis and medicine); they also play an important role in emergent domains as exemplified by their use in OLEDs, DSSCs and MOF-based applications; *ii) the challenges and opportunities* – there are fields (e.g. artificial photosynthesis, molecular devices; novel diagnostic and therapy methods) in which the use of coordination complexes is only at the fundamental research or prototype level, but in the future development of which they could play an important role.

Trends in the study of coordination complexes and their applications were also identified. Driven by the general evolution/ progress of our society, research in modern coordination chemistry evolves *toward complexity at the molecular level*, with Nature representing a major source of inspiration as shown by artificial photosynthesis and mellosupramolecular chemistry. Advancing from the fundamental study of coordination complexes and proofs-of-principle in academic research, all the way to prototypes, and full-scale applications can be extremely slow (e.g. clinical approval of new drugs) or unexpectedly fast (e.g. OLEDs). However, there is no doubt that coordination compounds can present answers to real problems. Innovative vision is therefore necessary for new discoveries to be made and to use what has already been discovered in new original ways. At the same time, the study of coordination complexes nurtures scientific curiosity, and multidisciplinary approaches open fascinating new worlds, while pushing the frontiers of knowledge to unprecedented depths.

1.1.2. Key Concepts – Theoretical Framework

The context of this work from a conceptual/ theoretical perspective is presented in Figure 1.1-6. Selected relevant concepts are emphasised in this section: coordination compound/ metallic complex; bonding/ metal-ligand interaction; ligand design; properties of coordination complexes (experimental *vs.* calculated); structure – properties relationship; molecular/ supramolecular approaches; mixed valence systems; supramolecular coordination architectures.

▪ The term **coordination compound** is used in accordance with the IUPAC definition of ***coordination entity***:[74] '*an assembly consisting of a **central atom** (usually metallic) to which is attached a surrounding array of other groups of atoms (**ligands**)*'. In inorganic/ coordination chemistry, the **central atom** is **a metal ion** and the **ligand** is '***the atoms or groups joined to the central atom***'.[75] The terms **coordination compound** and **coordination complex** are used interchangeably within this work. Related to the distinction between organometallic compounds ('*compounds having bonds between one or more metal atoms and one or more carbon atoms of an organyl group*'[76]) and coordination compounds, the classification principle given in *Comprehensive Coordination Chemistry II* is formally adopted: '*any coordination compound in which the number of metal–carbon bonds is at least half the coordination number of the metal is deemed to be ''organometallic'' and nominally outside the scope of coverage.*'[77] However, as more advanced experimental and theoretical tools are becoming available for in depth analyses of the nature of metal-ligand bonding, it could be useful to abandon these intermediary level classifications/ distinctions, in favour of new terminologies which allowed the direct assessment of the specificities of a system within a general conceptual framework.

▪ The IUPAC definition of the **chemical bond** could be considered to set the above-mention type of general conceptual framework: '*There is a chemical bond between two atoms or groups of atoms in the case that the forces acting between them are such as to lead to the formation of an aggregate with sufficient stability to make it convenient for the chemist to consider it as an independent 'molecular species'.*'[78] Within this general concept, **the bonding in coordination compounds** has as core notion **the metal-ligand interaction**.
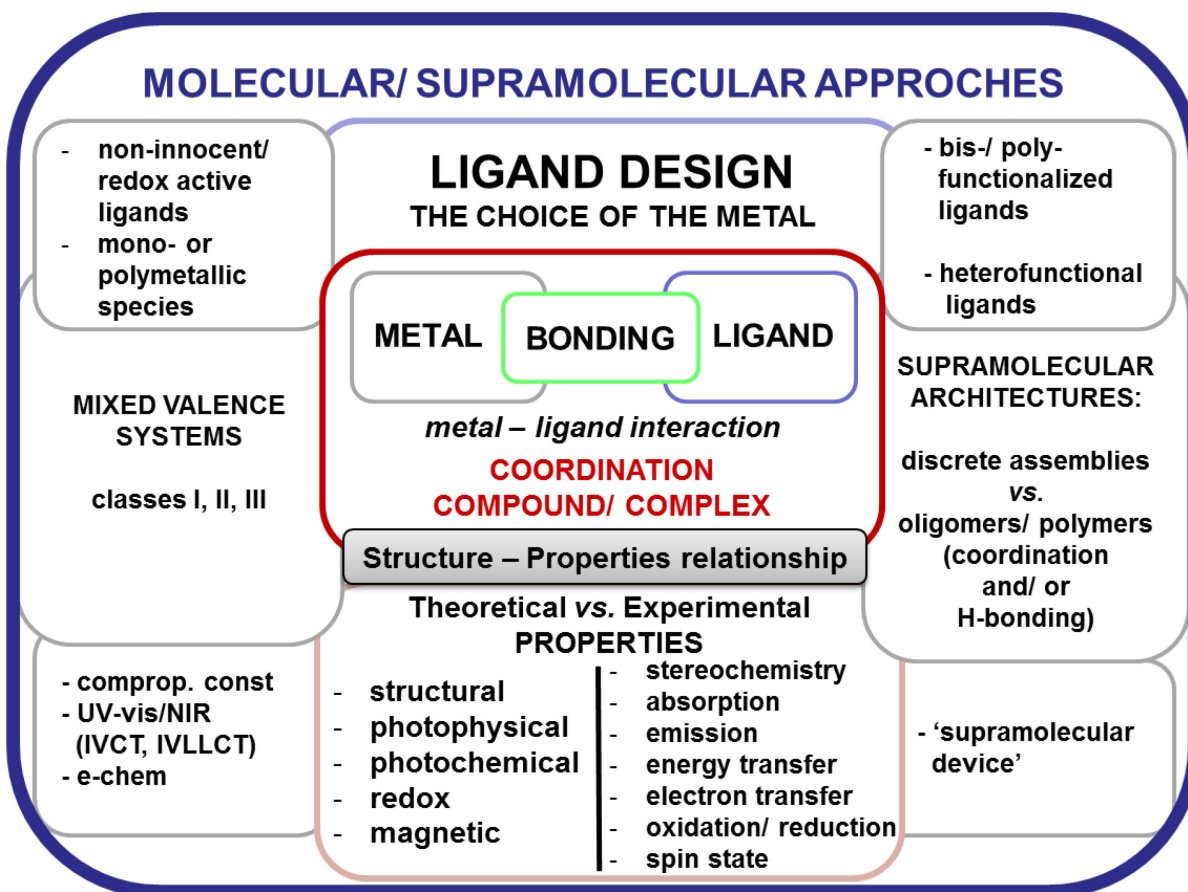
Figure 1.1-6. Conceptual/ theoretical context of the thesis

One of the main tasks is therefore to probe and to adequately describe this interaction and its influence on the structure and the properties of the compounds (geometry; stereochemistry; spin state, photophysical and redox properties, stability/ reactivity; chemistry). Aspects of crystal field, ligand field, and molecular orbital (MO) theories[79] will be used for describing and discussing the specificities of the systems under study. From a classical perspective, the metal-ligand interaction can be seen as a combination of specific contributions from the metal, the ligand, and the environment (Figure 1.1-7).
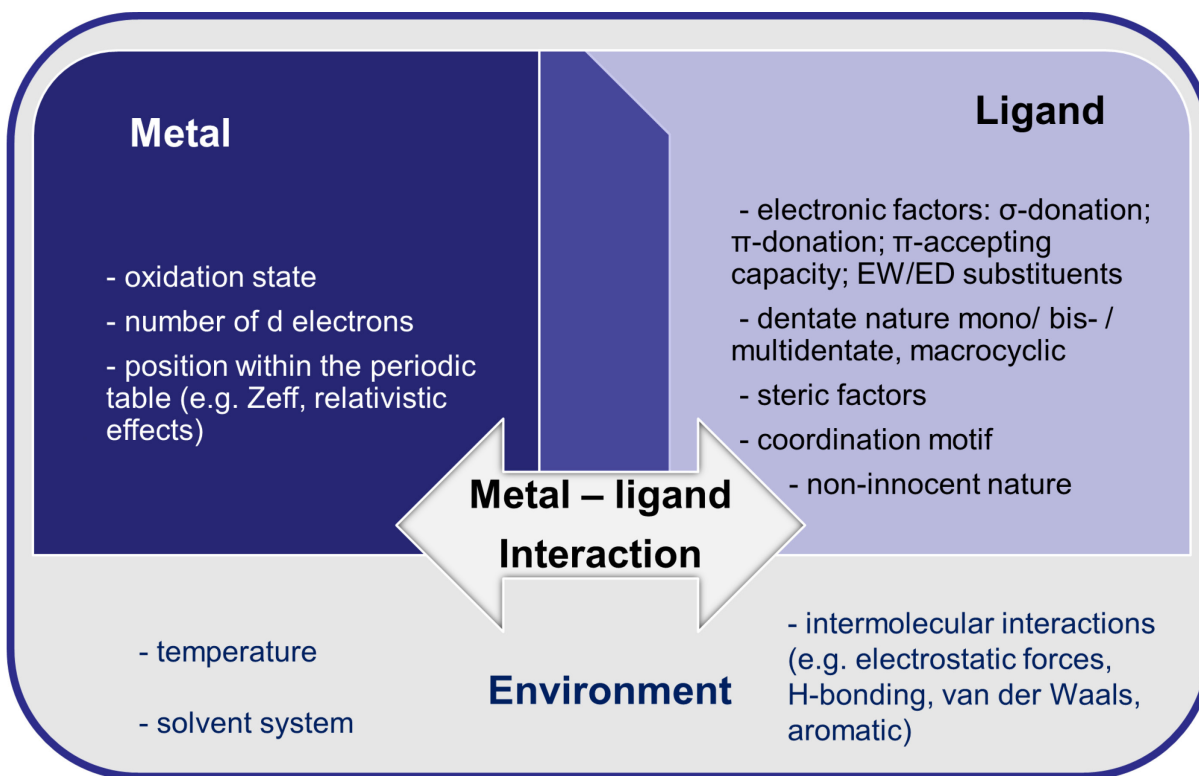
Figure 1.1-7. Metal-ligand interaction: metal, ligand and environment factors

In addition, multidisciplinary experimental characterization techniques (e.g. X-ray crystallography, nuclear magnetic resonance (NMR), electron paramagnetic resonance (EPR),[80] vibrational spectroscopy (IR/ Raman),[81] UV/vis/NIR and X-ray absorption spectroscopy (XAS),[82] Mössbauer spectroscopy, X-ray photoelectron spectroscopy (XPS), magnetic circular dichroism (MCD), SQUID magnetometry, electrochemical techniques (e.g. cyclic voltammetry (CV)), spectroelectrochemistry) and advanced theoretical chemistry tools[83] (e.g. DFT,[84] TD-DFT)[85] allow one to probe, interpret, and fully describe the specificities of bonding and the properties in each individual case. This is particularly insightful and necessary for coordination complexes with ligands displaying non-innocent behaviour (e.g. NO, quinones/ semiquinones/ catecholates, *α*-diimines, *α*-dithiolenes, porphyrines, chlorins, corroles, azo ligands).[86] The term *non-innocent* describes particular cases of coordination compounds in which uncertainty with respect to the oxidation-state assignment of the metal centre exists, as the ligands involved are redox-active in the same electrochemical range of potentials of the metal.[86c] However, the *innocent* or *non-innocent* behaviour of a ligand is coordination situation, and condition dependent.[86c, 87] Therefore, the

necessity to use terms such as *non-innocent behaviour* rather than *non-innocent ligand* is stressed.[86c] The description of bonding in complexes with redox-active ligands has been debated for a long time[86a], but significant success has been obtained in the last decade by using the above-mentioned combination of multidisciplinary experimental techniques and theoretical calculations.[86b, 88] The properties of these complexes (e.g. multi-electron reservoirs, electron transfer) have brought them into the spotlight, placing them as potential candidates for application in catalysis[89] and materials chemistry.[90]

The influence of the metal-ligand interaction on the structure of the coordination compounds is dictated by a combination of metal and ligand electronic factors, as well as steric effects. The latter concerns the ligand repulsions resulting in the stabilization of the lowest energy geometry.[91] While translating ligand electronic and steric effects in accessible models is a possible, but rather a complex task (e.g. Brown's metric oxidation states of redox-active ligands,[92] Lever's electrochemical ligand parameter[93]), metal electronic factors can be easily interpreted based on crystal field theory.
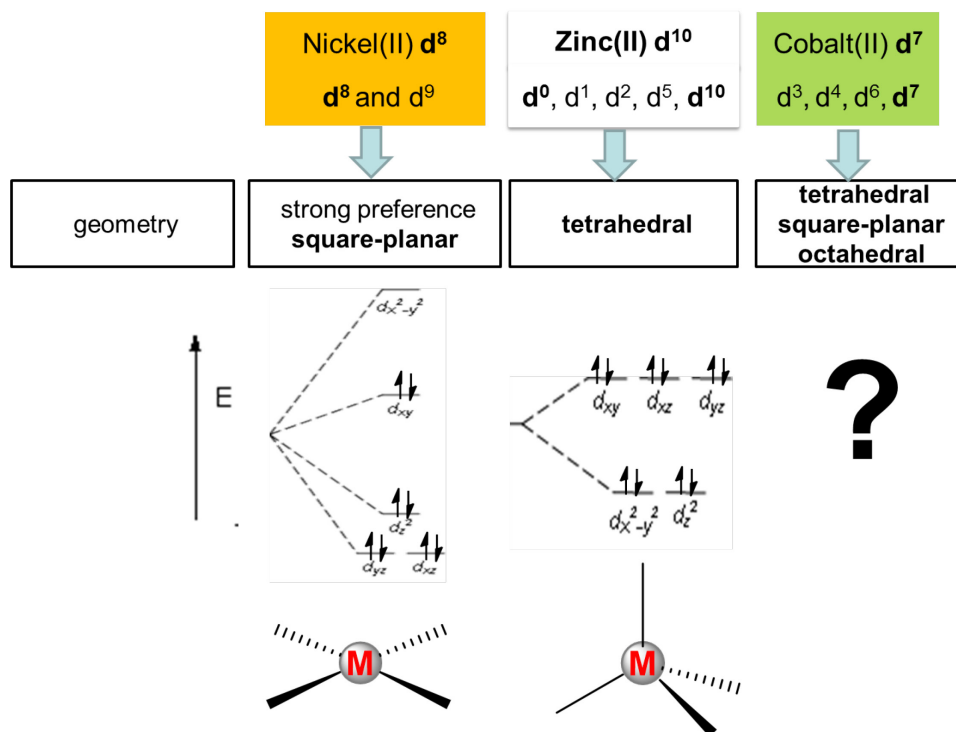
Figure 1.1-8. Geometry preferences as a function of the metal oxidation state/ number of *d* electrons.[94]

Thus, geometry preferences as a function of the metal oxidation state/ number of d electrons were identified,[91] (Figure 1.1.-8) and were experimentally confirmed.[94b, 94c] Considerable research also focuses on prediction and control of stereochemistry and spin states (Figure 1.1-9).[94c]
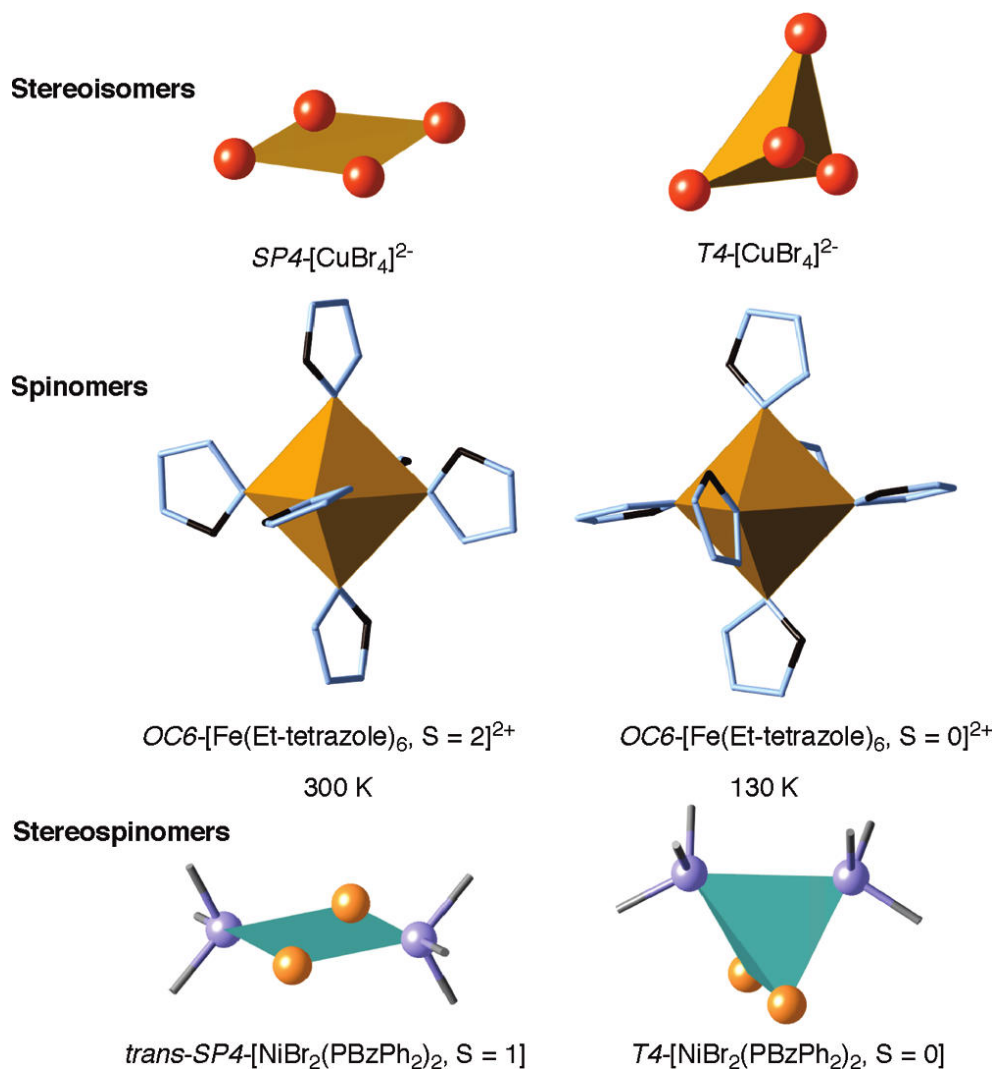
Figure 1.1-9. Isomerism examples: coordination geometry isomers (stereoisomers), spin isomers (spinomers), and both (stereospinomers). (Reproduced with permission from reference [94c])

▪ **Ligand design** is one of the central theme in coordination chemistry and also a key concept in this thesis. It is defined by Collins as: '*the process by which the components are varied either for curiosity's sake or to control the properties of a targeted system*'.[95] It is also

considered by the same author as a '*a collection of adjustable components*':[95] type of chelate ring (cyclic/ macrocyclic; denticity) and size; ring substituents and their electronic and steric effects; donor atoms and donor functional groups; coordination site(s) (Figure 1.1-10 left). Tuning these parameters results in modulating the intrinsic **chelation capacity** of the ligand for different metal-ions. If 'the choice of metal' is added as a supplementary adjustable component to this tool-kit, the concept could be extended to **the design of metallic complexes** (Figure 1.1.-10). The choice of metal-ion generates specific properties, which are fine-tuned by ligand design. Redox-active ligand design has lately received particular attention.[87a, 96] The surrounding environment (Figure 1.1-7) can also be seen as an adjustable component.
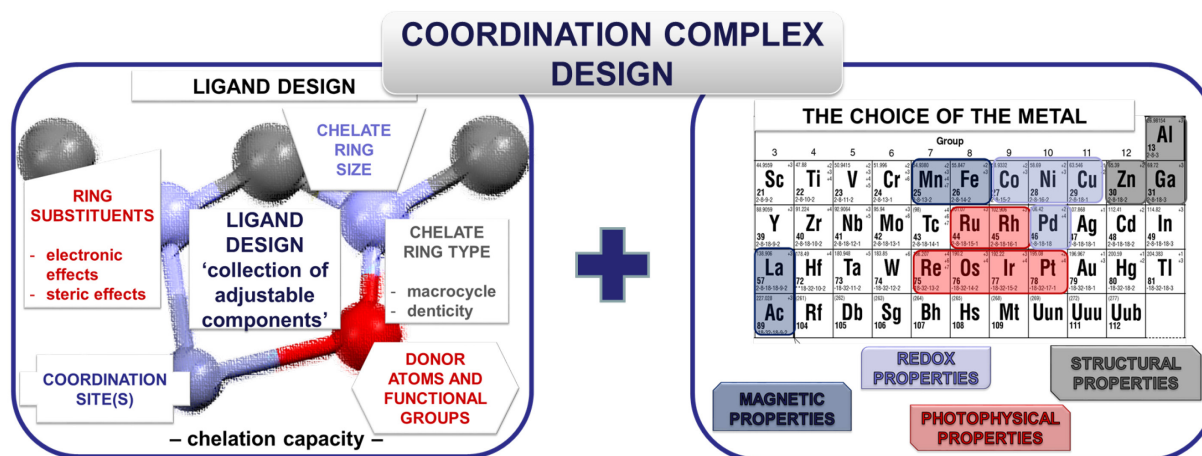
Figure 1.1-10. Coordination complex design as '*collection of adjustable components*'[95] (the ligand design figure was realized using the concepts presented in reference [95])

▪   As emphasized in section 1.1.1, coordination complexes are of interest due to their specific **properties**, which make them interesting candidates for a large variety of applications. Therefore their photophysical, photochemical, redox and magnetic properties have been comprehensively investigated by experimental and/ or theoretical methods.[97] Theories have been developed and **structure – properties relationships** have been derived for different classes of compounds, with the aim of synthesizing coordination complexes with tailor-made properties for specific applications. Light-induced processes in coordination compounds (e.g. charge separation) are among the most relevant in their study and application (in devices and processes). A schematic representation of photophysical fundamentals is therefore given in Figure 1.1-11.

Owing to their optical, electrical, and magnetic properties,[98] coordination complexes involving two or more redox-active centres (**mixed-valence compounds**) are also of interest for applications as well as from fundamental research perspective. Three types of behaviour can be identified for these compounds, based on the degree of electronic interaction between the redox centres: non-interacting/ localization (class I), partially-interacting/ partial-localization (class II), and fully interacting/ complete delocalization (class III).[22, 98]

(a)   (b)
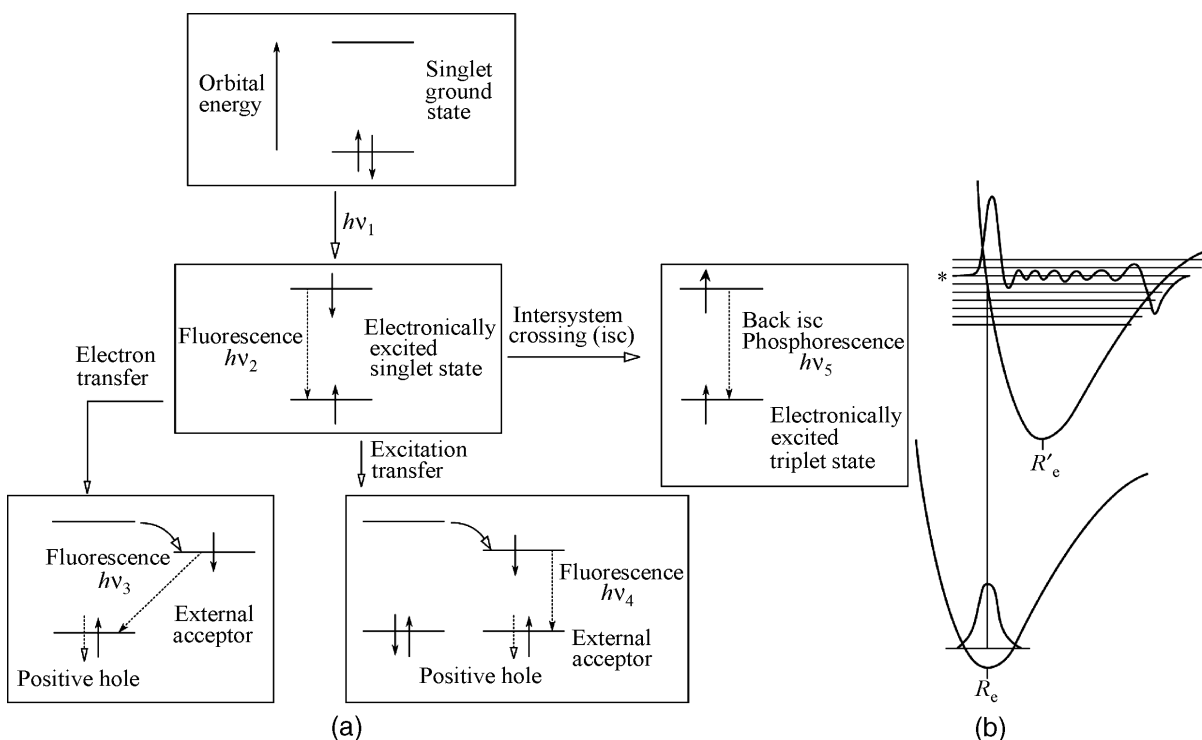
Figure 1.1-11. (a) Photoexcitation and possible radiative events in the excited state, (b) Following photoexcitation an electron is promoted into a vibrationally and electronically excited state. Experiencing a new force field after the transition occurred, the molecule starts vibrating. (Reproduced with permission from reference [22]).

For class II compounds, new properties arising from the intervalence interaction between the redox centers can be monitored by spectroelectrochemical techniques (characteristic optical intervalence (IV) bands).[22, 98] The theories of mixed-valence complexes were developed initially for bi- and multimetallic species, considering the electronic interaction between metal centres. However, the notion has been extended to encompass the cases of coordination compounds with two or more redox-active ligands, in which the electronic interaction takes

place between the ligand radicals 'bridged' by the metal. Characteristic ligand-to-ligand intervalence charge transfer (LLIVCT) transitions are observed in these class II systems.[86c]

▪ As briefly mentioned in the previous section (1.1.1), **the molecular/ supramolecular approaches** of Atwood and Steed illustrated by the concept of *'the supramolecular device'*[22] are interesting to be considered from the perspective of coordination compounds. The 'structural' base of the classical definition of supramolecular chemistry is extended to encompass a 'functional' one. Exemplification using photochemical and electrochemical classification criteria is presented in Figure 1.1-12. [22]

+/- Indicates a charge-separated excited state
☀ Indicates an electronically excited state
◄► Indicates any kind of connector or bond that keeps together the two components
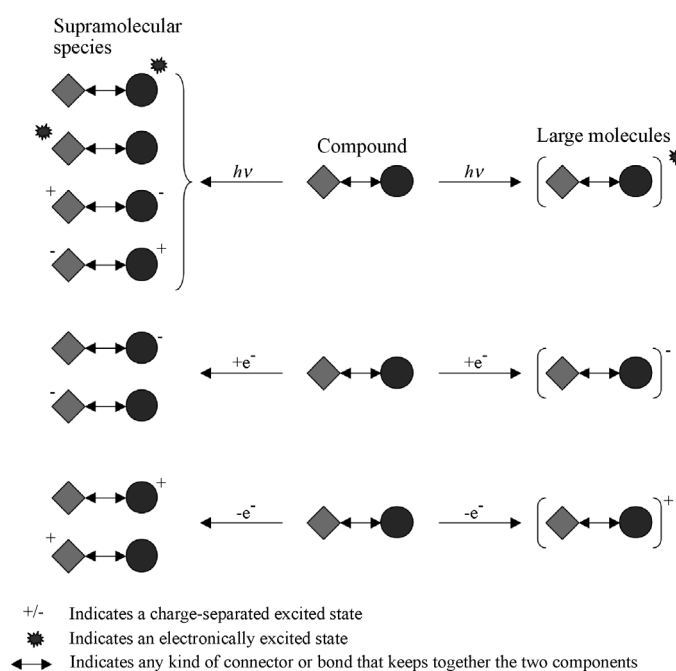
Figure 1.1-12. Supramolecular device *vs.* large molecule: photochemical and electrochemical classification criteria. (Reproduced with permission from reference [22])

'If light excitation of a molecule (♦↔●) results in the formation of excited states that are substantially localised on one of the two components (♦ or ●) or causes electron transfer from one to the other, then the molecule is said to be supramolecular. If the excited state is substantially delocalised across both components, then the complex is best thought of as being simply a large single molecule. Analogous arguments apply to redox processes'.[22] Considering the mixed-valence complexes from this perspective, the ones in class I and II are classified as supramolecular, while those in class III are large molecules. The coordination

complexes with redox-active ligands presenting localized and partial-localized charge also become 'supramolecular entities' within this approach.

Considering J. M. Lehn's classical definition of supramolecular chemistry: '*the chemistry beyond the molecule, bearing on organized entities of higher complexity that result from the association of two or more chemical species held together ...*',[99] coordination bonds can be identified in the supramolecular interactions tool-kit alongside ion-ion, ion-dipole, and dipole-dipole interactions, hydrogen bonding,[100] cation-π, anion-π, π-π interactions, van der Waals forces and crystal packing, closed shell interactions (e.g. metalophilic interactions, halogen bonding,[101]).[23, 60a] The tools and strategies from general host-guest and self-assembly chemistry (recognition at the molecular level, use of pre-existent affinities/ compatibilities, preorganization and complementarity, reversibility) have been successfully applied to coordination compounds, resulting in the fascinating field of metallosupramolecular chemistry.[23, 59-60, 99] The associated sub-fields and corresponding literature references were presented at the end of section 1.1.1 (page IV-V)., together with their relevance for different type of applications. It is also important to emphasise the importance of ligand design from supramolecular chemistry perspective.[59] Selected examples of research strategies in this direction are: targeting specificity and selectivity through the design of (hetero)multifunctional ligands;[102] identifying and exploiting the effect of metal-ligand coordination on tuning the intermolecular interaction;[103] using complementary combinations coordination/ H-bonding in order to harness the synergy, cooperativity and emergence resulting from this association.[104]

The key theoretical concepts discussed herein are exemplified in section 1.2 with selected relevant metal-ion – N,O ligand systems, aiming to set the specific context for the work presented in this thesis.

1.2. Specific Context: 'Preparing the Way for the AMOXs' – Relevant Examples of Coordination Complexes with N,O Ligands

1.2.1. Probing 'the Design of Coordination Complexes as '*a Collection of Adjustable Components*' within the Coordination Chemistry of N,O Ligands

Aspects of the coordination chemistry of N,O ligands will be presented from the perspective of **the design of coordination complexes** as '*a collection of adjustable components*'[95] (Figure 1.1-10, section 1.1.2). The following 'adjustable components' will be emphasized: the ligand design (the chelate ring type (denticity; cyclic/ macrocyclic) and the chelate ring size; the donor atoms and the donor functional groups; the ring substituents and their electronic and steric effects; the coordination site(s)/ mode(s)); the choice of the metal ion; the environment (e.g. secondary interactions, solvent).

The diversity of chelate ring sizes and types in the coordination chemistry of N,O ligands is highlighted by selected examples of classic metallic complexes of this class (Figure 1.2-1). In the 6-membered chelate ring category, the salicylaldimine- (**52**),[105] the *β*-ketoaminato- (**53**),[106] and the salen-type (**54**)[107] complexes have been among the most studied, especially in catalysis.[108] Macrocyclic [N$_2$O$_2$]-type complexes (**55**)[109] have also attracted research interest.[109-110] Typical examples in the 5-membered chelate ring class include quinolin-8-olato- (**56**)[111] *o*-aminophenolato- (**57**),[87a, 90, 112] pyridine-2-carboxylato-,[113] pyridine-2,6-dicarboxylato-type (**58**)[114] complexes. N,O ligands which form four- and three-membered chelate rings with metal ions also exist (e.g. Ti(IV) (**59**),[115] Co(II) (**59**,[116] **60**,[117] **61[118]**), Zn(II) (**60**,[119] **61[120]**). All these classes of compounds have been extensively reviewed (several references are given above). The five-membered ring class will be further discussed in section 1.2.2.

To assess the influence/ impact of the nature of the donor atoms and the donor functional groups on the properties of the complexes, noteworthy examples are the studies on

the anti-cancer activity of iridium and ruthenium arene complexes with (N,N'), (N,O) and (O,O') bidentate coordinated ligands. It was found that the cytotoxicity of the complex (in some cases comparable with that of cisplatin (**cpd**. **13**, Figure 1.1-1) correlates with the type of bidentate ligand.[121] The effects of (N,N') *vs*. (N,O) bidentate ligands were also investigated with respect to the activation of manganese(I) and rhenium(I) carbonyl complexes towards substitution. It was found that the anionic (N,O) donor ligands (e.g. 2-picolinate; 2,4-quinolinate) activate the metal centre faster than the neutral (N,N') ones (e.g. 1,10-phenantroline; 2,2'-bipyridine).[122] Pure theoretical studies have also investigated the influence of the donor atoms on different properties of the complexes. For example, in the electronic series of $[Ru(en)_2L_{NN}]^{n+}$ (n = +2, +1, 0), (L_{NN} = *o*-phenylenediamide) replacing the NH in L_{NN} with oxygen atoms in L_{NO} and L_{OO} generated an easier reduction by 0.5 V per NH to O substitution (explained by the authors by the higher electronegativity of oxygen *vs*. nitrogen).[87a]
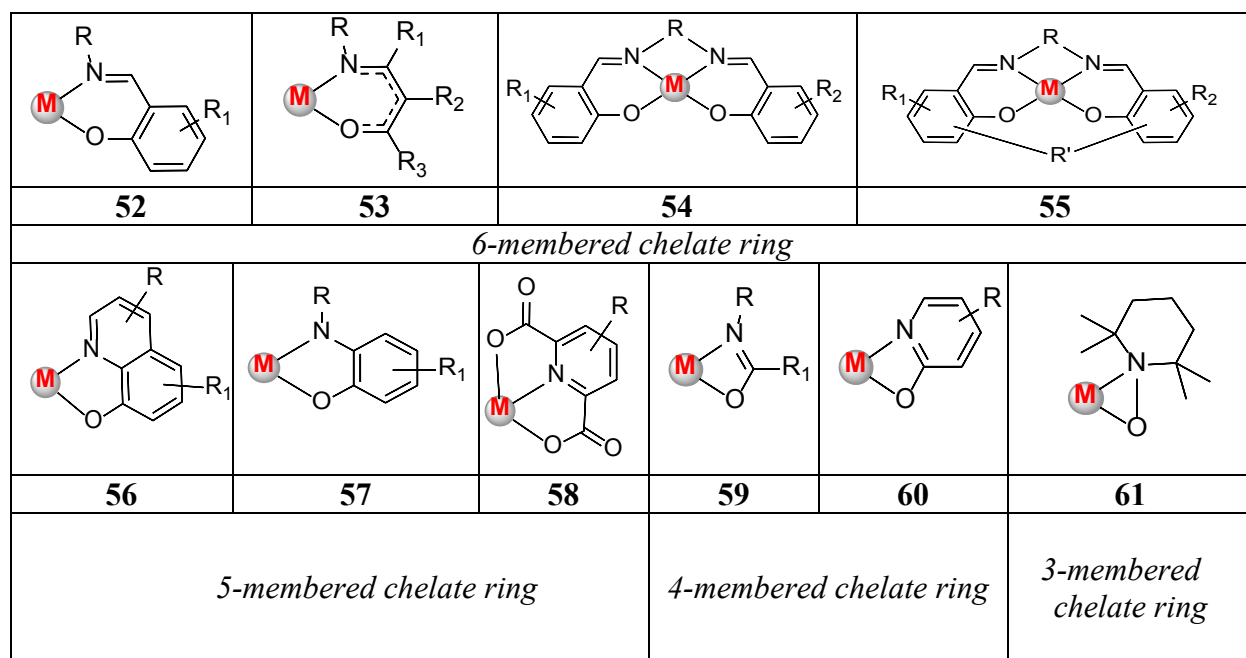
Figure 1.2-1 Structures of selected complexes of N,O ligands highlighting diverse chelate ring sizes and types (cyclic/ macrocyclic, different denticities)

The compounds which are the most significant for setting the specific context of this work are tetracoordinated homoleptic monomeric complexes of internal, N,O bis(chelates), forming five-membered rings with the metal ion (see Fig. 1.3-1). Therefore, the effect of the

donor atom functional groups, the influence of the ring substituents and their electronic and steric effects, as well as the importance of the choice of metal-ion and the effect of the environment will be analysed within this class of compounds (section 1.2.2.).

1.2.2. Tetracoordinated Homoleptic Five-Membered Ring Bis(chelates) of Transition Metal Complexes with Bidentate N,O Ligands

1.2.2.1. CSD search – summary, classification, and discussion of the results

In order to identify the compounds of interest, a Cambridge Structural Database (CSD)[123] search was performed using the criteria shown in Figure 1.2-2a. Data selection procedure is given in the figure caption.
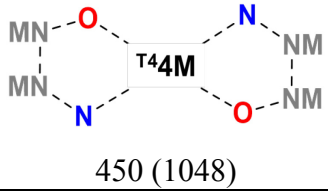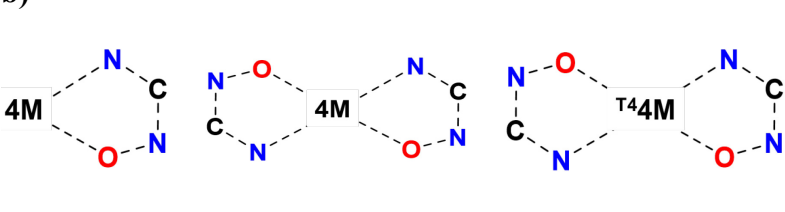
Figure 1.2-2 – CSD[124] search criteria and number of results after and before data selection (total number of results is given in parenthesis). Data selection procedure: the entries without 3D coordinates were not considered; only monometallic structures with bidentate N,O ligands were retained (multimetallic structures and structures giving coordination polymers were excluded – selected dinuclear and higher nuclearity systems are presented in section 1.2.2.2); multiple determination of the same structures were removed manually.

Thus, 450 structures of monomeric tetracoordinated homoleptic five-membered ring bis(chelates) of transition metal complexes with bidentate N,O ligands where identified after data selection. The majority of the structures contains monoanionic ligands, generating neutral

bis(chelates) with metal(II) [M(II)] ions. The distribution of the results by metal ion is illustrated in Figure 1.2-3. Over 90% of the compounds are based on transition metals of groups 10, 11 and 12. The copper(II) complexes are counting for almost half (47%) of the structures, followed by those of Pd(II) (18%), Ni(II) (10%), and Pt(II) (8%). 3% of the results are found for each of the cobalt(II) and the zinc(II) ions.

Metal	Nb. of structures
Cu	211
Pd	83
Ni	43
Pt	38
Ag	22
Co	15
Zn	12
Sn	8
Ge	4
Pb	3
Hg	2
Cr	2
Mn	2
Au	2
Be	1
In	1
Fe	1
Sb	1
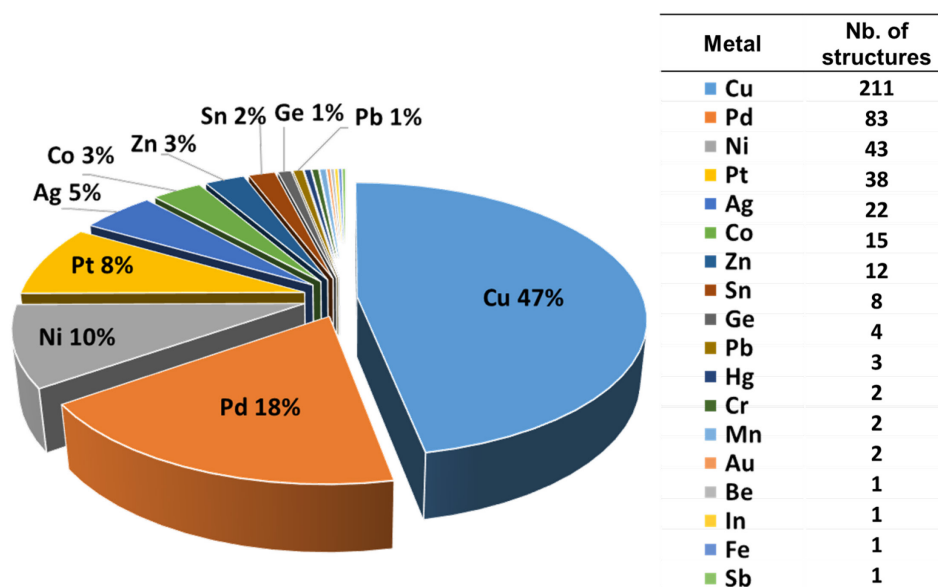
Figure 1.2-3. Distribution of the CSD search (Figure 1.2.-2) results by type of metal.

The distribution of the results by nature of chelate and by ligand type are presented in Figures 1.2-4 and 1.2-5, respectively. The nature of the κ^2-(N,O) chelate was defined based on the identity of the two other atoms in the ring (e.g. OCCN; OCNN; ONNN; ONCN; others (OCPN, OPCN, OSCN)). The classification by type of N,O ligand considers the chemical nature of the ligand. Thus, over 20 generic categories were identified (Figure 1.2-5 and Appendix-1.2). In 1971, in their study on the stereochemistry of bis(chelate) metal(II) complexes, in a same type of structural analysis, Holm and O'Connor identified only three categories of N,O ligands (all OCCN-type: 8-hydroxyquinoline; α-hydroxyamidine, and alkanolamine). They also noted at that time that '*the chemistry of this group* [5-membered ring M-N_2O_2 bis(chelates)] *is poorly developed*'.[106a] Therefore, the 450 solid-state structures reported at this moment (October 2015) evidence the advancement in the chemistry of this class of complexes over the last 45 years. The analysis of the distribution by ligand type shows that the complexes of amino-acids (1) are found in the highest number, followed by those of 8-

hydroxyquinolines (2). This is in line with the extensive study of these complexes in medicine (1 and 2),[111b, 111f, 125] materials[111c, 126] and extraction industry (2).[6] The next three classes, in descending order, but with similar number of structures, are the pyridine-2-carboxylato- and derivates (3), alkanolamine- (4), and amido-phenolato-type (5) complexes. The carbohydrazonato compounds (12) are the most important class of OCNN-type, whereas the triazene-1-oxide-based complexes (14) are the only ones of ONNN-type.

Chelate ring type	Nb. of structures
■ OCCN	371
■ OCNN	47
■ ONNN	18
■ ONCN	11
■ other	3
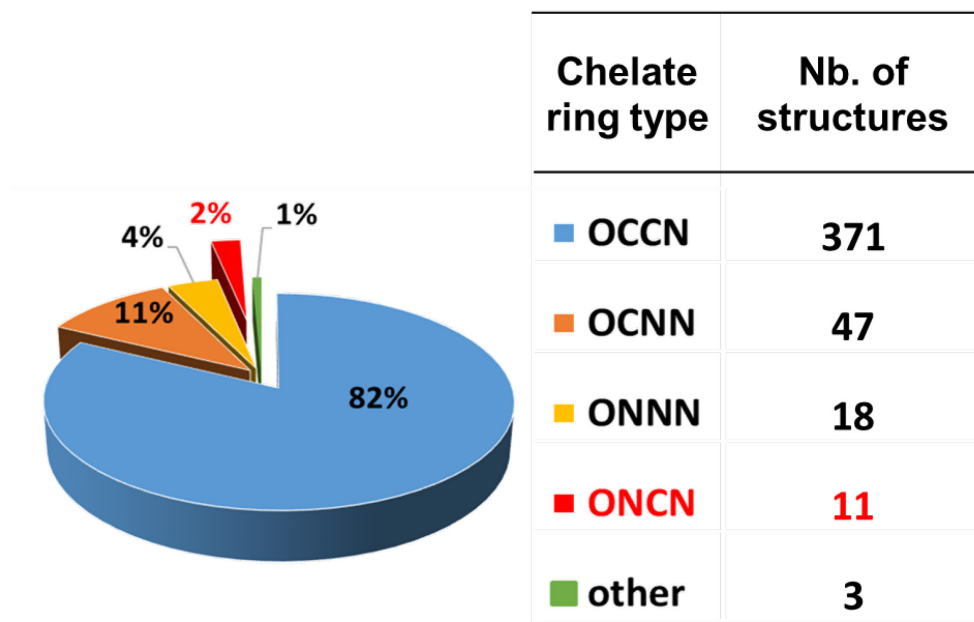
Figure 1.2-4. Distribution of the CSD search (Figure 1.2-2) results by chelate ring type (OCCN; OCNN; ONNN; ONCN; others (OCPN, OPCN, OSCN))

The smallest number of compounds is found in the ONCN category. They are bis(chelates) of the structures 15 to 19 (Figure 1.2-5; 17 = nitroimidazolato-type).

The studies of systematic series of complexes of the same metal but with different ligand substitution pattern allow structure-properties relationships to be derived, reflecting the important role of ring substituents and their electronic and steric effects. The example of triazene-1-oxide family of cobalt(II) complexes is given in this direction, based on its relevance with respect to the prediction and control of stereochemistry and spin-states in tetra-coordinated transition metal complexes. The isomerization from square-planar (low-spin) to tetrahedral (high-spin) coordination geometry is observed for this class of compounds, and it was shown that in solution of non-coordinating solvents (e.g. dichloromethane) the

equilibrium of the isomerization process is controlled by the nature of the substituents.[127] The importance of the environment (non-coordinating solvent) is also noteworthy in this case.
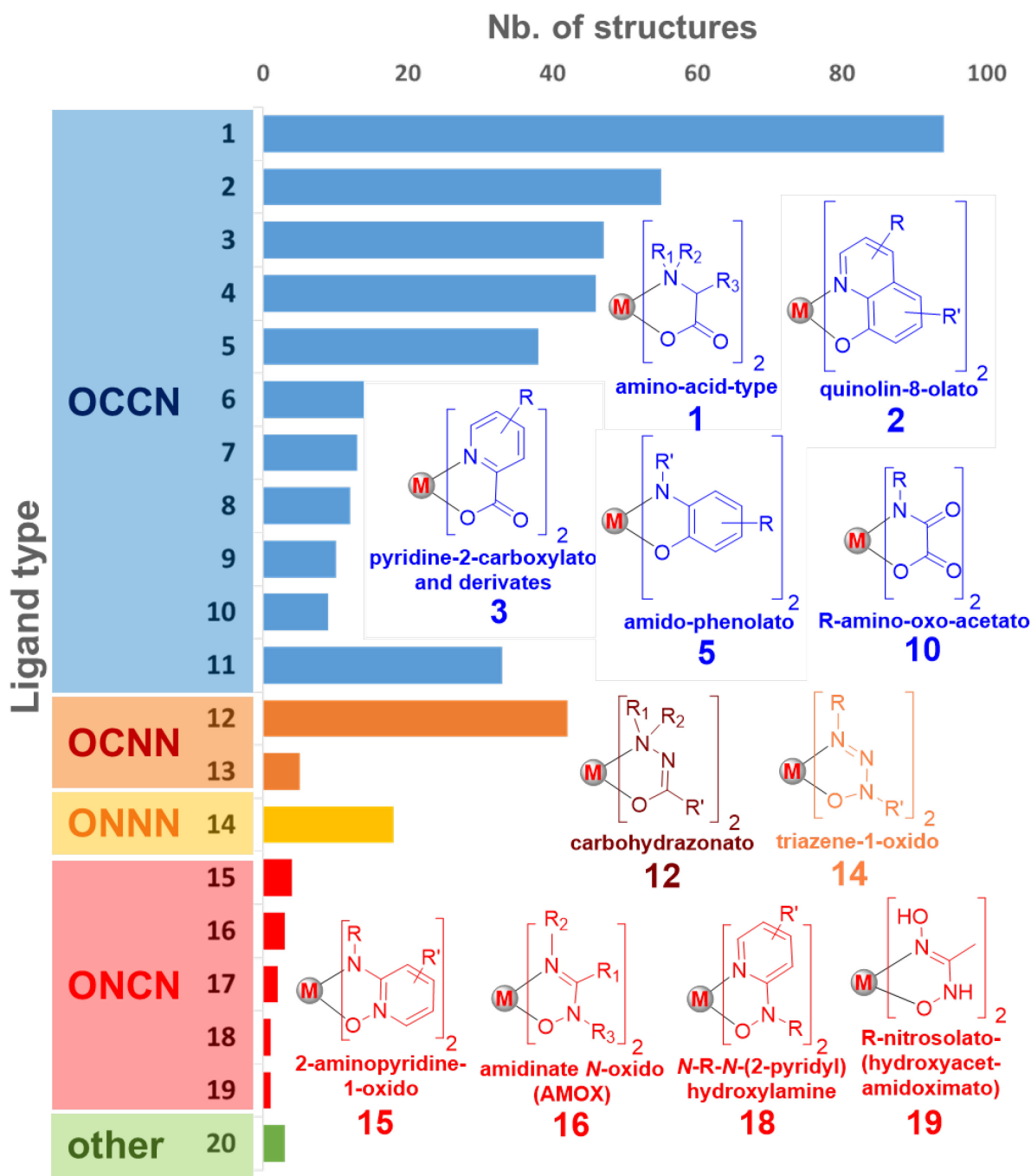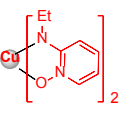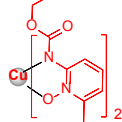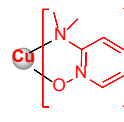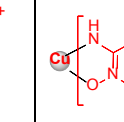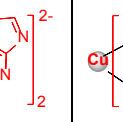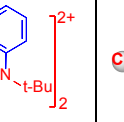
Figure 1.2-5. Distribution of the CSD search (Figure 1.2-2) results by ligand type. Generic structures for the main classes of compounds are given in this figure. For the complete list of the structures see Appendix-1.2. Category 11 regroups several ligand types ('other OCCN').

The impact of the metal choice on the properties of the compounds is highlighted by studying complexes of the same ligand with different metal-ions. The type of the metal, by its intrinsic characteristics, dictates specific (but not mutually exclusive) properties for the complex (e.g. Re(I), Ru(II), Ir(III), Eu(III) – photophysical properties; Co(II/III), Ni(II), Cu(II) – redox properties; Mn(II/III), Fe(II/III), Gd(III) – magnetic properties). In series of complexes with the same ligand and different metal ions (in the same environment/ medium), the structure of the complex (geometry/ coordination mode) and its reactivity have been found to be metal-ion dependent.[128] It has also been shown that the nature of the metal-ion can impact the degree of non-innocent behaviour of the ligand.[88k]

The type of donor atom functional group (nature of atoms, saturated *vs.* unsaturated, neutral *vs.* charged) determines the degree of electron-density delocalization within the chelate ring and onto the ligand, allowing the modulation of the σ-donation, π-donation, and π-acceptance capacity, with direct effect on the metal-ligand interaction, and hence on the properties of the compound. The variation in structural properties of different donor atom functional groups is followed within a series of reported copper(II) complexes of ONCN-type, classes 15 and 18 (Figure 1.2-5), 2-aminopyridine-1-oxido and *N*-R-*N*-(2-pyridyl)hydroxylamine,[129] respectively (Table 1.2-1). Significant differences are observed at the level of the bond lengths in the chelate ring among the complexes under study. The variations are in accordance with the nature of the bonds, the amount of electronic delocalization, the geometry at the metal centre, and the charge of the complex. On the other hand, the bite angles and the bite distances have similar values (even though not all are statistically equivalent), as expected on the basis that all the complexes have five-membered ONCN chelate rings. Related to the copper(II) complexes of type 18, it is worth mentioning that the analogues with 2-pyridyl-nitroxide radical ligands (both L• and mixed-valence compounds with one L• and one L⁻) have been prepared and investigated for their magnetic properties.[129-130] The N-O bond length in the radical complexes (1.29-1.30Å) is distinctively shorter than those in the copper(II) complexes with ligand-type 15 and 18.

Table 1.2-1. The variation in structural properties in a series of copper(II) complexes of ONCN-type.[131]

Bond lengths (Å) / angles (°)						
	Cu(15-1)$_2$	Cu(15-2)$_2$	[Cu(15-3)$_2$]$^+$ 2(ClO$_4$)$^-$	[Cu(15-4)$_2$]$^-$ 2(Na)$^+$	[Cu(18-1)$_2$]$^+$ 2(BF$_4$)$^-$	Cu(18-2)$_2$
Ref. CSD	DUKNUS	HATNEV	MAPOCU	CUHJUK	YUKCOX	YUKCOX
Cu-O1	1.917(3)	1.906(5)^{av}	1.987(1)	1.949(3)	1.923(2)	1.917(2)
Cu-N2	1.900(3)	1.941(3) 1.916(3)	2.052(1)	1.898(3)	1.930(2)	1.936(2)
N1-C1	1.312(3)	1.375(7) ^{av}	1.435(1)	1.304(5)	1.353(2)	1.348(2)
C1-N2	1.378(3)	1.372(4) 1.412(5)	1.352(10	1.384(4)	1.415(2)	1.419(2)
N1-O1	1.350(3)	1.330(5) 1.356(4)	1.351(1)	1.377(4)	1.440(2)	1.444(2)
Bite distance	2.543(2)	2.252(4) 2.543(5)	2.624(4)	2.564(3)	2.542(2)	2.543(2)
Bite angle	83.5(1)	82.2(1) 83.3(1)	83.2(1)	83.6(1)	82.6(1)	82.7(1)
τ_4	0.00	0.33	0.00	0.00	0.00	0.00

Given the relevance of the ONCN-type complexes for the work in this thesis, a CSD[123] search was also performed, in this particular case, for metallic bis(chelates) without restriction on coordination number, as well as for metallic monochelates (Figure 1.2.-2b), in order to identify all reported bidentate N,O ligands of ONCN-type complexed to metal-ions in κ^2-(N,O) fashion. In addition to the structures 15 – 19, metallic complexes of nitropyrazolato-,[132] 1,8-naphthyridine-1-oxide-,[133] and amidoxime-type[134] ligands were found.

1.2.2.2. Dinuclear and higher nuclearity systems with 5-membered chelate ring bidentate N,O ligands

For this class of compounds, an important number (around 500) of monomeric complexes with polydentate ligands, dimeric, trimeric, tetrameric, and higher nuclearity species as well as coordination polymers is reported in CSD. These structures feature the previously presented types of N,O ligands, which are designed/ connected to generate multiple coordination sites (e.g. chelating units (identical or not) bridged together (bis-R-amino-oxo-acetato-type ligands, Figure 1.2-6a); combination of functional groups in the ligand to

generate new additional binding sites for metals (e.g. pyridine-di-carboxylate, pyridine-amidoxime, pyrimidine-amidoxime ligands, Figure 1.2-6b). Supramolecular chemistry strategies are also used: the type of assembly is induced by the geometry of the metal ion, in combination with the coordination vectors of the ligand (e.g. octahedral metal + parallel coordination vectors = grid type assembly, Figure 1.2-6c).
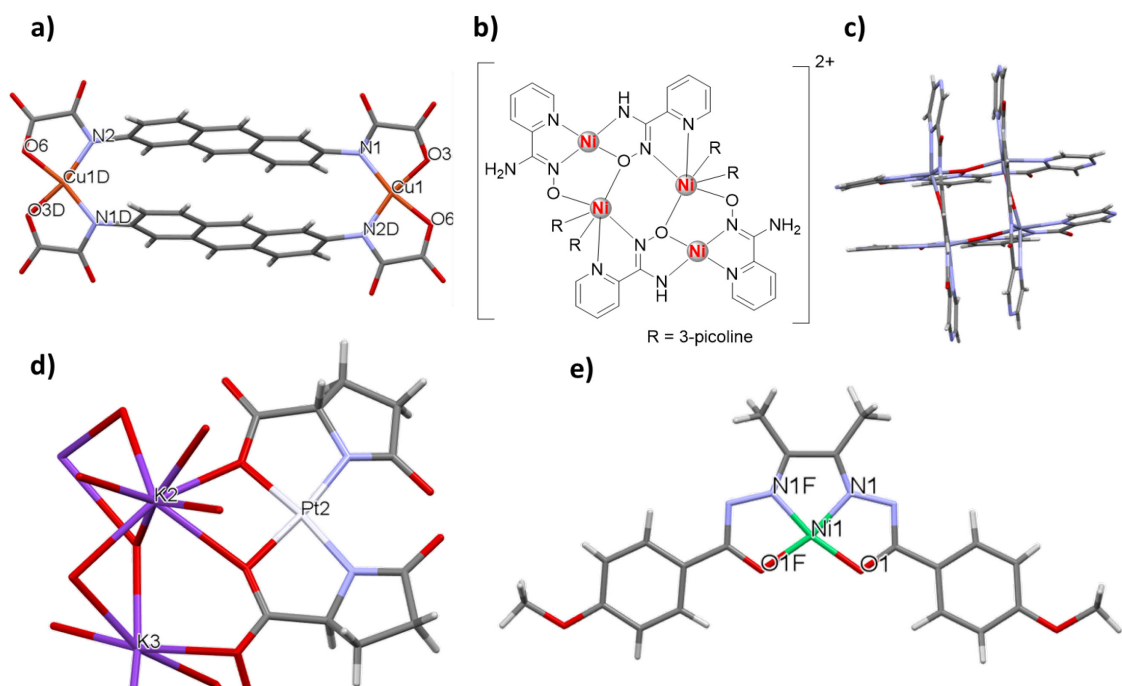
Figure 1.2-6. Selected examples of mononuclear, dinuclear and higher nuclearity systems: a) anthracene bridged amino-oxo-acetato-type units and dimer formation with copper(II)[135] – this family of compounds is of interest for their magnetic properties;[136] b) tetramer of nickel(II) formed by exploiting multiple coordination modes of the pyridine-amidoxime ligand;[137] c) Zinc-based grid type compound;[138] d) monomer with bidentate N,O-ligands in which the *cis* form is stabilized by interactions of the O atoms in the chelate ring with K$^+$ ions;[139] e) bridged N,O ligands, resulting in a M(NO)$_2$(NO)$_2$ tetracoordination motif and imposition of the *cis* form of the complex.[140]

The chelation capacity of the coordination sites, the 'compatibility' with the metal (considered within the framework of the hard and soft acid and base theory (HSAB)) as well as the effect of the environment determine the coordination modes and the stereochemistry in mono/ oligo/ polymetallic compounds. The following tendencies have been tabulated while

screening the multimetallic structures of compounds in this class. The macrocyclic ligands enforce square-planar geometry; the bridged dimers of N,O ligands, highlighting a $M(NO)_2(NO)_2$ tetracoordination motif, usually have the *cis* form upon complexation (Figure 1.2-6a, e). For the complexes of bidentate N,O ligands, the *trans* form is generally the norm, but there are however cases when the *cis* form is stabilized by interactions of the donor atoms in the chelate ring with cations (Figure 1.2-6d), or by H-bonding and other type of crystal packing forces – these situations also emphasize the important role of the medium/ environment.

1.2.3. Introducing the amidine *N*-oxide (AMOX) ligands

The amidine oxides (AMOXs), also known as α-aminonitrones, are the tautomeric forms of hydroxyamidines and amidoximes. (Figure 1.2-7b).[141] The amidoximes are hydroxyamides of imidic acids, which are tautomers of carboxyamides (Figure 1.2-7a). Therefore, amidoximes are formally classified as derivatives of carboximides.[141] The structures of the AMOXs are presented in Figure 1.2-7b, and are classified as a function of the substitution degree (e.g. unsubstituted, *N*-substituted, *N,N*-disubstituted, *N,N'*-disubstituted).
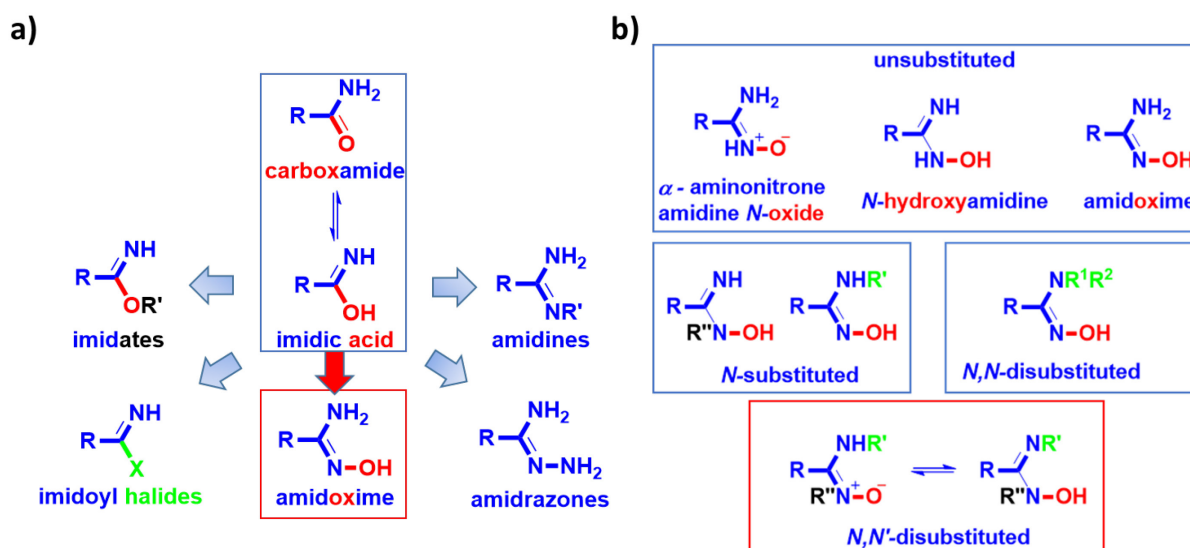
Figure1.2-7. The family of amidoximes: a) their precursors; b) the tautomeric forms and their classification function of the substitution degree.

The evolution of the number of publications containing any of the terms: *amidine oxide, hydroxyamidine, aminonitrone, amidoxime* shows a constant development over the period 1900-2015 (Figure 1.2-8a). However, when the total number of publications on AMOX-type compounds is compared with the results obtained for the terms *2,2'-bipyridine* and *8-hydroxyquinoline,* it can be seen that the AMOX-based research is in its infancy (Figure 1.2-8b). In this respect, it is important to note that very recently, amidoximes and their coordination complexes have been comprehensively reviewed by Kukushkin and co-workers.[142]
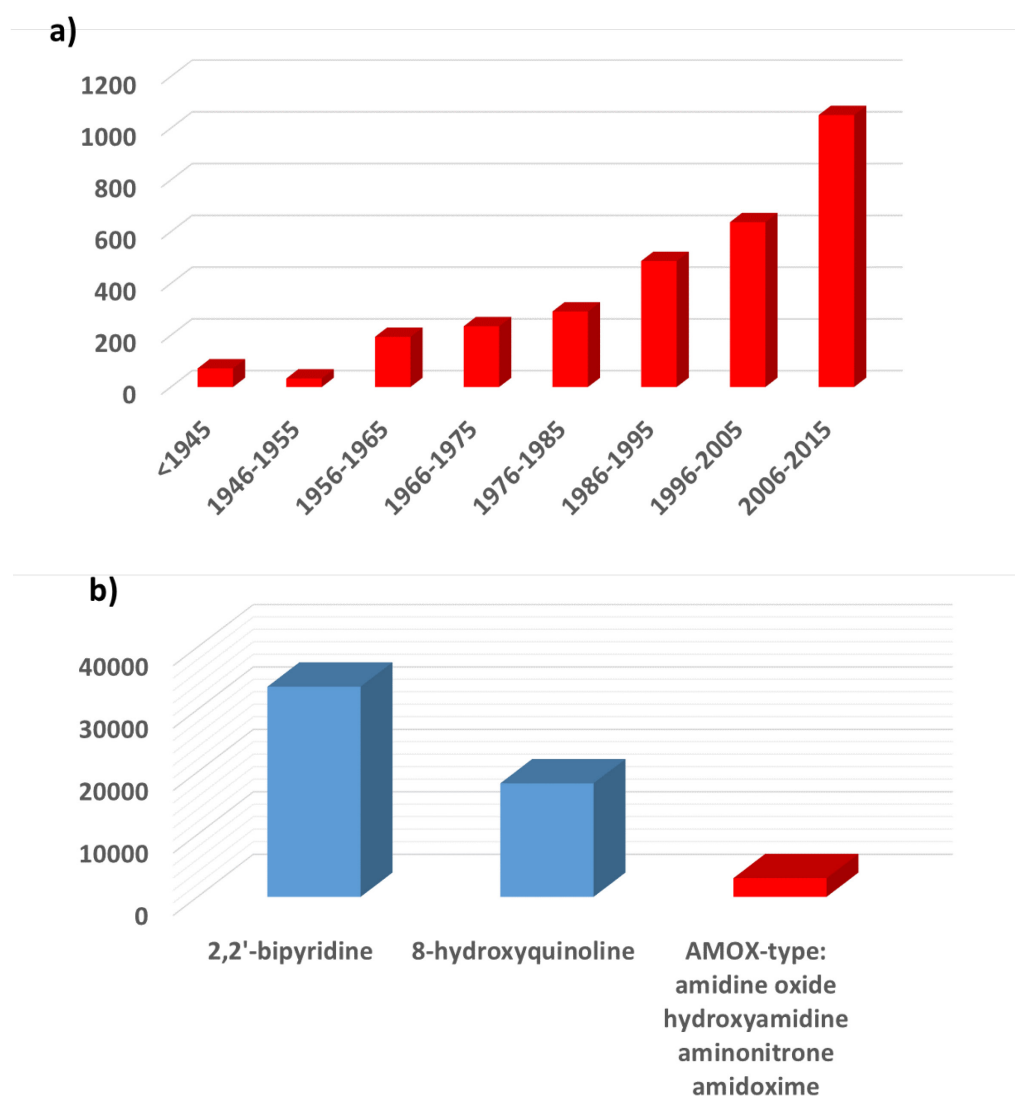
Figure1.2-8. The number of publications containing any of the terms: *amidine oxide*, *hydroxyamidine, aminonitrone, amidoxime* (Scifinder, December 2015): a) the evolution of the number of publications over the period 1900-2015; b) comparative presentation *vs.* the results obtained for the terms *2,2'-bipyridine* and *8-hydroxyquinoline*.

1.3. Research Objective, Directions and Methodology

1.3.1. Research Objective and Directions

The general objective of the work reported in this thesis is the study of *N,N'*-disubstituted amidine *N*-oxide (AMOX) ligands (also known as *N,N'*-disubstituted *N*-hydroxyamidines/ α-aminonitrones, Figure 1.2.-7) from coordination and supramolecular chemistry perspectives [Figure 1.3-1 (left)]. As choice of metals, the late first series transition metal ions, in particular cobalt(II) and zinc(II) are targeted.
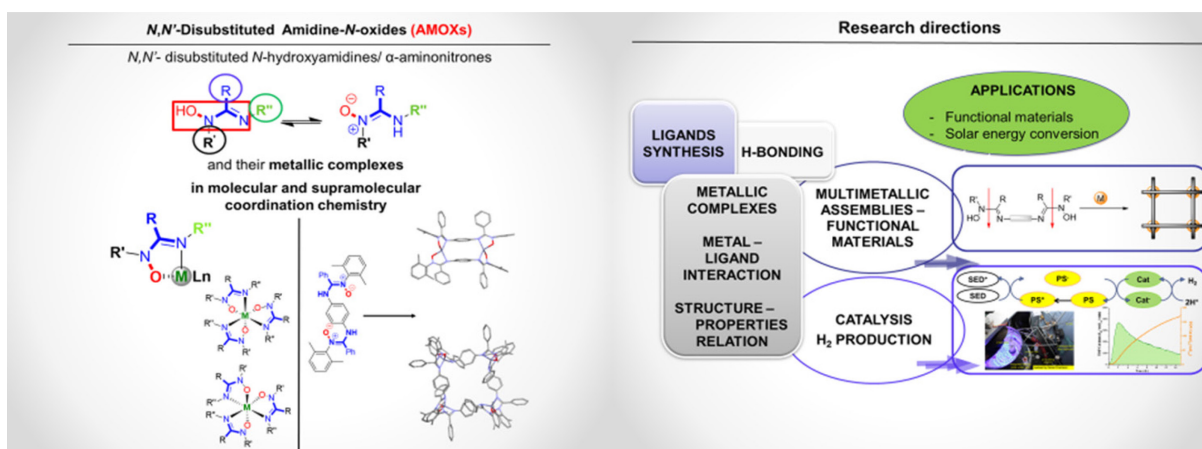
Figure 1.3.-1. General objective of the thesis and research directions

The following research directions were pursued [Figure 1.3-1 (right)]:

- ligands: synthesis and characterization;

- metallic complexes: synthesis and characterization; the study of the influence of the ligand substitution pattern on the metal-ligand interaction and identification of structure-properties relationships;

- AMOX-based compounds in supramolecular systems: multimetallic assemblies – toward functional materials and photocatalytic systems for solar-energy conversion (more

specifically photocatalysis for H_2 production). The study of H-bonding patterns in AMOX-based compounds is also one of the point of interest of this work.

1.3.2. Note on Methodology

The general methodology used in this thesis is outlined in Figure 1.4.-1 (left). The specific techniques used for compound characterization and investigation of their properties are shown in Figure 1.3.-2 (right).
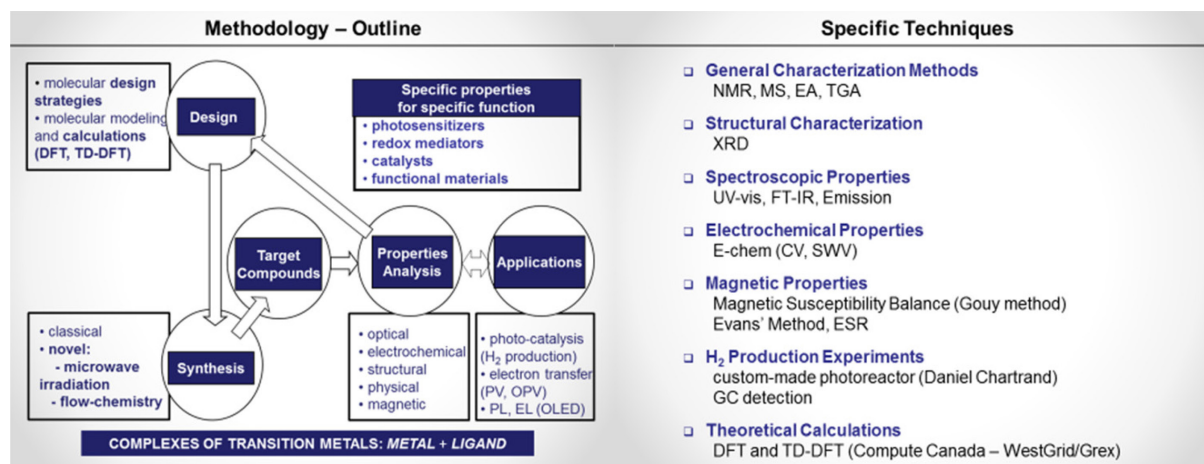
Figure 1.3.-2. Methodology: outline (left) and specific techniques (right)

The tests for the performance of zinc-based AMOX complexes in OLEDs are done in collaboration with other research groups. As the work is in progress at the moment, the results as well as the methodology will be described in future joint publications. Preliminary results are however presented in chapter 6.

1.4. Outline of the Thesis

The thesis is divided in six chapters:

Chapter 1. To set the general context of this work, the importance of coordination compounds in applications is emphasised, and trends and future opportunities in their study and use in applications are identified. Relevant key concepts in molecular and supramolecular coordination chemistry are also presented (section 1.1). The specific context of this research is highlighted by selected aspects of the coordination chemistry of N,O ligands (section 1.2). The

research objective, directions and methodology are also described (section 1.3) as well as the outline of the thesis (section 1.4).

Chapter 2. This chapter presents: the properties of AMOX ligands (section 2.1.2), a general overview on the synthetic strategy used (section 2.1.3), and the results obtained on the family of *N,N'*-disubstituted-hydroxyformamidines (section 2.2).

Chapter 3. The cobalt(II) complexes of bulky *N,N'*-diarylformamidinate *N*-oxides are introduced (section 3.2) and the influence of the substitution pattern of the ligands on their properties is assessed (section 3.3).

Chapter 4. This chapter highlights a special case of hydrogen-bonding-induced geometry and spin change at a cobalt(II) centre within a same cobalt(II) bis(AMOX-chelate). The influence of the environment on the properties of the complex is thus revealed: weak interactions are the main factors responsible for biasing the system toward a specific geometry – spin state combination in the ground state.

Chapter 5. The results on the coordination chemistry of AMOX ligands with zinc(II) metal-ions are emphasised. First, the structure – properties relationship in the $Zn(AMOX)_2$ (AMOX = *N,N'*- diarylformamidinate-*N*-oxide) family of complexes is determined (section 5.2). The theoretical study (DFT/ TD-DFT) performed for the series $Zn(AMOX)_2$ (AMOX = *N,N'*-diarylbenzamidinate-*N*-oxide) to assess the influence of the ligand substitution pattern on the band gap of the complexes (section 5.3.1) is then presented. Finally, the AMOX-based Zn(II) coordination polymer obtained with *N*-bridged bis-AMOX ligands is described (section 5.3.2).

Chapter 6. The general conclusions of the thesis (section 6.1) and the perspectives of the AMOX ligands in molecular and supramolecular coordination chemistry (section 6.2) as well as final remarks (section 6.3) presented.

1.5. References

[1]   M. D. Ward, in *Comprehensive Coordination Chemistry II* (Ed.: Meyer, J. A.; McCleverty, T. J.), Pergamon, Oxford, **2003**, pp. xv-xvi.
[2]   C. E. Housecroft, A. G. Sharpe, in *Inorganic Chemistry, 4th Ed.*, Pearson, Harlow; New York, **2012**, pp. 639-847.
[3]   J. A. Meyer; T. J. McCleverty, in *Comprehensive Coordination Chemistry II* (Ed.: Meyer, J. A.; McCleverty, T. J.), Pergamon, Oxford, **2003**, pp. xix-xx.

[4]   R. Smalley, Humanity's top ten problems for next 50 years; http://cnst.rice.edu/content.aspx?id=246; accessed 10/2015.

[5]   a) P. Gregory, in *Comprehensive Coordination Chemistry II* (Ed.: Meyer, J. A.; McCleverty, T. J.), Pergamon, Oxford, **2003**, pp. 549-579; b) J. Kent, in *Riegel's Handbook of Industrial Chemistry* (Ed.: Kent, J.), Springer US, **2003**, pp. 880-962.

[6]   P. A. Tasker, P. G. Plieger, L. C. West, in *Comprehensive Coordination Chemistry II* (Ed.: Meyer, J. A.; McCleverty, T. J.), Pergamon, Oxford, **2003**, pp. 759-808.

[7]   a) C. E. Housecroft, A. G. Sharpe, in *Inorganic Chemistry, 4th Ed.*, Pearson, Halrow, **2012**, pp. 940-975; b) V. C. Gibson, E. L. Marshall, in *Comprehensive Coordination Chemistry II* (Ed.: Meyer, J. A.; McCleverty, T. J.), Pergamon, Oxford, **2003**, pp. 1-74; c) C. Pettinari, F. Marchetti, D. Martini, in *Comprehensive Coordination Chemistry II* (Ed.: Meyer, J. A.; McCleverty, T. J.), Pergamon, Oxford, **2003**, pp. 75-139; d) R. H. Morris, *Acc. Chem. Res.* **2015**, *48*, 1494-1502; e) R. Noyori, M. Yamakawa, S. Hashiguchi, *J. Org. Chem.* **2001**, *66*, 7931-7944; f) P. W. N. M. Van Leeuwen, C. Claver, in *Comprehensive Coordination Chemistry II* (Ed.: Meyer, J. A.; McCleverty, T. J.), Pergamon, Oxford, **2003**, pp. 141-206; g) S. Hübner, J. G. de Vries, V. Farina, *Advanced Synthesis & Catalysis* **2016**, *358*, 3-25; h) I. P. Beletskaya, A. V. Cheprakov, in *Comprehensive Coordination Chemistry II* (Ed.: Meyer, J. A. and McCleverty, T. J.), Pergamon, Oxford, **2003**, pp. 305-368.

[8]   a) J. J. Wilson, S. J. Lippard, *Chem. Rev.* **2014**, *114*, 4470-4495; b) N. Farrell, in *Comprehensive Coordination Chemistry II* (Ed.: Meyer, J. A. and McCleverty, T. J.), Pergamon, Oxford, **2003**, pp. 809-840; c) A. Erxleben, in *Reference Module in Chemistry, Molecular Sciences and Chemical Engineering*, Elsevier, **2015**.

[9]   a) K. J. Franz, *Curr. Opin. Chem. Biol.* **2013**, *17*, 143-149; b) P. V. Bernhardt, *Dalton Trans.* **2007**, 3214-3220; c) http://www.rsc.org/education/eic/issues/2009Jan/iron-antibiotic-siderophore-oxygen-microbe.asp#; consulted december 2015; d) S. J. S. Flora, in *Comprehensive Inorganic Chemistry II (Second Edition)* (Ed.: Poeppelmeier, J. R.), Elsevier, Amsterdam, **2013**, pp. 987-1013.

[10]   I. Bertini, H. B. Gray, S. J. Lippard, J. S. Valentine, *Bioinorganic Chemistry*, Univ. Sci. Books, **1994**, 505 - 583

[11]   a) É. Tóth, L. Helm, A. E. Merbach, in *Comprehensive Coordination Chemistry II* (Ed.: Meyer, J. A. and McCleverty, T. J.), Pergamon, Oxford, **2003**, pp. 841-881; b) S. Z. Lever, J. D. Lydon, C. S. Cutler, S. S. Jurisson, in *Comprehensive Coordination Chemistry II* (Ed.: Meyer, J. A. M. J.), Pergamon, Oxford, **2003**, pp. 883-911; c) É. Tóth, L. Helm, A. E. Merbach, in *Reference Module in Chemistry, Molecular Sciences and Chemical Engineering*, Elsevier, **2015**; d) A. Duatti, in *Reference Module in Chemistry, Molecular Sciences and Chemical Engineering*, Elsevier, **2013**.

[12]   a) M. Nazeeruddin, M. Grätzel, in *Comprehensive Coordination Chemistry II* (Ed.: Meyer, J. A. and McCleverty, T. J.), Pergamon, Oxford, **2003**, pp. 719-758; b) K. Kalyanasundaram, *Dye-sensitized Solar Cells*, EFPL Press, **2010**, ; c) http://www.dyesol.com/products/dsc-materials/dyes.html; consulted november 2015; d) S. Mathew, A. Yella, P. Gao, R. Humphry-Baker, F. E. CurchodBasile, N. Ashari-Astani, I. Tavernelli, U. Rothlisberger, K. NazeeruddinMd, M. Grätzel, *Nat. Chem.* **2014**, *6*, 242-247; e) K.-L. Wu, W.-P. Ku, J. N. Clifford, E. Palomares, S.-T. Ho, Y. Chi, S.-H. Liu, P.-T. Chou, M. K. Nazeeruddin, M. Gratzel, *Energy Environ. Sci.* **2013**, *6*, 859-870.

[13]   a) I. Omae, *Coord. Chem. Rev*; b) E. Holder, B. M. W. Langeveld, U. S. Schubert, *Advanced Materials* **2005**, *17*, 1109-1121; c) Sigma Aldrich; OLED eFabricator; http://www.sigmaaldrich.com/materials-science/learning-center/oled-efabricator.html?cm_sp=Insite-_-MatSci-_-oledPDP; consulted december 2015; d) R. C. Evans, P. Douglas, C. J. Winscom, *Coord. Chem. Rev.* **2006**, *250*, 2093-2126; e) T.-Y. Li, Y.-M. Jing, X. Liu, Y. Zhao, L. Shi, Z. Tang, Y.-X. Zheng, J.-L. Zuo, *Scientific Reports* **2015**, *5*, 14912; f) C. Pérez-Bolívar, S.-y. Takizawa, G. Nishimura, V. A. Montes, P. Anzenbacher, *Chem. Eur. J.* **2011**, *17*, 9076-9082.

[14]   a) P. Silva, S. M. F. Vilela, J. P. C. Tome, F. A. Almeida Paz, *Chem. Soc. Rev.* **2015**, *44*, 6774-6803; b) Y.-B. Zhang, H. Furukawa, N. Ko, W. Nie, H. J. Park, S. Okajima, K. E. Cordova, H. Deng, J. Kim, O. M. Yaghi, *J. Am. Chem. Soc.* **2015**, *137*, 2641-2650; c) A. U. Czaja, N. Trukhan, U. Muller, *Chem. Soc. Rev.* **2009**, *38*, 1284-1293.

[15]   http://www.sony.net/Products/SC-HP/cx_news_archives/img/pdf/vol_56/sideview56.pdf; consulted december 2015.

[16]   a) http://www.digitaltrends.com/home-theater/value-electronics-tv-shootout-2015-lg-oled-winner/; consulted december 2015; b) http://www.displaymate.com/Galaxy_S6_ShootOut_1.htm; consulted december 2015; c) http://www.oled-info.com/history; consulted december 2015.

[17]   a) PubChem, http://pubchem.ncbi.nlm.nih.gov/compound/157443#section=Top; accessed 21-12-2015; b) http://www.accessdata.fda.gov/scripts/cder/drugsatfda/index.cfm?fuseaction=Search.SearchAction&SearchType=BasicSearch&searchTerm=NET&Search_Button=Submitaccessed; accessed on 21-12-2015.

[18]   S. Mathew, A. Yella, P. Gao, R. Humphry-Baker, F. E. CurchodBasile, N. Ashari-Astani, I. Tavernelli, U. Rothlisberger, K. NazeeruddinMd, M. Grätzel, *Nat Chem* **2014**, *6*, 242-247.

[19]   http://www.remm.nlm.gov/dimercaprol.htm

[20]   Information on Gadolinium-based Contrast Agents (GBCA): http://www.fda.gov/Drugs/DrugSafety/PostmarketDrugSafetyInformationforPatientsandProviders/ucm142882.htm; consulted 22-12-2015

[21]   http://www.chemtube3d.com/solidstate/MOF-home.html; consulted december 2015.

[22]   J. W. Steed, J. L. Atwood, in *Supramolecular Chemistry*, John Wiley & Sons, Ltd, **2009**, pp. 707-775.

[23]   J. W. Steed, J. L. Atwood, in *Supramolecular Chemistry*, John Wiley & Sons, Ltd, **2009**, pp. 1-48.

[24]   J. W. Steed, J. L. Atwood, in *Supramolecular Chemistry*, John Wiley & Sons, Ltd, **2009**, pp. 49-104.

[25]   a) G. F. Swiegers, in *Bioinspiration and Biomimicry in Chemistry* (Ed.: Swiegers, G. F.), John Wiley & Sons, Inc., **2012**, pp. i-xxvii; b) J. W. Steed, J. L. Atwood, in *Supramolecular Chemistry*, John Wiley & Sons, Ltd, **2009**, pp. 777-827; c) M. Zhang, Z.-Y. Gu, M. Bosch, Z. Perry, H.-C. Zhou, *Coord. Chem. Rev.* **2015**, *293–294*, 327-356.

[26]   a) W. Lubitz, H. Ogata, O. Rüdiger, E. Reijerse, *Chem. Rev.* **2014**, *114*, 4081-4148; b) T. Xu, D. Chen, X. Hu, *Coord. Chem. Rev.* **2015**, *303*, 32-41; c) G. Berggren, A. Adamska, C. Lambertz, T. R. Simmons, J. Esselborn, M. Atta, S. Gambarelli, J. M.

Mouesca, E. Reijerse, W. Lubitz, T. Happe, V. Artero, M. Fontecave, *Nature* **2013**, *499*, 66.

[27] M. Hoarau, C. Hureau, E. Gras, P. Faller, *Coord. Chem. Rev.* **2016**, *308*, 445-459.

[28] A. P. Alivisatos, M. J. Blaser, E. L. Brodie, M. Chun, J. L. Dangl, T. J. Donohue, P. C. Dorrestein, J. A. Gilbert, J. L. Green, J. K. Jansson, R. Knight, M. E. Maxon, M. J. McFall-Ngai, J. F. Miller, K. S. Pollard, E. G. Ruby, S. A. Taha, *Science* **2015**, *350*, 507-508.

[29] H. B. Gray, *Nat. Chem.* **2009**, *1*, 7.

[30] a) G. Caserta, S. Roy, M. Atta, V. Artero, M. Fontecave, *Curr. Opin. Chem. Biol.* **2015**, *25*, 36-47; b) M. Bacchi, G. Berggren, J. Niklas, E. Veinberg, M. W. Mara, M. L. Shelby, O. G. Poluektov, L. X. Chen, D. M. Tiede, C. Cavazza, M. J. Field, M. Fontecave, V. Artero, *Inorg. Chem.* **2014**, *53*, 8071.

[31] a) T. W. Woolerton, S. Sheard, Y. S. Chaudhary, F. A. Armstrong, *Energy Environ. Sci.* **2012**, *5*, 7470-7490; b) E. M. Nichols, J. J. Gallagher, C. Liu, Y. Su, J. Resasco, Y. Yu, Y. Sun, P. Yang, M. C. Y. Chang, C. J. Chang, *Proc. Natl. Acad. Sci.* **2015**, *112*, 11461-11466.

[32] a) J. R. McKone, N. S. Lewis, H. B. Gray, *Chem. Mater.* **2014**, *26*, 407-414; b) C. E. Lubner, R. Grimme, D. A. Bryant, J. H. Golbeck, *Biochemistry* **2010**, *49*, 404-414; c) N. S. Lewis, D. G. Nocera, *Proc. Natl. Acad. Sci. U. S. A.* **2006**, *103*, 15729-15735; d) R. L. House, N. Y. M. Iha, R. L. Coppo, L. Alibabaei, B. D. Sherman, P. Kang, M. K. Brennaman, P. G. Hoertz, T. J. Meyer, *J. Photochem. Photobiol. C: Photochem. Rev.* **2015**, *25*, 32-45; e) L. Hammarström, S. Hammes-Schiffer, *Acc. Chem. Res.* **2009**, *42*, 1859-1860; f) R. Eisenberg, *Science* **2009**, *324*, 44-45; g) J. Barber, *Chem. Soc. Rev.* **2009**, *38*, 185-196; h) V. Balzani, A. Credi, M. Venturi, *ChemSusChem* **2008**, *1*, 26-58; i) N. Armaroli, V. Balzani, *Angew. Chem., Int. Ed.* **2007**, *46*, 52-66.

[33] S. Berardi, S. Drouet, L. Francas, C. Gimbert-Surinach, M. Guttentag, C. Richmond, T. Stoll, A. Llobet, *Chem. Soc. Rev.* **2014**, *43*, 7501-7519.

[34] J. D. Hughes, *Nature* **2013**, *494*, 307-308.

[35] K. R. Ramsayer, C., http://climate.nasa.gov/news/2364/; consulted 12-2015.

[36] D. G. Nocera, *Acc. Chem. Res.* **2012**, *45*, 767-776.

[37] H. Shaftel, http://climate.nasa.gov/news/2373/; consulted december 2015.

[38] A. Fujishima, K. Honda, *Bull. Chem. Soc. Jap.* **1971**, *44*, 1148-1150.

[39] A. Hagfeldt, G. Boschloo, L. Sun, L. Kloo, H. Pettersson, *Chem. Rev.* **2010**, *110*, 6595-6663.

[40] Y. Jiao, Y. Zheng, M. Jaroniec, S. Z. Qiao, *Chem. Soc. Rev.* **2015**, *44*, 2060-2086.

[41] a) F. E. Osterloh, *Chem. Soc. Rev.* **2013**, *42*, 2294-2320; b) T. Hisatomi, J. Kubota, K. Domen, *Chem. Soc. Rev.* **2014**, *43*, 7520-7535; c) J. Ronge, T. Bosserez, D. Martel, C. Nervi, L. Boarino, F. Taulelle, G. Decher, S. Bordiga, J. A. Martens, *Chem. Soc. Rev.* **2014**, *43*, 7963-7981; d) Z. Li, W. Luo, M. Zhang, J. Feng, Z. Zou, *Energy Environ. Sci.* **2013**, *6*, 347-370.

[42] a) L. Sun, F. Li, Z. Yu, *Energy Environ. Sci.* **2015**, *8*, 760-775; b) M. Wang, K. Han, S. Zhang, L. Sun, *Coord. Chem. Rev.* **2015**, *287*, 1-14; c) V. Artero, M. Fontecave, *Chem. Soc. Rev.* **2013**, *42*, 2338.

[43] N. Queyriaux, N. Kaeffer, A. Morozan, M. Chavarot-Kerlidou, V. Artero, *J. Photochem. Photobiol., C* **2015**, Ahead of Print.

[44]   F. Li, K. Fan, B. Xu, E. Gabrielsson, Q. Daniel, L. Li, L. Sun, *J. Am. Chem. Soc.* **2015**, *137*, 9153-9159.

[45]   P. Chawla, M. Tripathi, *International Journal of Energy Research* **2015**, *39*, 1579-1596.

[46]   D. L. Ashford, M. K. Gish, A. K. Vannucci, M. K. Brennaman, J. L. Templeton, J. M. Papanikolas, T. J. Meyer, *Chem. Rev.* **2015**, *115*, 13006-13049.

[47]   a) M. Wang, L. Sun *ChemSusChem* **2010**, *3*, 551-554; b) M. Wang, L. Chen, L. Sun, *Energy Environ. Sci.* **2012**, *5*, 6763-6778; c) V. S. Thoi, Y. Sun, J. R. Long, C. J. Chang, *Chem. Soc. Rev.* **2013**, *42*, 2388-2400; d) T. Lazarides, T. McCormick, P. Du, G. Luo, B. Lindley, R. Eisenberg, *J. Am. Chem. Soc.* **2009**, *131*, 9192-9194; e) J. L. Dempsey, J. R. Winkler, H. B. Gray, in *Comprehensive Inorganic Chemistry II (Second Edition)* (Ed.: Poeppelmeier, J. R.), Elsevier, Amsterdam, **2013**, pp. 553-565.

[48]   a) M. E. Louis, T. G. Fenton, J. Rondeau, T. Jin, G. Li, *Comments on Inorganic Chemistry* **2016**, *36*, 38-60; b) W.-H. Wang, Y. Himeda, J. T. Muckerman, G. F. Manbeck, E. Fujita, *Chem. Rev.* **2015**; c) M. Rakowski Dubois, D. L. Dubois, *Acc. Chem. Res.* **2009**, *42*, 1974-1982; d) R. Angamuthu, P. Byers, M. Lutz, A. L. Spek, E. Bouwman, *Science* **2010**, *327*, 313-315; e) C. Costentin, M. Robert, J.-M. Saveant, *Chem. Soc. Rev.* **2013**, *42*, 2423-2436.

[49]   M. D. Kärkäs, O. Verho, E. V. Johnston, B. Åkermark, *Chem. Rev.* **2014**, *114*, 11863-12001.

[50]   T. C. B. Harlang, Y. Liu, O. Gordivska, L. A. Fredin, C. S. Ponseca Jr, P. Huang, P. Chábera, K. S. Kjaer, H. Mateos, J. Uhlig, R. Lomoth, R. Wallenberg, S. Styring, P. Persson, V. Sundström, K. Wärnmark, *Nat. Chem.* **2015**, *7*, 883-889.

[51]   a) P. Zhang, M. Wang, Y. Na, X. Q. Li, Y. Jiang, L. C. Sun, *Dalton Trans.* **2010**, *39*, 1204-1206; b) M. Wang, L. Chen, X. Li, L. Sun, *Dalton Trans.* **2011**, *40*, 12793-12800.

[52]   a) N. Queyriaux, R. T. Jane, J. Massin, V. Artero, M. Chavarot-Kerlidou, *Coord. Chem. Rev.* **2015**, *304-305*, 3-19; b) V. Artero, M. Chavarot-Kerlidou, M. Fontecave, *Angew. Chem., Int. Ed.* **2011**, *50*, 7238-7266.

[53]   a) A. Das, Z. Han, W. W. Brennessel, P. L. Holland, R. Eisenberg, *ACS Catalysis* **2015**, *5*, 1397-1406; b) S. Wiese, U. J. Kilgore, M.-H. Ho, S. Raugei, D. L. DuBois, R. M. Bullock, M. L. Helm, *ACS Catal.* **2013**, *3*, 2527-2535.

[54]   a) H. Lei, H. Fang, Y. Han, W. Lai, X. Fu, R. Cao, *ACS Catalysis* **2015**, *5*, 5145-5153; b) X. Liu, H. Zheng, Z. Sun, A. Han, P. Du, *ACS Catalysis* **2015**, *5*, 1530-1538.

[55]   a) X. Li, M. Wang, D. Zheng, K. Han, J. Dong, L. Sun, *Energy Environ. Sci.* **2012**, *5*, 8220-8224; b) T. M. McCormick, B. D. Calitree, A. Orchard, N. D. Kraut, F. V. Bright, M. R. Detty, R. Eisenberg, *J. Am. Chem. Soc.* **2010**, *132*, 15480-15483.

[56]   E. Verlage, S. Hu, R. Liu, R. J. R. Jones, K. Sun, C. Xiang, N. S. Lewis, H. A. Atwater, *Energ. Environ. Sci.* **2015**, *8*, 3166-3172.

[57]   J. Newman, P. G. Hoertz, C. A. Bonino, J. A. Trainham, *J. Electrochem. Soc.* **2012**, *159*, A1722-A1729.

[58]   J.-M. Lehn, in *Constitutional Dynamic Chemistry, Vol. 322* (Ed.: Barboiu, M.), Springer Berlin Heidelberg, **2012**, pp. 1-32.

[59]   E. C. Constable, C. E. Housecroft, in *Comprehensive Inorganic Chemistry II (Second Edition)* (Ed.: Poeppelmeier, J. R.), Elsevier, Amsterdam, **2013**, pp. 1-29.

[60] a) J. W. Steed, J. L. Atwood, in *Supramolecular Chemistry*, John Wiley & Sons, Ltd, **2009**, pp. 591-706; b) K. Harris, Q. F. Sun, M. Fujita, in *Comprehensive Inorganic Chemistry II (Second Edition)* (Ed.: Poeppelmeier, J. R.), Elsevier, Amsterdam, **2013**, pp. 31-57.

[61] J. W. Steed, J. L. Atwood, in *Supramolecular Chemistry*, John Wiley & Sons, Ltd, **2009**, pp. 829-859.

[62] M. R. Axet, O. Dechy-Cabaret, J. Durand, M. Gouygou, P. Serp, *Coord. Chem. Rev.* **2016**, *308*, 236-345.

[63] L. Valade, D. de Caro, C. Faulmann, K. Jacob, *Coord. Chem. Rev.* **2016**, *308*, 433-444.

[64] a) R. Chakrabarty, P. S. Mukherjee, P. J. Stang, *Chem. Rev.* **2011**, *111*, 6810-6918; b) T. R. Cook, Y.-R. Zheng, P. J. Stang, *Chem. Rev.* **2013**, *113*, 734-777; c) T. R. Cook, P. J. Stang, *Chem. Rev.* **2015**, *115*, 7001-7045; d) M. Yoshizawa, J. K. Klosterman, M. Fujita, *Angew. Chem. Intl. Ed.* **2009**, *48*, 3418-3438; e) R. S. Forgan, J.-P. Sauvage, J. F. Stoddart, *Chem. Rev.* **2011**, *111*, 5434-5464.

[65] a) N. A. Khan, S. H. Jhung, *Coord. Chem. Rev.* **2015**, *285*, 11-23; b) A. Karmakar, A. V. Desai, S. K. Ghosh, *Coord. Chem. Rev.* **2016**, *307, Part 2*, 313-341; c) J. W. Steed, J. L. Atwood, in *Supramolecular Chemistry*, John Wiley & Sons, Ltd, **2009**, pp. 537-589; d) M. Li, D. Li, M. O'Keeffe, O. M. Yaghi, *Chem. Rev.* **2014**, *114*, 1343-1370; e) H. Furukawa, K. E. Cordova, M. O'Keeffe, O. M. Yaghi, *Science* **2013**, *341*; f) S. Kitagawa, K. Uemura, *Chem. Soc. Rev.* **2005**, *34*, 109.

[66] a) C. Amiens, D. Ciuculescu-Pradines, K. Philippot, *Coord. Chem. Rev*; b) J. W. Steed, J. L. Atwood, in *Supramolecular Chemistry*, John Wiley & Sons, Ltd, **2009**, pp. 899-939.

[67] J. W. Steed, J. L. Atwood, in *Supramolecular Chemistry*, John Wiley & Sons, Ltd, **2009**, pp. 441-536.

[68] A. J. McConnell, C. S. Wood, P. P. Neelakandan, J. R. Nitschke, *Chem. Rev.* **2015**, *115*, 7729-7793.

[69] a) M. D. Manrique-Juárez, S. Rat, L. Salmon, G. Molnár, C. M. Quintero, L. Nicu, H. J. Shepherd, A. Bousseksou, *Coord. Chem. Rev*; b) P. G. Lacroix, I. Malfant, C. Lepetit, *Coord. Chem. Rev*; c) A. Bianchi, E. Delgado-Pinar, E. García-España, F. Pina, in *Comprehensive Inorganic Chemistry II (Second Edition)* (Ed.: Poeppelmeier, J. R.), Elsevier, Amsterdam, **2013**, pp. 969-1037.

[70] L. Wang, Y. Han, X. Feng, J. Zhou, P. Qi, B. Wang, *Coord. Chem. Rev.* **2016**, *307, Part 2*, 361-381.

[71] a) A. K. Bar, C. Pichon, J.-P. Sutter, *Coord. Chem. Rev*; b) L. K. Thompson, L. N. Dawe, *Coord. Chem. Rev.* **2015**, *289–290*, 13-31; c) M. Castellano, R. Ruiz-García, J. Cano, J. Ferrando-Soria, E. Pardo, F. R. Fortea-Pérez, S.-E. Stiriba, W. P. Barros, H. O. Stumpf, L. Cañadillas-Delgado, J. Pasán, C. Ruiz-Pérez, G. de Munno, D. Armentano, Y. Journaux, F. Lloret, M. Julve, *Coord. Chem. Rev.* **2015**, *303*, 110-138.

[72] a) C. J. Brown, F. D. Toste, R. G. Bergman, K. N. Raymond, *Chem. Rev.* **2015**, *115*, 3012-3035; b) P. Ballester, P. van Leeuwer, A. Vidal-Ferran, in *Reference Module in Chemistry, Molecular Sciences and Chemical Engineering*, Elsevier, **2015**.

[73] G.-Y. Li, R.-L. Guan, L.-N. Ji, H. Chao, *Coord. Chem. Rev.* **2014**, *281*, 100-113.

[74] IUPAC Golden Book: (http://goldbook.iupac.org/C01330.html); consulted 10-2015

[75] IUPAC Golden Book: (http://goldbook.iupac.org/L03518.html); consulted 10-2015

[76] IUPAC Golden Book: (http://goldbook.iupac.org/O04328.html; consulted 12-2015

[77]   J. A. McCleverty, T. J. Meyer, in *Comprehensive Coordination Chemistry II* (Ed.: Meyer, J. A. M. J.), Pergamon, Oxford, **2003**, pp. xv-xxiv.

[78]   IUPAC Golden Book: (http://goldbook.iupac.org/B00697.html); consulted 10-2015

[79]   a) J. R. Gispert, in *Coordination Chemistry*, Wiley, **2008**, pp. 3-29; b) C. Lepetit, V. Maraval, Y. Canac, R. Chauvin, *Coord. Chem. Rev.*

[80]   M. Goswami, A. Chirila, C. Rebreyend, B. de Bruin, *Top. Catal.* **2015**, *58*, 719-750.

[81]   M. Wächtler, J. Guthmuller, L. González, B. Dietzek, *Coord. Chem. Rev.* **2012**, *256*, 1479-1508.

[82]   G. Smolentsev, V. Sundström, *Coord. Chem. Rev.* **2015**, *304–305*, 117-132.

[83]   C. Daniel, *Coord. Chem. Rev.* **2015**, *282–283*, 19-32.

[84]   a) A. Caneschi, D. Gatteschi, F. Totti, *Coord. Chem. Rev.* **2015**, *289–290*, 357-378; b) A. C. Tsipis, *Coord. Chem. Rev.* **2014**, *272*, 1-29; c) M. Bruschi, C. Greco, P. Fantucci, L. De Gioia, *Inorg. Chem.* **2008**, *47*, 6056-6071; d) M. Atanasov, C. Daul, H. U. Güdel, T. A. Wesolowski, M. Zbiri, *Inorg. Chem.* **2005**, *44*, 2954-2963; e) A. C. Tsipis, A. T. Chaviara, *Inorg. Chem.* **2004**, *43*, 1273-1286.

[85]   C. Adamo, T. Le Bahers, M. Savarese, L. Wilbraham, G. García, R. Fukuda, M. Ehara, N. Rega, I. Ciofini, *Coord. Chem. Rev.* **2015**, *304–305*, 166-178.

[86]   a) B. Butschke, K. L. Fillman, T. Bendikov, L. J. W. Shimon, Y. Diskin-Posner, G. Leitus, S. I. Gorelsky, M. L. Neidig, D. Milstein, *Inorg. Chem.* **2015**, *54*, 4909-4926; b) K. Ray, T. Petrenko, K. Wieghardt, F. Neese, *Dalton Trans.* **2007**, 1552-1566; c) W. Kaim, *Inorg. Chem.* **2011**, *50*, 9752-9765.

[87]   a) G. Skara, B. Pinter, P. Geerlings, F. De Proft, *Chem. Sci.* **2015**, *6*, 4109-4117; b) W. Kaim, *Eur. J. Inorg. Chem.* **2012**, *2012*, 343-348.

[88]   a) M. M. Khusniyarov, E. Bill, T. Weyhermueller, E. Bothe, K. Wieghardt, *Angew. Chem., Int. Ed.* **2011**, *50*, 1652-1655, S1652/1651-S1652/1610; b) P. J. Chirik, K. Wieghardt, *Science* **2010**, *327*, 794-795; c) K. Ray, S. DeBeer George, E. I. Solomon, K. Wieghardt, F. Neese, *Chem. Eur. J.* **2007**, *13*, 2783-2797; d) R. Kapre, K. Ray, I. Sylvestre, T. Weyhermueller, S. DeBeer George, F. Neese, K. Wieghardt, *Inorg. Chem.* **2006**, *45*, 3499-3509; e) K. Ray, E. Bill, T. Weyhermueller, K. Wieghardt, *J. Am. Chem. Soc.* **2005**, *127*, 5641-5654; f) S. Kokatam, T. Weyhermuller, E. Bothe, P. Chaudhuri, K. Wieghardt, *Inorg. Chem.* **2005**, *44*, 3709-3717; g) K. S. Min, T. Weyhermueller, K. Wieghardt, *Dalton Trans.* **2004**, 178-186; h) K. S. Min, T. Weyhermueller, E. Bothe, K. Wieghardt, *Inorg. Chem.* **2004**, *43*, 2922-2931; i) D. Herebian, E. Bothe, F. Neese, T. Weyhermueller, K. Wieghardt, *J. Am. Chem. Soc.* **2003**, *125*, 9116-9128; j) D. Herebian, E. Bothe, E. Bill, T. Weyhermueller, K. Wieghardt, *J. Am. Chem. Soc.* **2001**, *123*, 10012-10023; k) P. Chaudhuri, C. N. Verani, E. Bill, E. Bothe, T. Weyhermueller, K. Wieghardt, *J. Am. Chem. Soc.* **2001**, *123*, 2213-2223; l) B. De Bruin, E. Bill, E. Bothe, T. Weyhermueller, K. Wieghardt, *Inorg. Chem.* **2000**, *39*, 2936-2947; m) A. Das, P. Ghosh, S. Plebst, B. Schwederski, S. M. Mobin, W. Kaim, G. K. Lahiri, *Inorg. Chem.* **2015**, *54*, 3376-3386; n) A. Paretzki, M. Bubrin, J. Fiedler, S. Zalis, W. Kaim, *Chem. Eur. J.* **2014**, *20*, 5414-5422; o) M. M. R. Choudhuri, W. Kaim, B. Sarkar, R. J. Crutchley, *Inorg. Chem.* **2013**, *52*, 11060-11066; p) A. K. Das, R. Hubner, B. Sarkar, J. Fiedler, S. Zalis, G. K. Lahiri, W. Kaim, *Dalton Trans.* **2012**, *41*, 8913-8921; q) A. B. P. Lever, *Coord. Chem. Rev.* **2010**, *254*, 1397-1405; r) D. Kalinina, C. Dares, H. Kaluarachchi, P. G. Potvin, A. B. P. Lever, *Inorg. Chem.* **2008**, *47*, 10110-10126; s) S. I. Gorelsky, A. B. P. Lever, M. Ebadi, *Coord.*

Chem. Rev. **2002**, *230*, 97-105; t) R. Santana da Silva, S. I. Gorelsky, E. S. Dodsworth, E. Tfouni, A. B. P. Lever, *Dalton Trans.* **2000**, 4078-4088; u) A. B. P. Lever, S. I. Gorelsky, *Coord. Chem. Rev.* **2000**, *208*, 153-167; v) R. A. Metcalfe, A. B. P. Lever, *Inorg. Chem.* **1997**, *36*, 4762-4771; w) H. Masui, A. B. P. Lever, E. S. Dodsworth, *Inorg. Chem.* **1993**, *32*, 258-267; x) M. Haga, E. S. Dodsworth, A. B. P. Lever, *Inorg. Chem.* **1986**, *25*, 447-453; y) R. Sarkar, K. K. Rajak, *J. Organomet. Chem.* **2015**, *779*, 1-13; z) N. Deibel, M. G. Sommer, S. Hohloch, J. Schwann, D. Schweinfurth, F. Ehret, B. Sarkar, *Organometallics* **2014**, *33*, 4756-4765; aa) N. Deibel, S. Hohloch, D. Schweinfurth, F. Weisser, A. Grupp, B. Sarkar, *Chem. Eur. J.* **2014**, *20*, 15178-15187; ab) S. Bellinger-Buckley, T.-C. Chang, S. Bag, D. Schweinfurth, W. Zhou, B. Torok, B. Sarkar, M.-K. Tsai, J. Rochford, *Inorg. Chem.* **2014**, *53*, 5556-5567.

[89] a) O. R. Luca, R. H. Crabtree, *Chem. Soc. Rev.* **2013**, *42*, 1440-1459; b) V. Lyaskovskyy, B. de Bruin, *ACS Catal.* **2012**, *2*, 270-279.

[90] D. L. J. Broere, R. Plessius, J. I. van der Vlugt, *Chem. Soc. Rev.* **2015**, *44*, 6886-6915.

[91] J. R. Gispert, *Coordination Chemistry*, Wiley, **2008**, 59-93

[92] S. N. Brown, *Inorg. Chem.* **2012**, *51*, 1251-1260.

[93] A. B. P. Lever, *Inorg. Chem.* **1990**, *29*, 1271-1285.

[94] a) J. R. Gispert, Wiley, **2008**, pp. 59-93; b) J. Cirera, P. Alemany, S. Alvarez, *Chem. - Eur. J.* **2004**, *10*, 190-207; c) J. Cirera, E. Ruiz, S. Alvarez, *Inorg. Chem.* **2008**, *47*, 2871-2889.

[95] T. J. Collins, *Acc. Chem. Res.* **1994**, *27*, 279-285.

[96] J. W. Jurss, R. S. Khnayzer, J. A. Panetier, K. A. El Roz, E. M. Nichols, M. Head-Gordon, J. R. Long, F. N. Castellano, C. J. Chang, *Chem. Sci.* **2015**, *6*, 4954-4972.

[97] Comprehensive Coordination Chemistry II (Ed.: J. A. McCleverty, J. Meyer), Pergamon, Oxford, 2003

[98] J. R. Gispert, in *Coordination Chemistry*, Wiley, **2008**, pp. 403-435.

[99] J. R. Gispert, in *Coordination Chemistry*, Wiley, **2008**, pp. 439-476.

[100] G. R. Desiraju, T. Steiner, *The Weak Hydrogen Bond in Structural Chemistry and Biology*, **2001**,

[101] L. C. Gilday, S. W. Robinson, T. A. Barendt, M. J. Langton, B. R. Mullaney, P. D. Beer, *Chem. Rev.* **2015**, *115*, 7118-7195.

[102] a) L. Zhang, Y.-J. Lin, Z.-H. Li, G.-X. Jin, *J. Am. Chem. Soc.* **2015**, *137*, 13670-13678; b) R. Sheng, L. Tang, L. Jiang, L. Hong, Y. Shi, N. Zhou, Y. Hu, *ACS Chem. Neurosci.* **2015**.

[103] Y. Gao, X. Zhang, C. Ma, X. Li, J. Jiang, *J. Am. Chem. Soc.* **2008**, *130*, 17044-17052.

[104] a) U. Gellrich, J. Huang, W. Seiche, M. Keller, M. Meuwly, B. Breit, *J. Am. Chem. Soc.* **2011**, *133*, 964-975; b) S. K. Sommer, L. N. Zakharov, M. D. Pluth, *Inorg. Chem.* **2015**, *54*, 1912-1918; c) S. K. Sommer, E. A. Henle, L. N. Zakharov, M. D. Pluth, *Inorg. Chem.* **2015**, *54*, 6910-6916.

[105] a) A. D. Garnovskii, I. S. Vasilchenko, D. A. Garnovskii, B. I. Kharisov, *J. Coord. Chem.* **2009**, *62*, 151-204; b) A. Blagus, D. Cincic, T. Friscic, B. Kaitner, V. Stilinovic, *Macedonian Journal of Chemistry and Chemical Engineering* **2010**, *29*, 117-138.

[106] a) R. H. Holm, M. J. O'Connor, *Progr. Inorg. Chem.* **1971**, *14*, 241-401; b) R. H. Holm, G. W. Everett, Jr., A. Chakravorty, *Prog. Inorg. Chem.* **1966**, *7*, 83-214.

[107] C. J. Whiteoak, G. Salassa, A. W. Kleij, *Chem. Soc. Rev.* **2012**, *41*, 622-631.

[108] a) K. C. Gupta, A. K. Sutar, *Coord. Chem. Rev.* **2008**, *252*, 1420-1450; b) R. Drozdzak, B. Allaert, N. Ledoux, I. Dragutan, V. Dragutan, F. Verpoort, *Coord. Chem. Rev.* **2005**, *249*, 3055-3074; c) T. Katsuki, *Chem. Soc. Rev.* **2004**, *33*, 437-444; d) P. G. Cozzi, *Chem. Soc. Rev.* **2004**, *33*, 410-421; e) D. J. Darensbourg, *Chem. Rev.* **2007**, *107*, 2388-2410; f) H. Chen, Z. Sun, S. Ye, D. Lu, P. Du, *J. Mater. Chem. A* **2015**, *3*, 15729-15737.

[109] S. Akine, T. Nabeshima, *Dalton Trans.* **2009**, 10395-10408.

[110] a) E. L. Gavey, M. Pilkington, *Coord. Chem. Rev.* **2015**, *296*, 125-152; b) M. Rezaeivala, H. Keypour, *Coord. Chem. Rev.* **2014**, *280*, 203-253.

[111] a) Y. n. Song, H. Xu, W. Chen, P. Zhan, X. Liu, *MedChemComm* **2015**, *6*, 61-74; b) V. Prachayasittikul, S. Prachayasittikul, S. Ruchirawat, V. Prachayasittikul, *Drug. Des. Devel. Ther.* **2013**, *7*, 1157-1178; c) N. Thejo Kalyani, S. J. Dhoble, *Renewable Sustainable Energy Rev.* **2012**, *16*, 2696-2723; d) Z. Yin, B. Wang, G. Chen, M. Zhan, *J. Mater. Sci.* **2011**, *46*, 2397-2409; e) P. J. Jadhav, B. N. Limketkai, M. A. Baldo, *Adv. Polym. Sci.* **2010**, *223*, 29-44; f) W.-Q. Ding, S. E. Lind, *IUBMB Life* **2009**, *61*, 1013-1018; g) M. Elhabiri, A.-M. Albrecht-Gary, *Coord. Chem. Rev.* **2008**, *252*, 1079-1092; h) M. Albrecht, M. Fiege, O. Osetska, *Coord. Chem. Rev.* **2008**, *252*, 812-824.

[112] a) B. Sarkar, D. Schweinfurth, N. Deibel, F. Weisser, *Coord. Chem. Rev.* **2015**, *293–294*, 250-262; b) E. Bill, E. Bothe, P. Chaudhuri, K. Chlopek, D. Herebian, S. Kokatam, K. Ray, T. Weyhermuller, F. Neese, K. Wieghardt, *Chem. Eur. J.* **2005**, *11*, 204-224; c) X. Sun, H. Chun, K. Hildenbrand, E. Bothe, T. Weyhermüller, F. Neese, K. Wieghardt, *Inorg. Chem.* **2002**, *41*, 4295-4303.

[113] P. Teo, T. S. A. Hor, *Coord. Chem. Rev.* **2011**, *255*, 273-289.

[114] P. Banerjee, *Coord. Chem. Rev.* **1999**, *190-192*, 19-28.

[115] P. R. Payne, R. K. Thomson, D. M. Medeiros, G. Wan, L. L. Schafer, *Dalton Trans.* **2013**, *42*, 15670-15677.

[116] J. Li, C. Wang, X. Li, H. Sun, *Dalton Trans.* **2012**, *41*, 8715-8722.

[117] A. J. Blake, L. M. Gilby, S. Parsons, J. M. Rawson, D. Reed, G. A. Solan, R. E. P. Winpenny, *J. Chem. Soc., Dalton Trans.* **1996**, 3575-3581.

[118] P. Jaitner, W. Huber, A. Gieren, H. Betz, *J. Organomet. Chem.* **1986**, *311*, 379-385.

[119] C. G. Mowat, S. Parsons, G. A. Solan, R. E. P. Winpenny, *Acta Crystallogr. Sect. C* **1997**, *53*, 282-283.

[120] Z. Zhu, J. C. Fettinger, M. M. Olmstead, P. P. Power, *Organometallics* **2009**, *28*, 2091-2095.

[121] a) S. J. Lucas, R. M. Lord, R. L. Wilson, R. M. Phillips, V. Sridharan, P. C. McGowan, *Dalton Trans.* **2012**, *41*, 13800-13802; b) A. Habtemariam, M. Melchart, R. Fernández, S. Parsons, I. D. H. Oswald, A. Parkin, F. P. A. Fabbiani, J. E. Davidson, A. Dawson, R. E. Aird, D. I. Jodrell, P. J. Sadler, *J. Med. Chem.* **2006**, *49*, 6858-6868.

[122] a) T. N. Twala, M. Schutte-Smith, A. Roodt, H. G. Visser, *Dalton Trans.* **2015**, *44*, 3278-3288; b) A. Brink, H. G. Visser, A. Roodt, *Inorg. Chem.* **2013**, *52*, 8950-8961; c) M. Schutte, G. Kemp, H. G. Visser, A. Roodt, *Inorg. Chem.* **2011**, *50*, 12486-12498.

[123] F. Allen, *Acta Crystallogr. Sect. B* **2002**, *58*, 380-388.

[124] CSD search performed in october 2015

[125] T. Storr, in *Ligand Design in Medicinal Inorganic Chemistry*, John Wiley & Sons, Ltd, **2014**, pp. i-xvii.

[126] P. K. Petrova, R. L. Tomova, R. T. Stoycheva-Topalova, InTech, **2011**, pp. 161-193.

[127] J. A. Wolny, M. F. Rudolf, Z. Ciunik, K. Gatner, S. Wolowiec, *J. Chem. Soc., Dalton Trans.* **1993**, 1611-1622.

[128] L. C. Kalutarage, P. D. Martin, M. J. Heeg, C. H. Winter, *J. Am. Chem. Soc.* **2013**, *135*, 12588-12591.

[129] A. Okazawa, T. Ishida, *Chem. Phys. Lett.* **2009**, *480*, 198-202.

[130] a) A. Okazawa, D. Hashizume, T. Ishida, *J. Am. Chem. Soc.* **2010**, *132*, 11516-11524; b) A. Okazawa, Y. Nagaichi, T. Nogami, T. Ishida, *Inorg. Chem.* **2008**, *47*, 8859-8868.

[131] a) D. X. West, S. F. Pavkovic, J. N. Brown, *Acta Crystallogr. Sect. B* **1980**, *36*, 143-145; b) D. X. West, E. J. Zaluzec, S. F. Pavkovic, *Acta Crystallogr. Sect. C* **1994**, *50*, 173-175; c) P. Knuuttila, H. Knuuttila, *Acta Crystallogr. Sect. C* **1986**, *42*, 989-991; d) E. Sletten, T. Marthinsen, J. Sletten, *Inorg. Chimica Acta* **1984**, *93*, 37-41.

[132] F.-Q. Z. Ying-Lei Wang, Yue-Ping Ji, Jian-Hua Yi, Ting An, Wei-Xiao Liu, *Chinese Chemical Letters* **2014**, *25*, 902-906.

[133] T. Minyu, *Bull. Chem. Soc. Jpn.* **1989**, *62*.

[134] A. Krajete, G. Steiner, H. Kopacka, K.-H. Ongania, K. Wurst, Marc O. Kristen, P. Preishuber-Pflügl, B. Bildstein, *Eur. J. Inorg. Chem.* **2004**, *2004*, 1740-1752.

[135] M. Castellano, J. Ferrando-Soria, E. Pardo, M. Julve, F. Lloret, C. Mathoniere, J. Pasan, C. Ruiz-Perez, L. Canadillas-Delgado, R. Ruiz-Garcia, J. Cano, *Chem. Comm.* **2011**, *47*, 11035-11037.

[136] M. Castellano, R. Ruiz-García, J. Cano, J. Ferrando-Soria, E. Pardo, F. R. Fortea-Pérez, S.-E. Stiriba, M. Julve, F. Lloret, *Acc. Chem. Res.* **2015**, *48*, 510-520.

[137] H.-Z. Kou, G.-Y. An, C.-M. Ji, B.-W. Wang, A.-L. Cui, *Dalton Trans.* **2010**, *39*, 9604-9610.

[138] W.-J. Ma, Z.-Y. Gao, S. Zhu, B.-L. Wu, *Polyhedron* **2014**, *73*, 59-66.

[139] B. Viossat, N. Rodier, N.-H. Dung, O. Guillard, *Acta Crystallogr. Sect. C* **1986**, *42*, 659-662.

[140] A. Bacchi, M. Carcelli, O. Francescangeli, F. Neve, P. Pelagatti, C. Pelizzi, *Inorg. Chem. Commun.* **1999**, *2*, 255-257.

[141] *The Chemistry of amidines and imidates / edited by Saul Patai*, Wiley, London ; New York, **1975**, 85-155

[142] D. S. Bolotin, N. A. Bokach, V. Y. Kukushkin, *Coord. Chem. Rev.* **2016**, *313*, 62-93.

Annexe-1.2 / Appendix-1.2

amino-acid-type
1

quinolin-8-olato
2

pyridine-2-carboxylato
and derivatives
3

alkanolamine-type
4

amido-phenolato
5

nitrosophenolato-type
and derivatives
6

imidazole-4-carboxylato
and derivatives
7

R-imino-cyclohepta-
1,3,5-trien-1-olato
8

9

R-amino-oxo-acetato
10

other OCCN ligands e.g.,
11

carbohydrazonato
12

hydrazine-
carboxamide-type
13

triazene-1-oxido
14

2-aminopyridine-
1-oxido
15

amidinate N-oxido
(AMOX)
16

nitroimidazole-type
17

N-R-N-(2-pyridyl)
hydroxylamine
18

R-nitrosolato-
(hydroxyacet-
amidoximato)
19

Appendix-2.1 – Chapter 2: *N,N'*-Disubstituted AMOX Ligands

2.1. Introduction

2.1.1. Outline

This chapter presents:

- the answer to the question *Why the N,N'-disubstituted AMOX ligands*? in form of analysis of AMOX ligands form the perspective of ligand design as '*collection of adjustable components*'[1] **(section 2.1.2)** – Appendix-2.1

- a general overview on the synthetic strategy used **(section 2.1.3)** – Appendix 2.1

- the results obtained on the family of *N,N'*-disubstituted-hydroxyformamidines, which were published in the article: *Synlett*, **2011**, 3, 405-409 – *Communication* **(section 2.2)**

2.1.2. Why *N,N'*-Disubstituted AMOX Ligands?

The interest in *N,N'*-disubstituted AMOX ligands stems from their properties (Figure 2.1-1). The same perspective of the ligand design as '*collection of adjustable components*'[1] will be used to highlight these properties.

N,N'-disubstituted AMOXs are bidentate N,O ligands which form 5-membered ring with metal ions. From the perspective of the atom donor and atom donor functional groups, AMOXs combine the σ-donation of the O and N atoms, with the π-donation of the O atom and π-acceptance of the amidine functionality. They present electron-density delocalization in the ONCN backbone which can be modulated by modification of the substitution pattern. AMOXs show enhanced electronic tunability and steric modularity, as substituents can be introduced in three positions (the two N atoms and the central C atom) directly on the backbone of the molecule ('primary' substitution positions) 'Secondary' substitution positions can also be identified (e.g. those on the *N,N'*-diaryl or *N,N'*-dialkyl substituents and *C*-aryl or *C*-alkyl substituents) (Figure 2.1-1). Furthermore, AMOXs are robust and present synthetic advantage

for the preparation of substituted analogues, over the fused type ligands (e.g. 8-hydroxyquinoline).
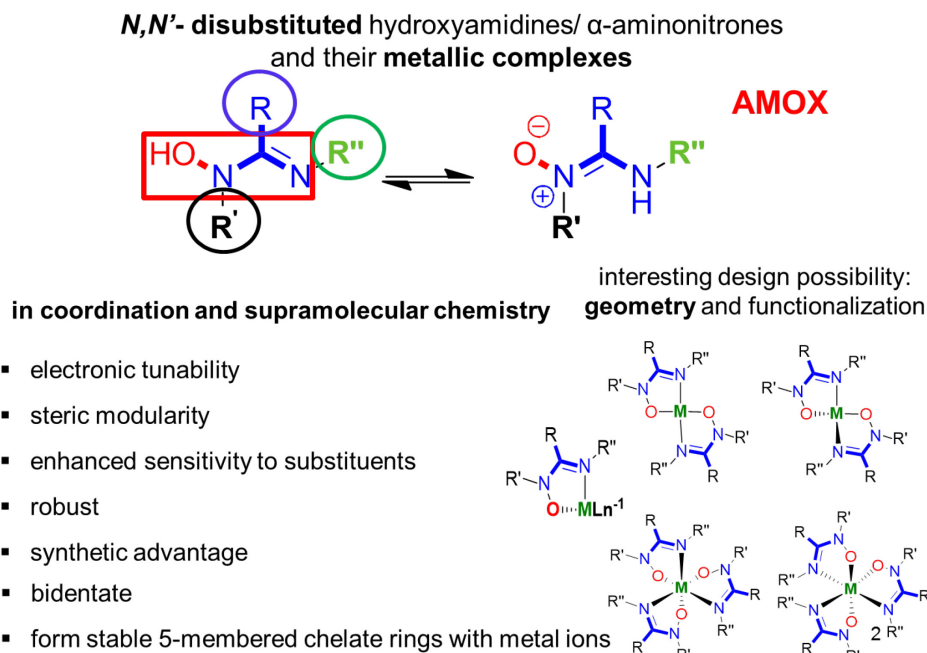
Figure 2.1-1. Why AMOX ligands?

N,N'-Disubstituted AMOXs present additional 'adjustable components' for the design tool-kit: their rich acid-base properties (basicity of oxime N atom, basicity of the HO group, and basicity of the N' atom);[2] the tautomerism (*N,N'*-disubstituted-hydroxyamidine/ *N,N'*-disubstituted α-aminonitrone (*N,N'*-disubstituted amidine-*N*-oxide)[2] (Figure 1.2-7), and their restricted rotation on the amidine moiety resulting in EE/EZ/ZE/ZZ isomers).[3] As *N,N'*-disubstituted AMOXs are very good chelators (they have been used extensively to trace metal ions in analytical chemistry) they allow the direct modulation of their chelation capacity for specific targets.

2.1.3. Synthetic Strategies – General Overview

The synthetic strategy used for preparation of AMOX ligand in this work is illustrated in Figure 2.1-2 (top).
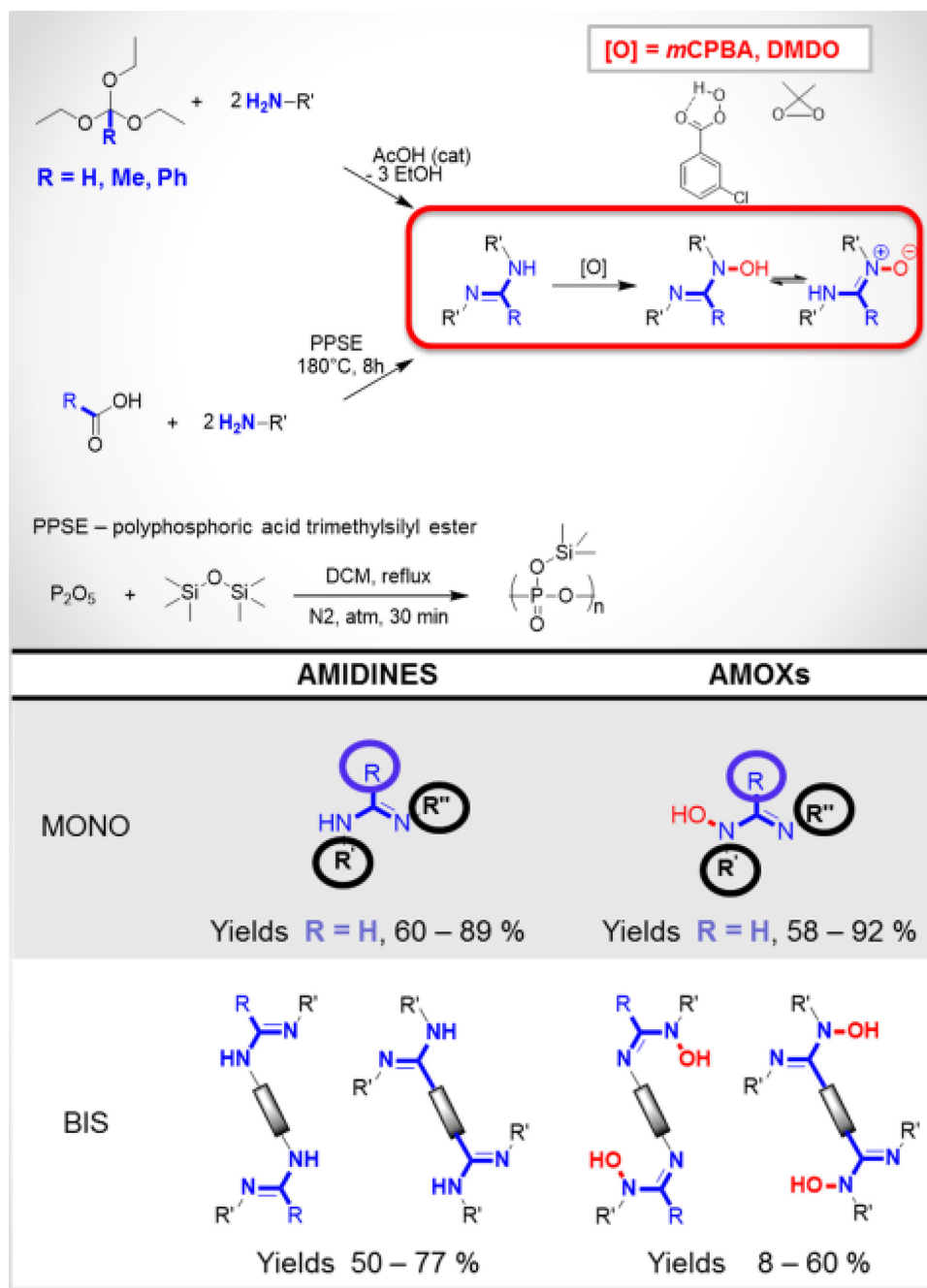
Figure 2.1-2. Synthetic strategy (top) for obtaining the AMOX ligands (bottom).

The *N*-oxidation of *N,N'*-disubstituted amidines with *m*-CPBA[4] was developed as the method of choice for the synthesis of the corresponding AMOXs. This method was integrated with different techniques of obtaining the parent amidines (classical condensation of orthoesters with amines (by distillation or adapted to microwave activation) and the direct condensation of carboxylic acids and amines using polyphosphoric acid trimethyl ester

(PPSE)).[5] Thus, a general 'synthetic strategy' for AMOXs preparation resulted. The method was initially used for mono-AMOXs synthesis, but it was successfully extended to the preparation of *N*-bridged-bis-AMOXs and *C*-bridged-bis-AMOXs. (Figure 2.1-2 (bottom). The *N*-bridged-bis-AMOX ligands and their bis-amidine precursors are presented in section 5.3.2 chapter 5), together with the results on their coordination chemistry with zinc(II) ions.

The major concern for the *N*-oxidation reaction is the protonation of the substrate by the acid produced, with the formation of a stable ion-pair, which prevents total conversion to be reached. (Figure 2.1-3) The efficiency of the *N*-oxidation method is therefore very substrate sensitive. The attempts to *N*-oxidize amidines bearing alkyl groups as *N*-substituents failed, as these substrates are too basic and they form peracid salts with the *m*-CPBA. The method was mainly used for the synthesis of symmetric AMOXs. Using it for obtaining the non-symmetric AMOXs would give information on the selectivity of the *N*-oxidation. The proposed mechanism of the *N*-oxidation reaction is illustrated in Figure 2.1-4. It was adapted from the alkene epoxidation mechanism.[6]
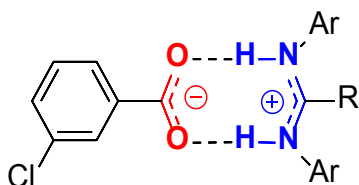
Figure 2.1-3. Proposed inhibition for the reaction of *N*-oxidation of amidines with *m*-CPBA
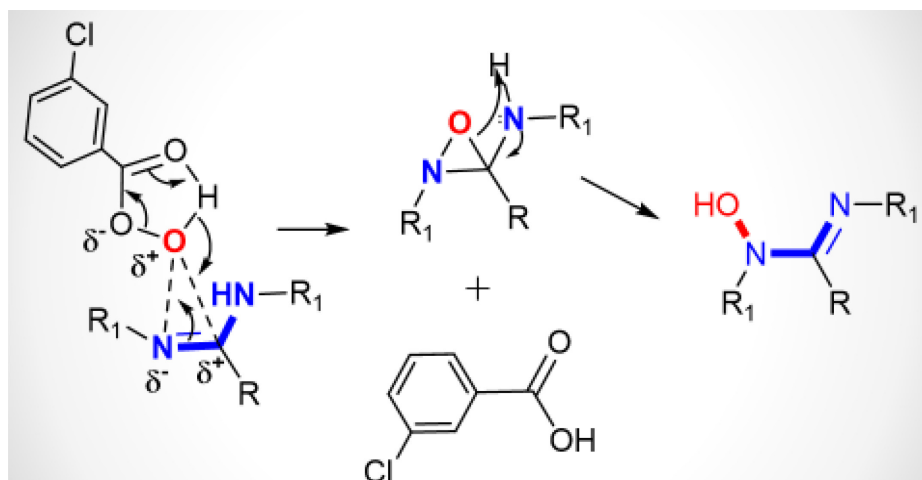
Figure 2.1-4. Proposed mechanism for the *N*-oxidation of amidines with *m*-CPBA.[6]

It is important to state that the primary aim of this work is the study of the coordination chemistry of the AMOXs. The synthesis and the characterization of AMOX ligands has been an important part of the project, and effort was invested in optimization of synthetic protocols. However, the full investigation of the ligands (clarification of tautomeric processes, isomerization processes, reaction mechanisms, etc.) were secondary in importance for this project. Several specific reports on these topics exist in the literature, in particular for amidoximes,[3] but these themes are not fully clarified in the case of *N,N'*-disubstituted AMOXs. Therefore they would be interesting to pursue as future developments of the project.

2.1.4. References

[1]   T. J. Collins, *Acc. Chem. Res.* **1994**, *27*, 279-285.
[2]   *The Chemistry of amidines and imidates / edited by Saul Patai*, Wiley, London ; New York, **1975**, 85-155
[3]   D. S. Bolotin, N. A. Bokach, V. Y. Kukushkin, *Coord. Chem. Rev.*
[4]   a) E. Baranowska, I. Panfil, C. Belzecki, *Bull. Acad. Pol. Sci., Ser. Sci. Chim.* **1977**, *25*, 93-99; b) C. Belzecki, I. Panfil, *Bull. Acad. Pol. Sci., Ser. Sci. Chim.* **1975**, *23*, 119-123.
[5]   a) M. Kakimoto, S. Ogata, A. Mochizuki, Y. Imai, *Chem. Lett.* **1984**, 821-824; b) S. Ogata, A. Mochizuki, M. Kakimoto, Y. Imai, *Bull. Chem. Soc. Jpn.* **1986**, *59*, 2171-2177.
[6]   P. D. Bartlett, *Rec. Chem. Prog.*, **1950**, 11 47.

Appendix-2.2-SI

Supporting Information

for

Facile Synthesis of Hydroxyformamidines by the *N*-Oxidation of Their Corresponding Formamidines

Mihaela Cibian, Sophie Langis-Barsetti, Garry S. Hanan*

Département of Chemistry, Université de Montréal, Montréal, Québec, H3T-1J4, Canada

Contents

1) Materials and Instrumentation

Nuclear magnetic resonance (NMR) spectra were recorded in CDCl$_3$ and C$_6$D$_6$ at room temperature (r.t.) on the following spectrometers: Bruker AV-400, AV-300, DRX-400, and ARX-300 MHz. Chemical shifts (δ) are reported in part per million (ppm) relative to TMS, using the residual solvent protons (7.26 ppm for CDCl$_3$ and 7.15 for C$_6$D$_6$) as reference. The microanalysis and the mass spectrometry analysis were done by the Elemental Analysis Service and the Regional Mass Spectrometry Center at Université de Montréal. Solvents, purchased from VRW and Fisher, were removed under reduced pressure using a rotary evaporator, unless otherwise stated. The anilines and triethylorthoformate, from Aldrich, were used without further purification with the exception of **1a**, which was purified by distillation, and **1c** and **1d** purified by sublimation. The *m*-CPBA form Acros Organics was dried under vacuum before being used.

2) General procedures:

 2.1) *N,N'*-Disubstituted Formamidines (**2a, 2e-i**)

Method A: According to the classical procedure,[1] the ethanol was distilled from a mixture of aniline, triethylorthoformate (2:1), and a catalytic amount of glacial acetic acid at 120-160 °C. The reactions times ranges form 1h (**2h**) to overnight. Solids were formed which where further purified as described below.

Method B: According to a modified literature procedure,[2] a mixture of aniline, triethylorthoformate (2:1), and a catalytic amount of glacial acetic acid (molecular sieves 4 Å were also added) was microwave (MW) activated at 130 °C for 10 minutes. At the end of the reactions, oily solids were obtained, which were taken in DCM (**2a-e** and **2g-i**) or hexane (**2f**). The solvents were evaporated under vacuum to afford solids or oils that were further purified by recrystallization in DCM/ hexane (1:1) (**2a-e** and **2g**), boiling hexane (**2f**, **2i**) or by trituration/ sonication with hexane (**2h**). Colourless solids were obtained in all cases. Except for compound **2f**, all of the formamidines are known compounds, and their characterization is similar to what has been reported (reference 1).

***N,N'*-Bis(2-isopropylphenyl)formamidine (2f)**

Compound **1f** (7.5 ml, 51 mmol, 2 eq.), triethylorthoformate (4.0 ml, 25 mmol, 1 eq.) and a catalytic amount of glacial acetic acid (0.30 ml, 5.1 mmol, 0.2 eq.) were reacted following the general procedure (method B). After purification by trituration with cold pentane and recrystallization in hot hexane, colorless crystals were obtained.

Yield: 5.56 g, 78%.

^{1}H-NMR (CDCl$_3$, 300 MHz) δ, ppm: 8.00 (s, 1H, -NH-C***H***=N-), 7.29 (d, J^d = 8 Hz, 2H, -C$_6$***H***$_4$), 7.20-7.08 (m, 4H, C$_6$***H***$_4$), 7.02 (d, J^d = 8 Hz, 2H, C$_6$***H***$_4$), 3.29 (sept, J^{sept}=7 Hz, 2H –C***H***(CH$_3$)$_2$), 1.26 (d, J^d = 7 Hz, 12H, -CH(C***H***$_3$)$_2$).

^{1}H-NMR (C$_6$D$_6$, 300 MHz) δ ppm : 7.78 (s, 1H, NH-C***H***=N-), 7.19-7.17 (m, 2H, - C$_6$***H***$_4$), 7.08-6.99 (m, 4H -C$_6$***H***$_4$), 6.87 (m, 2H, - C$_6$***H***$_4$), 3.17 (sept, J^{sept} = 7 Hz, 2H –C***H***(CH$_3$)$_2$), 1.13 (d, J= 7 Hz, 12H -CH(C***H***$_3$)$_2$).

^{13}C {^{1}H} NMR (CDCl$_3$, 75 MHz) δ, ppm: 148.6, 139.5 126.7, 125.9, 124.0, 118.7, 27.73, 23.21.

^{13}C {^{1}H} NMR (C$_6$D$_6$, 75 MHz) δ, ppm: 148.6, 140.1, 127.5, 126.5, 124.7, 119.4, 28.51, 23.70.

Elemental Analysis: *calc.* (%) for C$_{19}$H$_{24}$N$_2$: C 81.38, H 8.63, N 9.99; *found*: C 81.62, H 9.27, N 10.17.

2.2.) *N,N'*-Disubstituted Hydroxyformamidines (**3a-i**)

N-oxidation of amidines with *m*-CPBA: A solution of *m*-CPBA (1eq.) in DCM was added drop-wise by addition funnel to a solution of amidine (1 eq.) and NaHCO$_3$ (1.0-1.5 eq.) in the same solvent, at 0 °C (ice bath) to room temperature. The reaction mixture was stirred for other 30 to 60 minutes at room temperature and was washed with an aqueous solution of K$_2$CO$_3$ (5%) (2 *x* 25 mL). The combined organic fractions were dried over anhydrous MgSO$_4$ or Na$_2$SO$_4$ and filtered. The solvent was removed by evaporation, to afford solids or oils that were further purified by recrystallization or flash chromatography on silica, as described below. Final products were dried under vacuum overnight.

N-Hydroxy-N,N'-diphenylformamidine (3a)

Compound **2a** (0.10 g, 0.51 mmol, 1 eq.) and NaHCO$_3$ (0.07 g, 0.76 mmol, 1.5 eq.) in DCM (6 mL) and *m*-CPBA (0.11 g, 0.51 mmol, 1 eq.) in DCM (6 mL) were reacted following the general procedure. An oily solid was obtained after solvent evaporation. Recrystallization in AcOEt/ hexane (1:1) at 4 °C afforded a pale-yellow oily solid. The product is sensitive to air and humidity and decomposes on silica column.

Yield: 0.02 g, 20%.

^{1}H NMR (CDCl$_3$, 300 MHz,) δ 8.38 (s, 1H, -NH-C**H**=N-), 7.64 (d, J^d = 8 Hz, 2H, C$_6$**H**$_5$), 7.43 (t, J^t = 7 Hz, 2H, C$_6$**H**$_5$), 7.35 (t, J^t = 8 Hz, 3H, C$_6$**H**$_5$), 7.15-7.07 (m, 3H, C$_6$**H**$_5$), 3.99 (bs, O**H**).

^{13}C {^{1}H} NMR (CDCl$_3$, 75 MHz) δ, ppm: 145.6, 137.9, 134.2, 129.9 (2C), 129.5 (2C), 128.4, 124.4, 119.8 (2C), 117.2 (2C).

N/A – product sensitive to air and humidity

MS (ESI-HRMS AcOEt/ hexane) (m/z): [M+H]$^+$ C$_{13}$H$_{13}$N$_2$O: *calc.* 213.1022; *found* 213.1017.

N-Hydroxy-N,N'-di(*para*-bromophenyl)formamidine (3b)

Compound **2b** (0.30 g, 0.85 mmol, 1 eq.) and NaHCO$_3$ (0.11 g, 1.2 mmol, 1.5 eq.) in DCM (25 mL) and *m*-CPBA (0.19 g, 0.85 mmol, 1 eq.) in DCM (20 mL) were reacted following the general procedure. A brown-orange oily solid was obtained after solvent evaporation. Recrystallization in AcOEt/ hexane (1:1) at -10°C afforded a pale-yellow solid. The product is sensitive to air and humidity and decomposes on silica column.

Yield: 0.04 g, 13%.

^{1}H NMR (CDCl$_3$, 400 MHz) δ 8.34 (s, 1H, -NH-C**H**=N-), 7.54 (m, 4H, C$_6$**H**$_4$), 7.45 (d, J^d = 7 Hz, 2H, C$_6$**H**$_4$), 7.01 (d, J^d = 8 Hz, 2H, C$_6$**H**$_4$).

^{13}C {^{1}H} NMR (CDCl$_3$, 101MHz) δ, ppm: 144.9, 142.2, 137.5, 132.9 (2C), 132.5 (2C), 124.4, 121.0 (2C), 118.8 (2C), 105.3.

Elemental Analysis: *calc.* (%) for C$_{13}$H$_{10}$Br$_2$N$_2$O: C 42.20, H 2.72, N 7.57; *found*: C 41.42, H 2.26, N 7.37 (product sensitive to air and humidity).

MS (ESI-HRMS DCM) (m/z): [M+H]$^+$ C$_{13}$H$_{11}$Br$_2$N$_2$O: *calc.* 368.9233; *found* 368.9240.

_N_-Hydroxy-_N,N'_-di(_para_-anisidyl)formamidine (3c)

Compound **2c** (0.10 g, 0.39 mmol, 1 eq.) and NaHCO$_3$ (0.07 g, 0.58 mmol, 1.5 eq.) in DCM (6 mL) and _m_-CPBA (0.11 g, 0.39 mmol, 1 eq.) in DCM (6 mL) were reacted following the general procedure. A brown oil was obtained after solvent evaporation. Recrystallization in AcOEt/ hexane (1:1) at 4°C afforded a pale-beige solid. The product is sensitive to air and humidity and decomposes on silica column.

Yield: 0.015 g, 15%.

^{1}H-NMR (CDCl$_3$, 300 MHz) δ 8.15 (s, 1H, -NH-C**_H_**=N-), 7.57 (d, J^d = 9 Hz, 2H, C$_6$**_H_**$_4$), 7.01 (d, J^d = 9 Hz, 2H, C$_6$**_H_**$_4$), 6.93 (d, J^d = 9 Hz, 2H, C$_6$**_H_**$_4$), 6.88 d, J^d = 9 Hz, 2H, C$_6$**_H_**$_4$), 3.83 (s, 3H, O-C**_H_**$_3$), 3.79 (s, 3H, O-C**_H_**$_3$), 3.51(bs, O**_H_**).

^{13}C {^{1}H} NMR (CDCl$_3$, 75 MHz) δ, ppm: 159.5, 156.6, 133.4, 131.5, 131.4, 121.33 (2C), 118.55 (2C), 115.22 (2C), 114.45 (2C), 55.75 (2C, -O**_C_**H$_3$)

Elemental Analysis: _calc._ (%) for C$_{15}$H$_{16}$N$_2$O$_3$: C 66.16, H 5.92, N 10.29; _found_: C 66.07, H 5.73, N 10.26 (product sensitive to air and humidity).

MS (ESI-HRMS AcOEt/ hexane) (m/z): [M+H]$^+$ C$_{15}$H$_{17}$N$_2$O$_3$: _calc._ 273.1234; _found_ 273.1238.

_N_-Hydroxy-_N,N'_-di(_para_-tolyl)formamidine (3d)

Compound **2d** (0.10 g, 0.45 mmol, 1 eq.) and NaHCO$_3$ (0.07 g, 0.67 mmol, 1.5 eq.) in DCM (6 mL) and _m_-CPBA (0.11 g, 0.39 mmol, 1 eq.) in DCM (6 mL) were reacted following the general procedure. A brown-yellow solid was obtained after solvent evaporation. Recrystallization in AcOEt/ hexane (1:1) at 4°C afforded a pale-yellow solid. The product is sensitive to air and humidity and decomposes on silica column.

Yield: 0.024 g, 22%.

^{1}H NMR (CDCl$_3$, 400 MHz) δ 8.29 (s, 1H, -NH-C**_H_**=N-), 7.54 (d, J^d = 8 Hz, 2H, C$_6$**_H_**$_4$), 7.22 (d, J^d = 8 Hz, 2H, C$_6$**_H_**$_4$), 7.14 (d, J^d = 8 Hz, 2H, C$_6$**_H_**$_4$), 6.68 d, J^d = 8 Hz, 2H, C$_6$**_H_**$_4$), 4.24(bs, O**_H_**), 2.38 (s, 3H, C**_H_**$_3$), 2.32 (s, 1H, C**_H_**$_3$).

^{13}C {^{1}H} NMR (CDCl$_3$, 75 MHz) δ, ppm: 150.8, 138.2, 136.0, 133.6, 131.8, 130.5 (2C), 129.8 (2C), 119.7 (2C), 116.9 (2C), 21.21 (1C), 20.89 (1C).

Elemental Analysis: _calc._ (%) for C$_{15}$H$_{16}$N$_2$O: C 74.97, H 6.71, N 11.66; _found_: C 74.79, H

6.68, N 11.62 (product sensitive to air and humidity).

MS (ESI-HRMS AcOEt/ hexane) (m/z): $[M+H]^+$ $C_{15}H_{17}N_2O$: *calc.* 241.1335; *found* 241.1336.

N-Hydroxy-N,N'-di(*ortho*-tolyl)formamidine (3e)

Compound **2e** (1.0 g, 4.5 mmol, 1 eq.) in DCM (30 mL)and *m*-CPBA (1.0 g, 4.5 mmol, 1 eq.) in DCM (20 mL) were reacted following the general procedure modified as follows: the reaction temperature was -10 °C (ice/ MeOH bath) to r.t. and diisopropylethylamine (DIPEA) (0.78 mL, 4.5 mmol, 1 eq.) was added. The base used for washing was KOH aq. (5%) (2 *x* 20 mL). An oily solid (brown) was obtained after solvent evaporation. Purification by flash chromatography on silica (gradient of eluants: AcOEt 100%, AcOEt/ MeOH (9:1)) yielded a pale yellow oily solid, which was dried under vacuum overnight.

Yield: 0.45 g, 41%.

^{1}H NMR (CDCl$_3$, 400MHz) δ 7.99 (s, 1H, -NH-C***H***=N-), 7.36-7.28 (m, 4H, C$_6$***H***$_4$), 7.23 (d, J^d = 8 Hz, 1H, C$_6$***H***$_4$), 7.18 (td, J^{td} = 8, 1 Hz, 1H, C$_6$***H***$_4$), 7.01 (td, J^{td} = 7.7, 1 Hz, 1H, C$_6$***H***$_4$), 6.96 (d, J^d = 8 Hz, 1H, C$_6$***H***$_4$), 2.46 (s, 3H, C***H***$_3$), 2.40 (s, 3H, C***H***$_3$).

^{13}C {^{1}H} NMR (CDCl$_3$, 75 MHz) δ, ppm: 152.75, 147.75, 136.25, 133.99, 131.55, 131.49, 130.79, 130.62, 129.58, 127.24, 126.76, 125.03, 123.93, 77.00, 17.53, 17.51.

N/A (product sensitive to air and humidity)

MS (ESI-HRMS AcOEt/ hexane) (m/z): $[M+H]^+$ $C_{15}H_{17}N_2O$: *calc.* 241.1335; *found* 241.1340.

N-Hydroxy-N,N'-bis(2-isopropylphenyl)formamidine (3f)

Compound **2f** (2.0 g, 7.1 mmol, 1 eq.) and NaHCO$_3$ (0.61 g, 7.1 mmol, 1 eq.) in DCM (50 mL) and *m*-CPBA (1.6 g, 7.1 mmol, 1 eq.) in DCM (50 mL) were reacted following the general procedure with modified reaction temperature: -10 °C (ice/ MeOH bath) to r.t. After purification by flash chromatography on silica (gradient of eluants: hexane/ AcOEt (2:8), AcOEt/ MeOH (9:1), DCM 100%) and recrystallization in hot hexane, a colorless solid was obtained.

Yield: 0.92 g, 58%

^{1}H-NMR (CDCl$_3$, 300 MHz) δ, ppm: 7.93 (s, 1H, -NH-C***H***=N-), 7.45-7.39 (m, 2H, -C$_6$***H***$_4$), 7.34-7.31 (m, 2H, , -C$_6$***H***$_4$), 7.28-7.08 (m, 3H, -C$_6$***H***$_4$), 6.96 (d, J^d = 8 Hz, 1H, -C$_6$***H***$_4$), 3.67 (bs,

O$\boldsymbol{H}$), 3.40 (sept, J^{sept} = 7 Hz, 1H, -C$\boldsymbol{H}$(CH$_3$)$_2$), 3.27 (sept, J^{sept} = 7 Hz, 1H, –C$\boldsymbol{H}$(CH$_3$)$_2$), 1.33-1.29 (m, 12H, -CH(C$\boldsymbol{H}$)$_2$)

^{13}C {^{1}H} NMR (CDCl$_3$, 75 MHz) δ, ppm: 145.0, 142.1, 137.4, 136.2, 135.3, 130.1, 127.1, 127.0, 126.7, 126.7, 125.5, 124.3, 116.2, 28.12, 27.61, 24.27 (2C), 23.08 (2C).

Elemental Analysis: *calc.* (%) for C$_{19}$H$_{24}$N$_2$O: C 76.99, H 8.16, N 9.45; *found*: C 76.80, H 8.23, N 9.40.

MS (ESI-HRMS DCM) (m/z): [M+H]$^+$ C$_{19}$H$_{25}$N$_2$O: *calc.* 297.1961; *found* 297.1971.

N-Hydroxy-N,N'-bis(2-diphenyl)formamidine (3g)

Compound **2g** (1.5 g, 4.3 mmol, 1 eq.) and NaHCO$_3$ (0.38 g, 4.3 mmol, 1 eq.) in DCM (50 mL) and *m*-CPBA (0.96 g, 4.3 mmol, 1 eq.) in DCM (50 mL) were reacted following the general procedure with modified reaction temperature: -10 °C (ice/ MeOH bath) to r.t.. After purification by flash chromatography on silica (gradient of eluants: hexane/ AcOEt (2:8), AcOEt/ MeOH (9:1), DCM 100%) and recrystallization in DCM/ hexane (1:1), a colorless solid was obtained.

Yield: 0.93 g, 59%.

^{1}H-NMR (CDCl$_3$, 400 MHz) δ, ppm: δ 7.85 – 7.78 (m, 1H, -C$_6$$\boldsymbol{H}$$_4$), 7.55 – 7.32 (m, 14H, -C$_6$$\boldsymbol{H}$$_5$, -C$_6$$\boldsymbol{H}$$_4$, and -NH-C$\boldsymbol{H}$=N-), 7.21 (dd, J = 7, 2 Hz, 1H, -C$_6$$\boldsymbol{H}$$_4$), 7.11 (td, J = 8, 2 Hz, 1H, -C$_6$$\boldsymbol{H}$$_4$), 7.05 (td, J = 7, 1 Hz, 1H, -C$_6$$\boldsymbol{H}$$_4$), 6.17 (d, J = 8 Hz, 1H, -C$_6$$\boldsymbol{H}$$_4$)., 3.67 (bs, O$\boldsymbol{H}$).

^{13}C {^{1}H} NMR (CDCl$_3$, 75 MHz) δ, ppm: 142.0, 138.2, 137.5, 136.9, 135.7, 135.2, 131.7, 131.40, 130.7, 129.4 (2C), 129.24 (2C), 129.19 (2C), 129.1 (2C), 128.8, 128.6, 128.5 (2C), 128.3, 128.1, 126.1, 123.7, 115.4.

Elemental Analysis: *calc.* (%) for C$_{25}$H$_{20}$N$_2$O: C 82.39, H 5.53, N 7.69; *found*: C 82.33, H 5.52, N 7.73

MS (ESI-HRMS DCM) (m/z): [M+H]$^+$ C$_{25}$H$_{21}$N$_2$O: *calc.* 365.1648; *found* 365.1655

N-Hydroxy-N,N'-bis(2,6-dimethyl)formamidine (3h)

Compound **2h** (1.0 g, 4.0 mmol, 1 eq.) in DCM (20 mL) and *m*-CPBA (0.89 g, 4.0 mmol, 1 eq.) in DCM (20 mL) were reacted following the general procedure with modified reaction time (15 – 30 min) and without using NaHCO$_3$. After recrystallization in DCM/ hexane (1:1)

at -10 °C, a colorless solid was obtained.

Yield: 0.98 g, 92%.

^{1}H-NMR (CDCl$_3$, 400 MHz) δ 7.34 (s, 1H, -NH-CH=N-), 7.20 (t, J^{t} = 8 Hz 1H, -C$_6$$H_3$), 7.15-7.06 (m, 5H, -C$_6$$H_3$), 3.51 (bs, OH), 2.38 (d, J^{d} = 3 Hz, 12H, -CH_3)

^{13}C {^{1}H} NMR (CDCl$_3$, 75 MHz) δ, ppm: 142.1, 140.4, 135.8, 134.8 (2C), 133.4, 129.3, 129.0 (2C), 128.6 (2C), 126.7, 18.81 (2C), 17.26 (2C).

Elemental Analysis: *calc.* (%) for (C$_{17}$H$_{20}$N$_2$O)$_2$CH$_2$Cl$_2$: C 67.62, H 6.81, N 9.01; *found*: C 68.19, H 6.81, N 9.00.

MS (ESI - DCM) (m/z): 269.2 [M+H]$^{+}$ (100%).

N-Hydroxy-N,N'-bis(2,6-diisopropylphenyl)formamidine (3i)

Compound **2i** (1.5 g, 4.1 mmol, 1eq.) in DCM (10 mL) and *m*-CPBA (0.9 g, 4.1 mmol) in DCM (40 mL) were reacted following the general procedure with modified reaction time (15 – 30 min) and without using NaHCO$_3$. The green-white solid obtained after solvent evaporation was taken in EtOH, as the formamidine **2i** has low solubility in this solvent. After filtration, EtOH evaporation, and drying under vacuum, a pale-yellow solid was obtained.

Yield: 1.4 g, 88%

^{1}H-NMR (CDCl$_3$, 300 MHz) δ, ppm: 7.39 – 7.32 (m, 1H, C$_6$$H_3$), 7.32 – 7.26 (m, 1H, C$_6$$H_3$), 7.25 – 7.21 (m, 2H, C$_6$$H_3$ and -NH-CH=N-), 7.20 (d, J^{d} = 2 Hz, 2H, C$_6$$H_3$), 7.18 (d, J^{d} = 1 Hz, 1H, C$_6$$H_3$), 3.37 (sept, J^{sept} = 7 Hz, 2H, –CH(CH$_3$)$_2$), 3.25 (sept, J^{sept} = 7 Hz, 2H, –CH(CH$_3$)$_2$), 1.37 (d, J^{d} = 7 Hz, 6H, -CH(CH_3)$_2$), 1.23 (d, J^{d} = 7 Hz, 12H, -CH(CH_3)$_2$), 1.18 (d, J^{d} = 7 Hz, 6H, -CH(CH_3)$_2$).

^{13}C {^{1}H} NMR (CDCl$_3$, 75 MHz) δ, ppm: 146.6, 146.0, 141.7, 133.2, 132.5, 130.6, 128.8 (2C), 124.8 (2C), 124.7 (2C), 29.28 (2C) 29.1 (2C), 25.98 (2C), 25.05 (2C), 24.87 (4C).

Elemental Analysis: *calc.* (%) for C$_{25}$H$_{36}$N$_2$O: C 78.90, H 9.53, N 7.36; *found*: C 78.79, H 9.43, N 7.21

MS (ESI - DCM) (m/z): 381.3 [M+H]$^{+}$ (100%)

m.p. 165-167 °C.
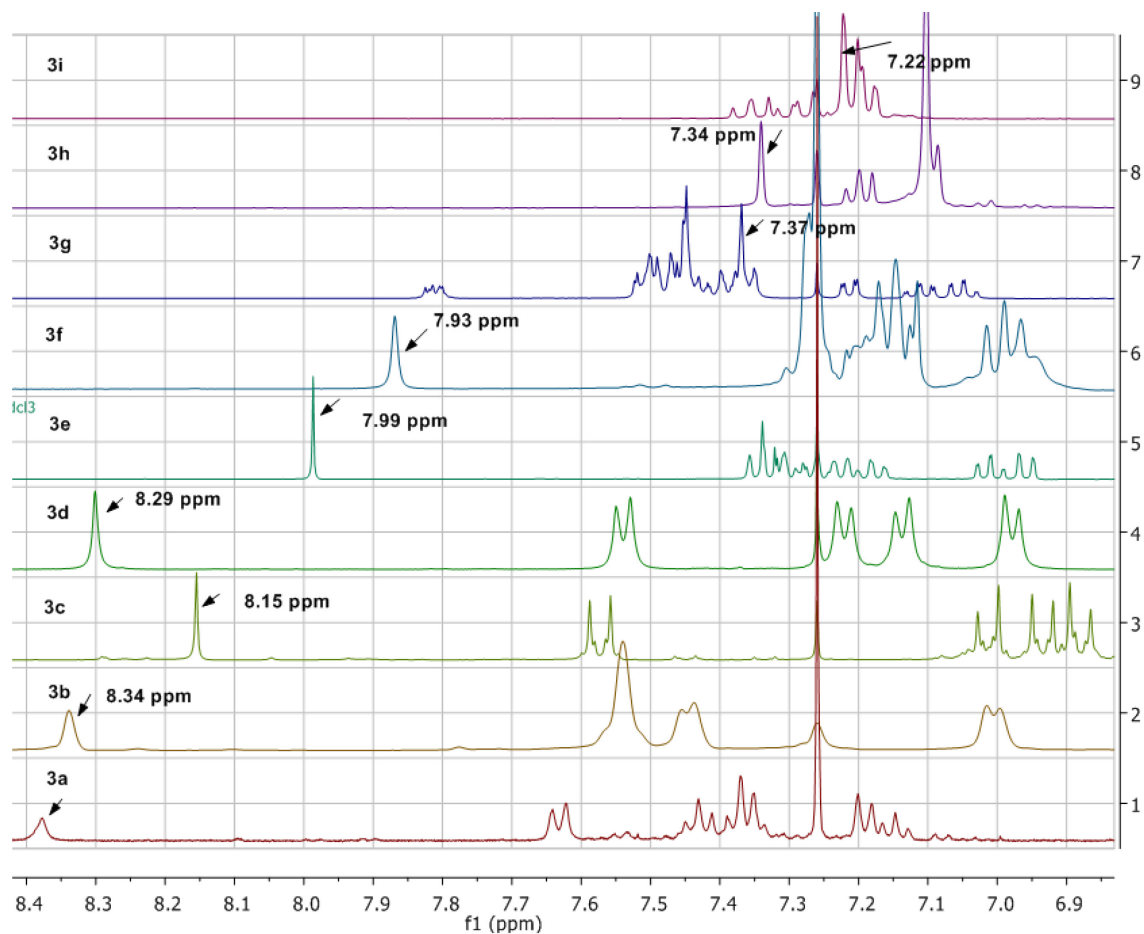
Figure S1 ^{1}H NMR (CDCl$_3$) (aromatic region) of compounds **3a-i**: function of the substitution on *N,N'*-aryl rings, the shielding of formamidine H increases in the series **3i**, **3h**, **3g**, **3f**, **3e**, **3c**, **3d**, **3b**, **3a**.

NMR-¹H CDCl₃ 400 MHz

NMR-¹H CDCl₃ 300 MHz
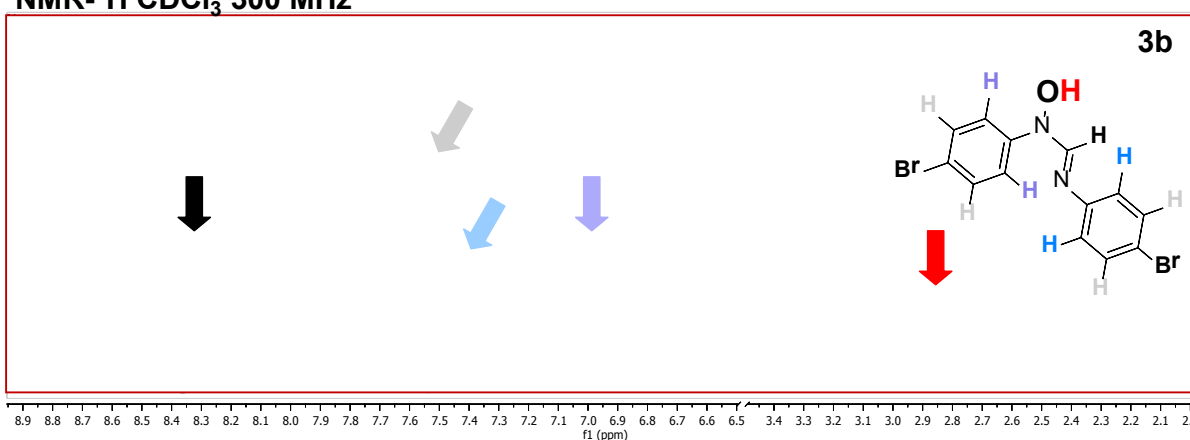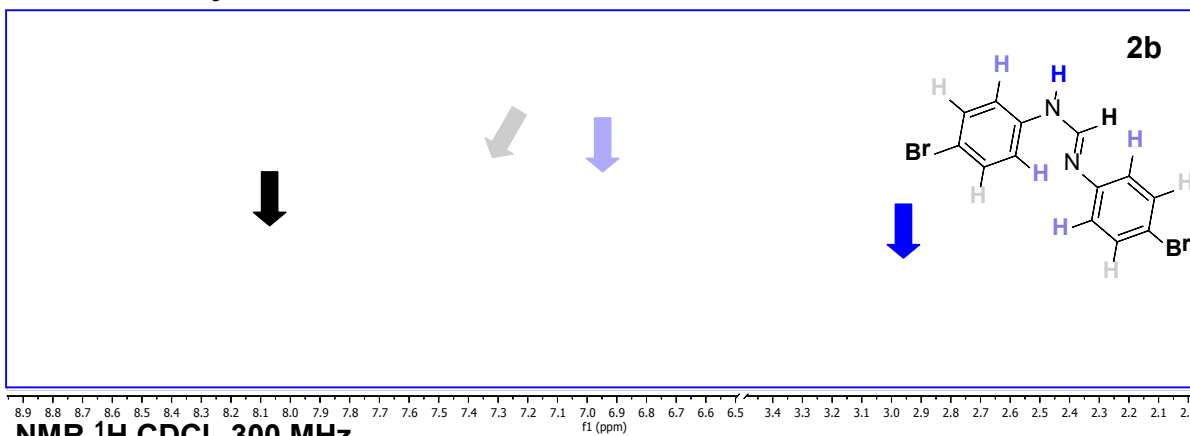
Figure S2 ^{1}H NMR (CDCl₃) of the compounds **2b** vs. **3b** as example of a common feature in the ^{1}H NMR of the hydroxyamidines vs. their corresponding amidines: the splitting of the signals due to the asymmetry introduced in the molecule by the presence of the hydroxyl group.

References

[1]   a) Hirano, K.; Urban, S.; Wang, C.; Glorius, F. *Org. Lett.* **2009**, *11*, 1019. b) Krahulic, K. E.; Enright, G. D.; Parvez, M.; Roesler, R. *J. Am. Chem. Soc.* **2005**, *127*, 4142. c) Roberts, R. M. *J. Org. Chem.* **1949**, 14, 277. d) Cole, M. L.; Deacon, G. B.; Forsyth, C. M.; Konstas, K.; Junk, P. C. *Dalton Trans.* **2006**, *27*, 3360. e) Cole, M. L.; Junk, P. C.; Louis, L. M. *Dalton Trans.* **2002**, *20*, 3906

[2]   Harding, P.; Harding, D. J.; Adams, H.; Youngme, S. *Synth. Commun.* **2007**, *37*, 2655

Appendix-3.2-SI

Supporting Information

for

Synthesis and Crystal Structure of a Rare Square-Planar Co(II) Complex of a Hydroxyamidinate Ligand

Mihaela Cibian, Sofia Derossi, and Garry S. Hanan*

Département of Chemistry, Université de Montréal, Montréal, Québec, H3T-1J4, Canada

Contents

1) Materials and Instrumentation

Nuclear magnetic resonance (NMR) spectra were recorded in $CDCl_3$ at room temperature (r.t.) on the following spectrometers: Bruker AV-400, AV-300, DRX-400, and ARX-300 MHz. Chemical shifts (δ) are reported in part per million (ppm) relative to TMS, using the residual solvent protons (7.26 ppm) as reference. Absorption spectra were measured in DCM at r.t. on a Cary 500i UV-Vis-NIR Spectrophotometer. Electrochemical measurements were carried out in argon-purged dry DCM at room temperature with a BAS CV50W multipurpose equipment interfaced to a PC. The working electrode was a glassy carbon electrode. The counter electrode was a Pt wire, and the pseudo-reference electrode was a silver wire. The reference was set using an internal 1 mM ferrocene/ferrocinium sample at 475 mV vs. SCE in DCM. The concentration of the compounds was about 1 mM. Tetrabutylammonium hexafluorophosphate (TBAP) was used as supporting electrolyte and its concentration was 0.10 M. Cyclic voltammograms were obtained at scan rates of 50, 100, 200, and 500 mV/s. For irreversible oxidation processes, the cathodic peak was used as E. Accurate mass measurements were performed on a LC-MSD-Tof instrument from Agilent Technologies in positive electrospray. For the ligand, aliquots of 0.1 uL were injected into the mass spectrometer using a 0.5 mL/min flow of 75% methanol/ 25% water mixture. The capillary voltage was set at 3000 V and mass spectra were acquired from 100 to 3000 m/z. Protonated molecular ions $[M+H]^+$ were used for empirical formula confirmation. For the complex, the sample was infused into the mass spectrometer at a flow rate of 20 uL/min, the capillary voltage was set at 3500 V, and mass spectra were acquired from 105 to 3200 m/z. Both the molecular ion $[M]^+$ and the sodium adduct $[M+Na]^+$ were used for empirical formula confirmation. The microanalyses were done by the Elemental Analysis Service at Université de Montréal. Solvents, purchased from VRW and Fisher, were removed under reduced pressure using a rotary evaporator, unless otherwise stated. The m-CPBA from Acros Organics and the aniline, triethylorthoformate, and metal salt from Aldrich, were used without further purification.

2) Experimental procedure for compounds **2** and **3**

***N*-Hydroxy-*N,N'*-bis(2,6-dimethyl)formamidine** (**2**): A solution of *m*-CPBA (0.89 g, 4.0 mmol, 1 eq.) in DCM (20 mL) was added drop-wise by addition funnel to a solution of compound **1** (1.0 g, 4.0 mmol, 1 eq.) in DCM (20mL) at 0 °C (ice bath). The reaction mixture was allowed to warm to room temperature and was stirred for other 30 minutes and then was washed with an aqueous solution of K_2CO_3 (5%) (2 *x* 25 mL). The combined organic fractions were dried over anhydrous $MgSO_4$ and filtered. The solvent was removed by evaporation to afford a solid that was further purified by recrystallization in DCM/ hexane (1:1) at -10 °C. A colorless solid was obtained and was dried under vacuum overnight.

Yield: 0.98 g, 92%. ^{1}H-NMR (CDCl$_3$, 400 MHz) δ 7.34 (s, 1H, -NH-C***H***=N-), 7.20 (t, J^t = 8 Hz 1H, -C6***H***3), 7.15-7.06 (m, 5H, -C6***H***3), 3.51 (bs, OH), 2.38 (d, J^d = 3 Hz, 12H, C***H***3). ^{13}C {1H} NMR (CDCl$_3$, 75 MHz) δ, ppm: 142.1, 140.4, 135.8, 134.8 (2C), 133.4, 129.3, 129.0 (2C), 128.6 (2C), 126.7, 18.81 (2C), 17.26 (2C). Elemental Analysis: *calc.* (%) for $C_{17}H_{20}N_2O\_0.5CH_2Cl_2$: C 67.62, H 6.81, N 9.01; *found*: C 68.19, H 6.81, N 9.00. MS (ESI - DCM) (m/z): 269.2 [M+H]$^+$ (100%).

Bis(*N*-hydroxy-*N,N'*-Bis(2,6-dimethylphenyl)formamidinate)cobalt(II) (3): A solution of the ligand **2** (0.10 g, 0.37 mmol, 2 eq.) in aq. EtOH 90% was slowly added to a solution of metal salt Co(OAc)$_2$·4H$_2$O (0.046 g, 0.19 mmol, 1 eq.) in water. The formation of a green precipitate is observed almost instantly. After stirring for 90 min. at r.t., water was added and the reaction mixture was kept at 4°C for 2 h, before being filtered. The resulted solid was washed with hot water and aq. EtOH 50%, and was taken in DCM and dried over MgSO$_4$. A second filtration and solvent evaporation yielded the desired product as a green X-ray quality crystals obtained by slow diffusion of hexane in DCM at -10 °C.

Yield: 0.090 g, 81%. ^{1}H NMR paramagnetic compound Co(II) d^7: (CDCl$_3$, 300 MHz) δ, ppm: 47,39; 36,92; 23,20; 7,28; -0,31; -5,62; -45,38; -50,84. IR (ATR, solid sample, cm^{-1}) 3008, 2968, 2947, 2913, 2851, 1601, 1578, 1466, 1269, 1227, 1202, 1092, 987, 928, 918, 892, 821, 777, 755, 741, 694, 639, 527, 497, 488. Elemental Analysis: calc. (%) for $C_{34}H_{38}CoN_4O_2$: C 68.79, H 6.45, N 9.44; found: C 68.52, H 6.42, N 9.27. MS (ESI-HRMS DCM − no acid) (m/z): [M]$^+$ $C_{34}H_{38}CoN_4O_2$: calc. 593.2321; found 593.2305. [M+Na]$^+$ $C_{34}H_{38}CoN_4NaO_2$:

calc. 616.2219; found 616.2212. UV-vis: (DCM, 5 x 10^{-4} M) [λ, nm (ε, $M^{-1}cm^{-1}$)]: 540 (79), 622 (12), 942 (29), 1233 (27). E-chem (values vs. SCE) (in 0.1 M TBAPF$_6$ in DCM; scan rate is 100 mV s^{-1}) Co$^{II/III}$, +0.47 V (r); ligand, +1.70 V (irr); no reduction observed.

Figure S1 The ^{1}H NMR of **3** in CDCl$_3$ showing a characteristically expanded paramagnetic spectrum (50 to -50 ppm) in line with the oxidation state of the metal (Co^{II}, d^7) and the tentative assignation of the signals (impurities and/or solvents are marked with an asterisk).
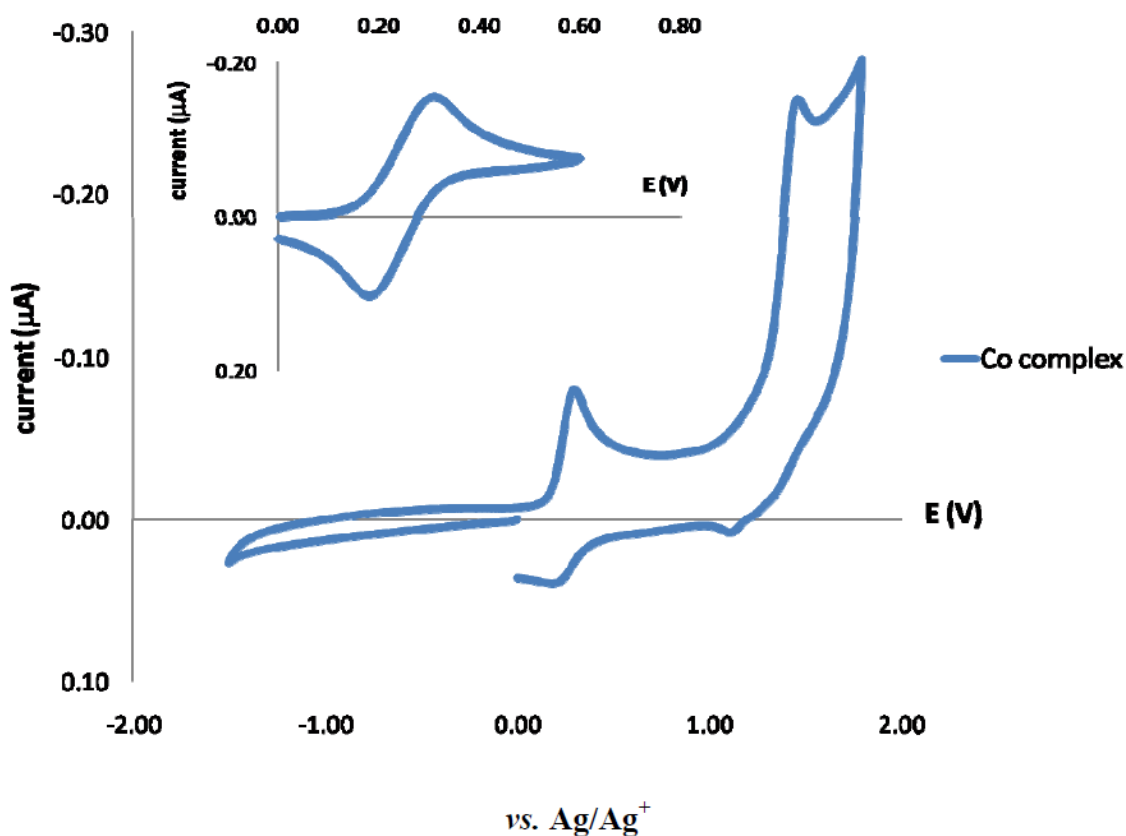
Figure S2 The CV of **3** showing the reversible oxidation of metal (+0.47 V *vs.* SCE) and the irreversible oxidation of the ligand (+1.70 V *vs.* SCE) (the plot is *vs.* Ag/Ag$^+$); conditions: 0.1 M TBAPF$_6$ in DCM, scan rate 100 mV s^{-1}, [complex] = 1 mM.

Table S1. Selected geometric parameters for compound **3** (in Å and °)

Co1-O1	1.8341(9)	O1-Co1-N2	84.5(1)
Co1-N2	1.8856(11)	N1-O1-Co1	111.5(1)
N1-O1	1.392(2)	N1-Co1-N2	116.8(3)
C1-N1	1.319(2)	C1-N1-O1	115.1(2)
C1-N2	1.312(2)	N2-Co1-O1-N1	179.0(1)
N1-C11	1.428(2)	Co1-N2-C1-N1	1.3(2)
N2-C21	1.430(2)	Co1-O1-N1-C11	177.0(1)
C26-C16	1.395(2)	O1-Co1-N2-C21	178.5(2)

Table S2. Crystal data and structure refinement for compound **3**

Empirical formula	C39 H43 Co N5 O2
Formula weight	672.71
Temperature	200K
Wavelength	0.71073 Å
Crystal system	Monoclinic
Space group	C2/c
Unit cell dimensions	$a = 10.3179(19)$ Å $\alpha = 90°$
	$b = 29.712(5)$ Å $\beta = 125.309(8)°$
	$c = 14.5167(19)$ Å $\gamma = 90°$
Volume	3631.7(10) Å^3
Z	4
Density (calculated)	1.230 g/cm^3
Absorption coefficient	0.512 mm^{-1}
F(000)	1420
Crystal size	0.09 x 0.07 x 0.03 mm
Theta range for data collection	1.37 to 27.49°
Index ranges	$-13 \leq h \leq 13$, $-38 \leq k \leq 38$, $-18 \leq l \leq 18$
Reflections collected	37392
Independent reflections	4187 [Rint = 0.103]
Absorption correction	Semi-empirical from equivalents
Max. and min. transmission	0.9848 and 0.7078
Refinement method	Full-matrix least-squares on F^2
Data / restraints / parameters	4187 / 0 / 218
Goodness-of-fit on F^2	1.042
Final R indices [I>2sigma(I)]	$R_1 = 0.0587$, $wR_2 = 0.1475$
Largest diff. peak and hole	$R_1 = 0.1169$, $wR_2 = 0.1744$
R indices (all data)	0.828 and -0.273 e/Å^3
Largest diff. peak and hole	

Table S3. Crystal data and structure refinement for compound **4**

Empirical formula	C39 H43 Co N5 O2
Formula weight	672.71
Temperature	200K
Wavelength	0.71073 Å
Crystal system	Monoclinic
Space group	C2/c
Unit cell dimensions	$a = 10.3179(19)$ Å $\alpha = 90°$
	$b = 29.712(5)$ Å $\beta = 125.309(8)°$
	$c = 14.5167(19)$ Å $\gamma = 90°$
Volume	3631.7(10) Å^3
Z	4
Density (calculated)	1.230 g/cm^3
Absorption coefficient	0.512 mm^{-1}
F(000)	1420
Crystal size	0.09 x 0.07 x 0.03 mm
Theta range for data collection	1.37 to 27.49°
Index ranges	$-13 \leq h \leq 13, -38 \leq k \leq 38, -18 \leq l \leq 18$
Reflections collected	37392
Independent reflections	4187 [Rint = 0.103]
Absorption correction	Semi-empirical from equivalents
Max. and min. transmission	0.9848 and 0.7078
Refinement method	Full-matrix least-squares on F^2
Data / restraints / parameters	4187 / 0 / 218
Goodness-of-fit on F^2	1.042
Final R indices [I>2sigma(I)]	R$_1$ = 0.0587, wR$_2$ = 0.1475
Largest diff. peak and hole	R$_1$ = 0.1169, wR$_2$ = 0.1744
R indices (all data)	0.828 and -0.273 e/Å^3
Largest diff. peak and hole	

Table S4. Selected geometric parameters for compound **4** (in Å and º)

Co1-O1	1.954(2)	N1-C11	1.425(4)
Co1-N2	2.126(2)	N2-C21	1.426(4)
Co1-N5	2.090(4)	O1-Co1-N2	97.21(9)
N1-O1	1.383(3)	N1-O1-Co1	112.32(17)
C1-N1	1.321(4)	O1-Co1-N5	110.20(8)
C1-N2	1.296(4)	C1-N1-O1	118.0(3)

Appendix-3.3-SI

Supporting Information

for

Influence of Ligand Substitution Pattern on Structure in Cobalt(II) Complexes of Bulky *N,N'*-Diarylformamidinate *N*-Oxides

Mihaela Cibian, Sophie Langis-Barsetti, Fernanda Gomes de Mendonça, Sammy Touaibia, Sofia Derossi, Denis Spasyuk, and Garry S. Hanan*

Département of Chemistry, Université de Montréal, Montréal, Québec, H3T-1J4, Canada

Contents

2a-c

a $R_1 = R_2 = Me$
b $R_1 = R_2 = iPr$
c $R_1 = iPr; R_2 = H$

Scheme S1. Structure of **2a-c** with notation of the protons.

1HC:/Users/admin/Documents/Chemistry/RMN/Co-article/T1/gsh-mc-CIBM-225_T1/gsh-mc-CIBM-225/1/fid
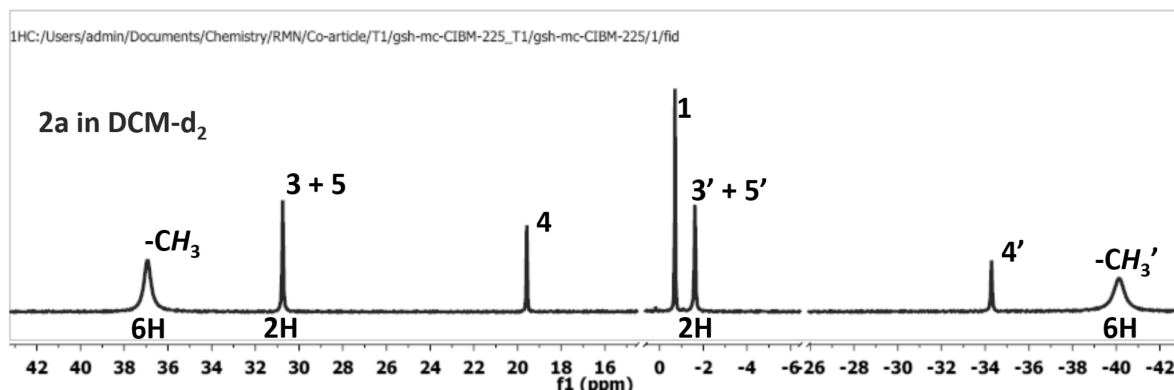
2a in DCM-d$_2$

Figure S1. a) ^{1}H-NMR spectra for **2a** in DCM-d$_2$ (tentative assignment based on the integration ratio, 2D COSY and T1 relaxation time measurement experiments, and proximity of the proton to the paramagnetic metallic centre).

gsh-cibmslb07-f-DCM.1.fid
C:/Users/Mihaela/Desktop/MC/Co/gsh-cibmslb07-f-DCM/1/fid
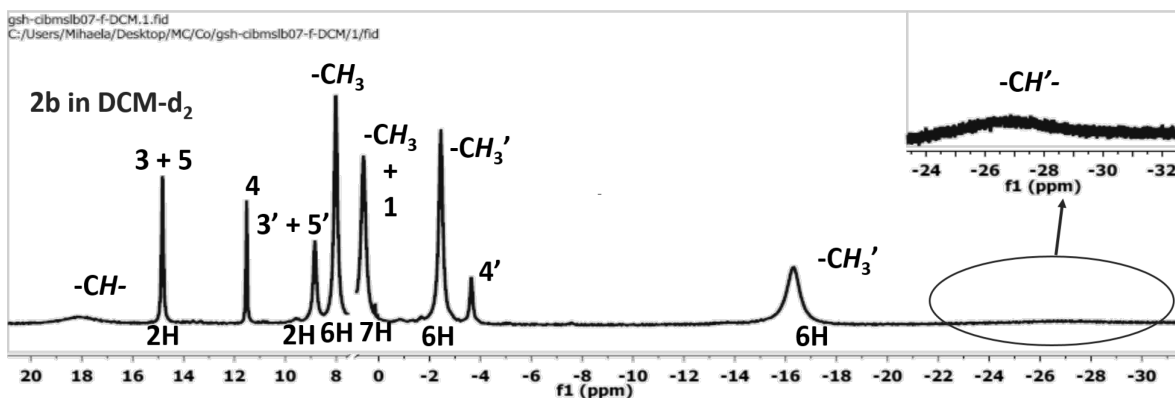
2b in DCM-d$_2$

Figure S1. b) ^{1}H-NMR spectra for **2b** in DCM-d$_2$ (tentative assignment based on the integration ratio, 2D COSY and T1 relaxation time measurement experiments, and proximity of the proton to the paramagnetic metallic centre).

gsh-dbm320.1.fid
H:/RMN/Co_complexes/gsh-cibm320/1/fid
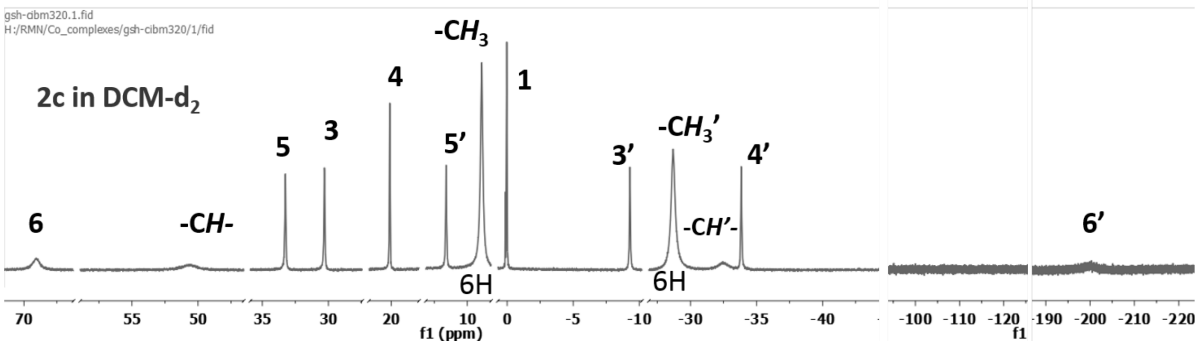
2c in DCM-d$_2$

Figure. S1. c) ^{1}H-NMR spectra for **2c** in DCM-d$_2$ (tentative assignment based on the integration ratio, 2D COSY and T1 relaxation time measurement experiments, and proximity of the proton to the paramagnetic metallic centre).
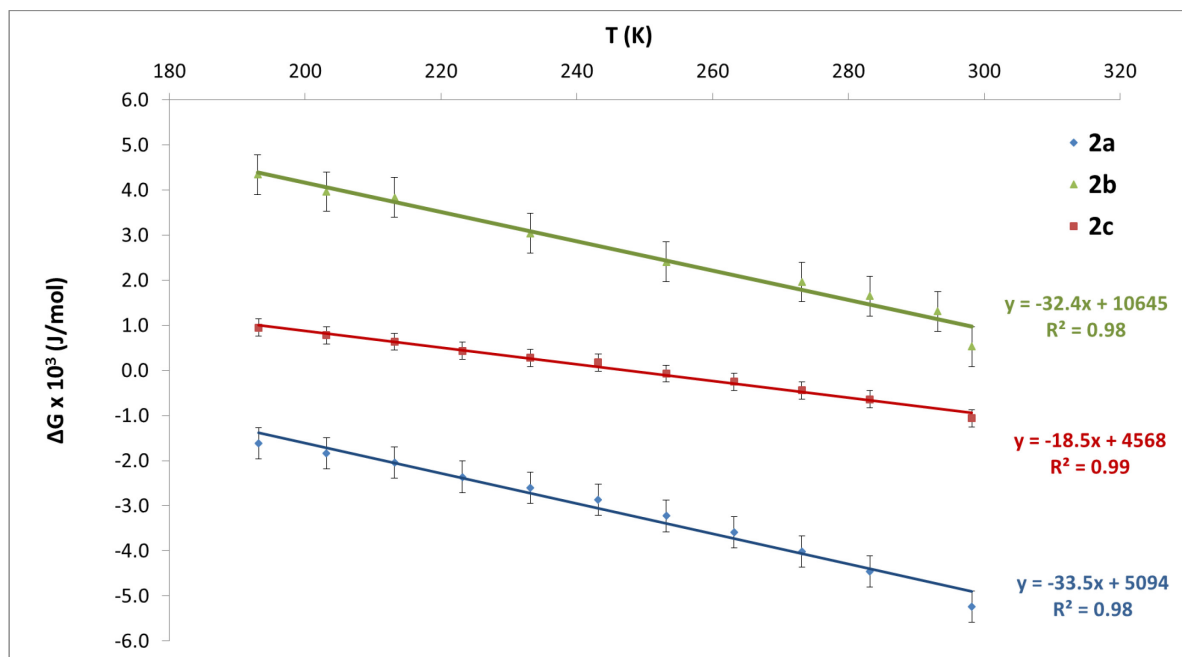
Figure S2. Determination of thermodynamic parameters. Changes in free energy are plotted versus temperature. They were determined from variation in magnetic susceptibility (magnetic moments) with temperature (see Fig. S3). Using $\Delta G = \Delta H - T\Delta S$, the changes in enthalpy (ΔH) and entropy (ΔS) are obtained from the least square fit of ΔG *vs.* T. Errors are estimated as follows: ±4% for the magnetic moments; ±15% for ΔG values (considering an error of 10% on the magnetic moment assumed for the pure tetrahedral form (eq. 2 in the article); ±18% for ΔH and ΔS values.
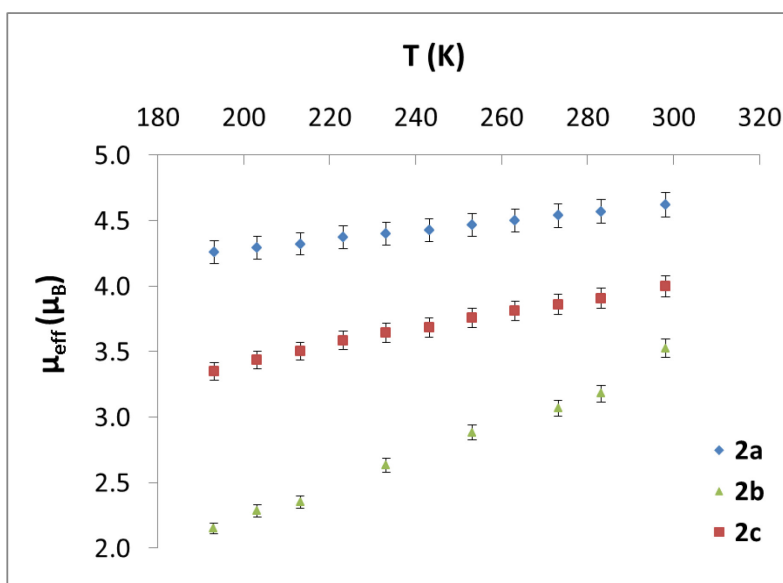
Figure S3. Plots of the magnetic moments vs. temperature for **2a-c**. Measurements were

performed by Evans' method in CD_2Cl_2 (10% v/v TMS), at variable temperature (193–298 K). Magnetic moments were calculated using: $\mu = 0.0618(\Delta\upsilon T/2fM)^{1/2}$, where $\Delta\upsilon$ is the difference in frequency (Hz) between the reference signals, T is the absolute temperature, M is the molar concentration of the sample, and f is the frequency (MHz) of the spectrometer.[1] The standard diamagnetic corrections using Pascal constants were applied,[2] as well as corrections for the change in solvent density with temperature.[3, 4] Error on the determined values is estimated at ± 4%.
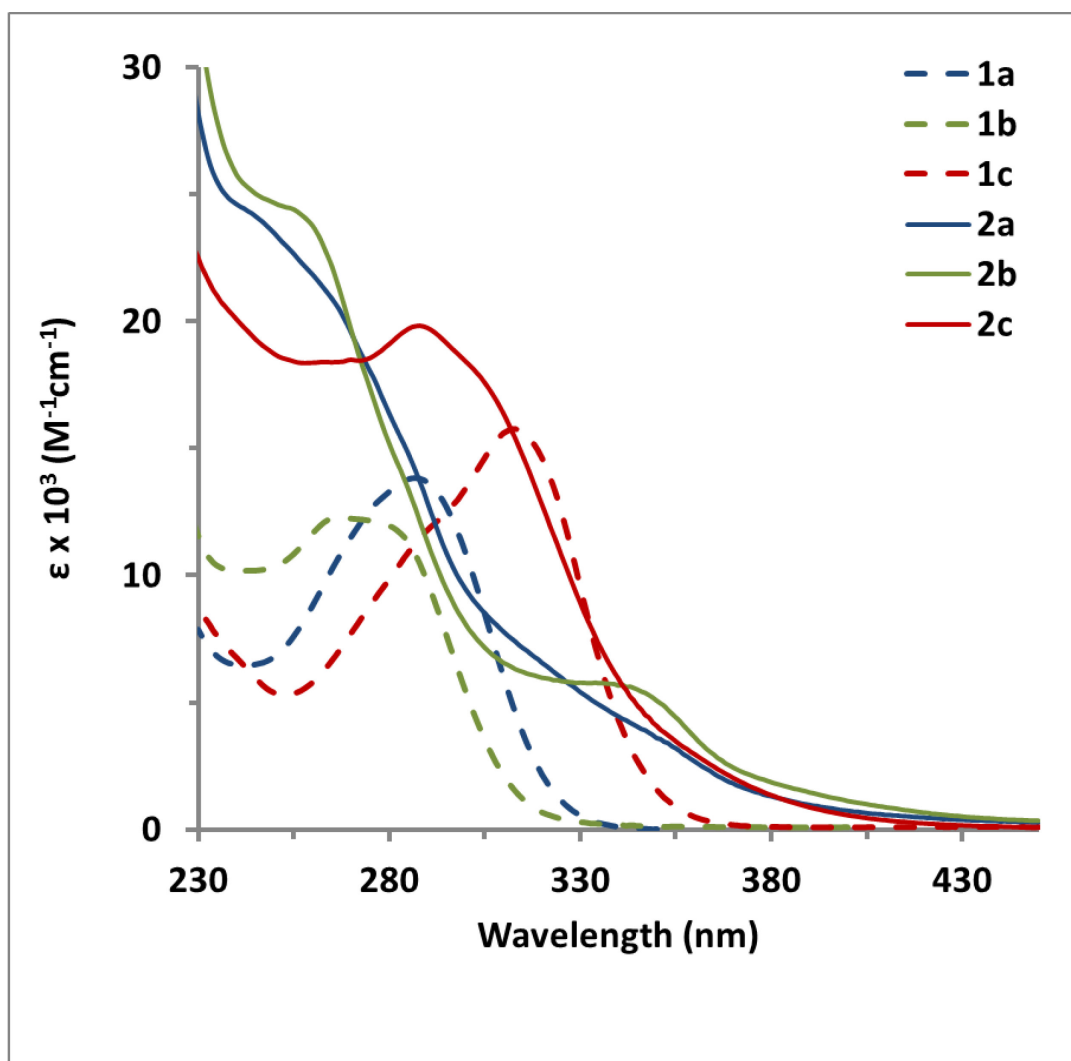
Figure S4. UV-vis absorption spectra for AMOX ligands **1a-c** and Co(AMOX)$_2$ complexes **2a-c** (in DCM)
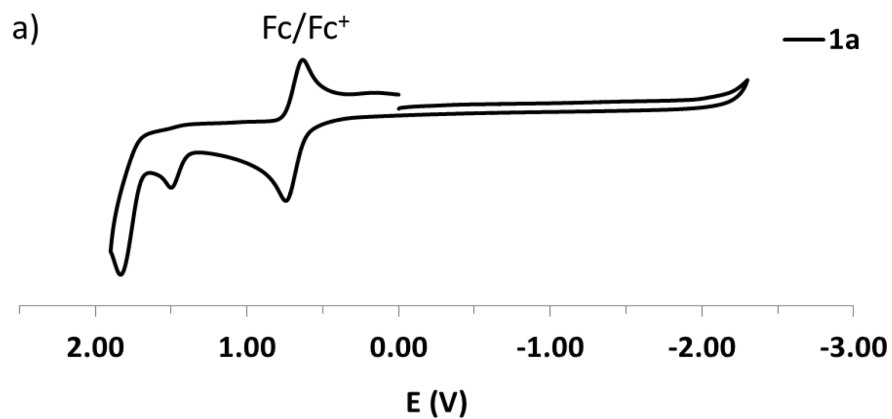
Figure S5. a) Cyclic voltammogram of **1a i**n dry DMF; scan rate of 100 mV/s; potential *vs.* silver wire; in [nBu$_4$N]PF$_6$ 0.1M, compound concentration about 1mM, glassy carbon electrode, room temperature, Ar atmosphere.
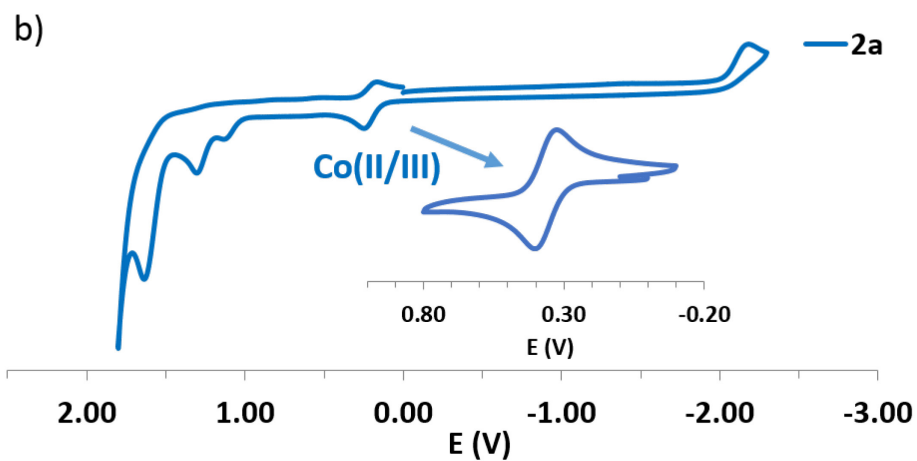
Figure S5. b) Cyclic voltammogram of **2a i**n dry DMF; scan rate of 100 mV/s; potential *vs.* silver wire; (same conditions as in **a)**)
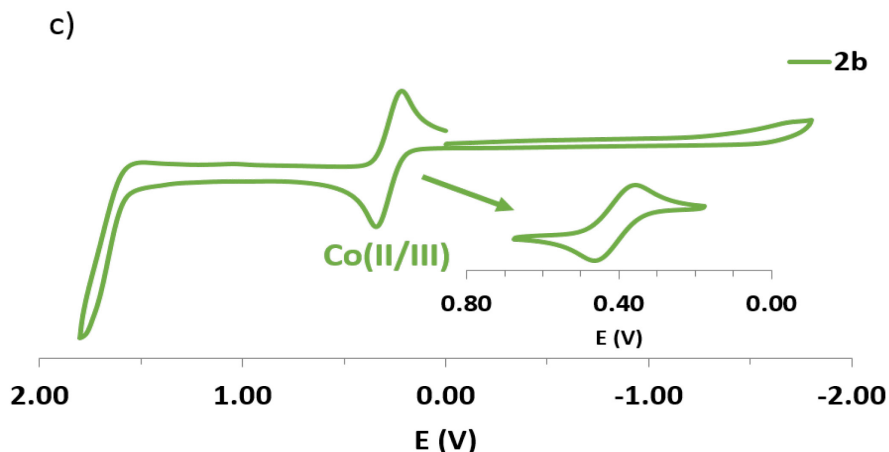
Figure S5. c) Cyclic voltammogram of **2b** in dry DCM; scan rate of 100 mV/s; potential *vs.* silver wire; (same conditions as in **a)**)

DFT calculations

As previously reported,[5] uB3LYP/ LANL2DZ[6-9] level of theory gives close agreement with the experimental trends in systems of the type studied herein. This combination of functional and basis set and CPCM CH_2Cl_2 solvatation model were used in the present study. In our case, the calculation results reporduced the experimental observation for **2a** (preference for tetrahedral form). For **2b**, the energy comparison between the two isomers (**2b-sqpl** and **2b-tetra**) is unfortunately inconclusive, as the **2b-sqpl** was not successfully optimized to its minimum. The optimization of the structure was started from the cif and fully converged, but the frequency calculation gives always one imaginary frequency despite our efforts to use very tight convergence criteria and/ or to manually displace the atoms in the direction of the vibration and reoptimize the structure.

Table S1. Total energy values for the optimized structures of the two isomers (square-planar – multiplicity doublet, and tetrahedral – multiplicity quadruplet) of **2a** and **2b**. Single point calculations at theory level: uB3LYP/ genecp LANL2DZ ECP (Co), 6311-G(d,p) (C, H, N, O), CPCM: CH_2Cl_2, were ran on the structures optimized at uB3LYP/LANL2DZ (all atoms), CPCM: CH_2Cl_2

Cpd.	Total energy (E)		
	a. u	kcal mol^{-1}	kJ mol^{-1}
2a-sqpl	-1833.49163259	-1.149582E+06	-4.813832E+06
2a-tetra	-1833.49846599	-1.149587E+06	-4.813850E+06
2b-sqpl*	-2462.65289562	-1.544061E+06	-6.465695E+06
2b-tetra	-2462.65837081	-1.544064E+06	-6.465710E+06
ΔE_{2a} $(E_{2a-sqpl} - E_{2a-tetra})$	**0.0068**	**4.3**	**18**
ΔE_{2b}* $(E_{2b-sqpl} - E_{2b-tetra})$	**0.0055***	**3.4***	**14***
* Note: *the optimization of the structure was started from the cif and fully converged, but the frequency calculation gives always one imaginary frequency despite our efforts to use very tight convergence criteria and/ or to manually displace the atoms in the direction of the vibration and reoptimize the structure. Thus, it is not possible to conclude if this structure is at its minimum, and the energy comparison is therefore inconclusive.*			

Table S2. Mulliken spin density values for each of the two isomers (square-planar – multiplicity doublet, and tetrahedral – multiplicity quadruplet) of **2a** and **2b**. Level of theory: uB3LYP/ LANL2DZ CPCM: CH_2Cl_2)

Cpd.	Mulliken spin density			
	Co	O	N	Other
2a-sqpl	0.935 (93%)	0.085 (9%)	0.013 (1%)	-0.032 (-3%)
2a-tetra	2.629 (88%)	0.204 (6%)	0.177 (6%)	-0.001
2b-sqpl*	0.979 (98%)	0.026 (3%)	-0.001	-0.003
2b-tetra	2.617 (87%)	0.212 (7%)	0.179 (6%)	-0.008

* Note: *the optimization of the structure was started from the cif and fully converged, but the frequency calculation gives always one imaginary frequency despite our efforts to use very tight convergence criteria and/ or to manually displace the atoms in the direction of the vibration and reoptimize the structure. Thus, it is not possible to conclude if this structure is at its minimum.*

Table S3. Spin contamination monitoring for the DFT calculations of the two isomers (square-planar – multiplicity doublet, and tetrahedral – multiplicity quadruplet) of **2a** and **2b**. Level of theory: uB3LYP/ LANL2DZ CPCM: CH_2Cl_2

Cpd.	S**2		
	Before annihilation	After annihilation	% change
2a-sqpl	0.8447	0.7506	13
2a-tetra	3.7593	3.7500	2
2b-sqpl*	0.8510	0.7506	13
2b-tetra	3.7589	3.7500	2

* Note: *the optimization of the structure was started from the cif and fully converged, but the frequency calculation gives always one imaginary frequency despite our efforts to use very tight convergence criteria and/ or to manually displace the atoms in the direction of the vibration and reoptimize the structure. Thus, it is not possible to conclude if this structure is at its minimum.*

Table S4. Atomic coordinates for DFT optimization of **2a-sqpl** (multiplicity: doublet) uB3LYP/ LANL2DZ CPCM: CH_2Cl_2

Center Number	Atomic Number	Atomic Type	Coordinates (Angstroms)		
			X	Y	Z
1	27	0	0	0	0
2	8	0	-0.016892	0.055039	1.881642
3	7	0	1.321555	0.051631	2.412365
4	7	0	1.925147	-0.013515	0.207792
5	6	0	2.290216	0.013928	1.485625
6	1	0	3.323740	0.001490	1.819060
7	6	0	1.460542	0.112134	3.840026
8	6	0	1.855478	1.331614	4.445745
9	6	0	1.969683	1.366284	5.852631
10	1	0	2.270593	2.291174	6.338716
11	6	0	1.685829	0.226614	6.625890
12	1	0	1.773380	0.271036	7.708711
13	6	0	1.282893	-0.970193	6.003300
14	1	0	1.063499	-1.848241	6.605773
15	6	0	1.163826	-1.048566	4.600590
16	6	0	2.148887	2.571139	3.620854
17	1	0	2.119178	3.467404	4.249159
18	1	0	1.423967	2.692716	2.807830
19	1	0	3.146408	2.523032	3.162683
20	6	0	0.731289	-2.335628	3.927767
21	1	0	0.650238	-3.148849	4.656208
22	1	0	1.444326	-2.638625	3.149857
23	1	0	-0.240287	-2.211239	3.434508
24	6	0	2.924466	-0.071528	-0.827148
25	6	0	3.409341	1.136285	-1.393525
26	6	0	4.369402	1.060820	-2.425475
27	1	0	4.746141	1.980413	-2.868123
28	6	0	4.838206	-0.183440	-2.885922
29	1	0	5.577060	-0.226772	-3.682632
30	6	0	4.343247	-1.371637	-2.317587
31	1	0	4.700057	-2.334555	-2.676693
32	6	0	3.382607	-1.335005	-1.283898
33	6	0	2.902155	2.481438	-0.909503
34	1	0	3.275439	3.291198	-1.545880
35	1	0	3.221321	2.688740	0.121126
36	1	0	1.805342	2.509978	-0.912285
37	6	0	2.847498	-2.621444	-0.683627

38	1	0	3.198083	-3.491235	-1.249794
39	1	0	1.750275	-2.625693	-0.679102
40	1	0	3.168743	-2.747771	0.359499
41	8	0	0.016892	-0.055039	-1.881642
42	7	0	-1.321555	-0.051631	-2.412365
43	7	0	-1.925147	0.013515	-0.207792
44	6	0	-2.290216	-0.013928	-1.485625
45	1	0	-3.323740	-0.001490	-1.819060
46	6	0	-1.460542	-0.112134	-3.840026
47	6	0	-1.855478	-1.331614	-4.445745
48	6	0	-1.969683	-1.366284	-5.852631
49	1	0	-2.270593	-2.291174	-6.338716
50	6	0	-1.685829	-0.226614	-6.625890
51	1	0	-1.773380	-0.271036	-7.708711
52	6	0	-1.282893	0.970193	-6.003300
53	1	0	-1.063499	1.848241	-6.605773
54	6	0	-1.163826	1.048566	-4.600590
55	6	0	-2.148887	-2.571139	-3.620854
56	1	0	-2.119178	-3.467404	-4.249159
57	1	0	-1.423967	-2.692716	-2.807830
58	1	0	-3.146408	-2.523032	-3.162683
59	6	0	-0.731289	2.335628	-3.927767
60	1	0	-0.650238	3.148849	-4.656208
61	1	0	-1.444326	2.638625	-3.149857
62	1	0	0.240287	2.211239	-3.434508
63	6	0	-2.924466	0.071528	0.827148
64	6	0	-3.409341	-1.136285	1.393525
65	6	0	-4.369402	-1.060820	2.425475
66	1	0	-4.746141	-1.980413	2.868123
67	6	0	-4.838206	0.183440	2.885922
68	1	0	-5.577060	0.226772	3.682632
69	6	0	-4.343247	1.371637	2.317587
70	1	0	-4.700057	2.334555	2.676693
71	6	0	-3.382607	1.335005	1.283898
72	6	0	-2.902155	-2.481438	0.909503
73	1	0	-3.275439	-3.291198	1.545880
74	1	0	-3.221321	-2.688740	-0.121126
75	1	0	-1.805342	-2.509978	0.912285
76	6	0	-2.847498	2.621444	0.683627
77	1	0	-3.198083	3.491235	1.249794
78	1	0	-1.750275	2.625693	0.679102
79	1	0	-3.168743	2.747771	-0.359499

Table S5. Atomic coordinates for DFT optimization of **2a-tetra** (multiplicity: quadruplet) uB3LYP/ LANL2DZ CPCM: CH_2Cl_2

Center Number	Atomic Number	Atomic Type	Coordinates (Angstroms)		
			X	Y	Z
1	8	0	1.6574350	-1.2299360	0.6393210
2	8	0	-1.6574960	-1.2333120	-0.6295690
3	7	0	2.7517370	-0.8483330	-0.1936420
4	7	0	1.2761120	0.5284080	-1.3232270
5	7	0	-1.2768040	0.5400920	1.3188140
6	7	0	-2.7514870	-0.8478010	0.2018950
7	6	0	2.5090310	0.0459410	-1.1640310
8	1	0	3.3467190	0.3290670	-1.7968210
9	6	0	4.0126560	-1.4968180	0.0640000
10	6	0	4.2057580	-2.8158920	-0.4188470
11	6	0	5.4334930	-3.4502130	-0.1385640
12	1	0	5.6047650	-4.4615860	-0.4989410
13	6	0	6.4334670	-2.7874670	0.5985320
14	1	0	7.3749850	-3.2897130	0.8069990
15	6	0	6.2164220	-1.4813930	1.0725730
16	1	0	6.9881920	-0.9776730	1.6495070
17	6	0	4.9983080	-0.8140000	0.8178260
18	6	0	3.1260800	-3.5220020	-1.2151210
19	1	0	2.1821830	-3.5469060	-0.6579730
20	1	0	3.4225750	-4.5493670	-1.4497120
21	1	0	2.9250410	-3.0026790	-2.1621860
22	6	0	4.7644100	0.5913890	1.3396420
23	1	0	4.8804050	1.3390340	0.5430090
24	1	0	5.4840220	0.8358420	2.1278580
25	1	0	3.7524470	0.7039350	1.7450940
26	6	0	1.0050390	1.5166790	-2.3326600
27	6	0	0.3190650	1.1245610	-3.5147160
28	6	0	0.0106420	2.1107890	-4.4759280
29	1	0	-0.5118130	1.8191200	-5.3845170
30	6	0	0.3710470	3.4563130	-4.2753010
31	1	0	0.1260760	4.2046690	-5.0252270
32	6	0	1.0435860	3.8303310	-3.0978470
33	1	0	1.3151400	4.8713140	-2.9356260
34	6	0	1.3682960	2.8734830	-2.1116150
35	6	0	-0.0753890	-0.3223190	-3.7436680
36	1	0	0.8034700	-0.9811550	-3.7611920
37	1	0	-0.6017570	-0.4341110	-4.6982790

38	1	0	-0.7297730	-0.6883210	-2.9413380
39	6	0	2.0723500	3.3008650	-0.8361860
40	1	0	3.1154480	2.9570760	-0.8086010
41	1	0	1.5775230	2.8834760	0.0501470
42	1	0	2.0827540	4.3925250	-0.7469490
43	6	0	-2.5092150	0.0547510	1.1647270
44	1	0	-3.3466530	0.3417860	1.7960710
45	6	0	-4.0117640	-1.4995650	-0.0502900
46	6	0	-5.0014760	-0.8207130	-0.8024200
47	6	0	-6.2188310	-1.4915360	-1.0518280
48	1	0	-6.9935770	-0.9908750	-1.6274320
49	6	0	-6.4312510	-2.7971070	-0.5744120
50	1	0	-7.3722140	-3.3020550	-0.7788190
51	6	0	-5.4273400	-3.4558940	0.1609100
52	1	0	-5.5951100	-4.4668800	0.5240110
53	6	0	-4.2002640	-2.8181040	0.4360050
54	6	0	-4.7728520	0.5840740	-1.3282370
55	1	0	-4.8914060	1.3335610	-0.5337060
56	1	0	-5.4936680	0.8236750	-2.1168450
57	1	0	-3.7614890	0.6992810	-1.7344080
58	6	0	-3.1164640	-3.5200220	1.2302980
59	1	0	-2.1763100	-3.5503010	0.6671020
60	1	0	-3.4128410	-4.5452400	1.4742530
61	1	0	-2.9082740	-2.9939710	2.1720680
62	6	0	-1.0060660	1.5376440	2.3191780
63	6	0	-0.3204840	1.1565970	3.5050600
64	6	0	-0.0117520	2.1518960	4.4567830
65	1	0	0.5105020	1.8687690	5.3681860
66	6	0	-0.3716670	3.4955610	4.2432370
67	1	0	-0.1264400	4.2509930	4.9859500
68	6	0	-1.0442520	3.8584670	3.0623370
69	1	0	-1.3157280	4.8978870	2.8902580
70	6	0	-1.3692230	2.8923170	2.0853060
71	6	0	0.0730350	-0.2882360	3.7481300
72	1	0	-0.8063350	-0.9461760	3.7726610
73	1	0	0.5997930	-0.3909730	4.7035420
74	1	0	0.7266730	-0.6628290	2.9491820
75	6	0	-2.0735960	3.3076530	0.8060920
76	1	0	-3.1162480	2.9622890	0.7813740
77	1	0	-1.5781790	2.8832050	-0.0765590
78	1	0	-2.0853630	4.3984750	0.7073200
79	27	0	0.0001210	-0.2949600	0.0015500

Table S6. Atomic coordinates for DFT optimization of **2b-sqpl** (multiplicity: doublet) uB3LYP/ LANL2DZ CPCM: CH_2Cl_2 Note: the optimization of the structure started from the cif fully converged, but the frequency calculation gives always one imaginary frequency despite our efforts to use very tight convergence criteria and/ or to manually displace the atoms in the direction of the vibration and reoptimize the structure.

Center Number	Atomic Number	Atomic Type	Coordinates (Angstroms)		
			X	Y	Z
1	27	0	0.000000	0.000000	0.005008
2	8	0	-1.799468	0.564241	-0.122134
3	7	0	-2.695242	-0.563558	-0.138581
4	7	0	-0.767271	-1.778988	0.067747
5	6	0	-2.093791	-1.756145	-0.019738
6	1	0	-2.714965	-2.646353	0.007465
7	6	0	-0.084488	-3.031810	0.291724
8	6	0	0.446085	-3.749874	-0.815465
9	6	0	0.297281	-3.248923	-2.254481
10	1	0	-0.186181	-2.266884	-2.220477
11	6	0	1.675143	-3.062105	-2.938799
12	1	0	2.301018	-2.374450	-2.358145
13	1	0	1.544657	-2.646368	-3.947291
14	1	0	2.209289	-4.016428	-3.037564
15	6	0	-0.608304	-4.193845	-3.088351
16	1	0	-0.165910	-5.195653	-3.171027
17	1	0	-0.739449	-3.798206	-4.104636
18	1	0	-1.600801	-4.299242	-2.63177
19	6	0	1.116008	-4.967661	-0.567921
20	1	0	1.523562	-5.533185	-1.402607
21	6	0	1.261837	-5.464063	0.737826
22	1	0	1.777424	-6.406085	0.909279
23	6	0	0.738289	-4.740024	1.821591
24	1	0	0.854598	-5.130209	2.829888
25	6	0	0.063685	-3.515791	1.623529
26	6	0	-0.502485	-2.761298	2.831838
27	1	0	-0.869838	-1.789729	2.484287
28	6	0	-1.703063	-3.524200	3.453966
29	1	0	-2.499017	-3.687237	2.715651
30	1	0	-2.125692	-2.954153	4.29213
31	1	0	-1.390931	-4.505803	3.834922
32	6	0	0.579391	-2.481643	3.905966

33	1	0	0.977519	-3.411076	4.333418
34	1	0	0.150496	-1.893214	4.72822
35	1	0	1.418093	-1.916308	3.481634
36	6	0	-4.099391	-0.299419	-0.314633
37	6	0	-4.689075	-0.496507	-1.593669
38	6	0	-3.886481	-0.979421	-2.805569
39	1	0	-2.822318	-0.963880	-2.544148
40	6	0	-4.070907	-0.050479	-4.033046
41	1	0	-5.106349	-0.060690	-4.396447
42	1	0	-3.426568	-0.387027	-4.855841
43	1	0	-3.804469	0.985347	-3.791702
44	6	0	-4.264991	-2.440505	-3.171041
45	1	0	-4.104135	-3.121459	-2.325516
46	1	0	-3.655973	-2.792082	-4.013774
47	1	0	-5.321208	-2.509271	-3.462937
48	6	0	-6.073860	-0.254147	-1.723773
49	1	0	-6.557528	-0.407860	-2.68464
50	6	0	-6.836162	0.191434	-0.631952
51	1	0	-7.900804	0.375423	-0.753915
52	6	0	-6.227099	0.402585	0.616383
53	1	0	-6.828388	0.749525	1.452579
54	6	0	-4.849369	0.162322	0.800573
55	6	0	-4.213978	0.376287	2.176364
56	1	0	-3.135729	0.208680	2.084247
57	6	0	-4.767384	-0.642930	3.207905
58	1	0	-5.847112	-0.510858	3.357147
59	1	0	-4.272941	-0.505814	4.178661
60	1	0	-4.593775	-1.675362	2.878557
61	6	0	-4.418293	1.829882	2.676445
62	1	0	-3.993165	2.554517	1.970631
63	1	0	-3.925279	1.967925	3.647395
64	1	0	-5.482602	2.064459	2.807081
65	8	0	1.799468	-0.564240	-0.122139
66	7	0	2.695243	0.563559	-0.138579
67	7	0	0.767271	1.778988	0.067751
68	6	0	2.093791	1.756145	-0.019733
69	1	0	2.714965	2.646353	0.007474
70	6	0	0.084488	3.031809	0.29173
71	6	0	-0.063689	3.515787	1.623535
72	6	0	0.502479	2.761291	2.831844
73	1	0	0.869832	1.789723	2.484291
74	6	0	-0.579399	2.481633	3.905969

75	1	0	-1.418100	1.916300	3.481635
76	1	0	-0.150505	1.893202	4.728223
77	1	0	-0.977527	3.411065	4.333422
78	6	0	1.703056	3.524192	3.453975
79	1	0	1.390923	4.505794	3.834933
80	1	0	2.125684	2.954143	4.292139
81	1	0	2.499011	3.687230	2.715662
82	6	0	-0.738294	4.740019	1.821599
83	1	0	-0.854605	5.130202	2.829896
84	6	0	-1.261839	5.464061	0.737834
85	1	0	-1.777427	6.406082	0.909288
86	6	0	-1.116007	4.967661	-0.567913
87	1	0	-1.523559	5.533188	-1.402599
88	6	0	-0.446083	3.749876	-0.815459
89	6	0	-0.297276	3.248928	-2.254476
90	1	0	0.186186	2.266889	-2.220473
91	6	0	0.608311	4.193852	-3.088342
92	1	0	1.600807	4.299248	-2.631758
93	1	0	0.739458	3.798216	-4.104627
94	1	0	0.165917	5.195660	-3.171016
95	6	0	-1.675136	3.062111	-2.938798
96	1	0	-2.209282	4.016434	-3.037562
97	1	0	-1.544648	2.646376	-3.94729
98	1	0	-2.301012	2.374455	-2.358147
99	6	0	4.099392	0.299421	-0.314629
100	6	0	4.849368	-0.162324	0.800577
101	6	0	4.213974	-0.376292	2.176366
102	1	0	3.135725	-0.208684	2.084247
103	6	0	4.418287	-1.829888	2.676444
104	1	0	5.482595	-2.064467	2.807081
105	1	0	3.925270	-1.967933	3.647392
106	1	0	3.993160	-2.554521	1.970626
107	6	0	4.767379	0.642922	3.207911
108	1	0	4.593771	1.675354	2.878566
109	1	0	4.272933	0.505803	4.178666
110	1	0	5.847106	0.510848	3.357155
111	6	0	6.227098	-0.402586	0.616389
112	1	0	6.828386	-0.749528	1.452586
113	6	0	6.836163	-0.191432	-0.631944
114	1	0	7.900805	-0.375421	-0.753905
115	6	0	6.073863	0.254152	-1.723765
116	1	0	6.557533	0.407866	-2.684632

117	6	0	4.689078	0.496511	-1.593663
118	6	0	3.886487	0.979428	-2.805564
119	1	0	2.822323	0.963887	-2.544145
120	6	0	4.264998	2.440514	-3.171031
121	1	0	5.321215	2.509280	-3.462925
122	1	0	3.655982	2.792092	-4.013765
123	1	0	4.104140	3.121465	-2.325506
124	6	0	4.070914	0.050490	-4.033043
125	1	0	3.804475	-0.985337	-3.791702
126	1	0	3.426577	0.387039	-4.855838
127	1	0	5.106357	0.060701	-4.396442

Table S7. Atomic coordinates for DFT optimization of **2b-tetra** (multiplicity: quadruplet) uB3LYP/ LANL2DZ CPCM: CH_2Cl_2

			Standard orientation:		
Center Number	Atomic Number	Atomic Type	Coordinates (Angstroms)		
			X	Y	Z
1	8	0	-1.525829	-1.360128	0.561126
2	8	0	1.526659	-1.359711	-0.560765
3	7	0	-2.699860	-0.981445	-0.151915
4	7	0	-1.449187	0.728021	-1.095853
5	7	0	2.700799	-0.979885	0.151568
6	7	0	1.448666	0.727825	1.096630
7	6	0	-3.824767	-1.882286	-0.059418
8	6	0	-4.818705	-1.650801	0.926697
9	6	0	-5.907266	-2.548000	0.985706
10	1	0	-6.691605	-2.393721	1.722165
11	6	0	-5.989629	-3.642524	0.109581
12	1	0	-6.835746	-4.322659	0.170908
13	6	0	-4.978808	-3.866803	-0.840317
14	1	0	-5.049895	-4.725270	-1.503270
15	6	0	-3.873598	-2.995717	-0.941138
16	6	0	-2.608456	0.076389	-0.972071
17	1	0	-3.506880	0.355222	-1.517022
18	6	0	-1.395729	1.910994	-1.922764
19	6	0	-1.967234	3.133460	-1.460220
20	6	0	-1.889066	4.270140	-2.295012
21	1	0	-2.325440	5.208562	-1.960979
22	6	0	-1.257131	4.213425	-3.547031
23	1	0	-1.209286	5.099291	-4.175827
24	6	0	-0.687799	3.005845	-3.983747

25	1	0	-0.203620	2.966305	-4.956504
26	6	0	-0.744663	1.841283	-3.189190
27	6	0	-4.740741	-0.481118	1.910163
28	1	0	-3.802889	0.055912	1.728928
29	6	0	-4.714014	-0.981722	3.378168
30	1	0	-4.596371	-0.132399	4.063492
31	1	0	-3.879664	-1.674220	3.545626
32	1	0	-5.645419	-1.499562	3.641532
33	6	0	-5.907820	0.517749	1.693468
34	1	0	-5.914999	0.904543	0.666849
35	1	0	-5.809815	1.369458	2.379326
36	1	0	-6.878479	0.041493	1.883979
37	6	0	-2.768789	-3.276639	-1.963373
38	1	0	-2.014308	-2.486808	-1.885229
39	6	0	-3.316528	-3.262980	-3.414207
40	1	0	-3.797635	-2.304610	-3.648579
41	1	0	-4.054371	-4.060411	-3.571392
42	1	0	-2.497158	-3.418210	-4.128220
43	6	0	-2.054645	-4.619668	-1.655272
44	1	0	-1.638415	-4.620228	-0.640086
45	1	0	-1.231199	-4.779487	-2.363761
46	1	0	-2.744494	-5.469239	-1.742616
47	6	0	-2.666370	3.259019	-0.100678
48	1	0	-2.559490	2.309062	0.433769
49	6	0	-2.015695	4.352469	0.785895
50	1	0	-0.951181	4.147828	0.952165
51	1	0	-2.513337	4.389058	1.764302
52	1	0	-2.104564	5.346723	0.329109
53	6	0	-4.183989	3.535120	-0.274867
54	1	0	-4.669245	2.751596	-0.871399
55	1	0	-4.353293	4.494880	-0.780665
56	1	0	-4.679914	3.576377	0.703797
57	6	0	-0.158383	0.531504	-3.723938
58	1	0	-0.148914	-0.194747	-2.904535
59	6	0	-1.055589	-0.052164	-4.849335
60	1	0	-2.081201	-0.216561	-4.494190
61	1	0	-0.655918	-1.014170	-5.197705
62	1	0	-1.100435	0.628927	-5.709883
63	6	0	1.300481	0.693605	-4.217812
64	1	0	1.944958	1.095799	-3.425401
65	1	0	1.365414	1.367002	-5.082511
66	1	0	1.704744	-0.279933	-4.523820

XC

67	6	0	3.826228	-1.880073	0.059029
68	6	0	3.876189	-2.993083	0.941227
69	6	0	4.981928	-3.863484	0.840299
70	1	0	5.053865	-4.721615	1.503599
71	6	0	5.992176	-3.638971	-0.110155
72	1	0	6.838710	-4.318583	-0.171548
73	6	0	5.908713	-2.544883	-0.986716
74	1	0	6.692627	-2.390392	-1.723583
75	6	0	4.819588	-1.648371	-0.927614
76	6	0	2.608586	0.077574	0.972138
77	1	0	3.506988	0.357286	1.516688
78	6	0	1.394244	1.910957	1.923211
79	6	0	1.965117	3.133701	1.460617
80	6	0	1.886014	4.270464	2.295217
81	1	0	2.321897	5.209103	1.961152
82	6	0	1.253723	4.213580	3.547044
83	1	0	1.205124	5.099537	4.175654
84	6	0	0.684927	3.005739	3.983760
85	1	0	0.200419	2.966077	4.956346
86	6	0	0.742746	1.841091	3.189412
87	6	0	2.772105	-3.274258	1.964179
88	1	0	2.016774	-2.485278	1.885710
89	6	0	2.059198	-4.618292	1.657621
90	1	0	1.642467	-4.620208	0.642645
91	1	0	1.236267	-4.778319	2.366664
92	1	0	2.749962	-5.467074	1.745395
93	6	0	3.320554	-3.258805	3.414732
94	1	0	3.800762	-2.299737	3.648080
95	1	0	4.059341	-4.055319	3.572163
96	1	0	2.501727	-3.414329	4.129301
97	6	0	4.740491	-0.479071	-1.911441
98	1	0	3.802312	0.057339	-1.730077
99	6	0	4.713705	-0.980136	-3.379283
100	1	0	3.879785	-1.673257	-3.546322
101	1	0	5.645396	-1.497413	-3.642750
102	1	0	4.595302	-0.131095	-4.064829
103	6	0	5.906915	0.520704	-1.695386
104	1	0	5.914120	0.907800	-0.668882
105	1	0	5.808083	1.372135	-2.381468
106	1	0	6.877861	0.045092	-1.886050
107	6	0	2.664437	3.259565	0.101190
108	1	0	2.558195	2.309531	-0.433251

109	6	0	2.013324	4.352575	-0.785609
110	1	0	2.511037	4.389218	-1.763977
111	1	0	2.101702	5.346954	-0.329000
112	1	0	0.948922	4.147411	-0.951929
113	6	0	4.181865	3.536552	0.275670
114	1	0	4.667489	2.753291	0.872250
115	1	0	4.350476	4.496373	0.781578
116	1	0	4.677957	3.578183	-0.702896
117	6	0	0.157066	0.531025	3.724102
118	1	0	0.147804	-0.195128	2.904616
119	6	0	1.054703	-0.052334	4.849333
120	1	0	2.080335	-0.216255	4.494032
121	1	0	0.655493	-1.014534	5.197699
122	1	0	1.099356	0.628745	5.709901
123	6	0	-1.301781	0.692409	4.218249
124	1	0	-1.946549	1.094629	3.426093
125	1	0	-1.366837	1.365475	5.083201
126	1	0	-1.705630	-0.281388	4.523995
127	27	0	0.000147	-0.183389	-0.000339

X-ray diffraction measurements and structure determination

Crystallographic data for **2b-c** were collected at 150 K, from single crystal samples, which were mounted on a loop fiber. Data were collected using a Bruker Microstar diffractometer equipped with a Platinum 135 CCD Detector, Helios optics and a Kappa goniometer. The initial unit cell parameters were determined by a least-squares fit of the angular setting of strong reflections, collected by a 10.0 degree scan in 33 frames over three different parts of the reciprocal space (99 frames total). For determination of cell parameters, cell refinement and data reduction APEX2 was used.[10] Absorption corrections were applied using SADABS.[11] Structure solution was performed using direct methods with SHELXS97 and refined on F^2 by full-matrix least squares using SHELXL97.[12] All non-H atoms were refined by full-matrix least-squares with anisotropic displacement parameters. The H-atoms were included in calculated positions and treated as riding atoms: aromatic C—H 0.95 Å, methyl C—H 0.98 Å, with $U_{iso}(H) = k \times U_{eq}$ (parent C-atom), where k = 1.2 for the aromatic H-atoms and 1.5 for the methyl H-atoms. The following software were used to prepare material for publication: PLATON, UdMX and Mercury.[13, 14, 15]. Figures were generated using ORTEP3 and POV-

Ray.[16, 17] Data were deposited in CCDC under the deposit numbers: 963737-963738. For compound **2b**, checkCIF/ PLATON routine gives two A alerts related to the completeness %, which is lower than the threshold considered. As also mentioned in the comments in the cif, the low completeness value is due to geometrical constraints of the instrument and the use of copper radiation. Data completeness percentages lower than 100% were obtained, in dependence of the crystal system and the orientation of the mounted crystal, even with appropriate data collection routines. This situation existed in the past with the instrument that we used, but it has been corrected. In case of **2b**, the data were collected while this situation still existed. Nevertheless, the data set and the structural parameters for **2b** are very good (R_{int} is 4.84%, R_1 is 3.27%), validating the crystallographic data.

References

1.   D. F. Evans and D. A. Jakubovic, *Journal of the Chemical Society, Dalton Transactions*, 1988, 2927-2933.
2.   C. J. O'Connor, *Prog. Inorg. Chem.*, 1982, **29**, 203-283.
3.   D. Ostfeld and I. A. Cohen, *J. Chem. Educ.*, 1972, **49**, 829.
4.   D. R. Lide, *CRC Handbook of Chemistry and Physics - Internet Version, 9th edition*, 2014, 6-158 - 156-162.
5.   S. A. Carabineiro, L. C. Silva, P. T. Gomes, L. C. J. Pereira, L. F. Veiros, S. I. Pascu, M. T. Duarte, S. Namorado and R. T. Henriques, *Inorg. Chem.*, 2007, **46**, 6880-6890.
6.   P. J. Hay and W. R. Wadt, *J. Chem. Phys.*, 1985, **82**, 270-283.
7.   P. J. Hay and W. R. Wadt, *J. Chem. Phys.*, 1985, **82**, 299-310.
8.   T. H. D. J. a. P. J. Hay, in *Methods of Electronic Structure Theory*, ed. H. F. S. III, PLENUM PRESS 1977, vol. 2.
9.   W. R. Wadt and P. J. Hay, *J. Chem. Phys.*, 1985, **82**, 284-298.
10. *APEX2, Bruker AXS*, (2009-2011), Madison, WI 53719-1173.
11. G. M. Sheldrick, *SADABS*, (1996).
12. *SHELXTL, Bruker AXS* (2001), Madison, WI 53719-1173.
13. A. L. Spek, *PLATON*, (2003).
14. T. Maris, *UdMX*, (2004-2013).
15. CCDC, *Mercury 3.1*, (2001-2012).
16. L. J. Farrugia, *J. Appl. Crystallogr.*, 1997, **30**, 565.
17. *POV-Ray* (2004) Persistence of Vision Pty. Ltd., retrieved from http://www.povray.org/download/.

Appendix-4-SI

Supporting Information

for

Geometry and Spin Change at the Heart of a Cobalt(II) Complex: A Special Case of Solvatomorphism

Mihaela Cibian and Garry S. Hanan*

Département of Chemistry, Université de Montréal, Montréal, Québec, H3T-1J4, Canada

Contents

X-ray Crystallography

*Refinement details for **1-orange***

Despite many crystallization attempts, only poor quality crystals (clusters of non-separable fine needles) were obtained for **1-orange**. Inspection of the morphology of the crystals and of the diffraction patterns indicated twinning. Numerous crystal samples were tried, and all presented the same characteristics. Complete data collection was carried out for two different samples. In both cases, the same procedure was applied for solving and refining the structure, and very similar values were obtained for the final models. The best model is described herein. The structure was solved without difficulties using *SHELXT*,[1] but the twinning was confirmed by the large values of the confidence factors (R_1=0.1278, wR_2=0.3289), the large residual electron densities (highest peak 5.3 e/Å^3), and the $F_o^2 \gg F_c^2$ (in the .lst file). Using the TWINROTMAT routine implemented in *PLATON* (Spek, 2009),[2] the following twin law was detected (1 0 0 0 -1 0 0 0 -1), with a BASF value of 0.40. When it was introduced in the refinement, the BASF parameter converged to 0.405(9), and the confidence factors improved (R_1=0.0954 and wR_2 = 0.2347), but the residual density was still large (at 4.9 e/Å^3). An HKLF 5 type file was also generated with *PLATON* (Spek, 2009),[2] and used in the refinement, but the model did not improve. The *CELL_NOW/ TWINABS* (Bruker 2001)[3] procedure was also tried with 2 twin domains and 3 twin domains, but no better model was obtained. The parameters for the best models found are summarized in the table below.

MODEL	A	B	C	D	E
Procedure	1 domain TwinRotMat (PLATON) TWIN LAW/ BASF/ HKLF 4	**1 domain** **TwinRotMat (PLATON)** **BASF/ HKLF 5**	2 domains Cell_now/ Twinabs TWIN LAW/ BASF/ HKLF 4	2 domains Cell_now/ Twinabs BASF/ HKLF 5	3 domains Cell_now/ Twinabs BASF/ HKLF 5
$R_{1[I > 2\sigma(I)]}$	0.0954	**0.0954**	0.1088	0.1254	0.1115
$R_{1(all\ data)}$	0.0991	**0.0991**	0.1119	0.1399	0.1169
wR_2	0.2347	**0.2347**	0.2603	0.3127	0.2958
GooF	1.051	**1.051**	1.188	1.121	1.3490
Residual density (highest peak) (e/Å3)	4.9	**4.9**	5.7	5.5	4.7
BASF	0.405(9)	**0.405(9)**	0.406(10)	0.349(11)	0.300(7); 0.101(8)

Model B was chosen as final model, and it is considered acceptable for confidently discussing the geometry around the metal centre. The large residual density is the result of the twinning, and it is localized far from the metal centre (3.87 Å), being the closest to the C1 atom (2.01 Å). No solvent voids and no corresponding residual density were identified using SQUEEZE routine in *PLATON* (Spek, 2009),[2] (this routine was used as a test, and it is not applied to the final model). In order to improve the model, the reflections (hkl: 3 5 0; 18 1 0; 2 7 0) with $|F_o - F_c| > 5\sigma(F_o)$ were omitted from the refinement. Mild displacement parameter (U^{ij}) restraints were also applied to the final model.

CCDC 1041637 (for **1-green**) and CCDC 1041638 (for **1-orange**) contain the supplementary crystallographic data for the structures. These data can be obtained free of charge from The Cambridge Crystallographic Data Centre via www.ccdc.cam.ac.uk/data_request/cif.

Table S1. Cambridge Structural Database (CSD)[4] search for cases of a same cobalt bis(chelate) structurally characterized in different geometries at the metal centre.

Square-planar geometry				Pseudo-tetrahedral geometry			
Compound formula	τ_4[5]	CSD refcode	Ref.	Complex	τ_4[5]	CSD refcode	Ref.
i) different substitution pattern of the ligand; neutral complexes with minor modifications in ligand substitution							
iminopyrrolyl-type ligands							
$(C_{18}H_{23}N_2)_2Co$	0.00	LILZAI	[6]	$(C_{17}H_{21}N_2)_2Co$	0.73	LILYOV	[6]
				$(C_9H_{13}N_2)_2Co$	0.78	BPYACO10	[7]
triazene 1-oxide-type ligand							
$(C_8H_{10}N_3O)_2Co$ $[(Ph)N–N=N(Et)O]^-$	0.00	GESTED	[8]	$(C_8H_{10}N_3O)_2Co$ $[(p\text{-Tol})N–N=N(Me)O]^-$	0.73	YANWOZ	[9]
ii) different oxidation state of the metal and/ or the ligands							
$[(C_2H_4S_2)_2Co]^{2-}$ td, $[(C_2H_4S_2)_2Co]^-$ **sq-pl**, $3([(CH_3)_4N]^+)$	0.07	CUWLOV10	[10]	$[(C_2H_4S_2)_2Co]^{2-}$ **td**, $[(C_2H_4S_2)_2Co]^-$ sq-pl, $3([(CH_3)_4N]^+)$	0.85	CUWLOV10	[10]
$[(C_{26}H_{24}P_2)_2Co]^+$, $[C_{60}]^-$, $2(C6H4Cl2)$	0.21	UTAYOE	[11]	$[C_{20}H_{40}KO_8]^+$, $[C_{12}H_{24}KO_6]^+$, $2([(C_{26}H_{24}P_2)_2Co]^-)$	0.80	AFITUE	[12]
iii) secondary interactions (e. g., hydrogen bonding, electrostatic interactions); the same anionic ion complex with different cations							
$[C_6F_{12}O_2)_2Co]^{2-}$, $2([(C_4H_9)_4N]^+)$	0.00	XIYPIG	[13]	$[C_6F_{12}O_2)_2Co]^{2-}$, $2([(CH_3)_4N]^+)$	0.40	XIYPEC	[13]
$[C_6F_{12}O_2)_2Co]^{2-}$, $2([(C_4H_{10}O_2)_2K]^+)$	0.00	GATWOP	[14]	$[C_6F_{12}O_2)_2Co]^{2-}$, $[(Ph_3P)_2N]^+$, $[(CH_3OH)_4Li]^+$	0.51	SEWMAK	[15]

Note: The search was performed all types of bidentate ligands forming five- or six-membered chelate rings with the cobalt ion. From the 679 hits obtained (192 for five-membered chelate ring and 487 for six-membered chelate ring), **the monomeric complexes of bis(chelates)** were screened for **cases of the same neutral complex or ion complex appearing in different geometries**. **For neutral complexes, no case of a same compound structurally characterized in both geometries was identified**. For bidentate ligands forming five-membered chelate rings with the cobalt ion, the cases of complexes with the same type of ligand and minor modification in ligand substitution were considered [point i)]. For ion complexes, the cases of the same ion complex in identical and/ or in different oxidation state, with the same and/ or with different counter ions, were all considered [points ii) and iii)]. The classification of the results is function of the factors that play the main role in the change of geometry: i) the substitution pattern of the ligand; ii) the oxidation state of the metal and/ or the ligand; iii) the secondary interactions (e. g., hydrogen bonding, electrostatic interactions).

Table S2. Solid state structure and refinement data for compounds **1-green** and **1-orange**

Compound	1-green	1-orange
Formula	$C_{50}H_{38}CoN_4O_2(CH_2Cl_2)_2$	$C_{50}H_{38}CoN_4O_2$
M_w (g/mol)	955.63	785.77
Temperature (K)	100	100
Wavelength (Å)	1.54178	1.54178
Crystal System	Triclinic	Orthorhombic
a (Å)	11.1312(6)	19.3735(3)
b (Å)	13.8245(7)	7.8837(1)
c (Å)	15.9000(8)	24.7792(4)
α (°)	82.436(2)	90
β (°)	87.176(3)	90
γ (°)	68.936(2)	90
Unit cell volume (Å^3)	2263.4(2)	3784.6(1)
Space Group	P-1	P$ca2_1$
Z	2	4
$d_{calcd.}$ (g/cm^3)	1.402	1.379
μ (mm^{-1})	5.511	3.934
F(000)	986	1636
Reflections collected	33236	51028
Independent reflections	8387	7220
GoF	1.046	1.051
$R_1(F)$ [$I > 2\sigma(I)$]	0.0350	0.0954
$wR(F^2)$ [$I > 2\sigma(I)$]	0.0966	0.2281
$R_1(F)$ (all data)	0.0370	0.0991
$wR(F^2)$ (all data)	0.0975	0.2347
Largest diff. peak and hole (e/Å^3)	0.43 and -0.39	4.87 and -0.79

Figure S1. ORTEP view of **1-green** with atom labels. Ellipsoids are shown at 50% probability level. Hydrogen atoms and co-crystallized DCM molecules were removed for clarity.

Figure S2. ORTEP view of **1-orange** with atom labels. Ellipsoids are shown at 50% probability level. Hydrogen atoms were removed for clarity.
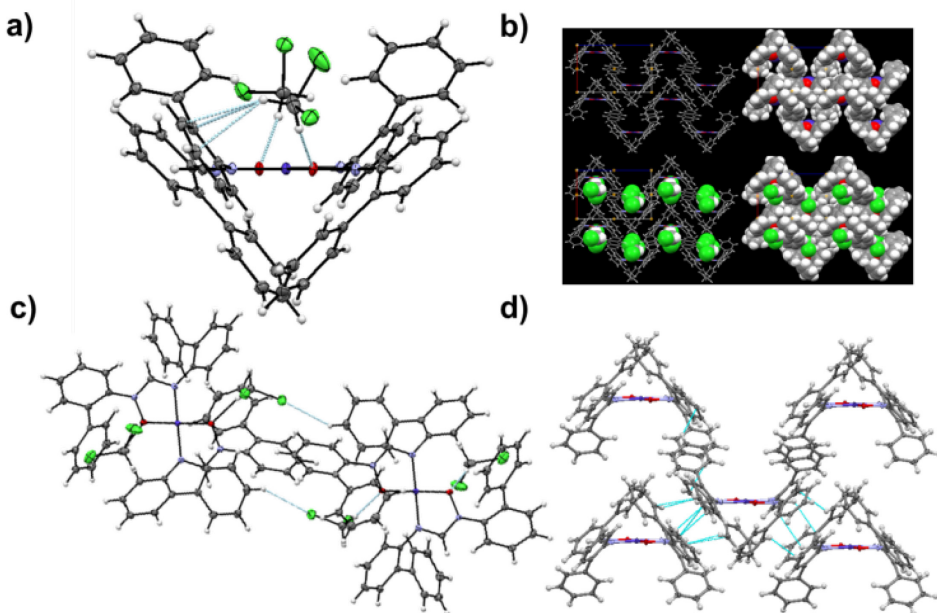
Figure S3. Hydrogen bonding and packing interactions in **1-green**: ORTEP view highlighting the hydrogen-bonding between the co-crystallized DCM molecules and the compound (a and c) – ellipsoids are shown at 50% probability level; capped-sticks and space-fill models with and without co-crystallized solvent (b); packing interactions (d) – co-crystallized DCM molecules were removed for clarity.
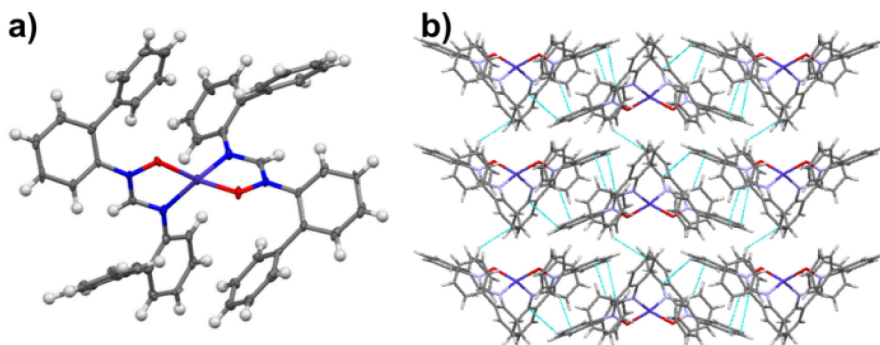
Figure S4. Hydrogen bonding and packing interactions in **1-orange**: (a) ORTEP view with ellipsoids shown at 50% probability level; (b) packing interactions

Table S3. Cambridge Structural Database (CSD)[4] search for intermolecular contacts of type O···H-CHCl$_2$, with O atom part of a five- or six-membered metal chelate ring, and directly linked to the metal ion

Metal	Coordination	No. hits	The shortest interactions found				
			Compound formula	$d(\text{H}\cdots\text{O})$ (Å)	$\theta(\text{C–H}\cdots\text{O})$ (°)	**CSD refcode**	**Ref.**
Five-membered chelate ring							
any	any	115	[C$_{48}$H$_{96}$CsFe$_8$N$_8$O$_{24}$]$^+$, Cl$^-$, 2(CH$_2$Cl$_2$), 2(CHCl$_3$)	1.70	139	NEWRIQ	[16]
			C$_{26}$H$_{20}$Cl$_4$MnN$_3$O$_4$, 1.5(CH$_2$Cl$_2$)	2.00	166	EBUCEK	[17]
			C$_{30}$H$_{39}$FeN$_8$O$_{14}$, CH$_2$Cl$_2$, 3.5(CH$_4$O)	2.00	153	OYEYUN	[18]
any	4	17	C$_{18}$H$_{26}$ClFeNO$_2$PtS, CH$_2$Cl$_2$, 0.5(H$_2$O)	2.06	150	PEPDAQ	[19]
			C$_{21}$H$_{32}$N$_2$O$_4$Pd, CH$_2$Cl$_2$	2.16	149	VASVOB	[20]
Co	any	0	-	-	-	-	-
Co	4	0	-	-	-	-	-
Six-membered chelate ring							
any	any	173	C$_{25}$H$_{37}$N$_2$OPPd, CH$_2$Cl$_2$	1.93	171	EZETUY	[21]
any	4	38					
Co	any	9	C$_{44}$H$_{46}$Co$_2$N$_4$O$_6$, 4(CH$_2$Cl$_2$)	2.10	163	NUHLIL	[22]
Co	4	1	C$_{22}$H$_{18}$CoN$_2$O$_4$, 2(CH$_2$Cl$_2$)	2.34	135	ROLSIV	[23]
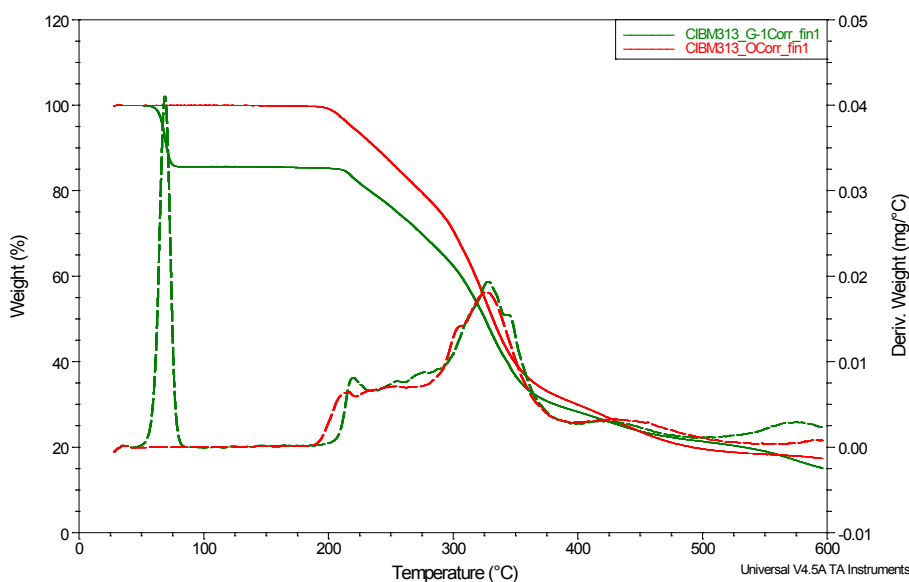
Figure S5. TGA analysis of **1_green** (in green) and **1_orange** (in red).
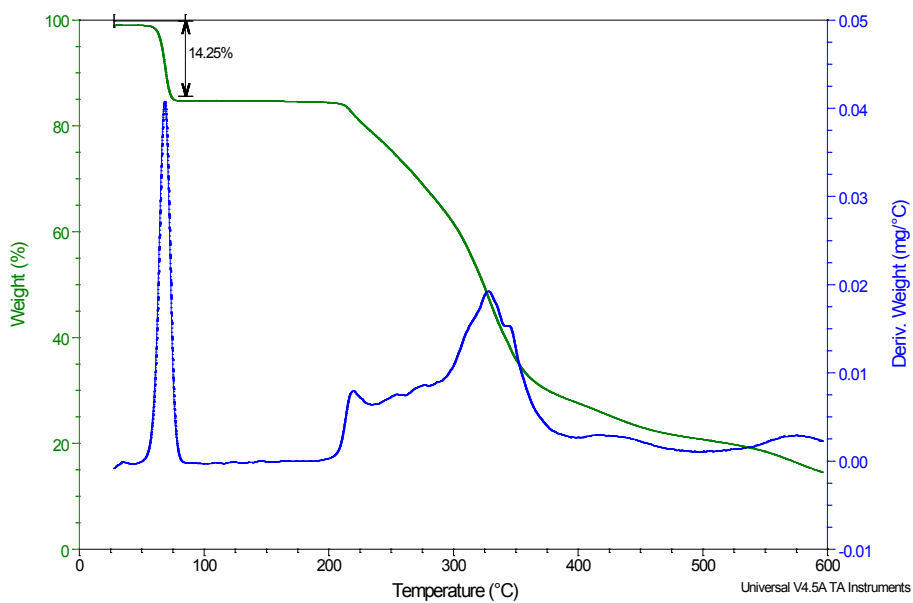
Figure S6. TGA analysis of **1_green**.
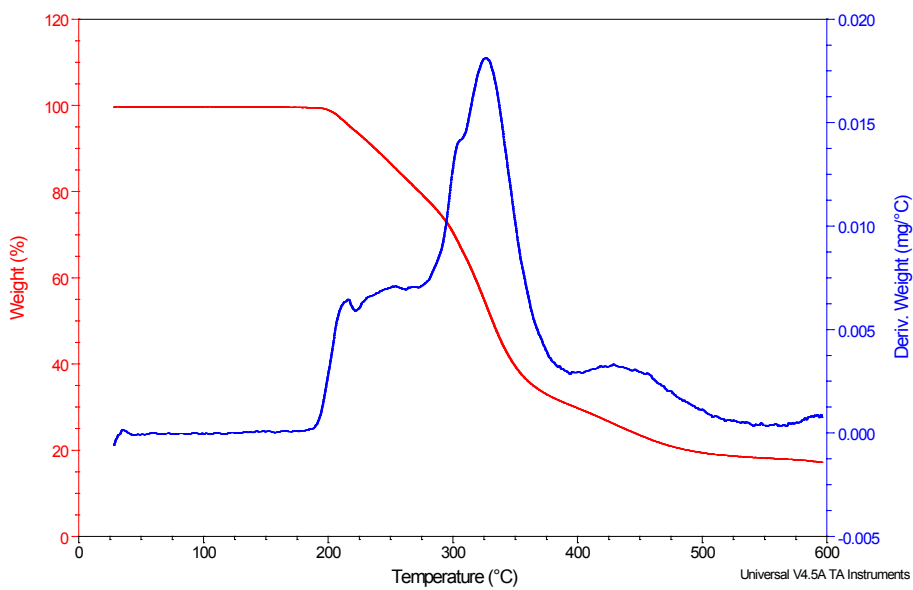
Figure S7. TGA analysis of **1-orange**.
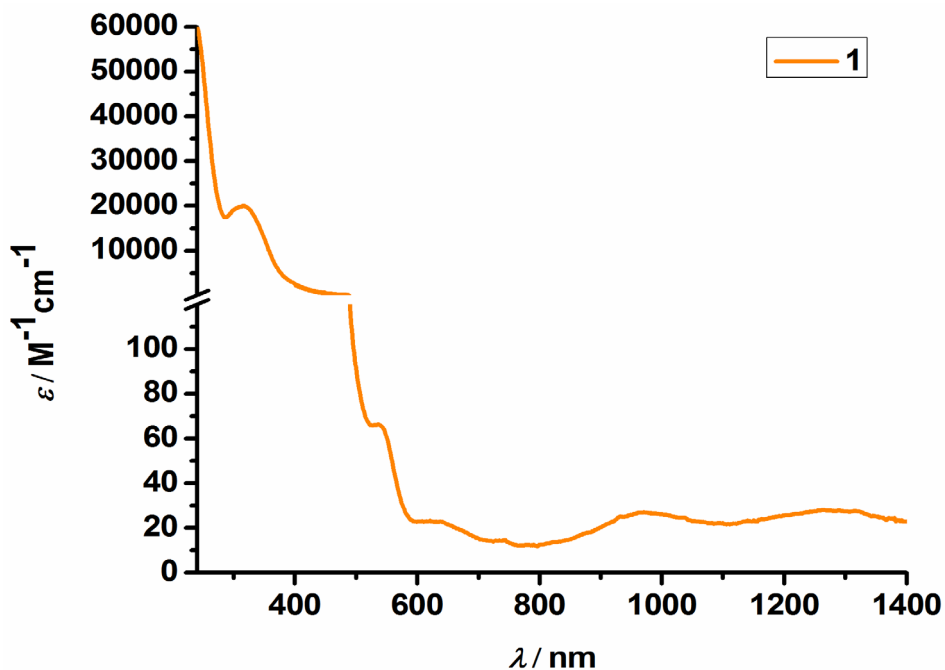
Figure S8. Electronic spectrum of **1** in DCM at room temperature. λ_{max}/ nm (ε/ M^{-1} cm^{-1}): 317 (20000), 540 (66); 642 (22); 970 (25); 1266 (26).
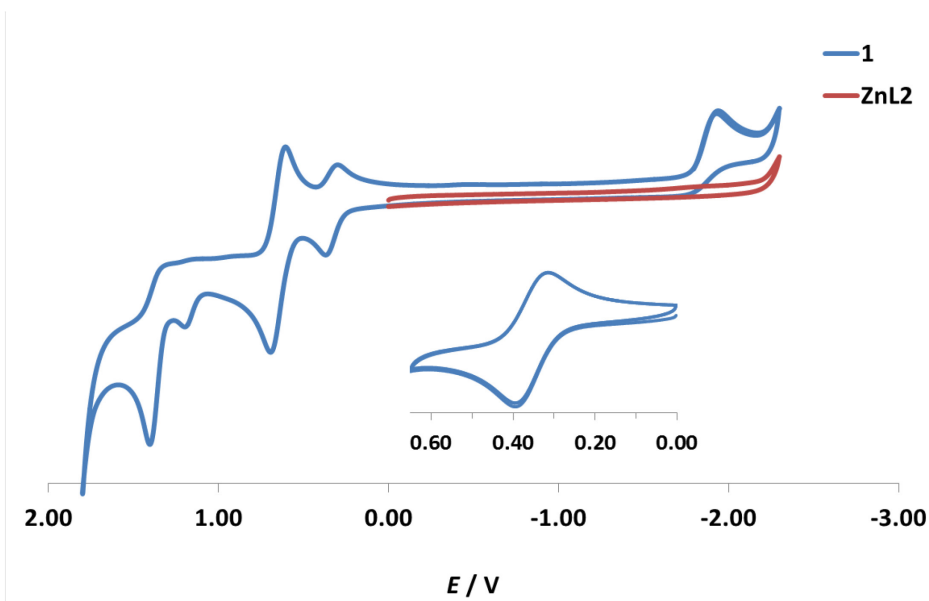
Figure S9. Cyclic voltammograms of complex **1** in dry DMF. The CV of the zinc analogue (**ZnL₂**) (negative potentials only) is shown for comparative purpose. Conditions: scan rate of 100 mV/s; potential *vs.* silver wire; in [nBu₄N]PF₆ 0.1M, compound concentration about 1 mM, glassy carbon electrode, room temperature, Ar atmosphere.

DFT Calculations

Gaussian09, Revision D.01[24] was used for all theoretical calculations discussed herein, with restricted open shell and spin-unrestricted B3LYP[25] DFT methods and LANL2DZ ECP[26] basis set. The calculations were performed for the ground states, in gas-phase and using the PCM (CH_2Cl_2) solvation model. Initial atom coordinates for geometry optimization were taken from XRD data (cif) of the corresponding structures. No symmetry constraints were used for the geometry optimization. Details on optimized structures are given in Tables S4-S15. No imaginary frequencies were obtained when frequency calculations on optimized geometries were performed. The values of $<S^2>$ were monitored, and didn't show major spin contamination (Tables S8-S9). The total energy values used for calculating energy differences were obtained from single point calculations on the optimized structures using a mixed basis set: LANL2DZ ECP for the Co atom, and 6-311g(d,p) for the N, O, C, H, Cl atoms. GaussView 3.0.9[27] and Chemissian 2.200[28] software were used for data analysis, visualisation, and surface plots.

DFT optimized structures of **1** were calculated for the following forms: square-planar (**1-green**), square-planar without the molecules of DCM (**1-green⊃2DCM**) and tetrahedral (**1-orange**) (Figure S10-S12 and Tables S4-S15; SI). The optimized calculated structures of **1** (Figure S11) are in agreement with the XRD data (Table S3).
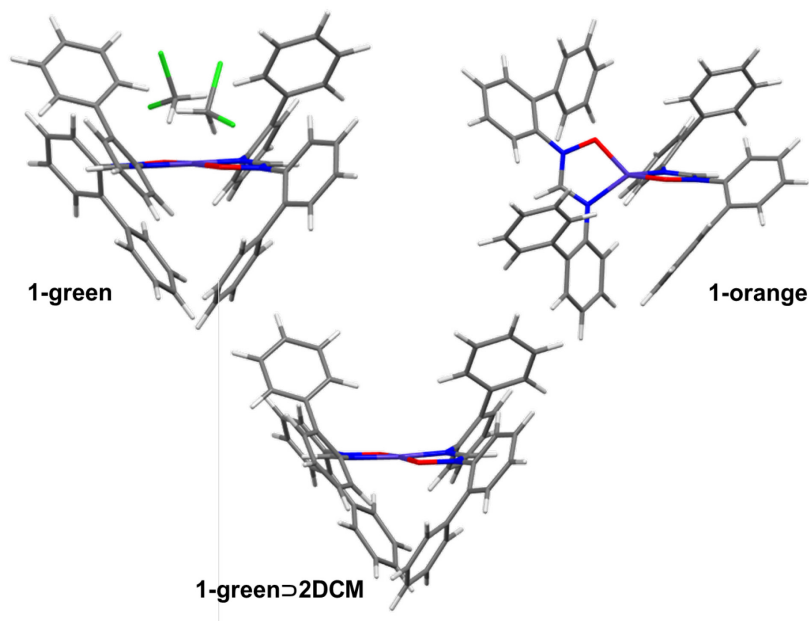
Figure S10. DFT optimized structures of **1** (square-planar – doublet (**1-green**); square-planar without the two molecules of DCM – doublet (**1-green⊃2DCM**), and tetrahedral – quadruplet (**1-orange**)); theory level: uB3LYP/LANL2DZ (all atoms), gas-phase.
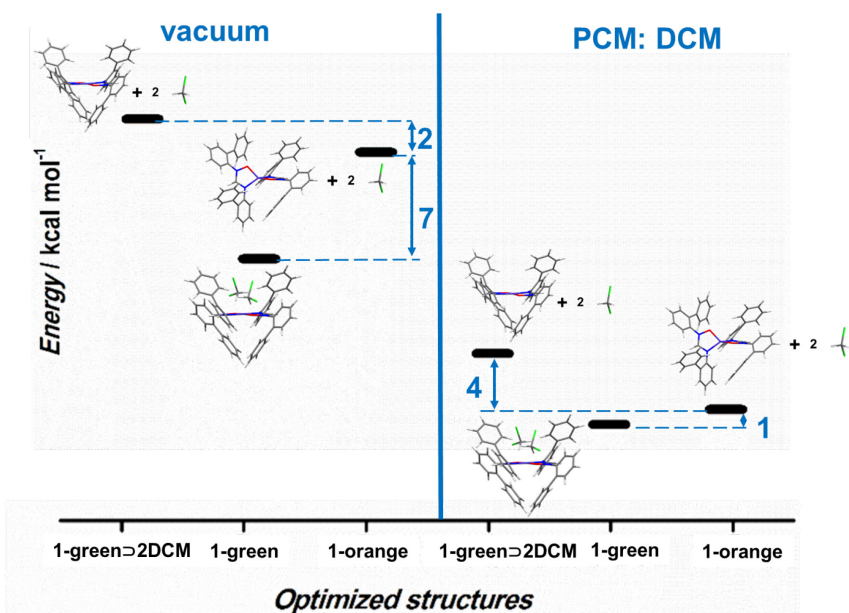
Figure. S11 – Balance of energy for the three forms calculated for **1** (square-planar – doublet (**1-green**); square-planar without the two molecules of DCM – doublet (**1-green⊃2DCM**), and

tetrahedral – quadruplet (**1-orange**)). Single point calculations at theory level: uB3LYP/ genecp LANL2DZ ECP (Co), 6311-G(d,p) (C, H, N, O, Cl), were ran on the structures optimized at uB3LYP/LANL2DZ (all atoms), in both gas-phase and PCM: DCM.
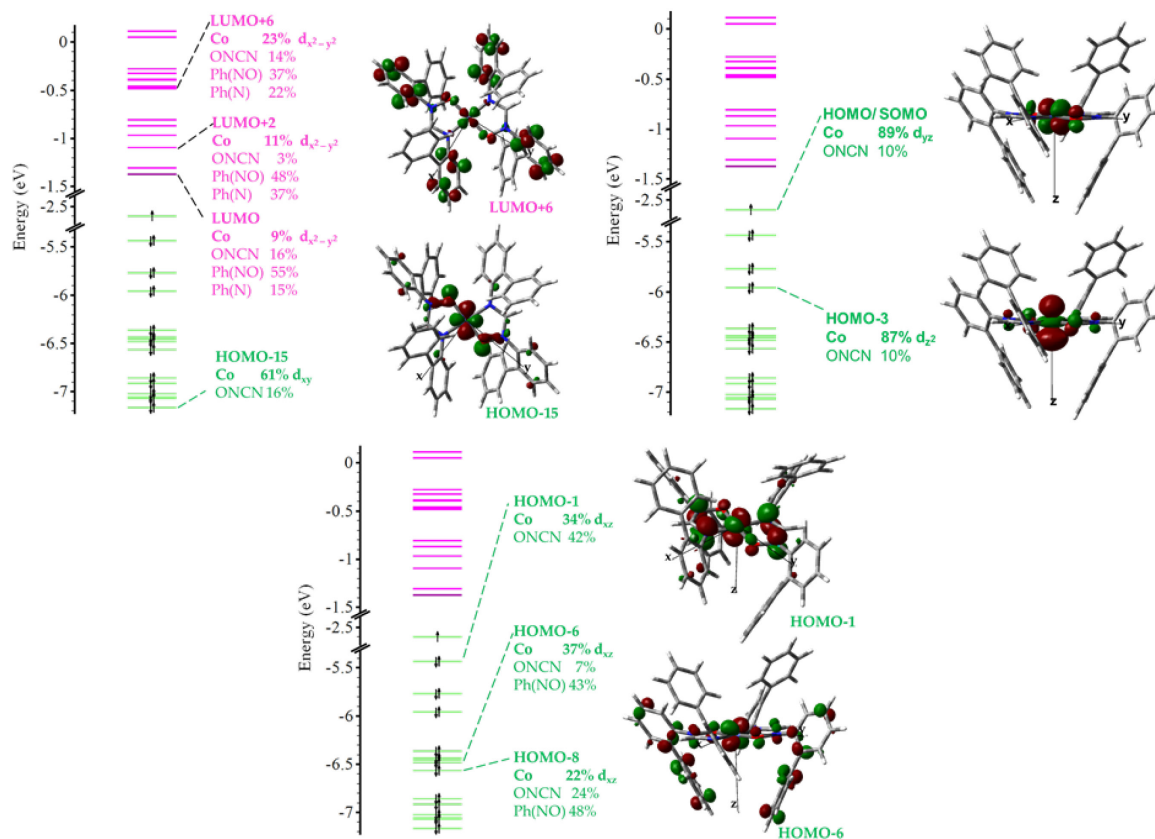
Figure S12. MO diagram for **1-green⊃2DCM** (doublet) roB3LYP/LANL2DZ PCM: CH₂Cl₂

Table S4. Total energy values for the optimized structures of the three forms of **1** (square-planar – doublet (**1-green**); square-planar without the two molecules of DCM – doublet (**1-green⊃2DCM**), and tetrahedral – quadruplet (**1-orange**)). Single point calculations at theory level: uB3LYP/ genecp LANL2DZ ECP (Co), 6311-G(d,p) (C, H, N, O, Cl), gas phae, were ran on the structures optimized at uB3LYP/LANL2DZ (all atoms), gas-phase

Cpd.	Total energy (E)		
	a. u	kcal mol^{-1}	kJ mol^{-1}
1-green⊃2DCM	-2443.28196	-1.531915E+06	-6.414837E+06
1-green	-4362.82284	-2.735450E+06	-1.145459E+07
1-orange	-2443.28546	-1.531917E+06	-6.414846E+06
DCM	-959.76303	-6.017626E+05	-2.519858E+06
ΔE₁ (E$_{1-green⊃2DCM}$ − E$_{1-orange}$)	**0.0035**	**2**	**9**
ΔE₂ [(E$_{1-green⊃2DCM}$ + 2E$_{DCM}$) − E$_{1-green}$]	**0.0148**	**9**	**39**
ΔE₃ [(E$_{1-orange}$ + 2E$_{DCM}$) − E$_{1-green}$]	**0.0113**	**7**	**30**

Table S5. Total energy values for the optimized structures of the three forms of **1** (square-planar – doublet (**1-green**); square-planar without the two molecules of DCM – doublet (**1-green⊃2DCM**), and tetrahedral – quadruplet (**1-orange**)). Single point calculations at theory level: uB3LYP/ genecp LANL2DZ ECP (Co), 6311-G(d,p) (C, H, N, O, Cl), PCM: CH$_2$Cl$_2$, were ran on the structures optimized at uB3LYP/LANL2DZ (all atoms), PCM: CH$_2$Cl$_2$

Cpd.	Total energy (E)		
	a. u	kcal mol^{-1}	kJ mol^{-1}
1-green⊃2DCM	-2443.29999	-1.531927E+06	-6.414884E+06
1-green	-4362.84039	-2.735461E+06	-1.145464E+07
1-orange	-2443.30594	-1.531930E+06	-6.414900E+06
DCM	-959.76645	-6.017647E+05	-2.519867E+06
ΔE₁ (E$_{1-green⊃2DCM}$ − E$_{1-orange}$)	**0.0060**	**4**	**16**
ΔE₂ [(E$_{1-green⊃2DCM}$ + 2E$_{DCM}$) − E$_{1-green}$]	**0.0076**	**5**	**20**
ΔE₃ [(E$_{1-orange}$ + 2E$_{DCM}$) − E$_{1-green}$]	**0.0016**	**1**	**4**

Table S6. Mulliken spin density values for the three forms of **1** (square-planar – doublet (**1-green**); square-planar without the two molecules of DCM – doublet (**1-green⊃2DCM**), and tetrahedral – quadruplet (**1-orange**)). Level of theory: uB3LYP/ LANL2DZ, gas-phase)

Cpd.	Mulliken spin density			
	Co	O	N	Other
1-green⊃2DCM	0.965 (97%)	0.060 (6%)	-0.004 (0%)	-0.022 (-2%)
1-green	0.943 (94%)	0.074 (7%)	0.004 (0%)	-0.021 (-2%)
1-orange	2.604 (87%)	0.220 (7%)	0.182 (6%)	-0.006 (0%)

Table S7. Mulliken spin density values for the three forms of **1** (square-planar – doublet (**1-green**); square-planar without the two molecules of DCM – doublet (**1-green⊃2DCM**), and tetrahedral – quadruplet (**1-orange**)). Level of theory: uB3LYP/ LANL2DZ, PCM: CH_2Cl_2)

Cpd.	Mulliken spin density			
	Co	O	N	Other
1-green⊃2DCM	0.971 (97%)	0.055 (6%)	-0.005 (0%)	-0.021 (-2%)
1-green	0.945 (95%)	0.072 (7%)	0.004 (0%)	-0.021 (-2%)
1-orange	2.639 (88%)	0.210 (7%)	0.161 (5%)	-0.010 (0%)

Table S8. Spin contamination monitoring for each of the calculated forms of **1** (square-planar – doublet (**1-green**); square-planar without the two molecules of DCM – doublet (**1-green⊃2DCM**), and tetrahedral – quadruplet (**1-orange**)). Level of theory: uB3LYP/ LANL2DZ, gas-phase

Cpd.	S**2		
	Before annihilation	After annihilation	% change
1-green⊃2DCM	0.8432	0.7506	12
1-green	0.8681	0.7507	16
1-orange	3.7601	3.7500	0.3

Table S9. Spin contamination monitoring for each of the calculated forms of **1** (square-planar – doublet (**1-green**); square-planar without the two molecules of DCM – doublet (**1-green⊃2DCM**), and tetrahedral – quadruplet (**1-orange**)). Level of theory: uB3LYP/ LANL2DZ, PCM: CH_2Cl_2

Cpd.	S**2		
	Before annihilation	After annihilation	% change
1-green⊃2DCM	0.8540	0.7506	14
1-green	0.8886	0.7508	18
1-orange	3.7592	3.7500	0.2

Table S10. DFT Optimization of **1-green⊃2DCM** (doublet) uB3LYP/LANL2DZ, gas-phase

Standard orientation:

```
---------------------------------------------------------------------------------
Center          Atomic          Atomic                Coordinates (Angstroms)
Number          Number          Type          X             Y             Z
---------------------------------------------------------------------------------
    1             27              0          0.000002     -0.000001      0.093294
    2              8              0         -1.786786     -0.569297      0.156537
    3              8              0          1.786863      0.569249      0.156484
    4              7              0         -2.681480      0.543808      0.144117
    5              7              0         -0.762465      1.783108      0.027846
    6              7              0          2.681542     -0.543864      0.144029
    7              7              0          0.762510     -1.783143      0.027856
    8              6              0         -4.085439      0.277546      0.103556
    9              6              0         -4.712616     -0.552529      1.072920
   10              6              0         -6.097104     -0.799053      0.909062
   11              1              0         -6.606725     -1.410530      1.648722
   12              6              0         -6.837938     -0.235699     -0.143116
   13              1              0         -7.902330     -0.440528     -0.225503
   14              6              0         -6.200808      0.599838     -1.078613
   15              1              0         -6.759740      1.039803     -1.900187
   16              6              0         -4.822909      0.839197     -0.959901
   17              1              0         -4.302500      1.432311     -1.707401
   18              6              0         -4.015868     -1.128099      2.262617
   19              6              0         -3.102750     -0.368048      3.030138
   20              1              0         -2.857721      0.645941      2.729919
   21              6              0         -2.511435     -0.904670      4.185709
   22              1              0         -1.815371     -0.299104      4.761466
   23              6              0         -2.816281     -2.216175      4.599697
   24              1              0         -2.355882     -2.631164      5.493195
   25              6              0         -3.720404     -2.985045      3.842416
   26              1              0         -3.960829     -4.001080      4.147596
   27              6              0         -4.314140     -2.444255      2.688110
   28              1              0         -4.992700     -3.056569      2.098757
   29              6              0         -2.092120      1.747004      0.060733
   30              1              0         -2.720730      2.631169      0.047914
   31              6              0         -0.091297      3.044270     -0.108996
   32              6              0         -0.414296      3.970784     -1.145369
```

33	6	0	0.246715	5.223094	-1.146993
34	1	0	0.021349	5.929958	-1.941876
35	6	0	1.214600	5.549246	-0.184103
36	1	0	1.711385	6.515822	-0.218629
37	6	0	1.555290	4.605410	0.803608
38	1	0	2.318168	4.829599	1.544260
39	6	0	0.905949	3.362739	0.835663
40	1	0	1.161655	2.622468	1.585178
41	6	0	-1.368825	3.669242	-2.259701
42	6	0	-2.331027	4.628286	-2.656778
43	1	0	-2.408046	5.565074	-2.109117
44	6	0	-3.199773	4.381076	-3.736258
45	1	0	-3.933552	5.131996	-4.020656
46	6	0	-3.122096	3.166164	-4.443448
47	1	0	-3.790424	2.972901	-5.279281
48	6	0	-2.165735	2.203884	-4.059703
49	1	0	-2.091372	1.264234	-4.602348
50	6	0	-1.300039	2.451835	-2.980878
51	1	0	-0.561688	1.706878	-2.698081
52	6	0	4.085505	-0.277623	0.103432
53	6	0	4.712723	0.552458	1.072764
54	6	0	6.097208	0.798963	0.908859
55	1	0	6.606859	1.410448	1.648492
56	6	0	6.838005	0.235579	-0.143329
57	1	0	7.902396	0.440393	-0.225753
58	6	0	6.200836	-0.599969	-1.078790
59	1	0	6.759739	-1.039960	-1.900370
60	6	0	4.822937	-0.839304	-0.960036
61	1	0	4.302497	-1.432418	-1.707514
62	6	0	4.016027	1.128044	2.262485
63	6	0	4.314361	2.444184	2.687985
64	1	0	4.992923	3.056480	2.098616
65	6	0	3.720684	2.984981	3.842318
66	1	0	3.961155	4.001004	4.147501
67	6	0	2.816561	2.216134	4.599621
68	1	0	2.356208	2.631128	5.493141
69	6	0	2.511652	0.904645	4.185627
70	1	0	1.815587	0.299098	4.761401
71	6	0	3.102907	0.368017	3.030028
72	1	0	2.857830	-0.645959	2.729805
73	6	0	2.092167	-1.747055	0.060677
74	1	0	2.720765	-2.631227	0.047824
75	6	0	0.091324	-3.044296	-0.108994
76	6	0	0.414194	-3.970736	-1.145470
77	6	0	-0.246815	-5.223049	-1.147093
78	1	0	-0.021551	-5.929859	-1.942053
79	6	0	-1.214575	-5.549267	-0.184103
80	1	0	-1.711360	-6.515843	-0.218628
81	6	0	-1.555145	-4.605498	0.803716
82	1	0	-2.317930	-4.829739	1.544447
83	6	0	-0.905804	-3.362827	0.835769
84	1	0	-1.161416	-2.622603	1.585363
85	6	0	1.368594	-3.669120	-2.259891
86	6	0	1.299792	-2.451624	-2.980916
87	1	0	0.561517	-1.706657	-2.697945
88	6	0	2.165371	-2.203594	-4.059816
89	1	0	2.090998	-1.263873	-4.602337
90	6	0	3.121629	-3.165884	-4.443795
91	1	0	3.789868	-2.972559	-5.279684
92	6	0	3.199319	-4.380886	-3.736760
93	1	0	3.933017	-5.131816	-4.021338

```
    94              6           0        2.330691   -4.628174   -2.657203
    95              1           0        2.407724   -5.565031   -2.109664
 -------------------------------------------------------------------------------------
```

Annihilation of the first spin contaminant:
S**2 before annihilation   0.8432,   after   0.7506

Table S11. DFT Optimization of **1-green⊃2DCM**   (doublet) uB3LYP/LANL2DZ, PCM: CH₂Cl₂

Standard orientation:

Center Number	Atomic Number	Atomic Type	X	Y	Z
1	27	0	0.000003	0.000019	0.145951
2	8	0	-1.829223	-0.450710	0.140977
3	8	0	1.829228	0.450749	0.141037
4	7	0	-2.646892	0.726040	0.103101
5	7	0	-0.644089	1.829051	0.101928
6	7	0	2.646901	-0.726000	0.103186
7	7	0	0.644100	-1.829014	0.101963
8	6	0	-4.062164	0.550851	-0.026721
9	6	0	-4.810572	-0.170246	0.943455
10	6	0	-6.190951	-0.354746	0.687394
11	1	0	-6.790790	-0.890078	1.418164
12	6	0	-6.813775	0.174292	-0.456552
13	1	0	-7.878476	0.021495	-0.611199
14	6	0	-6.059244	0.909181	-1.390401
15	1	0	-6.528649	1.323945	-2.277967
16	6	0	-4.681184	1.079694	-1.178517
17	1	0	-4.072437	1.598795	-1.914188
18	6	0	-4.235536	-0.694692	2.219131
19	6	0	-3.373441	0.090897	3.021055
20	1	0	-3.087504	1.085774	2.693297
21	6	0	-2.892334	-0.393849	4.249909
22	1	0	-2.236122	0.228929	4.853150
23	6	0	-3.261162	-1.676844	4.703079
24	1	0	-2.887227	-2.051637	5.652694
25	6	0	-4.119166	-2.467933	3.913998
26	1	0	-4.408857	-3.460590	4.250318
27	6	0	-4.603370	-1.978937	2.686709
28	1	0	-5.251524	-2.606771	2.080088
29	6	0	-1.973270	1.885108	0.066266
30	1	0	-2.538923	2.810541	0.037371
31	6	0	0.119269	3.042486	0.041029
32	6	0	-0.016960	3.979422	-1.026495
33	6	0	0.732177	5.180243	-0.954275
34	1	0	0.648158	5.898401	-1.766070
35	6	0	1.606538	5.446121	0.112270
36	1	0	2.173253	6.373414	0.131988
37	6	0	1.759138	4.493531	1.139194
38	1	0	2.444173	4.674401	1.963269
39	6	0	1.018103	3.302378	1.096776
40	1	0	1.121112	2.557849	1.879388

41	6	0	-0.872184	3.741097	-2.232991
42	6	0	-1.699651	4.774308	-2.735333
43	1	0	-1.751696	5.723893	-2.207712
44	6	0	-2.471286	4.584953	-3.897659
45	1	0	-3.103801	5.391105	-4.261683
46	6	0	-2.428240	3.355530	-4.584103
47	1	0	-3.023321	3.206475	-5.481690
48	6	0	-1.605173	2.319741	-4.095483
49	1	0	-1.558689	1.368482	-4.620238
50	6	0	-0.836966	2.509806	-2.933276
51	1	0	-0.201987	1.706251	-2.571227
52	6	0	4.062173	-0.550810	-0.026620
53	6	0	4.810550	0.170267	0.943588
54	6	0	6.190954	0.354701	0.687621
55	1	0	6.790770	0.890007	1.418429
56	6	0	6.813822	-0.174357	-0.456293
57	1	0	7.878538	-0.021603	-0.610878
58	6	0	6.059314	-0.909210	-1.390191
59	1	0	6.528754	-1.323995	-2.277728
60	6	0	4.681236	-1.079677	-1.178383
61	1	0	4.072513	-1.598769	-1.914079
62	6	0	4.235438	0.694714	2.219226
63	6	0	4.603371	1.978885	2.686926
64	1	0	5.251689	2.606670	2.080430
65	6	0	4.119064	2.467867	3.914180
66	1	0	4.408841	3.460464	4.250603
67	6	0	3.260844	1.676842	4.703092
68	1	0	2.886826	2.051626	5.652679
69	6	0	2.891896	0.393929	4.249785
70	1	0	2.235508	-0.228794	4.852891
71	6	0	3.373111	-0.090805	3.020969
72	1	0	3.087074	-1.085616	2.693094
73	6	0	1.973282	-1.885069	0.066342
74	1	0	2.538937	-2.810502	0.037477
75	6	0	-0.119260	-3.042446	0.041046
76	6	0	0.017013	-3.979410	-1.026449
77	6	0	-0.732141	-5.180220	-0.954238
78	1	0	-0.648088	-5.898399	-1.766010
79	6	0	-1.606563	-5.446061	0.112267
80	1	0	-2.173292	-6.373347	0.131975
81	6	0	-1.759206	-4.493445	1.139159
82	1	0	-2.444287	-4.674288	1.963203
83	6	0	-1.018154	-3.302303	1.096752
84	1	0	-1.121189	-2.557755	1.879342
85	6	0	0.872306	-3.741132	-2.232907
86	6	0	0.837132	-2.509870	-2.933245
87	1	0	0.202134	-1.706298	-2.571268
88	6	0	1.605408	-2.319855	-4.095415
89	1	0	1.558956	-1.368618	-4.620213
90	6	0	2.428499	-3.355667	-4.583946
91	1	0	3.023632	-3.206650	-5.481505
92	6	0	2.471499	-4.585062	-3.897451
93	1	0	3.104029	-5.391233	-4.261407
94	6	0	1.699796	-4.774368	-2.735161
95	1	0	1.751806	-5.723932	-2.207501

Annihilation of the first spin contaminant:
S**2 before annihilation   0.8540,   after   0.7506

Table S12. DFT Optimization of **1-green** (doublet) uB3LYP/LANL2DZ gas-phase

Standard orientation:

```
---------------------------------------------------------------------------------------
Center          Atomic         Atomic                Coordinates (Angstroms)
Number          Number         Type          X               Y               Z
---------------------------------------------------------------------------------------
   1              27              0        -0.000006        0.000009        0.457007
   2               8              0         1.885380        0.074848        0.522438
   3               8              0        -1.885382       -0.074843        0.522581
   4               7              0         2.450405       -1.237685        0.608461
   5               7              0         0.274415       -1.930181        0.431954
   6               7              0        -2.450445        1.237684        0.607896
   7               7              0        -0.274486        1.930222        0.431179
   8               6              0         1.564377       -2.240008        0.532327
   9               1              0         1.936946       -3.257640        0.577825
  10               6              0        -1.564478        2.240020        0.531390
  11               1              0        -1.937111        3.257646        0.576453
  12               6              0         3.876625       -1.365055        0.663015
  13               6              0         4.640035       -0.726713        1.677561
  14               6              0         6.046004       -0.872908        1.612717
  15               1              0         6.652686       -0.410021        2.386359
  16               6              0         6.670849       -1.635109        0.611843
  17               1              0         7.753521       -1.731002        0.602347
  18               6              0         5.893620       -2.273997       -0.370621
  19               1              0         6.364297       -2.858116       -1.156524
  20               6              0         4.498832       -2.121972       -0.350910
  21               1              0         3.888451       -2.558006       -1.137374
  22               6              0         4.047004        0.041821        2.813081
  23               6              0         2.938492       -0.447204        3.542583
  24               1              0         2.474044       -1.385198        3.253825
  25               6              0         2.436763        0.258667        4.648845
  26               1              0         1.587041       -0.139980        5.198242
  27               6              0         3.031744        1.470835        5.050234
  28               1              0         2.642426        2.016889        5.906154
  29               6              0         4.135345        1.968814        4.331492
  30               1              0         4.602058        2.904864        4.629816
  31               6              0         4.637598        1.259597        3.225808
  32               1              0         5.478259        1.662189        2.665537
  33               6              0        -0.686727       -2.984554        0.273971
  34               6              0        -0.545991       -4.002316       -0.719251
  35               6              0        -1.518463       -5.031940       -0.755720
  36               1              0        -1.429245       -5.803300       -1.516643
  37               6              0        -2.606448       -5.057008        0.132131
  38               1              0        -3.339820       -5.857029        0.071108
  39               6              0        -2.746312       -4.029877        1.085376
  40               1              0        -3.586421       -4.024578        1.774084
  41               6              0        -1.791353       -3.004323        1.152256
  42               1              0        -1.887953       -2.205068        1.877736
  43               6              0         0.553082       -4.028973       -1.738236
  44               6              0         0.880327       -2.888107       -2.510211
  45               1              0         0.338045       -1.960307       -2.356561
  46               6              0         1.888445       -2.946472       -3.487833
  47               1              0         2.122626       -2.056404       -4.065571
  48               6              0         2.588992       -4.147758       -3.718180
  49               1              0         3.367109       -4.190960       -4.476591
  50               6              0         2.269146       -5.291275       -2.961398
  51               1              0         2.801971       -6.224436       -3.129792
  52               6              0         1.260524       -5.230628       -1.981795
```

```
 53          1          0          1.030052    -6.115578    -1.392470
 54          6          0         -3.876664     1.364979     0.662928
 55          6          0         -4.639620     0.727242     1.678190
 56          6          0         -6.045631     0.873259     1.613779
 57          1          0         -6.651973     0.410839     2.387965
 58          6          0         -6.670917     1.634727     0.612624
 59          1          0         -7.753602     1.730510     0.603460
 60          6          0         -5.894119     2.273042    -0.370561
 61          1          0         -6.365162     2.856586    -1.156671
 62          6          0         -4.499310     2.121170    -0.351269
 63          1          0         -3.889236     2.556759    -1.138218
 64          6          0         -4.046049    -0.040435     2.814007
 65          6          0         -2.937307     0.449269     3.542696
 66          1          0         -2.473137     1.387146     3.253113
 67          6          0         -2.434980    -0.255759     4.649223
 68          1          0         -1.585079     0.143399     5.197972
 69          6          0         -3.029591    -1.467745     5.051700
 70          1          0         -2.639815    -2.013155     5.907822
 71          6          0         -4.133430    -1.966392     4.333785
 72          1          0         -4.599862    -2.902311     4.632956
 73          6          0         -4.636280    -1.258018     3.227830
 74          1          0         -5.477127    -1.661118     2.668205
 75          6          0          0.686579     2.984595     0.272737
 76          6          0          0.545694     4.002008    -0.720818
 77          6          0          1.518113     5.031671    -0.757736
 78          1          0          1.428782     5.802762    -1.518918
 79          6          0          2.606181     5.057103     0.129999
 80          1          0          3.339500     5.857148     0.068633
 81          6          0          2.746193     4.030303     1.083583
 82          1          0          3.586363     4.025279     1.772216
 83          6          0          1.791299     3.004719     1.150902
 84          1          0          1.888023     2.205707     1.876633
 85          6          0         -0.553485     4.028267    -1.739692
 86          6          0         -1.261028     5.229801    -1.983568
 87          1          0         -1.030526     6.114963    -1.394574
 88          6          0         -2.269783     5.290056    -2.963055
 89          1          0         -2.802683     6.223130    -3.131696
 90          6          0         -2.589676     4.146257    -3.719397
 91          1          0         -3.367902     4.189156    -4.477712
 92          6          0         -1.889028     2.945093    -3.488735
 93          1          0         -2.123237     2.054809    -4.066131
 94          6          0         -0.880767     2.887121    -2.511234
 95          1          0         -0.338407     1.959410    -2.357339
 96         17          0          5.230236     1.581624    -1.866637
 97         17          0          2.623533     1.083152    -3.426345
 98          6          0          3.379876     1.725663    -1.847389
 99          1          0          3.134620     2.780879    -1.782655
100          1          0          2.991171     1.124766    -1.028001
101         17          0         -2.624270    -1.084320    -3.425748
102         17          0         -5.230927    -1.582580    -1.865896
103          6          0         -3.380539    -1.726314    -1.846559
104          1          0         -3.135121    -2.781463    -1.781396
105          1          0         -2.991940    -1.125037    -1.027407
```

Annihilation of the first spin contaminant:
S**2 before annihilation   0.8681,   after   0.7507

Table S13. DFT Optimization of **1-green** (doublet) uB3LYP/LANL2DZ PCM: CH$_2$Cl$_2$

Standard orientation:

Center Number	Atomic Number	Atomic Type	Coordinates (Angstroms)		
			X	Y	Z
1	27	0	0.003437	−0.002460	0.396346
2	8	0	1.895793	−0.021927	0.441450
3	8	0	−1.888786	0.015958	0.438036
4	7	0	2.394403	−1.363243	0.524923
5	7	0	0.184540	−1.946293	0.386251
6	7	0	−2.388356	1.356933	0.521737
7	7	0	−0.178596	1.941614	0.387599
8	6	0	1.459422	−2.320259	0.468581
9	1	0	1.781806	−3.354545	0.521202
10	6	0	−1.453972	2.314568	0.468017
11	1	0	−1.777370	3.348470	0.521454
12	6	0	3.813526	−1.553573	0.597689
13	6	0	4.578895	−0.994264	1.656957
14	6	0	5.981410	−1.177641	1.606266
15	1	0	6.590821	−0.769749	2.408038
16	6	0	6.598856	−1.909913	0.577088
17	1	0	7.677682	−2.040056	0.579493
18	6	0	5.818207	−2.479266	−0.446342
19	1	0	6.283978	−3.046087	−1.247436
20	6	0	4.427479	−2.282917	−0.440938
21	1	0	3.814511	−2.669902	−1.250746
22	6	0	3.982728	−0.275011	2.823462
23	6	0	2.867209	−0.797448	3.520022
24	1	0	2.408076	−1.724257	3.189263
25	6	0	2.353179	−0.140662	4.651798
26	1	0	1.498383	−0.562201	5.175201
27	6	0	2.944607	1.053522	5.111598
28	1	0	2.545799	1.561982	5.985887
29	6	0	4.058056	1.581212	4.428369
30	1	0	4.522527	2.502190	4.772358
31	6	0	4.572707	0.920818	3.297304
32	1	0	5.423683	1.345194	2.770062
33	6	0	−0.828539	−2.956072	0.265399
34	6	0	−0.779750	−3.971797	−0.737998
35	6	0	−1.791495	−4.964838	−0.726481
36	1	0	−1.771556	−5.737862	−1.490228
37	6	0	−2.833641	−4.952482	0.215608
38	1	0	−3.598724	−5.723750	0.189867
39	6	0	−2.887574	−3.923115	1.176340
40	1	0	−3.693094	−3.889793	1.904658
41	6	0	−1.889271	−2.936806	1.196681
42	1	0	−1.915813	−2.139490	1.930724
43	6	0	0.256373	−4.025749	−1.819655
44	6	0	0.598457	−2.879232	−2.578088
45	1	0	0.125523	−1.927113	−2.355989
46	6	0	1.537735	−2.959911	−3.621089
47	1	0	1.784131	−2.067408	−4.190409
48	6	0	2.155112	−4.189169	−3.931221
49	1	0	2.882164	−4.249664	−4.737242
50	6	0	1.821205	−5.337512	−3.186613
51	1	0	2.291956	−6.291068	−3.413428
52	6	0	0.880376	−5.254946	−2.142625

53	1	0	0.641011	-6.145819	-1.566592
54	6	0	-3.807811	1.545491	0.594327
55	6	0	-4.571163	0.990056	1.656926
56	6	0	-5.974025	1.170410	1.606961
57	1	0	-6.581813	0.765127	2.411283
58	6	0	-6.593743	1.895995	0.574466
59	1	0	-7.672827	2.024027	0.577056
60	6	0	-5.815219	2.461199	-0.452906
61	1	0	-6.282945	3.022736	-1.256584
62	6	0	-4.424012	2.268001	-0.447669
63	1	0	-3.812302	2.652570	-1.259532
64	6	0	-3.972316	0.276525	2.825605
65	6	0	-2.859245	0.805527	3.521089
66	1	0	-2.404059	1.733543	3.188249
67	6	0	-2.342554	0.153636	4.654512
68	1	0	-1.489664	0.580081	5.177051
69	6	0	-2.928927	-1.041978	5.117036
70	1	0	-2.528112	-1.546647	5.992604
71	6	0	-4.040031	-1.576069	4.434948
72	1	0	-4.500599	-2.498208	4.781070
73	6	0	-4.557302	-0.920644	3.302196
74	1	0	-5.406364	-1.349829	2.775802
75	6	0	0.834402	2.952111	0.272546
76	6	0	0.785892	3.974441	-0.724173
77	6	0	1.798072	4.966932	-0.706485
78	1	0	1.778106	5.744850	-1.465251
79	6	0	2.840318	4.948313	0.235435
80	1	0	3.605537	5.719601	0.214701
81	6	0	2.893612	3.913021	1.189838
82	1	0	3.698720	3.875039	1.918394
83	6	0	1.895026	2.926908	1.203902
84	1	0	1.921293	2.125115	1.933029
85	6	0	-0.250842	4.036766	-1.804867
86	6	0	-0.877146	5.267916	-2.115628
87	1	0	-0.639137	6.153524	-1.530969
88	6	0	-1.818275	5.359002	-3.158647
89	1	0	-2.290790	6.313870	-3.376091
90	6	0	-2.149931	4.217434	-3.914583
91	1	0	-2.876986	4.284518	-4.720089
92	6	0	-1.530093	2.986395	-3.616665
93	1	0	-1.774281	2.099269	-4.195305
94	6	0	-0.590748	2.897100	-2.574404
95	1	0	-0.114948	1.944106	-2.362659
96	17	0	5.407862	1.611987	-1.557342
97	17	0	3.029182	0.979851	-3.402461
98	6	0	3.557934	1.663695	-1.748520
99	1	0	3.259115	2.706164	-1.722687
100	1	0	3.110977	1.042030	-0.974667
101	17	0	-3.122900	-0.935256	-3.403200
102	17	0	-5.402674	-1.669874	-1.473860
103	6	0	-3.561321	-1.666461	-1.743445
104	1	0	-3.234558	-2.700823	-1.751425
105	1	0	-3.098737	-1.048256	-0.975790

Annihilation of the first spin contaminant:
S**2 before annihilation   0.8886,   after   0.7508

Table S14. DFT Optimization of **1-orange** (quadruplet) uB3LYP/LANL2DZ, PCM: gas-phase

Standard orientation:

Center Number	Atomic Number	Atomic Type	Coordinates (Angstroms)		
			X	Y	Z
1	27	0	0.000162	-0.000015	0.220458
2	8	0	-1.266239	1.207759	-0.711573
3	8	0	1.266504	-1.207928	-0.711501
4	7	0	-0.937691	2.547719	-0.401065
5	7	0	0.703300	1.710489	0.999252
6	7	0	0.937654	-2.547848	-0.401164
7	7	0	-0.703074	-1.710448	0.999331
8	6	0	-1.650756	3.583220	-1.093126
9	6	0	2.920890	-5.614239	-2.562526
10	1	0	3.424987	-6.395951	-3.125124
11	6	0	1.516217	-5.581750	-2.493807
12	1	0	0.918137	-6.326421	-3.012242
13	6	0	3.731672	3.722667	-2.682950
14	1	0	3.919644	4.010579	-3.714812
15	6	0	-0.886869	4.554990	-1.772359
16	1	0	0.197224	4.477358	-1.764207
17	6	0	-5.950460	1.218768	-0.377079
18	1	0	-6.815522	0.809301	-0.893612
19	6	0	1.650690	-3.583417	-1.093152
20	6	0	3.675550	-4.635031	-1.895080
21	1	0	4.760616	-4.685989	-1.926194
22	6	0	-0.072863	-2.757846	0.459959
23	1	0	-0.323741	-3.787779	0.697374
24	6	0	4.549918	-1.377790	1.604314
25	1	0	4.329705	-1.091376	2.629861
26	6	0	-3.012836	-2.566096	1.432433
27	6	0	1.711279	1.484747	3.209726
28	1	0	0.790404	0.996214	3.517330
29	6	0	3.919902	4.651459	-1.641479
30	1	0	4.253835	5.662458	-1.864697
31	6	0	-4.549923	1.377420	1.604209
32	1	0	-4.329674	1.090977	2.629740
33	6	0	-3.923661	-2.356416	3.711818
34	1	0	-4.736173	-2.529756	4.413122
35	6	0	3.056400	2.037696	-1.046292
36	1	0	2.748032	1.018892	-0.826206
37	6	0	-3.732098	-3.722656	-2.682518
38	1	0	-3.920237	-4.010634	-3.714332
39	6	0	3.071237	-3.604172	-1.135877
40	6	0	-2.753662	-1.691543	4.127123
41	1	0	-2.649821	-1.349331	5.154088
42	6	0	3.233481	2.967798	0.007137
43	6	0	0.886769	-4.555130	-1.772420
44	1	0	-0.197316	-4.477399	-1.764348
45	6	0	-3.920335	-4.651336	-1.640942
46	1	0	-4.254407	-5.662315	-1.864042
47	6	0	-3.946151	2.634276	-0.411084
48	6	0	-1.711011	-1.484207	3.209726
49	1	0	-0.790086	-0.995690	3.517207
50	6	0	3.923879	2.357240	3.711570

```
51          1          0       4.736393    2.530786    4.412820
52          6          0       4.043478    2.780951    2.377335
53          1          0       4.962420    3.257813    2.044608
54          6          0      -3.233537   -2.967613    0.007453
55          6          0      -4.043334   -2.780381    2.377671
56          1          0      -4.962344   -3.257196    2.045059
57          6          0      -3.071302    3.603860   -1.135969
58          6          0      -5.683678    0.851215    0.954883
59          1          0      -6.340053    0.158653    1.476302
60          6          0       3.674058    4.274378   -0.307482
61          1          0       3.811044    4.999562    0.492367
62          6          0       2.753940    1.692361    4.127051
63          1          0       2.650164    1.350360    5.154092
64          6          0       0.072833    2.757816    0.460034
65          1          0       0.323517    3.787773    0.697562
66          6          0      -1.817141   -1.929050    1.874934
67          6          0      -3.056443   -2.037628   -1.046076
68          1          0      -2.747907   -1.018847   -0.826119
69          6          0      -3.674313   -4.274169   -0.307004
70          1          0      -3.811309   -4.999260    0.492929
71          6          0      -3.691966    2.259960    0.928361
72          1          0      -2.822822    2.658640    1.443772
73          6          0       1.817348    1.929322    1.874843
74          6          0       5.683623   -0.851525    0.954952
75          1          0       6.339975   -0.158921    1.476345
76          6          0       3.012959    2.566400    1.432177
77          6          0       3.946110   -2.634622   -0.410976
78          6          0      -3.302880   -2.415017   -2.377311
79          1          0      -3.162938   -1.685813   -3.171509
80          6          0       5.950378   -1.219063   -0.377022
81          1          0       6.815402   -0.809551   -0.893584
82          6          0      -5.090461    2.103905   -1.050948
83          1          0      -5.289703    2.357765   -2.089647
84          6          0       3.302649    2.414998   -2.377584
85          1          0       3.162711    1.685714   -3.171709
86          6          0       3.691966   -2.260351    0.928485
87          1          0       2.822851   -2.659067    1.443919
88          6          0       5.090390   -2.104228   -1.050870
89          1          0       5.289615   -2.358098   -2.089570
90          6          0      -1.516344    5.581541   -2.493824
91          1          0      -0.918281    6.326261   -3.012205
92          6          0      -2.921010    5.613905   -2.562661
93          1          0      -3.425132    6.395542   -3.125340
94          6          0      -3.675638    4.634650   -1.895245
95          1          0      -4.760705    4.685532   -1.926435
 ---------------------------------------------------------------------------------------------
```

Annihilation of the first spin contaminant:
S**2 before annihilation   3.7601,   after   3.7500

Table S15. DFT Optimization of **1-orange** (quadruplet) uB3LYP/LANL2DZ PCM: CH$_2$Cl$_2$

Standard orientation:

```
---------------------------------------------------------------------
Center          Atomic          Atomic          Coordinates (Angstroms)
Number          Number          Type          X          Y          Z
---------------------------------------------------------------------
   1              27              0        0.000060     0.000066    -0.150228
   2               8              0       -0.542803     1.605196     0.919974
   3               8              0        0.542533    -1.605629     0.919479
   4               7              0       -1.840654     2.011354     0.520809
   5               7              0       -1.858114     0.200709    -0.922863
   6               7              0        1.840645    -2.011400     0.520870
   7               7              0        1.858096    -0.200928    -0.923019
   8               6              0       -2.422001     3.124129     1.220983
   9               6              0        3.589073    -5.180154     2.740590
  10               1              0        4.029472    -5.982884     3.325848
  11               6              0        4.227091    -3.928301     2.658992
  12               1              0        5.159755    -3.746818     3.185693
  13               6              0       -5.884104    -0.859119     2.281250
  14               1              0       -6.397770    -0.786458     3.236699
  15               6              0       -3.630587     2.899127     1.911664
  16               1              0       -4.080172     1.910067     1.886400
  17               6              0        1.670360     5.803927     0.424179
  18               1              0        2.461990     6.354453     0.926707
  19               6              0        2.422043    -3.124080     1.221147
  20               6              0        2.380659    -5.396187     2.055006
  21               1              0        1.912371    -6.375688     2.098828
  22               6              0        2.476851    -1.261491    -0.392162
  23               1              0        3.476310    -1.572058    -0.680622
  24               6              0       -0.777052    -4.725054    -1.565304
  25               1              0       -0.873983    -4.444436    -2.611199
  26               6              0        3.852664     1.200697    -1.540345
  27               6              0       -1.949677    -0.943696    -3.067780
  28               1              0       -0.968905    -0.522390    -3.265146
  29               6              0       -6.573038    -0.594023     1.081258
  30               1              0       -7.622857    -0.311622     1.105601
  31               6              0        0.777437     4.724356    -1.565452
  32               1              0        0.874368     4.443674    -2.611330
  33               6              0        3.874600     2.246754    -3.775560
  34               1              0        4.385714     2.857041    -4.515401
  35               6              0       -3.854889    -1.314114     0.997392
  36               1              0       -2.808675    -1.605893     0.973412
  37               6              0        5.883616     0.860130     2.281320
  38               1              0        6.397213     0.787689     3.236823
  39               6              0        1.773643    -4.387834     1.268174
  40               6              0        2.588123     1.734991    -4.035336
  41               1              0        2.092862     1.940908    -4.980868
  42               6              0       -4.536290    -1.046459    -0.215636
  43               6              0        3.630589    -2.898900     1.911858
  44               1              0        4.080063    -1.909791     1.886564
  45               6              0        6.572710     0.595027     1.081423
  46               1              0        7.622583     0.312839     1.105894
  47               6              0       -0.527325     4.713418     0.510646
  48               6              0        1.949735     0.943078    -3.068136
  49               1              0        0.969117     0.521459    -3.265603
  50               6              0       -3.874789    -2.246986    -3.775245
  51               1              0       -4.385973    -2.857242    -4.515064
  52               6              0       -4.486024    -1.980849    -2.538339
```

```
53          1          0      -5.459963    -2.412420    -2.321211
54          6          0       4.535986     1.046894    -0.215702
55          6          0       4.485740     1.980961    -2.538532
56          1          0       5.459549     2.412796    -2.321344
57          6          0      -1.773466     4.387815     1.267916
58          6          0       1.808990     5.445766    -0.931101
59          1          0       2.705314     5.719070    -1.482338
60          6          0      -5.904467    -0.689422    -0.154400
61          1          0      -6.443605    -0.472607    -1.073852
62          6          0      -2.588141    -1.735602    -4.034935
63          1          0      -2.092804    -1.941826    -4.980359
64          6          0      -2.476790     1.261447    -0.392266
65          1          0      -3.476102     1.572209    -0.681036
66          6          0       2.568559     0.647586    -1.833487
67          6          0       3.854430     1.314580     0.997231
68          1          0       2.808169     1.606173     0.973108
69          6          0       5.904229     0.690143    -0.154308
70          1          0       6.443495     0.473348    -1.073690
71          6          0      -0.378389     4.362761    -0.851984
72          1          0      -1.168939     3.815904    -1.358089
73          6          0      -2.568613    -0.647824    -1.833277
74          6          0      -1.808506    -5.446607    -0.930960
75          1          0      -2.704753    -5.720111    -1.482223
76          6          0      -3.852886    -1.200574    -1.540196
77          6          0       0.527613    -4.713739     0.510849
78          6          0       4.521523     1.222779     2.231617
79          1          0       3.981195     1.438289     3.150148
80          6          0      -1.669876    -5.804643     0.424356
81          1          0      -2.461430    -6.355278     0.926888
82          6          0       0.511011     5.443722     1.135818
83          1          0       0.423781     5.709599     2.186634
84          6          0      -4.522077    -1.222032     2.231707
85          1          0      -3.981865    -1.437524     3.150311
86          6          0       0.378667    -4.363189    -0.851800
87          1          0       1.169132    -3.816200    -1.357900
88          6          0      -0.510626    -5.444184     1.136023
89          1          0      -0.423408    -5.709975     2.186862
90          6          0      -4.227009     3.928669     2.658679
91          1          0      -5.159725     3.747351     3.185345
92          6          0      -3.588865     5.180460     2.740167
93          1          0      -4.029208     5.983292     3.325331
94          6          0      -2.380389     5.396313     2.054623
95          1          0      -1.911987     6.375760     2.098396
```

Annihilation of the first spin contaminant:
S**2 before annihilation   3.7592,   after   3.7500

References

[1]   G. M. Sheldrick, *Acta Crystallogr., Sect. A: Found. Crystallogr.* **2008**, *64*, 112-122.
[2]   A. L. Spek, *Acta Crystallogr., Sect. D: Biol. Crystallogr.* **2009**, *65*, 148-155.
[3]   Bruker, **2001,** *SADABS and TWINABS,* Bruker AXS Inc., Madison, Wisconsin, USA.
[4]   F. Allen, *Acta Crystallogr., Sect. B: Struct. Sci.* **2002**, *58*, 380-388.
[5]   L. Yang, D. R. Powell, R. P. Houser, *Dalton Trans.* **2007**, 955-964.

[6] S. A. Carabineiro, L. C. Silva, P. T. Gomes, L. C. J. Pereira, L. F. Veiros, S. I. Pascu, M. T. Duarte, S. Namorado, R. T. Henriques, *Inorg. Chem.* **2007**, *46*, 6880-6890.

[7] C. H. Wei, *Inorg. Chem.* **1972**, *11*, 1100-1105.

[8] M. F. Rudolf, J. Wolny, Z. Ciunik, P. Chmielewski, *J. Chem. Soc., Chem. Commun.* **1988**, 1006.

[9] J. A. Wolny, M. F. Rudolf, Z. Ciunik, K. Gatner, S. Wolowiec, *J. Chem. Soc., Dalton Trans.* **1993**, 1611-1622.

[10] C. P. Rao, J. R. Dorfman, R. H. Holm, *Inorg. Chem.* **1986**, *25*, 428-439.

[11] D. V. Konarev, A. V. Kuzmin, S. V. Simonov, S. S. Khasanov, E. I. Yudanova, R. N. Lyubovskaya, *Dalton Trans.* **2011**, *40*, 4453-4458.

[12] W. W. Brennessel, J. V. G. Young, J. E. Ellis, *Angew. Chem. Int. Ed.* **2002**, *41*, 1211-1215.

[13] L. Tahsini, S. E. Specht, J. S. Lum, J. J. M. Nelson, A. F. Long, J. A. Golen, A. L. Rheingold, L. H. Doerrer, *Inorg. Chem.* **2013**, *52*, 14050-14063.

[14] S. A. Cantalupo, S. R. Fiedler, M. P. Shores, A. L. Rheingold, L. H. Doerrer, *Angew. Chem., Int. Ed.* **2012**, *51*, 1000-1005.

[15] X. Wurzenberger, C. Neumann, P. Klüfers, *Angew. Chem., Int. Ed.* **2013**, *52*, 5159-5161.

[16] R. W. Saalfrank, I. Bernt, E. Uller, F. Hampel, *Angew. Chem. Int. Ed.* **1997**, *36*, 2482-2485.

[17] N. Reddig, D. Pursche, B. Krebs, A. Rompel, *Inorg. Chim. Acta* **2004**, *357*, 2703-2712.

[18] M. R. Seyedsayamdost, M. F. Traxler, S.-L. Zheng, R. Kolter, J. Clardy, *J. Am. Chem. Soc.* **2011**, *133*, 11434-11437.

[19] C. López, A. Caubet, S. Pérez, X. Solans, M. Font-Bardía, E. Molins, *Eur. J. Inorg. Chem.* **2006**, *2006*, 3974-3984.

[20] P. Braunstein, O. Siri, J.-p. Taquet, M.-M. Rohmer, M. Bénard, R. Welter, *J. Am. Chem. Soc.* **2003**, *125*, 12246-12256.

[21] A. W. Waltman, R. H. Grubbs, *Organometallics* **2004**, *23*, 3105-3107.

[22] R. Blaauw, J. L. van der Baan, S. Balt, M. W. G. de Bolster, G. W. Klumpp, H. Kooijman, A. L. Spek, *Chem. Commun.* **1998**, 1295-1296.

[23] A. Nabei, T. Kuroda-Sowa, T. Okubo, M. Maekawa, M. Munakata, *Acta Crystallogr., Sect. E: Struct. Rep. Online* **2009**, *65*, m188-m189.

[24] G. W. T. M. J. Frisch, H. B. Schlegel, G. E. Scuseria, M. A. Robb, J. R. Cheeseman, G. Scalmani, V. Barone, B. Mennucci, G. A. Petersson, H. Nakatsuji, M. Caricato, X. Li, H. P. Hratchian, A. F. Izmaylov, J. Bloino, G. Zheng, J. L. Sonnenberg, M. Hada, M. Ehara, K. Toyota, R. Fukuda, J. Hasegawa, M. Ishida, T. Nakajima, Y. Honda, O. Kitao, H. Nakai, T. Vreven, J. A. Montgomery, Jr., J. E. Peralta, F. Ogliaro, M. Bearpark, J. J. Heyd, E. Brothers, K. N. Kudin, V. N. Staroverov, R. Kobayashi, J. Normand, K. Raghavachari, A. Rendell, J. C. Burant, S. S. Iyengar, J. Tomasi, M. Cossi, N. Rega, J. M. Millam, M. Klene, J. E. Knox, J. B. Cross, V. Bakken, C. Adamo, J. Jaramillo, R. Gomperts, R. E. Stratmann, O. Yazyev, A. J. Austin, R. Cammi, C. Pomelli, J. W. Ochterski, R. L. Martin, K. Morokuma, V. G. Zakrzewski, G. A. Voth, P. Salvador, J. J. Dannenberg, S. Dapprich, A. D. Daniels, Ö. Farkas, J. B. Foresman, J. V. Ortiz, J. Cioslowski, and D. J. Fox, **2009,** *Gaussian09,* Gaussian, Inc.; Wallingford CT.

[25] a) C. Lee, W. Yang, R. G. Parr, *Phys. Rev. B: Condens. Matter* **1988**, *37*, 785-789; b) B. Miehlich, A. Savin, H. Stoll, H. Preuss, *Chem. Phys. Lett.* **1989**, *157*, 200-206.

[26] a) P. J. Hay, W. R. Wadt, *J. Chem. Phys.* **1985**, *82*, 270-283; b) P. J. Hay, W. R. Wadt, *J. Chem. Phys.* **1985**, *82*, 299-310; c) T. H. D. J. a. P. J. Hay, in *Methods of Electronic Structure Theory, Vol. 2* (Ed.: H. F. S. III), Plenum Press New York, **1977**; d) W. R. Wadt, P. J. Hay, *J. Chem. Phys.* **1985**, *82*, 284-298.

[27] R. D. K. Dennington II, T.; Millam, J.; Eppinnett, K.; Hovell, W. L.; Gilliland, R., **2003**, *GaussView 3.0.9,* Semichem, Inc.; Shawnee Mission, KS.

[28] L. Skripnikov, **2005 - 2014,** *Chemissian V4.01,*

Appendix-5.2-SI

Supporting Information

for

The Relationship between Structure and Properties in Zn[II] Complexes of Bulky *N,N'*-Diarylformamidinate *N*-Oxides

Mihaela Cibian, Sophie Langis-Barsetti, Janaina G. Ferreira, and Garry S. Hanan*

Département of Chemistry, Université de Montréal, Montréal, Québec, H3T-1J4, Canada

Contents

Scheme S1. Synthesis of AMOX ligands **2a-d** and their corresponding Zn(AMOX)$_2$ complexes **3a-d.** The structures of **3a-d** are presented with notation of the protons.
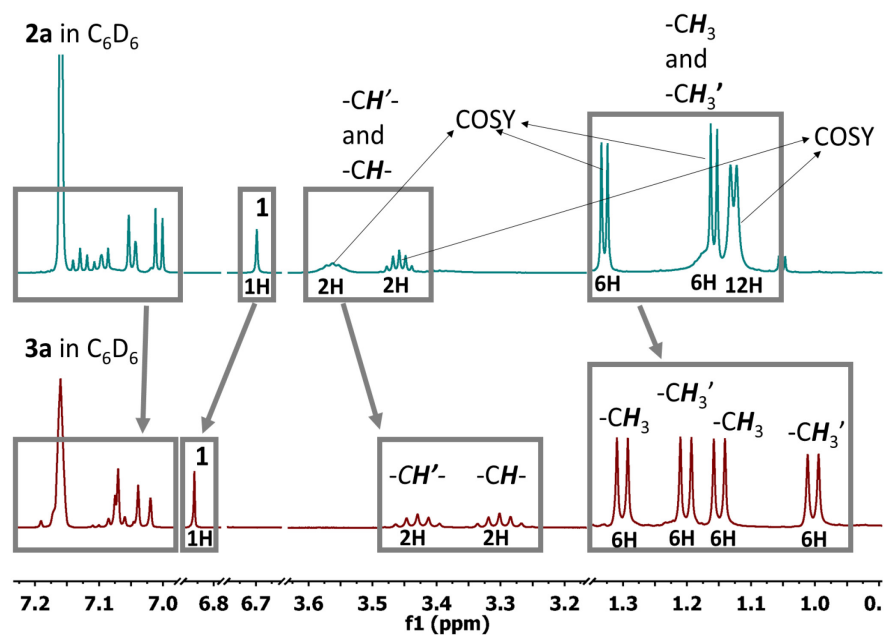
Figure S1. ^{1}H-NMR spectra for **2a** and **3a** in C_6D_6 (tentative assignment based on the integration ratio, 2D COSY, NOESY, and HMQC, and proximity of the proton to the metallic centre).
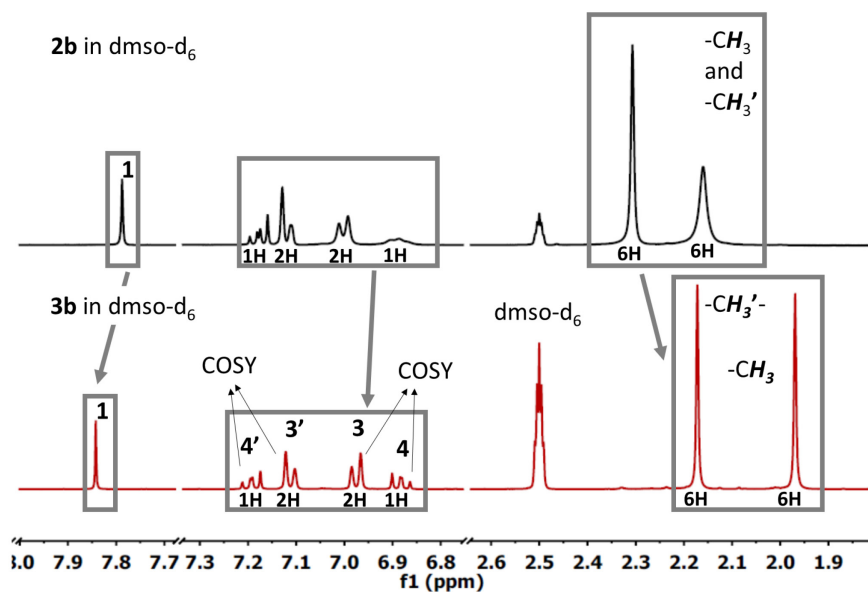
Figure S2. ^{1}H-NMR spectra for **2b** and **3b** in dmso-d_6 (tentative assignment based on the integration ratio, 2D COSY, NOESY, and HMQC, and proximity of the proton to the metallic centre).
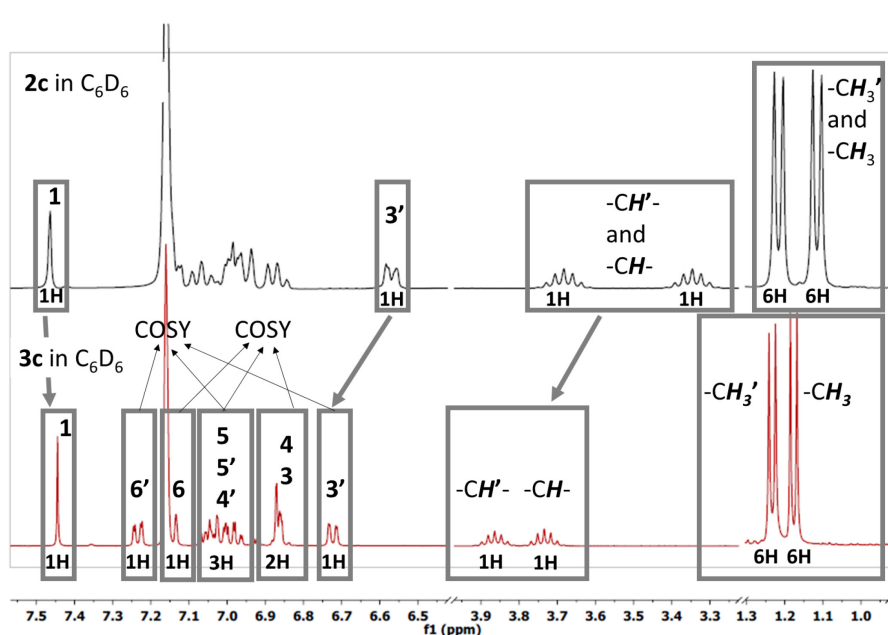
Figure S3. ^{1}H-NMR spectra for 2c and 3c in C_6D_6 (tentative assignment based on the integration ratio, 2D COSY, NOESY, and HMQC, and proximity of the proton to the metallic centre).

X-Ray diffraction measurements and structure determination

Crystallographic data for **3a** and **3b** were collected at 200 K and 150 K, respectively, from single crystals which were mounted on loop fibers. Data were collected using a Bruker Platform diffractometer, a Bruker SMART 4K Charged-Coupled Device (CCD) Area Detector, and a Nonius FR591 rotating anode equipped with a Montel 200 optics. The crystal-to-detector distance was 5.0 cm, and the data collection was carried out in 512 x 512 pixel mode. The initial unit cell parameters were determined by a least-squares fit of the angular setting of strong reflections, collected by a 10.0 degree scan in 33 frames over three different parts of the reciprocal space (99 frames total). Crystallographic data for **3d** were collected at 100 K using a Bruker Venture diffractometer configured with a Metal Jet liquid-metal source, a Photon 100 CMOS-based area detector, a Helios MX optics and a Kappa goniometer. The crystal-to-detector distance was 4.0 cm, and the data collection was carried out in 1024 x 1024 pixel mode. For data collection, determination of cell parameters, cell refinement, and data reduction *APEX2* and *SAINT* (Bruker, 2007) were used.[1] Absorption corrections were applied using *SADABS* (Bruker 2001).[2] Structure solution was performed using direct methods with *SHELXS*

or *SHELXT* (Sheldrick, 2008; Sheldrick, 2015)[3] and refined on F^2 by full-matrix least squares using *SHELXL97* and *SHELXL2014* (Sheldrick, 2008; Sheldrick, 2015).[3] *OLEX2* (Dolomanov *et al.*, 2009),[4] *ORTEP-3 for Windows* (Farrugia, 2012),[5] and POV-ray (2013)[6] were used for molecular graphics. The material was prepared for publication using *PLATON* (Spek, 2009),[7] Mercury,[8] UdMX,[9] and *publCIF* (Westrip, 2010).[10] All non-H atoms were refined by full-matrix least-squares with anisotropic displacement parameters. The H-atoms were included in calculated positions and treated as riding atoms: aromatic C—H 0.95 Å, methyl C—H 0.98 Å, with $U_{iso}(H) = k \times U_{eq}$ (parent C-atom), where k = 1.2 for the aromatic H-atoms and 1.5 for the methyl H-atoms. Data were deposited in CCDC under the deposit numbers: 963739 (for **3b**), 963740 (for **3a**), and 1426815 (for **3d**). For compound **3a**, the structure contains two co-crystallized solvent molecules (methanol), which are slightly disordered. checkCIF/ PLATON routine gives a B alert related to the completeness %, which is lower than the threshold considered. As also mentioned in the comments in the cif, the low completeness value is due to geometrical constraints of the instrument and the use of copper radiation. Data completeness percentages lower than 100% were obtained, in dependence of the crystal system and the orientation of the mounted crystal, even with appropriate data collection routines. This situation existed in the past with the instrument that we used, but it has been corrected. In case of **3a**, the data were collected while this situation still existed. Nevertheless, the data set and the structure factors for **3a** are good (R_{int} is 4.36%, R_1 is 4.91%), validating the crystallographic data. Solvent accessible void of 34 Å^3 is reported. This void is too small to accommodate molecules bigger than water, and water didn't fit. For compound **3d**, a residual electron density pic (1.17 e/Å^3) exists. The closest atom to it is C31 (1.57 Å). This residual electron density doesn't make chemical sense. Relevant atomic sites have been checked and they were found to be consistent with the chemistry performed. No twinning was detected using *CELL_NOW* (Bruker 2001)[2] and TwinRotMat routine implemented in *PLATON* (Spek, 2009).[7] No solvent voids and no corresponding residual density were identified with *SQUEEZE* routine in *PLATON* (Spek, 2009)[7] (this routine was used as a test, and it is not applied to the present model). The crystal was poor quality (very small and fine needle). For **3d**, The Flack parameter was refined using TWIN/ BASF to give 0.49(3). As the compound crystallized in the polar space group *Pca2₁*, it indicates the orientation of the molecule vs. the polar axis.
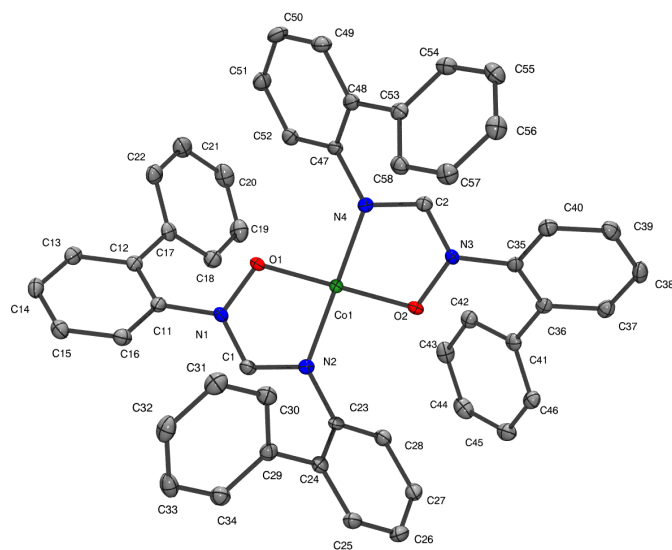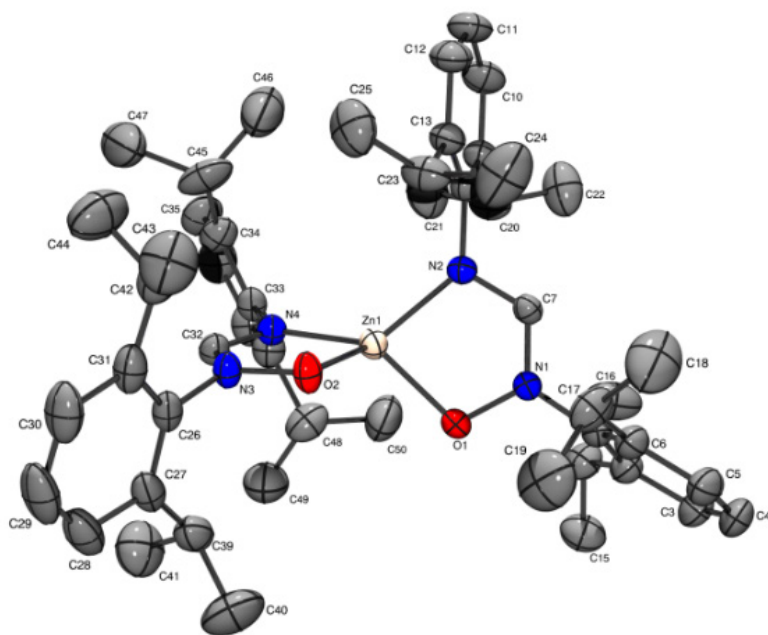
Figure S4. ORTEP view of **3a** with labels. Ellipsoids are shown at 50% probability level. Hydrogen atoms and co-crystallized solvent molecules were omitted for clarity.
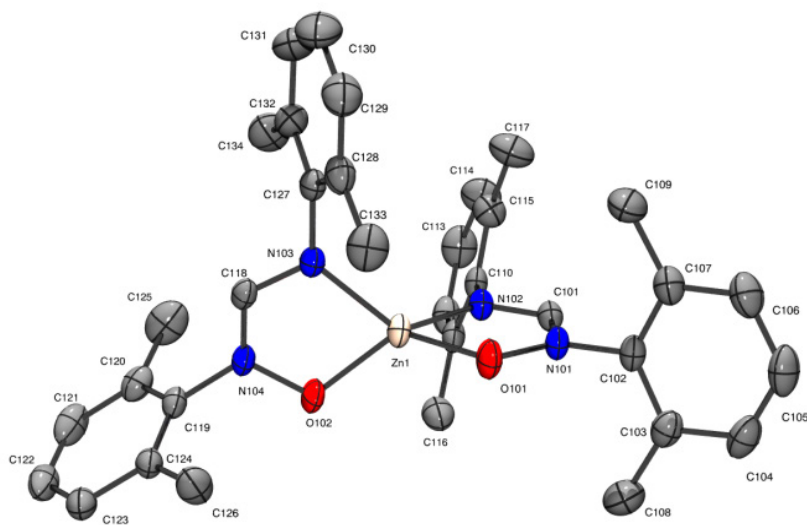
Figure S5. ORTEP view of **3b** with labels. Ellipsoids are shown at 50% probability level. Hydrogen atoms were omitted for clarity.
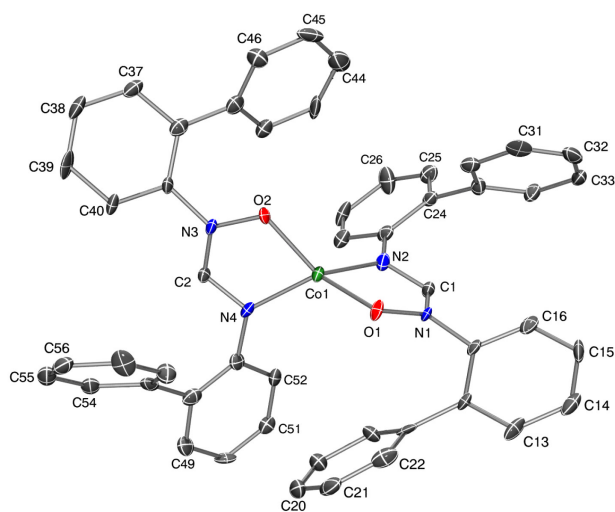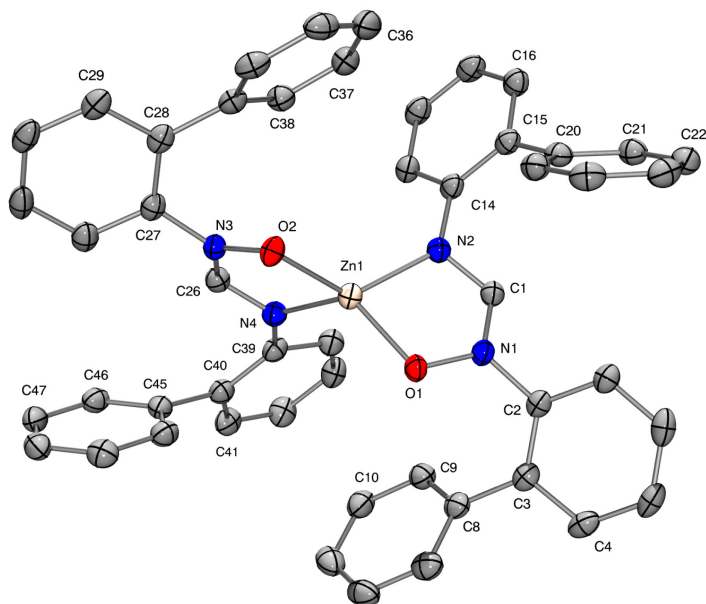
Figure S6. ORTEP view of **3d** with labels. Ellipsoids are shown at 50% probability level. Hydrogen atoms were omitted for clarity.
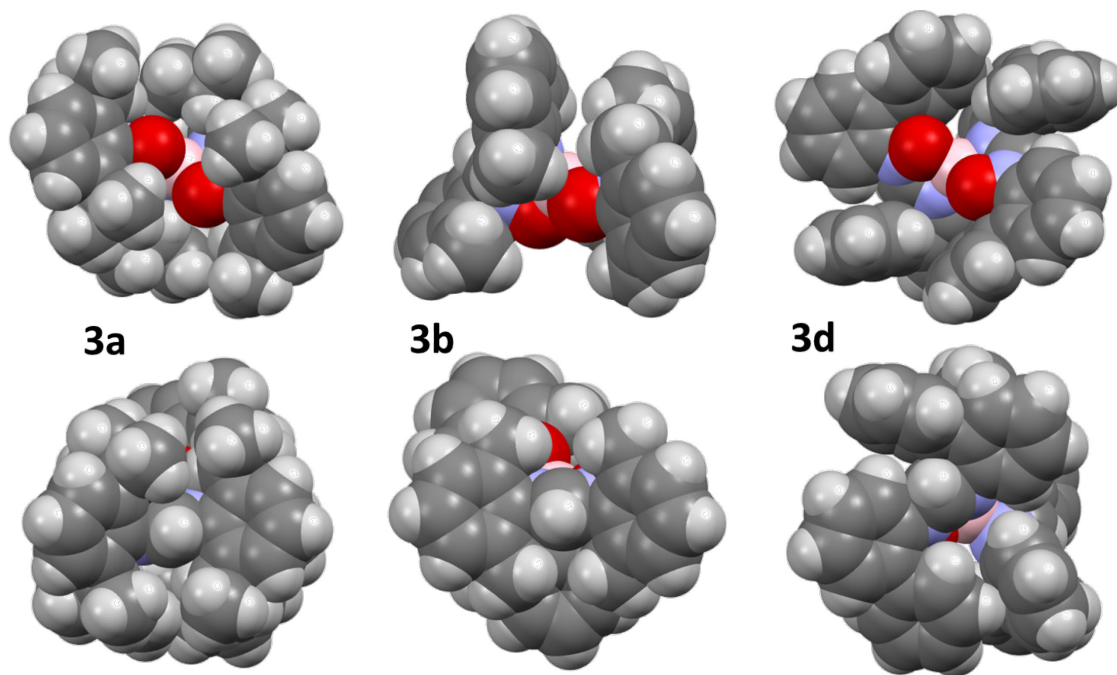

Figure S7. Spacefill views of **3a**, **3b**, and **3d**.
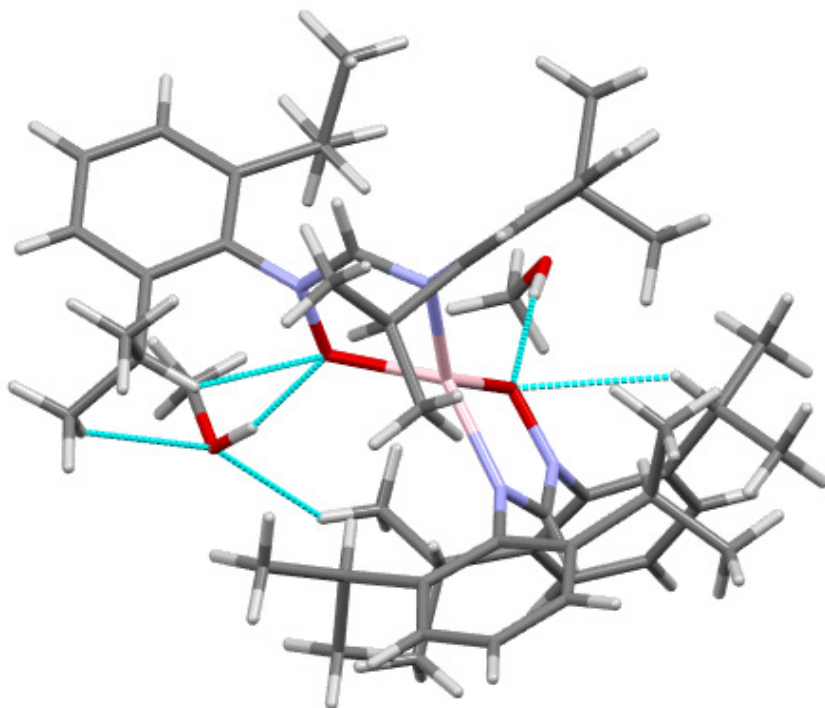
Figure S8. H-bonding-type interactions in **3a**
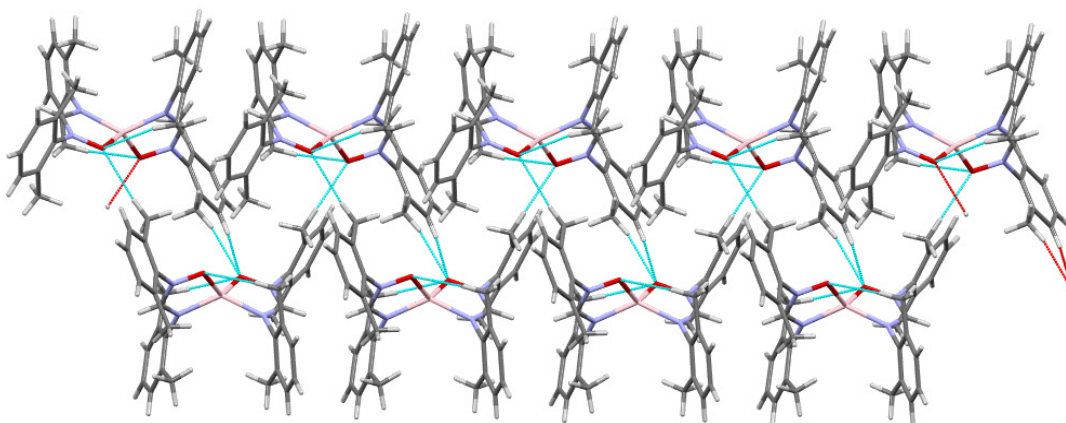
Figure S9. H-bonding-type interactions in **3b**.
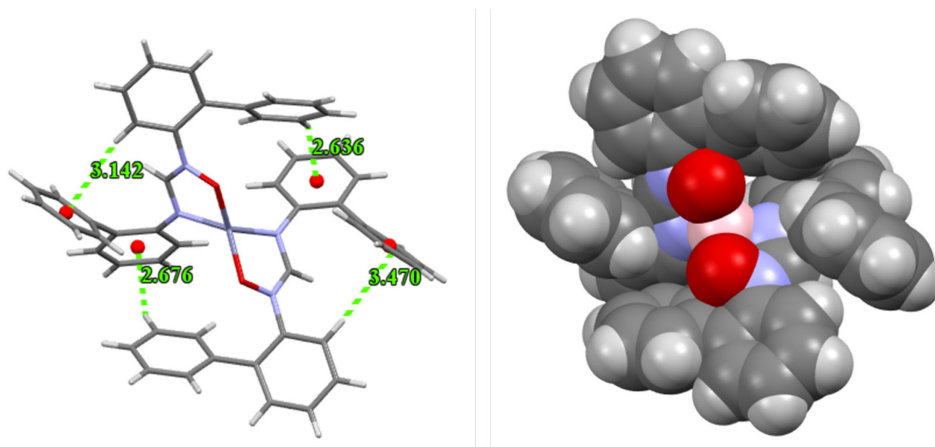
Figure S10. Intramolecular interactions in **3d** – capped sticks view (left) and spacefill view (right**)**.
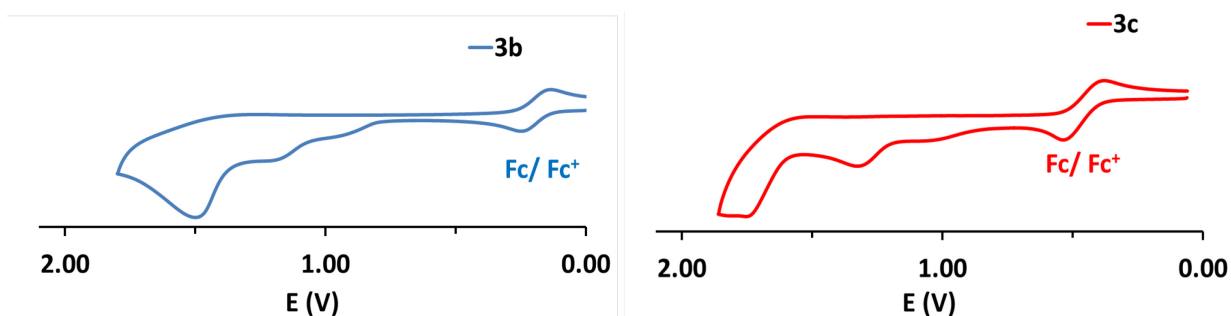
Figure S11. Cyclic voltammogram of **3b** (left) and **3c** (right) **i**n dry CH_2Cl_2; scan rate of 100 mV/s; potential *vs*. silver wire; in [nBu₄N]PF₆ 0.1M, compound concentration about 1mM, glassy carbon electrode, room temperature, Ar atmosphere.

Computational details

Gaussian09, Revision D.01[11] was used for all theoretical calculations discussed herein, with B3LYP[12] DFT method, 6,31-g(d,p)[13] basis set, and PCM[14] (CH_2Cl_2) solvation model. Initial atom coordinates for geometry optimization were taken from XRD data (cif) of the corresponding structures. No symmetry constraints were used for the geometry optimization. Details on optimized structures are given in Tables S5-S7. Selected molecular orbital surfaces are presented in Table S1. No imaginary frequencies were obtained when frequency calculations on optimized geometries were performed. TD-DFT[15] calculations (for the first 30 (**3a**, **3b**) and 50 (**3d**) singlet states) were performed, starting with the optimized geometries of

the ground states. (Figures S12-15 and Table S2). GaussView 3.0.9[16] Gaussum[17] and Chemissian V.4.36[18] software were used for data analysis, visualisation, and surface plots.
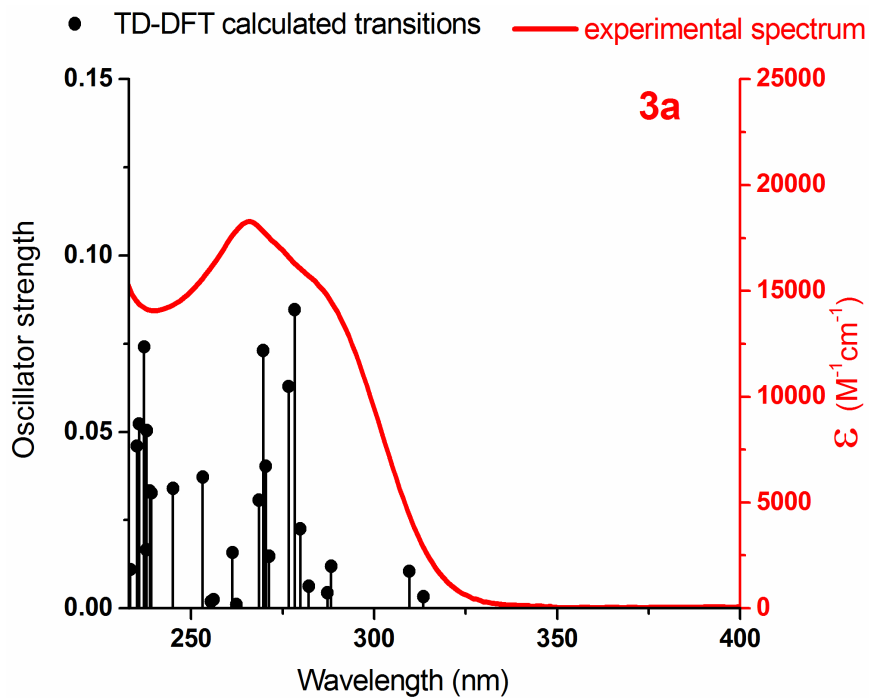
Figure S12. Electronic spectrum of **3a** in CH_2Cl_2: experimental spectrum (in red) and TD-DFT calculated transitions (in black), theory level: B3LYP/ 6,31-g(d,p), PCM: CH_2Cl_2
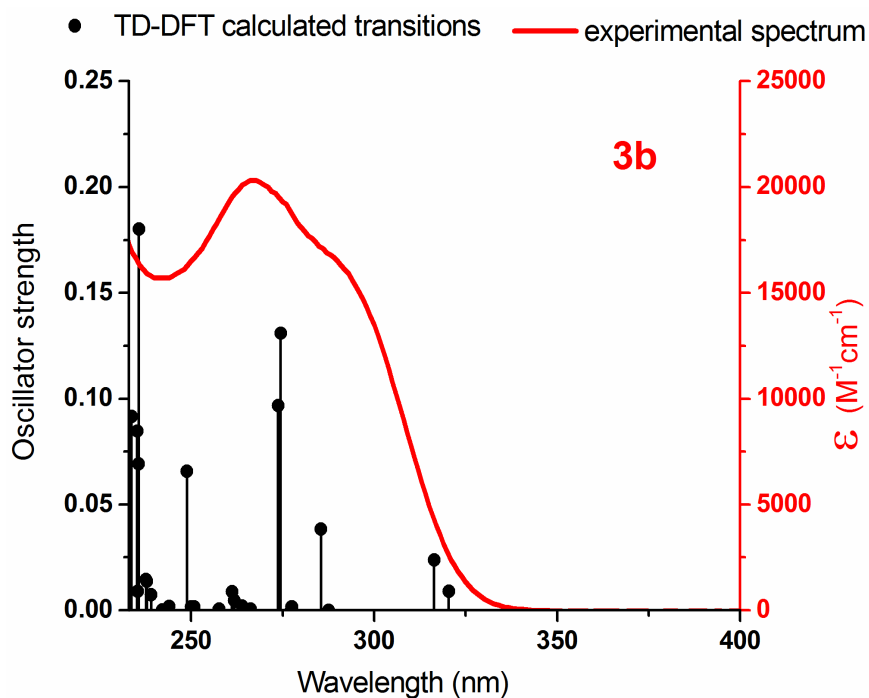
Figure S13. Electronic spectrum of **3b** in CH_2Cl_2: experimental spectrum (in red) and TD-DFT calculated transitions (in black), theory level: B3LYP/ 6,31-g(d,p), PCM: CH_2Cl_2
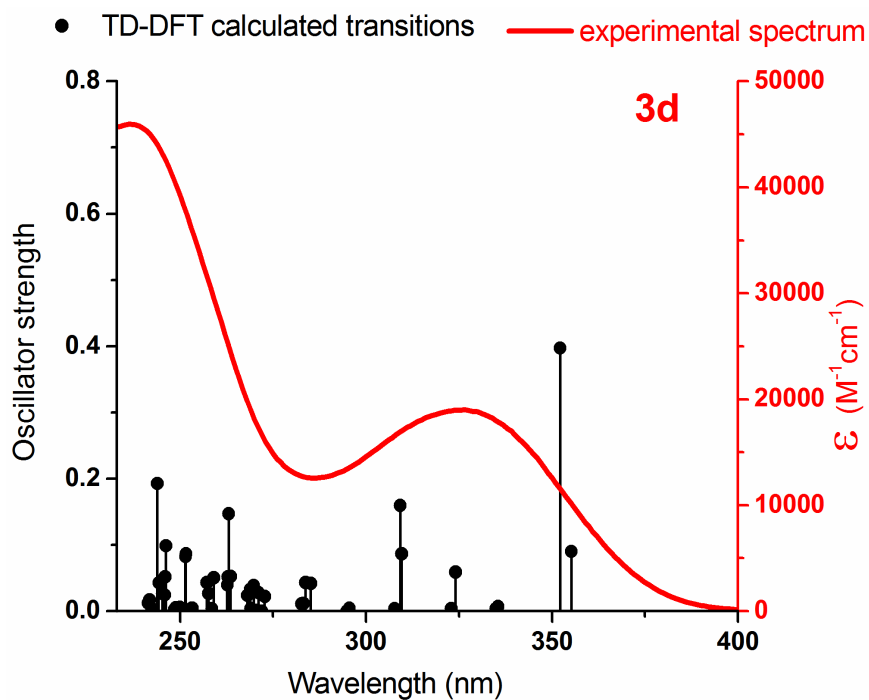
Figure S14. Electronic spectrum of **3d** in CH$_2$Cl$_2$: experimental spectrum (in red) and TD-DFT calculated transitions (in black), theory level: B3LYP/ 6,31-g(d,p), PCM: CH$_2$Cl$_2$
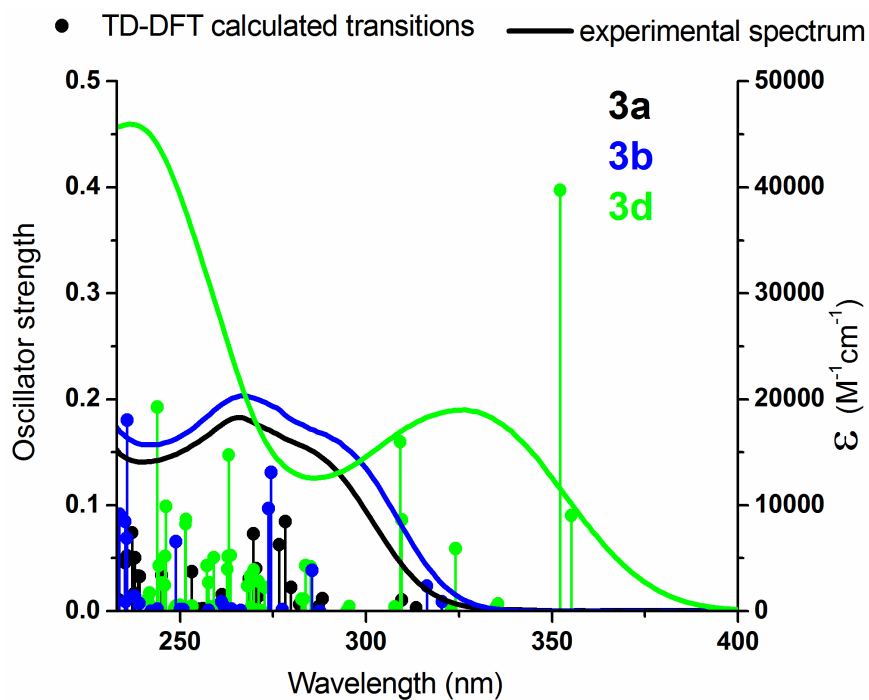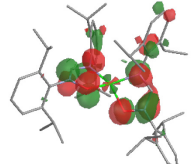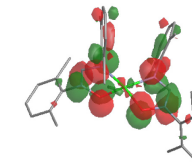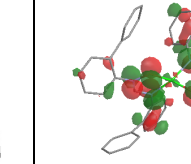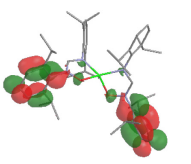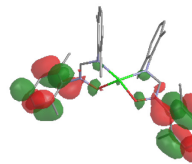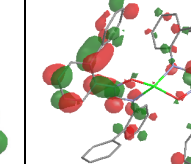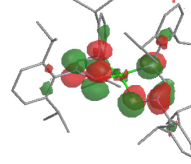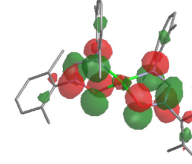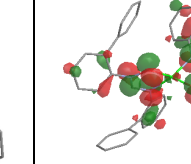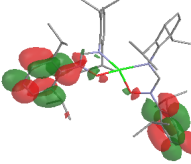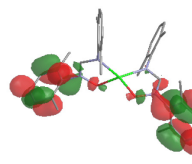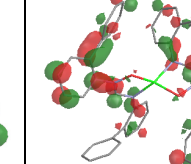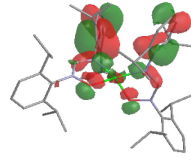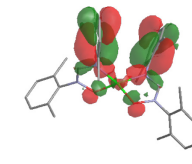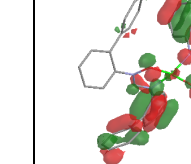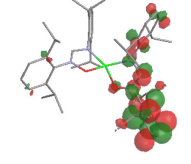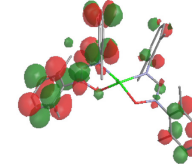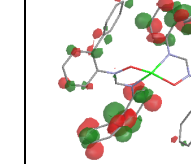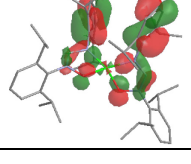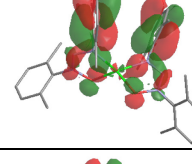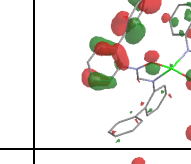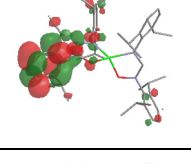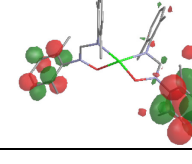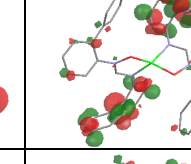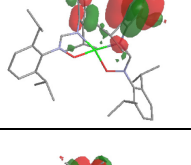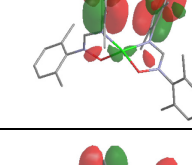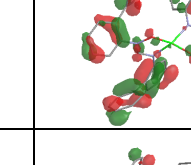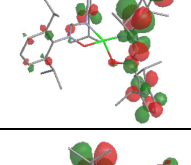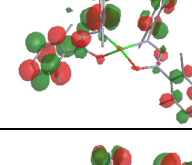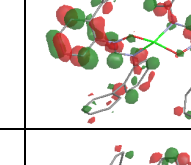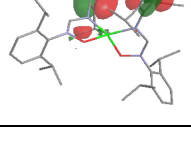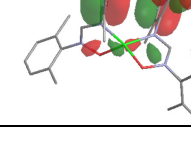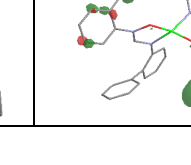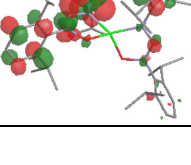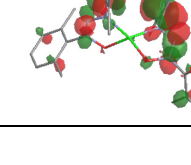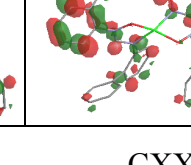
Figure S15. Electronic spectra of **3a-d** in CH$_2$Cl$_2$: experimental spectra and TD-DFT calculated transitions (vertical lines), theory level: B3LYP/ 6,31-g(d,p), PCM: CH$_2$Cl$_2$

Table S1. Molecular orbital surfaces (isovalue 0.03) for **3a**, **3b**, and **3d** (theory level: B3LYP[12]/ 6,31-g(d,p)[13] PCM[14] CH_2Cl_2)

Molecular orbital	Compound			Molecular orbital	Compound		
	3a	**3b**	**3c**		**3a**	**3b**	**3c**
HOMO				**LUMO**			
H-1				**L+1**			
H-2				**L+2**			
H-3				**L+3**			
H-4				**L+4**			
H-5				**L+5**			
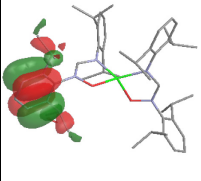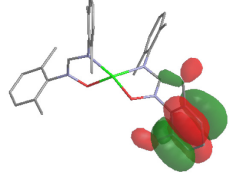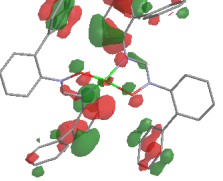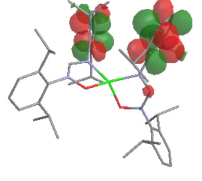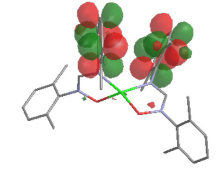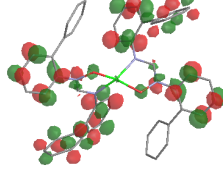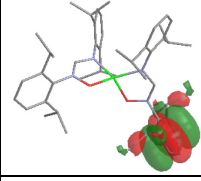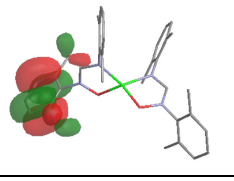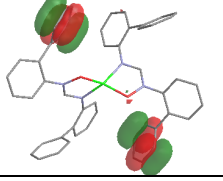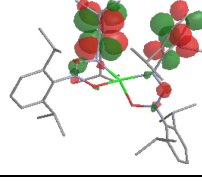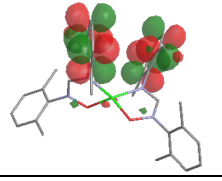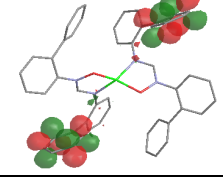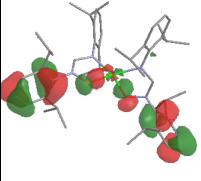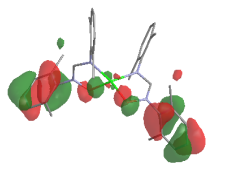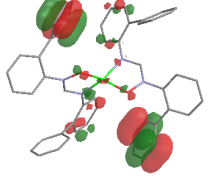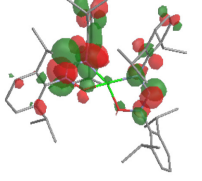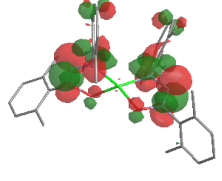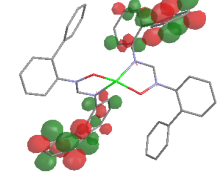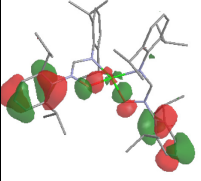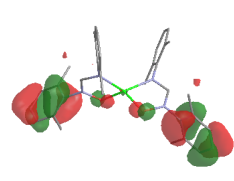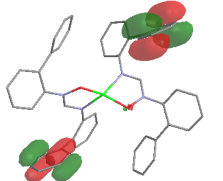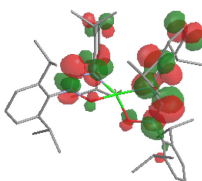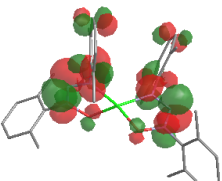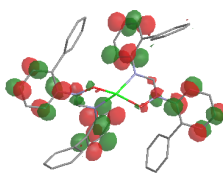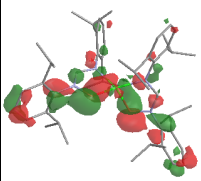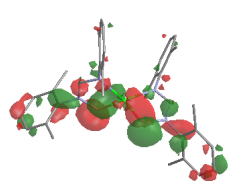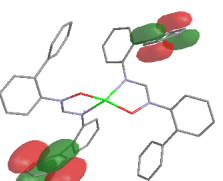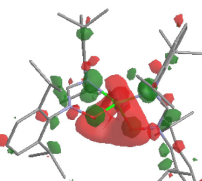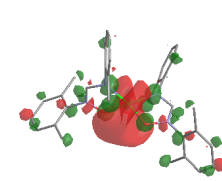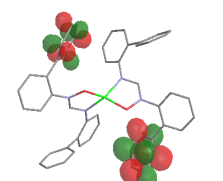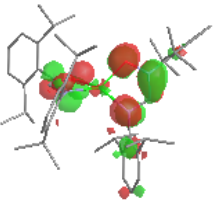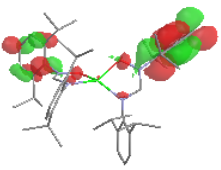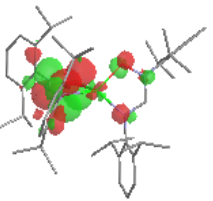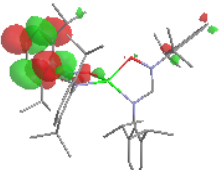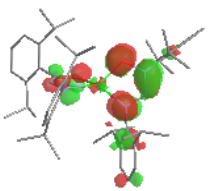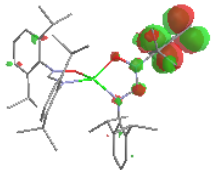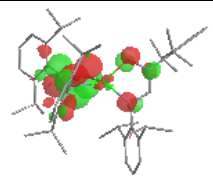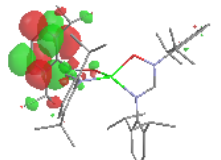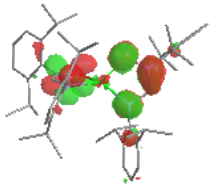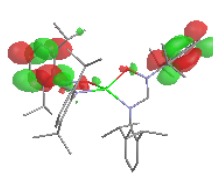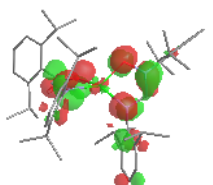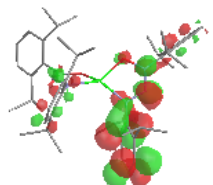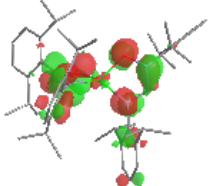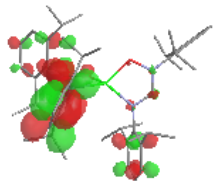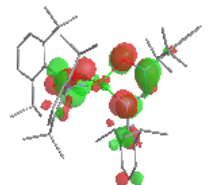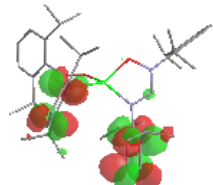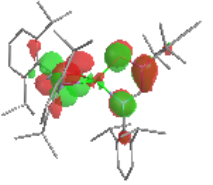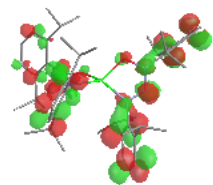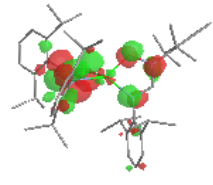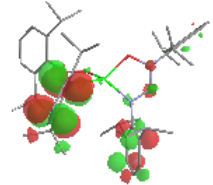
Molecular orbital	Compound			Molecular orbital	Compound		
	3a	3b	3c		3a	3b	3c
H-6				L+6			
H-7				L+7			
H-8				L+8			
H-9				L+9			
H-10				L+10			
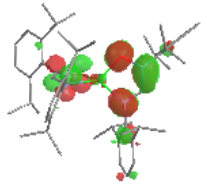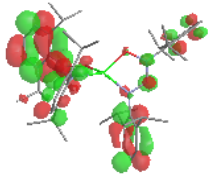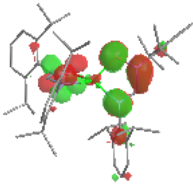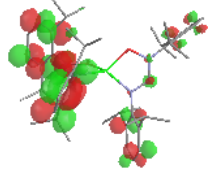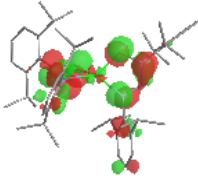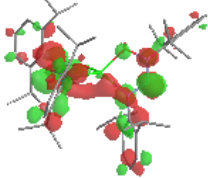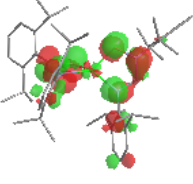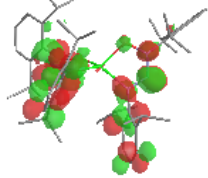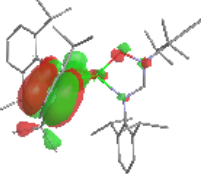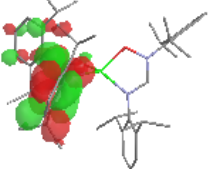
Table S2. TD-DFT calculated singlet transitions (first 30) for **3a** (theory level: B3LYP/ 6,31-g(d,p) PCM: CH_2Cl_2)

Wavelength (nm)	Oscillator strength	Major contributions		NTO surfaces	
		Transition	Contr. (%)	'Hole'	'Particle'
313	0.0033	HOMO->LUMO	76		
		H-1->L+1	19		
310	0.0105	HOMO->L+1	55		
		H-1->LUMO	39		
288	0.0119	HOMO->L+2	75		
		H-1->L+2	11		
287	0.0044	HOMO->L+3	73		
		H-1->L+3	14		
282	0.0063	H-1->LUMO	51		
		HOMO->L+1	37		
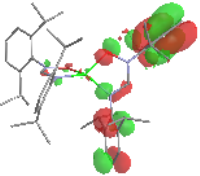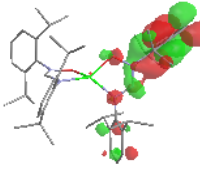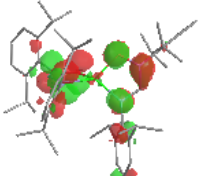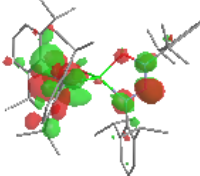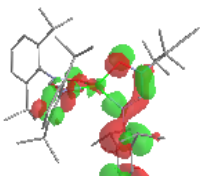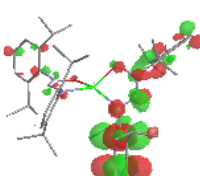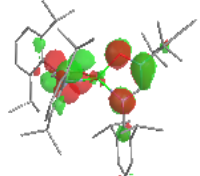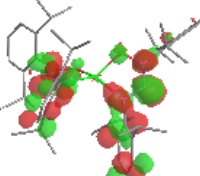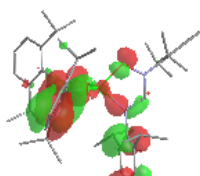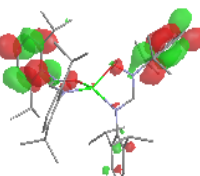
280	0.0225	H-1->L+1	69		
		HOMO->LUMO	18		
278	0.0847	HOMO->L+4	73		
277	0.0629	HOMO->L+5	69		
271	0.0148	HOMO->L+6	75		
270	0.0403	H-1->L+2	51		
		H-1->L+4	19		
		H-1->L+3	11		
270	0.0731	HOMO->L+7	73		
		H-1->L+6	12		

269	0.0307	H-1->L+3	49		
		H-1->L+2	11		
262	0.0011	H-1->L+4	66		
261	0.0158	H-1->L+5	76		
256	0.0025	H-1->L+6	76		
		HOMO->L+7	15		
255	0.0019	H-1->L+7	81		
		HOMO->L+6	11		
253	0.0372	HOMO->L+8	77		
245	0.0340	HOMO->L+9	77		
239	0.0327	H-1->L+8	18		
		H-2->L+5	12		

239	0.0333	H-7->LUMO	22		
		H-7->L+1	13		
238	0.0504	H-1->L+8	30		
		H-7->LUMO	10		
238	0.0166	H-6->L+1	23		
		H-6->LUMO	23		
		H-8->L+3	11		
		H-9->L+3	11		
237	0.0741	H-1->L+8	23		
		H-2->L+6	11		
236	0.0523	H-1->L+9	56		
		HOMO->L+10	14		
		H-2->LUMO	14		
235	0.0460	H-2->LUMO	53		
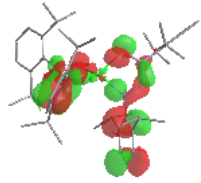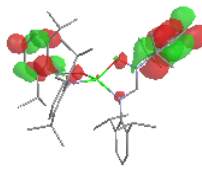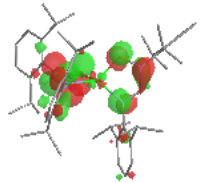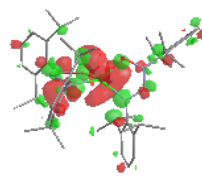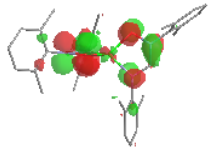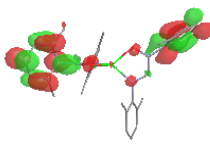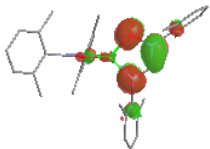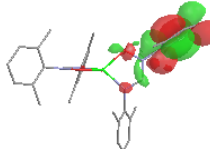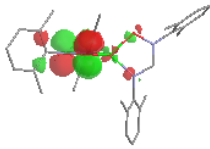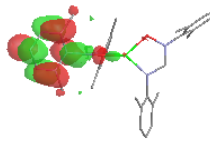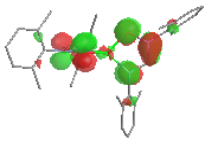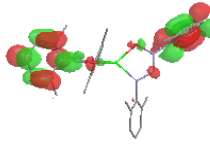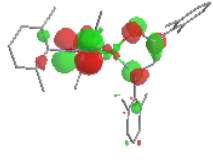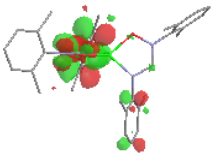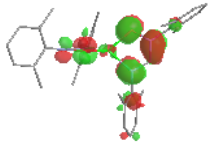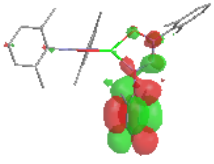
233	0.0110	H-3->LUMO	47		
		H-2->L+1	35		
231	0.1200	HOMO->L+10	51		
		H-1->L+9	12		
229	0.0045	H-2->L+1	29		
		H-3->LUMO	27		
227	0.0098	H-1->L+10	49		
		H-3->L+1	14		
		H-2->L+1	11		
227	0.0111	H-2->L+2	41		
		H-1->L+10	19		
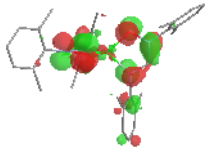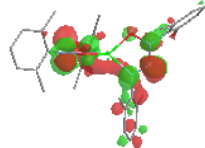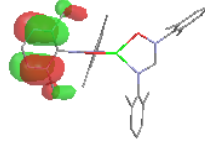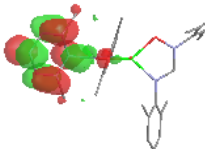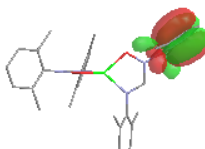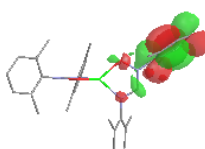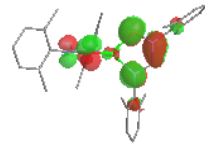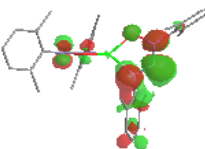
Table S3. TD-DFT calculated singlet transitions (first 30) for **3b** (theory level: B3LYP/ 6,31-g(d,p) PCM: CH_2Cl_2)

Wavelength (nm)	Oscillator strength	Major contributions		NTO surfaces	
		Transition	Contr. (%)	'Hole'	'Particle'
320	0.0089	HOMO->LUMO	75		
		H-1->L+1	23		
316	0.0238	HOMO->L+1	48		
		H-1->LUMO	49		
288	0.0001	HOMO->L+1	50		
		H-1->LUMO	47		
285	0.0383	H-1->L+1	75		
		HOMO->LUMO	23		
278	0.0016	HOMO->L+2	34		
		H-1->L+3	28		
		HOMO->L+4	26		
277	0.0001	HOMO->L+3	57		
		H-1->L+2	18		
		H-1->L+4	13		

274	0.1309	HOMO->L+4	45		
		HOMO->L+2	37		
274	0.0966	HOMO->L+5	65		
		H-1->L+4	11		
266	0.0005	H-1->L+2	39		
		H-1->L+4	32		
		HOMO->L+5	18		
264	0.0021	H-1->L+5	74		
262	0.0047	HOMO->L+6	80		
		H-1->L+7	10		
261	0.0088	HOMO->L+7	78		
		H-1->L+6	13		
258	0.0005	HOMO->L+3	29		
		H-1->L+3	21		
		H-1->L+4	21		
		H-1->L+2	20		
258	0.0003	H-1->L+3	35		
		HOMO->L+4	18		
		H-1->L+4	13		
		HOMO->L+2	13		
		H-1->L+2	10		
251	0.0017	H-1->L+6	81		
		HOMO->L+7	14		
250	0.0016	H-1->L+7	87		
		HOMO->L+6	10		

249	0.0657	HOMO->L+8	82		
244	0.0019	H-2->LUMO	58		
		HOMO->L+9	28		
242	0.0002	HOMO->L+9	33		
		H-2->LUMO	32		
		H-1->L+8	31		
239	0.0073	H-2->L+1	59		
		H-3->LUMO	34		
238	0.0138	H-7->LUMO	37		
		H-7->L+1	28		
238	0.0145	H-6->LUMO	36		
		H-6->L+1	27		
		H-8->L+3	11		
236	0.1802	H-1->L+8	35		
		HOMO->L+9	16		
236	0.0691	H-2->L+6	14		
		H-1->L+8	12		
		H-4->L+5	11		
235	0.0090	H-2->L+7	17		
		H-4->L+4	10		
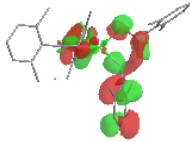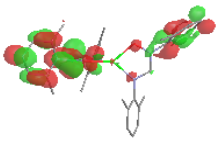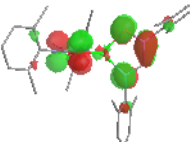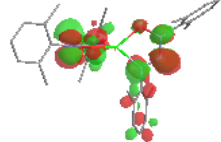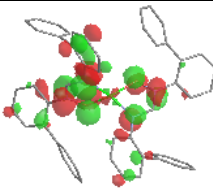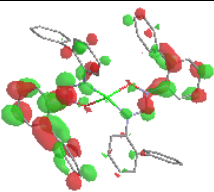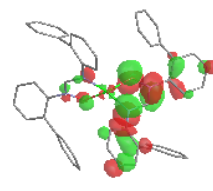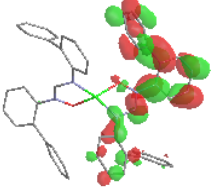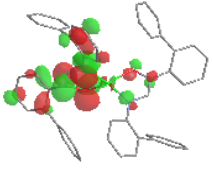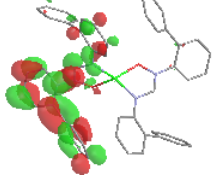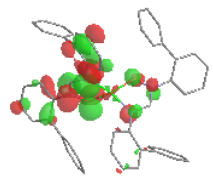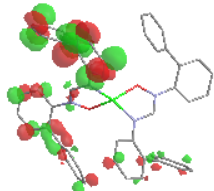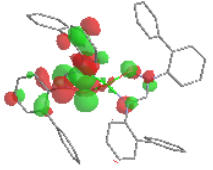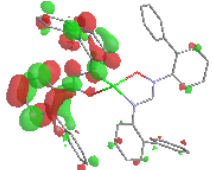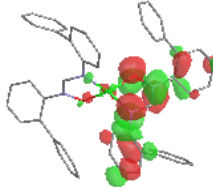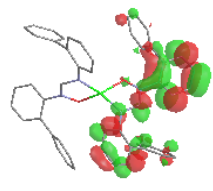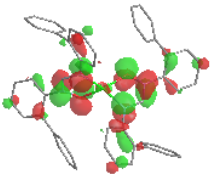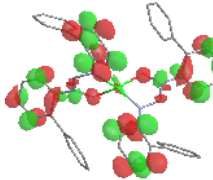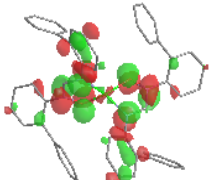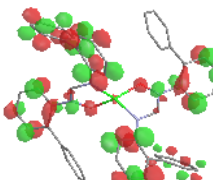
		H-3->L+6	10		
235	0.0847	H-3->LUMO	36		
		H-1->L+9	27		
		H-2->L+1	14		
234	0.0916	H-1->L+9	46		
		H-2->L+1	17		
		H-3->LUMO	18		
		HOMO->L+10	11		
231	0.0004	H-3->L+1	90		
228	0.0001	H-4->LUMO	95		
227	0.0060	H-5->LUMO	94		
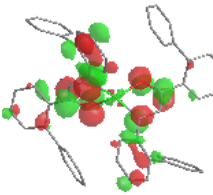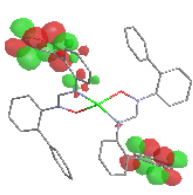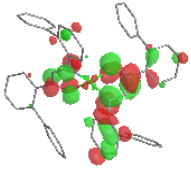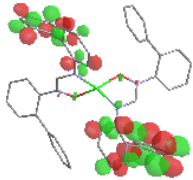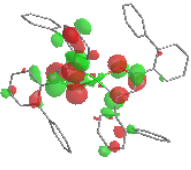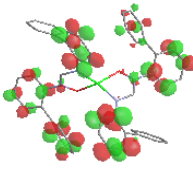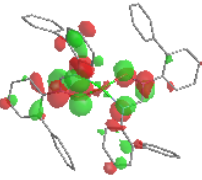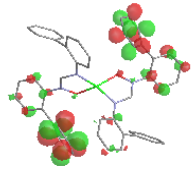
Table S4. TD-DFT calculated singlet transitions (first 50) for **3d** (theory level: B3LYP/ 6,31-g(d,p) PCM: CH_2Cl_2)

Wavelength (nm)	Oscillator strength	Major contributions		NTO surfaces	
		Transition	Contr. (%)	'Hole'	'Particle'
355	0.0902	HOMO->LUMO	67		
		H-1->L+1	30		
352	0.3973	HOMO->L+1	53		
		H-1->LUMO	44		
335	0.0069	H-1->LUMO	52		
		HOMO->L+1	40		
335	0.0037	H-1->L+1	64		
		HOMO->LUMO	28		
324	0.0590	HOMO->L+2	61		
		H-1->L+3	36		
323	0.0037	HOMO->L+3	51		
		H-1->L+2	44		
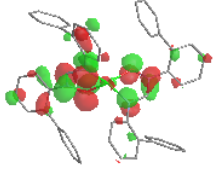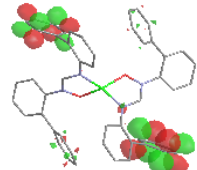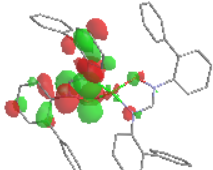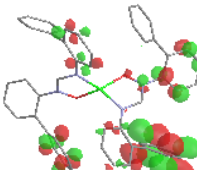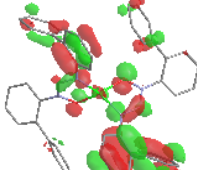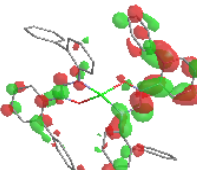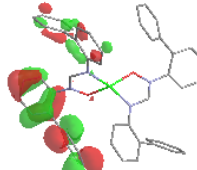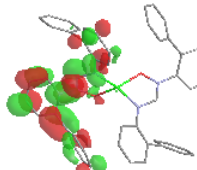
310	0.0864	HOMO->L+4	59		
		H-1->L+5	24		
309	0.1597	H-1->L+4	46		
		HOMO->L+5	42		
308	0.0005	H-1->L+3	58		
		HOMO->L+2	37		
308	0.0040	H-1->L+2	49		
		HOMO->L+3	43		
295	0.0046	HOMO->L+5	49		
		H-1->L+4	46		
295	0.0003	H-1->L+5	63		
		HOMO->L+4	31		
285	0.0418	H-1->L+6	69		
		HOMO->L+9	16		
284	0.0432	HOMO->L+6	77		
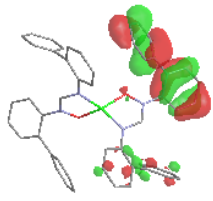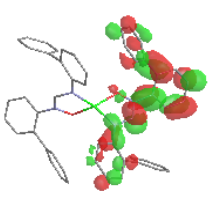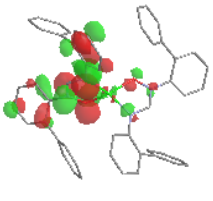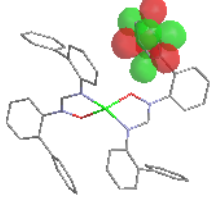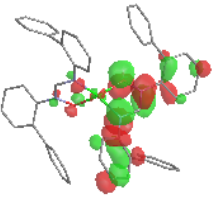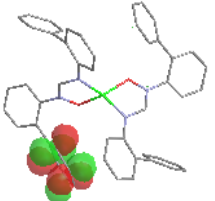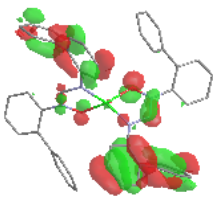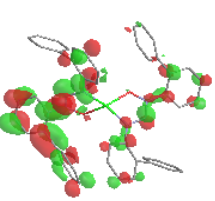
283	0.0116	HOMO->L+7	60		
		H-1->L+8	35		
283	0.0112	HOMO->L+8	59		
		H-1->L+7	37		
273	0.0223	HOMO->L+9	52		
		HOMO->L+10	13		
		H-1->L+8	10		
272	0.0003	H-1->L+9	35		
		HOMO->L+11	22		
		H-1->L+10	19		
271	0.0283	HOMO->L+10	38		
		H-1->L+11	22		
		H-2->LUMO	14		
271	0.0010	HOMO->L+11	28		
		H-1->L+10	20		
		H-1->L+7	18		
		HOMO->L+8	14		
		H-1->L+9	13		
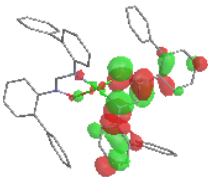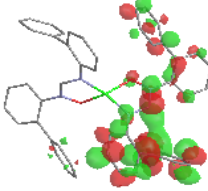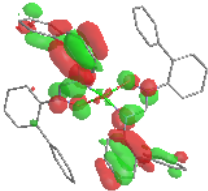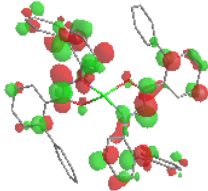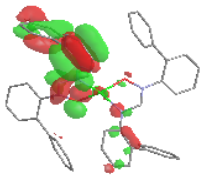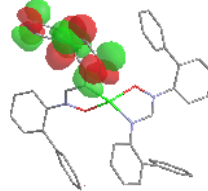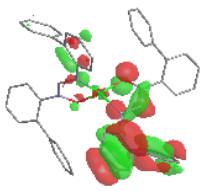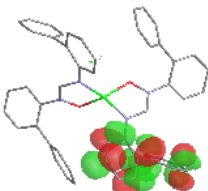
270	0.0390	H-1->L+8	32		
		H-2->LUMO	27		
		HOMO->L+7	20		
269	0.0037	H-1->L+7	23		
		H-1->L+9	20		
		H-2->L+1	16		
		HOMO->L+8	12		
		HOMO->L+6	10		
269	0.0331	H-2->LUMO	33		
		HOMO->L+9	15		
		HOMO->L+7	12		
		H-1->L+8	10		
268	0.0239	H-2->L+1	49		
		H-1->L+9	15		
		H-3->LUMO	11		
264	0.0527	H-4->LUMO	29		
		H-3->LUMO	25		
		H-5->L+1	15		
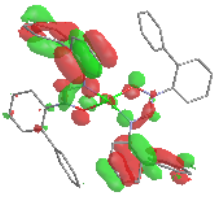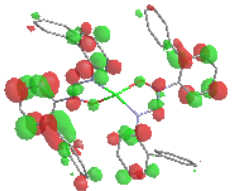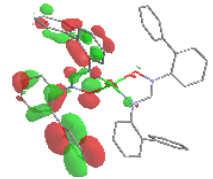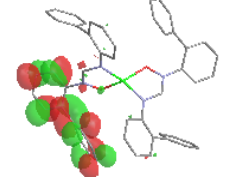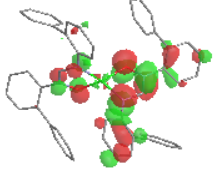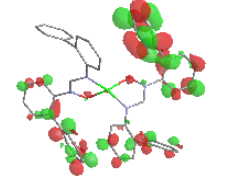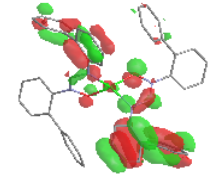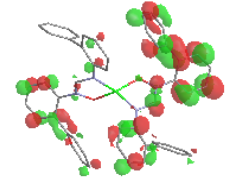
263	0.1473	H-5->LUMO	32		
		H-5->L+1	16		
		HOMO->L+10	11		
263	0.0518	H-1->L+10	43		
		HOMO->L+11	24		
		H-5->LUMO	11		
263	0.0397	H-1->L+11	57		
		HOMO->L+10	19		
		HOMO->L+11	12		
259	0.0506	HOMO->L+12	26		
		H-4->L+1	24		
		H-3->L+1	17		
259	0.0040	H-4->LUMO	39		
		H-3->LUMO	24		
		H-2->L+1	24		
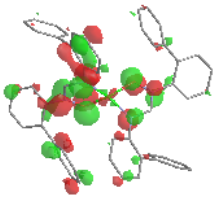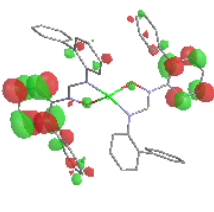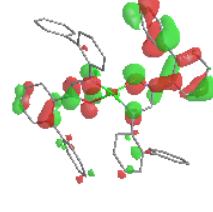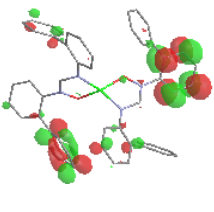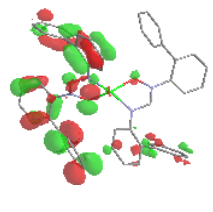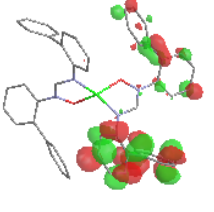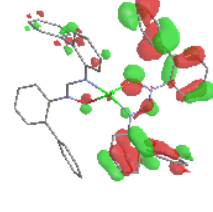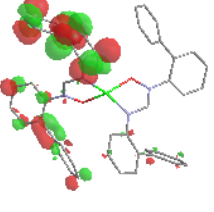
258	0.0271	H-1->L+12	36		
		HOMO->L+13	35		
257	0.0432	HOMO->L+12	37		
		H-4->L+1	20		
		H-3->L+1	14		
		H-2->LUMO	11		
		H-1->L+13	11		
253	0.0047	H-4->L+1	23		
		H-3->L+1	22		
		H-4->LUMO	15		
		H-3->LUMO	14		
		H-5->L+1	13		
253	0.0048	H-5->LUMO	41		
		H-5->L+1	32		
252	0.0865	H-2->L+3	30		
		H-2->L+2	16		
251	0.0823	H-2->L+2	34		

		H-2->L+3	14		
250	0.0056	HOMO->L+13	52		
		H-1->L+12	39		
249	0.0008	H-6->LUMO	13		
		H-8->L+1	12		
		H-1->L+13	10		
249	0.0051	H-1->L+13	59		
		HOMO->L+12	14		
249	0.0024	H-6->L+1	14		
		H-8->LUMO	14		
		H-9->L+1	10		
246	0.0988	H-1->L+14	18		
		H-2->L+4	13		
246	0.0519	H-2->L+4	18		
246	0.0245	HOMO->L+14	35		
		H-1->L+15	11		
245	0.0266	H-2->L+5	22		
		H-2->L+2	16		

244	0.0430	HOMO->L+14	25		
		H-5->L+2	10		
244	0.1928	H-1->L+14	27		
		HOMO->L+15	14		
243	0.0040	H-2->L+7	13		
		H-11->L+2	11		
		H-2->L+8	10		
242	0.0022	H-2->L+7	11		
		H-2->L+8	10		
242	0.0170	H-3->L+2	40		
		H-2->L+3	14		
		H-5->L+3	13		
		H-3->L+3	10		
241	0.0123	H-3->L+3	46		
		H-5->L+2	16		

Table S5. Atomic coordinates for DFT optimization of **3a** (theory level: B3LYP/ 6,31-g(d,p) PCM: CH_2Cl_2)

```
                          Standard orientation:
---------------------------------------------------------------------
Center     Atomic     Atomic           Coordinates (Angstroms)
Number     Number     Type          X           Y           Z
---------------------------------------------------------------------
   1         30         0        0.000484    -0.191503    0.003708
   2          8         0       -1.519883    -1.310143    0.592783
   3          8         0        1.550224    -1.275321   -0.565109
   4          7         0       -2.623167    -0.970493   -0.155264
   5          7         0       -1.395656     0.701595   -1.146947
   6          7         0        2.636734    -0.903452    0.191771
   7          7         0        1.368028     0.764456    1.136938
   8          6         0       -3.727921    -1.887552   -0.097173
   9          6         0       -4.824035    -1.599943    0.739773
  10          6         0       -5.877221    -2.524454    0.774015
  11          1         0       -6.742023    -2.325092    1.399500
  12          6         0       -5.828182    -3.698551    0.029232
  13          1         0       -6.652683    -4.404304    0.074377
  14          6         0       -4.719918    -3.974479   -0.769123
  15          1         0       -4.689056    -4.899109   -1.337506
  16          6         0       -3.647867    -3.079192   -0.850603
  17          6         0       -2.529632     0.037204   -1.017547
  18          1         0       -3.423639     0.266428   -1.593813
  19          6         0       -1.344440     1.844585   -2.000731
  20          6         0       -1.949427     3.064401   -1.611757
  21          6         0       -1.847519     4.165390   -2.474682
  22          1         0       -2.313340     5.105106   -2.191202
  23          6         0       -1.157278     4.082313   -3.678653
  24          1         0       -1.090550     4.947383   -4.332290
  25          6         0       -0.544041     2.883464   -4.037968
  26          1         0       -0.000287     2.826677   -4.975291
  27          6         0       -0.618921     1.754201   -3.216264
  28          6         0       -4.894248    -0.343098    1.598725
  29          1         0       -3.957404     0.205501    1.465401
  30          6         0       -5.010557    -0.692248    3.094772
  31          1         0       -4.991758     0.220829    3.698941
  32          1         0       -4.182529    -1.330766    3.416535
  33          1         0       -5.946633    -1.216649    3.314849
  34          6         0       -6.048447     0.577140    1.158576
  35          1         0       -5.955472     0.859168    0.105450
  36          1         0       -6.055522     1.494503    1.756620
  37          1         0       -7.019542     0.087389    1.289117
  38          6         0       -2.434180    -3.413917   -1.709956
```

39	1	0	−1.791583	−2.530851	−1.745211
40	6	0	−2.823600	−3.763502	−3.157576
41	1	0	−3.401833	−2.958441	−3.622121
42	1	0	−3.422017	−4.679285	−3.209409
43	1	0	−1.923697	−3.924877	−3.760117
44	6	0	−1.607295	−4.544660	−1.067240
45	1	0	−1.287099	−4.261440	−0.061130
46	1	0	−0.713804	−4.751387	−1.666238
47	1	0	−2.187681	−5.471555	−0.996791
48	6	0	−2.691751	3.234858	−0.288064
49	1	0	−2.639591	2.287435	0.254198
50	6	0	−2.026140	4.298623	0.606332
51	1	0	−0.980701	4.049757	0.809995
52	1	0	−2.549933	4.370000	1.565914
53	1	0	−2.052878	5.289447	0.140093
54	6	0	−4.180228	3.564648	−0.511607
55	1	0	−4.674685	2.799046	−1.118127
56	1	0	−4.302045	4.523757	−1.026641
57	1	0	−4.707790	3.632371	0.445725
58	6	0	0.025126	0.437929	−3.642128
59	1	0	0.280273	−0.108433	−2.728914
60	6	0	−0.973632	−0.427243	−4.437525
61	1	0	−1.882649	−0.625487	−3.862178
62	1	0	−0.525102	−1.390859	−4.703290
63	1	0	−1.267910	0.076809	−5.365249
64	6	0	1.326367	0.617909	−4.439738
65	1	0	2.034787	1.264968	−3.912715
66	1	0	1.147986	1.049099	−5.430802
67	1	0	1.805291	−0.354193	−4.592142
68	6	0	3.768379	−1.787114	0.147653
69	6	0	3.814193	−2.875440	1.044477
70	6	0	4.926396	−3.723760	0.982024
71	1	0	4.994790	−4.566778	1.663099
72	6	0	5.943479	−3.508337	0.055356
73	1	0	6.799528	−4.176310	0.025265
74	6	0	5.859499	−2.445727	−0.840340
75	1	0	6.652689	−2.296135	−1.566612
76	6	0	4.765854	−1.570723	−0.823411
77	6	0	2.517904	0.122720	1.027047
78	1	0	3.403015	0.384504	1.602914
79	6	0	1.300027	1.939075	1.943735
80	6	0	1.958162	3.129856	1.547882
81	6	0	1.848370	4.259108	2.372378
82	1	0	2.354862	5.176016	2.084081
83	6	0	1.098706	4.234241	3.542887
84	1	0	1.027924	5.120604	4.166863
85	6	0	0.430595	3.066176	3.905041

86	1	0	-0.159483	3.053400	4.815817
87	6	0	0.511049	1.910120	3.122325
88	6	0	2.694840	-3.160259	2.039552
89	1	0	1.950873	-2.364650	1.949924
90	6	0	1.979067	-4.482840	1.702114
91	1	0	1.575986	-4.461455	0.685475
92	1	0	1.147634	-4.650352	2.394967
93	1	0	2.658895	-5.338268	1.781168
94	6	0	3.204839	-3.162222	3.492608
95	1	0	3.695499	-2.216829	3.745510
96	1	0	3.924570	-3.969311	3.666334
97	1	0	2.370516	-3.307608	4.186523
98	6	0	4.684381	-0.433307	-1.833976
99	1	0	3.721888	0.067334	-1.694957
100	6	0	4.717484	-0.963424	-3.279862
101	1	0	3.911321	-1.681990	-3.454802
102	1	0	5.667330	-1.459017	-3.507174
103	1	0	4.596887	-0.137123	-3.987961
104	6	0	5.800056	0.603594	-1.604109
105	1	0	5.762701	1.012214	-0.589950
106	1	0	5.700051	1.435397	-2.309610
107	1	0	6.790946	0.159783	-1.750403
108	6	0	2.759554	3.245422	0.252146
109	1	0	2.702585	2.287754	-0.271036
110	6	0	2.160812	4.304238	-0.694331
111	1	0	2.723971	4.335562	-1.633540
112	1	0	2.197039	5.305902	-0.252816
113	1	0	1.117130	4.079282	-0.932965
114	6	0	4.247090	3.539264	0.527155
115	1	0	4.698352	2.770585	1.163325
116	1	0	4.375645	4.502490	1.032712
117	1	0	4.811562	3.578159	-0.410346
118	6	0	-0.192695	0.629405	3.559976
119	1	0	-0.373110	0.033526	2.661004
120	6	0	0.716066	-0.199966	4.489168
121	1	0	1.671661	-0.432382	4.010266
122	1	0	0.233756	-1.145743	4.760134
123	1	0	0.929739	0.348748	5.413692
124	6	0	-1.558547	0.872772	4.221511
125	1	0	-2.206257	1.489107	3.589873
126	1	0	-1.466185	1.367628	5.194378
127	1	0	-2.063467	-0.083115	4.392592

Table S6. Atomic coordinates for DFT optimization of **3b** (theory level: B3LYP/ 6,31-g(d,p) PCM: CH₂Cl₂)

```
                              Standard orientation:
---------------------------------------------------------------------
Center     Atomic      Atomic          Coordinates (Angstroms)
Number     Number      Type         X           Y           Z
---------------------------------------------------------------------
   1         30          0       0.000772    -0.349312    0.004616
   2          8          0      -1.607223    -1.317191   -0.619585
   3          8          0       1.609823    -1.317097    0.626723
   4          7          0      -2.681396    -0.870637    0.118268
   5          7          0      -1.286223     0.559822    1.249679
   6          7          0       1.287351     0.560269   -1.240370
   7          7          0       2.683217    -0.873624   -0.114029
   8          6          0      -2.491200     0.063553    1.042317
   9          1          0      -3.368956     0.368472    1.608409
  10          6          0      -3.934866    -1.522877   -0.126868
  11          6          0      -4.189628    -2.749977    0.511655
  12          6          0      -5.405194    -3.387264    0.241781
  13          1          0      -5.625541    -4.335119    0.724675
  14          6          0      -6.327744    -2.821742   -0.638634
  15          1          0      -7.265970    -3.330905   -0.839086
  16          6          0      -6.046394    -1.611440   -1.269685
  17          1          0      -6.762826    -1.180876   -1.963547
  18          6          0      -4.839920    -0.941435   -1.030536
  19          6          0      -3.183718    -3.350708    1.461983
  20          1          0      -2.186362    -3.362749    1.014163
  21          1          0      -3.462646    -4.372643    1.729170
  22          1          0      -3.114914    -2.768992    2.388809
  23          6          0      -4.527380     0.364830   -1.719292
  24          1          0      -4.668326     1.218672   -1.046053
  25          1          0      -5.184071     0.513362   -2.579894
  26          1          0      -3.490256     0.391156   -2.063506
  27          6          0      -1.102549     1.577877    2.227965
  28          6          0      -0.418934     1.254476    3.420424
  29          6          0      -0.194121     2.265058    4.361830
  30          1          0       0.326625     2.019488    5.283794
  31          6          0      -0.628504     3.570257    4.134511
  32          1          0      -0.445764     4.343573    4.875042
  33          6          0      -1.290624     3.879220    2.948262
  34          1          0      -1.619598     4.898078    2.760547
  35          6          0      -1.532823     2.899088    1.977078
  36          6          0       0.048520    -0.157311    3.680021
  37          1          0      -0.795219    -0.855717    3.728182
  38          1          0       0.589330    -0.217720    4.628282
```

39	1	0	0.706954	-0.518043	2.882070
40	6	0	-2.218552	3.267553	0.682149
41	1	0	-3.226481	2.843184	0.608783
42	1	0	-1.658455	2.900925	-0.184530
43	1	0	-2.314879	4.352715	0.593851
44	6	0	2.491467	0.060370	-1.038582
45	1	0	3.367101	0.362106	-1.609583
46	6	0	3.935497	-1.530052	0.125110
47	6	0	4.881034	-0.915951	0.963556
48	6	0	6.086545	-1.591395	1.194642
49	1	0	6.833323	-1.135764	1.838708
50	6	0	6.327615	-2.838281	0.621681
51	1	0	7.265118	-3.351027	0.816274
52	6	0	5.365253	-3.435498	-0.193038
53	1	0	5.554532	-4.411125	-0.631826
54	6	0	4.150810	-2.793725	-0.455146
55	6	0	4.615039	0.428637	1.596285
56	1	0	4.774213	1.247960	0.885168
57	1	0	5.287142	0.595136	2.441651
58	1	0	3.584142	0.502373	1.951978
59	6	0	3.105827	-3.425652	-1.340503
60	1	0	2.126512	-3.409662	-0.854933
61	1	0	3.368338	-4.459467	-1.576703
62	1	0	3.005601	-2.880067	-2.286364
63	6	0	1.101295	1.573294	-2.223806
64	6	0	0.435559	1.238770	-3.423064
65	6	0	0.208210	2.244775	-4.368843
66	1	0	-0.298958	1.991049	-5.296147
67	6	0	0.622709	3.555902	-4.138612
68	1	0	0.438247	4.325585	-4.882499
69	6	0	1.267086	3.875619	-2.945383
70	1	0	1.580632	4.898993	-2.755876
71	6	0	1.511171	2.900193	-1.970003
72	6	0	-0.011657	-0.179315	-3.684088
73	1	0	0.841397	-0.866459	-3.730910
74	1	0	-0.549648	-0.247136	-4.633441
75	1	0	-0.666607	-0.548476	-2.887183
76	6	0	2.178172	3.277835	-0.668131
77	1	0	3.186447	2.857370	-0.579396
78	1	0	1.608330	2.912720	0.192843
79	1	0	2.268882	4.363773	-0.583545

Table S7. Atomic coordinates for DFT optimization of **3d** (theory level: B3LYP/ 6,31-g(d,p) PCM: CH$_2$Cl$_2$)

```
                          Standard orientation:
---------------------------------------------------------------------
Center     Atomic      Atomic            Coordinates (Angstroms)
Number     Number      Type         X           Y           Z
---------------------------------------------------------------------
   1         30          0       -0.001634    0.005544   -0.084323
   2          8          0       -0.895018   -1.455342   -1.049123
   3          8          0        0.900907    1.458222   -1.052528
   4          7          0       -2.158538   -1.598143   -0.549159
   5          7          0       -1.794073    0.208318    0.821617
   6          7          0        2.163025    1.599185   -0.548027
   7          7          0        1.785180   -0.196776    0.832340
   8          6          0       -2.591721   -0.749176    0.380460
   9          1          0       -3.595346   -0.914283    0.757095
  10          6          0       -2.984096   -2.608554   -1.125619
  11          6          0       -2.518925   -3.931720   -1.302621
  12          6          0       -3.395026   -4.840547   -1.919050
  13          1          0       -3.063810   -5.866041   -2.048416
  14          6          0       -4.678419   -4.478317   -2.325603
  15          1          0       -5.326864   -5.216007   -2.787897
  16          6          0       -5.120389   -3.170654   -2.131700
  17          1          0       -6.111895   -2.867064   -2.452415
  18          6          0       -4.266145   -2.236552   -1.549912
  19          1          0       -4.575846   -1.201328   -1.452936
  20          6          0       -1.189015   -4.424137   -0.847640
  21          6          0       -0.712459   -4.170183    0.448445
  22          1          0       -1.303899   -3.564662    1.127835
  23          6          0        0.504947   -4.696788    0.876849
  24          1          0        0.856138   -4.486286    1.882290
  25          6          0        1.272443   -5.486901    0.016794
  26          1          0        2.222685   -5.892951    0.350653
  27          6          0        0.810146   -5.747920   -1.273789
  28          1          0        1.400424   -6.355988   -1.953231
  29          6          0       -0.410902   -5.223774   -1.700000
  30          1          0       -0.756791   -5.419657   -2.710641
  31          6          0       -2.266926    1.143153    1.771267
  32          6          0       -3.538085    1.772481    1.700407
  33          6          0       -3.910643    2.640419    2.741119
  34          1          0       -4.882201    3.122513    2.683885
  35          6          0       -3.061256    2.929546    3.806797
  36          1          0       -3.380358    3.611842    4.588451
  37          6          0       -1.790265    2.353077    3.838647
  38          1          0       -1.102679    2.577010    4.648877
```

39	6	0	−1.404889	1.475113	2.829916
40	1	0	−0.421838	1.017463	2.854820
41	6	0	−4.476360	1.614431	0.549871
42	6	0	−5.823191	1.281240	0.767150
43	1	0	−6.165569	1.082496	1.778731
44	6	0	−6.720366	1.191072	−0.299122
45	1	0	−7.756837	0.927808	−0.108873
46	6	0	−6.287188	1.435839	−1.603385
47	1	0	−6.983898	1.367429	−2.433507
48	6	0	−4.949970	1.773721	−1.832814
49	1	0	−4.604983	1.976399	−2.842491
50	6	0	−4.053268	1.861464	−0.768206
51	1	0	−3.019826	2.136834	−0.953645
52	6	0	2.589279	0.753739	0.387793
53	1	0	3.592827	0.915791	0.766125
54	6	0	2.994752	2.602245	−1.128657
55	6	0	2.537635	3.927640	−1.308903
56	6	0	3.417199	4.828924	−1.931157
57	1	0	3.091580	5.855831	−2.063692
58	6	0	4.697411	4.457213	−2.339430
59	1	0	5.349207	5.189102	−2.806214
60	6	0	5.132064	3.147751	−2.141200
61	1	0	6.121127	2.837145	−2.462741
62	6	0	4.273557	2.220841	−1.554010
63	1	0	4.577304	1.184186	−1.453408
64	6	0	1.212441	4.429409	−0.850396
65	6	0	0.431182	5.223119	−1.705274
66	1	0	0.770838	5.407800	−2.720139
67	6	0	−0.785000	5.755661	−1.275546
68	1	0	−1.378176	6.358909	−1.956752
69	6	0	−1.238831	5.509385	0.020969
70	1	0	−2.185326	5.921961	0.357437
71	6	0	−0.467553	4.725896	0.883631
72	1	0	−0.811895	4.527165	1.893817
73	6	0	0.745102	4.191021	0.451933
74	1	0	1.339943	3.590825	1.133155
75	6	0	2.251251	−1.131363	1.785514
76	6	0	3.517037	−1.771489	1.715760
77	6	0	3.882607	−2.640256	2.758261
78	1	0	4.850025	−3.130699	2.701719
79	6	0	3.031317	−2.919506	3.825074
80	1	0	3.344896	−3.602755	4.608133
81	6	0	1.765572	−2.331543	3.856497
82	1	0	1.076642	−2.547415	4.667765
83	6	0	1.387231	−1.452763	2.845819
84	1	0	0.408403	−0.986194	2.870571
85	6	0	4.456209	−1.623706	0.564578

```
86          6          0        4.031470   -1.873087   -0.752502
87          1          0        2.996451   -2.143217   -0.936724
88          6          0        4.928623   -1.794607   -1.817469
89          1          0        4.582347   -1.998858   -2.826388
90          6          0        6.267882   -1.464022   -1.589336
91          1          0        6.964909   -1.402811   -2.419758
92          6          0        6.702714   -1.217336   -0.285981
93          1          0        7.740823   -0.959864   -0.096742
94          6          0        5.805070   -1.298146    0.780646
95          1          0        6.148728   -1.097983    1.791517
 ----------------------------------------------------------------
```

References

[1]   Bruker, **2007,** *APEX2 and SAINT,* Bruker AXS Inc., Madison, Wisconsin, USA.

[2]   Bruker, **2001,** *SADABS and TWINABS,* Bruker AXS Inc., Madison, Wisconsin, USA.

[3]   a) G. M. Sheldrick, *Acta Crystallogr., Sect. A: Found. Crystallogr.* **2008**, *64*, 112-122; b) G. M. Sheldrick, *Acta Crystallogr., Sect. A* **2015**, *71*, 3-8.

[4]   O. V. Dolomanov, Bourhis, L. J., Gildea, R. J., Howard, J. A. K., Puschmann, H., *J. Appl. Cryst.* **2009**, *42*, 339-341.

[5]   L. J. Farrugia, *J. Appl. Crystallogr.* **1997**, *30*, 565.

[6]   POV-Ray, **2013,** *POV-Ray 3.7.0,* Persistence of Vision Pty. Ltd., Persistence of Vision Raytracer, retrieved from http://www.povray.org/download/,

[7]   A. L. Spek, *Acta Crystallogr., Sect. D: Biol. Crystallogr.* **2009**, *65*, 148-155.

[8]   CCDC, **2001-2013,** *Mercury 3.1 - 3.3,*

[9]   T. Maris, **2004-2014,** *UdMX,*

[10]   S. P. Westrip, *J. Appl. Crystallogr.* **2010**, *43*, 920-925.

[11]   M. J. Frisch, G. W. Trucks, H. B. Schlegel, G. E. Scuseria, M. A. Robb, J. R. Cheeseman, G. Scalmani, V. Barone, B. Mennucci, G. A. Petersson, H. Nakatsuji, M. Caricato, X. Li, H. P. Hratchian, A. F. Izmaylov, J. Bloino, G. Zheng, J. L. Sonnenberg, M. Hada, M. Ehara, K. Toyota, R. Fukuda, J. Hasegawa, M. Ishida, T. Nakajima, Y. Honda, O. Kitao, H. Nakai, T. Vreven, J. A. Montgomery, J. E. Peralta, F. Ogliaro, M. Bearpark, J. J. Heyd, E. Brothers, K. N. Kudin, V. N. Staroverov, R. Kobayashi, J. Normand, K. Raghavachari, A. Rendell, J. C. Burant, S. S. Iyengar, J. Tomasi, M. Cossi, N. Rega, J. M. Millam, M. Klene, J. E. Knox, J. B. Cross, V. Bakken, C. Adamo, J. Jaramillo, R. Gomperts, R. E. Stratmann, O. Yazyev, A. J. Austin, R. Cammi, C. Pomelli, J. W. Ochterski, R. L. Martin, K. Morokuma, V. G. Zakrzewski, G. A. Voth, P. Salvador, J. J. Dannenberg, S. Dapprich, A. D. Daniels, O. Farkas, J. B. Foresman, J. V. Ortiz, J. Cioslowski, D. J. Fox, *Gaussian 09*, **2009**,

[12]   a) C. Lee, W. Yang, R. G. Parr, *Phys. Rev. B: Condens. Matter* **1988**, *37*, 785-789; b) B. Miehlich, A. Savin, H. Stoll, H. Preuss, *Chem. Phys. Lett.* **1989**, *157*, 200-206.

[13]   M. M. Francl, W. J. Pietro, W. J. Hehre, J. S. Binkley, M. S. Gordon, D. J. DeFrees, J. A. Pople, *J. Chem. Phys.* **1982**, *77*, 3654-3665.

[14]   J. Tomasi, B. Mennucci, R. Cammi, *Chem. Rev.* **2005**, *105*, 2999-3094.

[15]   a) M. E. Casida, C. Jamorski, K. C. Casida, D. R. Salahub, *J. Chem. Phys.* **1998**, *108*, 4439-4449; b) R. E. Stratmann, G. E. Scuseria, M. J. Frisch, *J. Chem. Phys.* **1998**, *109*, 8218-8224.

[16]   R. D. K. Dennington II, T.; Millam, J.; Eppinnett, K.; Hovell, W. L.; Gilliland, R., **2003,** *GaussView 3.0.9,* Semichem, Inc.; Shawnee Mission, KS.

[17]   N. M. T. O'Boyle, A. L.; Langner, K. M., *J. Comp. Chem.* **2008**, *29*, 839-845.

[18]   L. Skripnikov, **2005 - 2015,** *Chemissian V.4.36,*

Annexe-5.3 / Appendix-5.3

5.3. Additional Unpublished Results on Zn(II) Coordination Compounds of *N,N'*-diaryl-bezamidinate *N*-oxide Ligands

5.3.1. Zn(AMOX)₂ (AMOX = *N,N'*- diarylbenzamidinate-*N*-oxide) – theoretical study

The theoretical study (DFT/ TD-DFT) performed for the Zn(AMOX)$_2$ (AMOX = *N,N'*- diarylformamidinate-*N*-oxide) family of complexes and described in section 5.2, was extended to the series Zn(AMOX)$_2$ (AMOX = *N,N'*- diarylbenzamidinate-*N*-oxide) (Table 5.3-1), in order to further assess and rationalize the effect of the AMOX ligand substitution pattern on the band gap of the complexes. Details on the computational studies are given in Appendix-5.3-EXP. The frontier molecular orbital surfaces of compounds **Zn1 – Zn6 Zn8 – Zn10** are presented in Figure 5.3-1. As in the case of compounds **3** (section 5.2), the HOMO is localized on the ONCN moiety of the molecule, however, the localization of the LUMO changes to the *C*-aryl substituent.

Table 5.3-1. The compounds analyzed in this study.

Cpd.	*C*-aryl substituent R	*N,N'*-diaryl substituents R'	Obs.
Zn1	Ph	2,6-diiPrPh	
Zn2	Ph	2,6-diMePh	
Zn3	4-BrPh	2,6-diMePh	
Zn4	4-py	2,6-diMePh	
Zn5	4-CF3Ph	2,6-diMePh	
Zn6	4-OMePh	2,6-diMePh	
Zn7	4-N(Me2)Ph	2,6-diMePh	*didn't converge*
Zn8	4-py	2,6-diiPrPh	
Zn9	4-py	2-py	
Zn10	4-py	C$_6$F$_5$	

Cpd.	MO surfaces	
	HOMO	LUMO
Zn1		
Zn2		
Zn3		
Zn4		
Zn5		
Zn6		
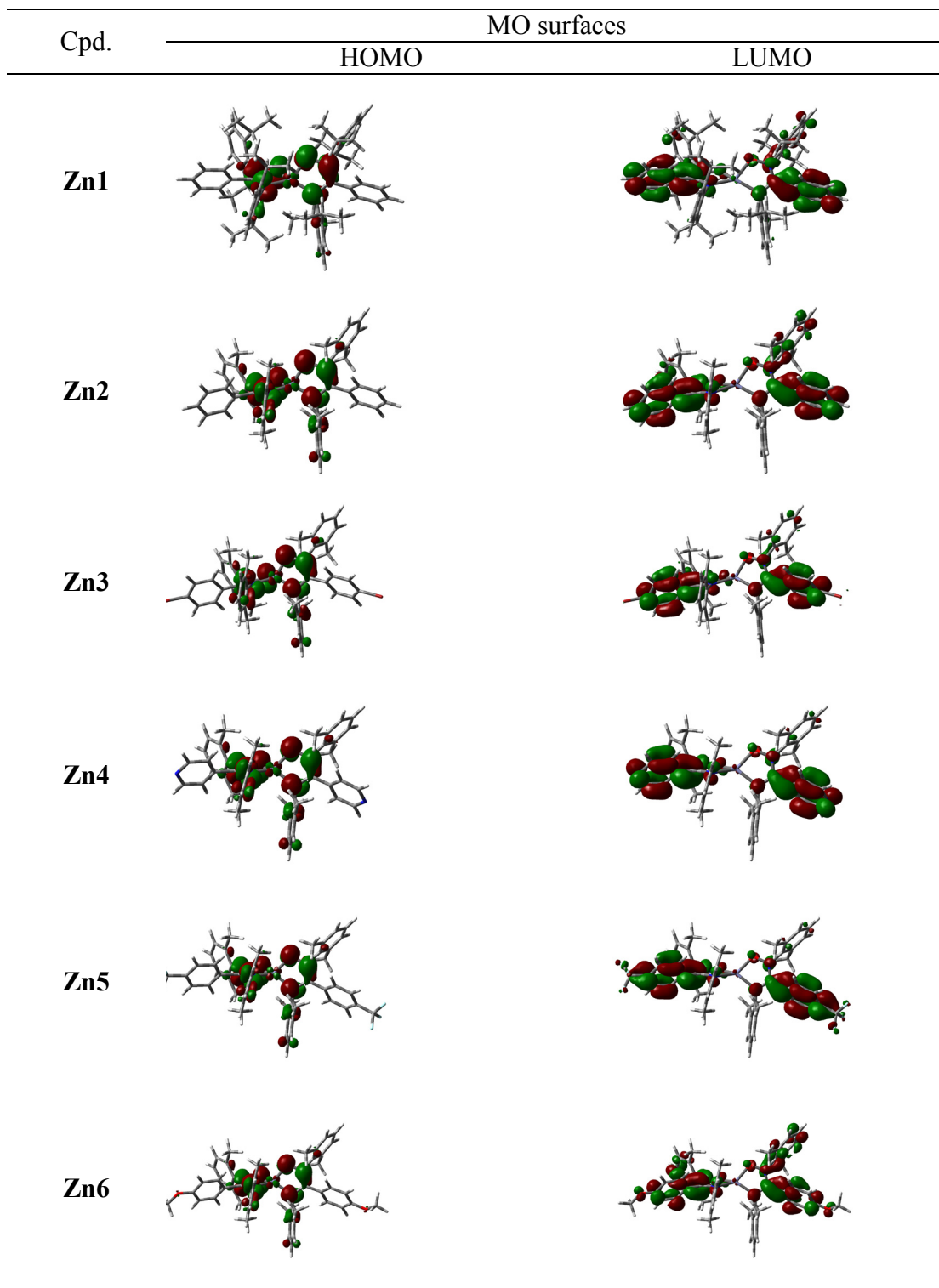
Figure 5.3-1a MO sufaces (HOMO and LUMO) for **Zn1 – Zn6**

Cpd.	MO surfaces	
	HOMO	LUMO/ LUMO+1
Zn8		
Zn9		
Zn10		
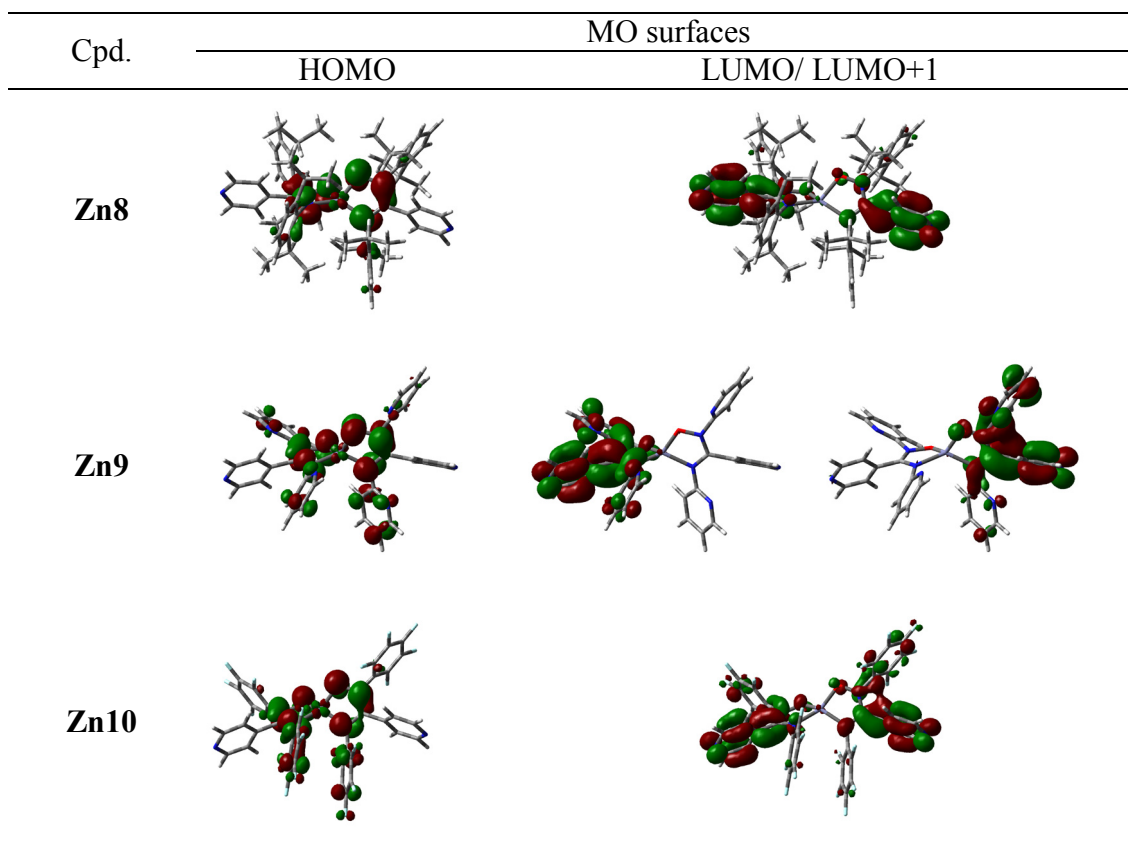
Figure 5.3-1b MO surfaces (HOMO et LUMO) for **Zn8 – Zn10**

The results are summarized in Table 5.3-2, Figure 5.3-3 (the influence of the substitution on the *C*-aryl ring), and Figure 5.3-4 (the influence of the substitution on the *N,N'*-aryl rings).

Table 5.3-2. Energy of HOMO and LUMO levels for **Zn1 – Zn6** and **Zn8 – Zn10** – theoretical values

Composé	E_{HOMO}[a] (eV)	E_{LUMO}[b] (eV)	$E_{g\,(TD\text{-}DFT)}$[c] (eV)	Composé	E_{HOMO} (eV)	E_{LUMO} (eV)	$E_{g\,(TD\text{-}DFT)}$ (eV)
Zn1	-5.05	-1.51	3.54	**Zn6**	-5.03	-1.38	3.65
Zn2	-5.09	-1.56	3.53	**Zn8**	-5.21	-1.99	3.22
Zn3	-5.17	-1.76	3.41	**Zn9**	-5.38	-2.21	3.17
Zn4	-5.25	-2.04	3.21	**Zn10**	-5.87	-2.42	3.45
Zn5	-5.21	-1.97	3.24				

[a] E_{HOMO} was obtained from DFT optimisation calculations, theory level: B3LYP/ 6-31g(d, p), PCM: CH₂Cl₂; [b] E_{LUMO} (eV) = E_{HOMO} (DFT) + $E_{g(TD\text{-}DFT)}$; [c] E_g(TD-DFT) is the first singlet calculated by TD-DFT, which correspond to the HOMO-LUMO transition; theory level: B3LYP/ 6-31g(d, p), PCM: CH₂Cl₂.

The stabilization of the LUMO increases with the strength of the EW substituent (a higher degree of delocalization on the *C*-aryl ring) (Figure 5.3-2). It was also found that substitution on the *C*-aryl ring has a minor effect on the HOMO energy level and a more important effect on the energy of the LUMO. The effect on the substitution on the *N,N'*-diaryl rings can be observed in Figure 5.3-3. The stabilization of both the HOMO and LUMO energy levels takes place, and the degree of stabilization also correlates with the nature of the substituent ED/EW. The band gap of the Zn(AMOX)$_2$ complexes is also compared with that of the Zn(BTZ)$_2$ (BTZ = 2-(2-benzothiazolyl)phenolato), an established compound for use in OLEDs.[1]

B3LYP/ 6-31g(d, p), PCM: DCM, Gaussian 09
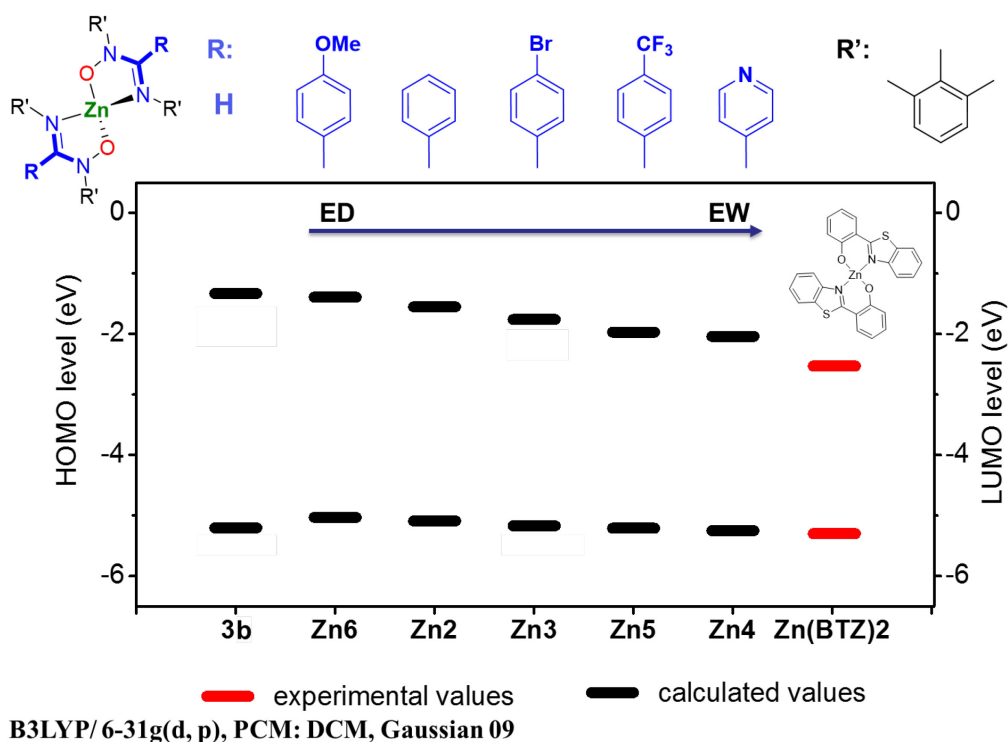
Figure 5.3-2. Calculated band gaps for **Zn2 − Zn6**. (The influence of the substitution on the *C*-aryl ring.)
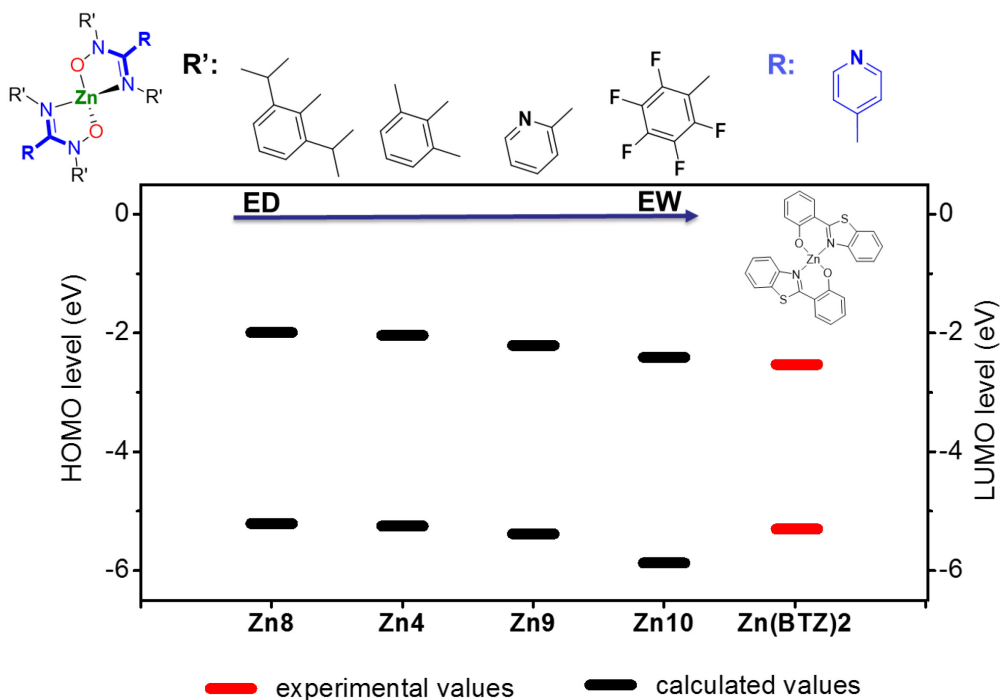
B3LYP/ 6-31g(d, p), PCM: DCM, Gaussian 09

Figure 5.3-3. Calculated band gaps for **Zn4**, **Zn8**, **Zn9**, **Zn10**. (The influence of the substitution on the *N,N'*-aryl rings.)

5.3.2. The [Zn(AMOX)₂]₂ dimers (AMOX = *N,N'*-diarylbenzamidinate-*N*-oxide)

The Figure 5.3-4 and Table S31, Appendix-5.3-EXP present the properties of the zinc(II) dimeric compound of type [Zn(AMOX)₂]₂ with AMOX = *N,N'*-diarylbenzamidinate-*N*-oxides: **D1** ([Zn(AMOX)₂]₂, AMOX = 4-bromo-*N,N'*-diphenylbenzamidinate-*N*-oxide) and **D2** ([Zn(AMOX)₂]₂, AMOX = 4-cyano-*N,N'*-diphenylbenzamidinate-*N*-oxide). The experimental details are given in Appendix-5.3-EXP. For **D1**, the solid state structure was obtained (Figure 5.3-4a and Tables S16-S18, Appendix-5.3-EXP). The Zn(II) centres are pentacoordinated and present a pseudo-square-pyramidal geometry. The AMOX ligands show two coordination modes to the zinc(II) ions: μ-AMOX-κN,κO:κO et AMOX-κN,κO. This type of complexes present potential interest in OLED applications.[2] The DFT calculations show for this compounds that the HOMO is localized on the ONCN moiety of the molecule, whereas the LUMO is found on the *C*-aryl substituents (Figure 5.3-4b). This distinction

indicates that the energy of the LUMO can be fine tuned by modifying the *C*-aryl substituent (introducing EW/ED groups). The stabilization of the LUMO level was observed for **D2** vs. **D1**, in line with the better EW character of the –CN group (**D2**) vs. the –Br group (**D1**). For **D1**, the theoretical value of its HOMO-LUMO gap determined by DFT/TD-DFT is close to the experimental value (Figure 5.3-4c). In addition, the experimental value is in line with that of Zn(BTZ)$_2$ (BTZ = 2-(2-benzothiazolyl)phenolato), a compound which was used in OLED fabrication.[1] **D1** is poorly emitting in solution, at low concentrations, but it is emissive in solid state. Its photoluminescence spectrum features a large emission band (400 – 800 nm) (Figure 5.3-4d). The AIE – Aggregation Induced Emission process is proposed for explaining this behaviour, and investigations are ongoing to prove it. The performance of these compounds as luminophores in WOLEDs (White OLEDs) is tested in collaboration with the research groupe of Professor Nunzi at Queens University. An example of preliminary results obtained for **D1** is shown in Figure 5.3-4e.
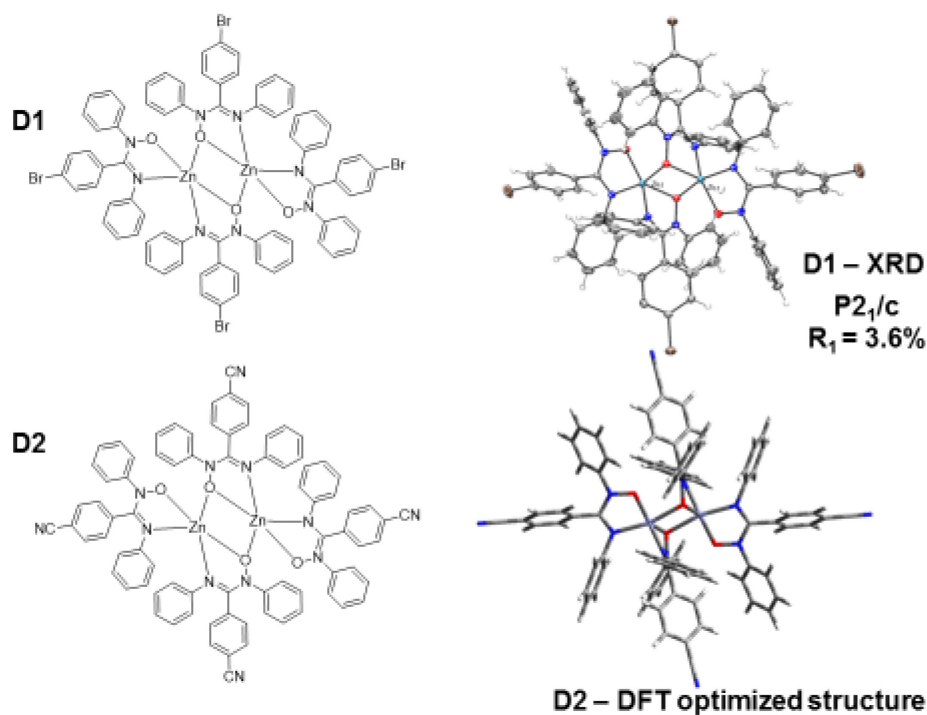
Figure 5.3-4a. ChemDraw structures of **D1** and **D2**, the solid state structure of **D1** (cristallography by Janaina Ferreira) and the DFT optimized structure of **D2**

B3LYP/ 6-31g(d, p), PCM: DCM, Gaussian 09
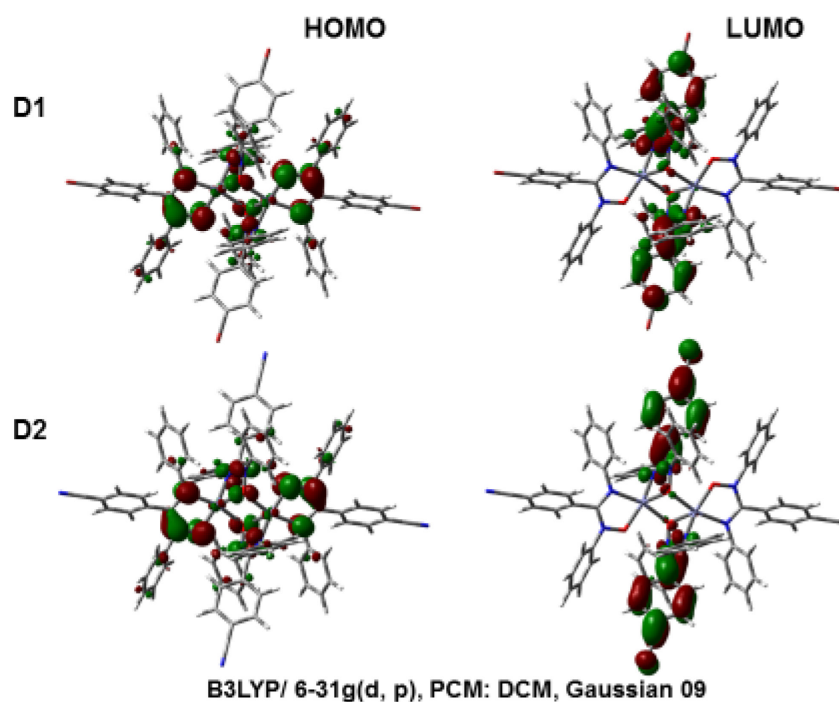
Figure 5.3-4b. The MO surfaces (HOMO and LUMO) for **D1** and **D2**
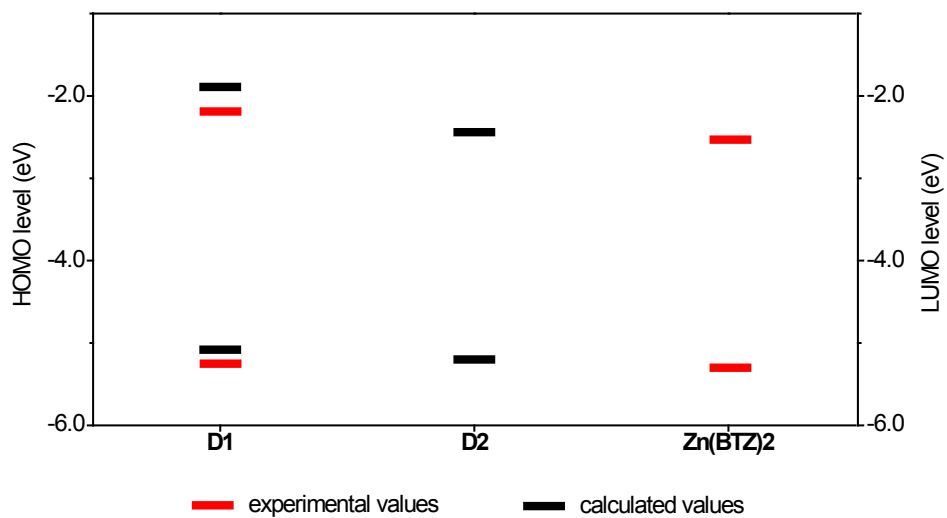
Figure 5.3-4c. The HOMO-LUMO gap for **D1** (calculated and experimental values) and for **D2** (calculated value); comparaison with Zn(BTZ)2

Cpd.	D1 (4-BrPh)
$\lambda_{max\ em}$ (nm)	556

λ_{exc} (nm) = 350
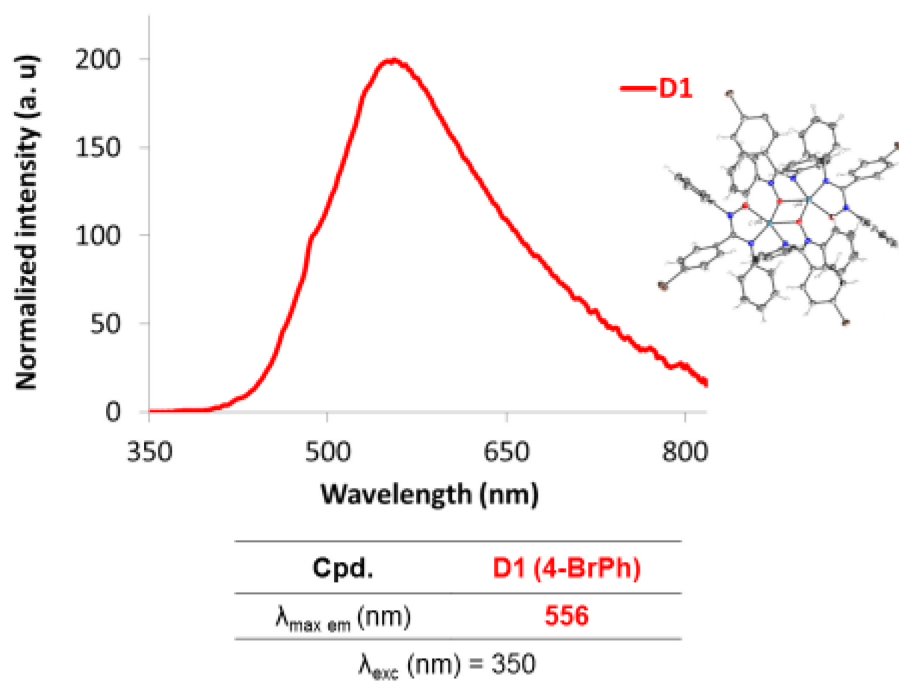
Figure 5.3-4d. Emission spectra (in solid state – powder) for **D1**
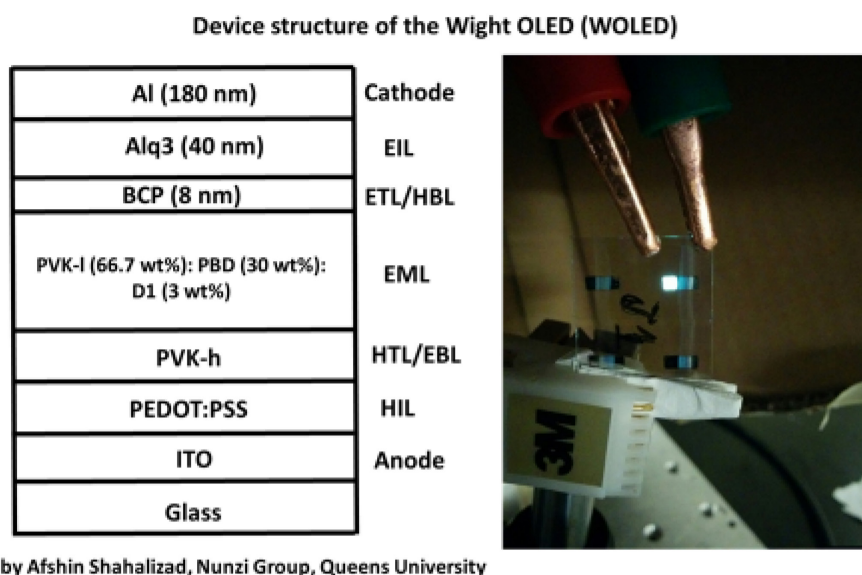
Figure 5.3-4e. The test with **D1** in WOLEDs

5.3.3. Coordination of *N*-bridged bis-AMOX ligands with Zn(II) ions

  N-bridged bis-AMOX ligands were synthesized (Figure 5.3-5) in order to be used as synthons for AMOX-based supramolecular architectures. The experimental details are given in Appendix-5.3-EXP.
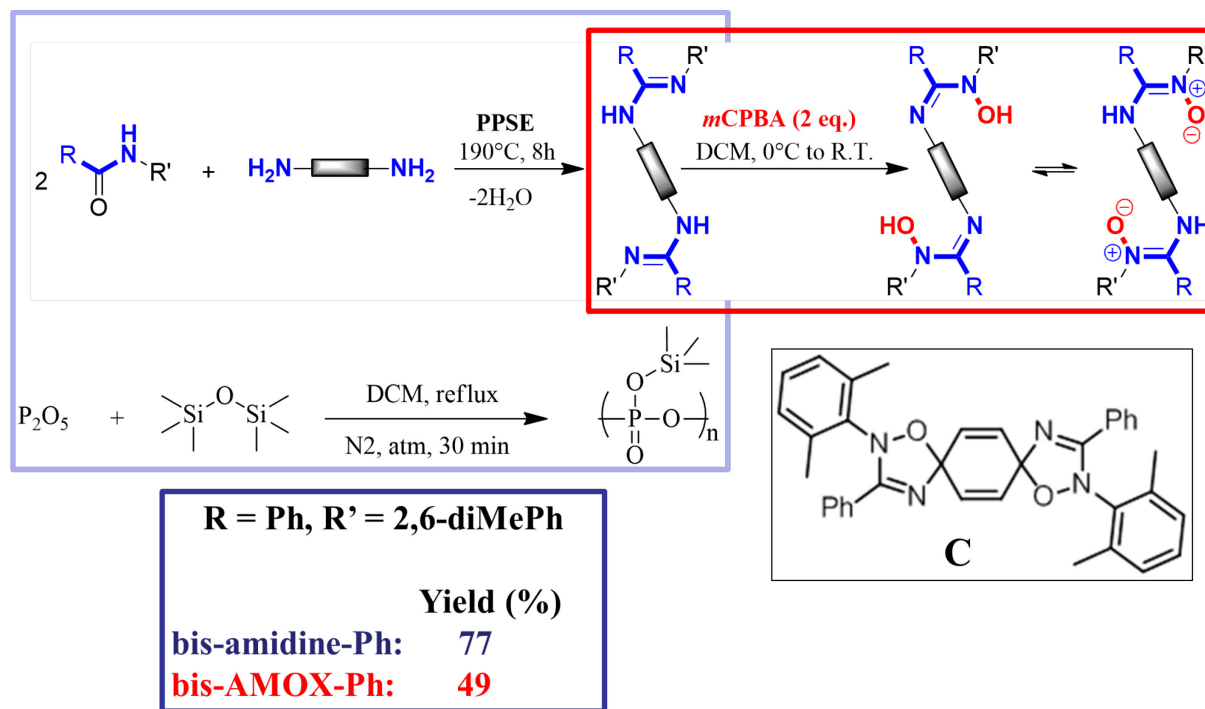
Figure 5.3-5. Synthesis of the *N*-bridged bis-AMOX ligands and their bis-amidine precursors

  The PPSE synthesis for yielding the *N*-bridged bis-amidine compounds was optimised to the conditions presented above (8h at 190°C); at shorter reaction times unreacted amidine is present, and at longer reaction times, secondary products are formed. The purification of the *N*-bridged bis-AMOXs is done by flash chromatography on silica, using the following eluant gradient: hexane/AcOEt 5/5, AcOEt 100%, AcOEt/EtOH 5/5, EtOH 100%; secondary products identified: mono-AMOX, oxidized bis-AMOX (product **C**, Figure 5.3-5 – its solid state structure is shown in Figure 5.3-8). ^{1}H NMR spectra of **bis-amidine-Ph** and **bis-AMOX-Ph** with proton resonance assignments are shown in Figure 5.3-6. The solid state structures of **bis-amidine-Ph**, **bis-AMOX-Ph**, and of compound **C** were obtained, and are presented in Figures 5.3-7, 5.3-8, 5.3-9, and Tables S19-S27, Appendix-5.3-EXP.
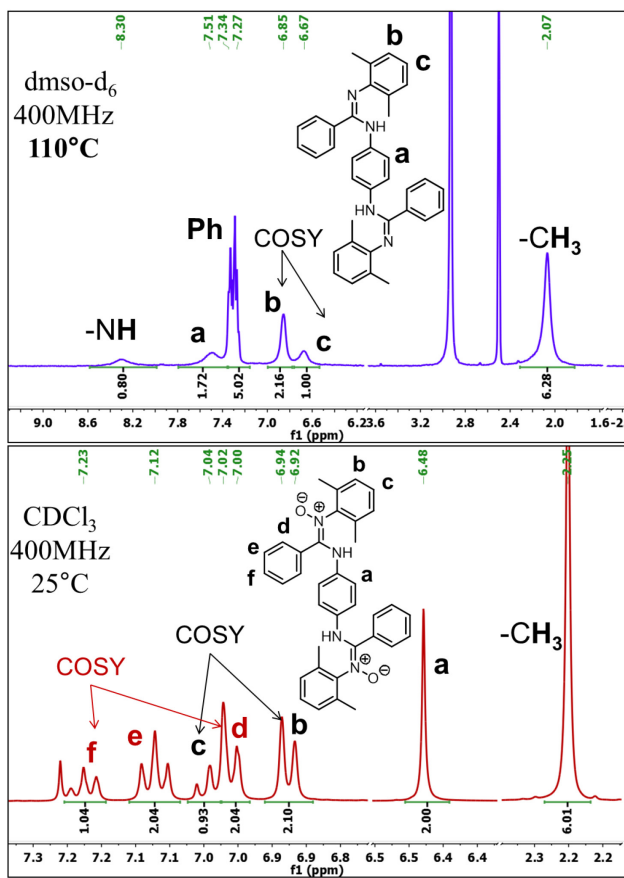
Figure 5.3-6. ^{1}H NMR spectrum of **bis-amidine-Ph** (top) and **bis-AMOX-Ph** (bottom) with proton resonance assignments.
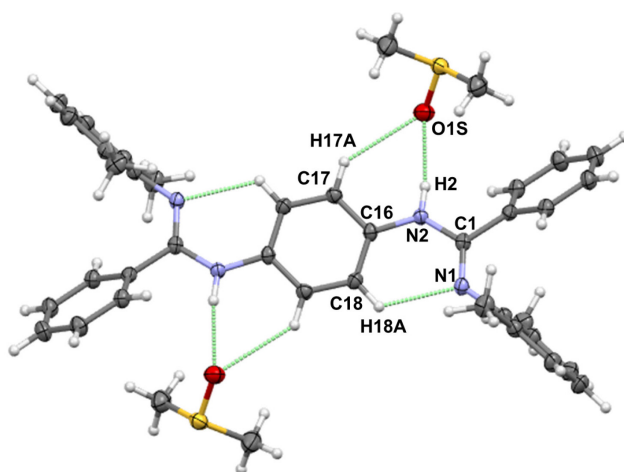
Figure 5.3-7. The solid state structure of **bis-amidine-Ph**: ORTEP view with ellipsoids at 50% probability level; the H-bonding pattern (intramolecular and with the co-crystallized solvent) is also showed.
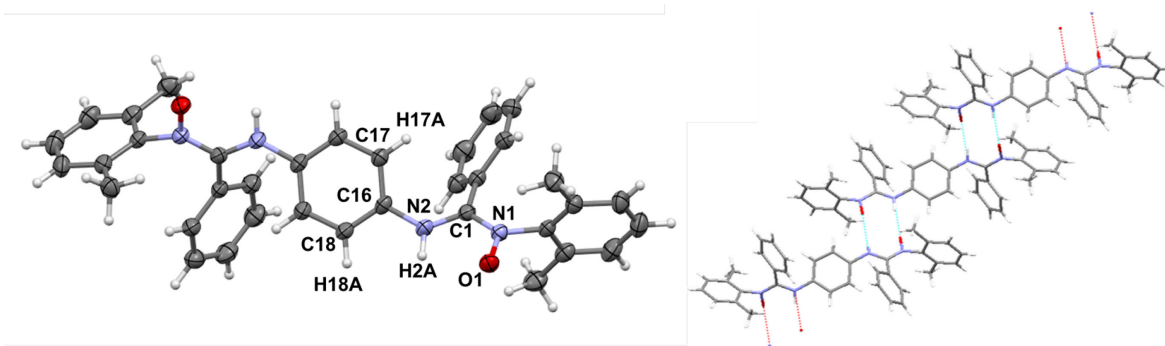
Figure 5.3-8. The solid state structure of **bis-AMOX-Ph**: ORTEP view with ellipsoids at 50% probability level (left) and H-bonding pattern (right) – cyclic dimeres *via* N-H⋯O (*d* = 1.977(1) bonds
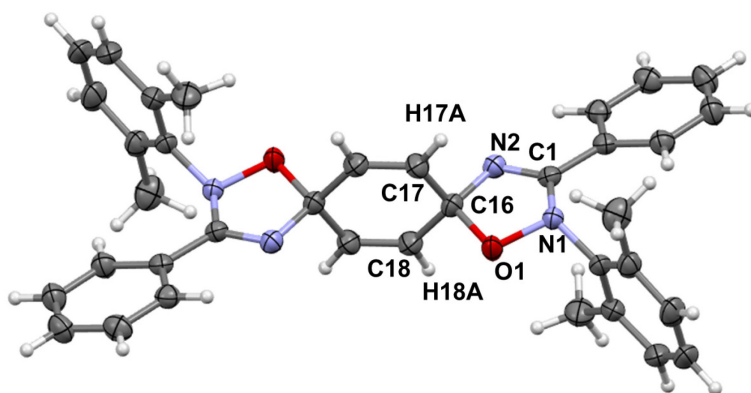
Figure 5.3-9. The solid state structure of **compound C**: ORTEP view with ellipsoids at 50% probability level

The complexation of the *N*-bridged bis-AMOX ligand (**bis-AMOX-Ph**) (presenting the possibility to have parallel coordination vectors) with Zn(II) metal-ions (tetrahedral geometry) was realized in an attempt to obtain grid-type compounds (Figure 5.3-10).
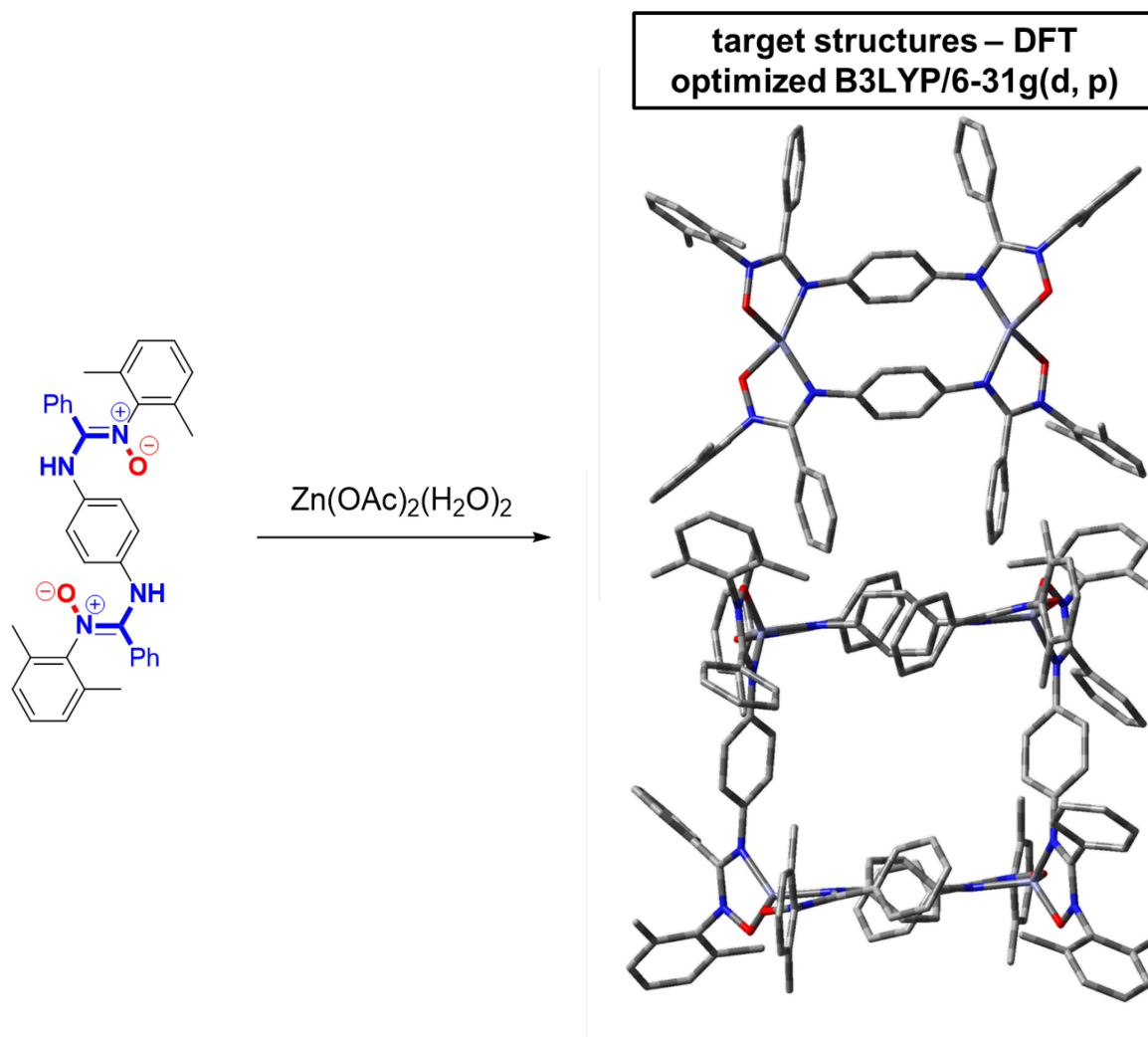
Figure 5.3-10. Coordination of *N*-bridged bis-AMOX ligand with Zn(II) metal-ions: expected grid structure (model)

However, the 1D-metallopolymer was obtained, as proved by its solid state structure (Figure 5.3-11 and Tables S28-S30, Appendix-5.3-EXP). The compound is a yellow solid, highly insoluble. Poor quality X-ray crystals (very thin yellow needles) were obtained from hot toluene, by slow evaporation. The solid state structure highlights a 1D coordination polymer, with a Zn---Zn distance of 9.6 Å. The zinc(II) metal-ions display pseudotetrahedral geometry ($\tau_4 = 0.74$).[3]
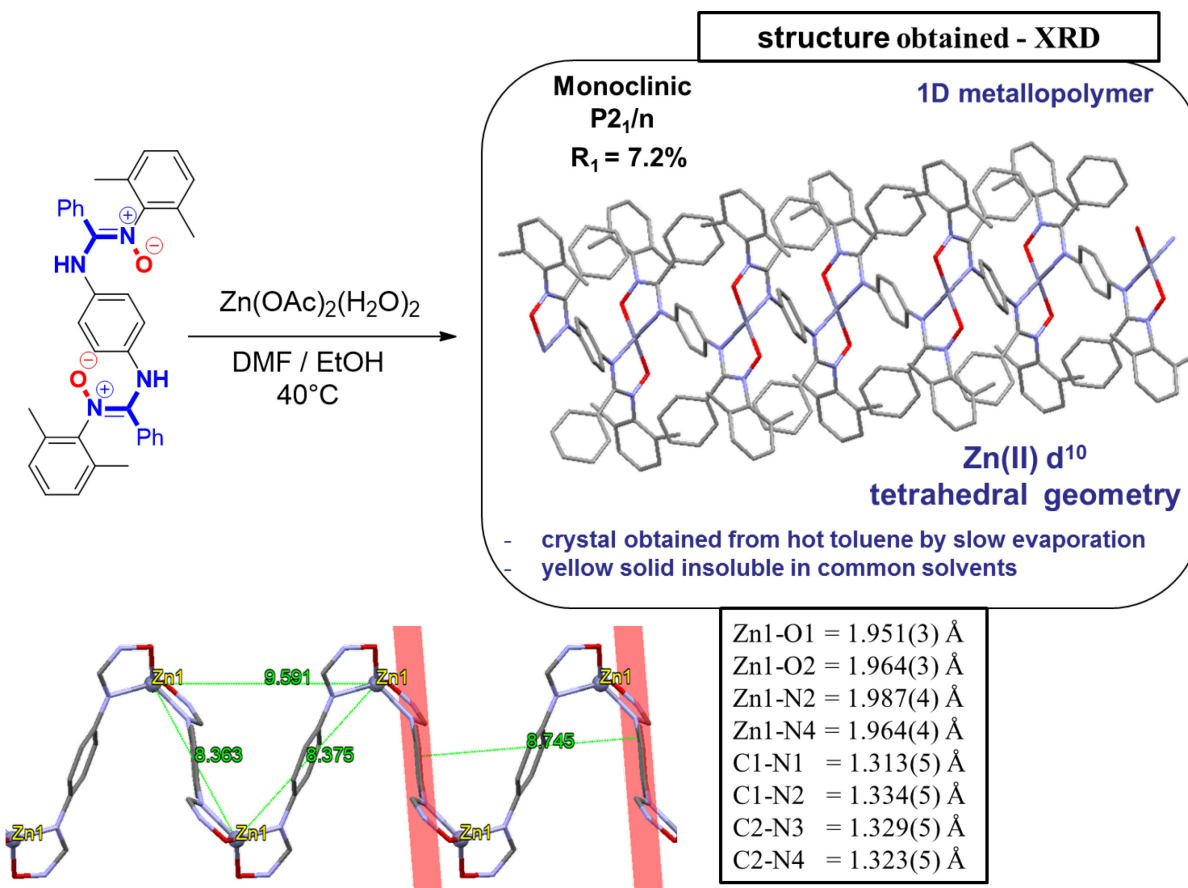
Figure 5.3-11. Synthesis of the Zn-metallopolymer and its X-ray structure. Hydrogen atoms and co-crystallized toluene molecules omitted for clarity

The high insolubility of the polymer hindered its full characterization. Its electronic spectrum is shown in Figure 5.3-12 together with those of the AMOX ligand and corresponding parent amidine. The Zn(II) metallopolymer is emissive (Figure 5.3-13) and it has good stability (decomposition temperature Td measured at 5% weight loss is 320 °C (Figure 5.3-14).
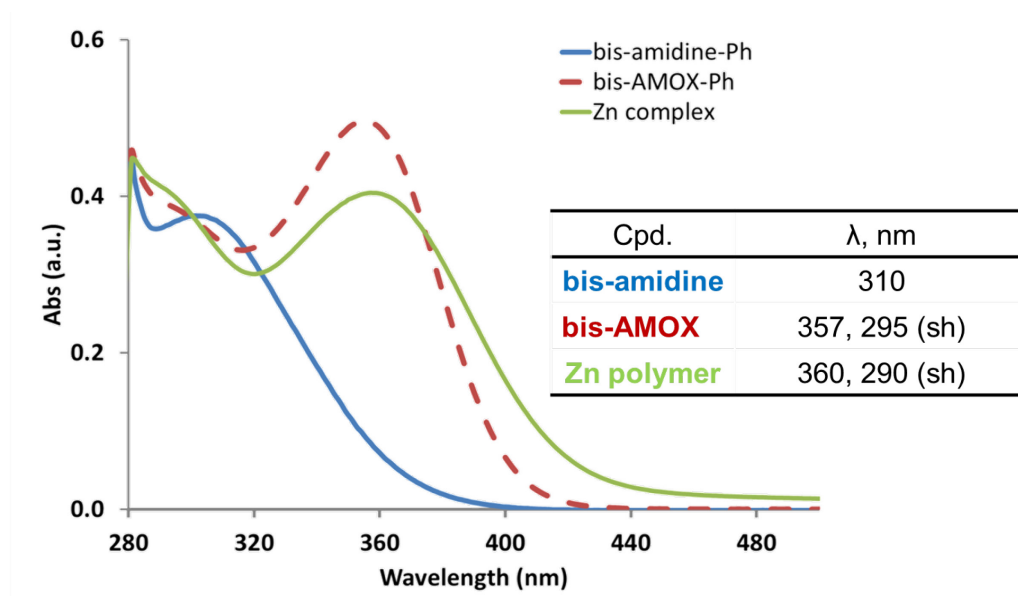
Figure 5.3-12. Electronic spectra of the Zn(II) metallopolymer, the *N*-bridged bis-AMOX ligand, and the *N*-bridged bis-amidine precursor (in toluene)
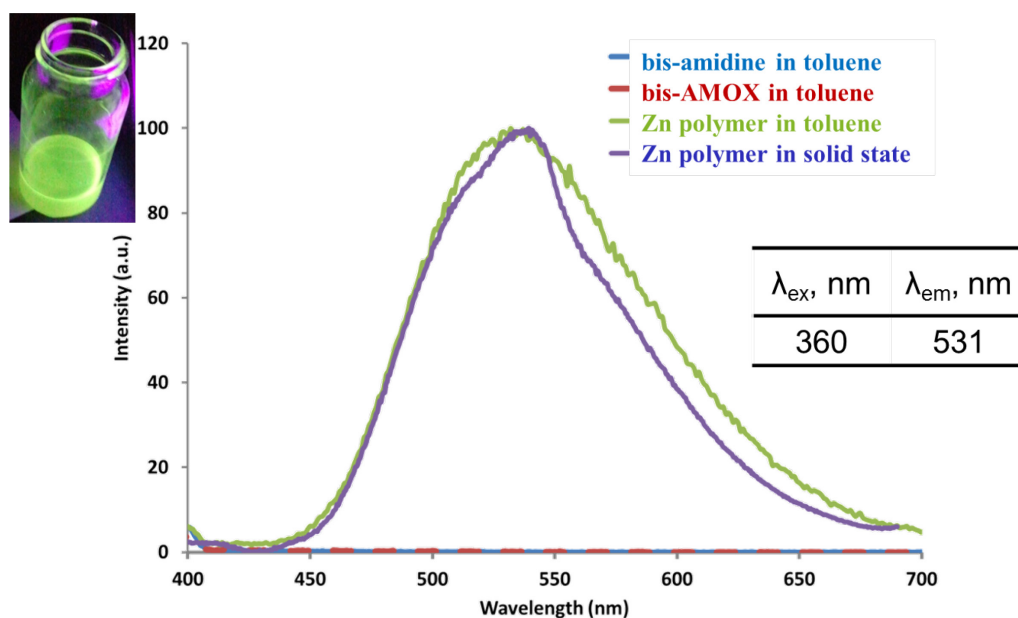
Figure 5.3-13. Emission spectra of the Zn(II) metallopolymer (in toluene solution and in the solid state), and of the *N*-bridged bis-AMOX ligand, and the *N*-bridged bis-amidine precursor (in toluene)
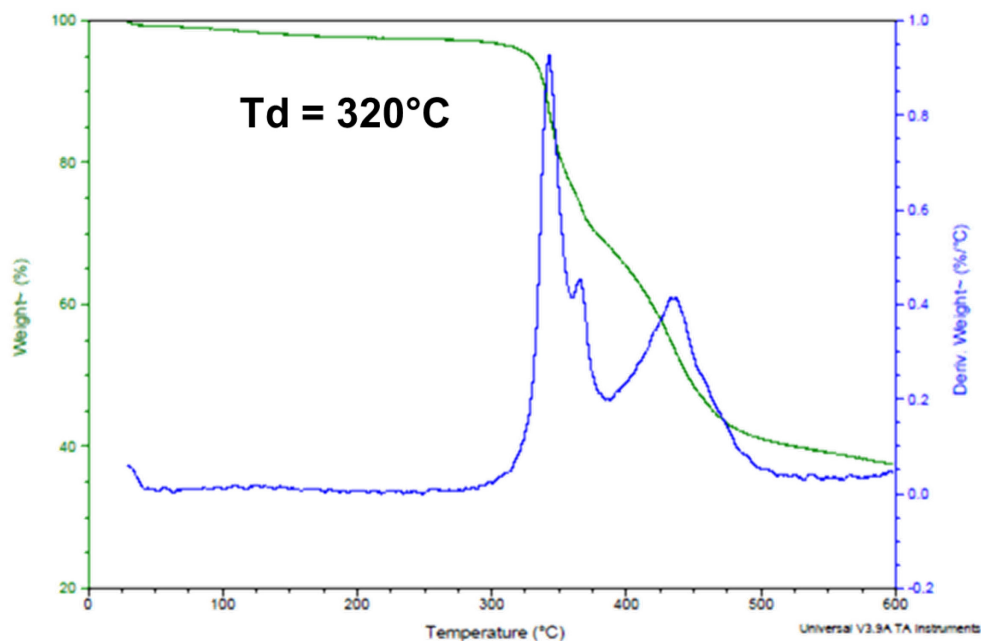
Figure 5.3-14. TGA profile for the Zn(II) metallopolymer (Td calculated at 5% weight loss).
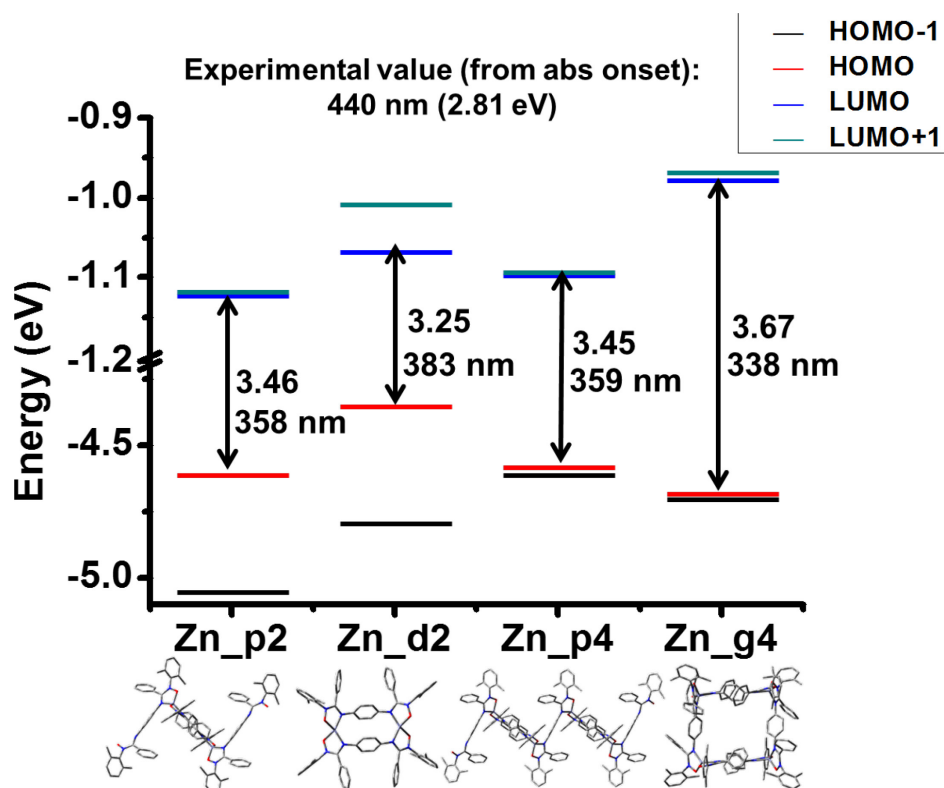
Figure 5.3-15. Calculated band gap for AMOX-based Zn(II) compounds of discrete and oligomeric type.

Calculated band gap for AMOX-based Zn(II) compounds of discrete and oligomeric type are presented in Figure 5.3-15, and the frontier MO surfaces of the corresponding optimized structures are highlighted in Figure 5.3-16. Localization of the LUMO on the *C*-aryl rings is observed in all cases, suggesting that tuning of the band gap for this type of compounds can also be achieved by modifying the substitution pattern of this specific group.
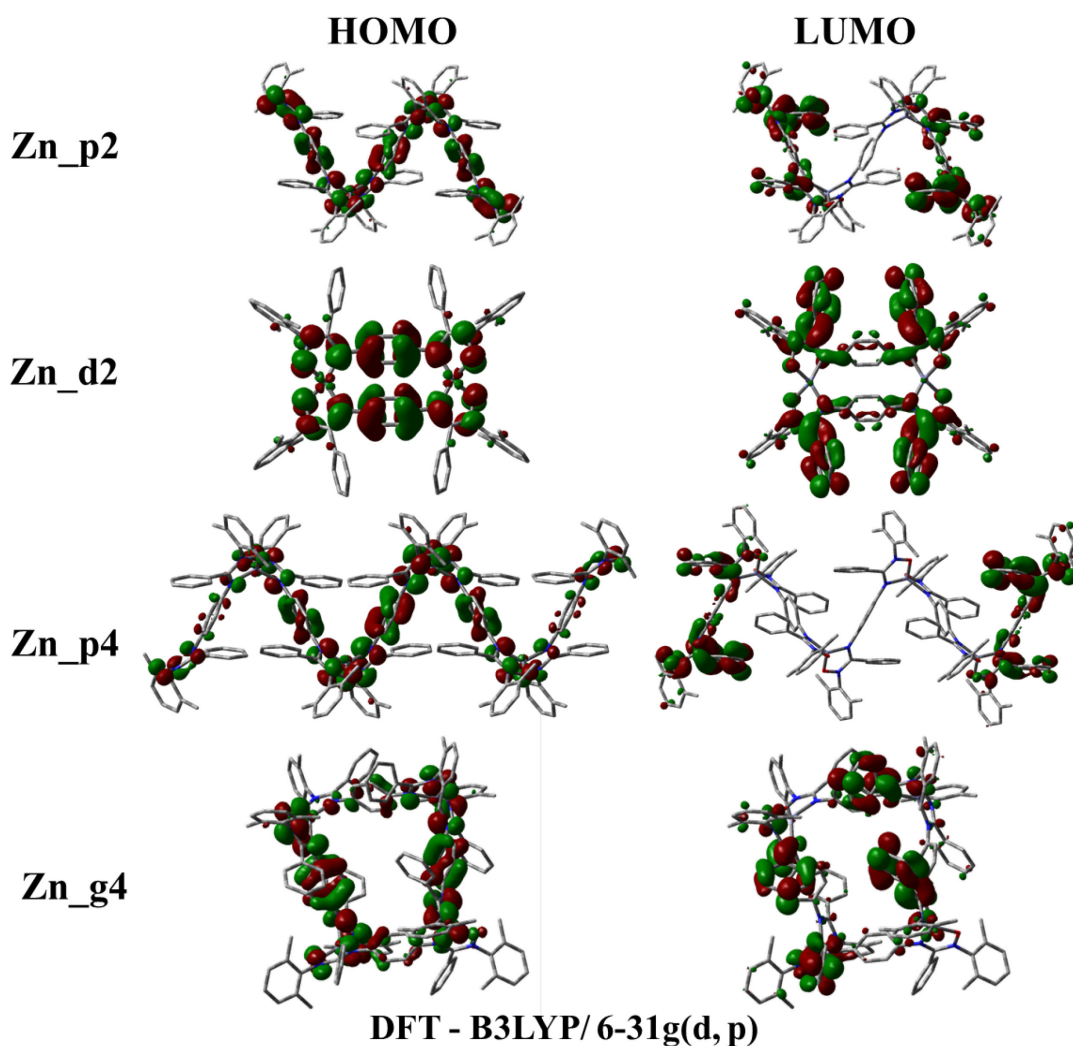
Figure 5.3-16. Frontier MO surfaces for AMOX-based Zn(II) compounds of discrete and oligomeric type.

5.3.5. References

[1]   R. Wang, L. Deng, M. Fu, J. Cheng, J. Li, *J. Mat. Chem.* **2012**, *22*, 23454-23460.
[2]   F. Borbone, U. Caruso, M. Causa, S. Fusco, B. Panunzi, A. Roviello, R. Shikler, A. Tuzi, *Eur. J. Inorg. Chem.* **2014**, *2014*, 2695-2703.
[3]   L. Yang, D. R. Powell, R. P. Houser, *Dalton Trans.* **2007**, 955-964.

Annexe-5.3-EXP/ Appendix-5.3-EXP

Materials and Instrumentation

Nuclear magnetic resonance (NMR) spectra were recorded in $CDCl_3$ and/ or dmso-d_6 at room temperature (r.t.) (unless otherwise stated) on the following spectrometers: Bruker AV-400, AV-300, DRX-400, and ARX-300 MHz. Chemical shifts (δ) are reported in part per million (ppm) relative to TMS, using the residual solvent protons (7.26 ppm and 2.50 ppm) as reference. Absorption spectra were measured in DCM (concentration range $10^{-4} – 10^{-6}$ M) at r.t. on a Cary 500i and a Cary 6000i UV-Vis-NIR Spectrophotometer. Luminescence spectra were obtained using a Perkin Elmer LS55 Luminescence Spectrometer equipped with an accessory for measuring solid state samples. Electrochemical measurements were carried out in argon-purged dry DCM at room temperature with a BAS CV50W multipurpose equipment interfaced to a PC. The working electrode was a glassy carbon electrode. The counter electrode was a Pt wire, and the pseudo-reference electrode was a silver wire. The reference was set using an internal 1 mM ferrocene/ferrocinium sample at 0.46 V *vs*. SCE in DCM. The concentration of the compounds was about 1 mM. Tetrabutylammonium hexafluorophosphate (TBAP) was used as supporting electrolyte and its concentration was 0.10 M. Cyclic voltammograms were obtained at scan rates of 50, 100, 200, and 500 mV/s. For irreversible oxidation processes, the anodic peak was used as E. Thermogravimetric analyses (TGA) were carried out on a TA Q-500 and a TGA2950 thermogravimetric analyzer (TA Instruments) under N_2 atmosphere, in the $25 – 600$ °C temperature range, at a heating rate of 10 °C/ min. The IR spectra were recorded on solid samples (powders) of the compounds, using a Perkin Elmer Spectrum Two FT-IR spectrometer equipped with a Universal Attenuated Total Reflectance Accessory (UATR). The mass spectrometry analyses and the microanalyses were done by the Mass Spectrometry Service and the Elemental Analysis Service at Université de Montréal. Solvents, purchased from VRW and Fisher, were removed under reduced pressure using a rotary evaporator, unless otherwise stated. The *m*-CPBA from Acros Organics and anilines, carboxylic acids, and metal salt from Aldrich, were used without further purification.

Experimental procedure

Synthesis of AMOX ligands (section 5.3.2)

The parent benzamidine (4-bromo-*N,N'*-diphenylbenzamidine) previously reported, was prepared in very good yield (97%) by condensation between the corresponding carboxylic acid and two equivalents of aniline, in polyphosphoric acid trimethylsilyl ester (PPSE), at 180 °C, followed by basic treatment.[1] The corresponding AMOX ligand was obtained by the *N*-oxidation of the parent amidine with *meta*-chloro-peroxybenzoic acid (*m*-CPBA) in dichloromethane at room temperature, following the general procedure reported in the previous chapters.

4-bromo-*N,N'*-diphenylbenzamidine-*N*-oxide

To a solution of the corresponding amidine (1.50 g, 4.3 mmol, 1 eq.) in DCM (100 mL), NaHCO$_3$ (0.39 g, 4.7 mmol, 1.1 eq.) was added as a solid, followed by the slow addition at r. t. of a solution of *m*-CPBA (0.81 g, 4.7 mmol, 1.1 eq) in DCM (50 mL). The reaction mixture was stirred for 24 h, then was filtered and washed with an aqueous solution of NaOH 1M (2 x 25 mL) and with water (2 x 25 mL). The combined organic layers were dried over anhydrous MgSO$_4$ and filtered. After filtration and solvent evaporation, a brown solid was obtained, further purified by flash chromatography on silica (gradient of eluants: hexane/ AcOEt (5:5), AcOEt 100%, AcOEt/ EtOH (9:1), EtOH 100%). The purification yielded a yellow solid, the desired product. Yield: 0.80 g, 51%. ^{1}H-NMR (DMSO-d$_6$, 400 MHz) δ, ppm: δ 7.43 (d, *J* = 8 Hz, 2H), 7.36 (d, J = 8 Hz, 2H), 7.29 (t, *J* = 8 Hz, 2H), 7.16-7.13 (m, 3H), 7.08 (t, *J* = 8 Hz 2H), 6.84 (t, *J* = 7 Hz, 1H), 6.64 (d, *J* = 8 Hz, 2H). ^{13}C NMR (DMSO-d$_6$, 126 MHz) δ, ppm: 153.5, 146.0, 144.6, 132.2 (2C), 131.5, 130.9, 128.9 (2C), 128.8 (2C), 126.2, 124.3 (2C), 122.9, 122.6, 122.2 (2C). MS (ESI - DCM) (m/z): 367.1 [M+H]$^+$ (100%). Elemental Analysis: *calc.* (%) for C$_{19}$H$_{15}$BrN$_2$O: C 62.14, H 4.12, N 7.63; *found*: C 61.95, H 3.73, N 7.54. IR (ATR, solid sample, cm^{-1}) 3099, 3053, 1592, 1569, 1556, 1504, 1487, 1449, 1423, 1394, 1356, 1318, 1298, 1245, 1201, 1142, 1085, 1068, 1028, 1013, 999, 981, 964, 933, 907, 841, 827, 803, 748, 739, 719, 695, 665, 642, 619, 610, 573, 527, 509, 494, 423, 412.

Synthesis of the complexes (section 5.3.2)

General procedure.[2] A solution of the AMOX ligand (2 eq.) in aqueous ethanol 90% was added to a solution of metal salt (1 eq.) in water, previously brought to pH 8 with an aqueous solution of KOH or NaOH. The formation of precipitate is observed almost instantly. The reaction mixture was

stirred at room temperature before water was added (reaction times are specified below for each compound), and was kept at 4°C for 1-2 h before being filtered. The resulted solid was washed with hot water and aqueous ethanol 50%, and was dissolved in DCM and dried over MgSO$_4$. A second filtration and evaporation of the solvent yielded the desired products as solids. When necessary, further purification by recrystallization was performed.

D1 – Bis[μ-(4-bromo-*N*,*N*'-diphenylbenzamidinate-*N*-oxide-κN,κO:κO)]bis[4-bromo-*N*,*N*'-diphenylbenzamidinate--*N*-oxide-κN,κO]dizinc(II, II)

Zn(AcO)$_2$·2H$_2$O (0.17 g, 0.79 mmol, 1 eq.) and the corresponding AMOX ligand **(**0.58 g, 1.6 mmol, 2 eq.) were reacted following the general procedure, for a total reaction time of 24 h. A pale beige-green solid was obtained which was further recrystallized in DCM/ hexane at -10 °C to yield the pure product as a pale beige solid. X-ray quality crystals were obtained in DCM/ hexane at -10 °C. Yield 0.44 g, 70%. T$_d$ (TGA, 5% weight loss): 243°C. ^{1}H NMR (DMSO-d_6, 300 MHz): ^{1}H NMR (300 MHz, DMSO) δ 7.33 (d, J = 8 Hz, 1H), 7.24 – 7.14 (m, 1H), 7.10 – 6.96 (m, 7H), 6.80 (t, J = 7 Hz, 1H), 6.70 (d, J = 7 Hz, 1H). ^{13}C NMR (DMSO-d_6, 75 MHz): 154.9, 147.6, 143.7, 132.2 (2C), 131.1 (2C), 130.9, 128.3 (2C), 128.0 (2C), 126.1, 126.0 (2C), 124.8 (2C), 122.2, 121.8, 39.52. Elemental Analysis: *calc.* (%) for C$_{76}$H$_{56}$Br$_4$N$_8$O$_4$Zn$_2$: C 57.21, H 3.54, N 7.02; *found*: C 57.26, H 3.48, N 6.95. IR (ATR, solide sample, cm^{-1}) 1592, 1563, 1487, 1459, 1426, 1213, 1071, 1044, 1014, 1000, 960, 828, 775, 760, 742, 695, 673, 611, 496, 464.

Synthesis of the bis-AMOX based compounds (section 5.3.3)

bis-amidine-Ph

The synthesis of **bis-amidine-Ph** was realized based on modified literature protocols for amidine synthesis by condensation between a carboxylic acid and two equivalents of aniline, in polyphosphoric acid trimethylsilyl ester (PPSE).[1] The PPSE was obtained as a colourless viscous liquid, by refluxing P$_2$O$_5$ with HMDS (hexamethyldisiloxane) (stoichiometry 1 to 1.5) in DCM for 30 min (under N2), followed by the evaporation of the solvent. For the synthesis of the **bis-amidine-Ph**, the *N*-(2,6-dimethylphenyl)-amide (previously reported)[3] was used as starting product (0.21 g, 0.92 mmol, 2 eq.), together with 1,4-phenylenediamine (0.05 g, 0.46 mmol, 1 eq.). These two compounds were mixed with PPSE (in excess) and the reaction mixture was heated at 185 °C for 6 h. The reaction was brought to r. t. and quenched with aqueous NaOH 1M (40 mL). A beige solid was obtained, which was further recrystallized in aqueous EtOH and dried under

vacuum, to give the pure compound, a colourless powder. X-ray quality single crystals were obtained at r. t. by slow evaporation from DMSO. Yield 0.19 g, 77%. ^{1}H NMR (400 MHz, dmso-d6, 110 °C) δ 8.30 (br. s, 2H), 7.49 (br. s, 4H) 7.35 – 7.25 (m, 10H), 6.85 (br. s, 4H), 6.67 (br. s, 2H), 2.07 (br. s, 12H). MS (ESI - DCM) (m/z): 323.3 [M+H]$^+$ (100%); 262.2 [M+2H]$^{2+}$ (17%). Elemental Analysis: *calc.* (%) for $C_{36}H_{34}N_4$: C 82.72, H 6.56, N 10.72; *found*: C 82.53, H 6.60, N 10.78.

bis-AMOX-Ph

To a solution of the **bis-amidine-Ph** (0. 64 g, 1.2 mmol, 1 eq.) in DCM (100 mL), NaHCO$_3$ (0.21 g, 2.4 mmol, 2 eq.) was added as solid, followed by the slow addition (at 0°C) of a solution of *m*-CPBA (0.43 g, 1.2 mmol, 1 eq) in DCM (100 mL). The reaction mixture was allowed to warm to room temperature and stirred for other 30 minutes, then was filtered and washed with an aqueous solution of NaOH 1M (2 x 50 mL) and with water (2 x 50 mL). The combined organic layers were dried over anhydrous MgSO$_4$ and filtered. Evaporation of the solvent yielded a yellow-brown solid, which was further purified by flash chromatography on silica (gradient of eluents: hexane/ AcOEt (5:5), AcOEt 100%, AcOEt/ EtOH (5:5), EtOH 100%). The pure desired product was obtained as a yellow powder, and was dried under vacuum overnight. X-ray quality yellow crystals were obtained by slow diffusion of hexane in a DCM solution of the compound at r. t. Yield: 0.69 g, 49%. ^{1}H-NMR (CDCl$_3$, 400 MHz) δ, ppm: 7.23 (t, *J* = 7.4 Hz, 2H) 7.12 (t, *J* = 7.7 Hz, 4H), 7.06 – 7.00 (m, 6H), 6.93 (d, *J* = 7.6 Hz, 4H), 6.48 (s, 4H), 2.25 (s, 12H). ^{13}C NMR (CDCl$_3$, 400 MHz) δ, ppm: 148.4 (2C), 141.2 (2C), 134.6 (2C), 134.2 (4C), 130.3(2C), 128.9 (4C), 128.8 (2C), 128.5 (8C), 127.1 (2C), 122.5 (4C), 17.6 (4C). MS (ESI - DCM) (m/z): 555.2 [M+H]$^+$ (100%). Elemental Analysis: *calc.* (%) for $C_{36}H_{34}N_4O_2$ (H$_2$O): C 75.50, H 6.34, N 9.78; *found*: C 75.82, H 6.22, N 9.88.

Compound C (Figure 5.3-5) was obtained as a secondary product in the reaction for the synthesis of bis-AMOX-Ph. X-ray quality yellow single crystals were formed at r. t., by diffusion of hexane in a DCM solution of the compound. Its solid state structure is presented in Figure 5.3-8 and Tables S25-S27. Its full characterization is in progress.

Zn(II) bis-AMOX-Ph coordination polymer

The synthesis of this compound is based on a previously reported protocol.[4]

A solution of the bis-AMOX-Ph ligand (55 mg, 0.1 mmol, 1 eq.) in DMF (5 mL) and EtOH (2 mL) was added over 30 min. (syringe pump), at 40°C, to a solution of Zn(AcO)$_2$·2H$_2$O (23 mg, 0.1 mmol, 1 eq.) in DMF (2 mL), which was previously prepared with heating at 40°C for 10 min. The

reaction was kept at this temperature for an additional 30 min., and left at r. t. overnight. A yellow precipitate formed, which was isolated by filtration as a yellow solid (42 mg obtained after drying under vacuum). The compound is very poorly soluble in common solvents. NMR characterization was hindered by its poor solubility. T_d (TGA, 5% weight loss): 320°C. Very poor quality single crystals were obtained by slow evaporation of a hot toluene solution of the compound. The solid state structure is presented in Figure 5.3-11 and Tables S28-S30.

Computational details

Gaussian09, Revision D.01[5] was used for all theoretical calculations discussed herein, with B3LYP[6] DFT method, 6,31-g(d,p)[7] basis set, in gas phase or using PCM[8] (CH_2Cl_2) solvation model. No symmetry constraints were used for the geometry optimization. Initial atom coordinates for geometry optimization were taken from XRD data (cif) of the corresponding structures, when available. The atomic coordinates for the optimized structures are given in Tables S1-S15. No imaginary frequencies were obtained when frequency calculations on optimized geometries were performed. TD-DFT[9] calculations (for the first 30 singlet states) were performed, starting with the optimized geometries of the ground states. GaussView 3.0.9[10] Gaussum[11] and Chemissian V.4.36[12] software were used for data analysis, visualisation, and surface plots.

Table S1. Atomic coordinates for DFT optimization of **Zn1** (theory level: B3LYP/ 6,31-g(d,p) PCM: CH_2Cl_2)

```
                        Standard orientation:
 ---------------------------------------------------------------------
 Center     Atomic      Atomic           Coordinates (Angstroms)
 Number     Number       Type         X           Y           Z
 ---------------------------------------------------------------------
      1         30          0       0.000087   -0.021501   -0.000276
      2          8          0       1.216484   -1.212753   -0.993602
      3          8          0      -1.215884   -1.213209    0.992715
      4          7          0       2.512677   -1.000594   -0.591435
      5          7          0       1.755810    0.796613    0.618501
      6          7          0      -2.512308   -1.001005    0.591266
      7          7          0      -1.756070    0.796654   -0.618387
      8          6          0       2.780185    0.039936    0.218031
      9          6          0       4.205348    0.266608    0.606824
     10          6          0       4.582331    0.280237    1.957377
     11          1          0       3.836603    0.118099    2.724869
     12          6          0       5.914294    0.479956    2.319425
     13          1          0       6.190454    0.479861    3.369444
     14          6          0       6.887079    0.679152    1.337768
     15          1          0       7.923299    0.837382    1.620712
     16          6          0       6.519965    0.675883   -0.008982
     17          1          0       7.267983    0.834676   -0.779729
     18          6          0       5.188927    0.468931   -0.371605
     19          1          0       4.908764    0.478846   -1.418045
     20          6          0       3.373221   -2.137151   -0.817308
```

```
21      6       0       3.931637    -2.318930   -2.100294
22      6       0       4.741253    -3.441173   -2.311269
23      1       0       5.188985    -3.600393   -3.287152
24      6       0       4.977164    -4.360647   -1.293234
25      1       0       5.612723    -5.222562   -1.475071
26      6       0       4.379921    -4.186057   -0.048657
27      1       0       4.544453    -4.925588    0.728615
28      6       0       3.555083    -3.084859    0.214720
29      6       0       3.628118    -1.377883   -3.259914
30      1       0       3.158198    -0.480550   -2.846680
31      6       0       2.606404    -2.032688   -4.211447
32      1       0       3.004662    -2.961592   -4.634780
33      1       0       2.369903    -1.360485   -5.043295
34      1       0       1.680727    -2.264881   -3.678681
35      6       0       4.886330    -0.943277   -4.033433
36      1       0       5.644350    -0.510863   -3.372971
37      1       0       4.622359    -0.191726   -4.784783
38      1       0       5.348791    -1.782893   -4.562671
39      6       0       2.831390    -2.998522    1.555436
40      1       0       2.393473    -2.001520    1.647545
41      6       0       1.662343    -4.004144    1.593494
42      1       0       2.027966    -5.035059    1.529109
43      1       0       0.975310    -3.832840    0.760870
44      1       0       1.100293    -3.901782    2.527943
45      6       0       3.767368    -3.205394    2.759930
46      1       0       3.215640    -3.048370    3.692818
47      1       0       4.608690    -2.506958    2.740169
48      1       0       4.172103    -4.222403    2.790276
49      6       0       1.981857     2.025886    1.320784
50      6       0       2.403462     3.187958    0.623424
51      6       0       2.564159     4.381616    1.339547
52      1       0       2.888952     5.274113    0.812535
53      6       0       2.307949     4.453716    2.704261
54      1       0       2.438824     5.389984    3.239244
55      6       0       1.875472     3.314578    3.375338
56      1       0       1.667309     3.372790    4.439466
57      6       0       1.705468     2.093939    2.711041
58      6       0       2.643499     3.213761   -0.885277
59      1       0       2.568308     2.189855   -1.260584
60      6       0       1.555944     4.042467   -1.597333
61      1       0       0.554325     3.654599   -1.395524
62      1       0       1.712038     4.027815   -2.681519
63      1       0       1.584188     5.087813   -1.270331
64      6       0       4.041401     3.745784   -1.255224
65      1       0       4.152292     4.802268   -0.988773
66      1       0       4.201210     3.664819   -2.336161
67      1       0       4.833420     3.186166   -0.751451
68      6       0       1.200586     0.890138    3.502983
69      1       0       1.357546    -0.002481    2.890514
70      6       0       1.948390     0.681620    4.834640
71      1       0       3.034312     0.656602    4.700494
72      1       0       1.641430    -0.265540    5.290378
73      1       0       1.725212     1.475157    5.555478
74      6       0      -0.314025     1.002872    3.763990
75      1       0      -0.547248     1.921667    4.313212
76      1       0      -0.663340     0.153508    4.358788
77      1       0      -0.876243     1.006347    2.827027
78      6       0      -2.780178     0.039693   -0.217891
79      6       0      -4.205482     0.266197   -0.606339
80      6       0      -5.188900     0.468313    0.372285
81      1       0      -4.908545     0.478184    1.418673
82      6       0      -6.520032     0.675109    0.009918
83      1       0      -7.267940     0.833743    0.780805
84      6       0      -6.887395     0.678437   -1.336767
85      1       0      -7.923691     0.836562   -1.619490
86      6       0      -5.914768     0.479455   -2.318619
87      1       0      -6.191115     0.479404   -3.368588
88      6       0      -4.582709     0.279891   -1.956825
89      1       0      -3.837092     0.117945   -2.724469
90      6       0      -3.372603    -2.137756    0.817089
```

```
 91      6       0      -3.930946   -2.319782    2.100088
 92      6       0      -4.740259   -3.442248    2.310987
 93      1       0      -5.187941   -3.601668    3.286860
 94      6       0      -4.975952   -4.361724    1.292890
 95      1       0      -5.611271   -5.223823    1.474692
 96      6       0      -4.378794   -4.186883    0.048317
 97      1       0      -4.543145   -4.926383   -0.729022
 98      6       0      -3.554260   -3.085433   -0.214990
 99      6       0      -3.627689   -1.378733    3.259786
100      1       0      -3.157965   -0.481267    2.846626
101      6       0      -4.886023   -0.944451    4.033278
102      1       0      -5.644140   -0.512201    3.372815
103      1       0      -4.622258   -0.192852    4.784657
104      1       0      -5.348303   -1.784182    4.562495
105      6       0      -2.605876   -2.033329    4.211381
106      1       0      -3.003919   -2.962390    4.634570
107      1       0      -2.369701   -1.361127    5.043321
108      1       0      -1.680049   -2.265187    3.678741
109      6       0      -2.830715   -2.998764   -1.555762
110      1       0      -2.392844   -2.001718   -1.647676
111      6       0      -1.661649   -4.004338   -1.594190
112      1       0      -0.974496   -3.833159   -0.761639
113      1       0      -1.099753   -3.901792   -2.528709
114      1       0      -2.027222   -5.035277   -1.529928
115      6       0      -3.766842   -3.205413   -2.760182
116      1       0      -4.171463   -4.222461   -2.790728
117      1       0      -3.215268   -3.048079   -3.693109
118      1       0      -4.608245   -2.507085   -2.740108
119      6       0      -1.982441    2.025832   -1.320695
120      6       0      -2.404418    3.187807   -0.623352
121      6       0      -2.565408    4.381394   -1.339489
122      1       0      -2.890511    5.273808   -0.812531
123      6       0      -2.309103    4.453558   -2.704202
124      1       0      -2.440204    5.389799   -3.239176
125      6       0      -1.876234    3.314559   -3.375227
126      1       0      -1.667943    3.372818   -4.439335
127      6       0      -1.705952    2.093951   -2.710901
128      6       0      -2.644404    3.213532    0.885355
129      1       0      -2.569222    2.189609    1.260601
130      6       0      -1.556743    4.042160    1.597359
131      1       0      -0.555164    3.654253    1.395429
132      1       0      -1.712732    4.027476    2.681562
133      1       0      -1.584980    5.087514    1.270382
134      6       0      -4.042251    3.745560    1.255463
135      1       0      -4.153200    4.802042    0.989029
136      1       0      -4.201914    3.664604    2.336424
137      1       0      -4.834335    3.185918    0.751811
138      6       0      -1.200713    0.890295   -3.502835
139      1       0      -1.357237   -0.002354   -2.890294
140      6       0       0.313797    1.003563   -3.764144
141      1       0       0.663282    0.154305   -4.358975
142      1       0       0.876226    1.007242   -2.827286
143      1       0       0.546602    1.922425   -4.313443
144      6       0      -1.948700    0.681426   -4.834347
145      1       0      -3.034579    0.656023   -4.699986
146      1       0      -1.641479   -0.265645   -5.290096
147      1       0      -1.725945    1.475015   -5.555264
---------------------------------------------------------------------
```

Table S2. Atomic coordinates for DFT optimization of **Zn2** (theory level: B3LYP/ 6,31-g(d,p) PCM: CH_2Cl_2)

```
                      Standard orientation:
---------------------------------------------------------------------
Center     Atomic     Atomic           Coordinates (Angstroms)
Number     Number      Type          X           Y           Z
---------------------------------------------------------------------
   1         30          0         0.000075    0.485323    0.000447
   2          8          0        -1.346554    1.477515   -1.025008
   3          8          0         1.346904    1.477292    1.025649
   4          7          0        -2.606642    1.082949   -0.630683
   5          7          0        -1.614217   -0.454062    0.732886
   6          7          0         2.606980    1.082521    0.631390
   7          7          0         1.614212   -0.454010   -0.732471
   8          6          0        -2.735682    0.076544    0.254031
   9          6          0        -4.107544   -0.358714    0.653807
  10          6          0        -4.440399   -0.456057    2.014284
  11          1          0        -3.704750   -0.200108    2.767353
  12          6          0        -5.713224   -0.870700    2.404571
  13          1          0        -5.956241   -0.932822    3.460812
  14          6          0        -6.668418   -1.205167    1.442942
  15          1          0        -7.658038   -1.531822    1.747633
  16          6          0        -6.344321   -1.120168    0.087664
  17          1          0        -7.078969   -1.383186   -0.667128
  18          6          0        -5.074662   -0.698226   -0.305159
  19          1          0        -4.832966   -0.642038   -1.359978
  20          6          0        -3.638554    1.971781   -1.085097
  21          6          0        -4.013471    1.913700   -2.441767
  22          6          0        -4.990638    2.806347   -2.892110
  23          1          0        -5.302650    2.767505   -3.932031
  24          6          0        -5.560247    3.741248   -2.027502
  25          1          0        -6.318582    4.427224   -2.393466
  26          6          0        -5.142263    3.809249   -0.701038
  27          1          0        -5.565398    4.557185   -0.036268
  28          6          0        -4.163482    2.936833   -0.206717
  29          6          0        -3.364212    0.939489   -3.392223
  30          1          0        -2.322880    1.220990   -3.576211
  31          6          0        -3.688173    3.057243    1.220558
  32          1          0        -2.611280    2.884196    1.297725
  33          6          0        -1.579748   -1.636357    1.523013
  34          6          0        -1.847419   -2.901479    0.952699
  35          6          0        -1.725547   -4.040283    1.759254
  36          1          0        -1.932772   -5.014710    1.324181
  37          6          0        -1.328020   -3.945965    3.090826
  38          1          0        -1.236133   -4.841170    3.699015
  39          6          0        -1.029341   -2.695985    3.630986
  40          1          0        -0.702038   -2.615267    4.664378
  41          6          0        -1.140873   -1.531791    2.863099
  42          6          0        -2.221795   -3.047263   -0.502374
  43          1          0        -3.264173   -2.765688   -0.687311
  44          6          0        -0.795305   -0.188208    3.458789
  45          1          0        -1.660097    0.485802    3.483185
  46          6          0         2.735770    0.076302   -0.253645
  47          6          0         4.107499   -0.359196   -0.653570
  48          6          0         5.074649   -0.698769    0.305345
  49          1          0         4.833060   -0.642386    1.360172
  50          6          0         6.344185   -1.121012   -0.087536
  51          1          0         7.078856   -1.384059    0.667226
  52          6          0         6.668134   -1.206275   -1.442836
  53          1          0         7.657657   -1.533175   -1.747574
  54          6          0         5.712906   -0.871766   -2.404413
  55          1          0         5.955789   -0.934091   -3.460672
  56          6          0         4.440198   -0.456811   -2.014061
  57          1          0         3.704537   -0.200837   -2.767106
  58          6          0         3.639041    1.971416    1.085351
  59          6          0         4.013982    1.913854    2.442079
  60          6          0         4.991363    2.806428    2.891997
  61          1          0         5.303286    2.768100    3.931962
```

```
62          6          0          5.561320      3.740724      2.026907
63          1          0          6.319857      4.426635      2.392573
64          6          0          5.143328      3.808243      0.700458
65          1          0          5.566642      4.555744      0.035313
66          6          0          4.164183      2.935931      0.206564
67          6          0          3.364605      0.939963      3.392787
68          1          0          2.321464      1.217911      3.571628
69          6          0          3.688875      3.056035     -1.220742
70          1          0          2.612153      2.882061     -1.298079
71          6          0          1.579302     -1.635910     -1.523155
72          6          0          1.846580     -2.901374     -0.953478
73          6          0          1.724271     -4.039760     -1.760584
74          1          0          1.931182     -5.014468     -1.325992
75          6          0          1.326723     -3.944644     -3.092077
76          1          0          1.234497     -4.839512     -3.700715
77          6          0          1.028499     -2.694280     -3.631643
78          1          0          0.701251     -2.612975     -4.665003
79          6          0          1.140442     -1.530506     -2.863217
80          6          0          2.221069     -3.047961      0.501487
81          1          0          1.597217     -2.412729      1.138130
82          6          0          0.795246     -0.186512     -3.458181
83          1          0          1.659923      0.487678     -3.481169
84          1          0         -2.097407     -4.083152     -0.828235
85          1          0         -1.597969     -2.411592     -1.138600
86          1          0         -0.432511     -0.302026      4.483852
87          1          0         -0.023640      0.323106      2.872900
88          1          0         -3.903436      4.055302      1.610324
89          1          0         -4.186413      2.333252      1.875123
90          1          0         -3.893624      0.915611     -4.347577
91          1          0         -3.340100     -0.076336     -2.984797
92          1          0          3.903292      4.054328     -1.610384
93          1          0          4.187865      2.332568     -1.875324
94          1          0          3.890351      0.920841      4.350264
95          1          0          3.346216     -0.077208      2.988310
96          1          0          0.433482     -0.299581     -4.483695
97          1          0          0.022872      0.324215     -2.872674
98          1          0          2.096822     -4.084048      0.826768
99          1          0          3.263419     -2.766359      0.686512
-----------------------------------------------------------------------------------
```

Table S3. Atomic coordinates for DFT optimization of **Zn3** (theory level: B3LYP/ 6,31-g(d,p) PCM: CH$_2$Cl$_2$)

```
                    Standard orientation:
---------------------------------------------------------------------
Center      Atomic      Atomic          Coordinates (Angstroms)
Number      Number      Type          X           Y           Z
---------------------------------------------------------------------
   1          30          0      -0.000031      0.719186      0.000026
   2           8          0      -1.190288      1.706436     -1.205335
   3           8          0       1.190249      1.706132      1.205597
   4           7          0      -2.492627      1.318844     -0.986164
   5           7          0      -1.704367     -0.201947      0.524450
   6           7          0       2.492591      1.318726      0.986269
   7           7          0       1.704327     -0.201911     -0.524501
   8           6          0      -2.745116      0.325887     -0.113429
   9           6          0      -4.160894     -0.098744      0.098322
  10           6          0      -4.679330     -0.186575      1.399631
  11           1          0      -4.056993      0.064833      2.249643
  12           6          0      -5.995607     -0.586862      1.621436
  13           1          0      -6.388519     -0.643364      2.629640
  14           6          0      -6.797265     -0.912605      0.529987
  15           6          0      -6.307971     -0.844915     -0.772278
  16           1          0      -6.939730     -1.107004     -1.612610
  17           6          0      -4.991842     -0.436689     -0.980345
  18           1          0      -4.612794     -0.391416     -1.994020
  19           6          0      -3.448508      2.207666     -1.585928
```

CXC

20	6	0	-3.636448	2.136828	-2.980389
21	6	0	-4.536729	3.030985	-3.567089
22	1	0	-4.704932	2.983664	-4.639284
23	6	0	-5.211412	3.978478	-2.796848
24	1	0	-5.907608	4.665204	-3.269249
25	6	0	-4.977626	4.057540	-1.426617
26	1	0	-5.481434	4.814725	-0.832357
27	6	0	-4.081743	3.184043	-0.795844
28	6	0	-2.873905	1.147945	-3.826062
29	1	0	-1.812711	1.412224	-3.861371
30	6	0	-3.807143	3.313914	0.682445
31	1	0	-2.758929	3.107610	0.913881
32	6	0	-1.789600	-1.375521	1.324650
33	6	0	-1.978534	-2.645639	0.734478
34	6	0	-1.987823	-3.775002	1.562974
35	1	0	-2.136396	-4.753236	1.113001
36	6	0	-1.793531	-3.666335	2.937978
37	1	0	-1.802376	-4.554256	3.563363
38	6	0	-1.567761	-2.411900	3.502472
39	1	0	-1.398172	-2.320730	4.572198
40	6	0	-1.552661	-1.256597	2.713527
41	6	0	-2.129707	-2.806497	-0.758911
42	1	0	-3.120784	-2.497787	-1.109599
43	6	0	-1.282522	0.091553	3.337644
44	1	0	-2.120868	0.785071	3.201505
45	6	0	2.745092	0.325863	0.113431
46	6	0	4.160865	-0.098729	-0.098347
47	6	0	4.991826	-0.436673	0.980316
48	1	0	4.612790	-0.391434	1.993997
49	6	0	6.307959	-0.844872	0.772230
50	1	0	6.939723	-1.106967	1.612557
51	6	0	6.797252	-0.912543	-0.530037
52	6	0	5.995576	-0.586812	-1.621479
53	1	0	6.388480	-0.643314	-2.629688
54	6	0	4.679296	-0.186549	-1.399659
55	1	0	4.056943	0.064852	-2.249661
56	6	0	3.448452	2.207605	1.585998
57	6	0	3.636450	2.136731	2.980454
58	6	0	4.536776	3.030862	3.567123
59	1	0	4.705035	2.983522	4.639308
60	6	0	5.211449	3.978353	2.796862
61	1	0	5.907696	4.665046	3.269238
62	6	0	4.977604	4.057437	1.426647
63	1	0	5.481401	4.814617	0.832371
64	6	0	4.081680	3.183960	0.795896
65	6	0	2.873984	1.147826	3.826174
66	1	0	1.812771	1.412011	3.861523
67	6	0	3.807073	3.313821	-0.682395
68	1	0	2.758901	3.107371	-0.913874
69	6	0	1.789580	-1.375511	-1.324677
70	6	0	1.978562	-2.645625	-0.734507
71	6	0	1.987926	-3.774976	-1.563020
72	1	0	2.136513	-4.753214	-1.113059
73	6	0	1.793675	-3.666310	-2.938030
74	1	0	1.802576	-4.554232	-3.563414
75	6	0	1.567867	-2.411885	-3.502527
76	1	0	1.398326	-2.320711	-4.572259
77	6	0	1.552678	-1.256593	-2.713563
78	6	0	2.129717	-2.806516	0.758877
79	1	0	1.393804	-2.203081	1.299719
80	6	0	1.282529	0.091545	-3.337692
81	1	0	2.120971	0.785000	-3.201752
82	1	0	-1.991533	-3.851576	-1.047770
83	1	0	-1.393620	-2.203234	-1.299712
84	1	0	-1.103094	-0.008770	4.411374
85	1	0	-0.409150	0.574052	2.884522
86	1	0	-4.041063	4.324725	1.025809
87	1	0	-4.418070	2.618387	1.269132
88	1	0	-3.262868	1.127943	-4.846699
89	1	0	-2.924693	0.132937	-3.418525

```
90        1         0      4.040859    4.324673   -1.025733
91        1         0      4.418121    2.618393   -1.269075
92        1         0      3.262986    1.127904    4.846804
93        1         0      2.924889    0.132801    3.418678
94        1         0      1.102896   -0.008811   -4.411383
95        1         0      0.409302    0.574173   -2.884438
96        1         0      1.991321   -3.851564    1.047725
97        1         0      3.120886   -2.498022    1.109505
98       35         0      8.604425   -1.467365   -0.825833
99       35         0     -8.604431   -1.467472    0.825762
----------------------------------------------------------------
```

Table S4. Atomic coordinates for DFT optimization of **Zn4** (theory level: B3LYP/ 6,31-g(d,p) PCM: CH_2Cl_2)

```
                       Standard orientation:
---------------------------------------------------------------------
Center     Atomic     Atomic           Coordinates (Angstroms)
Number     Number      Type        X            Y            Z
---------------------------------------------------------------------
   1         30         0       0.000027     0.494556     0.000003
   2          8         0      -1.351848     1.491367    -1.016267
   3          8         0       1.351983     1.491100     1.016597
   4          7         0      -2.608744     1.088922    -0.630682
   5          7         0      -1.613018    -0.452669     0.729874
   6          7         0       2.608819     1.088645     0.630903
   7          7         0       1.612998    -0.452457    -0.730128
   8          6         0      -2.731340     0.081343     0.251607
   9          6         0      -4.102863    -0.355775     0.653885
  10          6         0      -4.446540    -0.460387     2.007881
  11          1         0      -3.735609    -0.211937     2.785648
  12          6         0      -5.729478    -0.885534     2.349615
  13          1         0      -6.010132    -0.964222     3.397656
  14          6         0      -6.332924    -1.120267     0.161000
  15          1         0      -7.100005    -1.393434    -0.560349
  16          6         0      -5.081161    -0.700980    -0.287056
  17          1         0      -4.879222    -0.654883    -1.349880
  18          6         0      -3.649544     1.969627    -1.083349
  19          6         0      -4.034572     1.899085    -2.436365
  20          6         0      -5.023795     2.780385    -2.882486
  21          1         0      -5.345199     2.733074    -3.919070
  22          6         0      -5.593511     3.715099    -2.017605
  23          1         0      -6.361245     4.391978    -2.380656
  24          6         0      -5.164790     3.795184    -0.695291
  25          1         0      -5.588992     4.543078    -0.031345
  26          6         0      -4.174270     2.934152    -0.204540
  27          6         0      -3.384855     0.924466    -3.386303
  28          1         0      -2.347333     1.213107    -3.580773
  29          6         0      -3.687370     3.065911     1.218046
  30          1         0      -2.610040     2.893359     1.288758
  31          6         0      -1.583284    -1.634192     1.523499
  32          6         0      -1.849204    -2.898969     0.952421
  33          6         0      -1.735022    -4.036539     1.761888
  34          1         0      -1.940880    -5.011374     1.327400
  35          6         0      -1.347053    -3.939863     3.095999
  36          1         0      -1.261159    -4.834006     3.706469
  37          6         0      -1.050308    -2.689610     3.636615
  38          1         0      -0.730613    -2.607982     4.672192
  39          6         0      -1.154243    -1.526444     2.866206
  40          6         0      -2.213832    -3.045991    -0.505210
  41          1         0      -3.256494    -2.770076    -0.698102
  42          6         0      -0.811462    -0.182206     3.462021
  43          1         0      -1.675392     0.493105     3.480485
  44          6         0       2.731378     0.081355    -0.251725
  45          6         0       4.102874    -0.355681    -0.654185
```

```
46          6          0         5.081243    -0.701185     0.286577
47          1          0         4.879392    -0.655422     1.349434
48          6          0         6.332980    -1.120318    -0.161695
49          1          0         7.100101    -1.393730     0.559518
50          6          0         5.729412    -0.884828    -2.350190
51          1          0         6.010023    -0.963105    -3.398274
52          6          0         4.446493    -0.459804    -2.008235
53          1          0         3.735536    -0.211033    -2.785872
54          6          0         3.649685     1.969190     1.083759
55          6          0         4.034802     1.898169     2.436723
56          6          0         5.024171     2.779209     2.883041
57          1          0         5.345661     2.731527     3.919582
58          6          0         5.593913     3.714144     2.018414
59          1          0         6.361772     4.390799     2.381620
60          6          0         5.165076     3.794721     0.696168
61          1          0         5.589286     4.542798     0.032433
62          6          0         4.174416     2.933957     0.205224
63          6          0         3.385045     0.923358     3.386443
64          1          0         2.347947     1.212745     3.582107
65          6          0         3.687440     3.066220    -1.217291
66          1          0         2.610210     2.893148    -1.288123
67          6          0         1.583161    -1.633976    -1.523770
68          6          0         1.848956    -2.898783    -0.952668
69          6          0         1.734604    -4.036351    -1.762097
70          1          0         1.940364    -5.011201    -1.327599
71          6          0         1.346580    -3.939658    -3.096202
72          1          0         1.260572    -4.833801    -3.706654
73          6          0         1.049952    -2.689390    -3.636822
74          1          0         0.730215    -2.607734    -4.672384
75          6          0         1.154057    -1.526213    -2.866436
76          6          0         2.213534    -3.045789     0.504976
77          1          0         1.587519    -2.409079     1.137901
78          6          0         0.811383    -0.181945    -3.462248
79          1          0         1.675430     0.493204    -3.481014
80          1          0        -2.084290    -4.081513    -0.829740
81          1          0        -1.588233    -2.408875    -1.138126
82          1          0        -0.455264    -0.294760     4.489369
83          1          0        -0.035482     0.327822     2.880865
84          1          0        -3.898971     4.067373     1.600679
85          1          0        -4.182205     2.349972     1.884266
86          1          0        -3.921315     0.891557    -4.337286
87          1          0        -3.350130    -0.089334    -2.974479
88          1          0         3.898519     4.068000    -1.599390
89          1          0         4.182691     2.350900    -1.883873
90          1          0         3.922291     0.889249     4.336944
91          1          0         3.349070    -0.090081     2.973864
92          1          0         0.454861    -0.294489    -4.489484
93          1          0         0.035687     0.328250    -2.880871
94          1          0         2.084503    -4.081418     0.829370
95          1          0         3.256021    -2.769352     0.698040
96          7          0         6.670726    -1.215171    -1.455239
97          7          0        -6.670744    -1.215552     1.454494
------------------------------------------------------------------
```

Table S5. Atomic coordinates for DFT optimization of **Zn5** (theory level: B3LYP/ 6,31-g(d,p) PCM: CH$_2$Cl$_2$)

```
                        Standard orientation:
------------------------------------------------------------------
Center     Atomic     Atomic            Coordinates (Angstroms)
Number     Number     Type          X            Y            Z
------------------------------------------------------------------
    1         30          0         0.000428     0.709217     0.000055
    2          8          0        -1.198876     1.686737    -1.204959
    3          8          0         1.193461     1.708554     1.193079
    4          7          0        -2.497843     1.291820    -0.984158
    5          7          0        -1.699816    -0.211488     0.539147
    6          7          0         2.495398     1.323319     0.972293
```

7	7	0	1.705136	-0.215507	-0.519906
8	6	0	-2.743174	0.305831	-0.102231
9	6	0	-4.157617	-0.123838	0.116384
10	6	0	-4.673446	-0.191513	1.419878
11	1	0	-4.050091	0.078131	2.263161
12	6	0	-5.985766	-0.598754	1.643399
13	1	0	-6.373515	-0.644977	2.654710
14	6	0	-6.797309	-0.955722	0.564327
15	6	0	-6.293942	-0.902888	-0.737540
16	1	0	-6.918486	-1.191513	-1.575389
17	6	0	-4.983284	-0.489078	-0.957707
18	1	0	-4.600434	-0.461073	-1.970317
19	6	0	-3.460876	2.164665	-1.596138
20	6	0	-3.648276	2.072656	-2.989412
21	6	0	-4.557167	2.950226	-3.587721
22	1	0	-4.725644	2.886501	-4.659006
23	6	0	-5.240239	3.901924	-2.830136
24	1	0	-5.943051	4.575477	-3.311584
25	6	0	-5.006772	4.002218	-1.461257
26	1	0	-5.517467	4.762786	-0.877310
27	6	0	-4.102679	3.145782	-0.818950
28	6	0	-2.876948	1.079780	-3.822405
29	1	0	-1.820435	1.360156	-3.872501
30	6	0	-3.829024	3.297848	0.657424
31	1	0	-2.779838	3.100373	0.892076
32	6	0	-1.779024	-1.376806	1.352515
33	6	0	-1.961949	-2.653920	0.775786
34	6	0	-1.966333	-3.774416	1.616307
35	1	0	-2.110263	-4.758064	1.176803
36	6	0	-1.772718	-3.650041	2.990019
37	1	0	-1.777724	-4.531159	3.624965
38	6	0	-1.552186	-2.388688	3.540999
39	1	0	-1.382700	-2.285395	4.609614
40	6	0	-1.541967	-1.241771	2.739816
41	6	0	-2.111256	-2.831687	-0.715911
42	1	0	-3.105284	-2.537012	-1.070393
43	6	0	-1.275897	0.113703	3.349738
44	1	0	-2.116483	0.803268	3.207578
45	6	0	2.746186	0.324108	0.106814
46	6	0	4.163832	-0.095139	-0.111580
47	6	0	4.999719	-0.429026	0.964634
48	1	0	4.623241	-0.381992	1.978886
49	6	0	6.314767	-0.829581	0.745295
50	1	0	6.951492	-1.081437	1.585792
51	6	0	6.812596	-0.898278	-0.557811
52	6	0	5.991015	-0.571727	-1.639072
53	1	0	6.378709	-0.617740	-2.650463
54	6	0	4.674737	-0.177551	-1.416275
55	1	0	4.045818	0.075407	-2.260615
56	6	0	3.452121	2.221143	1.557857
57	6	0	3.652658	2.159923	2.950952
58	6	0	4.554299	3.061793	3.523520
59	1	0	4.732571	3.022263	4.594371
60	6	0	5.217293	4.007480	2.740944
61	1	0	5.914649	4.700338	3.202528
62	6	0	4.970082	4.077328	1.372604
63	1	0	5.464343	4.833473	0.769127
64	6	0	4.072499	3.195715	0.755625
65	6	0	2.901090	1.174042	3.809874
66	1	0	1.838759	1.433058	3.850036
67	6	0	3.781723	3.316591	-0.720417
68	1	0	2.733012	3.100448	-0.940154
69	6	0	1.794074	-1.395388	-1.310952
70	6	0	1.993859	-2.658997	-0.710611
71	6	0	2.007863	-3.795191	-1.529676
72	1	0	2.164864	-4.768565	-1.072143
73	6	0	1.807720	-3.699264	-2.904754
74	1	0	1.820487	-4.592273	-3.522758
75	6	0	1.570818	-2.451285	-3.478895
76	1	0	1.396298	-2.370401	-4.548633

```
 77         6          0        1.550587    -1.289508    -2.699672
 78         6          0        2.151666    -2.806647     0.783575
 79         1          0        1.415708    -2.201642     1.322536
 80         6          0        1.267857     0.051234    -3.333915
 81         1          0        2.102386     0.751448    -3.209350
 82         1          0       -1.962881    -3.878335    -0.993729
 83         1          0       -1.380898    -2.227139    -1.262952
 84         1          0       -1.095180     0.024844     4.424234
 85         1          0       -0.404209     0.594165     2.891231
 86         1          0       -4.068280     4.312143     0.986438
 87         1          0       -4.436764     2.607750     1.253801
 88         1          0       -3.273716     1.034398    -4.839209
 89         1          0       -2.908197     0.072140    -3.395398
 90         1          0        4.003218     4.327997    -1.070173
 91         1          0        4.392952     2.624523    -1.310849
 92         1          0        3.296740     1.164931     4.828062
 93         1          0        2.954635     0.155785     3.410939
 94         1          0        1.082590    -0.059746    -4.405574
 95         1          0        0.394201     0.532312    -2.879918
 96         1          0        2.018518    -3.849785     1.081526
 97         1          0        3.143110    -2.491908     1.127845
 98         6          0       -8.230992    -1.344913     0.798221
 99         6          0        8.215907    -1.380798    -0.801817
100         9          0       -8.412468    -1.909184     2.013117
101         9          0       -9.057553    -0.271562     0.739944
102         9          0       -8.674471    -2.225745    -0.126806
103         9          0        9.041679    -1.080648     0.225729
104         9          0        8.749915    -0.840579    -1.920314
105         9          0        8.263659    -2.726646    -0.959005
------------------------------------------------------------------
```

Table S6. Atomic coordinates for DFT optimization of **Zn6** (theory level: B3LYP/ 6,31-g(d,p) PCM: CH$_2$Cl$_2$)

```
                    Standard orientation:
---------------------------------------------------------------------
Center     Atomic     Atomic          Coordinates (Angstroms)
Number     Number      Type        X            Y            Z
---------------------------------------------------------------------
    1        30          0        0.000031     0.603562     0.000345
    2         8          0       -1.277811     1.589289    -1.109940
    3         8          0        1.278136     1.589227     1.110263
    4         7          0       -2.561986     1.202606    -0.789508
    5         7          0       -1.660300    -0.316880     0.654121
    6         7          0        2.562211     1.202665     0.789398
    7         7          0        1.660175    -0.317142    -0.653669
    8         6          0       -2.749946     0.205164     0.096561
    9         6          0       -4.141856    -0.227521     0.404214
   10         6          0       -4.570169    -0.348652     1.739661
   11         1          0       -3.888267    -0.114041     2.548240
   12         6          0       -5.860710    -0.755796     2.042871
   13         1          0       -6.191977    -0.839850     3.072475
   14         6          0       -6.764795    -1.068191     1.014770
   15         6          0       -6.352566    -0.964456    -0.320003
   16         1          0       -7.024231    -1.205856    -1.134271
   17         6          0       -5.054230    -0.545344    -0.610067
   18         1          0       -4.752439    -0.478159    -1.648650
   19         6          0       -3.555922     2.100550    -1.306006
   20         6          0       -3.842213     2.050978    -2.684482
   21         6          0       -4.776705     2.956799    -3.195194
   22         1          0       -5.018811     2.925305    -4.253861
   23         6          0       -5.391637     3.895776    -2.366830
   24         1          0       -6.115674     4.592139    -2.779704
   25         6          0       -5.061822     3.954072    -1.015216
   26         1          0       -5.519181     4.704762    -0.376701
   27         6          0       -4.127606     3.068968    -0.460896
   28         6          0       -3.143866     1.070940    -3.593247
   29         1          0       -2.083324     1.323804    -3.684353
```

```
30      6       0       -3.746063    3.179064    0.994993
31      1       0       -2.677327    3.000073    1.140897
32      6       0       -1.674685   -1.495846    1.448707
33      6       0       -1.902698   -2.764394    0.868477
34      6       0       -1.830334   -3.899189    1.686541
35      1       0       -2.007344   -4.876040    1.243561
36      6       0       -1.519834   -3.798034    3.040658
37      1       0       -1.465917   -4.690297    3.657683
38      6       0       -1.259233   -2.544887    3.593051
39      1       0       -0.999707   -2.458722    4.645102
40      6       0       -1.323292   -1.384621    2.813993
41      6       0       -2.182475   -2.917085   -0.607067
42      1       0       -3.205615   -2.620952   -0.862969
43      6       0       -1.018735   -0.037081    3.422938
44      1       0       -1.881051    0.638868    3.377532
45      6       0        2.749983    0.205059   -0.096498
46      6       0        4.141817   -0.227595   -0.404538
47      6       0        5.054519   -0.545375    0.609466
48      1       0        4.753082   -0.478155    1.648148
49      6       0        6.352769   -0.964486    0.319012
50      1       0        7.024679   -1.205851    1.133089
51      6       0        6.764589   -1.068266   -1.015882
52      6       0        5.860189   -0.755884   -2.043710
53      1       0        6.191149   -0.839936   -3.073413
54      6       0        4.569738   -0.348750   -1.740113
55      1       0        3.887602   -0.114140   -2.548489
56      6       0        3.556261    2.100504    1.305888
57      6       0        3.842669    2.050785    2.684332
58      6       0        4.777208    2.956556    3.195048
59      1       0        5.019404    2.924969    4.253690
60      6       0        5.392071    3.895607    2.366714
61      1       0        6.116135    4.591934    2.779598
62      6       0        5.062148    3.954031    1.015133
63      1       0        5.519461    4.704777    0.376653
64      6       0        4.127870    3.068995    0.460810
65      6       0        3.144416    1.070626    3.593030
66      1       0        2.083823    1.323323    3.684020
67      6       0        3.746158    3.179247   -0.995023
68      1       0        2.677311    3.000745   -1.140746
69      6       0        1.674460   -1.496244   -1.448037
70      6       0        1.902714   -2.764672   -0.867639
71      6       0        1.830193   -3.899628   -1.685471
72      1       0        2.007401   -4.876384   -1.242360
73      6       0        1.519285   -3.798748   -3.039511
74      1       0        1.465245   -4.691132   -3.656352
75      6       0        1.258442   -2.545718   -3.592065
76      1       0        0.998625   -2.459767   -4.644062
77      6       0        1.322676   -1.385300   -2.813251
78      6       0        2.182920   -2.917083    0.607854
79      1       0        1.509269   -2.295861    1.206786
80      6       0        1.017981   -0.037882   -3.422392
81      1       0        1.880315    0.638068   -3.377293
82      1       0       -2.052540   -3.957392   -0.916538
83      1       0       -1.508494   -2.296155   -1.205931
84      1       0       -0.732481   -0.143044    4.472835
85      1       0       -0.204610    0.467206    2.890522
86      1       0       -3.981914    4.175748    1.376427
87      1       0       -4.288656    2.452970    1.610770
88      1       0       -3.592627    1.075124   -4.589353
89      1       0       -3.183035    0.049270   -3.201266
90      1       0        3.982407    4.175815   -1.376509
91      1       0        4.288304    2.452887   -1.610876
92      1       0        3.593117    1.074824    4.589157
93      1       0        3.183730    0.048965    3.201014
94      1       0        0.731524   -0.144054   -4.472214
95      1       0        0.203983    0.466540   -2.889911
96      1       0        2.052859   -3.957291    0.917601
97      1       0        3.206205   -2.621107    0.863367
98      8       0       -8.003827   -1.460159    1.414346
99      8       0        8.003493   -1.460250   -1.415835
```

```
100         6          0        8.967353    -1.790151    -0.416732
101         1          0        8.635299    -2.636205     0.195510
102         1          0        9.872730    -2.068370    -0.956295
103         1          0        9.180185    -0.933060     0.232129
104         6          0       -8.967383    -1.790067     0.414952
105         1          0       -8.635167    -2.636166    -0.197141
106         1          0       -9.872945    -2.068221     0.954239
107         1          0       -9.179969    -0.933001    -0.234023
-------------------------------------------------------------------
```

Table S7. Atomic coordinates for DFT optimization of **Zn8** (theory level: B3LYP/ 6,31-g(d,p) PCM: CH₂Cl₂)

```
                     Standard orientation:
---------------------------------------------------------------------
Center     Atomic     Atomic            Coordinates (Angstroms)
Number     Number     Type         X           Y           Z
---------------------------------------------------------------------
   1         30         0        0.000091    -0.032137     0.000400
   2          8         0        1.224376    -1.248446    -0.954449
   3          8         0       -1.224495    -1.248725     0.954205
   4          7         0        2.520516    -1.013768    -0.578311
   5          7         0        1.756123     0.792356     0.618098
   6          7         0       -2.520608    -1.013770     0.578053
   7          7         0       -1.755891     0.792581    -0.617820
   8          6         0        2.779468     0.034824     0.221295
   9          6         0        4.203621     0.269557     0.612765
  10          6         0        4.592360     0.289139     1.957011
  11          1         0        3.873384     0.127116     2.748666
  12          6         0        5.934014     0.502076     2.270861
  13          1         0        6.249633     0.511386     3.311932
  14          6         0        6.512675     0.690886     0.071744
  15          1         0        7.294740     0.857870    -0.665901
  16          6         0        5.199305     0.481211    -0.347137
  17          1         0        4.960261     0.496205    -1.402747
  18          6         0        3.400570    -2.134844    -0.811018
  19          6         0        3.971808    -2.294402    -2.091159
  20          6         0        4.804401    -3.399763    -2.302647
  21          1         0        5.264064    -3.543637    -3.275224
  22          6         0        5.047641    -4.322597    -1.289355
  23          1         0        5.701185    -5.170653    -1.472129
  24          6         0        4.435184    -4.170868    -0.049094
  25          1         0        4.606189    -4.914174     0.723066
  26          6         0        3.587645    -3.087469     0.215118
  27          6         0        3.657326    -1.352386    -3.247375
  28          1         0        3.176106    -0.461556    -2.832242
  29          6         0        2.644460    -2.017517    -4.201720
  30          1         0        3.056011    -2.939228    -4.627785
  31          1         0        2.399932    -1.345418    -5.031201
  32          1         0        1.721257    -2.265162    -3.671669
  33          6         0        4.909187    -0.899938    -4.021090
  34          1         0        5.666181    -0.464616    -3.361334
  35          1         0        4.635181    -0.146169    -4.766408
  36          1         0        5.377953    -1.731290    -4.557509
  37          6         0        2.845137    -3.024861     1.546646
  38          1         0        2.388672    -2.036202     1.642049
  39          6         0        1.691627    -4.049110     1.557969
  40          1         0        2.074327    -5.072965     1.483083
  41          1         0        1.010876    -3.875884     0.720453
  42          1         0        1.118713    -3.968429     2.487880
  43          6         0        3.768092    -3.228625     2.761596
  44          1         0        3.202531    -3.086135     3.688376
  45          1         0        4.601254    -2.519908     2.758666
  46          1         0        4.186139    -4.240184     2.789219
  47          6         0        1.983361     2.021805     1.322148
  48          6         0        2.401902     3.184266     0.624350
  49          6         0        2.564524     4.376538     1.342534
  50          1         0        2.886820     5.270410     0.816565
```

```
 51        6        0        2.313805     4.444948     2.708360
 52        1        0        2.446389     5.380077     3.244736
 53        6        0        1.885437     3.304248     3.379623
 54        1        0        1.682755     3.360350     4.444785
 55        6        0        1.713203     2.084926     2.713653
 56        6        0        2.637115     3.212145    -0.885238
 57        1        0        2.565371     2.188273    -1.261904
 58        6        0        1.543654     4.036210    -1.593658
 59        1        0        0.544427     3.643384    -1.389867
 60        1        0        1.697447     4.023572    -2.678118
 61        1        0        1.567906     5.081118    -1.265219
 62        6        0        4.031036     3.751934    -1.259363
 63        1        0        4.134989     4.810310    -0.998270
 64        1        0        4.190450     3.666457    -2.339851
 65        1        0        4.828468     3.202026    -0.753202
 66        6        0        1.212899     0.877621     3.503290
 67        1        0        1.379323    -0.014183     2.891938
 68        6        0        1.954429     0.673808     4.839140
 69        1        0        3.041535     0.657974     4.712700
 70        1        0        1.652465    -0.276373     5.291642
 71        1        0        1.720287     1.464464     5.559509
 72        6        0       -0.303934     0.979426     3.756400
 73        1        0       -0.545512     1.893659     4.309512
 74        1        0       -0.651035     0.124511     4.344335
 75        1        0       -0.861768     0.986184     2.816819
 76        6        0       -2.779312     0.035027    -0.221381
 77        6        0       -4.203462     0.270004    -0.612812
 78        6        0       -5.198980     0.481972     0.347196
 79        1        0       -4.959799     0.496948     1.402780
 80        6        0       -6.512351     0.691872    -0.071549
 81        1        0       -7.294306     0.859085     0.666159
 82        6        0       -5.933999     0.502670    -2.270717
 83        1        0       -6.249733     0.511945    -3.311753
 84        6        0       -4.592343     0.289469    -1.957003
 85        1        0       -3.873497     0.127199    -2.748731
 86        6        0       -3.400966    -2.134517     0.810964
 87        6        0       -3.971914    -2.293925     2.091302
 88        6        0       -4.804826    -3.398983     2.302994
 89        1        0       -5.264266    -3.542755     3.275691
 90        6        0       -5.048615    -4.321758     1.289757
 91        1        0       -5.702342    -5.169632     1.472726
 92        6        0       -4.436423    -4.170240     0.049364
 93        1        0       -4.607807    -4.913535    -0.722723
 94        6        0       -3.588631    -3.087080    -0.215091
 95        6        0       -3.656511    -1.352274     3.247558
 96        1        0       -3.174691    -0.461759     2.832439
 97        6        0       -4.907879    -0.898996     4.021591
 98        1        0       -5.664715    -0.463095     3.362038
 99        1        0       -4.633180    -0.145487     4.766923
100        1        0       -5.377112    -1.730061     4.558047
101        6        0       -2.643962    -2.018317     4.201633
102        1        0       -3.056404    -2.939445     4.628109
103        1        0       -2.398333    -1.346277     5.030836
104        1        0       -1.721274    -2.267178     3.671287
105        6        0       -2.846455    -3.024686    -1.546789
106        1        0       -2.389804    -2.036121    -1.642314
107        6        0       -1.693169    -4.049183    -1.558378
108        1        0       -1.012150    -3.876020    -0.721064
109        1        0       -1.120504    -3.968681    -2.488452
110        1        0       -2.076079    -5.072951    -1.483319
111        6        0       -3.769782    -3.228231    -2.761495
112        1        0       -4.188138    -4.239664    -2.789002
113        1        0       -3.204408    -3.085924    -3.688418
114        1        0       -4.602741    -2.519276    -2.758373
115        6        0       -1.983044     2.021884    -1.322209
116        6        0       -2.401190     3.184622    -0.624605
117        6        0       -2.563738     4.376756    -1.343014
118        1        0       -2.885764     5.270809    -0.817181
119        6        0       -2.313314     4.444808    -2.708910
120        1        0       -2.445823     5.379847    -3.245465
```

```
121        6        0       -1.885363    3.303862   -3.380003
122        1        0       -1.682889    3.359677   -4.445223
123        6        0       -1.713232    2.084644   -2.713801
124        6        0       -2.636115    3.212932    0.885008
125        1        0       -2.564261    2.189167    1.261933
126        6        0       -1.542533    4.037281    1.592935
127        1        0       -0.543310    3.644568    1.388916
128        1        0       -1.695990    4.024858    2.677446
129        1        0       -1.567043    5.082117    1.264275
130        6        0       -4.029935    3.752849    1.259263
131        1        0       -4.133960    4.811124    0.997785
132        1        0       -4.189089    3.667796    2.339823
133        1        0       -4.827503    3.202760    0.753506
134        6        0       -1.213300    0.877142   -3.503338
135        1        0       -1.379983   -0.014605   -2.891986
136        6        0        0.303562    0.978457   -3.756403
137        1        0        0.650418    0.123360   -4.344171
138        1        0        0.861331    0.985165   -2.816771
139        1        0        0.545420    1.892554   -4.309640
140        6        0       -1.954809    0.673565   -4.839232
141        1        0       -3.041936    0.658414   -4.712939
142        1        0       -1.653344   -0.276835   -5.291602
143        1        0       -1.720092    1.464000   -5.559668
144        7        0       -6.893345    0.702999   -1.356211
145        7        0        6.893525    0.702078    1.356444
```

Table S8. Atomic coordinates for DFT optimization of **Zn9** (theory level: B3LYP/ 6,31-g(d,p) PCM: CH$_2$Cl$_2$)

```
                   Standard orientation:
-----------------------------------------------------------------
Center     Atomic     Atomic            Coordinates (Angstroms)
Number     Number      Type         X            Y            Z
-----------------------------------------------------------------
   1         30         0       -0.002720    0.340878    0.160072
   2          8         0       -1.216098    1.312608   -1.066169
   3          8         0        1.319730    1.143058    1.357952
   4          7         0       -2.509950    1.111184   -0.678354
   5          7         0       -1.737829   -0.524524    0.698406
   6          7         0        2.571316    0.865086    0.892620
   7          7         0        1.630132   -0.391628   -0.753571
   8          6         0       -2.785414    0.107281    0.180378
   9          6         0       -4.203232   -0.237207    0.488224
  10          6         0       -4.661060   -0.261090    1.809400
  11          1         0       -4.010030    0.016414    2.630845
  12          6         0       -5.980752   -0.635492    2.051280
  13          1         0       -6.360406   -0.649995    3.070615
  14          6         0       -6.391556   -0.975410   -0.171348
  15          1         0       -7.098953   -1.271319   -0.943154
  16          6         0       -5.093629   -0.609819   -0.524309
  17          1         0       -4.785468   -0.619814   -1.564313
  18          6         0       -3.405344    2.127004   -1.121716
  19          6         0       -3.189679    2.690548   -2.386037
  20          6         0       -4.056924    3.694479   -2.799772
  21          1         0       -3.929759    4.154695   -3.774557
  22          6         0       -5.091030    4.097484   -1.950419
  23          1         0       -5.785950    4.879190   -2.236419
  24          6         0       -5.202810    3.473348   -0.710171
  25          1         0       -5.984042    3.765039   -0.012092
  26          6         0       -1.787396   -1.734921    1.411496
  27          6         0       -2.619285   -2.815827    1.064267
  28          6         0       -2.535298   -3.987592    1.807621
  29          1         0       -3.167119   -4.833892    1.555315
  30          6         0       -1.625442   -4.067240    2.863374
  31          1         0       -1.527740   -4.964197    3.464737
  32          6         0       -0.823165   -2.955500    3.110419
  33          1         0       -0.084113   -2.976260    3.908615
```

```
34        6         0        2.738616    0.052160   -0.160218
35        6         0        4.130526   -0.228594   -0.616478
36        6         0        5.087139   -0.776919    0.243607
37        1         0        4.835449   -1.034786    1.266135
38        6         0        6.375043   -0.996487   -0.242121
39        1         0        7.132054   -1.427525    0.409637
40        6         0        5.835438   -0.180958   -2.307647
41        1         0        6.160090    0.052486   -3.319496
42        6         0        4.520241    0.073656   -1.926156
43        1         0        3.817404    0.500655   -2.633280
44        6         0        3.587329    1.669222    1.510978
45        6         0        4.704038    2.194603    3.426975
46        1         0        4.865019    1.982849    4.481421
47        6         0        5.422877    3.209684    2.792457
48        1         0        6.148447    3.794654    3.346859
49        6         0        5.179127    3.448638    1.441330
50        1         0        5.707414    4.233866    0.910270
51        6         0        4.231562    2.668630    0.780201
52        6         0        1.615570   -1.440325   -1.683967
53        6         0        2.432079   -3.440638   -2.465358
54        1         0        3.171363   -4.231161   -2.348174
55        6         0        1.481444   -3.514555   -3.479654
56        1         0        1.469349   -4.355183   -4.164668
57        6         0        0.546860   -2.478114   -3.573682
58        1         0       -0.217104   -2.489446   -4.345488
59        6         0        0.608464   -1.426467   -2.669893
60        7         0        6.761781   -0.707638   -1.492849
61        7         0       -6.845723   -0.991742    1.089745
62        7         0       -4.369118    2.512351   -0.286575
63        7         0       -0.890414   -1.817529    2.408475
64        7         0        3.799276    1.428594    2.804952
65        7         0        2.504554   -2.439485   -1.576071
66        1         0       -3.299181   -2.742269    0.225114
67        1         0       -2.371534    2.341581   -3.001475
68        1         0       -0.092195   -0.598383   -2.703295
69        1         0        3.995366    2.826946   -0.265378
-------------------------------------------------------------------
```

Table S9. Atomic coordinates for DFT optimization of **Zn10** (theory level: B3LYP/ 6,31-g(d,p) PCM: CH₂Cl₂)

```
                     Standard orientation:
-------------------------------------------------------------------
Center    Atomic    Atomic           Coordinates (Angstroms)
Number    Number    Type        X           Y           Z
-------------------------------------------------------------------
   1        30        0        0.000022    0.834162   -0.000263
   2         8        0       -1.499812    1.860752   -0.716923
   3         8        0        1.499972    1.861330    0.715669
   4         7        0       -2.675454    1.295858   -0.301972
   5         7        0       -1.483189   -0.343626    0.722974
   6         7        0        2.675535    1.296116    0.300989
   7         7        0        1.483122   -0.343625   -0.723262
   8         6        0       -2.671734    0.167309    0.423118
   9         6        0       -3.979811   -0.396885    0.855914
  10         6        0       -4.262755   -0.558859    2.216233
  11         1        0       -3.545958   -0.268479    2.976134
  12         6        0       -5.500745   -1.090159    2.577173
  13         1        0       -5.748658   -1.218345    3.628261
  14         6        0       -6.151090   -1.308296    0.393921
  15         1        0       -6.918595   -1.619503   -0.310926
  16         6        0       -4.948437   -0.784001   -0.076540
  17         1        0       -4.768014   -0.687860   -1.141345
  18         6        0       -3.797513    2.144454   -0.475912
  19         6        0       -4.353289    2.318292   -1.745878
  20         6        0       -5.390495    3.220617   -1.953403
  21         6        0       -5.870675    3.975920   -0.884567
  22         6        0       -5.326792    3.818459    0.388316
```

23	6	0	-1.339320	-1.627455	1.260706
24	6	0	-1.835802	-2.781567	0.636089
25	6	0	-1.598568	-4.054655	1.142702
26	6	0	-0.816022	-4.211893	2.283482
27	6	0	-0.280655	-3.088598	2.908157
28	6	0	2.671749	0.167285	-0.423544
29	6	0	3.979808	-0.397230	-0.856016
30	6	0	4.948152	-0.784477	0.076668
31	1	0	4.767496	-0.688296	1.141427
32	6	0	6.150836	-1.308962	-0.393497
33	1	0	6.918101	-1.620330	0.311539
34	6	0	5.501006	-1.090856	-2.576901
35	1	0	5.749143	-1.219088	-3.627931
36	6	0	4.263028	-0.559309	-2.216262
37	1	0	3.546473	-0.268830	-2.976350
38	6	0	3.797759	2.144396	0.475415
39	6	0	5.389953	3.220732	1.953599
40	6	0	5.870736	3.975880	0.884912
41	6	0	5.327576	3.818221	-0.388243
42	6	0	4.284427	2.918197	-0.580976
43	6	0	1.339185	-1.627550	-1.260797
44	6	0	1.598039	-4.054786	-1.142022
45	6	0	0.815873	-4.212205	-2.283033
46	6	0	0.280922	-3.088993	-2.908209
47	6	0	0.541651	-1.821790	-2.397562
48	7	0	6.437395	-1.464251	-1.693877
49	7	0	-6.437390	-1.463454	1.694372
50	6	0	-0.541405	-1.821514	2.397238
51	6	0	-4.283580	2.918429	0.580625
52	6	0	1.835256	-2.781583	-0.635693
53	6	0	4.352830	2.318416	1.745665
54	9	0	2.094229	-5.130897	-0.518325
55	9	0	0.577069	-5.433928	-2.772431
56	9	0	-0.474843	-3.231055	-4.003884
57	9	0	5.796544	4.542374	-1.409045
58	9	0	6.866807	4.841016	1.079676
59	9	0	5.929371	3.365525	3.167850
60	9	0	0.475477	-3.230448	4.003601
61	9	0	-0.577260	-5.433533	2.773108
62	9	0	-2.095155	-5.130878	0.519507
63	9	0	-5.795211	4.542786	1.409248
64	9	0	-6.866825	4.841063	-1.078885
65	9	0	-5.930581	3.365193	-3.167383
66	9	0	0.006903	-0.757954	-3.018596
67	9	0	2.537140	-2.666523	0.504928
68	9	0	-2.538085	-2.666717	-0.504303
69	9	0	-0.006281	-0.757553	3.017784
70	9	0	3.759220	2.777681	-1.802722
71	9	0	3.917384	1.576422	2.767761
72	9	0	-3.918467	1.576089	-2.768084
73	9	0	-3.757732	2.778025	1.802116

Table S10. Atomic coordinates for DFT optimization of **D1** (theory level: B3LYP/ 6,31-g(d,p) PCM: CH_2Cl_2)

			Standard orientation:		
Center Number	Atomic Number	Atomic Type	Coordinates (Angstroms)		
			X	Y	Z
1	30	0	-0.272487	-0.535271	1.492879
2	35	0	-0.052546	-0.741490	10.511706
3	35	0	8.808713	-0.586599	0.870406
4	8	0	1.320177	-1.337872	2.345345
5	8	0	0.641266	-1.175424	-0.401177
6	7	0	1.334880	-1.213839	3.709238
7	7	0	-0.726814	-0.255202	3.553075

CCI

```
 8      7      0       2.011861   -1.364075   -0.400412
 9      7      0       2.160525    0.886850   -0.736017
10      6      0       0.248870   -0.711298    4.325688
11      6      0       0.200278   -0.720967    5.818867
12      6      0       0.009117    0.474952    6.525017
13      1      0      -0.080810    1.412165    5.986722
14      6      0      -0.060563    0.476261    7.916641
15      1      0      -0.198311    1.404272    8.459264
16      6      0       0.048164   -0.733653    8.599953
17      6      0       0.226569   -1.937636    7.921980
18      1      0       0.303432   -2.870639    8.468105
19      6      0       0.304281   -1.923802    6.530328
20      1      0       0.445973   -2.857922    5.996877
21      6      0       2.574104   -1.580559    4.311391
22      6      0       3.245074   -0.721619    5.189382
23      1      0       2.816061    0.241786    5.438944
24      6      0       4.468810   -1.110754    5.736108
25      1      0       4.983085   -0.442051    6.419635
26      6      0       5.039452   -2.337652    5.392778
27      1      0       5.994120   -2.633343    5.816644
28      6      0       4.378100   -3.179553    4.492779
29      1      0       4.817174   -4.132995    4.214967
30      6      0       3.150643   -2.805628    3.949415
31      1      0       2.635288   -3.443590    3.240836
32      6      0      -1.990540    0.057285    4.112008
33      6      0      -2.794716   -0.927819    4.711840
34      1      0      -2.421784   -1.944554    4.785167
35      6      0      -4.055589   -0.607351    5.215173
36      1      0      -4.659197   -1.382921    5.678214
37      6      0      -4.541511    0.699581    5.126108
38      1      0      -5.521799    0.948803    5.520645
39      6      0      -3.752258    1.681138    4.522605
40      1      0      -4.115234    2.702229    4.447951
41      6      0      -2.491620    1.363689    4.013896
42      1      0      -1.878967    2.127058    3.545377
43      6      0       2.774261   -0.245663   -0.436442
44      6      0       4.230006   -0.345576   -0.132752
45      6      0       5.175613    0.180424   -1.023773
46      1      0       4.851045    0.638727   -1.951990
47      6      0       6.536120    0.105188   -0.732464
48      1      0       7.269941    0.501142   -1.424606
49      6      0       6.939632   -0.486327    0.463913
50      6      0       6.016259   -1.003663    1.370385
51      1      0       6.345221   -1.452295    2.300590
52      6      0       4.658707   -0.934451    1.063474
53      1      0       3.922108   -1.326094    1.755864
54      6      0       2.428091   -2.724012   -0.436775
55      6      0       1.647804   -3.676811    0.234701
56      1      0       0.780433   -3.347403    0.788249
57      6      0       2.007893   -5.021905    0.197871
58      1      0       1.396091   -5.748929    0.723969
59      6      0       3.141895   -5.437668   -0.504968
60      1      0       3.418503   -6.487156   -0.530837
61      6      0       3.906965   -4.489447   -1.185115
62      1      0       4.780224   -4.797120   -1.752801
63      6      0       3.550083   -3.140739   -1.167563
64      1      0       4.133441   -2.424029   -1.729172
65      6      0       2.720129    2.159701   -0.496335
66      6      0       3.299837    2.513171    0.735484
67      1      0       3.362216    1.774609    1.527244
68      6      0       3.775985    3.806386    0.947406
69      1      0       4.219228    4.058467    1.906721
70      6      0       3.675595    4.775898   -0.053178
71      1      0       4.044759    5.782428    0.117813
72      6      0       3.083123    4.437045   -1.271955
73      1      0       2.992072    5.180296   -2.059099
74      6      0       2.605654    3.145630   -1.491238
75      1      0       2.152239    2.882172   -2.441412
76     30      0       0.272487    0.535271   -1.492879
77     35      0       0.052546    0.741490  -10.511706
```

78	35	0	-8.808713	0.586599	-0.870406
79	8	0	-1.320177	1.337872	-2.345345
80	8	0	-0.641266	1.175424	0.401177
81	7	0	-1.334880	1.213839	-3.709238
82	7	0	0.726814	0.255202	-3.553075
83	7	0	-2.011861	1.364075	0.400412
84	7	0	-2.160525	-0.886850	0.736017
85	6	0	-0.248870	0.711298	-4.325688
86	6	0	-0.200278	0.720967	-5.818867
87	6	0	-0.009117	-0.474952	-6.525017
88	1	0	0.080810	-1.412165	-5.986722
89	6	0	0.060563	-0.476261	-7.916641
90	1	0	0.198311	-1.404272	-8.459264
91	6	0	-0.048164	0.733653	-8.599953
92	6	0	-0.226569	1.937636	-7.921980
93	1	0	-0.303432	2.870639	-8.468105
94	6	0	-0.304281	1.923802	-6.530328
95	1	0	-0.445973	2.857922	-5.996877
96	6	0	-2.574104	1.580559	-4.311391
97	6	0	-3.245074	0.721619	-5.189382
98	1	0	-2.816061	-0.241786	-5.438944
99	6	0	-4.468810	1.110754	-5.736108
100	1	0	-4.983085	0.442051	-6.419635
101	6	0	-5.039452	2.337652	-5.392778
102	1	0	-5.994120	2.633343	-5.816644
103	6	0	-4.378100	3.179553	-4.492779
104	1	0	-4.817174	4.132995	-4.214967
105	6	0	-3.150643	2.805628	-3.949415
106	1	0	-2.635288	3.443590	-3.240836
107	6	0	1.990540	-0.057285	-4.112008
108	6	0	2.794716	0.927819	-4.711840
109	1	0	2.421784	1.944554	-4.785167
110	6	0	4.055589	0.607351	-5.215173
111	1	0	4.659197	1.382921	-5.678214
112	6	0	4.541511	-0.699581	-5.126108
113	1	0	5.521799	-0.948803	-5.520645
114	6	0	3.752258	-1.681138	-4.522605
115	1	0	4.115234	-2.702229	-4.447951
116	6	0	2.491620	-1.363689	-4.013896
117	1	0	1.878967	-2.127058	-3.545377
118	6	0	-2.774261	0.245663	0.436442
119	6	0	-4.230006	0.345576	0.132752
120	6	0	-5.175613	-0.180424	1.023773
121	1	0	-4.851045	-0.638727	1.951990
122	6	0	-6.536120	-0.105188	0.732464
123	1	0	-7.269941	-0.501142	1.424606
124	6	0	-6.939632	0.486327	-0.463913
125	6	0	-6.016259	1.003663	-1.370385
126	1	0	-6.345221	1.452295	-2.300590
127	6	0	-4.658707	0.934451	-1.063474
128	1	0	-3.922108	1.326094	-1.755864
129	6	0	-2.428091	2.724012	0.436775
130	6	0	-1.647804	3.676811	-0.234701
131	1	0	-0.780433	3.347403	-0.788249
132	6	0	-2.007893	5.021905	-0.197871
133	1	0	-1.396091	5.748929	-0.723969
134	6	0	-3.141895	5.437668	0.504968
135	1	0	-3.418503	6.487156	0.530837
136	6	0	-3.906965	4.489447	1.185115
137	1	0	-4.780224	4.797120	1.752801
138	6	0	-3.550083	3.140739	1.167563
139	1	0	-4.133441	2.424029	1.729172
140	6	0	-2.720129	-2.159701	0.496335
141	6	0	-3.299837	-2.513171	-0.735484
142	1	0	-3.362216	-1.774609	-1.527244
143	6	0	-3.775985	-3.806386	-0.947406
144	1	0	-4.219228	-4.058467	-1.906721
145	6	0	-3.675595	-4.775898	0.053178
146	1	0	-4.044759	-5.782428	-0.117813
147	6	0	-3.083123	-4.437045	1.271955

148	1	0	-2.992072	-5.180296	2.059099
149	6	0	-2.605654	-3.145630	1.491238
150	1	0	-2.152239	-2.882172	2.441412

Table S11. Atomic coordinates for DFT optimization of **D2** (theory level: B3LYP/ 6,31-g(d,p) PCM: CH$_2$Cl$_2$)

Standard orientation:

Center Number	Atomic Number	Atomic Type	Coordinates (Angstroms)		
			X	Y	Z
1	30	0	-0.272078	-0.532257	1.491525
2	8	0	1.330151	-1.319874	2.344973
3	8	0	0.633878	-1.183308	-0.401785
4	7	0	1.338969	-1.202418	3.708190
5	7	0	-0.731135	-0.258775	3.550774
6	7	0	2.002849	-1.377367	-0.399144
7	7	0	2.161792	0.874442	-0.731574
8	6	0	0.248876	-0.707249	4.321504
9	6	0	0.199614	-0.716872	5.815681
10	6	0	0.000235	0.480812	6.518674
11	1	0	-0.092485	1.415044	5.976691
12	6	0	-0.072581	0.480682	7.906382
13	1	0	-0.216339	1.409233	8.447334
14	6	0	0.227651	-1.935855	7.911938
15	1	0	0.308270	-2.869854	8.456562
16	6	0	0.308339	-1.922287	6.524309
17	1	0	0.455267	-2.853036	5.987397
18	6	0	2.580441	-1.554764	4.315699
19	6	0	3.246153	-0.677444	5.178837
20	1	0	2.814143	0.289757	5.408388
21	6	0	4.470190	-1.052752	5.734931
22	1	0	4.981268	-0.370753	6.407474
23	6	0	5.044704	-2.283780	5.414078
24	1	0	5.999274	-2.569082	5.845047
25	6	0	4.388218	-3.144183	4.527755
26	1	0	4.831005	-4.101069	4.268675
27	6	0	3.160499	-2.784315	3.975816
28	1	0	2.647468	-3.437194	3.279076
29	6	0	-1.997034	0.044817	4.111752
30	6	0	-2.794766	-0.947587	4.707565
31	1	0	-2.416993	-1.963039	4.774833
32	6	0	-4.056883	-0.635977	5.213728
33	1	0	-4.655982	-1.416690	5.673769
34	6	0	-4.549371	0.668811	5.131208
35	1	0	-5.530330	0.911135	5.528183
36	6	0	-3.765883	1.657634	4.531887
37	1	0	-4.133970	2.677339	4.463933
38	6	0	-2.504110	1.349300	4.020401
39	1	0	-1.895056	2.118299	3.556331
40	6	0	2.768361	-0.262459	-0.437007
41	6	0	4.226384	-0.368975	-0.137270
42	6	0	5.169263	0.148726	-1.037487
43	1	0	4.839703	0.599442	-1.967178
44	6	0	6.526444	0.071748	-0.748454
45	1	0	7.258694	0.460689	-1.447071
46	6	0	6.006649	-1.022009	1.367163
47	1	0	6.334568	-1.465775	2.300625
48	6	0	4.652107	-0.951813	1.063937
49	1	0	3.912433	-1.334526	1.757498
50	6	0	2.416810	-2.738350	-0.433730
51	6	0	1.647279	-3.686418	0.256277
52	1	0	0.787182	-3.354358	0.819722
53	6	0	2.009448	-5.030887	0.224053
54	1	0	1.406972	-5.755486	0.763887
55	6	0	3.134725	-5.449315	-0.491514

CCIV

56	1	0	3.412924	-6.498401	-0.513196
57	6	0	3.888585	-4.505595	-1.189806
58	1	0	4.753966	-4.816303	-1.767611
59	6	0	3.528524	-3.157518	-1.177853
60	1	0	4.100285	-2.444187	-1.755809
61	6	0	2.730309	2.142859	-0.485924
62	6	0	3.311452	2.485017	0.748153
63	1	0	3.363578	1.743435	1.537958
64	6	0	3.799856	3.772774	0.966146
65	1	0	4.244372	4.016674	1.926897
66	6	0	3.709335	4.747094	-0.030446
67	1	0	4.087860	5.749292	0.145042
68	6	0	3.114227	4.419464	-1.251093
69	1	0	3.030667	5.167155	-2.034745
70	6	0	2.624854	3.133703	-1.476533
71	1	0	2.169315	2.878658	-2.427939
72	30	0	0.272078	0.532257	-1.491525
73	8	0	-1.330151	1.319874	-2.344973
74	8	0	-0.633878	1.183308	0.401785
75	7	0	-1.338969	1.202418	-3.708190
76	7	0	0.731135	0.258775	-3.550774
77	7	0	-2.002849	1.377367	0.399144
78	7	0	-2.161792	-0.874442	0.731574
79	6	0	-0.248876	0.707249	-4.321504
80	6	0	-0.199614	0.716872	-5.815681
81	6	0	-0.000235	-0.480812	-6.518674
82	1	0	0.092485	-1.415044	-5.976691
83	6	0	0.072581	-0.480682	-7.906382
84	1	0	0.216339	-1.409233	-8.447334
85	6	0	-0.227651	1.935855	-7.911938
86	1	0	-0.308270	2.869854	-8.456562
87	6	0	-0.308339	1.922287	-6.524309
88	1	0	-0.455267	2.853036	-5.987397
89	6	0	-2.580441	1.554764	-4.315699
90	6	0	-3.246153	0.677444	-5.178837
91	1	0	-2.814143	-0.289757	-5.408388
92	6	0	-4.470190	1.052752	-5.734931
93	1	0	-4.981268	0.370753	-6.407474
94	6	0	-5.044704	2.283780	-5.414078
95	1	0	-5.999274	2.569082	-5.845047
96	6	0	-4.388218	3.144183	-4.527755
97	1	0	-4.831005	4.101069	-4.268675
98	6	0	-3.160499	2.784315	-3.975816
99	1	0	-2.647468	3.437194	-3.279076
100	6	0	1.997034	-0.044817	-4.111752
101	6	0	2.794766	0.947587	-4.707565
102	1	0	2.416993	1.963039	-4.774833
103	6	0	4.056883	0.635977	-5.213728
104	1	0	4.655982	1.416690	-5.673769
105	6	0	4.549371	-0.668811	-5.131208
106	1	0	5.530330	-0.911135	-5.528183
107	6	0	3.765883	-1.657634	-4.531887
108	1	0	4.133970	-2.677339	-4.463933
109	6	0	2.504110	-1.349300	-4.020401
110	1	0	1.895056	-2.118299	-3.556331
111	6	0	-2.768361	0.262459	0.437007
112	6	0	-4.226384	0.368975	0.137270
113	6	0	-5.169263	-0.148726	1.037487
114	1	0	-4.839703	-0.599442	1.967178
115	6	0	-6.526444	-0.071748	0.748454
116	1	0	-7.258694	-0.460689	1.447071
117	6	0	-6.006649	1.022009	-1.367163
118	1	0	-6.334568	1.465775	-2.300625
119	6	0	-4.652107	0.951813	-1.063937
120	1	0	-3.912433	1.334526	-1.757498
121	6	0	-2.416810	2.738350	0.433730
122	6	0	-1.647279	3.686418	-0.256277
123	1	0	-0.787182	3.354358	-0.819722
124	6	0	-2.009448	5.030887	-0.224053
125	1	0	-1.406972	5.755486	-0.763887

```
126          6          0       -3.134725    5.449315    0.491514
127          1          0       -3.412924    6.498401    0.513196
128          6          0       -3.888585    4.505595    1.189806
129          1          0       -4.753966    4.816303    1.767611
130          6          0       -3.528524    3.157518    1.177853
131          1          0       -4.100285    2.444187    1.755809
132          6          0       -2.730309   -2.142859    0.485924
133          6          0       -3.311452   -2.485017   -0.748153
134          1          0       -3.363578   -1.743435   -1.537958
135          6          0       -3.799856   -3.772774   -0.966146
136          1          0       -4.244372   -4.016674   -1.926897
137          6          0       -3.709335   -4.747094    0.030446
138          1          0       -4.087860   -5.749292   -0.145042
139          6          0       -3.114227   -4.419464    1.251093
140          1          0       -3.030667   -5.167155    2.034745
141          6          0       -2.624854   -3.133703    1.476533
142          1          0       -2.169315   -2.878658    2.427939
143          6          0       -6.949752    0.513479   -0.457836
144          6          0       -0.040015    0.730964   -8.609485
145          6          0        6.949752   -0.513479    0.457836
146          6          0        0.040015   -0.730964    8.609485
147          6          0        0.037914    0.737907  -10.040822
148          6          0       -8.348844    0.589550   -0.761330
149          6          0       -0.037914   -0.737907   10.040822
150          6          0        8.348844   -0.589550    0.761330
151          7          0        0.100141    0.743719  -11.202877
152          7          0       -9.484579    0.652530   -1.007533
153          7          0        9.484579   -0.652530    1.007533
154          7          0       -0.100141   -0.743719   11.202877
------------------------------------------------------------------------
```

Table S12. Atomic coordinates for DFT optimization of **Zn_p2** (theory level: B3LYP/ 6,31-g(d,p), gas phase)

```
                      Standard orientation:
---------------------------------------------------------------------
Center     Atomic     Atomic           Coordinates (Angstroms)
Number     Number     Type          X          Y          Z
---------------------------------------------------------------------
    1         30          0       3.067670    2.759453    0.958305
    2          8          0       3.380270    3.097995    2.855397
    3          8          0       2.863935    4.109997   -0.436597
    4          7          0       1.482794    1.767090    1.637110
    5          7          0       4.553335    2.120788   -0.207582
    6          7          0       2.298652    2.650223    3.572895
    7          7          0       3.900263    3.994858   -1.326794
    8          6          0       1.338082    1.942140    2.950102
    9          6          0       0.714986    0.870321    0.861945
   10          6          0       4.754765    2.961089   -1.223770
   11          6          0       5.191566    0.871441   -0.061340
   12          6          0       2.248316    3.190695    4.902832
   13          6          0       4.026853    5.138513   -2.187107
   14          6          0       0.159115    1.469700    3.732609
   15          6          0       0.389456   -0.435098    1.265043
   16          6          0       0.320973    1.282250   -0.421270
   17          6          0       5.898920    2.869185   -2.177030
   18          6          0       5.525844    0.456230    1.237953
   19          6          0       5.439109   -0.019860   -1.119938
   20          6          0       1.408304    4.282032    5.181660
   21          6          0       3.138547    2.668584    5.859983
   22          6          0       3.108707    5.271593   -3.245483
   23          6          0       4.972609    6.133434   -1.888380
   24          6          0       0.300843    0.736238    4.918550
   25          6          0      -1.132022    1.743597    3.252619
   26          1          0       0.701571   -0.791175    2.240721
   27          6          0      -0.320973   -1.282250    0.421270
```

```
28        6        0       -0.389456    0.435098   -1.265043
29        1        0        0.575891    2.287677   -0.744456
30        6        0        7.200362    2.735709   -1.666279
31        6        0        5.714016    2.890774   -3.566378
32        1        0        5.327488    1.132296    2.064828
33        6        0        6.113038   -0.782213    1.477469
34        6        0        6.014255   -1.263047   -0.882325
35        1        0        5.163995    0.254596   -2.131941
36        6        0        1.418408    4.799265    6.483272
37        6        0        0.538004    4.903533    4.117558
38        6        0        3.119092    3.219484    7.143753
39        6        0        4.104620    1.567340    5.501950
40        6        0        3.206448    6.402668   -4.059697
41        6        0        2.034069    4.238379   -3.474269
42        6        0        5.037920    7.248002   -2.734038
43        6        0        5.875742    6.027525   -0.684792
44        1        0        1.290979    0.506784    5.294994
45        6        0       -0.824045    0.293163    5.613598
46        6        0       -2.254047    1.305519    3.952340
47        1        0       -1.250873    2.293302    2.325323
48        1        0       -0.575891   -2.287677    0.744456
49        6        0       -0.714986   -0.870321   -0.861945
50        1        0       -0.701571    0.791175   -2.240721
51        1        0        7.350267    2.700423   -0.592470
52        6        0        8.291358    2.642105   -2.527530
53        6        0        6.807353    2.789082   -4.425952
54        1        0        4.714617    2.981743   -3.975729
55        1        0        6.385491   -1.055829    2.489901
56        6        0        6.365005   -1.663427    0.415955
57        1        0        6.186343   -1.945720   -1.710042
58        1        0        0.770917    5.638837    6.720908
59        6        0        2.257181    4.269451    7.459262
60        1        0        0.256004    5.920690    4.401735
61        1        0       -0.386096    4.334273    3.966695
62        1        0        1.060491    4.949671    3.158081
63        1        0        3.792541    2.823606    7.898964
64        1        0        3.591758    0.678645    5.116694
65        1        0        4.695707    1.268585    6.371199
66        1        0        4.779462    1.903168    4.709409
67        1        0        2.512962    6.519510   -4.887949
68        6        0        4.171777    7.379171   -3.815494
69        1        0        2.450383    3.240980   -3.657069
70        1        0        1.411080    4.506969   -4.331199
71        1        0        1.402894    4.152390   -2.585283
72        1        0        5.766984    8.026017   -2.524732
73        1        0        5.338815    5.615972    0.174357
74        1        0        6.260309    7.012584   -0.408090
75        1        0        6.737064    5.379060   -0.880918
76        1        0       -0.698586   -0.275095    6.530454
77        6        0       -2.103430    0.578437    5.134922
78        1        0       -3.244736    1.527546    3.567430
79        7        0       -1.482794   -1.767090   -1.637110
80        1        0        9.292168    2.544497   -2.117986
81        6        0        8.098050    2.667776   -3.909989
82        1        0        6.648825    2.805324   -5.500105
83        1        0        2.254583    4.686719    8.462124
84        1        0        4.234254    8.252794   -4.457928
85        1        0       -2.978390    0.235424    5.679308
86        6        0       -1.338082   -1.942140   -2.950102
87        1        0        8.948446    2.590279   -4.580857
88        7        0       -2.298652   -2.650223   -3.572895
89        6        0       -0.159115   -1.469700   -3.732609
90        8        0       -3.380270   -3.097995   -2.855397
91        6        0       -2.248316   -3.190695   -4.902832
92        6        0       -0.300843   -0.736238   -4.918550
93        6        0        1.132022   -1.743597   -3.252619
94        6        0       -1.408304   -4.282032   -5.181660
95        6        0       -3.138547   -2.668584   -5.859983
96        1        0       -1.290979   -0.506784   -5.294994
97        6        0        0.824045   -0.293163   -5.613598
```

98	6	0	2.254047	-1.305519	-3.952340
99	1	0	1.250873	-2.293302	-2.325323
100	6	0	-1.418408	-4.799265	-6.483272
101	6	0	-0.538004	-4.903533	-4.117558
102	6	0	-3.119092	-3.219484	-7.143753
103	6	0	-4.104620	-1.567340	-5.501950
104	1	0	0.698586	0.275095	-6.530454
105	6	0	2.103430	-0.578437	-5.134922
106	1	0	3.244736	-1.527546	-3.567430
107	1	0	-0.770917	-5.638837	-6.720908
108	6	0	-2.257181	-4.269451	-7.459262
109	1	0	-0.256004	-5.920690	-4.401735
110	1	0	0.386096	-4.334273	-3.966695
111	1	0	-1.060491	-4.949671	-3.158081
112	1	0	-3.792541	-2.823606	-7.898964
113	1	0	-3.591758	-0.678645	-5.116694
114	1	0	-4.695707	-1.268585	-6.371199
115	1	0	-4.779462	-1.903168	-4.709409
116	1	0	2.978390	-0.235424	-5.679308
117	1	0	-2.254583	-4.686719	-8.462124
118	7	0	6.973172	-2.926100	0.570625
119	6	0	7.136100	-3.675303	1.704150
120	7	0	8.198817	-4.476706	1.644596
121	6	0	6.128584	-3.717773	2.781329
122	6	0	8.500681	-5.532454	2.587330
123	6	0	4.764308	-3.722242	2.434982
124	6	0	6.480009	-3.738430	4.140990
125	6	0	9.592570	-5.346250	3.451191
126	6	0	7.786484	-6.737293	2.515316
127	1	0	4.481399	-3.694718	1.388309
128	6	0	3.783358	-3.767232	3.422158
129	6	0	5.493824	-3.783751	5.124800
130	1	0	7.524076	-3.713664	4.429131
131	6	0	9.917379	-6.392349	4.319309
132	6	0	10.389810	-4.065042	3.425218
133	6	0	8.146020	-7.756917	3.405003
134	6	0	6.691559	-6.938808	1.496979
135	1	0	2.735994	-3.778164	3.135702
136	6	0	4.143903	-3.800091	4.770913
137	1	0	5.783654	-3.800109	6.171182
138	1	0	10.753305	-6.270675	5.002789
139	6	0	9.193639	-7.584710	4.306277
140	1	0	9.834186	-3.228622	3.868209
141	1	0	11.321362	-4.176878	3.985287
142	1	0	10.618908	-3.789861	2.392377
143	1	0	7.605089	-8.698705	3.373370
144	1	0	6.979415	-6.508326	0.533421
145	1	0	6.492139	-8.003924	1.353885
146	1	0	5.754124	-6.462970	1.807790
147	1	0	3.378348	-3.834401	5.540351
148	1	0	9.461771	-8.388650	4.985633
149	8	0	8.999076	-4.421629	0.596402
150	30	0	-3.067670	-2.759453	-0.958305
151	8	0	-2.863935	-4.109997	0.436597
152	7	0	-4.553335	-2.120788	0.207582
153	7	0	-3.900263	-3.994858	1.326794
154	6	0	-4.754765	-2.961089	1.223770
155	6	0	-5.191566	-0.871441	0.061340
156	6	0	-4.026853	-5.138513	2.187107
157	6	0	-5.898920	-2.869185	2.177030
158	6	0	-5.439109	0.019860	1.119938
159	6	0	-5.525844	-0.456230	-1.237953
160	6	0	-3.108707	-5.271593	3.245483
161	6	0	-4.972609	-6.133434	1.888380
162	6	0	-7.200362	-2.735709	1.666279
163	6	0	-5.714016	-2.890774	3.566378
164	6	0	-6.014255	1.263047	0.882325
165	1	0	-5.163995	-0.254596	2.131941
166	1	0	-5.327488	-1.132296	-2.064828
167	6	0	-6.113038	0.782213	-1.477469

```
168        6         0        -3.206448    -6.402668    4.059697
169        6         0        -2.034069    -4.238379    3.474269
170        6         0        -5.037920    -7.248002    2.734038
171        6         0        -5.875742    -6.027525    0.684792
172        1         0        -7.350267    -2.700423    0.592470
173        6         0        -8.291358    -2.642105    2.527530
174        6         0        -6.807353    -2.789082    4.425952
175        1         0        -4.714617    -2.981743    3.975729
176        6         0        -6.365005     1.663427   -0.415955
177        1         0        -6.186343     1.945720    1.710042
178        1         0        -6.385491     1.055829   -2.489901
179        1         0        -2.512962    -6.519510    4.887949
180        6         0        -4.171777    -7.379171    3.815494
181        1         0        -2.450383    -3.240980    3.657069
182        1         0        -1.411080    -4.506969    4.331199
183        1         0        -1.402894    -4.152390    2.585283
184        1         0        -5.766984    -8.026017    2.524732
185        1         0        -5.338815    -5.615972   -0.174357
186        1         0        -6.260309    -7.012584    0.408090
187        1         0        -6.737064    -5.379060    0.880918
188        1         0        -9.292168    -2.544497    2.117986
189        6         0        -8.098050    -2.667776    3.909989
190        1         0        -6.648825    -2.805324    5.500105
191        7         0        -6.973172     2.926100   -0.570625
192        1         0        -4.234254    -8.252794    4.457928
193        1         0        -8.948446    -2.590279    4.580857
194        6         0        -7.136100     3.675303   -1.704150
195        1         0        -7.704490     3.198109    0.094599
196        7         0        -8.198817     4.476706   -1.644596
197        6         0        -6.128584     3.717773   -2.781329
198        8         0        -8.999076     4.421629   -0.596402
199        6         0        -8.500681     5.532454   -2.587330
200        6         0        -4.764308     3.722242   -2.434982
201        6         0        -6.480009     3.738430   -4.140990
202        6         0        -9.592570     5.346250   -3.451191
203        6         0        -7.786484     6.737293   -2.515316
204        1         0        -4.481399     3.694718   -1.388309
205        6         0        -3.783358     3.767232   -3.422158
206        6         0        -5.493824     3.783751   -5.124800
207        1         0        -7.524076     3.713664   -4.429131
208        6         0        -9.917379     6.392349   -4.319309
209        6         0       -10.389810     4.065042   -3.425218
210        6         0        -8.146020     7.756917   -3.405003
211        6         0        -6.691559     6.938808   -1.496979
212        1         0        -2.735994     3.778164   -3.135702
213        6         0        -4.143903     3.800091   -4.770913
214        1         0        -5.783654     3.800109   -6.171182
215        1         0       -10.753305     6.270675   -5.002789
216        6         0        -9.193639     7.584710   -4.306277
217        1         0        -9.834186     3.228622   -3.868209
218        1         0       -11.321362     4.176878   -3.985287
219        1         0       -10.618908     3.789861   -2.392377
220        1         0        -7.605089     8.698705   -3.373370
221        1         0        -6.979415     6.508326   -0.533421
222        1         0        -6.492139     8.003924   -1.353885
223        1         0        -5.754124     6.462970   -1.807790
224        1         0        -3.378348     3.834401   -5.540351
225        1         0        -9.461771     8.388650   -4.985633
226        1         0         7.704490    -3.198109   -0.094599
      ----------------------------------------------------------------
```

Table S13. Atomic coordinates for DFT optimization of **Zn_d2** (theory level: B3LYP/ 6,31-g(d,p), gas phase)

```
                        Standard orientation:
---------------------------------------------------------------------
Center     Atomic     Atomic          Coordinates (Angstroms)
Number     Number     Type          X           Y           Z
---------------------------------------------------------------------
   1          6          0      -1.421624   -1.832448    0.555619
   2          6          0      -0.693380   -2.622227   -0.350251
   3          6          0       0.693411   -2.622250   -0.350194
   4          6          0       1.421602   -1.832500    0.555744
   5          6          0       0.697107   -1.065987    1.480742
   6          6          0      -0.697189   -1.065960    1.480681
   7          7          0      -2.827139   -1.698953    0.449111
   8          7          0       2.827138   -1.699031    0.449399
   9          6          0       3.595252   -2.749374    0.122717
  10          7          0       4.726049   -2.487713   -0.550625
  11          6          0       3.286937   -4.145814    0.541202
  12          6          0      -3.595246   -2.749311    0.122491
  13          7          0      -4.725967   -2.487683   -0.551003
  14          6          0      -3.287068   -4.145693    0.541244
  15          8          0      -4.980595   -1.210348   -0.965362
  16          6          0       5.842389   -3.371114   -0.755719
  17          8          0       4.980741   -1.210355   -0.964863
  18          6          0      -5.842362   -3.371032   -0.756023
  19          6          0      -2.844314   -4.367816    1.855955
  20          6          0      -2.551483   -5.656290    2.295952
  21          6          0      -2.684193   -6.741365    1.427469
  22          6          0      -3.110257   -6.528788    0.115872
  23          6          0      -3.411361   -5.241247   -0.325061
  24          6          0       3.411133   -5.241196   -0.325338
  25          6          0       3.109840   -6.528789    0.115306
  26          6          0       2.683682   -6.741587    1.426840
  27          6          0       2.551075   -5.656685    2.295550
  28          6          0       2.844095   -4.368152    1.855841
  29          6          0      -6.672360   -3.709105    0.325840
  30          6          0      -7.769555   -4.541173    0.069883
  31          6          0      -8.046009   -4.989739   -1.218234
  32          6          0      -7.233908   -4.599034   -2.282529
  33          6          0      -6.123750   -3.776965   -2.073936
  34          6          0       6.672232   -3.709496    0.326177
  35          6          0       7.769394   -4.541586    0.070170
  36          6          0       8.045985   -4.989877   -1.218018
  37          6          0       7.234045   -4.598875   -2.282319
  38          6          0       6.123910   -3.776776   -2.073683
  39          6          0      -6.419261   -3.179727    1.715877
  40          6          0      -5.258805   -3.328229   -3.225675
  41          6          0       5.259116   -3.327786   -3.225436
  42          6          0       6.419021   -3.180409    1.716305
  43         30          0      -3.773955    0.000003   -0.000466
  44         30          0       3.773876   -0.000056   -0.000132
  45          6          0       1.421652    1.832500   -0.555821
  46          6          0       0.693476    2.622124    0.350239
  47          6          0      -0.693316    2.622151    0.350277
  48          6          0      -1.421566    1.832560   -0.555750
  49          6          0      -0.697144    1.066183   -1.480913
  50          6          0       0.697152    1.066154   -1.480948
  51          7          0       2.827185    1.698985   -0.449485
  52          7          0      -2.827098    1.699075   -0.449338
  53          6          0      -3.595238    2.749362   -0.122567
  54          7          0      -4.726189    2.487571    0.550470
  55          6          0      -3.286810    4.145908   -0.540622
  56          6          0       3.595333    2.749285   -0.122750
  57          7          0       4.726192    2.487546    0.550454
  58          6          0       3.286976    4.145776   -0.541032
  59          8          0       4.980945    1.210131    0.964480
  60          6          0      -5.842508    3.370996    0.755613
  61          8          0      -4.981066    1.210094    0.964214
```

62	6	0	5.842533	3.370944	0.755586
63	6	0	3.411156	5.241042	0.325652
64	6	0	3.109823	6.528688	-0.114811
65	6	0	2.683647	6.741654	-1.426310
66	6	0	2.551061	5.656867	-2.295170
67	6	0	2.844118	4.368282	-1.855640
68	6	0	-2.843862	4.368616	-1.855162
69	6	0	-2.550739	5.657267	-2.294460
70	6	0	-2.683347	6.741912	-1.425430
71	6	0	-3.109614	6.528744	-0.113992
72	6	0	-3.411012	5.241034	0.326238
73	6	0	6.124146	3.776438	2.073579
74	6	0	7.234291	4.598520	2.282238
75	6	0	8.046148	4.989662	1.217927
76	6	0	7.769468	4.541530	-0.070299
77	6	0	6.672297	3.709463	-0.326329
78	6	0	-6.672162	3.709696	-0.326327
79	6	0	-7.769318	4.541780	-0.070283
80	6	0	-8.046086	4.989759	1.217977
81	6	0	-7.234337	4.598443	2.282307
82	6	0	-6.124215	3.776333	2.073635
83	6	0	5.259447	3.327285	3.225340
84	6	0	6.418992	3.180520	-1.716494
85	6	0	-5.259634	3.326984	3.225410
86	6	0	-6.418745	3.180955	-1.716549
87	1	0	-1.222508	-3.199268	-1.101322
88	1	0	1.222574	-3.199308	-1.101226
89	1	0	1.237184	-0.440735	2.185930
90	1	0	-1.237304	-0.440684	2.185819
91	1	0	-2.731936	-3.522092	2.525651
92	1	0	-2.217610	-5.812223	3.317422
93	1	0	-2.452754	-7.745770	1.769606
94	1	0	-3.207701	-7.366215	-0.568522
95	1	0	-3.735775	-5.086875	-1.347155
96	1	0	3.735625	-5.086633	-1.347378
97	1	0	3.207201	-7.366089	-0.569256
98	1	0	2.452089	-7.746035	1.768747
99	1	0	2.217134	-5.812795	3.316970
100	1	0	2.731787	-3.522551	2.525705
101	1	0	-8.421397	-4.819738	0.893354
102	1	0	-8.905943	-5.628627	-1.397620
103	1	0	-7.464010	-4.929076	-3.291858
104	1	0	8.421112	-4.820389	0.893658
105	1	0	8.905902	-5.628778	-1.397437
106	1	0	7.464247	-4.928696	-3.291698
107	1	0	-5.605205	-3.718318	2.213858
108	1	0	-6.150626	-2.119685	1.691449
109	1	0	-7.314606	-3.288858	2.333224
110	1	0	-5.691872	-3.637361	-4.180207
111	1	0	-5.148214	-2.240964	-3.212658
112	1	0	-4.247679	-3.750191	-3.165238
113	1	0	5.692338	-3.636663	-4.179981
114	1	0	4.248008	-3.749832	-3.165255
115	1	0	5.148462	-2.240533	-3.212156
116	1	0	6.150358	-2.120370	1.692078
117	1	0	5.604944	-3.719119	2.214122
118	1	0	7.314326	-3.289649	2.333689
119	1	0	1.222651	3.199039	1.101372
120	1	0	-1.222428	3.199092	1.101433
121	1	0	-1.237272	0.441043	-2.186161
122	1	0	1.237220	0.440995	-2.186226
123	1	0	3.735666	5.086348	1.347668
124	1	0	3.207170	7.365896	0.569865
125	1	0	2.452025	7.746143	-1.768079
126	1	0	2.217110	5.813110	-3.316566
127	1	0	2.731823	3.522768	-2.525615
128	1	0	-2.731545	3.523213	-2.525274
129	1	0	-2.216715	5.813668	-3.315808
130	1	0	-2.451671	7.746451	-1.767017
131	1	0	-3.206979	7.365842	0.570815

```
 132          1          0        -3.735595     5.086176     1.348206
 133          1          0         7.464567     4.928212     3.291642
 134          1          0         8.906073     5.628549     1.397363
 135          1          0         8.421124     4.820443    -0.893800
 136          1          0        -8.420895     4.820825    -0.893801
 137          1          0        -8.905996     5.628663     1.397422
 138          1          0        -7.464683     4.928017     3.291733
 139          1          0         4.248343     3.749363     3.165324
 140          1          0         5.148771     2.240036     3.211897
 141          1          0         5.692764     3.635998     4.179894
 142          1          0         7.314228     3.289903    -2.333954
 143          1          0         6.150417     2.120456    -1.692354
 144          1          0         5.604822     3.719218    -2.214173
 145          1          0        -5.693111     3.635438     4.179975
 146          1          0        -5.148869     2.239747     3.211731
 147          1          0        -4.248560     3.749168     3.165638
 148          1          0        -5.604606     3.719805    -2.214115
 149          1          0        -6.150066     2.120916    -1.692542
 150          1          0        -7.313963     3.290331    -2.334036
 ----------------------------------------------------------------------
```

Table S14. Atomic coordinates for DFT optimization of **Zn_p4** (theory level: B3LYP/ 6,31-g(d,p),
gas phase)

```
                      Standard orientation:
 ---------------------------------------------------------------------
 Center     Atomic     Atomic              Coordinates (Angstroms)
 Number     Number     Type            X           Y           Z
 ---------------------------------------------------------------------
    1          30         0        -8.701135     2.842342     0.763577
    2           8         0        -8.402269     3.179237     2.664884
    3           8         0        -9.019991     4.197802    -0.606821
    4           7         0       -10.215400     1.737757     1.443142
    5           7         0        -7.168460     2.358744    -0.406260
    6           7         0        -9.455900     2.669513     3.378880
    7           7         0        -7.957924     4.208778    -1.476540
    8           6         0       -10.373507     1.907878     2.756722
    9           6         0       -10.918556     0.794455     0.665731
   10           6         0        -7.021332     3.246404    -1.390089
   11           6         0        -6.438828     1.154101    -0.305436
   12           6         0        -9.530090     3.193158     4.714903
   13           6         0        -7.902248     5.401334    -2.275498
   14           6         0       -11.530368     1.384244     3.539552
   15           6         0       -11.225791    -0.510358     1.089633
   16           6         0       -11.257349     1.153964    -0.649052
   17           6         0        -5.856484     3.275253    -2.321627
   18           6         0        -6.028489     0.738322     0.971601
   19           6         0        -6.168282     0.308852    -1.394135
   20           6         0       -10.412016     4.248179     5.002115
   21           6         0        -8.620491     2.697305     5.667561
   22           6         0        -8.814154     5.523491    -3.340813
   23           6         0        -7.032621     6.443648    -1.913338
   24           6         0       -11.356760     0.647503     4.719306
   25           6         0       -12.832724     1.619413     3.069570
   26           1         0       -10.952731    -0.832325     2.088036
   27           6         0       -11.856229    -1.406106     0.233128
   28           6         0       -11.899564     0.263946    -1.503708
   29           1         0       -11.017435     2.157069    -0.990386
   30           6         0        -4.559818     3.184709    -1.789390
   31           6         0        -6.014248     3.365696    -3.711495
   32           1         0        -6.244439     1.382063     1.820092
   33           6         0        -5.354640    -0.464465     1.156447
   34           6         0        -5.494768    -0.893820    -1.209269
   35           1         0        -6.496010     0.591143    -2.388658
   36           6         0       -10.422677     4.753615     6.308375
   37           6         0       -11.304787     4.844436     3.942131
   38           6         0        -8.662323     3.234906     6.956375
   39           6         0        -7.611376     1.638695     5.298854
```

```
40        6         0      -8.787231    6.698719   -4.095739
41        6         0      -9.808603    4.429733   -3.639049
42        6         0      -7.036554    7.601817   -2.701079
43        6         0      -6.136383    6.341851   -0.704097
44        1         0     -10.357097    0.449242    5.088246
45        6         0     -12.461865    0.162390    5.417824
46        6         0     -13.935058    1.140457    3.774116
47        1         0     -12.974431    2.174464    2.148356
48        1         0     -12.073124   -2.415628    0.571824
49        6         0     -12.204787   -1.035780   -1.074488
50        1         0     -12.171300    0.585669   -2.502176
51        1         0      -4.428927    3.095936   -0.716522
52        6         0      -3.447640    3.198268   -2.627736
53        6         0      -4.899390    3.374152   -4.549221
54        1         0      -7.008442    3.423759   -4.138975
55        1         0      -5.027683   -0.747697    2.150983
56        6         0      -5.084160   -1.309768    0.067438
57        1         0      -5.282557   -1.538653   -2.057644
58        1         0     -11.102157    5.565444    6.552948
59        6         0      -9.564734    4.247666    7.280378
60        1         0     -11.624102    5.848505    4.233239
61        1         0     -12.207379    4.242553    3.787438
62        1         0     -10.784433    4.916498    2.983131
63        1         0      -7.973891    2.859458    7.708513
64        1         0      -8.088418    0.720943    4.935905
65        1         0      -6.987589    1.379414    6.157998
66        1         0      -6.971982    1.997206    4.487139
67        1         0      -9.476846    6.808122   -4.928252
68        6         0      -7.897072    7.727178   -3.787648
69        1         0      -9.317512    3.471587   -3.844823
70        1         0     -10.425568    4.687528   -4.503469
71        1         0     -10.456358    4.266715   -2.773092
72        1         0      -6.366212    8.416817   -2.442163
73        1         0      -6.652232    5.855995    0.128833
74        1         0      -5.821719    7.336458   -0.377706
75        1         0      -5.231424    5.762533   -0.918705
76        1         0     -12.312343   -0.409058    6.329026
77        6         0     -13.752847    0.409711    4.949750
78        1         0     -14.936304    1.334494    3.401644
79        7         0     -12.863511   -1.990645   -1.876349
80        1         0      -2.453073    3.127671   -2.198124
81        6         0      -3.614536    3.293229   -4.010811
82        1         0      -5.037251    3.443522   -5.624175
83        7         0      -4.358257   -2.516513    0.167593
84        1         0      -9.584044    4.655527    8.286906
85        1         0      -7.888989    8.634649   -4.384588
86        1         0     -14.612377    0.032563    5.495831
87        6         0     -13.011596   -2.018156   -3.236645
88        1         0     -13.629121   -2.532875   -1.462952
89        1         0      -2.747620    3.301969   -4.665010
90        6         0      -4.507293   -3.403798    1.151092
91       30         0      -2.821768   -2.998841   -1.001157
92        7         0     -14.105553   -2.672114   -3.624068
93        6         0     -11.965350   -1.535161   -4.158447
94        7         0      -3.574161   -4.369894    1.235659
95        6         0      -5.670540   -3.428774    2.084971
96        8         0      -2.514477   -4.364044    0.363831
97        8         0      -3.096280   -3.335004   -2.906280
98        7         0      -1.315796   -1.875846   -1.658825
99        8         0     -14.941984   -3.138651   -2.715610
100       6         0     -14.416464   -3.044089   -4.987624
101       6         0     -12.264644   -0.821918   -5.330981
102       6         0     -10.616224   -1.785302   -3.844171
103       6         0      -3.632000   -5.561276    2.035879
104       6         0      -6.967852   -3.328183    1.555992
105       6         0      -5.510836   -3.524497    3.474305
106       7         0      -2.042662   -2.805064   -3.608019
107       6         0      -1.142101   -2.034683   -2.970819
108       6         0      -0.631105   -0.923692   -0.873246
109       6         0     -13.754697   -4.136868   -5.566340
```

```
110        6        0        -15.469600    -2.367983    -5.625927
111        1        0        -13.295684    -0.602416    -5.580907
112        6        0        -11.242754    -0.389197    -6.174119
113        6        0         -9.599465    -1.349556    -4.689639
114        1        0        -10.373973    -2.325690    -2.935621
115        6        0         -2.717797    -5.685495     3.098962
116        6        0         -4.505668    -6.601241     1.676961
117        1        0         -7.100422    -3.234906     0.483725
118        6        0         -8.078107    -3.336440     2.396981
119        6        0         -6.623894    -3.528868     4.314511
120        1        0         -4.516207    -3.590194     3.899561
121        6        0         -1.947875    -3.319559    -4.945672
122        6        0          0.016149    -1.485624    -3.734246
123        6        0         -0.250292    -1.296369     0.426095
124        6        0         -0.378007     0.396762    -1.280825
125        6        0        -14.124435    -4.502931    -6.866258
126        6        0        -12.705096    -4.908842    -4.805623
127        6        0        -15.806727    -2.770267    -6.921240
128        6        0        -16.211823    -1.256619    -4.924994
129        1        0        -11.491968     0.160260    -7.076998
130        6        0         -9.908654    -0.651270    -5.858837
131        1        0         -8.564799    -1.556812    -4.433570
132        6        0         -2.746463    -6.859799     3.855179
133        6        0         -1.719373    -4.594080     3.392937
134        6        0         -4.503662    -7.758569     2.465942
135        6        0         -5.403434    -6.497425     0.469037
136        1        0         -9.073064    -3.255762     1.969843
137        6        0         -7.909398    -3.437368     3.779412
138        1        0         -6.484260    -3.603259     5.388905
139        6        0         -1.044309    -4.356281    -5.232466
140        6        0         -2.857766    -2.833627    -5.903313
141        6        0         -0.150305    -0.756294    -4.919597
142        6        0          1.313737    -1.685349    -3.235331
143        6        0          0.378007    -0.396762     1.280825
144        1        0         -0.452469    -2.312609     0.753801
145        1        0         -0.682844     0.722857    -2.269083
146        6        0          0.250292     1.296369    -0.426095
147        1        0        -13.623330    -5.342718    -7.339773
148        6        0        -15.132906    -3.821437    -7.543008
149        1        0        -12.545712    -5.889924    -5.260335
150        1        0        -11.742122    -4.385451    -4.796066
151        1        0        -13.014177    -5.055148    -3.766505
152        1        0        -16.612775    -2.258510    -7.439918
153        1        0        -15.606240    -0.344172    -4.851379
154        1        0        -17.128462    -1.002415    -5.462844
155        1        0        -16.462606    -1.561573    -3.905705
156        1        0         -9.115199    -0.310626    -6.517383
157        1        0         -2.054830    -6.970904     4.685811
158        6        0         -3.640889    -7.885624     3.550536
159        1        0         -2.206795    -3.636980     3.612249
160        1        0         -1.091906    -4.859358     4.247634
161        1        0         -1.083514    -4.424995     2.519344
162        1        0         -5.176960    -8.571890     2.209379
163        1        0         -4.886443    -6.014920    -0.365129
164        1        0         -5.722775    -7.491187     0.144537
165        1        0         -6.305416    -5.913536     0.684064
166        1        0         -8.774807    -3.442675     4.435660
167        6        0         -1.013899    -4.853243    -6.541717
168        6        0         -0.148525    -4.942029    -4.169118
169        6        0         -2.796152    -3.362452    -7.194934
170        6        0         -3.885936    -1.792821    -5.536549
171        1        0         -1.146107    -0.584995    -5.311643
172        6        0          0.957331    -0.243727    -5.594304
173        6        0          2.419029    -1.177537    -3.914254
174        1        0          1.450026    -2.233172    -2.309266
175        6        0          0.631105     0.923692     0.873246
176        1        0          0.682844    -0.722857     2.269083
177        1        0          0.452469     2.312609    -0.753801
178        1        0        -15.409868    -4.122854    -8.549081
179        1        0         -3.650320    -8.792501     4.148337
```

180	1	0	-0.317499	-5.650787	-6.785739
181	6	0	-1.873234	-4.357083	-7.517561
182	1	0	0.196071	-5.936065	-4.465728
183	1	0	0.738865	-4.321659	-4.000136
184	1	0	-0.676612	-5.033811	-3.215997
185	1	0	-3.484820	-2.994321	-7.950541
186	1	0	-3.424805	-0.867656	-5.171710
187	1	0	-4.511529	-1.542892	-6.397200
188	1	0	-4.520878	-2.162549	-4.726452
189	1	0	0.813106	0.320595	-6.510894
190	6	0	2.243587	-0.454461	-5.095814
191	1	0	3.414934	-1.342713	-3.514742
192	7	0	1.315796	1.875846	1.658825
193	1	0	-1.838466	-4.758420	-8.526329
194	1	0	3.105055	-0.056436	-5.624041
195	30	0	2.821768	2.998841	1.001157
196	6	0	1.142101	2.034683	2.970819
197	8	0	3.096280	3.335004	2.906280
198	8	0	2.514477	4.364044	-0.363831
199	7	0	4.358257	2.516513	-0.167593
200	7	0	2.042662	2.805064	3.608019
201	6	0	-0.016149	1.485624	3.734246
202	7	0	3.574161	4.369894	-1.235659
203	6	0	4.507293	3.403798	-1.151092
204	6	0	5.084160	1.309768	-0.067438
205	6	0	1.947875	3.319559	4.945672
206	6	0	0.150305	0.756294	4.919597
207	6	0	-1.313737	1.685349	3.235331
208	6	0	3.632000	5.561276	-2.035879
209	6	0	5.670540	3.428774	-2.084971
210	6	0	5.494768	0.893820	1.209269
211	6	0	5.354640	0.464465	-1.156447
212	6	0	1.044309	4.356281	5.232466
213	6	0	2.857766	2.833627	5.903313
214	1	0	1.146107	0.584995	5.311643
215	6	0	-0.957331	0.243727	5.594304
216	6	0	-2.419029	1.177537	3.914254
217	1	0	-1.450026	2.233172	2.309266
218	6	0	2.717797	5.685495	-3.098962
219	6	0	4.505668	6.601241	-1.676961
220	6	0	6.967852	3.328183	-1.555992
221	6	0	5.510836	3.524497	-3.474305
222	1	0	5.282557	1.538653	2.057644
223	6	0	6.168282	-0.308852	1.394135
224	6	0	6.028489	-0.738322	-0.971601
225	1	0	5.027683	0.747697	-2.150983
226	6	0	1.013899	4.853243	6.541717
227	6	0	0.148525	4.942029	4.169118
228	6	0	2.796152	3.362452	7.194934
229	6	0	3.885936	1.792821	5.536549
230	1	0	-0.813106	-0.320595	6.510894
231	6	0	-2.243587	0.454461	5.095814
232	1	0	-3.414934	1.342713	3.514742
233	6	0	2.746463	6.859799	-3.855179
234	6	0	1.719373	4.594080	-3.392937
235	6	0	4.503662	7.758569	-2.465942
236	6	0	5.403434	6.497425	-0.469037
237	1	0	7.100422	3.234906	-0.483725
238	6	0	8.078107	3.336440	-2.396981
239	6	0	6.623894	3.528868	-4.314511
240	1	0	4.516207	3.590194	-3.899561
241	1	0	6.496010	-0.591143	2.388658
242	6	0	6.438828	-1.154101	0.305436
243	1	0	6.244439	-1.382063	-1.820092
244	1	0	0.317499	5.650787	6.785739
245	6	0	1.873234	4.357083	7.517561
246	1	0	-0.196071	5.936065	4.465728
247	1	0	-0.738865	4.321659	4.000136
248	1	0	0.676612	5.033811	3.215997
249	1	0	3.484820	2.994321	7.950541

```
250      1       0       3.424805    0.867656    5.171710
251      1       0       4.511529    1.542892    6.397200
252      1       0       4.520878    2.162549    4.726452
253      1       0      -3.105055    0.056436    5.624041
254      1       0       2.054830    6.970904   -4.685811
255      6       0       3.640889    7.885624   -3.550536
256      1       0       2.206795    3.636980   -3.612249
257      1       0       1.091906    4.859358   -4.247634
258      1       0       1.083514    4.424995   -2.519344
259      1       0       5.176960    8.571890   -2.209379
260      1       0       4.886443    6.014920    0.365129
261      1       0       5.722775    7.491187   -0.144537
262      1       0       6.305416    5.913536   -0.684064
263      1       0       9.073064    3.255762   -1.969843
264      6       0       7.909398    3.437368   -3.779412
265      1       0       6.484260    3.603259   -5.388905
266      7       0       7.168460   -2.358744    0.406260
267      1       0       1.838466    4.758420    8.526329
268      1       0       3.650320    8.792501   -4.148337
269      1       0       8.774807    3.442675   -4.435660
270      6       0       7.021332   -3.246404    1.390089
271     30       0       8.701135   -2.842342   -0.763577
272      7       0       7.957924   -4.208778    1.476540
273      6       0       5.856484   -3.275253    2.321627
274      8       0       9.019991   -4.197802    0.606821
275      8       0       8.402269   -3.179237   -2.664884
276      7       0      10.215400   -1.737757   -1.443142
277      6       0       7.902248   -5.401334    2.275498
278      6       0       4.559818   -3.184709    1.789390
279      6       0       6.014248   -3.365696    3.711495
280      7       0       9.455900   -2.669513   -3.378880
281      6       0      10.373507   -1.907878   -2.756722
282      6       0      10.918556   -0.794455   -0.665731
283      6       0       8.814154   -5.523491    3.340813
284      6       0       7.032621   -6.443648    1.913338
285      1       0       4.428927   -3.095936    0.716522
286      6       0       3.447640   -3.198268    2.627736
287      6       0       4.899390   -3.374152    4.549221
288      1       0       7.008442   -3.423759    4.138975
289      6       0       9.530090   -3.193158   -4.714903
290      6       0      11.530368   -1.384244   -3.539552
291      6       0      11.257349   -1.153964    0.649052
292      6       0      11.225791    0.510358   -1.089633
293      6       0       8.787231   -6.698719    4.095739
294      6       0       9.808603   -4.429733    3.639049
295      6       0       7.036554   -7.601817    2.701079
296      6       0       6.136383   -6.341851    0.704097
297      1       0       2.453073   -3.127671    2.198124
298      6       0       3.614536   -3.293229    4.010811
299      1       0       5.037251   -3.443522    5.624175
300      6       0      10.412016   -4.248179   -5.002115
301      6       0       8.620491   -2.697305   -5.667561
302      6       0      11.356760   -0.647503   -4.719306
303      6       0      12.832724   -1.619413   -3.069570
304      6       0      11.899564   -0.263946    1.503708
305      1       0      11.017435   -2.157069    0.990386
306      1       0      10.952731    0.832325   -2.088036
307      6       0      11.856229    1.406106   -0.233128
308      1       0       9.476846   -6.808122    4.928252
309      6       0       7.897072   -7.727178    3.787648
310      1       0       9.317512   -3.471587    3.844823
311      1       0      10.425568   -4.687528    4.503469
312      1       0      10.456358   -4.266715    2.773092
313      1       0       6.366212   -8.416817    2.442163
314      1       0       6.652232   -5.855995   -0.128833
315      1       0       5.821719   -7.336458    0.377706
316      1       0       5.231424   -5.762533    0.918705
317      1       0       2.747620   -3.301969    4.665010
318      6       0      10.422677   -4.753615   -6.308375
319      6       0      11.304787   -4.844436   -3.942131
```

```
320        6        0        8.662323    -3.234906    -6.956375
321        6        0        7.611376    -1.638695    -5.298854
322        1        0       10.357097    -0.449242    -5.088246
323        6        0       12.461865    -0.162390    -5.417824
324        6        0       13.935058    -1.140457    -3.774116
325        1        0       12.974431    -2.174464    -2.148356
326        6        0       12.204787     1.035780     1.074488
327        1        0       12.171300    -0.585669     2.502176
328        1        0       12.073124     2.415628    -0.571824
329        1        0        7.888989    -8.634649     4.384588
330        1        0       11.102157    -5.565444    -6.552948
331        6        0        9.564734    -4.247666    -7.280378
332        1        0       11.624102    -5.848505    -4.233239
333        1        0       12.207379    -4.242553    -3.787438
334        1        0       10.784433    -4.916498    -2.983131
335        1        0        7.973891    -2.859458    -7.708513
336        1        0        8.088418    -0.720943    -4.935905
337        1        0        6.987589    -1.379414    -6.157998
338        1        0        6.971982    -1.997206    -4.487139
339        1        0       12.312343     0.409058    -6.329026
340        6        0       13.752847    -0.409711    -4.949750
341        1        0       14.936304    -1.334494    -3.401644
342        7        0       12.863511     1.990645     1.876349
343        1        0        9.584044    -4.655527    -8.286906
344        1        0       14.612377    -0.032563    -5.495831
345        6        0       13.011596     2.018156     3.236645
346        1        0       13.629121     2.532875     1.462952
347        7        0       14.105553     2.672114     3.624068
348        6        0       11.965350     1.535161     4.158447
349        8        0       14.941984     3.138651     2.715610
350        6        0       14.416464     3.044089     4.987624
351        6        0       12.264644     0.821918     5.330981
352        6        0       10.616224     1.785302     3.844171
353        6        0       13.754697     4.136868     5.566340
354        6        0       15.469600     2.367983     5.625927
355        1        0       13.295684     0.602416     5.580907
356        6        0       11.242754     0.389197     6.174119
357        6        0        9.599465     1.349556     4.689639
358        1        0       10.373973     2.325690     2.935621
359        6        0       14.124435     4.502931     6.866258
360        6        0       12.705096     4.908842     4.805623
361        6        0       15.806727     2.770267     6.921240
362        6        0       16.211823     1.256619     4.924994
363        1        0       11.491968    -0.160260     7.076998
364        6        0        9.908654     0.651270     5.858837
365        1        0        8.564799     1.556812     4.433570
366        1        0       13.623330     5.342718     7.339773
367        6        0       15.132906     3.821437     7.543008
368        1        0       12.545712     5.889924     5.260335
369        1        0       11.742122     4.385451     4.796066
370        1        0       13.014177     5.055148     3.766505
371        1        0       16.612775     2.258510     7.439918
372        1        0       15.606240     0.344172     4.851379
373        1        0       17.128462     1.002415     5.462844
374        1        0       16.462606     1.561573     3.905705
375        1        0        9.115199     0.310626     6.517383
376        1        0       15.409868     4.122854     8.549081
---------------------------------------------------------------
```

Table S15. Atomic coordinates for DFT optimization of **Zn_g4** (theory level: B3LYP/ 6,31-g(d,p) PCM: CH₂Cl₂)

```
                  Standard orientation:
---------------------------------------------------------------------
Center     Atomic      Atomic          Coordinates (Angstroms)
Number     Number      Type         X           Y           Z
---------------------------------------------------------------------
   1          6           0      -1.354459    4.118025   -0.922689
   2          6           0      -0.313417    3.201487   -1.146473
   3          6           0       0.833661    3.216279   -0.355199
   4          6           0       0.985922    4.134298    0.696506
   5          6           0      -0.057521    5.049887    0.920549
   6          6           0      -1.205189    5.032696    0.132908
   7          7           0      -2.573304    4.115634   -1.642980
   8          7           0       2.203169    4.160121    1.416690
   9          6           0       2.253863    4.328461    2.741156
  10          7           0       3.442876    4.661067    3.268113
  11          6           0       1.111374    4.048629    3.660760
  12          6           0      -2.646511    4.097783   -2.972463
  13          7           0      -3.867976    3.955827   -3.514236
  14          6           0      -1.482420    4.306530   -3.883673
  15          8           0      -4.966075    3.826255   -2.696820
  16          6           0       3.789344    4.736964    4.661284
  17          8           0       4.519886    4.852195    2.441233
  18          6           0      -4.219491    4.084127   -4.902146
  19          6           0      -0.727006    5.483400   -3.763157
  20          6           0       0.349436    5.719228   -4.616664
  21          6           0       0.696876    4.775233   -5.586079
  22          6           0      -0.035761    3.592020   -5.695491
  23          6           0      -1.121383    3.359298   -4.851254
  24          6           0       0.667560    4.971952    4.617289
  25          6           0      -0.384172    4.648822    5.474647
  26          6           0      -1.002270    3.399684    5.390031
  27          6           0      -0.573073    2.477548    4.432309
  28          6           0       0.471652    2.801379    3.568170
  29          6           0      -4.557941    2.916728   -5.611412
  30          6           0      -4.945094    3.051993   -6.948587
  31          6           0      -5.010324    4.307778   -7.551798
  32          6           0      -4.714126    5.452532   -6.815488
  33          6           0      -4.328612    5.365024   -5.471685
  34          6           0       3.978812    6.012959    5.224990
  35          6           0       4.364109    6.085047    6.567090
  36          6           0       4.572144    4.926155    7.315519
  37          6           0       4.420008    3.675204    6.722364
  38          6           0       4.040235    3.555588    5.379110
  39          6           0      -4.511195    1.559065   -4.953492
  40          6           0      -4.058622    6.613929   -4.669333
  41          6           0       3.925928    2.198789    4.730374
  42          6           0       3.783347    7.264363    4.404339
  43         30           0      -4.408308    3.971610   -0.827951
  44         30           0       4.039764    4.306664    0.616662
  45          6           0      -5.021009   -1.479569   -0.120516
  46          6           0      -4.050546   -0.635505   -0.678314
  47          6           0      -4.017289    0.720306   -0.365647
  48          6           0      -4.963175    1.301775    0.499893
  49          6           0      -5.930388    0.448818    1.064208
  50          6           0      -5.939399   -0.915125    0.774689
  51          7           0      -5.028599   -2.878282   -0.387205
  52          7           0      -4.926037    2.705236    0.648672
  53          6           0      -5.405853    3.384863    1.694190
  54          7           0      -5.526884    4.714876    1.549948
  55          6           0      -5.695004    2.794331    3.035878
  56          6           0      -5.610158   -3.386465   -1.470209
  57          7           0      -5.457691   -4.704276   -1.691343
  58          6           0      -6.395812   -2.587515   -2.458585
  59          8           0      -4.701597   -5.454858   -0.816964
  60          6           0      -5.966298    5.660712    2.540687
  61          8           0      -5.182086    5.312768    0.364605
```

62	6	0	-6.187551	-5.506721	-2.634311
63	6	0	-7.545847	-1.888843	-2.059555
64	6	0	-8.271429	-1.137846	-2.983893
65	6	0	-7.853958	-1.066607	-4.314232
66	6	0	-6.703815	-1.748545	-4.716141
67	6	0	-5.978067	-2.502577	-3.794210
68	6	0	-6.960954	2.867777	3.633060
69	6	0	-7.180153	2.305742	4.890876
70	6	0	-6.136533	1.673742	5.569508
71	6	0	-4.872862	1.595536	4.979475
72	6	0	-4.653951	2.143472	3.715982
73	6	0	-5.486704	-6.062969	-3.721173
74	6	0	-6.191671	-6.880165	-4.610137
75	6	0	-7.545961	-7.150892	-4.414928
76	6	0	-8.207595	-6.627805	-3.307078
77	6	0	-7.538732	-5.810426	-2.386270
78	6	0	-7.270448	6.179109	2.420465
79	6	0	-7.680333	7.141340	3.348057
80	6	0	-6.815802	7.585078	4.349159
81	6	0	-5.518004	7.085845	4.422389
82	6	0	-5.061767	6.124284	3.510758
83	6	0	-4.015471	-5.798134	-3.921905
84	6	0	-8.259440	-5.297461	-1.163856
85	6	0	-3.642679	5.620074	3.578654
86	6	0	-8.198162	5.716391	1.323309
87	30	0	-4.039814	-4.306781	0.616686
88	6	0	5.021001	1.479464	-0.120550
89	6	0	4.050593	0.635382	-0.678423
90	6	0	4.017338	-0.720434	-0.365769
91	6	0	4.963174	-1.301888	0.499838
92	6	0	5.930334	-0.448917	1.064216
93	6	0	5.939336	0.915031	0.774715
94	7	0	5.028581	2.878187	-0.387199
95	7	0	4.926105	-2.705351	0.648587
96	6	0	5.405912	-3.384960	1.694117
97	7	0	5.527000	-4.714971	1.549881
98	6	0	5.695015	-2.794412	3.035815
99	6	0	5.610158	3.386402	-1.470189
100	7	0	5.457654	4.704209	-1.691312
101	6	0	6.395941	2.587512	-2.458509
102	8	0	4.701501	5.454752	-0.816961
103	6	0	5.966341	-5.660818	2.540643
104	8	0	5.182144	-5.312905	0.364565
105	6	0	6.187502	5.506704	-2.634254
106	6	0	7.545957	1.888868	-2.059361
107	6	0	8.271697	1.137954	-2.983640
108	6	0	7.854413	1.066775	-4.314041
109	6	0	6.704295	1.748685	-4.716069
110	6	0	5.978385	2.502631	-3.794194
111	6	0	6.960950	-2.867810	3.633035
112	6	0	7.180095	-2.305759	4.890852
113	6	0	6.136440	-1.673771	5.569444
114	6	0	4.872788	-1.595607	4.979373
115	6	0	4.653928	-2.143575	3.715884
116	6	0	5.486686	6.062799	-3.721207
117	6	0	6.191633	6.880032	-4.610157
118	6	0	7.545867	7.150945	-4.414834
119	6	0	8.207466	6.628010	-3.306887
120	6	0	7.538623	5.810597	-2.386099
121	6	0	7.270449	-6.179321	2.420422
122	6	0	7.680273	-7.141552	3.348040
123	6	0	6.815715	-7.585195	4.349160
124	6	0	5.517951	-7.085875	4.422383
125	6	0	5.061778	-6.124310	3.510726
126	6	0	4.015509	5.797751	-3.922054
127	6	0	8.259278	5.297783	-1.163591
128	6	0	3.642727	-5.619997	3.578598
129	6	0	8.198171	-5.716733	1.323211
130	30	0	4.408352	-3.971789	-0.827989
131	6	0	1.354433	-4.118097	-0.922714

```
132        6          0        0.313368    -3.201594    -1.146504
133        6          0       -0.833704    -3.216412    -0.355217
134        6          0       -0.985939    -4.134420     0.696497
135        6          0        0.057523    -5.049994     0.920536
136        6          0        1.205183    -5.032775     0.132887
137        7          0        2.573280    -4.115698    -1.642998
138        7          0       -2.203191    -4.160248     1.416681
139        6          0       -2.253908    -4.328477     2.741162
140        7          0       -3.442941    -4.660974     3.268141
141        6          0       -1.111410    -4.048604     3.660749
142        6          0        2.646493    -4.097775    -2.972467
143        7          0        3.867991    -3.955964    -3.514227
144        6          0        1.482407    -4.306304    -3.883726
145        8          0        4.966112    -3.826593    -2.696794
146        6          0       -3.789361    -4.736867     4.661317
147        8          0       -4.519953    -4.852155     2.441256
148        6          0        4.219486    -4.084126    -4.902149
149        6          0        0.726910    -5.483134    -3.763385
150        6          0       -0.349602    -5.718722    -4.616870
151        6          0       -0.697042    -4.774513    -5.586074
152        6          0        0.035694    -3.591344    -5.695322
153        6          0        1.121392    -3.358864    -4.851114
154        6          0       -0.667604    -4.971876     4.617331
155        6          0        0.384166    -4.648731     5.474635
156        6          0        1.002323    -3.399631     5.389902
157        6          0        0.573133    -2.477544     4.432130
158        6          0       -0.471644    -2.801385     3.568058
159        6          0        4.558095    -2.916686    -5.611271
160        6          0        4.945223    -3.051841    -6.948465
161        6          0        5.010266    -4.307561    -7.551838
162        6          0        4.713900    -5.452361    -6.815669
163        6          0        4.328409    -5.364962    -5.471851
164        6          0       -3.978964    -6.012849     5.225007
165        6          0       -4.364194    -6.084913     6.567127
166        6          0       -4.572035    -4.926009     7.315591
167        6          0       -4.419784    -3.675065     6.722454
168        6          0       -4.040079    -3.555472     5.379177
169        6          0        4.511538    -1.559094    -4.953192
170        6          0        4.058221    -6.613928    -4.669659
171        6          0       -3.925626    -2.198675     4.730463
172        6          0       -3.783734    -7.264257     4.404308
173        1          0       -0.406344     2.466197    -1.939031
174        1          0        1.623572     2.493245    -0.534102
175        1          0        0.038117     5.792427     1.705474
176        1          0       -1.997874     5.752684     0.314959
177        1          0       -0.987972     6.212851    -3.003735
178        1          0        0.916106     6.640024    -4.522619
179        1          0        1.535980     4.960008    -6.249762
180        1          0        0.234587     2.849297    -6.439839
181        1          0       -1.683888     2.436982    -4.939096
182        1          0        1.137559     5.945702     4.689231
183        1          0       -0.718381     5.373989     6.210172
184        1          0       -1.815875     3.148112     6.063391
185        1          0       -1.047818     1.503667     4.359696
186        1          0        0.800866     2.087167     2.820830
187        1          0       -5.204810     2.162752    -7.516308
188        1          0       -5.314140     4.394998    -8.590916
189        1          0       -4.798000     6.432304    -7.277446
190        1          0        4.508075     7.060193     7.023793
191        1          0        4.872677     4.999784     8.356600
192        1          0        4.613871     2.774377     7.298030
193        1          0       -4.889598     1.607995    -3.930253
194        1          0       -5.112125     0.838966    -5.513613
195        1          0       -3.489170     1.162770    -4.907750
196        1          0       -2.986388     6.832704    -4.614778
197        1          0       -4.547763     7.476510    -5.128830
198        1          0       -4.427314     6.514563    -3.644849
199        1          0        4.489814     1.454505     5.297237
200        1          0        2.884183     1.861449     4.681688
201        1          0        4.313934     2.212523     3.708291
```

```
202       1          0          2.725782     7.443728     4.175733
203       1          0          4.158036     8.140111     4.939390
204       1          0          4.306248     7.179611     3.448375
205       1          0         -3.321993    -1.047270    -1.370284
206       1          0         -3.251644     1.352813    -0.804671
207       1          0         -6.696648     0.847546     1.716658
208       1          0         -6.692374    -1.552984     1.228433
209       1          0         -7.874874    -1.936742    -1.028159
210       1          0         -9.162700    -0.607795    -2.662658
211       1          0         -8.419696    -0.480748    -5.032186
212       1          0         -6.370291    -1.696096    -5.748108
213       1          0         -5.079091    -3.020203    -4.109045
214       1          0         -7.778191     3.352824     3.111823
215       1          0         -8.166650     2.364328     5.340207
216       1          0         -6.307275     1.243636     6.551684
217       1          0         -4.055555     1.108348     5.502256
218       1          0         -3.673156     2.079180     3.256169
219       1          0         -5.667886    -7.312620    -5.458148
220       1          0         -8.078667    -7.788392    -5.114542
221       1          0         -9.253336    -6.867842    -3.135728
222       1          0         -8.684590     7.549527     3.277030
223       1          0         -7.149562     8.334850     5.060538
224       1          0         -4.836740     7.454277     5.184361
225       1          0         -3.480336    -5.846001    -2.971055
226       1          0         -3.586315    -6.531490    -4.609137
227       1          0         -3.832065    -4.805419    -4.349850
228       1          0         -8.666591    -4.293895    -1.329740
229       1          0         -9.097222    -5.953076    -0.912758
230       1          0         -7.593127    -5.245513    -0.299005
231       1          0         -3.576043     4.678987     4.134915
232       1          0         -3.232908     5.436584     2.582283
233       1          0         -3.001656     6.345159     4.086186
234       1          0         -7.670295     5.667641     0.367927
235       1          0         -8.600200     4.715542     1.523114
236       1          0         -9.048217     6.395911     1.225480
237       1          0          3.322076     1.047140    -1.370435
238       1          0          3.251738    -1.352954    -0.804856
239       1          0          6.696576    -0.847627     1.716697
240       1          0          6.692274     1.552891     1.228518
241       1          0          7.874837     1.936730    -1.027917
242       1          0          9.162946     0.607923    -2.662313
243       1          0          8.420279     0.480988    -5.031954
244       1          0          6.370917     1.696281    -5.748086
245       1          0          5.079431     3.020235    -4.109126
246       1          0          7.778215    -3.352836     3.111829
247       1          0          8.166576    -2.364318     5.340220
248       1          0          6.307151    -1.243644     6.551617
249       1          0          4.055458    -1.108408     5.502109
250       1          0          3.673139    -2.079316     3.256053
251       1          0          5.667871     7.312363    -5.458245
252       1          0          8.078557     7.788472    -5.114435
253       1          0          9.253159     6.868196    -3.135454
254       1          0          8.684491    -7.549830     3.277008
255       1          0          7.149422    -8.334977     5.060554
256       1          0          4.836666    -7.454242     5.184369
257       1          0          3.480293     5.845529    -2.971244
258       1          0          3.586280     6.531050    -4.609301
259       1          0          3.832281     4.805013    -4.350026
260       1          0          9.096983     5.953486    -0.912469
261       1          0          7.592899     5.245833    -0.298792
262       1          0          8.666527     4.294240    -1.329379
263       1          0          3.576157    -4.678908     4.134861
264       1          0          3.232997    -5.436475     2.582218
265       1          0          3.001635    -6.345031     4.086112
266       1          0          8.600541    -4.716034     1.523099
267       1          0          9.048012    -6.396494     1.225195
268       1          0          7.670222    -5.667718     0.367889
269       1          0          0.406265    -2.466302    -1.939064
270       1          0         -1.623641    -2.493406    -0.534115
271       1          0         -0.038090    -5.792528     1.705467
```

```
272          1          0        1.997890    -5.752742     0.314919
273          1          0        0.987862    -6.212746    -3.004112
274          1          0       -0.916328    -6.639496    -4.522954
275          1          0       -1.536231    -4.959078    -6.249710
276          1          0       -0.234643    -2.848462    -6.439515
277          1          0        1.683968    -2.436579    -4.938828
278          1          0       -1.137641    -5.945600     4.689361
279          1          0        0.718367    -5.373860     6.210201
280          1          0        1.815979    -3.148061     6.063201
281          1          0        1.047934    -1.503696     4.359424
282          1          0       -0.800857    -2.087208     2.820684
283          1          0        5.205063    -2.162566    -7.516075
284          1          0        5.314057    -4.394694    -8.590970
285          1          0        4.797615    -6.432090    -7.277749
286          1          0       -4.508277    -7.060047     7.023820
287          1          0       -4.872522    -4.999626     8.356686
288          1          0       -4.613501    -2.774225     7.298148
289          1          0        4.889903    -1.608199    -3.929947
290          1          0        5.112592    -0.839024    -5.513212
291          1          0        3.489574    -1.162644    -4.907438
292          1          0        2.985955    -6.832561    -4.615144
293          1          0        4.547247    -7.476521    -5.129256
294          1          0        4.426914    -6.514741    -3.645158
295          1          0       -4.489391    -1.454322     5.297357
296          1          0       -2.883836    -1.861474     4.681748
297          1          0       -4.313663    -2.212341     3.708392
298          1          0       -2.726169    -7.443989     4.175982
299          1          0       -4.158870    -8.139911     4.939201
300          1          0       -4.306362    -7.179260     3.448218
------------------------------------------------------------------
```

X-Ray diffraction measurements and structure determination

Crystallographic data for the solid state structures presented herein were collected at 100 K or 150 K, from single crystal samples, which were mounted on a loop fiber. The data were collected using using a Bruker Microstar diffractometer equipped with a Platinum 135 CCD Detector, Helios optics and a Kappa goniometer. The initial unit cell parameters were determined by a least-squares fit of the angular setting of strong reflections, collected by a 10.0 degree scan in 33 frames over three different parts of the reciprocal space (99 frames total). For determination of cell parameters, cell refinement and data reduction APEX2 was used.[13] Absorption corrections were applied using SADABS.[14] Structure solution was performed using direct methods with SHELXS97 and refined on F^2 by full-matrix least squares using SHELXL97.[15] All non-H atoms were refined by full-matrix least-squares with anisotropic displacement parameters. The H-atoms were included in calculated positions and treated as riding atoms: aromatic C—H 0.95 Å, methyl C—H 0.98 Å, with $U_{iso}(H) = k \times U_{eq}$ (parent C-atom), where k = 1.2 for the aromatic H-atoms and 1.5 for the methyl H-atoms. The following software were used to prepare material and generate the figures: PLATON, UdMX, Mercury, and OLEX2.[16], [17], [18] [19]

The crystal structure determination and refinement data for **D1** (co-crystallized DCM solvent) (C79H62Br4Cl6N8O4Zn2) are given in Tables S16 - S18.

CCXXII

Table S16. Crystal data and structure refinement for **D1** (C79H62Br4Cl6N8O4Zn2)

Identification code	jana29
Empirical formula	C79 H62 Br4 Cl6 N8 O4 Zn2
Formula weight	1850.45
Temperature	150K
Wavelength	1.54178 Å
Crystal system	Monoclinic
Space group	P21/c
Unit cell dimensions	a = 10.6205(2) Å α = 90°
	b = 19.7985(4) Å β = 90.758(1)°
	c = 18.0287(4) Å γ = 90°
Volume	3790.56(13) Å^3
Z	2
Density (calculated)	1.621 g/cm^3
Absorption coefficient	5.644 mm^{-1}
F(000)	1852
Crystal size	0.19 x 0.17 x 0.16 mm
Theta range for data collection	3.32 to 72.51°
Index ranges	$-13 \leq h \leq 12$, $-24 \leq k \leq 24$, $-21 \leq l \leq 22$
Reflections collected	49126
Independent reflections	7289 [R_{int} = 0.031]
Absorption correction	Multi-scan
Max. and min. transmission	0.4053 and 0.3388
Refinement method	Full-matrix least-squares on F^2
Data / restraints / parameters	7289 / 0 / 479
Goodness-of-fit on F^2	1.053
Final R indices [I>2sigma(I)]	R_1 = 0.0364, wR_2 = 0.0979
R indices (all data)	R_1 = 0.0378, wR_2 = 0.0990
Extinction coefficient	0.00100(5)
Largest diff. peak and hole	2.498 and -0.806 e/Å^3

Table S17. Bond lengths [Å] and angles [°] for **D1** (C79H62Br4Cl6N8O4Zn2)

_____

Zn(1)-O(1)	1.9964(17)	C(27)-C(28)	1.401(4)
Zn(1)-N(4)	2.073(2)	C(28)-C(29)	1.383(4)
Zn(1)-N(2)	2.075(2)	C(28)-H(28)	0.9500
Zn(1)-O(10)#1	2.0759(17)	C(29)-C(30)	1.385(5)
Zn(1)-O(10)	2.1516(17)	C(29)-H(29)	0.9500
Zn(1)-Zn(1)#1	3.0915(6)	C(30)-C(31)	1.385(5)
Br(1)-C(5)	1.906(2)	C(30)-H(30)	0.9500
Br(2)-C(24)	1.906(2)	C(31)-C(32)	1.394(4)
O(1)-N(1)	1.378(2)	C(31)-H(31)	0.9500
O(10)-N(3)	1.392(2)	C(32)-H(32)	0.9500
O(10)-Zn(1)#1	2.0759(17)	C(33)-C(38)	1.387(4)
N(1)-C(1)	1.334(3)	C(33)-C(34)	1.394(3)
N(1)-C(8)	1.431(3)	C(34)-C(35)	1.393(4)
N(2)-C(1)	1.318(3)	C(34)-H(34)	0.9500
N(2)-C(14)	1.423(3)	C(35)-C(36)	1.384(4)
N(3)-C(20)	1.348(3)	C(35)-H(35)	0.9500
N(3)-C(27)	1.422(3)	C(36)-C(37)	1.391(4)
N(4)-C(20)#1	1.314(3)	C(36)-H(36)	0.9500
N(4)-C(33)	1.419(3)	C(37)-C(38)	1.392(4)
C(1)-C(2)	1.498(3)	C(37)-H(37)	0.9500
C(2)-C(3)	1.393(4)	C(38)-H(38)	0.9500
C(2)-C(7)	1.393(4)	C(01)-Cl(1B)	1.755(4)
C(3)-C(4)	1.389(4)	C(01)-Cl(1A)	1.762(4)
C(3)-H(3)	0.9500	C(01)-H(01A)	0.9900
C(4)-C(5)	1.380(4)	C(01)-H(01B)	0.9900
C(4)-H(4)	0.9500	C(02)-Cl(2B)	1.402(10)
C(5)-C(6)	1.385(4)	C(02)-Cl(2A)	1.672(10)
C(6)-C(7)	1.394(4)	C(02)-H(02A)	0.9900
C(6)-H(6)	0.9500	C(02)-H(02B)	0.9900
C(7)-H(7)	0.9500		
C(8)-C(9)	1.385(4)	O(1)-Zn(1)-N(4)	150.78(8)
C(8)-C(13)	1.389(4)	O(1)-Zn(1)-N(2)	79.58(7)
C(9)-C(10)	1.399(4)	N(4)-Zn(1)-N(2)	99.36(8)
C(9)-H(9)	0.9500	O(1)-Zn(1)-O(10)#1	131.05(7)
		N(4)-Zn(1)-O(10)#1	76.92(7)
C(10)-C(11)	1.386(4)	N(2)-Zn(1)-O(10)#1	111.16(7)
C(10)-H(10)	0.9500	O(1)-Zn(1)-O(10)	87.41(6)
C(11)-C(12)	1.381(4)	N(4)-Zn(1)-O(10)	86.42(7)
C(11)-H(11)	0.9500	N(2)-Zn(1)-O(10)	162.66(7)
C(12)-C(13)	1.392(4)	O(10)#1-Zn(1)-O(10)	86.03(7)
C(12)-H(12)	0.9500	O(1)-Zn(1)-Zn(1)#1	114.17(5)
C(13)-H(13)	0.9500	N(4)-Zn(1)-Zn(1)#1	78.72(6)
C(14)-C(19)	1.395(4)	N(2)-Zn(1)-Zn(1)#1	155.05(6)
C(14)-C(15)	1.396(4)	O(10)#1-Zn(1)-Zn(1)#1	43.97(5)
C(15)-C(16)	1.386(4)	O(10)-Zn(1)-Zn(1)#1	42.06(4)
C(15)-H(15)	0.9500	N(1)-O(1)-Zn(1)	111.71(13)
C(16)-C(17)	1.387(5)	N(3)-O(10)-Zn(1)#1	107.04(12)
C(16)-H(16)	0.9500	N(3)-O(10)-Zn(1)	112.73(12)
C(17)-C(18)	1.385(5)	Zn(1)#1-O(10)-Zn(1)	93.97(7)
C(17)-H(17)	0.9500	C(1)-N(1)-O(1)	119.01(19)
C(18)-C(19)	1.393(4)	C(1)-N(1)-C(8)	127.2(2)
C(18)-H(18)	0.9500	O(1)-N(1)-C(8)	113.81(18)
C(19)-H(19)	0.9500	C(1)-N(2)-C(14)	120.4(2)
C(20)-N(4)#1	1.314(3)	C(1)-N(2)-Zn(1)	112.31(15)
C(20)-C(21)	1.489(3)	C(14)-N(2)-Zn(1)	125.57(15)
C(21)-C(26)	1.393(3)	C(20)-N(3)-O(10)	116.33(18)
C(21)-C(22)	1.404(3)	C(20)-N(3)-C(27)	129.1(2)
C(22)-C(23)	1.386(3)	O(10)-N(3)-C(27)	114.58(18)
C(22)-H(22)	0.9500	C(20)#1-N(4)-C(33)	122.7(2)
C(23)-C(24)	1.389(3)	C(20)#1-N(4)-Zn(1)	111.81(16)
C(23)-H(23)	0.9500	C(33)-N(4)-Zn(1)	125.46(15)
C(24)-C(25)	1.390(3)	N(2)-C(1)-N(1)	117.2(2)
C(25)-C(26)	1.388(3)	N(2)-C(1)-C(2)	123.8(2)
C(25)-H(25)	0.9500	N(1)-C(1)-C(2)	119.0(2)
C(26)-H(26)	0.9500	C(3)-C(2)-C(7)	119.6(2)
C(27)-C(32)	1.389(4)	C(3)-C(2)-C(1)	118.9(2)

C(7)-C(2)-C(1)	121.5(2)		C(22)-C(23)-C(24)	119.0(2)
C(4)-C(3)-C(2)	120.6(2)		C(22)-C(23)-H(23)	120.5
C(4)-C(3)-H(3)	119.7		C(24)-C(23)-H(23)	120.5
C(2)-C(3)-H(3)	119.7		C(23)-C(24)-C(25)	121.8(2)
C(5)-C(4)-C(3)	118.8(2)		C(23)-C(24)-Br(2)	118.58(18)
C(5)-C(4)-H(4)	120.6		C(25)-C(24)-Br(2)	119.65(18)
C(3)-C(4)-H(4)	120.6		C(26)-C(25)-C(24)	118.9(2)
C(4)-C(5)-C(6)	122.0(2)		C(26)-C(25)-H(25)	120.5
C(4)-C(5)-Br(1)	118.4(2)		C(24)-C(25)-H(25)	120.5
C(6)-C(5)-Br(1)	119.5(2)		C(25)-C(26)-C(21)	120.3(2)
C(5)-C(6)-C(7)	118.8(2)		C(25)-C(26)-H(26)	119.8
C(5)-C(6)-H(6)	120.6		C(21)-C(26)-H(26)	119.8
C(7)-C(6)-H(6)	120.6		C(32)-C(27)-C(28)	120.0(2)
C(2)-C(7)-C(6)	120.2(2)		C(32)-C(27)-N(3)	121.8(2)
C(2)-C(7)-H(7)	119.9		C(28)-C(27)-N(3)	118.1(2)
C(6)-C(7)-H(7)	119.9		C(29)-C(28)-C(27)	119.6(3)
C(9)-C(8)-C(13)	120.8(2)		C(29)-C(28)-H(28)	120.2
C(9)-C(8)-N(1)	120.9(2)		C(27)-C(28)-H(28)	120.2
C(13)-C(8)-N(1)	118.3(2)		C(28)-C(29)-C(30)	120.7(3)
C(8)-C(9)-C(10)	119.1(2)		C(28)-C(29)-H(29)	119.7
C(8)-C(9)-H(9)	120.4		C(30)-C(29)-H(29)	119.7
C(10)-C(9)-H(9)	120.4		C(31)-C(30)-C(29)	119.7(3)
C(11)-C(10)-C(9)	120.4(3)		C(31)-C(30)-H(30)	120.1
C(11)-C(10)-H(10)	119.8		C(29)-C(30)-H(30)	120.1
C(9)-C(10)-H(10)	119.8		C(30)-C(31)-C(32)	120.5(3)
C(12)-C(11)-C(10)	119.8(2)		C(30)-C(31)-H(31)	119.7
C(12)-C(11)-H(11)	120.1		C(32)-C(31)-H(31)	119.7
C(10)-C(11)-H(11)	120.1		C(27)-C(32)-C(31)	119.5(3)
C(11)-C(12)-C(13)	120.6(3)		C(27)-C(32)-H(32)	120.2
C(11)-C(12)-H(12)	119.7		C(31)-C(32)-H(32)	120.2
C(13)-C(12)-H(12)	119.7		C(38)-C(33)-C(34)	119.4(2)
C(8)-C(13)-C(12)	119.3(2)		C(38)-C(33)-N(4)	118.4(2)
C(8)-C(13)-H(13)	120.3		C(34)-C(33)-N(4)	122.0(2)
C(12)-C(13)-H(13)	120.3		C(35)-C(34)-C(33)	119.8(3)
C(19)-C(14)-C(15)	119.2(2)		C(35)-C(34)-H(34)	120.1
C(19)-C(14)-N(2)	119.1(2)		C(33)-C(34)-H(34)	120.1
C(15)-C(14)-N(2)	121.6(2)		C(36)-C(35)-C(34)	120.9(3)
C(16)-C(15)-C(14)	120.6(3)		C(36)-C(35)-H(35)	119.5
C(16)-C(15)-H(15)	119.7		C(34)-C(35)-H(35)	119.5
C(14)-C(15)-H(15)	119.7		C(35)-C(36)-C(37)	119.0(3)
C(15)-C(16)-C(17)	120.2(3)		C(35)-C(36)-H(36)	120.5
C(15)-C(16)-H(16)	119.9		C(37)-C(36)-H(36)	120.5
C(17)-C(16)-H(16)	119.9		C(36)-C(37)-C(38)	120.4(3)
C(18)-C(17)-C(16)	119.5(3)		C(36)-C(37)-H(37)	119.8
C(18)-C(17)-H(17)	120.2		C(38)-C(37)-H(37)	119.8
C(16)-C(17)-H(17)	120.2		C(33)-C(38)-C(37)	120.4(2)
C(17)-C(18)-C(19)	120.8(3)		C(33)-C(38)-H(38)	119.8
C(17)-C(18)-H(18)	119.6		C(37)-C(38)-H(38)	119.8
C(19)-C(18)-H(18)	119.6		Cl(1B)-C(01)-Cl(1A)	112.1(2)
C(18)-C(19)-C(14)	119.8(3)		Cl(1B)-C(01)-H(01A)	109.2
C(18)-C(19)-H(19)	120.1		Cl(1A)-C(01)-H(01A)	109.2
C(14)-C(19)-H(19)	120.1		Cl(1B)-C(01)-H(01B)	109.2
N(4)#1-C(20)-N(3)	117.2(2)		Cl(1A)-C(01)-H(01B)	109.2
N(4)#1-C(20)-C(21)	122.7(2)		H(01A)-C(01)-H(01B)	107.9
N(3)-C(20)-C(21)	120.1(2)		Cl(2B)-C(02)-Cl(2A)	140.5(6)
C(26)-C(21)-C(22)	119.8(2)		Cl(2B)-C(02)-H(02A)	101.9
C(26)-C(21)-C(20)	120.6(2)		Cl(2A)-C(02)-H(02A)	101.9
C(22)-C(21)-C(20)	119.4(2)		Cl(2B)-C(02)-H(02B)	101.9
C(23)-C(22)-C(21)	120.1(2)		Cl(2A)-C(02)-H(02B)	101.9
C(23)-C(22)-H(22)	119.9		H(02A)-C(02)-H(02B)	104.7
C(21)-C(22)-H(22)	119.9			

_____

Symmetry transformations used to generate equivalent atoms: #1 -x+2,-y+1,-z+2

Table S18. Torsion angles [°] for **D1** (C79H62Br4Cl6N8O4Zn2)

N(4)-Zn(1)-O(1)-N(1)	-92.8(2)		C(1)-N(1)-C(8)-C(13)	125.5(3)
N(2)-Zn(1)-O(1)-N(1)	-2.26(15)		O(1)-N(1)-C(8)-C(13)	-53.4(3)
O(10)#1-Zn(1)-O(1)-N(1)	106.79(16)		C(13)-C(8)-C(9)-C(10)	-1.6(4)
O(10)-Zn(1)-O(1)-N(1)	-170.76(16)		N(1)-C(8)-C(9)-C(10)	-179.2(2)
Zn(1)#1-Zn(1)-O(1)-N(1)	155.86(13)		C(8)-C(9)-C(10)-C(11)	1.6(4)
O(1)-Zn(1)-O(10)-N(3)	-21.13(14)		C(9)-C(10)-C(11)-C(12)	-1.1(4)
N(4)-Zn(1)-O(10)-N(3)	-172.55(14)		C(10)-C(11)-C(12)-C(13)	0.7(4)
N(2)-Zn(1)-O(10)-N(3)	-62.3(3)		C(9)-C(8)-C(13)-C(12)	1.2(4)
O(10)#1-Zn(1)-O(10)-N(3)	110.33(15)		N(1)-C(8)-C(13)-C(12)	178.8(2)
Zn(1)#1-Zn(1)-O(10)-N(3)	110.33(15)		C(11)-C(12)-C(13)-C(8)	-0.7(4)
O(1)-Zn(1)-O(10)-Zn(1)#1	-131.46(8)		C(1)-N(2)-C(14)-C(19)	128.6(2)
N(4)-Zn(1)-O(10)-Zn(1)#1	77.11(7)		Zn(1)-N(2)-C(14)-C(19)	-67.7(3)
N(2)-Zn(1)-O(10)-Zn(1)#1	-172.6(2)		C(1)-N(2)-C(14)-C(15)	-55.3(3)
O(10)#1-Zn(1)-O(10)-Zn(1)#1	0.0		Zn(1)-N(2)-C(14)-C(15)	108.4(2)
Zn(1)-O(1)-N(1)-C(1)	4.5(3)		C(19)-C(14)-C(15)-C(16)	-0.8(4)
Zn(1)-O(1)-N(1)-C(8)	-176.54(16)		N(2)-C(14)-C(15)-C(16)	-176.9(2)
O(1)-Zn(1)-N(2)-C(1)	0.03(17)		C(14)-C(15)-C(16)-C(17)	-0.1(4)
N(4)-Zn(1)-N(2)-C(1)	150.37(17)		C(15)-C(16)-C(17)-C(18)	0.7(4)
O(10)#1-Zn(1)-N(2)-C(1)	-130.13(16)		C(16)-C(17)-C(18)-C(19)	-0.4(4)
O(10)-Zn(1)-N(2)-C(1)	42.0(3)		C(17)-C(18)-C(19)-C(14)	-0.6(4)
Zn(1)#1-Zn(1)-N(2)-C(1)	-126.26(16)		C(15)-C(14)-C(19)-C(18)	1.2(4)
O(1)-Zn(1)-N(2)-C(14)	-164.7(2)		N(2)-C(14)-C(19)-C(18)	177.3(2)
N(4)-Zn(1)-N(2)-C(14)	-14.4(2)		O(10)-N(3)-C(20)-N(4)#1	-12.5(3)
O(10)#1-Zn(1)-N(2)-C(14)	65.1(2)		C(27)-N(3)-C(20)-N(4)#1	168.2(2)
O(10)-Zn(1)-N(2)-C(14)	-122.8(2)		O(10)-N(3)-C(20)-C(21)	167.30(19)
Zn(1)#1-Zn(1)-N(2)-C(14)	69.0(3)		C(27)-N(3)-C(20)-C(21)	-12.0(4)
Zn(1)#1-O(10)-N(3)-C(20)	31.1(2)		N(4)#1-C(20)-C(21)-C(26)	121.6(3)
Zn(1)-O(10)-N(3)-C(20)	-70.8(2)		N(3)-C(20)-C(21)-C(26)	-58.2(3)
Zn(1)#1-O(10)-N(3)-C(27)	-149.48(16)		N(4)#1-C(20)-C(21)-C(22)	-55.0(3)
Zn(1)-O(10)-N(3)-C(27)	108.58(18)		N(3)-C(20)-C(21)-C(22)	125.2(2)
O(1)-Zn(1)-N(4)-C(20)#1	171.70(15)		C(26)-C(21)-C(22)-C(23)	0.9(4)
N(2)-Zn(1)-N(4)-C(20)#1	86.34(17)		C(20)-C(21)-C(22)-C(23)	177.5(2)
O(10)#1-Zn(1)-N(4)-C(20)#	-23.37(16)		C(21)-C(22)-C(23)-C(24)	-1.1(4)
O(10)-Zn(1)-N(4)-C(20)#1	-110.12(16)		C(22)-C(23)-C(24)-C(25)	0.4(4)
Zn(1)#1-Zn(1)-N(4)-C(20)#	-68.37(15)		C(22)-C(23)-C(24)-Br(2)	-179.89(18)
O(1)-Zn(1)-N(4)-C(33)	-10.1(3)		C(23)-C(24)-C(25)-C(26)	0.6(4)
N(2)-Zn(1)-N(4)-C(33)	-95.51(19)		Br(2)-C(24)-C(25)-C(26)	-179.19(18)
O(10)#1-Zn(1)-N(4)-C(33)	154.8(2)			
O(10)-Zn(1)-N(4)-C(33)	68.04(19)		C(24)-C(25)-C(26)-C(21)	-0.8(4)
Zn(1)#1-Zn(1)-N(4)-C(33)	109.78(19)		C(22)-C(21)-C(26)-C(25)	0.1(4)
C(14)-N(2)-C(1)-N(1)	168.1(2)		C(20)-C(21)-C(26)-C(25)	-176.5(2)
Zn(1)-N(2)-C(1)-N(1)	2.4(3)		C(20)-N(3)-C(27)-C(32)	-37.1(4)
C(14)-N(2)-C(1)-C(2)	-14.3(4)		O(10)-N(3)-C(27)-C(32)	143.6(2)
Zn(1)-N(2)-C(1)-C(2)	-179.96(18)		C(20)-N(3)-C(27)-C(28)	146.4(2)
O(1)-N(1)-C(1)-N(2)	-4.7(3)		O(10)-N(3)-C(27)-C(28)	-32.8(3)
C(8)-N(1)-C(1)-N(2)	176.5(2)		C(32)-C(27)-C(28)-C(29)	0.9(4)
O(1)-N(1)-C(1)-C(2)	177.6(2)		N(3)-C(27)-C(28)-C(29)	177.4(2)
C(8)-N(1)-C(1)-C(2)	-1.3(4)		C(27)-C(28)-C(29)-C(30)	0.1(5)
N(2)-C(1)-C(2)-C(3)	-58.6(3)		C(28)-C(29)-C(30)-C(31)	-0.8(5)
N(1)-C(1)-C(2)-C(3)	119.0(3)		C(29)-C(30)-C(31)-C(32)	0.4(5)
N(2)-C(1)-C(2)-C(7)	119.0(3)		C(28)-C(27)-C(32)-C(31)	-1.3(4)
N(1)-C(1)-C(2)-C(7)	-63.4(3)		N(3)-C(27)-C(32)-C(31)	-177.7(2)
C(7)-C(2)-C(3)-C(4)	0.7(4)		C(30)-C(31)-C(32)-C(27)	0.7(4)
C(1)-C(2)-C(3)-C(4)	178.4(2)		C(20)#1-N(4)-C(33)-C(38)	-131.8(3)
			Zn(1)-N(4)-C(33)-C(38)	50.2(3)
C(2)-C(3)-C(4)-C(5)	-1.6(4)		C(20)#1-N(4)-C(33)-C(34)	53.9(3)
C(3)-C(4)-C(5)-C(6)	1.1(4)		Zn(1)-N(4)-C(33)-C(34)	-124.0(2)
C(3)-C(4)-C(5)-Br(1)	-176.7(2)		C(38)-C(33)-C(34)-C(35)	0.6(4)
C(4)-C(5)-C(6)-C(7)	0.3(4)		N(4)-C(33)-C(34)-C(35)	174.7(2)
Br(1)-C(5)-C(6)-C(7)	178.1(2)		C(33)-C(34)-C(35)-C(36)	0.2(4)
C(3)-C(2)-C(7)-C(6)	0.7(4)		C(34)-C(35)-C(36)-C(37)	-0.4(4)
C(1)-C(2)-C(7)-C(6)	-176.9(2)		C(35)-C(36)-C(37)-C(38)	-0.2(4)
C(5)-C(6)-C(7)-C(2)	-1.2(4)		C(34)-C(33)-C(38)-C(37)	-1.2(4)
C(1)-N(1)-C(8)-C(9)	-56.9(4)		N(4)-C(33)-C(38)-C(37)	-175.6(2)
O(1)-N(1)-C(8)-C(9)	124.2(3)		C(36)-C(37)-C(38)-C(33)	1.0(4)

Symmetry transformations used to generate equivalent atoms: #1 -x+2,-y+1,-z+2

The crystal structure determination and refinement data for **bis-amidine-Ph** (co-crystallized DMSO solvent) are given in Tables S19 - S21.

Table S19. Crystal data and structure refinement for **bis-amidine-Ph** (C40H46N4O2S2)

Identification code	MHAL92
Empirical formula	C40 H46 N4 O2 S2
Formula weight	678.93
Temperature	100K
Wavelength	1.54178 Å
Crystal system	Monoclinic
Space group	C 2/c
Unit cell dimensions	$a = 33.23(2)$ Å $\quad \alpha = 90°$
	$b = 6.8845(5)$ Å $\quad \beta = 123.552(2)°$
	$c = 19.2948(14)$ Å $\quad \gamma = 90°$
Volume	$3678.7(5) Å^3$
Z	4
Density (calculated)	1.226 g/cm^3
Absorption coefficient	1.616 mm^{-1}
F(000)	1448
Crystal size	0.26 x 0.21 x 0.10 mm
Theta range for data collection	3.191 to 69.694°
Index ranges	$-40 \leq h \leq 40$, $-6 \leq k \leq 8$, $-23 \leq \ell \leq 23$
Reflections collected	73405
Independent reflections	3467 [$R_{int} = 0.052$]
Absorption correction	Semi-empirical from equivalents
Max. and min. transmission	0.7532 and 0.5996
Refinement method	Full-matrix least-squares on F^2
Data / restraints / parameters	3467 / 0 / 221
Goodness-of-fit on F^2	1.038
Final R indices [I>2sigma(I)]	$R_1 = 0.0365$, $wR_2 = 0.0995$
R indices (all data)	$R_1 = 0.0373$, $wR_2 = 0.1005$
Extinction coefficient	n/a
Largest diff. peak and hole	0.263 and -0.326 e/Å^3

Table S20. Bond lengths [Å] and angles [°] for **bis-amidine-Ph** (C40H46N4O2S2)

_____

```
   S(1)-O(1)              1.5007(10)          C(1)-N(1)-C(8)          123.50(11)
   S(1)-C(20)             1.7718(17)          C(1)-N(1)-C(16)         129.09(11)
   S(1)-C(19)             1.7896(16)          C(18)-C(17)-C(16)       121.70(12)
   N(1)-C(1)              1.2860(17)          C(7)-C(2)-C(3)          119.26(12)
   N(1)-C(8)              1.4078(16)          C(7)-C(2)-C(1)          120.81(11)
   N(2)-C(1)              1.3683(16)          C(3)-C(2)-C(1)          119.93(11)
   N(2)-C(16)             1.4101(16)          C(12)-C(13)-C(8)        118.52(12)
   C(17)-C(18)            1.3883(18)          C(12)-C(13)-C(15)       120.10(12)
   C(17)-C(16)            1.3958(18)          C(8)-C(13)-C(15)        121.38(12)
   C(2)-C(7)              1.3925(18)          C(13)-C(8)-N(1)         121.61(11)
   C(2)-C(3)              1.3996(18)          C(13)-C(8)-C(9)         120.28(12)
   C(2)-C(1)              1.5004(17)          N(1)-C(8)-C(9)          117.59(11)
   C(13)-C(12)            1.3973(19)          C(17)-C(18)-C(16)#1     120.07(12)
   C(13)-C(8)             1.4072(18)          N(1)-C(1)-N(2)          121.68(11)
   C(13)-C(15)            1.5046(19)          N(1)-C(1)-C(2)          125.51(11)
   C(8)-C(9)              1.4095(18)          N(2)-C(1)-C(2)          112.81(11)
   C(18)-C(16)#1          1.3967(18)          C(4)-C(3)-C(2)          120.20(12)
   C(3)-C(4)              1.3889(19)          C(4)-C(5)-C(6)          120.00(13)
   C(5)-C(4)              1.387(2)            C(6)-C(7)-C(2)          120.37(12)
   C(5)-C(6)              1.390(2)            C(10)-C(9)-C(8)         119.07(12)
   C(7)-C(6)              1.3872(19)          C(10)-C(9)-C(14)        121.19(12)
   C(14)-C(9)             1.5018(19)          C(8)-C(9)-C(14)         119.74(12)
   C(9)-C(10)             1.3897(19)          C(11)-C(12)-C(13)       121.59(13)
   C(12)-C(11)            1.379(2)            C(12)-C(11)-C(10)       119.43(12)
   C(11)-C(10)            1.390(2)            C(7)-C(6)-C(5)          120.09(13)
   C(16)-C(18)#1          1.3968(18)          C(11)-C(10)-C(9)        121.09(13)
                                             C(5)-C(4)-C(3)          120.07(12)
   O(1)-S(1)-C(20)        106.82(7)           C(17)-C(16)-C(18)#1     118.23(12)
   O(1)-S(1)-C(19)        107.01(7)           C(17)-C(16)-N(2)        116.80(11)
   C(20)-S(1)-C(19)        97.75(8)           C(18)#1-C(16)-N(2)      124.96(11)
```

_____
```
Symmetry transformations used to generate equivalent atoms:
#1 -x+1/2,-y+1/2,-z+1
```

Table S21. Torsion angles [°] for **bis-amidine-Ph** (C40H46N4O2S2)

_____

```
  C(12)-C(13)-C(8)-N(1)   -170.32(12)        C(13)-C(8)-C(9)-C(10)       0.08(19)
  C(15)-C(13)-C(8)-N(1)      8.85(19)        N(1)-C(8)-C(9)-C(10)      171.88(11)
  C(12)-C(13)-C(8)-C(9)      1.15(19)        C(13)-C(8)-C(9)-C(14)    -179.72(12)
  C(15)-C(13)-C(8)-C(9)   -179.68(12)        N(1)-C(8)-C(9)-C(14)       -7.92(18)
  C(1)-N(1)-C(8)-C(13)     -71.17(17)        C(8)-C(13)-C(12)-C(11)     -1.3(2)
  C(1)-N(1)-C(8)-C(9)      117.15(14)        C(15)-C(13)-C(12)-C(11)  179.50(13)
  C(16)-C(17)-C(18)-C(16)#1  0.0(2)          C(13)-C(12)-C(11)-C(10)    0.2(2)
  C(8)-N(1)-C(1)-N(2)      174.25(11)        C(2)-C(7)-C(6)-C(5)        -0.7(2)
  C(8)-N(1)-C(1)-C(2)       -6.86(19)        C(4)-C(5)-C(6)-C(7)         1.0(2)
  C(16)-N(2)-C(1)-N(1)      -0.3(2)          C(12)-C(11)-C(10)-C(9)      1.0(2)
  C(16)-N(2)-C(1)-C(2)    -179.35(11)        C(8)-C(9)-C(10)-C(11)      -1.2(2)
  C(7)-C(2)-C(1)-N(1)      132.13(14)        C(14)-C(9)-C(10)-C(11)   178.60(13)
  C(3)-C(2)-C(1)-N(1)      -48.42(18)        C(6)-C(5)-C(4)-C(3)        -0.5(2)
  C(7)-C(2)-C(1)-N(2)      -48.89(16)        C(2)-C(3)-C(4)-C(5)        -0.4(2)
  C(3)-C(2)-C(1)-N(2)      130.56(12)        C(18)-C(17)-C(16)-C(18)#1   0.0(2)
  C(7)-C(2)-C(3)-C(4)        0.69(19)        C(18)-C(17)-C(16)-N(2)   179.65(11)
  C(1)-C(2)-C(3)-C(4)     -178.78(12)        C(1)-N(2)-C(16)-C(17)    168.99(12)
  C(3)-C(2)-C(7)-C(6)       -0.12(19)        C(1)-N(2)-C(16)-C(18)#1   -11.4(2)
  C(1)-C(2)-C(7)-C(6)      179.33(12)
```

_____
```
Symmetry transformations used to generate equivalent atoms: #1 -x+1/2,-y+1/2,-z+1
```

The crystal structure determination and refinement data for **bis-AMOX-Ph** (C36H34N4O2) are given in Tables S22 - S24.

Table S22. Crystal data and structure refinement for **bis-AMOX-Ph** (C36H34N4O2)

_____

Identification code	BROD04MC
Empirical formula	C36 H34 N4 O2
Formula weight	554.67
Temperature	100K
Wavelength	1.54178 Å
Crystal system	Monoclinic
Space group	P2/n
Unit cell dimensions	a = 13.9746(11) Å α = 90°
	b = 6.6772(6) Å β = 108.555(3)°
	c = 17.1658(14) Å γ = 90°
Volume	1518.5(2) Å^3
Z	2
Density (calculated)	1.213 g/cm^3
Absorption coefficient	0.600 mm^{-1}
F(000)	588
Crystal size	0.13 x 0.10 x 0.03 mm
Theta range for data collection	3.569 to 69.777°
Index ranges	$-16 \leq h \leq 16$, $-7 \leq k \leq 8$, $-20 \leq \ell \leq 20$
Reflections collected	62390
Independent reflections	2860 [R_{int} = 0.057]
Absorption correction	Multi-scan
Max. and min. transmission	0.7533 and 0.6320
Refinement method	Full-matrix least-squares on F^2
Data / restraints / parameters	2860 / 0 / 192
Goodness-of-fit on F^2	1.025
Final R indices [I>2sigma(I)]	R_1 = 0.0540, wR_2 = 0.1531
R indices (all data)	R_1 = 0.0573, wR_2 = 0.1575
Largest diff. peak and hole	0.40 and -0.20 e/Å^3

Table S23. Bond lengths [Å] and angles [°] for **bis-AMOX-Ph** (C36H34N4O2)

_____

```
O1- N(1)      1.3303(17)        C8-   C9          1.395(2)
N1- C1        1.327(2)          C8-   C13         1.397(2)
N1- C8        1.438(2)          C9-   C10         1.392(2)
N2- C1        1.344(2)          C9-   C14         1.503(3)
N2- C16       1.4092(19)        C10-  C11         1.388(3)
C1- C2        1.473(2)          C11-  C12         1.377(3)
C2- C3        1.394(2)          C12-  C13         1.397(3)
C2- C7        1.390(2)          C13-  C15         1.501(3)
C3- C4        1.391(3)          C16-  C17#1       1.400(2)
C4- C5        1.379(3)          C16-  C18         1.388(2)
C5- C6        1.378(3)          C17   C16#1       1.400(2)
C6- C7        1.376(3)          C17   C18         1.387(2)

O1- N1- C8    114.80(12)        C9-   C8-  C13    123.17(15)
C1- N1- O1    120.58(13)        C13-  C8-  N1     118.37(14)
C1- N1- C8    124.14(14)        C8-   C9-  C14    121.41(15)
C1- N2- C16   127.42(14)        C10-  C9-  C8     117.48(16)
N1- C1- N2    116.18(14)        C10-  C9-  C14    121.10(16)
N1- C1- C2    121.76(14)        C11-  C10-  C9    120.62(17)
N2- C1- C2    121.79(14)        C12-  C11-  C10   120.56(17)
C3- C2- C1    122.91(15)        C11-  C12-  C13   121.02(18)
C7- C2- C1    118.41(15)        C8-   C13-  C12   117.07(17)
C7- C2- C3    118.62(15)        C8-   C13-  C15   121.82(16)
C4- C3- C2    120.28(17)        C12-  C13-  C15   121.09(17)
C5- C4- C3    119.84(17)        C17#1-  C16-  N2  123.14(15)
C6- C5- C4    120.34(17)        C18-  C16-  N2    117.42(14)
C7- C6- C5    119.91(18)        C18-  C16-  C17#1 119.35(14)
C6- C7- C2    121.01(17)        C18-  C17-  C16#1 119.95(15)
C9- C8- N1    118.14(14)        C17-  C18-  C16   120.70(15)
```

_____

 Symmetry transformations used to generate equivalent atoms: #1 -x+3/2,y,-z+3/2

Table S24. Torsion angles [°] for **bis-AMOX-Ph** (C36H34N4O2)

_____

```
O1-N1- C1- N2        6.2(2)      C3-    C4- C5- C6       0.3(3)
O1-N1- C1- C2     -179.65(13)    C4-    C5- C6- C7      -0.1(3)
O1-N1- C8- C9       77.35(17)    C5-    C6- C7- C2       0.0(3)
O1-N1- C8- C13     -96.43(16)    C7-    C2- C3- C4       0.4(2)
N1-C1- C2- C3       52.7(2)      C8-    N1- C1- N2    -165.41(14)
N1-C1- C2- C7     -130.27(17)    C8-    N1- C1- C2       8.8(2)
N1-C8- C9- C10    -176.87(15)    C8-    C9- C10-C11      1.9(3)
N1-C8- C9- C14       2.5(2)      C9-    C8- C13-C12      2.6(2)
N1-C8- C13-C12     176.09(15)    C9-    C8- C13-C15   -175.74(16)
N1-C8- C13-C15      -2.3(2)      C9-    C10-C11-C12      0.2(3)
N2-C1- C2- C3     -133.46(17)    C10-   C11-C12-C13     -1.0(3)
N2-C1- C2- C7       43.6(2)      C11-   C12-C13-C8      -0.3(3)
N2-C16-C18-C17    -176.78(14)    C11-   C12-C13-C15    178.05(18)
C1-N1- C8- C9     -110.65(18)    C13-   C8- C9- C10     -3.4(2)
C1-N1- C8- C13      75.6(2)      C13-   C8- C9- C14    175.98(15)
C1-N2- C16-C17¹     25.8(3)      C14-   C9- C10-C11   -177.50(17)
C1-N2- C16-C18    -157.75(16)    C16-   N2- C1- N1    -158.03(15)
C1-C2- C3- C4      177.44(15)    C16-   N2- C1- C2      27.8(3)
C1-C2- C7- C6     -177.35(15)    C16#1-C17-C18-C16     -0.1(2)
C2-C3- C4- C5       -0.5(3)      C17#1-C16-C18-C17     -0.2(2)
C3-C2- C7- C6       -0.2(2)
```

_____

 Symmetry transformations used to generate equivalent atoms: #1 -x+3/2,y,-z+3/2

The crystal structure determination and refinement data for compound **C** are given in Tables S25 - S27.

Table S25. Crystal data and structure refinement for **compound C** (C36H32N4O2)

Identification code	MHAL99
Empirical formula	C36 H32 N4 O2
Formula weight	552.65
Temperature	150K
Wavelength	1.54178 Å
Crystal system	Monoclinic
Space group	P21/n
Unit cell dimensions	$a = 15.1954(10)$ Å $\quad \alpha = 90°$
	$b = 6.3722(4)$ Å $\quad \beta = 101.589(3)°$
	$c = 15.5411(10)$ Å $\quad \gamma = 90°$
Volume	$1474.14(16) Å^3$
Z	2
Density (calculated)	1.245 g/cm^3
Absorption coefficient	0.618 mm^{-1}
F(000)	584
Crystal size	0.18 x 0.08 x 0.08 mm
Theta range for data collection	3.712 to 69.739°
Index ranges	$-18 \leq h \leq 15$, $-7 \leq k \leq 7$, $-18 \leq \ell \leq 18$
Reflections collected	33056
Independent reflections	2771 [R_{int} = 0.048]
Absorption correction	Multi-scan
Max. and min. transmission	0.7533 and 0.6264
Refinement method	Full-matrix least-squares on F^2
Data / restraints / parameters	2771 / 0 / 192
Goodness-of-fit on F^2	1.044
Final R indices [I>2sigma(I)]	$R_1 = 0.0360$, $wR_2 = 0.0992$
R indices (all data)	$R_1 = 0.0384$, $wR_2 = 0.1018$
Extinction coefficient	n/a
Largest diff. peak and hole	0.187 and -0.166 $e/Å^3$

Table S26. Bond lengths [Å] and angles [°] for **compound C** (C36H32N4O2)

_____

N(1)-C(1)	1.3867(14)		C(10)-C(9)-C(14)	120.18(12)
N(1)-C(8)	1.4404(13)		C(8)-C(9)-C(14)	122.31(11)
N(1)-O(1)	1.4566(11)		C(6)-C(5)-C(4)	120.03(11)
N(2)-C(1)	1.2847(14)		C(6)-C(7)-C(2)	119.97(11)
N(2)-C(16)	1.4597(15)		C(7)-C(2)-C(3)	119.08(10)
O(1)-C(16)	1.4682(12)		C(7)-C(2)-C(1)	123.90(10)
C(9)-C(10)	1.3965(17)		C(3)-C(2)-C(1)	117.02(10)
C(9)-C(8)	1.3996(17)		N(2)-C(1)-N(1)	115.28(10)
C(9)-C(14)	1.5012(19)		N(2)-C(1)-C(2)	122.57(10)
C(5)-C(6)	1.3817(19)		N(1)-C(1)-C(2)	122.04(9)
C(5)-C(4)	1.3835(18)		C(4)-C(3)-C(2)	120.60(11)
C(7)-C(6)	1.3886(17)		N(2)-C(16)-O(1)	105.29(8)
C(7)-C(2)	1.3931(16)		N(2)-C(16)-C(18)	111.98(10)
C(2)-C(3)	1.3953(16)		O(1)-C(16)-C(18)	107.96(9)
C(2)-C(1)	1.4775(15)		N(2)-C(16)-C(17)	110.15(9)
C(3)-C(4)	1.3820(17)		O(1)-C(16)-C(17)	107.94(9)
C(16)-C(18)	1.4969(16)		C(18)-C(16)-C(17)	113.11(9)
C(16)-C(17)	1.4991(16)		C(18)#1-C(17)-C(16)	124.13(11)
C(17)-C(18)#1	1.3227(16)		C(8)-C(13)-C(12)	117.36(12)
C(13)-C(8)	1.3960(17)		C(8)-C(13)-C(15)	122.93(11)
C(13)-C(12)	1.3967(17)		C(12)-C(13)-C(15)	119.67(12)
C(13)-C(15)	1.5023(19)		C(13)-C(8)-C(9)	122.60(10)
C(18)-C(17)#1	1.3227(16)		C(13)-C(8)-N(1)	121.23(10)
C(12)-C(11)	1.380(2)		C(9)-C(8)-N(1)	116.09(10)
C(10)-C(11)	1.375(2)		C(17)#1-C(18)-C(16)	122.75(11)
			C(11)-C(12)-C(13)	121.11(13)
C(1)-N(1)-C(8)	126.56(9)		C(11)-C(10)-C(9)	121.01(13)
C(1)-N(1)-O(1)	104.21(8)		C(5)-C(6)-C(7)	120.36(12)
C(8)-N(1)-O(1)	108.60(7)		C(3)-C(4)-C(5)	119.96(12)
C(1)-N(2)-C(16)	106.89(9)		C(10)-C(11)-C(12)	120.39(12)
N(1)-O(1)-C(16)	104.05(7)			
C(10)-C(9)-C(8)	117.50(12)			

_____

Symmetry transformations used to generate equivalent atoms: #1 -x,-y,-z

Table S27. Torsion angles [°] for **compound C** (C36H32N4O2)

_____

C(1)-N(1)-O(1)-C(16)	-19.81(10)		C(15)-C(13)-C(8)-C(9)	177.31(12)
C(8)-N(1)-O(1)-C(16)	-157.00(9)		C(12)-C(13)-C(8)-N(1)	-177.13(10)
C(6)-C(7)-C(2)-C(3)	-0.60(17)		C(15)-C(13)-C(8)-N(1)	0.62(17)
C(6)-C(7)-C(2)-C(1)	179.87(11)		C(10)-C(9)-C(8)-C(13)	-0.76(17)
C(16)-N(2)-C(1)-N(1)	-1.38(13)		C(14)-C(9)-C(8)-C(13)	177.85(11)
C(16)-N(2)-C(1)-C(2)	-177.63(10)		C(10)-C(9)-C(8)-N(1)	176.10(10)
C(8)-N(1)-C(1)-N(2)	140.61(11)		C(14)-C(9)-C(8)-N(1)	-5.30(16)
O(1)-N(1)-C(1)-N(2)	13.92(12)		C(1)-N(1)-C(8)-C(13)	-55.34(15)
C(8)-N(1)-C(1)-C(2)	-43.11(15)		O(1)-N(1)-C(8)-C(13)	69.56(12)
O(1)-N(1)-C(1)-C(2)	-169.80(9)		C(1)-N(1)-C(8)-C(9)	127.76(12)
C(7)-C(2)-C(1)-N(2)	164.80(11)		O(1)-N(1)-C(8)-C(9)	-107.34(11)
C(3)-C(2)-C(1)-N(2)	-14.74(16)		N(2)-C(16)-C(18)-C(17)#1	-125.50(12)
C(7)-C(2)-C(1)-N(1)	-11.20(17)		O(1)-C(16)-C(18)-C(17)#1	119.05(12)
C(3)-C(2)-C(1)-N(1)	169.25(10)		C(17)-C(16)-C(18)-C(17)#1	-0.32(18)
C(7)-C(2)-C(3)-C(4)	1.08(17)		C(8)-C(13)-C(12)-C(11)	1.68(18)
C(1)-C(2)-C(3)-C(4)	-179.35(10)		C(15)-C(13)-C(12)-C(11)	-176.15(12)
C(1)-N(2)-C(16)-O(1)	-11.72(12)		C(8)-C(9)-C(10)-C(11)	0.77(18)
C(1)-N(2)-C(16)-C(18)	-128.78(10)		C(14)-C(9)-C(10)-C(11)	-177.87(12)
C(1)-N(2)-C(16)-C(17)	104.42(10)		C(4)-C(5)-C(6)-C(7)	0.4(2)
N(1)-O(1)-C(16)-N(2)	19.35(11)		C(2)-C(7)-C(6)-C(5)	-0.2(2)
N(1)-O(1)-C(16)-C(18)	139.12(9)		C(2)-C(3)-C(4)-C(5)	-0.81(18)
N(1)-O(1)-C(16)-C(17)	-98.29(10)		C(6)-C(5)-C(4)-C(3)	0.0(2)
N(2)-C(16)-C(17)-C(18)#1	126.49(12)		C(9)-C(10)-C(11)-C(12)	0.4(2)
O(1)-C(16)-C(17)-C(18)#1	-119.05(12)		C(13)-C(12)-C(11)-C(10)	-1.7(2)
C(18)-C(16)-C(17)-C(18)#1	0.33(18)			
C(12)-C(13)-C(8)-C(9)	-0.44(17)			

_____

Symmetry transformations used to generate equivalent atoms: #1 -x,-y,-z

The crystal structure determination and refinement data for the Zn(II) metallopolymer (co-crystallized toluene solvent) (C50H48N4O2Zn) are given in Tables S28 - S30.

Table S28 Crystal data and structure refinement for **the Zn(II) metallopolymer** (C50H48N4O2Zn)

Identification code	MHAL81
Empirical formula	C50 H48 N4 O2 Zn
Formula weight	802.29
Temperature	100K
Wavelength	1.54178 Å
Crystal system	Monoclinic
Space group	P21/n
Unit cell dimensions	a = 9.5906(6) Å α = 90°
	b = 22.2020(11) Å β = 99.741(4)°
	c = 20.2657(12) Å γ = 90°
Volume	4253.0(4)Å^3
Z	4
Density (calculated)	1.253 g/cm^3
Absorption coefficient	1.140 mm^{-1}
F(000)	1688
Crystal size	0.21 x 0.04 x 0.02 mm
Theta range for data collection	2.976 to 71.258°
Index ranges	$-11 \le h \le 10$, $-26 \le k \le 27$, $-24 \le \ell \le 24$
Reflections collected	57326
Independent reflections	8189 [R$_{int}$ = 0.105]
Absorption correction	Semi-empirical from equivalents
Max. and min. transmission	0.7534 and 0.4597
Refinement method	Full-matrix least-squares on F^2
Data / restraints / parameters	8189 / 0 / 520
Goodness-of-fit on F^2	1.031
Final R indices [I>2sigma(I)]	R$_1$ = 0.0720, wR$_2$ = 0.1863
R indices (all data)	R$_1$ = 0.1116, wR$_2$ = 0.2176
Largest diff. peak and hole	1.169 and -1.233 e/Å^3

Table S29 Bond lengths [Å] and angles [°] for for **the Zn(II) metallopolymer** (C50H48N4O2Zn)

_____

C(49)-C(50)	1.469(12)

Zn(1)-O(1)	1.951(3)
Zn(1)-N(4)	1.964(3)
Zn(1)-O(2)	1.964(3)
Zn(1)-N(1)	1.987(3)
O(1)-N(2)	1.382(4)
O(2)-N(3)	1.386(4)
N(1)-C(1)	1.313(5)
N(1)-C(16)	1.412(5)
N(2)-C(1)	1.334(5)
N(2)-C(8)	1.428(5)
N(3)-C(19)	1.329(5)
N(3)-C(29)	1.430(5)
N(4)-C(19)	1.323(5)
N(4)-C(20)	1.416(4)
C(1)-C(2)	1.500(5)
C(2)-C(7)	1.387(6)
C(2)-C(3)	1.391(6)
C(3)-C(4)	1.402(6)
C(4)-C(5)	1.373(7)
C(5)-C(6)	1.381(7)
C(6)-C(7)	1.391(6)
C(8)-C(13)	1.374(7)
C(8)-C(9)	1.410(6)
C(9)-C(10)	1.371(7)
C(9)-C(15)	1.493(8)
C(10)-C(11)	1.360(9)
C(11)-C(12)	1.401(9)
C(12)-C(13)	1.407(8)
C(13)-C(14)	1.501(7)
C(16)-C(18)#1	1.383(6)
C(16)-C(17)	1.403(5)
C(17)-C(18)	1.385(6)
C(18)-C(16)#1	1.382(6)
C(19)-C(23)	1.493(5)
C(20)-C(21)	1.384(6)
C(20)-C(22)#2	1.395(5)
C(21)-C(22)	1.395(5)
C(22)-C(20)#2	1.395(5)
C(23)-C(28)	1.388(6)
C(23)-C(24)	1.390(6)
C(24)-C(25)	1.393(6)
C(25)-C(26)	1.366(7)
C(26)-C(27)	1.388(7)
C(27)-C(28)	1.394(6)
C(29)-C(30)	1.381(6)
C(29)-C(34)	1.406(6)
C(30)-C(31)	1.393(6)
C(30)-C(36)	1.515(6)
C(31)-C(32)	1.390(7)
C(32)-C(33)	1.369(7)
C(33)-C(34)	1.416(6)
C(34)-C(35)	1.487(6)
C(37)-C(38)	1.500(8)
C(38)-C(39)	1.390(8)
C(38)-C(42)	1.393(7)
C(39)-C(40)	1.373(8)
C(40)-C(41)	1.355(8)
C(41)-C(43)	1.343(9)
C(42)-C(43)	1.377(8)
C(44)-C(45)	1.352(9)
C(44)-C(49)	1.364(11)
C(45)-C(46)	1.445(9)
C(46)-C(47)	1.328(9)
C(47)-C(50)	1.304(11)
C(47)-C(48)	1.592(12)

O(1)-ZN1-N(4)	122.87(14)
O(1)-ZN1-O(2)	128.99(11)
N(4)-ZN1-O(2)	83.85(12)
O(1)-ZN1-N(1)	83.31(12)
N(4)-ZN1-N(1)	116.05(12)
O(2)-ZN1-N(1)	126.27(14)
N(2)-O(1)-ZN1	108.6(2)
N(3)-O(2)-ZN1	107.4(2)
C(1)-N(1)-C(16)	124.9(3)
C(1)-N(1)-ZN1	111.0(2)
C(16)-N(1)-ZN1	122.2(3)
C(1)-N(2)-O(1)	119.4(3)
C(1)-N(2)-C(8)	126.6(3)
O(1)-N(2)-C(8)	112.9(3)
C(19)-N(3)-O(2)	120.3(3)
C(19)-N(3)-C(29)	124.7(3)
O(2)-N(3)-C(29)	114.8(3)
C(19)-N(4)-C(20)	124.1(3)
C(19)-N(4)-ZN1	111.6(2)
C(20)-N(4)-ZN1	122.9(2)
N(1)-C(1)-N(2)	117.5(3)
N(1)-C(1)-C(2)	123.7(3)
N(2)-C(1)-C(2)	118.5(4)
C(7)-C(2)-C(3)	119.3(4)
C(7)-C(2)-C(1)	117.8(4)
C(3)-C(2)-C(1)	122.8(4)
C(2)-C(3)-C(4)	120.6(4)
C(5)-C(4)-C(3)	119.2(5)
C(4)-C(5)-C(6)	120.7(4)
C(5)-C(6)-C(7)	120.3(4)
C(2)-C(7)-C(6)	119.9(4)
C(13)-C(8)-C(9)	123.2(4)
C(13)-C(8)-N(2)	119.7(4)
C(9)-C(8)-N(2)	116.8(4)
C(10)-C(9)-C(8)	117.6(5)
C(10)-C(9)-C(15)	121.3(5)
C(8)-C(9)-C(15)	121.1(4)
C(11)-C(10)-C(9)	120.4(6)
C(10)-C(11)-C(12)	122.5(5)
C(11)-C(12)-C(13)	118.3(6)
C(8)-C(13)-C(12)	117.9(5)
C(8)-C(13)-C(14)	121.3(5)
C(12)-C(13)-C(14)	120.8(5)
C(18)#1-C(16)-C(17)	117.9(4)
C(18)#1-C(16)-N(1)	118.5(3)
C(17)-C(16)-N(1)	123.4(4)
C(18)-C(17)-C(16)	120.2(4)
C(16)#1-C(18)-C(17)	121.9(3)
N(4)-C(19)-N(3)	116.8(3)
N(4)-C(19)-C(23)	124.0(3)
N(3)-C(19)-C(23)	119.1(3)
C(21)-C(20)-C(22)#2	118.7(3)
C(21)-C(20)-N(4)	117.8(3)
C(22)#2-C(20)-N(4)	123.3(4)
C(20)-C(21)-C(22)	121.0(4)
C(20)#2-C(22)-C(21)	120.2(4)
C(28)-C(23)-C(24)	119.2(3)
C(28)-C(23)-C(19)	123.0(4)
C(24)-C(23)-C(19)	117.8(4)
C(23)-C(24)-C(25)	120.2(4)
C(26)-C(25)-C(24)	120.5(4)
C(25)-C(26)-C(27)	119.9(4)
C(26)-C(27)-C(28)	120.1(4)
C(23)-C(28)-C(27)	120.1(4)

```
C(30)-C(29)-C(34)        123.4(4)
C(30)-C(29)-N(3)         119.0(4)
C(34)-C(29)-N(3)         117.6(4)
C(29)-C(30)-C(31)        118.2(4)
C(29)-C(30)-C(36)        120.7(4)
C(31)-C(30)-C(36)        121.0(4)
C(32)-C(31)-C(30)        119.9(5)
C(33)-C(32)-C(31)        121.1(4)
C(32)-C(33)-C(34)        121.1(4)
C(29)-C(34)-C(33)        116.0(4)
C(29)-C(34)-C(35)        121.1(4)
C(33)-C(34)-C(35)        123.0(4)
C(39)-C(38)-C(42)        117.6(5)
C(39)-C(38)-C(37)        121.0(6)
C(42)-C(38)-C(37)        121.3(6)
```

```
C(40)-C(39)-C(38)        120.5(5)
C(41)-C(40)-C(39)        120.9(5)
C(43)-C(41)-C(40)        119.6(5)
C(43)-C(42)-C(38)        119.8(5)
C(41)-C(43)-C(42)        121.6(5)
C(45)-C(44)-C(49)        120.2(8)
C(44)-C(45)-C(46)        119.9(6)
C(47)-C(46)-C(45)        117.9(7)
C(50)-C(47)-C(46)        124.8(9)
C(50)-C(47)-C(48)        119.2(8)
C(46)-C(47)-C(48)        115.5(8)
C(44)-C(49)-C(50)        118.9(7)
C(47)-C(50)-C(49)        117.9(8)
```

_____

```
Symmetry transformations used to generate equivalent atoms:
#1 -x,-y,-z    #2 -x+1,-y,-z
```

Table S30 Torsion angles [°] for **the Zn(II) metallopolymer** (C50H48N4O2Zn)

_____

```
ZN1-O(1)-N(2)-C(1)          4.2(4)
ZN1-O(1)-N(2)-C(8)       -164.3(3)
ZN1-O(2)-N(3)-C(19)         2.0(4)
ZN1-O(2)-N(3)-C(29)      -173.0(3)
C(16)-N(1)-C(1)-N(2)      162.1(4)
ZN1-N(1)-C(1)-N(2)         -2.6(4)
C(16)-N(1)-C(1)-C(2)      -23.6(6)
ZN1-N(1)-C(1)-C(2)        171.7(3)
O(1)-N(2)-C(1)-N(1)        -1.1(5)
C(8)-N(2)-C(1)-N(1)       165.5(4)
O(1)-N(2)-C(1)-C(2)      -175.7(3)
C(8)-N(2)-C(1)-C(2)        -9.0(6)
N(1)-C(1)-C(2)-C(7)       -47.4(5)
N(2)-C(1)-C(2)-C(7)       126.9(4)
N(1)-C(1)-C(2)-C(3)       130.3(4)
N(2)-C(1)-C(2)-C(3)       -55.4(5)
C(7)-C(2)-C(3)-C(4)        -1.2(6)
C(1)-C(2)-C(3)-C(4)      -178.9(4)
C(2)-C(3)-C(4)-C(5)         0.8(7)
C(3)-C(4)-C(5)-C(6)        -0.1(7)
C(4)-C(5)-C(6)-C(7)        -0.1(7)
C(3)-C(2)-C(7)-C(6)         1.0(6)
C(1)-C(2)-C(7)-C(6)       178.8(3)
C(5)-C(6)-C(7)-C(2)        -0.3(6)
C(1)-N(2)-C(8)-C(13)      104.8(5)
O(1)-N(2)-C(8)-C(13)      -87.7(4)
C(1)-N(2)-C(8)-C(9)       -81.5(5)
O(1)-N(2)-C(8)-C(9)        86.0(4)
C(13)-C(8)-C(9)-C(10)      -3.5(6)
N(2)-C(8)-C(9)-C(10)     -176.9(4)
C(13)-C(8)-C(9)-C(15)     176.4(4)
N(2)-C(8)-C(9)-C(15)        3.0(6)
C(8)-C(9)-C(10)-C(11)       1.5(7)
C(15)-C(9)-C(10)-C(11)   -178.4(5)
C(9)-C(10)-C(11)-C(12)      0.1(8)
C(10)-C(11)-C(12)-C(13)     0.1(8)
C(9)-C(8)-C(13)-C(12)       3.7(6)
N(2)-C(8)-C(13)-C(12)     176.9(4)
C(9)-C(8)-C(13)-C(14)    -175.2(4)
N(2)-C(8)-C(13)-C(14)      -1.9(6)
C(11)-C(12)-C(13)-C(8)     -1.9(7)
C(11)-C(12)-C(13)-C(14)   177.0(5)
C(1)-N(1)-C(16)-C(18)#1   153.2(4)
ZN1-N(1)-C(16)-C(18)#1    -43.7(5)
C(1)-N(1)-C(16)-C(17)     -32.0(6)
ZN1-N(1)-C(16)-C(17)      131.1(4)
C(18)#1-C(16)-C(17)-C(18)  -2.3(7)
```

```
N(1)-C(16)-C(17)-C(18)   -177.2(4)
C(16)-C(17)-C(18)-C(16)#1   2.4(7)
C(20)-N(4)-C(19)-N(3)     166.5(4)
ZN1-N(4)-C(19)-N(3)        -0.5(4)
C(20)-N(4)-C(19)-C(23)    -17.7(6)
ZN1-N(4)-C(19)-C(23)      175.3(3)
O(2)-N(3)-C(19)-N(4)       -1.1(5)
C(29)-N(3)-C(19)-N(4)     173.4(4)
O(2)-N(3)-C(19)-C(23)    -177.1(3)
C(29)-N(3)-C(19)-C(23)     -2.6(6)
C(19)-N(4)-C(20)-C(21)    149.6(4)
ZN1-N(4)-C(20)-C(21)      -44.9(5)
C(19)-N(4)-C(20)-C(22)#2  -35.2(6)
ZN1-N(4)-C(20)-C(22)#2    130.4(4)
C(22)#2-C(20)-C(21)-C(22)   2.0(7)
N(4)-C(20)-C(21)-C(22)    177.5(4)
C(20)-C(21)-C(22)-C(20)#2  -2.0(7)
N(4)-C(19)-C(23)-C(28)    124.4(4)
N(3)-C(19)-C(23)-C(28)    -59.9(5)
N(4)-C(19)-C(23)-C(24)    -53.4(5)
N(3)-C(19)-C(23)-C(24)    122.3(4)
C(28)-C(23)-C(24)-C(25)     0.1(5)
C(19)-C(23)-C(24)-C(25)   178.1(3)
C(23)-C(24)-C(25)-C(26)    -0.4(6)
C(24)-C(25)-C(26)-C(27)     0.1(6)
C(25)-C(26)-C(27)-C(28)     0.6(6)
C(24)-C(23)-C(28)-C(27)     0.6(5)
C(19)-C(23)-C(28)-C(27)  -177.3(3)
C(26)-C(27)-C(28)-C(23)    -0.9(6)
C(19)-N(3)-C(29)-C(30)    100.3(5)
O(2)-N(3)-C(29)-C(30)     -85.0(4)
C(19)-N(3)-C(29)-C(34)    -79.1(5)
O(2)-N(3)-C(29)-C(34)      95.6(4)
C(34)-C(29)-C(30)-C(31)     4.7(6)
N(3)-C(29)-C(30)-C(31)   -174.7(3)
C(34)-C(29)-C(30)-C(36)  -174.6(4)
N(3)-C(29)-C(30)-C(36)      6.0(6)
C(29)-C(30)-C(31)-C(32)    -0.4(6)
C(36)-C(30)-C(31)-C(32)   178.8(4)
C(30)-C(31)-C(32)-C(33)    -3.0(7)
C(31)-C(32)-C(33)-C(34)     2.3(7)
C(30)-C(29)-C(34)-C(33)    -5.2(6)
N(3)-C(29)-C(34)-C(33)    174.2(3)
C(30)-C(29)-C(34)-C(35)   174.5(4)
N(3)-C(29)-C(34)-C(35)     -6.1(5)
C(32)-C(33)-C(34)-C(29)     1.6(6)
C(32)-C(33)-C(34)-C(35)  -178.0(4)
```

```
C(42)-C(38)-C(39)-C(40)    1.2(8)        C(49)-C(44)-C(45)-C(46)     2.3(12)
C(37)-C(38)-C(39)-C(40) -179.3(5)        C(44)-C(45)-C(46)-C(47)    -2.3(12)
C(38)-C(39)-C(40)-C(41)   -1.5(9)        C(45)-C(46)-C(47)-C(50)     4.7(13)
 C(39)-C(40)-C(41)-C(43)   0.9(9)        C(45)-C(46)-C(47)-C(48)  176.0(8)
C(39)-C(38)-C(42)-C(43)   -0.4(8)        C(45)-C(44)-C(49)-C(50)    -4.2(13)
C(37)-C(38)-C(42)-C(43) -180.0(5)        C(46)-C(47)-C(50)-C(49)    -6.5(14)
C(40)-C(41)-C(43)-C(42)   -0.2(9)        C(48)-C(47)-C(50)-C(49) -177.6(9)
C(38)-C(42)-C(43)-C(41)   -0.1(9)        C(44)-C(49)-C(50)-C(47)     6.1(14)
```
_____

```
Symmetry transformations used to generate equivalent atoms:
#1 -x,-y,-z    #2 -x+1,-y,-z
```

Table S31. Photophysical[a], electrochemical[b] and theoretical[c] data for **D1** and **D2**

Cpd.	Experimental data						Theoretical data[c]		
	λ_{max} [nm] (ε x 10^2 [$M^{-1}cm^{-1}$])	E_{pa}(irr) [V] *vs.* SCE	E_{ox_onset} [V]	HOMO[d] [eV]	LUMO[e] [eV]	E_g[f] (λ_{abs_onset}) [eV] (nm)	HOMO[g] [eV]	LUMO[h] [eV]	E_g(TD-DFT)[i] [eV]
D1	240 (707) sh, 276 (493) sh, 336 (388)	0.97; 1.16	0.85	-5.25	-2.19	3.06 (405)	-5.08	-1.89	3.19 (388)
D2	-	-	-	-	-	-	-5.20	-2.44	2.76 (449)

[a] photophysical data were obtained in CH_2Cl_2, at room temperature; [b] electrochemical data were obtained using the following conditions: dry CH_2Cl_2, [nBu_4N]PF_6 0.1M, compound concentration about 1mM, glassy carbon electrode, scan rate 100 mV/s, room temperature, Ar atmosphere, ferrocene used as internal reference; [b]all potentials are reported in volt, *vs.* SCE (Fc/Fc^+ *vs.* SCE was considered 0.46V in DCM[20]); [c]theory level: B3LYP/ 6-31g(d, p), PCM: CH_2Cl_2. [d]HOMO level was determined using the equation: E_{HOMO} (eV) = -(4.4 + E_{ox_onset}); [e]no reduction process is observed for D1; LUMO level was determined using the equation: E_{LUMO} (eV) = E_{HOMO} + E_g; [f]E_g was obtained using the absorption edge technique: E_g = 1240/λ_{abs_onset}; [g]HOMO level was obtained from DFT optimization, theory level: B3LYP/ 6-31g(d, p), PCM: CH_2Cl_2; [h]LUMO level was obtained using E_{LUMO} (eV) = E_{HOMO} (DFT) + E_g(TD-DFT); [i]E_g(TD-DFT) is the TD-DFT calculated first singlet, which corresponds to the HOMO-LUMO transition; theory level: B3LYP/ 6-31g(d, p), PCM: CH_2Cl_2.

References

[1]   a) M. Kakimoto, S. Ogata, A. Mochizuki, Y. Imai, *Chem. Lett.* **1984**, 821-824; b) S. Ogata, A. Mochizuki, M. Kakimoto, Y. Imai, *Bull. Chem. Soc. Jpn.* **1986**, *59*, 2171-2177.

[2]   a) M. Cibian, S. Derossi, G. S. Hanan, *Dalton Trans.* **2011**, *40*, 1038-1040; b) A. N. Verma, S. B. Gholse, S. P. Sangal, *J. Indian Chem. Soc.* **1995**, *72*, 685-688.

[3]   R. K. Thomson, B. O. Patrick, L. L. Schafer, *Canadian Journal of Chemistry* **2005**, *83*, 1037-1042.

[4]   J. I. Clodt, R. Froehlich, M. Eul, E.-U. Wuerthwein, *Eur. J. Inorg. Chem.* **2012**, *2012*, 1210-1217.

[5]   M. J. Frisch, G. W. Trucks, H. B. Schlegel, G. E. Scuseria, M. A. Robb, J. R. Cheeseman, G. Scalmani, V. Barone, B. Mennucci, G. A. Petersson, H. Nakatsuji, M. Caricato, X. Li, H. P. Hratchian, A. F. Izmaylov, J. Bloino, G. Zheng, J. L. Sonnenberg, M. Hada, M. Ehara, K. Toyota, R. Fukuda, J. Hasegawa, M. Ishida, T. Nakajima, Y. Honda, O. Kitao, H. Nakai, T. Vreven, J. A. Montgomery, J. E. Peralta, F. Ogliaro, M. Bearpark, J. J. Heyd, E. Brothers, K. N. Kudin, V. N. Staroverov, R. Kobayashi, J. Normand, K. Raghavachari, A. Rendell, J. C. Burant, S. S. Iyengar, J. Tomasi, M. Cossi, N. Rega, J. M. Millam, M. Klene, J. E. Knox, J. B. Cross, V. Bakken, C. Adamo, J. Jaramillo, R. Gomperts, R. E. Stratmann, O. Yazyev, A. J. Austin, R. Cammi, C. Pomelli, J. W. Ochterski, R. L. Martin, K. Morokuma, V. G.

Zakrzewski, G. A. Voth, P. Salvador, J. J. Dannenberg, S. Dapprich, A. D. Daniels, O. Farkas, J. B. Foresman, J. V. Ortiz, J. Cioslowski, D. J. Fox, *Gaussian 09*, **2009**,

[6]   a) C. Lee, W. Yang, R. G. Parr, *Phys. Rev. B: Condens. Matter* **1988**, *37*, 785-789; b) B. Miehlich, A. Savin, H. Stoll, H. Preuss, *Chem. Phys. Lett.* **1989**, *157*, 200-206.

[7]   M. M. Francl, W. J. Pietro, W. J. Hehre, J. S. Binkley, M. S. Gordon, D. J. DeFrees, J. A. Pople, *J. Chem. Phys.* **1982**, *77*, 3654-3665.

[8]   J. Tomasi, B. Mennucci, R. Cammi, *Chem. Rev.* **2005**, *105*, 2999-3094.

[9]   a) M. E. Casida, C. Jamorski, K. C. Casida, D. R. Salahub, *J. Chem. Phys.* **1998**, *108*, 4439-4449; b) R. E. Stratmann, G. E. Scuseria, M. J. Frisch, *J. Chem. Phys.* **1998**, *109*, 8218-8224.

[10]   R. D. K. Dennington II, T.; Millam, J.; Eppinnett, K.; Hovell, W. L.; Gilliland, R., **2003**, *GaussView 3.0.9,* Semichem, Inc.; Shawnee Mission, KS.

[11]   N. M. T. O'Boyle, A. L.; Langner, K. M., *J. Comp. Chem.* **2008**, *29*, 839-845.

[12]   L. Skripnikov, **2005 - 2015,** *Chemissian V.4.36,*

[13]   **2009-2011,** *APEX2, Bruker AXS,* Madison, WI 53719-1173.

[14]   G. M. Sheldrick, **1996,** *SADABS,*

[15]   **2001,** *SHELXTL, Bruker AXS* Madison, WI 53719-1173.

[16]   A. L. Spek, **2003,** *PLATON,*

[17]   T. Maris, **2004-2014,** *UdMX,*

[18]   CCDC, **2001-2013,** *Mercury 3.1 - 3.3,*

[19]   O. V. Dolomanov, Bourhis, L. J., Gildea, R. J., Howard, J. A. K., Puschmann, H., *J. Appl. Cryst.* **2009**, *42*, 339-341.

[20]   N. G. Connelly, W. E. Geiger, *Chem. Rev.* **1996**, *96*, 877-910.

Annex-6 / Appendix-6 – Chapter 6: Conclusions and Perspectives

Following the format of the 'thesis by articles', concluding remarks are presented at the end of all the chapters/ sections describing published results. Therefore, in this final chapter, a general summary of the thesis is provided in order to reemphasize the main conclusions (**section 6.1**). In addition, the perspectives of the project and the work in progress are highlighted (**section 6.2**), and final remarks are presented (**section 6.3**).

6.1. Summary

Due to their properties, coordination compounds are suitable and attractive for a wide range of applications in fields ranging from catalysis and solar energy conversion/ storage to materials and life sciences. Examples of coordination compounds (from well-established fields, emergent domains and prototype level/ fundamental research) were given (Table 1.1-1 and Figure 1.1.-1, Chapter 1) in order to illustrate their importance in our daily lives. Trends in molecular coordination chemistry were also identified. Driven by the general progress of our society, research evolves *toward complexity at the molecular level*, with Nature representing a major source of inspiration as shown by artificial photosynthesis and metallosupramolecular chemistry. These examples set the general context for this thesis.

The theoretical framework of this work was fixed by key concepts, such as: coordination compound/ coordination complex; bonding/ metal-ligand interaction; ligand design; properties of coordination complexes (experimental *vs.* calculated); structure – properties relationship; molecular/ supramolecular approaches; mixed valence systems; and supramolecular coordination architectures. The design of coordination complexes is seen as a '*collection of adjustable components*' (e.g. ligand: donor atom functional groups, ring substituents and their electronic and steric effects, type and size of the chelate ring; metal-ion; environment). This concept is exemplified with aspects from the coordination chemistry of N,O ligands, in order to lay the ground work for the specific context of the thesis. The same concept is further applied to the research in this thesis.

First, the properties of the ligand system used (*N,N'*-disubstituted amidine oxides (AMOXs)/ α-aminonitrones/ hydroxyamidines) are presented from the same perspective of ligand design. Second, the influence of the ligand substitution pattern on the properties of the complex is investigated within series of bis(AMOX) complexes with different metal-ions (cobalt(II) and zinc(II)). The cobalt(II) bis(chelate) complexes are square-planar (low spin) in the solid state, but show square-planar (low spin) to tetrahedral (high spin) isomerization in solution of non-coordinating solvents. The isomerization equilibrium is highly sensitive to the substitution pattern on the ligand due to a combination of steric and electronic influences. Integration of theoretical studies (DFT/ TD-DFT) with experimental results, for model validation, showed that in the family of zinc(II) bis(AMOX) chelates, by specific modification of the ligands, the optical band gap can be fine-tuned for potential applications in optoelectronic devices. Third, the effect of the environment on the properties of the compounds is explored in a cobalt(II) bisAMOX complex, by examining the critical effect that weak forces and stimuli (e.g., hydrogen bonding, solvation, temperature) have on its final structure(s). Complete structural evidence of a hydrogen-bonding-induced geometry and spin change at a cobalt(II) centre within a same cobalt(II) bis(chelate) is presented. The weak interactions are identified as the main factors responsible for biasing the system toward a specific geometry – spin state combination in the ground state, in a similar fashion to allosteric control and host-guest interactions in biological systems. Thus, the system offers important insights into the role of weak recognition forces and co-operative effects with respect to stereochemistry and spin preferences in four-coordinated metal complexes. Given the relevance of the tetra-coordinate cobalt complexes in catalysis (e.g., radical polymerization, hydrogen production, oxygen transport) and magnetic materials, it could provide exciting new developments in these fields. In addition, preliminary studies were conducted toward AMOX-based supramolecular systems: from multimetallic assemblies to functional materials (sections 5.3.2, 5.3.3, and 6.2.3) and photocatalytic systems for solar energy-conversion (in particular photocatalysis for H_2 production) (section 6.2.3).

6.2. Perspectives and Work in Progress

This section presents the perspectives of the project and information on the work in progress. The results reported herein converge toward the general objective of the thesis stated in the introduction: the study of *N,N'*-disubstituted amidine *N*-oxides (AMOX) ligands from the perspectives of coordination and supramolecular chemistry. Three main directions have been identified for pursuing the research: the AMOX ligands (section 6.2.1), the coordination compounds of AMOX ligands (section 6.2.2), and the AMOX-based supramolecular systems (multimetallic assemblies – toward functional materials and photocatalytic systems for solar energy-conversion, in particular photocatalysis for H_2 production) (section 6.2.3). The progress realized in each of these directions as well as the opportunities for developments will be further assessed.

6.2.1. AMOX Ligands

The *N*-oxidation of the *N,N'*-disubstituted amidines with *m*-CPBA has been optimized, and it has been used as the method of choice for the synthesis of the corresponding AMOXs. Integration of this method with different techniques of obtaining the parent amidines has resulted in a general 'synthetic strategy' for AMOXs preparation (Figure 2.1-2, Chapter 2). It brings together classical (e.g. distillation, thermal reactions) and modern synthesis techniques (e.g. microwave activation). Specific variations of the method allow its application to a broad range of substrates (e.g. different functional groups and different degrees of steric bulk). The method was initially used for the synthesis of mono-AMOXs, but it was successfully extended to the preparation of *N*-bridged-bis-AMOXs and *C*-bridged-bis-AMOXs (Figure 2.1-2, Chapter 2). New AMOXs have thus been synthesized and characterized, which has allowed the development of this class of compound, and their further use in coordination chemistry.

As future developments, the method could be easily adapted for combinatorial synthesis, which would open the opportunity of screening a library of compounds in order to identify the best candidates with the desired properties. Preliminary tests were done for the integration of the *N*-oxidation step in flow chemistry.[1] The major concern for the *N*-oxidation reaction using *m*-CPBA is the protonation of the substrate by the acid produced, with the formation of a stable ion-pair, which prevents total conversion being reached. By using the

flow chemistry technique, the possibility to increase the conversion is envisaged, by optimization of the following parameters: concentration/ stoichiometry/ reactor residence time/ temperature. Additional advantages of using the flow technique are thought to exist for the synthesis of bis-AMOX compounds. In these reactions, besides the protonation issue, the mono-AMOX analogue is also formed. In addition, at concentrations of 0.1M, the formation (in majority) of the over-oxidized cyclic product (compound **C**, Figure 5.3-5 et Figure 5.3-9 section 5.3.3) is observed. In flow, the dilution conditions necessary to maximize the formation of the desired bis-AMOX can be reached, and also, the formation of the mono-AMOX product could be minimized by better control of the optimization parameters.

With respect to the solid-state structures of AMOXs, studies are in progress to identify factors (e.g. substituent effects: steric and/ or electronic, other type of supramolecular interactions) that are generating specific H-bonding patterns: cyclic dimers *via* –O-H---O– et –N-H---N– bonds, with the presence of both the hydroxyamidine and the α-aminonitrone tautomers (type 1); cyclic dimers *via* –O-H---N– bonds, with the presence of the hydroxamidine form only (type 2); cyclic dimers *via* des liens –N-H---O– with the presence of the α-aminonitrone form only (type 3); non-cyclic dimers *via* –O-H---O– bonds, with the presence of both the hydroxyamidine and the α-aminonitrone tautomers (type 4).[2] Understanding and rationalizing such a cause - effect relationship is important in order to efficiently use H-bonding as a crystal engineering design tool. Theoretical studies (e.g. DFT calculations) are also planned in this direction for comparison with experimental findings.

Other possible avenues to explore with AMOX ligands are: their reactivity and tests in catalysis; surface studies; hybrid systems: incorporation in polymers (e.g. as adsorbent for toxic ions); AMOX-QD (quantum dots); AMOX-nanoparticles; AMOX anchored on TiO_2 or POM (recent studies focus on connection of N,O moieties to semiconductors[3] and POM);[4] modulation of the chelation capacity for applications in medicine (chelation therapy),[5] extraction industry;[6] coordination versatility – ligand assistance in catalysis; other dynamic processes in bio-medical applications.

6.2.2. AMOX Coordination Complexes

Some of the avenues to further explore with respect to the AMOX coordination complexes are briefly emphasised below.

a) the AMOX complexes of Co(II) and Co(III) – in **Co(AMOX)₂ complexes** (AMOX = *N,N'*-bis(aryl)-formamidinate-*N*-oxide) the stabilization of the square-planar geometry at the cobalt(II) centre correlates with the presence of substituents in positions 2, 6 of the *N*-aryls, and the bulkiness of these substituents. When only 2-methylphenyl is used as substituent, the pseudo-octahedral Co(III) complex is formed (Figure S1 Appendix-6.2-EXP). The electrochemical properties of the Co(AMOX)₂ compounds, with the reversibility of the Co(II/III) couple, as well as their featureless UV/vis spectra and the steric bulk of the AMOX ligands suggest that these compounds could be suitable candidates for redox mediators in DSSCs.[7a] The characterization of **the family of Co(III)(AMOX)₂X compounds (X = halogen)** is in progress. Preliminary results indicate a possible interest in their magnetic properties. Preliminary tests with Co(AMOX)₂ complexes as catalysts for hydrogen production in photocatalytic systems were performed. The conclusion and the perspectives on this direction are presentd in section 6.2.3.

b) the dimers [Zn(AMOX)₂]₂ (Figure 5.3-4a-e, section 5.3.2) – represent another class of AMOX compounds with potential interest in applications. They are stable and their solubility in organic solvents represents an advantage for their processability in device fabrication. The performance of this type of compounds as luminophores in White OLEDs (WOLEDs) is presently being investigated in collaboration with prof. Nunzi's research group at Queens University. The example of a preliminary result is presented in Figure 5.3-4e, section 5.3.2. Work is currently being pursued for extending this family of compounds. As showed in section 5.3.2, the DFT calculations validated by experimental results revealed that tuning of the LUMO level can be realized by altering the *C*-aryl substituent with EW/ ED groups, in order to obtain the compounds with the desired properties.

c) the Al(AMOX)₃ complexes – are also promising compounds for OLED applications. The research of this family of compounds is in progress. The preliminary results on Al(AMOX)₃ (AMOX = *N,N'*-diphenyl-benzamidinate-*N*-oxide) suggest that these

complexes are soluble in organic solvents, eassy to process in thin films, stable, and emissive in solid state. The comparison of the band gap of Al(AMOX)$_3$ (AMOX = *N,N'*-diphenyl-benzamidinate-*N*-oxide) with those of Alq$_3$ and Zn(BTZ)$_2$ (classical compounds used in OLEDs)[7b] is presented in Figure S2, Appendix-6.2-EXP. Preliminary DFT/ TD-DFT studies suggest that, similar to the zinc(II) complexes, the band gap of the aluminium(III) complexes can be fine tuned by modifying the *C*-aryl substituent of the AMOX ligand.

d) the chemistry of Ru(II)/Re(I) with AMOX ligands – is of interest for the synthesis of photosensitizers and/or catalysts (e.g. for water oxidation, CO$_2$ reduction); Ru(II/III) compounds of AMOXs could be potentially used as photosensitizers in DSSCs – DFT calculations for [Ru(AMOX)(bpy)$_2$]$^+$ (Figure S3, Appendix-6.2-EXP) show the HOMO localized partially on the AMOX ligand, and the LUMO on the bpy moiety (which is the anchor to the semiconductor); this fact strongly suggests the possibility of electron injection, while also having a handle to tune the HOMO level by modifications of the AMOX ligand).

Additional projects include: AMOX complexes of Ni(II), Cu(II) – these projects are in progress; AMOX ligands with lanthanides and actinides; AMOX ligands with other metal ions (Fe(II/III), Mn(II/III/IV), Pt(II), Pd(II), Ir(III) etc.). Furthermore, AMOX ligands substituted with long alkyl chains that form neutral complexes with metal-ions could be exploited in liquid crystals. It would also worth exploring more the reactivity of the AMOX complexes in catalysis and/ or on the complex modifications.

6.2.3. AMOX–based supramolecular systems

6.2.3.1.   Multimetallic systems – toward functional materials

Different multimetallic architectures were obtained upon coordination of the *N*-bridged bis-AMOX ligands with metal-ions: an emissive 1D-metallopolymer with Zn(II) ions (presented in chapter 5, section 5.3.3) and a dinuclear discrete assembly with Ni(II) (work in progress – the solid state structure of the Ni$_2$(bis-AMOX-Ph)$_2$ compound is shown in comparison with that of the Zn(II) coordination polymer (Figure S4, Appendix-6.2-EXP) only to highlight the perspectives of the project on the direction of supramolecular chemistry of AMOX-based systems. The complete characterization of the Ni$_2$(bis-AMOX-Ph)$_2$ compound

is to be finalized. Analogous compounds with paramagnetic metals (e.g., Cu(II)) could be synthesized and investigated for their magnetic properties. The Zn(II) grid species is still to be obtained – screening of different conditions (solvent/ temperature/ stoichiometry) is being pursued. Examining H-bonding in bis-AMOX ligands as well as exploiting the cooperative effects of coordination and H-bonding in AMOX-amidine type compounds present importance from a crystal engineering point-of-view. Extending the ligand design to multifunctional AMOXs by structural variation (e.g. introducing pendant pyridine(s), phosphine(s), to the AMOX backbone) and the coordination to different metal ions could lead to new metallosupramolecular architectures; selective binding of metal ions by specific ligand design would also be of interest.

6.2.3.2.   Photocatalytic systems for hydrogen production

Co(AMOX)$_2$ (AMOX   =   *N*,*N'*-bis(2.6-dimethylphenyl)-formamidinate-*N*-oxide (**Co(2,6-diMe)$_2$**) and *N*,*N'*-bis(2-biphenyl)-formamidinate-*N*-oxide (**Co(2-Ph)$_2$**) complexes were tested as catalysts for H$_2$ production in Re(I)- and Ir(III)-based photocatalytic systems (Figure 6.2-1, Figure 6.2-2 et Figures S5-S11, Appendix-6.2-EXP.[8] A brief overview of these preliminary results is presented here, in order to introduce the perspectives of the project in this direction.

The H$_2$ production was monitored in real-time flow experiments by gas chromatography (Figures S8-S9, Appendix-6.2-EXP).[9] Different combinations of solvent system - proton source, sacrificial electron donor (SED), photosensitizer (PS) and catalyst were screened (Figure S7, Appendix-6.2-EXP).

As general observations, Co(AMOX)$_2$ complexes catalyze H$_2$ production in Re- and Ir-based photocatalystic systems, but with low TONs. The efficiency of the system is very condition dependent. The best results (TON 170) were obtained with Ir-PS, TEA as SED and Co(2-Ph)$_2$, in DMF, with a stoichiometry PS:Cat 5:1 (1:0.2) (Figure 6.2-2). As shown by PS addition tests, the Co(AMOX)$_2$ catalysts are robust (Figure S6, Appendix-6.2-EXP). However, the main drawback is their difficult Co(II/I) reduction. It is well establish in the literature, by experimental and theoretical studies, that the photogenerated Co(I) is the entry species into the cobalt-based H$_2$-production catalytic cycle (Figure S11, Appendix-6.2-EXP).[8a, 8c-e, 10] The

Co(I) species, under photocatalytic conditions, can be generated by oxidative or reductive quenching processes.[11] For Ir/TEA and Re/TEOA systems, it was shown that reductive quenching usually operates (Figure 6.2-1 – top).[8] In the systems under study, however, both the oxidative and the reductive processes are thermodynamically uphill for the electron transfer necessary to generate the Co(I) species (Table S3, Appendix-6.2-EXP). The best performing system (Ir-PS and Co(2-Ph)$_2$ catalyst) is the one with the lowest energy barrier (0.68 V).
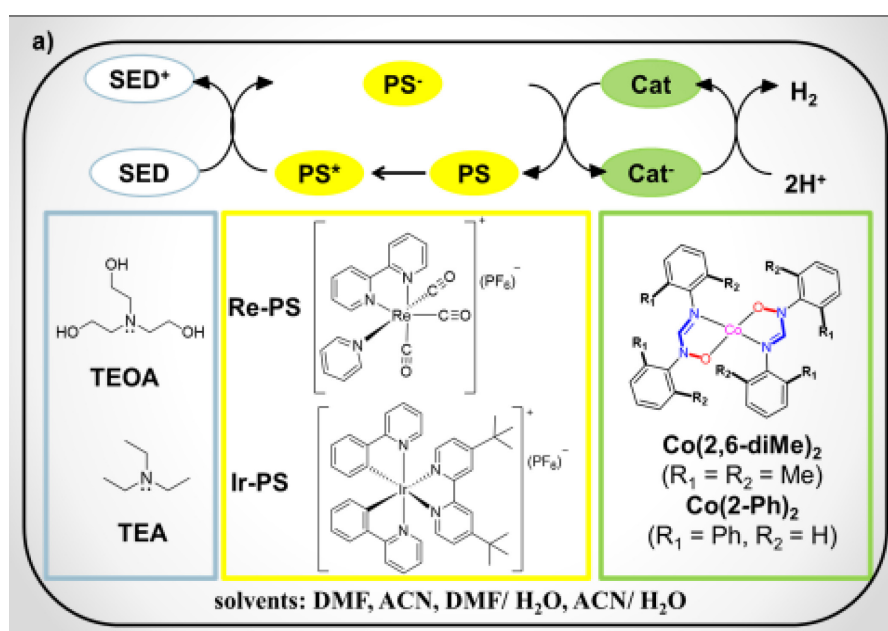
Figure 6.2-1. Photocatalytic systems under study[8]

Therefore, in order to improve the performance of these systems, it is necessary to tune the reduction potential of the Co(AMOX)$_2$ complexes toward more positive values. This can be done by the introduction of EW groups on the AMOX ligand. Modification of AMOX ligands to achieve water solubility of their complexes is another direction for the development of this project, as the final goal is the H$_2$ production in aqueous systems.
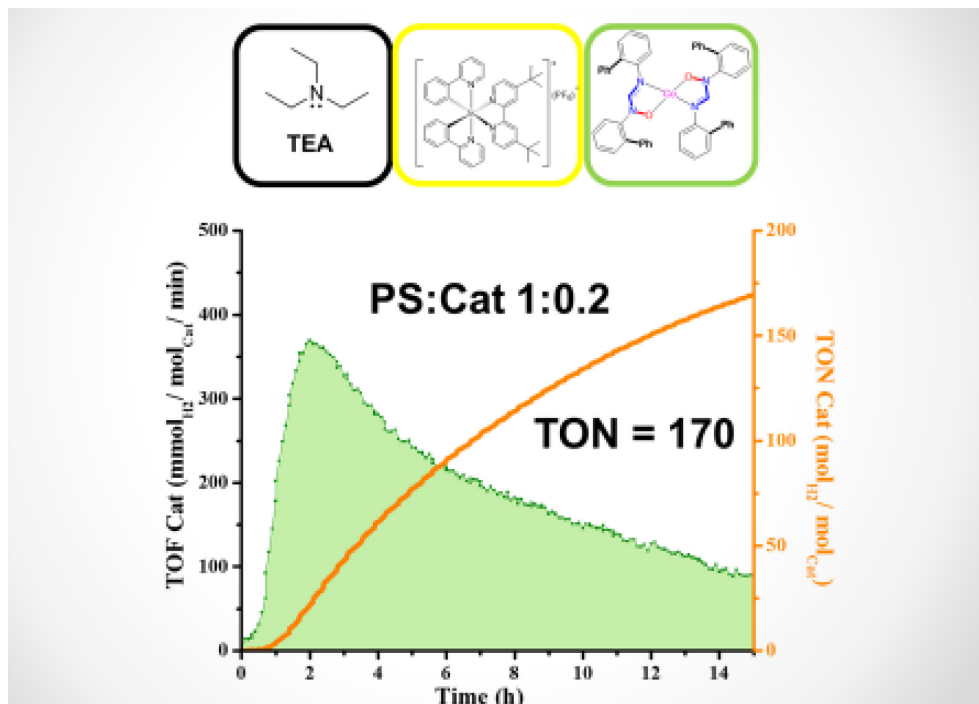
Figure 6.2-2. The best performing system in this study: photocatalytical H_2 production from 7.5 mL DMF solution containing TEA 1M, PS 0.1 mM, and a PS:Cat stoichiometry of 5:1 (1:0.2), at 20^0C (15 h irradiation at 394 nm). In a control experiment (PS only), same conditions, only traces of H_2 were produced.

6.3. Final Remarks

The exploratory nature of this project and the exciting results found thus far have led to multiple research directions that can be pursued. It is my hope that the results and the perspectives presented in this work motivate further developments in AMOX coordination chemistry.

As this project directly relates to modern coordination chemistry, key directions/ strategies in the study of coordination complexes and their use in applications are presented as final remarks. They are based on the results obtained as well as on the overall research experience and knowledge accumulated during this project:

- the development of design strategies for coordination complexes with emphasis on the ligand design; the final objective is to make use of structure – properties relationships to successfully design and synthetize compounds with tailor-made properties;

- the integration of theoretical studies (theoretical calculations e.g. DFT and TD-DFT methods) with synthesis and experimental work to validate theoretical models;

- the use of screening systems/ combinatorial approaches to conduct systematic studies of coordination complexes, as well as for systematic investigations of their performance in specific devices;

- the use of multidisciplinary approaches in synthesis, characterization methods, and device fabrication to generate hybrid systems which exploit pre-design and complementarity principles together with synergic effects, in order to gain enhanced efficiency;

- **the development of more efficient strategies and methods to link (designing/ predicting/ tuning/ adapting) the properties of coordination complexes with their performance in applications (in both devices and processes);**

- the pursuit of control at molecular level; attempts to better understand the behaviour of molecules at interfaces and on surfaces, water-solubility/ organic-solvent-solubility of coordination complexes;

- the development of new strategies to integrate the new discoveries (e.g. use of redox-active ligands).

And on a more general level:

- the improvement of the existing tools and the development of new ones (databases, research tools, software, etc) by integrating new technologies in order to cope with the extensive research and enormous progress as well as with the explosion of reported information;

- the search for trends in the study of coordination compounds and for lessons from the past and present; the development of a global, holistic approach for the study of coordination complexes based on the real needs of society and the values which respect ethics and prioritize

'life' and 'environment' – by extending it to the education in coordination chemistry and to collaboration initiatives (academia – government – industry);

- the investment in fundamental research, as breakthroughs in science happen by means of fundamental research.

~ ~ ~

'*There are things we do not know we don't know*' (Donald Rumsfeld, in a Press Conference at NATO Headquarters, Brussels, Belgium 2002); therefore as a researcher it is important to keep observing, to keep an open mind and pay attention, to be ready to welcome serendipity. It is also important to change perspective, to think dynamically, to look for 'the big picture' in specific situations and for specifics in general trends, as:

'*SCIENCE AT ITS BEST PROVIDES US WITH BETTER QUESTIONS, NOT ABSOLUTE ANSWERS*' (Norman Cousins, 1976) **and** '*THE REAL VOYAGE OF DISCOVERY CONSISTS NOT IN SEEKING NEW LANDSCAPES BUT IN HAVING NEW EYES*' (Marcel Proust).

6.4. References

[1]   D. T. McQuade, P. H. Seeberger, *J. Org. Chem.* **2013**, *78*, 6384-6389.
[2]   a) M. Cibian, S. Derossi, G. S. Hanan, *Acta Crystallogr. Sect. E* **2009**, *65*, o2485-o2485; b) A. Krajete, G. Steiner, H. Kopacka, K.-H. Ongania, K. Wurst, Marc O. Kristen, P. Preishuber-Pflügl, B. Bildstein, *Eur. J. Inorg. Chem.* **2004**, *2004*, 1740-1752.
[3]   L. Zhang, J. M. Cole, *ACS Appl. Mat. & Interf.* **2015**, *7*, 3427-3455.
[4]   B. Artetxe, S. Reinoso, L. San Felices, P. Vitoria, A. Pache, J. Martín-Caballero, J. M. Gutiérrez-Zorrilla, *Inorg. Chem.* **2015**, *54*, 241-252.
[5]   a) G. Crisponi, V. M. Nurchi, J. I. Lachowicz, M. Crespo-Alonso, M. A. Zoroddu, M. Peana, *Coord. Chem. Rev.* **2015**, *284*, 278-285; b) K. J. Franz, *Curr. Op. in Chem. Biol.* **2013**, *17*, 143-149; c) S. J. S. Flora, in *Comprehensive Inorganic Chemistry II (Second Edition)* (Ed.: Poeppelmeier, J. R.), Elsevier, Amsterdam, **2013**, pp. 987-1013.
[6]   P. A. Tasker, P. G. Plieger, L. C. West, in *Comprehensive Coordination Chemistry II* (Ed.: Meyer, J. A. and McCleverty, T. J.), Pergamon, Oxford, **2003**, pp. 759-808.
[7]   a) T. W. Hamann, *Dalton Trans.* **2012**, *41*, 3111; b) R. Wang, L. Deng, M. Fu, J. Cheng, J. Li, *J. Mat. Chem.* **2012**, *22*, 23454-23460.
[8]   a) P. Zhang, P.-A. Jacques, M. Chavarot-Kerlidou, M. Wang, L. Sun, M. Fontecave, V. Artero, *Inorg. Chem.* **2012**, *51*, 2115-2120; b) A. M. Soliman, D. Fortin, P. D. Harvey,

E. Zysman-Colman, *Chem. Commun.* **2012**, *48*, 1120-1122; c) B. Probst, M. Guttentag, A. Rodenberg, P. Hamm, R. Alberto, *Inorg. Chem.* **2011**, *50*, 3404-3412; d) B. Probst, A. Rodenberg, M. Guttentag, P. Hamm, R. Alberto, *Inorg. Chem.* **2010**, *49*, 6453-6460; e) B. Probst, C. Kolano, P. Hamm, R. Alberto, *Inorg. Chem.* **2009**, *48*, 1836-1843.

[9]   D. Chartrand, PhD Thesis: *Vers des assemblages de complexes métalliques oligonucléaires, servant d'antenne solaire au niveau moléculaire*, Université de Montréal, **2013**

[10]   a) S. Berardi, S. Drouet, L. Francas, C. Gimbert-Surinach, M. Guttentag, C. Richmond, T. Stoll, A. Llobet, *Chem. Soc. Rev.* **2014**, *43*, 7501-7519; b) B. H. Solis, Y. Yu, S. Hammes-Schiffer, *Inorg. Chem.* **2013**, *52*, 6994-6999; c) J. L. Dempsey, J. R. Winkler, H. B. Gray, in *Comprehensive Inorganic Chemistry II (Second Edition)* (Ed.: Poeppelmeier, J. R.), Elsevier, Amsterdam, **2013**, pp. 553-565.

[11]   V. Artero, M. Chavarot-Kerlidou, M. Fontecave, *Angew. Chem., Int. Ed.* **2011**, *50*, 7238-7266.

Annexe-6.2-EXP/ Appendix-6.2-EXP
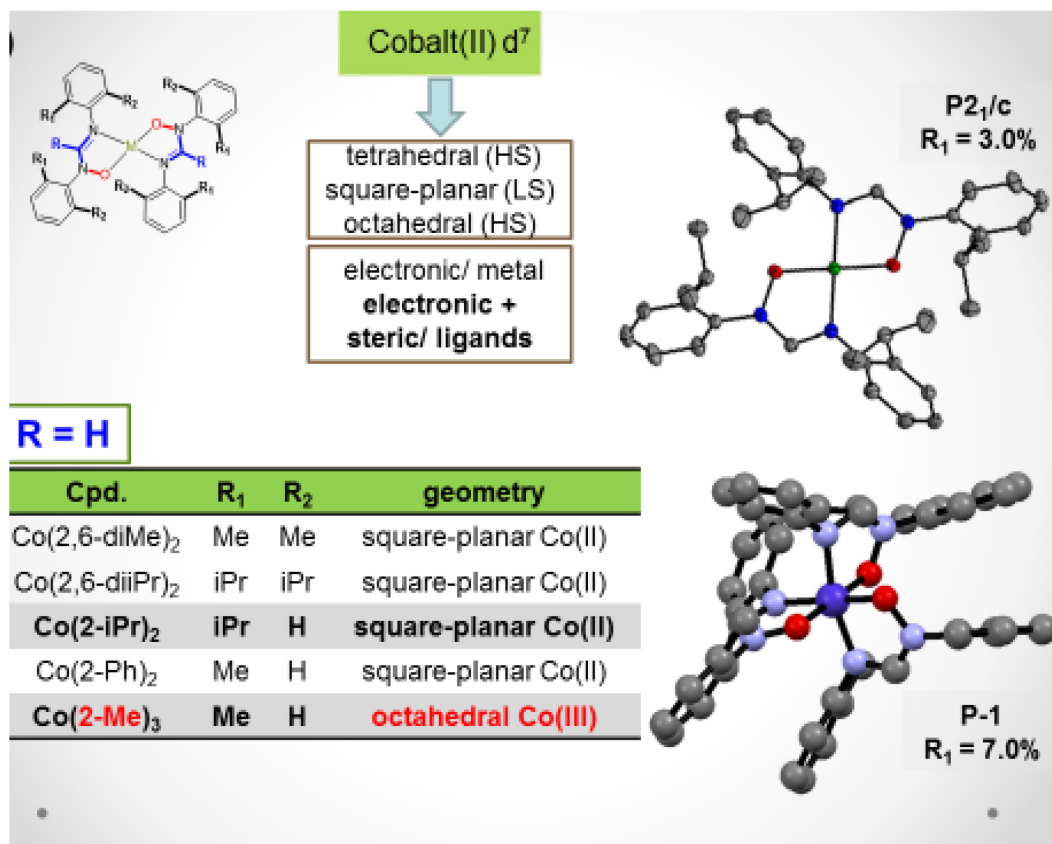
Figure S1. Cobalt(II) and cobalt(III) complexes of AMOX ligands – effect of the substitution pattern of the ligand on geometry and oxidation state of the metal ion. For Co(2-Me)₂ compound, the poor quality of the crystal allows only for the connectivity between the atoms to be observed (isotropic refinement).
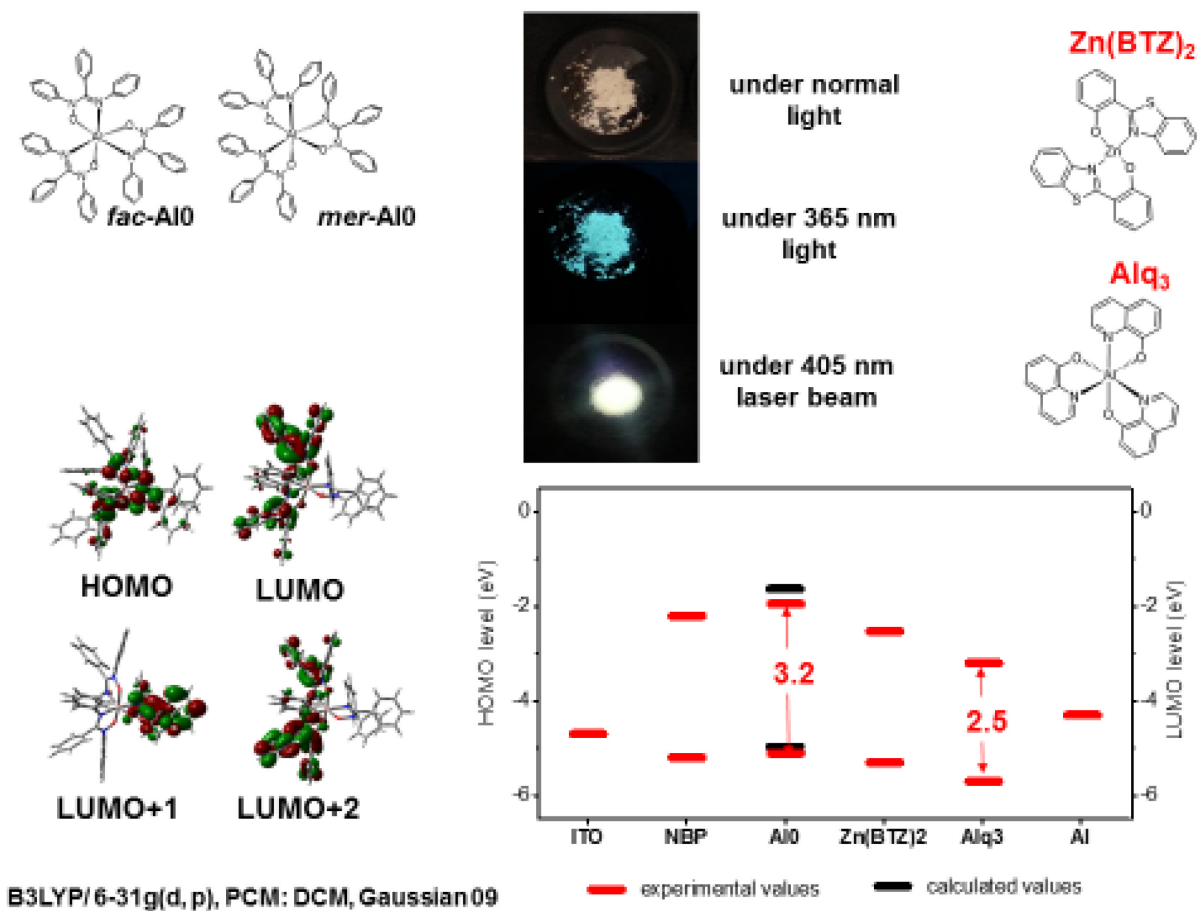
Figure S2. Highlights of Al(AMOX)₃ (AMOX = *N,N'*-diphenyl-benzamidinate-*N*-oxide): isomeric structures; emission (solid state); MO surfaces; calculated vs. experimental band gap and comparison with those of Alq₃ and Zn(BTZ)₂[1]

Computational details for Al(AMOX)₃ (AMOX = *N,N'*-diphenyl-benzamidinate-*N*-oxide) – same as reported in chapter 5.

Table S1. Atomic coordinates for DFT optimization of **Al(AMOX)₃** (AMOX = *N,N'*-diphenyl-benzamidinate-*N*-oxide) (theory level: B3LYP/ 6,31-g(d,p), PCM: CH₂Cl₂)

```
            Standard orientation:
---------------------------------------------------------------------
Center     Atomic     Atomic            Coordinates (Angstroms)
Number     Number     Type          X           Y           Z
---------------------------------------------------------------------
    1         13         0        0.167890   -0.226192    0.175118
    2          8         0       -0.601363   -1.496620   -0.992882
    3          8         0        0.729273    1.232460    1.242255
    4          7         0       -1.758013   -2.075751   -0.530064
    5          8         0        1.103469   -1.405629    1.325666
    6          7         0        0.407764    2.480059    0.769210
    7          6         0       -3.584877   -2.097446    1.103272
    8          6         0       -0.388046    2.528055   -0.312298
    9          6         0       -0.670966    4.248271   -2.111789
   10          6         0       -1.166126    5.469329   -2.567302
   11          6         0        1.031766    3.550755    1.469094
   12          6         0        1.652462    4.610396    0.796614
   13          1         0        1.655207    4.641340   -0.286340
   14          6         0        2.267805    5.625895    1.529248
   15          1         0        2.744436    6.446970    1.002247
   16          6         0        2.292250    5.578631    2.924114
   17          1         0        2.779991    6.367106    3.488927
   18          6         0        1.694374    4.503458    3.587802
   19          1         0        1.713574    4.454482    4.672471
   20          6         0        1.066929    3.489013    2.868474
   21          1         0        0.600843    2.649209    3.369844
   22          7         0        2.433807   -1.559610    1.011560
   23          7         0        1.933868   -0.392354   -0.862006
   24          6         0       -0.910039    3.839886   -0.791577
   25          7         0       -0.656656    1.352892   -0.870997
   26          6         0       -2.163898   -3.148591   -2.662911
   27          1         0       -1.888038   -2.214473   -3.137206
   28          6         0       -2.522109   -4.264112   -3.416206
   29          1         0       -2.527892   -4.196943   -4.500104
   30          6         0       -2.876080   -5.460863   -2.786400
   31          1         0       -3.155831   -6.327678   -3.377236
   32          6         0       -2.856289   -5.537761   -1.392875
   33          1         0       -3.110763   -6.467852   -0.893609
   34          6         0       -2.487529   -4.430608   -0.627698
   35          1         0       -2.448499   -4.502379    0.452487
   36          6         0       -2.163054   -3.226759   -1.264136
   37          6         0       -6.058247   -3.021324    2.036795
   38          1         0       -7.016742   -3.381055    2.398579
   39          6         0        2.167495   -0.026675   -2.216228
   40          6         0        2.299115    1.326685   -2.559075
   41          1         0        2.273378    2.072469   -1.771600
   42          6         0        2.475644    1.705066   -3.890881
   43          1         0        2.586398    2.756981   -4.138852
   44          6         0        2.516356    0.739361   -4.899596
   45          1         0        2.652016    1.034750   -5.935594
   46          6         0        2.381684   -0.609768   -4.563445
   47          1         0        2.409299   -1.369680   -5.339226
   48          6         0        2.205544   -0.992324   -3.232857
   49          1         0        2.086838   -2.038681   -2.971287
   50          6         0       -2.272018   -1.588113    0.613436
   51          6         0       -1.685648    1.243431   -1.849774
   52          6         0       -1.390760    0.738775   -3.124496
   53          1         0       -0.368556    0.469978   -3.362083
   54          6         0       -2.400344    0.596604   -4.077171
```

```
55          1          0      -2.152121     0.215073    -5.063808
56          6          0      -3.719527     0.944063    -3.773812
57          1          0      -4.502066     0.830933    -4.518138
58          6          0      -4.020164     1.438868    -2.503442
59          1          0      -5.040769     1.713180    -2.251433
60          6          0      -3.013174     1.584378    -1.547525
61          1          0      -3.249390     1.969160    -0.560986
62          6          0      -1.197267     0.089072     3.494595
63          1          0      -0.260381    -0.456675     3.481613
64          6          0      -1.595682     0.811249     4.619141
65          1          0      -0.962232     0.817566     5.501943
66          6          0      -2.801279     1.519150     4.617746
67          1          0      -3.108734     2.081213     5.494539
68          6          0      -3.604840     1.498358     3.476360
69          1          0      -4.541780     2.048125     3.458826
70          6          0      -3.211847     0.776729     2.347561
71          1          0      -3.839358     0.764680     1.462926
72          6          0      -2.007129     0.056541     2.348324
73          7          0      -1.543462    -0.653658     1.210410
74          6          0      -1.663942     4.660305     0.059323
75          6          0      -2.166866     5.875641    -0.403976
76          6          0      -1.915573     6.284525    -1.715524
77          1          0      -2.304568     7.232942    -2.073536
78          6          0      -4.922645    -3.123351     2.844189
79          6          0      -3.691711    -2.657616     2.384357
80          6          0       4.468676    -1.627476     2.405098
81          1          0       4.871394    -0.765664     1.887203
82          6          0       3.217066    -2.142415     2.045533
83          6          0       2.674685    -3.223284     2.753853
84          1          0       1.691714    -3.589570     2.483858
85          6          0       3.399380    -3.804590     3.791547
86          1          0       2.975499    -4.645566     4.332287
87          6          0       4.662577    -3.314681     4.134967
88          1          0       5.224817    -3.770431     4.944128
89          6          0       5.189945    -2.225813     3.438733
90          1          0       6.160998    -1.822798     3.710291
91          6          0      -5.958839    -2.452253     0.765432
92          6          0      -4.727466    -1.994223     0.297268
93          6          0       2.835125    -1.090374    -0.183761
94          6          0       4.609753    -2.738497    -0.830943
95          6          0       5.880380    -3.035790    -1.322422
96          6          0       6.760690    -2.005148    -1.658748
97          1          0       7.751215    -2.237716    -2.037925
98          6          0       6.363932    -0.674237    -1.508125
99          6          0       5.090764    -0.372648    -1.026319
100         6          0       4.207087    -1.404235    -0.677693
101         1          0       6.181786    -4.071861    -1.442399
102         1          0       3.926226    -3.539473    -0.568108
103         1          0       4.782099     0.661080    -0.913298
104         1          0       7.045317     0.130429    -1.766797
105         1          0      -2.754801     6.502385     0.259522
106         1          0      -1.859590     4.341841     1.078234
107         1          0      -0.969085     5.782611    -3.587975
108         1          0      -0.095650     3.610427    -2.774706
109         1          0      -4.649883    -1.549371    -0.689711
110         1          0      -6.839637    -2.364234     0.136765
111         1          0      -4.995098    -3.563639     3.833939
112         1          0      -2.811331    -2.730500     3.014447
---------------------------------------------------------------
```
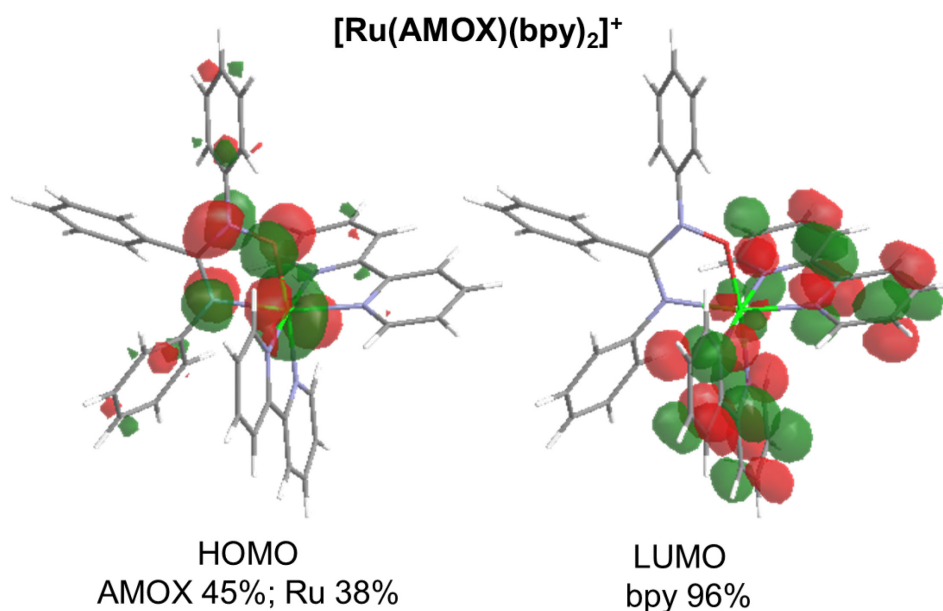
[Ru(AMOX)(bpy)₂]⁺

HOMO
AMOX 45%; Ru 38%

LUMO
bpy 96%

Figure S3. MO surfaces (HOMO and LUMO) for [Ru(AMOX)(bpy)₂]⁺ (B3LYP/ LANL2DZ/ PCM: acétonitrile/ Gaussian 09)

Computational details for [Ru(AMOX)(bpy)₂]⁺ – same as reported in chapter 3

Table S2. Atomic coordinates for DFT optimization of **[Ru(AMOX)(bpy)₂]⁺** (AMOX = *N,N'*-diphenyl-benzamidinate-*N*-oxide) (theory level: B3LYP/ LANL2DZ, PCM: CH₂Cl₂)

```
                    Standard orientation:
 ---------------------------------------------------------------------
 Center     Atomic      Atomic         Coordinates (Angstroms)
 Number     Number      Type        X           Y           Z
 ---------------------------------------------------------------------
    1         44          0      -0.920289   -0.351730    0.103789
    2          8          0       0.649168   -1.286248    1.106986
    3          7          0       0.736183    0.895901   -0.388866
    4          7          0       1.867689   -0.803136    0.649316
    5          7          0      -0.643802   -1.681361   -1.494158
    6          7          0      -1.346521    0.914117    1.711527
    7          7          0      -2.491686    0.822554   -0.659294
    8          7          0      -2.267235   -1.889601    0.575783
    9          6          0      -3.025244   -4.099405    0.005941
   10          6          0       3.214926    1.060467   -0.193799
   11          6          0      -1.331575   -2.855815   -1.409658
   12          6          0       0.610631    2.273671   -0.715740
   13          6          0       1.900214    0.385438    0.016197
   14          6          0       0.183812   -1.486904   -2.540006
   15          1          0       0.708947   -0.539863   -2.549273
   16          6          0       2.947117   -1.709937    0.843293
   17          6          0      -0.697305    0.879877    2.890083
   18          1          0       0.066502    0.113264    2.967243
   19          6          0       0.985293    3.286131    0.183440
```

```
20        1        0        1.411502     3.014623     1.143752
21        6        0       -3.089964    -1.910335     1.642913
22        1        0       -3.078887    -1.026191     2.268451
23        6        0        4.083310     1.276668     0.886956
24        1        0        3.800844     0.938605     1.878942
25        6        0       -2.233049    -2.974403    -0.249963
26        6        0        0.368129    -2.433765    -3.539891
27        6        0       -2.973664     1.779159     0.185614
28        6        0       -1.186757    -3.848838    -2.385381
29        1        0       -1.738731    -4.777080    -2.307951
30        6        0       -4.086684     1.504613    -2.322489
31        6        0       -2.660024     2.756271     2.510721
32        1        0       -3.436497     3.492315     2.344144
33        6        0       -3.045482     0.696889    -1.880488
34        1        0       -2.627144    -0.077849    -2.511843
35        6        0        3.040291    -2.381616     2.070267
36        1        0        2.309113    -2.175481     2.842925
37        6        0        0.806431     4.629513    -0.149907
38        1        0        1.104059     5.398940     0.557053
39        6        0       -2.323013     1.839998     1.508686
40        6        0        3.584795     1.506148    -1.471899
41        1        0        2.917542     1.345346    -2.312269
42        6        0        0.034885     2.638526    -1.943161
43        1        0       -0.264080     1.860499    -2.638043
44        6        0       -0.988224     1.763677     3.922991
45        6        0       -4.019650     2.623137    -0.202019
46        6        0        3.864651    -1.986647    -0.178616
47        1        0        3.771043    -1.494388    -1.139679
48        6        0       -1.987091     2.719224     3.728486
49        1        0       -2.239700     3.425429     4.512151
50        6        0        4.807501     2.148164    -1.665471
51        1        0        5.088428     2.481204    -2.660058
52        6        0       -4.582628     2.488442    -1.466843
53        1        0       -5.394391     3.137922    -1.776146
54        6        0        4.894934    -2.900482     0.046709
55        1        0        5.605274    -3.107608    -0.748186
56        6        0        5.301145     1.927513     0.691505
57        1        0        5.962734     2.095644     1.535879
58        6        0       -0.144362     3.982554    -2.270310
59        1        0       -0.584106     4.245601    -3.228273
60        6        0        5.667494     2.361800    -0.584990
61        1        0        6.617642     2.865037    -0.737038
62        6        0       -3.867531    -4.113914     1.112287
63        1        0       -4.484162    -4.981988     1.318845
64        6        0        0.242862     4.985951    -1.377519
65        1        0        0.103333     6.031801    -1.633974
66        6        0       -3.903250    -2.995285     1.945572
67        6        0       -0.330060    -3.639600    -3.460457
68        1        0       -0.210905    -4.403399    -4.221328
69        6        0        5.001549    -3.560414     1.273020
70        1        0        5.800572    -4.276142     1.440472
71        6        0        4.065931    -3.301705     2.279254
72        1        0        4.136438    -3.814777     3.233845
73        1        0       -4.494050     1.359185    -3.316484
74        1        0       -4.394184     3.377726     0.478306
75        1        0        1.048027    -2.225191    -4.358068
76        1        0       -2.985407    -4.957532    -0.652956
77        1        0       -4.544723    -2.957926     2.818618
78        1        0       -0.440125     1.700457     4.856221
    --------------------------------------------------------------------
```
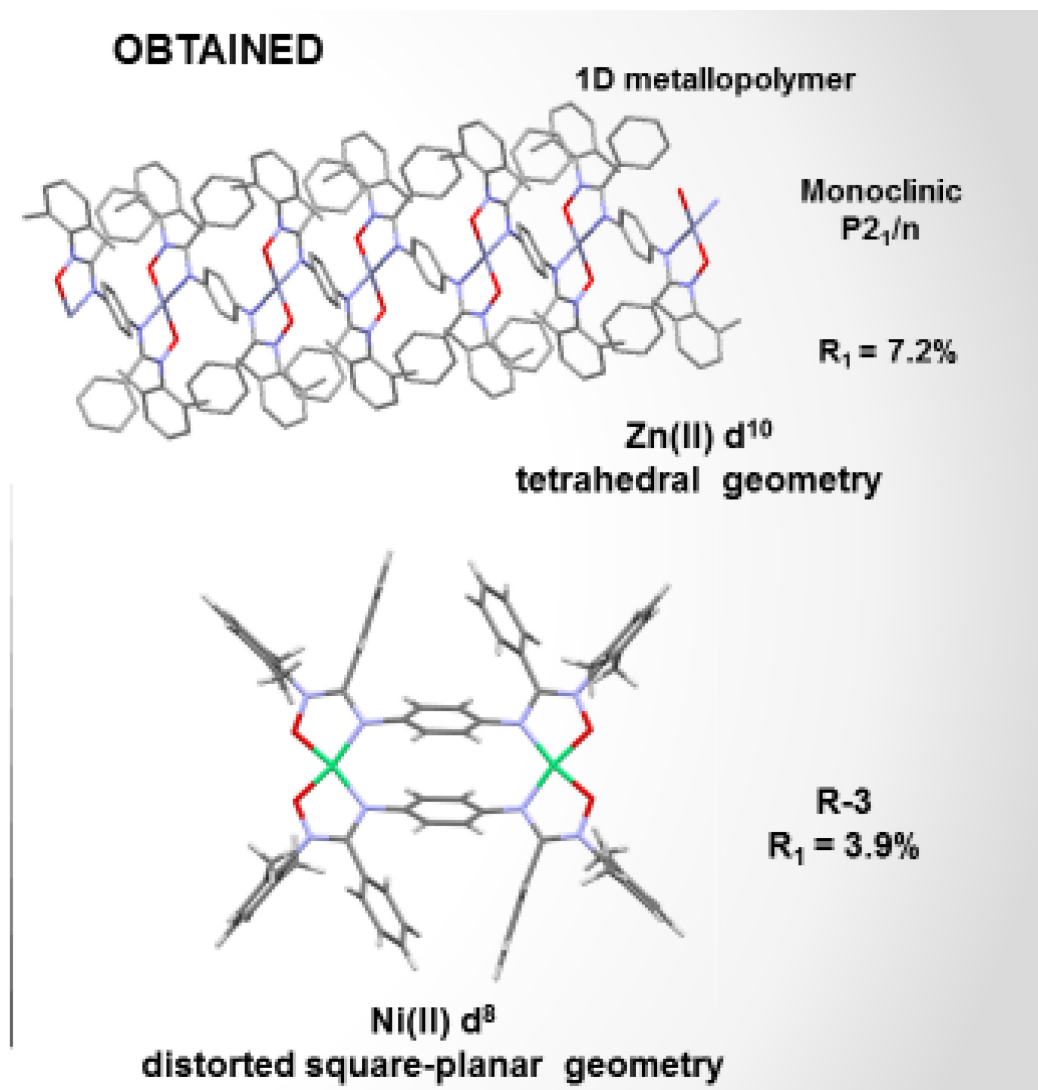
OBTAINED

1D metallopolymer

Monoclinic
P2$_1$/n

R$_1$ = 7.2%

Zn(II) d^{10}
tetrahedral geometry

R-3
R$_1$ = 3.9%

Ni(II) d^8
distorted square-planar geometry

Figure S4. Discreet assemblies and coordination polymers based on *N*-bridged bis-AMOX ligands

Details on initial H₂ production tests

The initial H$_2$ production tests were done using Re(bpy)(CO)$_3$(py) as photosensitizer (PS) and TEOA as SED in DMF. A TON of 6 was obtained vs. 0.2 in the control experiment without catalyst (Figure S5). However, PS addition tests showed Co(2,6-diMe)$_2$ to be more robust in the same conditions than the Co(dmgBF$_2$)$_2$ (Figure S6).

Photochemical H$_2$ production from 7.5 mL DMF solution containing TEOA 1M, PS 0.25 mM, and catalyst 0.25 mM, at 20^{0}C (6h irradiation at 394 nm). **Inset showing control experiment (PS only), same conditions**
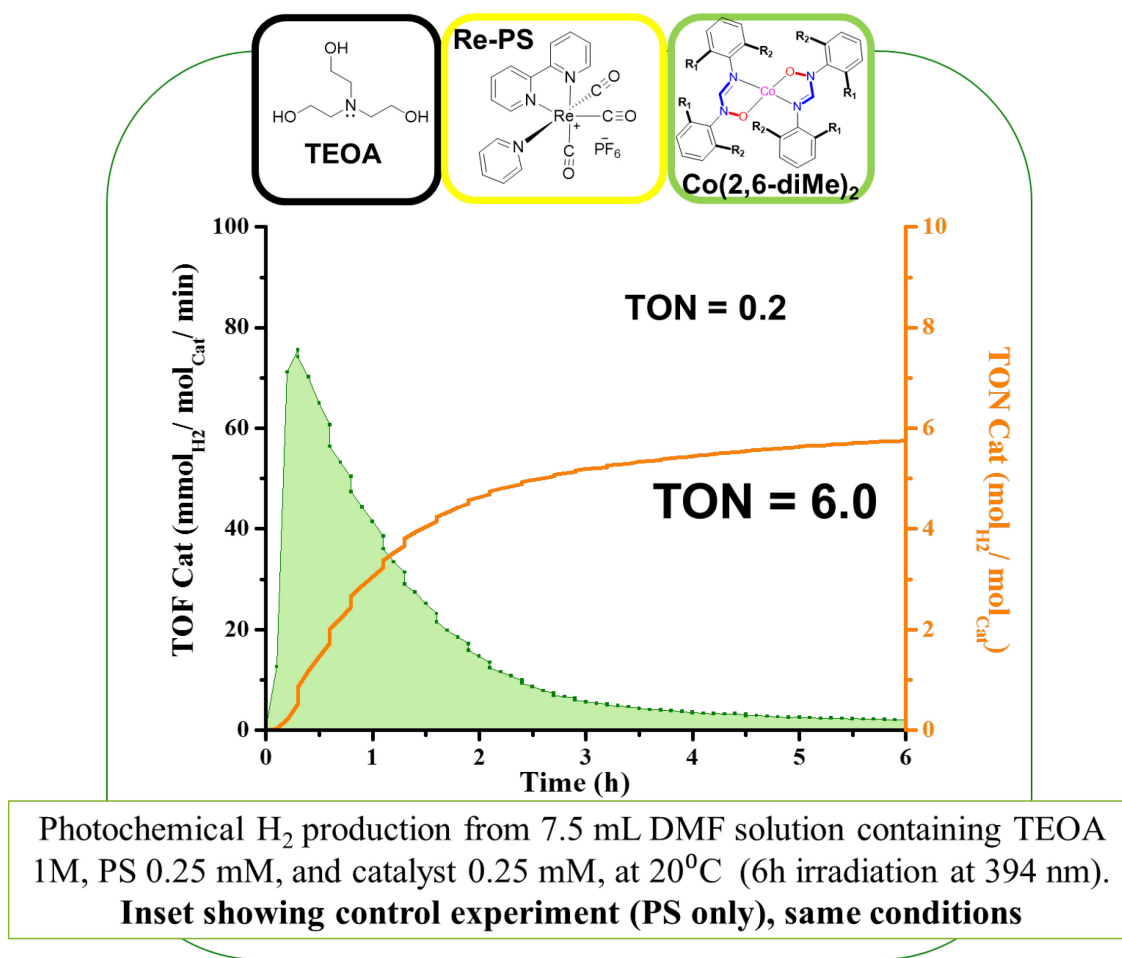
Figure S5. Initial H$_2$ production tests
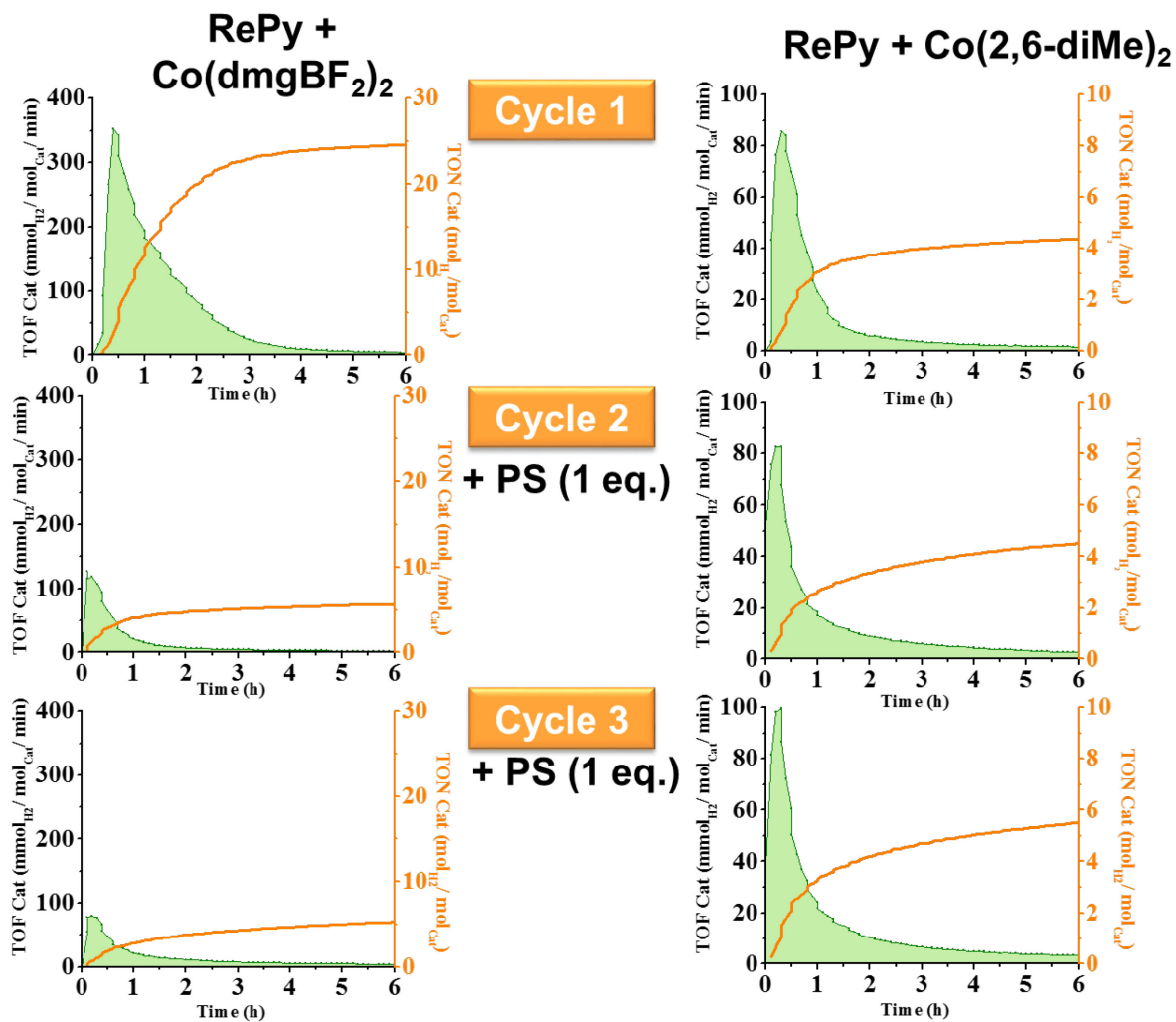
Figure S6. PS addition tests.

The results obtained using Ir-PS and Co(2,6-diMe)2, in different conditions are summarized in Figure S7.
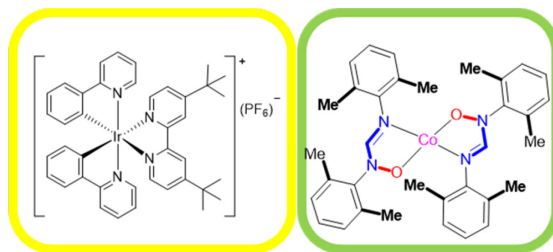
No.	Solvent system	SED (1 M)	PS:Cat	TOF$_{max}$ (time)	TON (time)
1[a]	DMF	TEOA	1:1	50 (30 min)	**6** (4 h)
2[a]	DMF	TEOA	1:2	130	**2**
3[a]	DMF/ H$_2$O (1/1)	TEOA	1:1	200 (15 min)	7 (4 h)
4[b]	DMF/ acid (0.1 M)	TEOA	1:1:	125 (2 min)	**<1** (1.5h)
5[b]	DMF	TEA	1:0.2	<10	**<1** (4 h)
6[b]	ACN/ H$_2$O (1/1) – pH 13.5	TEA	1:0.2	2250 (2 min)	**35** (6 h)
7[b*]	ACN/ H$_2$O (1/1) – pH 10.5	TEA	1:0.2	2750 (2 min)	**55** (6 h)

[a] [PS]=0.25 mM; [b] [PS]=0.1 mM; *control experiment (PS only) produced H$_2$ (half of the quantity produced in 7)

Figure S7. Photochemical H$_2$ production under various experimental conditions

Details on the experimental set-up for flow experiments – system designed and built by Daniel Chartrand, PhD Thesis: *Vers des assemblages de complexes métalliques oligonucléaires, servant d'antenne solaire au niveau moléculaire*, **2013**, p. 130
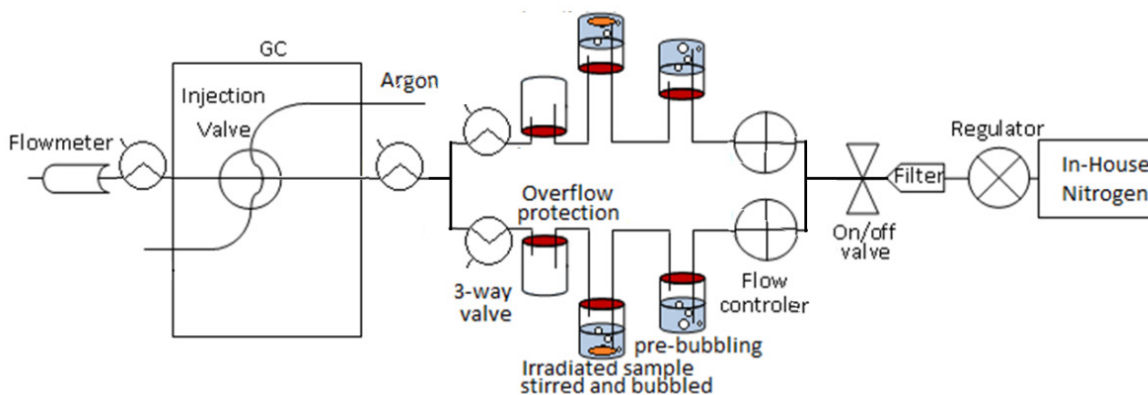
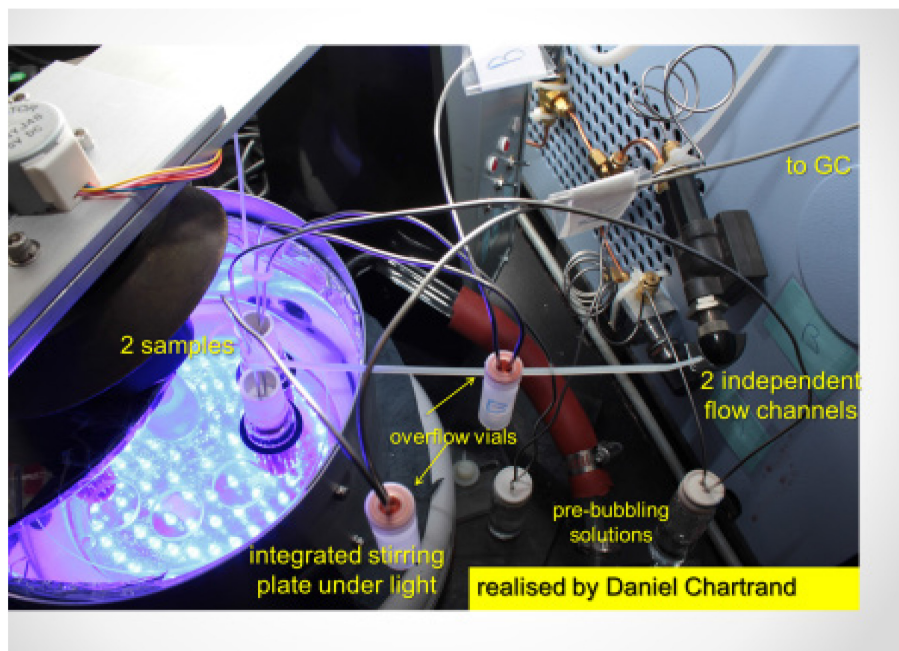**Figure S8.** Scheme of the flow system (2 channels) [2]

Figure S9. Experimental set-up for hydrogen production experiments (photoreactor and flow experiment set-up) – system designed and built by Daniel Chartrand.[2]
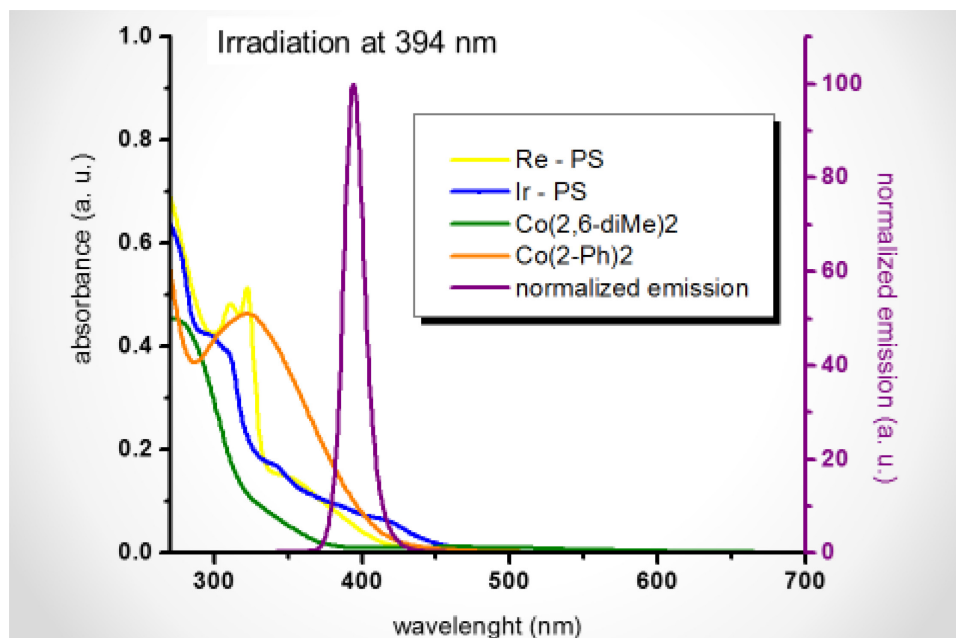

Figure S10. UV-vis spectra of PSs and catalysts in DMF, and emission spectrum of the UV-lamp used (irradiation at 394 nm)
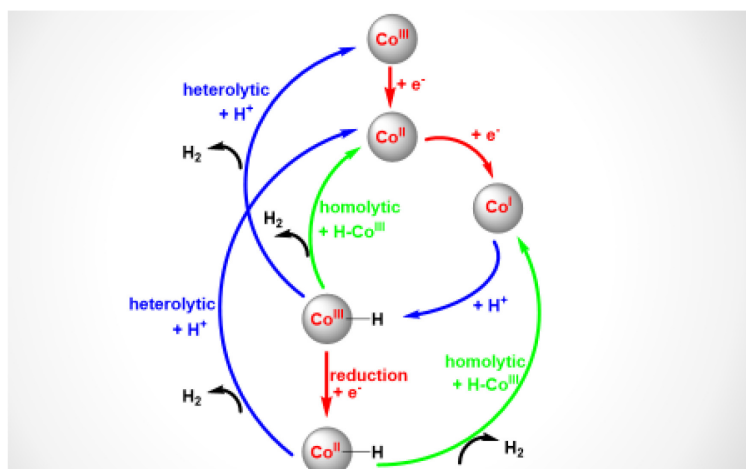
Figure S11. Cobalt-based catalytic cycle for hydrogen production.[3]

Table S3. Redox properties of PS and catalysts, and the free energies of formation (ΔG_1 and (ΔG_2) of Co^I species by oxidative and reductive quenching, respectively

PSs	Excited state energy (eV) and E (V)	
Ir*	2.16	
Ir $^{(IV/\,III)}$	+1.33	
$(bpy)_{Ir}/(bpy^{\bullet-})_{Ir}$	- 1.42	
Re*	2.19	
Re $^{(II/\,I)}$	> +1.60	
$(bpy)_{Re}/(bpy^{\bullet-})_{Re}$	- 1.26	
Catalysts	E (V) and ΔG (V)	
	Co(2-Ph)₂	**Co(2,6-diMe)₂**
$Co^{(II/\,I)}$	- 2.10	- 2.27
$Co^{(III/\,II)}$	+ 0.14	+ 0.14
ΔG_1 (Ir* → Co^I)	+ 0.85	+ 1.44
ΔG_2 ($(bpy)_{Ir}/(bpy^{\bullet-})_{Ir}$ → Co^I)	**+ 0.68**	+ 1.27
ΔG_1 (Re* → Co^I)	+ 1.01	+ 1.68
ΔG_2 ($(bpy)_{Re}/(bpy^{\bullet-})_{Re}$ → Co^I)	+ 0.84	+ 1.51

ΔG_1 (Ir* to Co^I) = E(Ir $^{(IV/\,III)}$) − E($Co^{(II/\,I)}$) − E(Ir*)
ΔG_2 ($(bpy)_{Ir}/(bpy^{\bullet-})_{Ir}$ → Co^I) = E(Ir $^{(IV/\,III)}$) − E($Co^{(II/\,I)}$) − E(Ir*)
ΔG_1 (Re* to Co^I) = E(Ir $^{(IV/\,III)}$) − E($Co^{(II/\,I)}$) − E(Ir*)
ΔG_2 ($(bpy)_{Re}/(bpy^{\bullet-})_{Re}$ → Co^I) = E(Ir $^{(IV/\,III)}$) − E($Co^{(II/\,I)}$) − E(Ir*)
Potentials are reported *vs.* SCE; they were measured during this work, in DMF, in the same conditions described in section 3.3.

References

[1]   R. Wang, L. Deng, M. Fu, J. Cheng, J. Li, *J. Mat. Chem.* **2012**, *22*, 23454-23460.

[2]   D. Chartrand, PhD Thesis: *Vers des assemblages de complexes métalliques oligonucléaires, servant d'antenne solaire au niveau moléculaire,* Université de Montréal, **2013**

[3]   a) P. Zhang, P.-A. Jacques, M. Chavarot-Kerlidou, M. Wang, L. Sun, M. Fontecave, V. Artero, *Inorg. Chem.* **2012**, *51*, 2115-2120; b) B. Probst, M. Guttentag, A. Rodenberg, P. Hamm, R. Alberto, *Inorg. Chem.* **2011**, *50*, 3404-3412; b) B. Probst, A. Rodenberg, M. Guttentag, P. Hamm, R. Alberto, *Inorg. Chem.* **2010**, *49*, 6453-6460; d) B. Probst, C. Kolano, P. Hamm, R. Alberto, *Inorg. Chem.* **2009**, *48*, 1836-1843; e) S. Berardi, S. Drouet, L. Francas, C. Gimbert-Surinach, M. Guttentag, C. Richmond, T. Stoll, A. Llobet, *Chem. Soc. Rev.* **2014**, *43*, 7501-7519; f) B. H. Solis, Y. Yu, S. Hammes-Schiffer, *Inorg. Chem.* **2013**, *52*, 6994-6999; g) J. L. Dempsey, J. R. Winkler, H. B. Gray, in *Comprehensive Inorganic Chemistry II (Second Edition)* (Ed.: J. R. Poeppelmeier), Elsevier, Amsterdam, **2013**, pp. 553-565; h) V. Artero, M. Chavarot-Kerlidou, M. Fontecave, *Angew. Chem., Int. Ed.* **2011**, *50*, 7238-7266.